

# The Brain

W. Reith

- 9.1 Anatomy – 57**
  - 9.1.1 Organisation of the Brain – 57
  - 9.1.2 Cranial Nerves and Cranial Nerve Nuclei – 59
  - 9.1.3 Mid-brain – 64
  - 9.1.4 Cerebral Peduncle – 65
  - 9.1.5 Cerebellum – 65
  - 9.1.6 Diencephalon – 65
  - 9.1.7 Functional Pathways of the Cerebrum – 66
  - 9.1.8 Blood Supply to the Brain – 69
  - 9.1.9 Cerebral Veins and Dural Venous Sinuses – 73
- 9.2 Developmental Disorders and Malformations of the Brain – 74**
  - 9.2.1 Embryogenesis of the Nervous System – 74
  - 9.2.2 Myelination of the Brain – 76
  - 9.2.3 Neural Tube Defects – 78
  - 9.2.4 Anomalies of the Medial Structures – 79
  - 9.2.5 Disturbances in Cortical Development – 82
  - 9.2.6 Schizencephaly, Porencephaly, Hemi-atrophy – 85
  - 9.2.7 Holoprosencephaly – 86
  - 9.2.8 Developmental Disorders of the Cerebellum and Brain Stem – 86
  - 9.2.9 Arachnoid Cysts – 88
  - 9.2.10 Neuro-cutaneous Syndromes (Phakomatoses) – 90
- 9.3 Vascular Diseases – 95**
  - 9.3.1 Intra-cerebral Vascular Malformations – 95
  - 9.3.2 Stroke – 113
  - 9.3.3 Rare Causes of Vascular Diseases – 129
- 9.4 Intra-cranial Tumours – 136**
  - 9.4.1 Basics – 136
  - 9.4.2 Infra-tentorial Tumours – 139
  - 9.4.3 Supra-tentorial Tumours – 148
  - 9.4.4 Extra-parenchymal Tumours – 163
  - 9.4.5 Malformation and Germ Cell Tumours – 167
  - 9.4.6 Other Rare Tumours of the Posterior Cranial Fossa and Base of the Skull – 169
  - 9.4.7 Tumours of the Sellar Region – 181
  - 9.4.8 Metastases – 188

<b>9.5</b>	<b>Cranio-cerebral Trauma – 190</b>
9.5.1	Basics – 190
9.5.2	Birth Trauma and Other Fractures in Children – 193
9.5.3	Other Consequences of Trauma – 198
9.5.4	Secondary Consequences of Trauma – 206
9.5.5	Child Abuse – 209
<b>9.6</b>	<b>Inflammatory Diseases of the Brain – 210</b>
9.6.1	Meningitis – 212
9.6.2	Complications in Meningitis or Intra-cerebral Infections – 214
9.6.3	CNS Infections in Immunosuppressed Patients – 219
9.6.4	Spongiform Encephalopathy – 232
9.6.5	Parasitic Infections – 234
9.6.6	Multiple Sclerosis and Related Diseases – 234
<b>9.7</b>	<b>Metabolic Disorders of the Central Nervous System – 243</b>
9.7.1	Basics, Definition – 243
9.7.2	Leukodystrophies with Primary Hypo-myelination – 243
9.7.3	Leukodystrophies with an Unknown Metabolic Defect – 244
9.7.4	Leukodystrophies with a Known Defect – 245
9.7.5	Peroxisomal Diseases – 246
9.7.6	Neurolipidoses – 247
9.7.7	Fatty Acid Oxidation Disorders – 249
9.7.8	Heteroglycanosis – 249
9.7.9	Disorders Affecting the Oxidative Phosphorylation System – 250
9.7.10	Metabolic Disorders of Amino Acids – 251
9.7.11	Wilson’s Disease – 252
<b>9.8</b>	<b>Disorders of the White Matter – 252</b>
9.8.1	Primary Demyelination – 252
9.8.2	Ischaemic Demyelination – 253
9.8.3	Demyelination Caused by Infections – 254
9.8.4	Toxic or Metabolically Related Demyelination – 254
9.8.5	Dysmyelinating Diseases – 256
<b>9.9</b>	<b>Neuro-degenerative Disorders – 259</b>
9.9.1	Alzheimer’s Disease – 259
9.9.2	Vascular Dementia, Differential Diagnosis from that of AD – 259
9.9.3	Fronto-temporal Dementia – 259
9.9.4	Parkinson’s Disease – 259
9.9.5	Multiple System Atrophy – 260
9.9.6	Huntington’s Disease – 262
9.9.7	Fahr’s Disease – 262
9.9.8	Other Diseases Associated with Degenerative Changes – 263
<b>9.10</b>	<b>Hydrocephalus and Intra-cranial Hypotension – 264</b>
9.10.1	Hydrocephalus – 264
9.10.2	Low CSF Pressure – 268
	<b>References – 268</b>

## 9.1 Anatomy

### 9.1.1 Organisation of the Brain

The brain can be divided into the following sections based on morphological, developmental, and functional aspects:

- Medulla oblongata
- Pons
- Mesencephalon
- Diencephalon
- Cerebellum
- Telencephalon

A further classification is into:

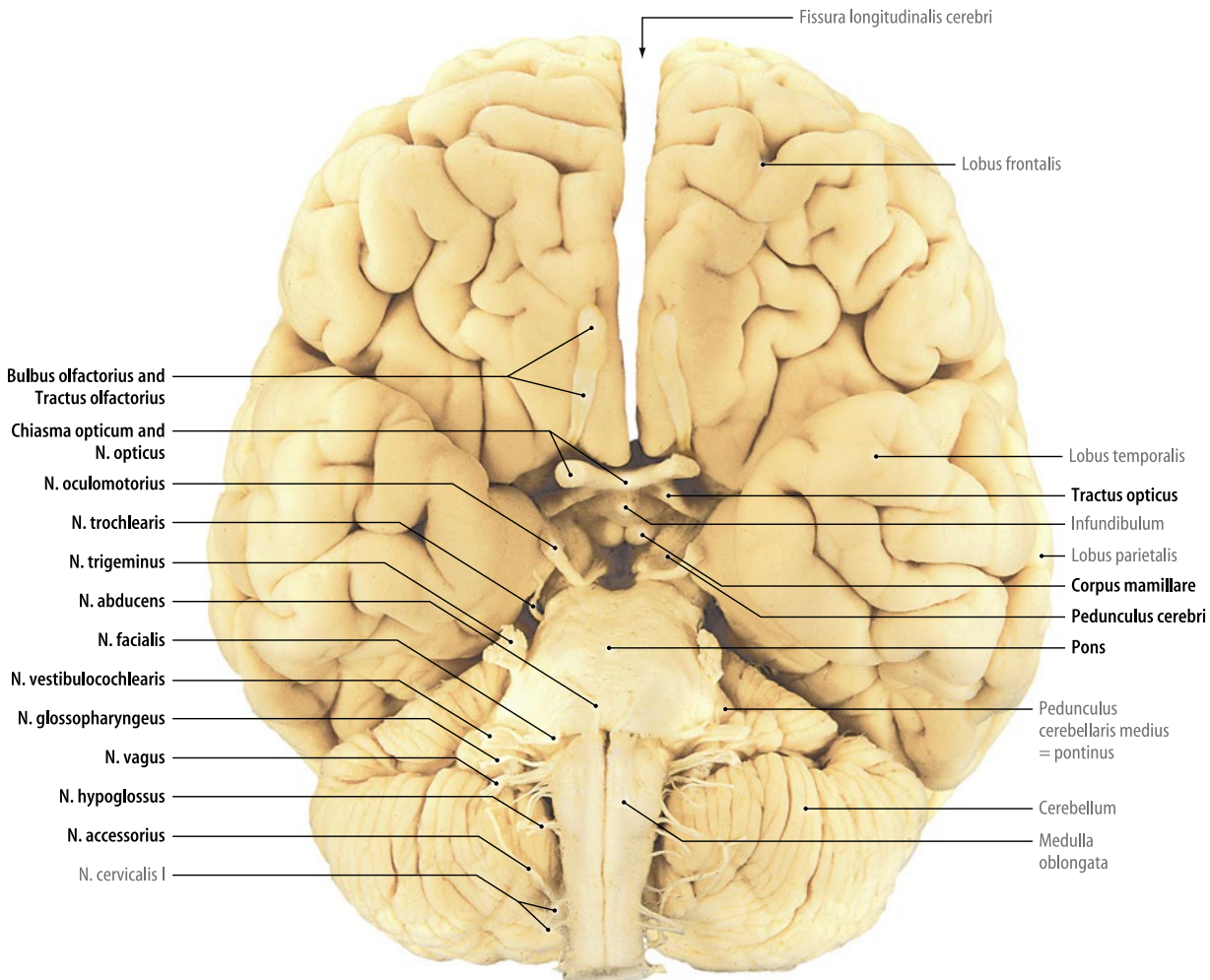
- Brain-stem
- Cerebellum
- Cerebrum

The brain stem includes the medulla oblongata, the pons and the mesencephalon. The medulla oblongata, pons and cerebellum are grouped together as the rhombencephalon (hind-brain).

In the **side-view** of the brain, the cerebral hemisphere takes up the most space. The cerebellum is located caudally. In front

of this are the medulla oblongata and the pons. The cerebrum comprises the frontal, parietal, temporal and occipital lobes. Sulci (grooves) divide the hemispherical surface into numerous gyri (convolutions). Particularly important are the central and lateral sulci in addition to the pre-central and post-central gyri. The central sulcus separates the frontal lobe from the parietal lobe, while the lateral sulcus (Sylvian fissure) separates the temporal lobe from the parietal and frontal lobes.

In the **basal view** (■ Fig. 9.1) of the brain, the entire brain-stem can be seen from the caudal to the cranial end, the medulla oblongata, pons and mid-brain. The branches of the cranial nerves can also be seen. At the mid-brain, they connect to the diencephalon. The basal portions of the diencephalon are formed by the hypothalamus. The mid-brain joins to the diencephalon, from which both mammillary corpora, the pituitary gland and the optic chiasm are visible. In the optic chiasm, both sides of the optic nerves meet and exchange fibres. In front of the optic chiasm, the olfactory tract can be found at the bottom of the frontal lobe; it ends anteriorly in a thickening in the olfactory bulb. Here, the first cranial nerve (olfactory nerve) enters the brain. In the brain-stem, the origin of the other cranial nerves can be seen from the caudal to the cranial end. The hypoglossal nerve, accessory nerve (from the spinal cord with only a small



■ Fig. 9.1 Basal view of the brain. (From: Tillmann 2009)

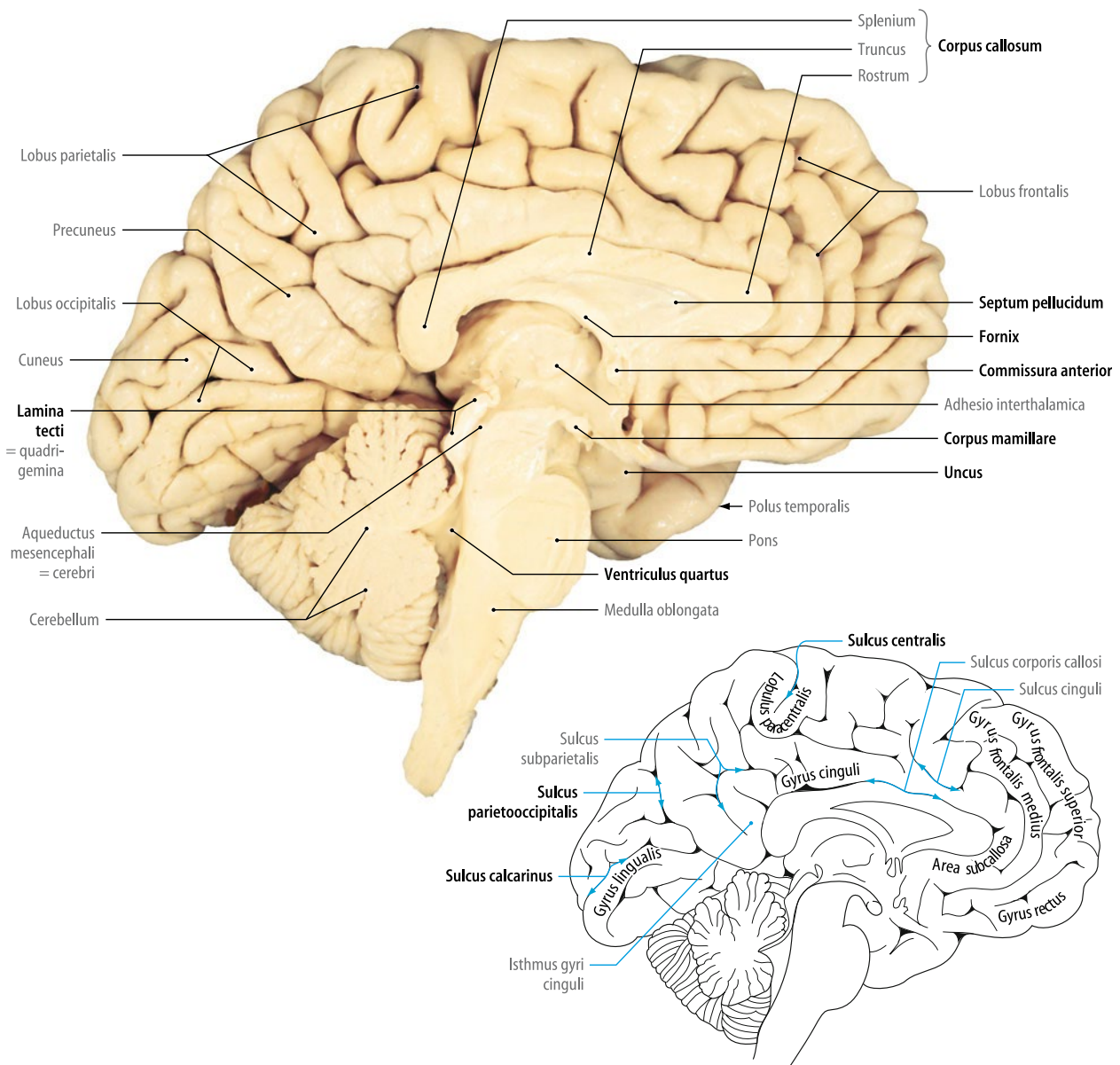


Fig. 9.2 Mid-sagittal section of the brain. (From: Tillmann 2009)

root from the brain-stem), vagus nerve, glosso-pharyngeal nerve, vestibulo-cochlear nerve, facial nerve, medial to the lower border of the pons abducens nerve, lateral from the large bulge of the pons trigeminal nerve, at the upper edge of the pons laterally forward or the trochlear nerve between the two cerebral peduncles of the oculo-motor nerve.

In the **medial view** (Fig. 9.2), the transversely severed corpus callosum can be seen. Above this, the cerebral hemisphere can be recognised. Below, one the diencephalon with the longitudinally sectioned third ventricle can be seen. Around the corpus callosum is the cingulate gyrus. Directly below runs a large fibre tract – the fornix – from the back to the front. It bulges out like a roof above the third ventricle, which is part of the mid-brain. On the back wall of the third ventricle the cone-shaped epiphysis can be seen. The base of the third ventricle is formed by the hypothalamus of the diencephalon. Caudal to the diencephalon, the mid-brain, the pons, and the medulla oblongata join up. The

cerebellum is connected to the mid-brain through the superior medullary velum (upper medullary velum) and the medulla oblongata through the inferior medullary velum (lower medullary velum).

The **brain-stem** consists of the medulla oblongata, the pons and the mid-brain and contains important functional structures. The medulla oblongata cannot be sharply demarcated from the spinal cord. In the cranial direction, the medulla oblongata extends to the beginning of the transverse, bead-like fibres of the pons. The pons is bordered above by the longitudinal fibres of the crura cerebri of the mesencephalon.

Together with the cerebellum, the medulla oblongata and pons form the **rhombencephalon**. Known outer structures are ventral to the two pyramids followed laterally by the olives in addition to the transverse fibre masses of the pons that form above the basilar part of the pons. The dorsal column nuclei can be recognised as the cuneate tubercle and the gracile tubercle. The

medulla and pons form the base of the fourth ventricle (rhomboid fossa), the roof of which is formed by the cerebellum and the medullary vela. In the medulla oblongata and the pons, numerous nerve nuclei can be found, of which the cranial nerve nuclei located there make up the largest proportion. The somato-motor nuclei are located more medially, and the somato-sensory nuclei are located more laterally. The visceromotor and viscerosensitive nuclei are in between. The nuclei of the third to the twelfth cranial nerves are located in the brain-stem.

### 9.1.2 Cranial Nerves and Cranial Nerve Nuclei

#### ■ First Cranial Nerve: Olfactory Nerve

The olfactory nerve (■ Fig. 9.3) is a viscerosensitive nerve composed of several fibres (olfactory fibres) that originate in the olfactory mucosa of the upper nasal concha. The primary sensory cells of the olfactory mucosa combine their unmyelinated projections along the olfactory fibres and run between the ethmoid sinuses through the base of the skull where the ethmoid bone penetrates into the lamina cribrosa ending in the olfactory bulb of the cerebrum. Here, they are connected for the first time so that the olfactory bulb can be considered the nucleus of the first cranial nerve. From here, the olfactory impulses are redirected to the primary olfactory cortex via the olfactory tract, which joins with the olfactory bulb dorsally as a long stalked structure.

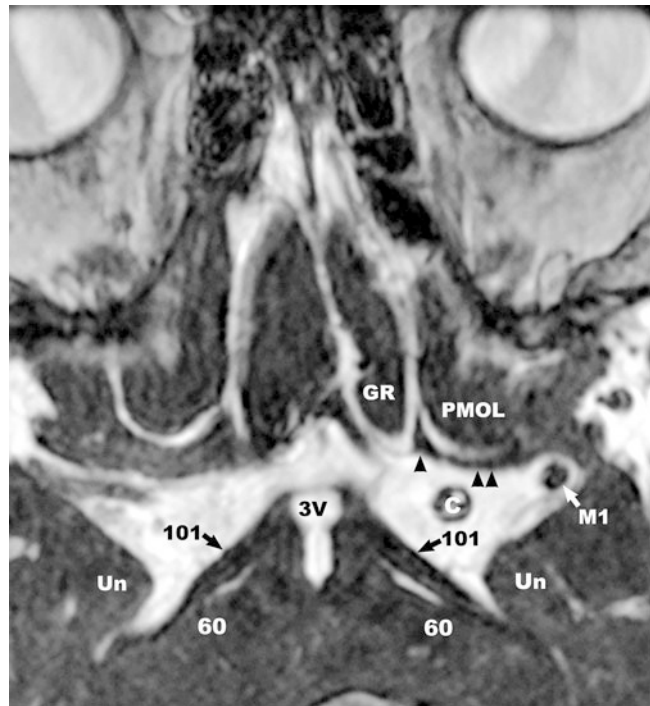
**Damage to the olfactory fibres** occurs in injuries to the base of the skull, which may lead to the avulsion of the fine fibres during their passage through the cribriform plate. This leads to anosmia, the inability to smell or anosmia (hyposmia). A characteristic feature is that patients can no longer perceive aromatic substances except for pungent agents, such as ammonia, which irritate the nasal mucosa and are thus perceived via the trigeminal nerve.

**Medical Imaging.** The olfactory bulb is best represented on coronary T1-weighted images.

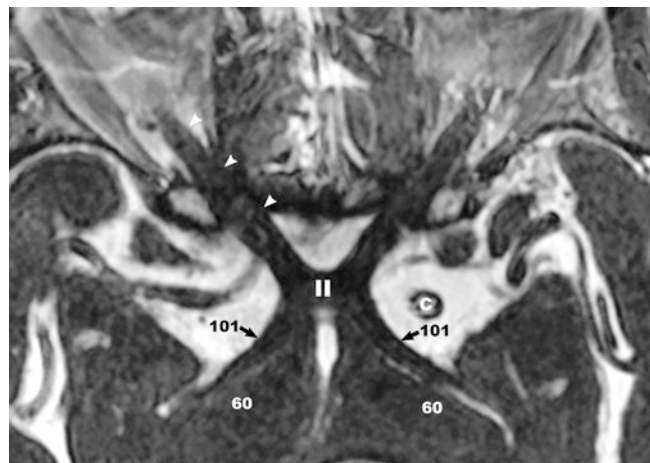
#### ■ Second Cranial Nerve: Optic Nerve

The optic nerve (■ Fig. 9.4) is a special somato-sensory nerve; it leads the fibres with the impulses of the sensory cells from the retina of the eye, i.e. the visual information. From a developmental perspective, it can be regarded as part of the diencephalon and is therefore not designated as a peripheral nerve. In the retina, the optic nerves do not directly begin on the sensory cells, but are rather composed of processes of the ganglion cells, which form the innermost light-facing cell layer in the retina. These processes are then bundled together in the optic nerve papilla and form the blind spot of the retina. They leave the eye slightly medially from the posterior pole of the bulb by breaking through the sclera in the dorsal direction. From there, they are medullated by oligodendrocytes, like all central nervous pathways, to which the optic nerve must usually be included as a brain component. Like the brain, it is also surrounded by soft meninges. The optic nerve has a diameter of about 4–5 mm and a length of about 5 cm.

The optic nerve leaves the eye socket along with the ophthalmic artery through the optic canal and moves into the medial



■ Fig. 9.3 Olfactory nerve (I) MR cisternography. (From: Naidich et al. 2009). Single black arrow bifurcation of the olfactory tract in stria medialis and stria lateralis, paired black arrows lateral olfactory stria, 3V third ventricle, C internal carotid artery, GR gyrus rectus, M1 medial cerebral artery, PMOL posteromedial orbital lobule, Un uncus, 60 cerebral peduncle, 101 optic tract



■ Fig. 9.4 Optic nerve (II), MR cisternography. (From: Naidich et al. 2009). White arrows: optic nerve (II), intra-orbital course and development in the optic canal, II optic chiasma

cranial cavity. Immediately above the pituitary gland, the ipsilateral optic nerve joins together with the contralateral side of the optic nerve in the optic chiasma. Up to the optic chiasma, the optic nerve itself can be divided into an intra-orbital, canicular, and intra-cranial component. In the optic chiasma the fibres coming from the medial half of the retina cross to the opposite side, while the fibres of the lateral half of the retina pass through the chiasma uncrossed. Crossed and uncrossed fibres then run laterally as the optic tract past the crura cerebri over to the lateral geniculate body of the thalamus, where they are once again connected so that they can pass to the visual cortex. In the

dorso-lateral direction, the optic tract is divided into a lateral part (which passes to the lateral geniculate nucleus) and a thinner medial portion, which extends to the superior colliculus. From the lateral geniculate nucleus, the optic radiation passes around the posterior horn to the calcarine sulcus and the visual cortex.

According to topically organised and intersecting fibre progressions, **clinical lesions of the visual pathway** can be fairly well localised. Damage to the optic nerve results in blindness to the eye on the affected side because the optic nerve guides all retinal fibres of the corresponding eye-ball. Damage in the chiasma, however, results in a so-called bi-temporal hemi-anopia (e.g. a pituitary tumour). A hemi-anopia is a loss of one half of the visual field. The term “bi-temporal” refers to the affected visual fields. A lesion of the total chiasma results in a lesion of all visual pathway fibres, which leads to complete blindness. Damage to the optic tract results in a homonymous hemi-anopia of the affected side, which means that both malfunctioning sides of the face point towards the same side.

Papilloedema can be seen with increased intra-cranial pressure. In multiple sclerosis (MS), the medullary sheath formed by the oligodendrocytes is destroyed, which results in a loss of function of the corresponding nerves. Because the optic nerve, as a central nervous fibre tract, is unmyelinated, this is often where this disease manifests. The result is a partial or possibly complete loss of function of the optic nerve.

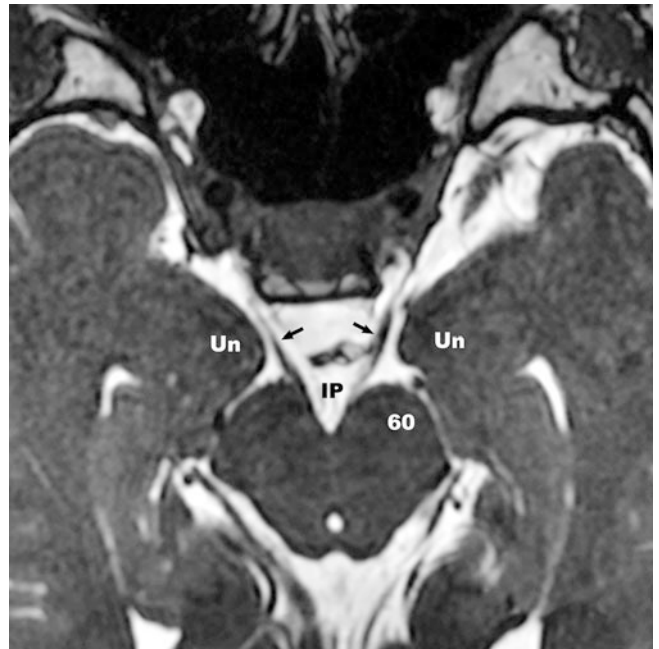
**Medical Imaging.** The optic nerve and the optic chiasma can be best displayed in axial and coronal orientations. For example, thin-layer, T1-weighted sequences are suitable here.

#### ■ Third Cranial Nerve: Oculo-motor Nerve

The oculo-motor nerve (■ Fig. 9.5) is a mixed somato- and visceromotor nerve, which, together with the fourth and sixth cranial nerves, is responsible for the innervation of the eye muscles. It originates in the mid-brain with two core complexes, a somato-motor complex for the movement of striated extra-ocular muscles and a visceromotor complex for the movement of the smooth inner eye muscles.

The oculo-motor nerve leaves the mid-brain at the front between the two cerebral peduncles in the inter-peduncular fossa and then runs anteriorly to the sella turcica. It breaks through the dura mater and enters the cavernous sinus. It then extends ventrally into the lateral wall. It finally extends medially through the superior orbital fissure into the orbital cavity, traverses the common annulus of Zinn (the tendinous ring) of the ocular muscle and forks into an upper and a lower branch. The smaller **superior branch** supplies the superior rectus muscle and the levator palpebrae superioris muscle; the larger **inferior branch** supplies the medial rectus muscle, the inferior rectus muscle, and the inferior oblique muscle. Another branch with para-sympathetic fibres innervates the internal eye muscles (the iris sphincter muscle and the ciliary muscle).

The third cranial nerve supplies all the extra-ocular muscles except the lateral rectus and the superior oblique muscle. It is therefore responsible for the movements of the eye (medial upward, medial and medial downward). The lateral movements of the eye are generated by other cranial nerves (the abducens and trochlear nerves).



■ Fig. 9.5 Oculo-motor nerve (III), 3-T MR cisternography. (From: Naidich et al. 2009). Black arrows oculo-motor nerve (III), cisternal segments, IP interpeduncular cistern, Un uncus, 60 cerebral peduncle

If the **oculo-motor nerve is damaged**, the affected eye moves outwards and downwards. This results in double images, which slope laterally downwards because of the deviation of the affected eye. Furthermore, because of failure of the levator palpebrae muscle on the affected side, the eyelid hangs limply (ptosis). In addition, failure of the para-sympathetic fibres leads to mydriasis and a lack of accommodative reactions so that sharp vision up close is no longer possible (e.g. reading with the affected eye). The core complex of the oculo-motor nerve is located in the mid-brain at the level of the superior colliculi near the median and ventral to the aqueduct, but is still partly embedded in the periaqueductal grey.

The oculo-motor nerve extends in the cisternal portion through the gap between the superior cerebellar artery and posterior cerebral artery and runs along the outermost edge of the posterior communicating artery. This close location to the posterior communicating artery is often the reason why aneurysms of the posterior communicating artery can result in irritation of the ocular nerve.

**Medical Imaging.** The cisternal pathway of the oculo-motor nerve can be detected on sagittal thin-slice scans. It can only be sectionally detected on axial imaging. The evaluation of the oculo-motor nerve in the sinus cavernous is best performed with coronary T1-weighted sequences after the administration of a contrast agent, because it appears as a dark spot.

#### ■ Fourth Cranial Nerve: Trochlear Nerve

The trochlear nerve (■ Fig. 9.6) is the thinnest of the 12 cranial nerves. As a purely somato-motor nerve, it only serves a single eye muscle. It originates in the core of the mid-brain. The trochlear nerve enters at the lower edge of the quadrigeminal plate, a single

nerve on the dorsal side of the brain. It then passes laterally to the cerebral peduncle and just above the bridge to the front, where it extends down through the sub-arachnoid space and the front end of the cerebellar tentorium into the dura. Below the dura, it then passes ventrally into the lateral wall of the cavernous sinus and meets with the ophthalmic nerve (first branch of the trigeminal nerve), the oculo-motor nerve, and the abducens nerve through the superior orbital fissure in the orbital cavity. It innervates the superior oblique muscle. As the only nerve responsible for eye movement, it does not extend through the annulus tendineus.

**Damage to the trochlear nerve** results in the eye being in an incorrect position, which is exactly opposite to the tensile direction of the superior oblique muscle in the primary position of the bulb, i.e. slightly medially above. Damage results in double images, and according to the deformity of the affected bulb, they turn obliquely above each other.

**Medical Imaging.** Because the cranial nerve is so thin, it is not easily represented on MRI. The most favourable method is 3D technology with a layer thickness of < 1 mm on a T1- or T2-weighted image (magnetisation-prepared rapid gradient-echo [MPRAGE], constructive interference steady state [CISS], true fast imaging with steady-state free precession [TRUFI]).

#### ■ Fifth Cranial Nerve: Trigeminal Nerve

The trigeminal nerve (■ Fig. 9.7) is a mixed sensory and motor nerve. The sensitive portion supplies the facial, oral and nasal mucosa in addition to the bulk of the cerebral membranes. A motor portion supplies the muscles of mastication. The trigeminal nerve has three sensitive nuclei in the central nervous system (CNS), in the upper cervical cord, in the medulla oblongata and a motor nucleus. The trigeminal nerve is the thickest nerve; it exits at the lateral side of the pons and extends forwards over the edge of the petrous pyramid, where it ends below the dura. It forms a dural pouch (trigeminal cavum), in which a large sensory ganglion (trigeminal ganglion or Gasserian ganglion) is situated. The trigeminal nerve subsequently forks out into **three large branches**

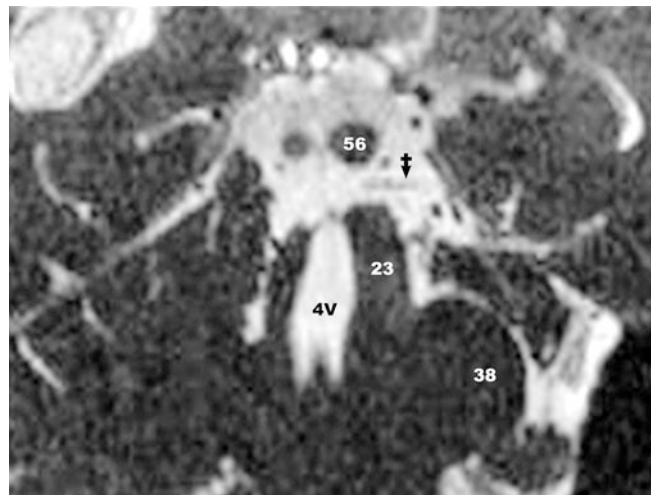
- Ophthalmic nerve (V1)
- Maxillary nerve (V2)
- Mandibular nerve (V3)

The three branches pass through separate openings of the base of the skull, and the sensory fibres supply separate areas of the facial skin and the head. The ophthalmic and maxillary nerves are purely sensory; the mandibular nerve also has motor fibres for the masticatory muscles. The nerves give off branches for the sensory innervation of the cerebral membranes.

#### ■ ■ Ophthalmic Nerve (V1)

After leaving Gasser's ganglion, the ophthalmic nerve runs ventrally along the lateral wall of the cavernous sinus. One branch leads to the meninges; upon entering the superior orbital fissure, it splits into three branches:

- Nasociliary nerve
- Frontal nerve
- Lacrimal nerve



■ Fig. 9.6 Trochlear nerve (IV), MR cisternography. (From: Naidich et al. 2009). *Black arrow* trochlear nerve (IV), cisternal segments; 4V fourth ventricle; 23 superior cerebellar peduncle; 38 medial cerebellar peduncle (brachium conjunctivum); 56: inferior colliculus



■ Fig. 9.7 Trigeminal nerve (V), MR cisternography. (From: Naidich et al. 2009). *Black arrows* trigeminal nerve (V), cisternal segment, *white arrows* lateral walls of the trigeminal cave, 38 medial cerebellar peduncle (brachium pontis), 227 posterior lobulus quadrangularis, 4V fourth ventricle, B basilar artery, C internal carotid artery

These three nerves branch out further into the orbital cavity and extend to their target organs. The ophthalmic nerve supplies the entire region of the orbital cavity and the eye, including the cornea, the skin of the forehead, and the nose in addition to the upper sinuses and the nasal septum with its mucosal branches.

#### ■ ■ Maxillary Nerve (V2)

The maxillary nerve extends ventrally into the baso-lateral wall of the sinus cavernosus and enters the foramen rotundum through the base of the skull. It is divided into:

- Rami ganglionares
- Zygomatic nerve
- Infra-orbital nerve

With its sensitive branches it supplies the facial skin, the cheek between the eye and lips, and the anterior temporal area lateral

to the eye. In addition, it supplies the mucous membranes of the nasal cavity and palate in addition to the bony upper jaw with all the maxillary teeth.

#### ■ ■ Mandibular Nerve (V3)

This nerve is the most powerful of the three trigeminal branches. It leaves the cranial cavity through the foramen ovale and enters the infra-temporal fossa. The sensitive portion is divided into:

- Auriculo-temporal nerve
- Inferior alveolar nerve
- Lingual nerve
- Buccal nerve

In addition, it supplies the facial skin over the chin and above the adjacent lower jaw up to the temple in addition to the anterior two thirds of the tongue, the lower jaw (with all the teeth) and the buccal mucosa.

The motor portion supplies all masticatory muscles via several branches.

**Medical Imaging.** The trigeminal nerve is best represented on T1- and T2-weighted layers in axial and coronary reconstruction. Clinically, hypersensitivity of the trigeminal nerve is most frequently observed. This is usually confined to one side or to individual branches and is referred to as trigeminal neuralgia. Even the smallest tactile stimuli can trigger violent attacks of pain in the skin area of the relevant trigeminal branch.

#### ■ Sixth Cranial Nerve: Abducens Nerve

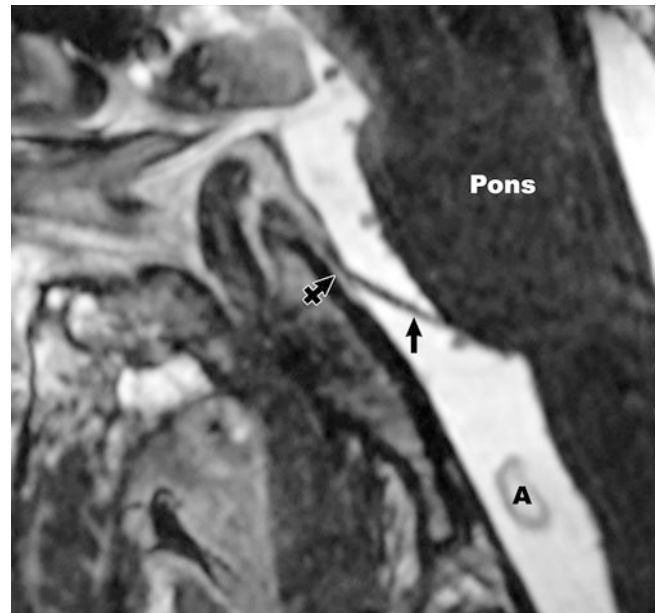
The abducens nerve (■ Fig. 9.8) is a pure somato-motor nerve. Its core is located in the pontine tegmentum near the median at the bottom of the fourth ventricle at the level of the facial colliculus. The nerve leaves the brain-stem medially at the lower edge of the bridge. In its course, it approaches the clivus, where it extends upwards below the dura and proceeds forward through the cavernous sinus to the superior orbital fissure. It supplies the lateral rectus muscle.

Damage to the abducens nerve may easily occur in the cavernous sinus. There, it is particularly vulnerable to pathological processes because as the only nerve, it extends directly through the lumen of this venous blood conductor. It can thus become damaged in the case of a basal skull fracture or basal meningitis. Damage results in visual deviation of the eye of the affected side corresponding to the loss of function of the lateral rectus muscle. This leads to side-by-side double images.

**Medical Imaging.** Because of the oblique course, it is not often possible to detect the nerve in its entire course. Thin-layer CISS or MPRAGE sequences are best suited to the representation of this nerve.

#### ■ Seventh Cranial Nerve: Facial Nerve

The facial nerve (■ Fig. 9.9) consists of two parts, a **motor-driven portion** and an **intermediate portion**. It supplies the mixed muscles and the viscerosensory gustatory fibres with the intermediate portion. The intermediate portion also contains para-sympathetic fibres. According to its three line categories, the facial



■ Fig. 9.8 Abducens nerve (VI), MR cisternography. (From: Naidich et al. 2009). *Black arrow* abducens nerve (VI), cisternal segments, *black arrow with cross* arachnoid and cerebrospinal fluid (CSF) around the abducens nerve, which penetrates the dura of the clivus, *A* vertebral artery

nerve has three cranial nerve nuclei in the brain-stem. The intermediate and fascial portion separately include the brain-stem at the lower edge of the pons and then join with the vestibulo-cochlear nerve through the internal acoustic meatus to the inner ear canal, where they accompany the vestibulo-cochlear nerve to the inner ear. In the facial canal of the temporal bone, the nerve bends backwards at nearly right angles. This point is referred to as the outer geniculi of the facial nerve. The ganglion geniculi for the sensory taste fibres is located here. The facial canal guides the facial fibres over the tympanic cavity downwards in an arc, where they appear in the stylo-mastoid foramen between the mastoid process and the styloid process of the base of the skull. In its course through the petrous bone, the para-sympathetic and gustatory fibres leave the nerve as the petrosal nerve and chorda tympani. In the parotid gland, the motor-driven fibres branch off and are drawn towards the mimetic muscles in the neck.

Because of its complex peripheral course, the facial nerve may be **damaged** at many sites. This results in a different pattern of symptoms, which allows a relatively accurate location of the injury. A cardinal symptom of facial lesioning is always the **flaccid paralysis of the facial muscles**. Here, the labial angle sags on the affected side, the wrinkles on the forehead are elapsed, and the eyelids cannot be closed.

**Medical Imaging.** In its course through the pre-mesencephalic cisterns and the internal acoustic meatus, the facial nerve may be mapped along with the superior vestibular nerve (upper dorsal), the cochlear nerve (lower ventral), and the inferior vestibular nerve (lower dorsal). Axial and coronal layers are best suited for this purpose. An enhancement contrast agent in the facial nerve is not necessarily synonymous with inflammation because this physiological contrast agent can accumulate, especially in the tympanic segment.



### ■ Eighth Cranial Nerve: Vestibulo-cochlear Nerve

The eighth cranial nerve (■ Fig. 9.9) is purely somato-sensory and consists of two portions:

- Vestibular nerve
- Cochlear nerve

It has two vestibular nuclei in the brain-stem, the cochlear nucleus and the vestibular nucleus. The cochlear nerve begins in the periphery of the perikarya in the ganglion cochlear, which is located in the inner ear. There, it follows the course of the cochlea close to the axis as a spiralised cellular ribbon. Peripheral dendritic processes of these bipolar ganglion cells terminate at the sensory cells of the organ of Corti, while the central processes in their entirety form the cochlear nucleus.

The vestibular nerve starts with the central processes of the perikarya, which are situated in the vestibular ganglion, found in a separate fundus at the base of the internal acoustic meatus. Both portions of the vestibulo-cochlear nerve then meet in the auditory canal of the petrous bone to form a nerve cord. The nerve passes onto the lower edge of the pons, immediately caudo-lateral to the facial nerve in the brain stem, where the cochlear and vestibular portions once again separate. Clinically, lesions of the vestibular and cochlear portion of the eighth cranial nerve can be differentiated. Lesions of the facial nerve are more frequent because the latter lies immediately on the eighth cranial nerve. Damage to the cochlear portion results in hearing impairment or deafness on the affected side. A lesion of the vestibular portion may result in vertigo, nausea, a tendency to fall to the affected side, and pathological nystagmus.

**Medical Imaging.** In T1- and T2-weighted axial and coronal sequences, the vestibulo-cochlear and facial nerves are clearly visible in the ponto-medullary cistern and internal auditory meatus. In sagittal cut through the cross section of the inner auditory canal, the individual nerves can be identified. The facial nerve lies ventrally and superiorly, the superior vestibular nerve lies dorsally, and the cochlear nerve lies ventrally and inferiorly – the inferior vestibular nerve lies dorsally from this.

### ■ Ninth Cranial Nerve: Glosso-pharyngeal Nerve

The glosso-pharyngeal nerve (■ Fig. 9.10) is a motor nerve responsible for the pharyngeal muscles and the posterior third of the tongue mucosa and the throat. It has four different cranial nerve nuclei in the brain-stem:

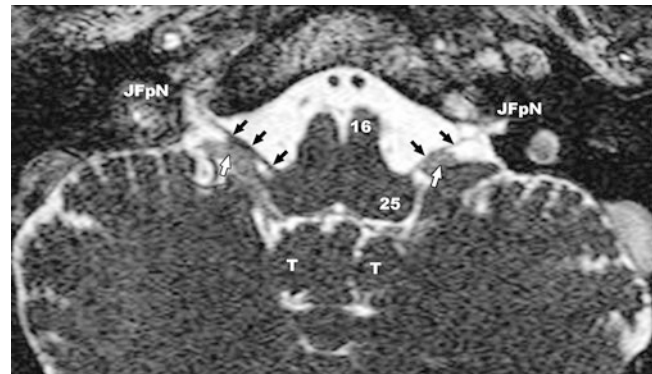
- Nucleus ambiguus
- Inferior salivatory nucleus
- Spinal nucleus of the trigeminal nerve
- Nucleus of the solitary tract

The nerve exits the brain stem between the eighth and tenth cranial nerves under the pons, is drawn obliquely downwards and ventrally through the sub-arachnoid space to the jugular foramen, through which it leaves the cranial cavity together with the vagus nerve and the accessory nerve. At this point, it forms the superior ganglion and the inferior ganglion caudally in the fossa petrosa.

An isolated failure of the glosso-pharyngeal nerve is rare, the 10th and 11th cranial nerves are frequently affected because they



■ Fig. 9.9 The facial nerve (VII) and vestibulo-cochlear nerve (VIII), MR cisternography. (From: Naidich et al. 2009). Black arrows the facial nerve (VII) and vestibulo-cochlear nerve (VIII) cisternal segments, black arrows with cross heads abducens nerve (VI), cisternal segments, 4V fourth ventricle, B basilar artery, Co cochlea (inner ear), Ve vestibulum, T cerebellar tonsil



■ Fig. 9.10 Glosso-pharyngeal nerve (IX), MR cisternography. (From: Naidich et al. 2009). Black arrows glosso-pharyngeal nerve (IX), cisternal segments, white arrow choroid plexus in the cerebellar ponto-medullary cistern; 16 pyramid the cortico-spinal tract extends therein, 25 inferior cerebellar peduncle, JFpN jugular fossa, pars nervosa, T cerebellar tonsil

all have a common exit point at the base of the skull in the jugular foramen. Here, they can be damaged by tumours in this area or injury to the base of the skull. A **glosso-pharyngeal lesion** leads to sensory deficits in the upper pharynx and the posterior third of the tongue, where the sensation of taste – especially bitterness – is lost on the affected side. As a rule, the uvula deviates to the healthy side. Even swallowing is limited.

**Medical Imaging.** On T1- and T2-weighted sequences, it can normally be detected on the axial slice orientation.

### ■ Tenth Cranial Nerve: Vagus Nerve

The vagus nerve (■ Fig. 9.11) has visceromotor portions and is the **largest para-sympathetic nerve** in the body. In addition, it also has motor fibres for the pharynx and laryngeal muscles for which it provides sensory innervation. An additional sensory area is located in the outer auditory canal.

The vagus nerve passes laterally behind the olive from the medulla oblongata and leaves the base of the skull through the

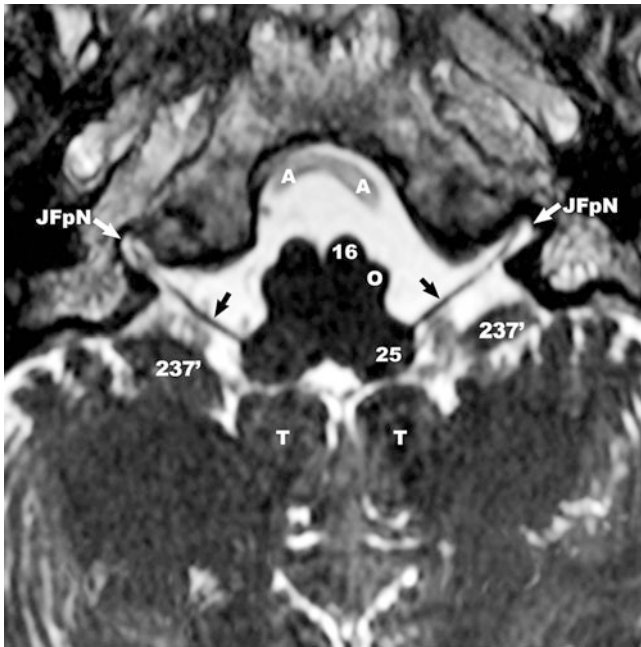


**Fig. 9.11** Vagus nerve (X), MR cisternography. (From: Naidich et al. 2009). Black arrows vagus nerve (X), cisternal segments, 16 pyramid, the cortico-spinal tract extends therein, 25 inferior cerebellar peduncle, 237' flocculus, A vertebral artery, JFpN jugular fossa, pars nervosa, O inferior olivary nucleus, T cerebellar tonsil

jugular foramen, forming from a smaller superior somato-sensory ganglion and a larger inferior viscerosensory ganglion.

It is the cranial nerve with the broadest innervation area and is the only one to extend as far as the pectoral and abdominal cavity. According to its line categories, it has four different cranial nerve areas in the brain-stem:

- Nucleus ambiguus
- Dorsal motor nucleus of the vagus nerve
- Spinal nucleus of the vagus nerve
- Nucleus of the solitary tract

An important nerve is the **recurrent laryngeal nerve**, which, because of its specific course and important function, **is of great clinical importance**. It can be compressed by the pulmonary hilum into mediastinal lymph node metastases. Even in the case of an aortic aneurysm, it can become damaged. This manifests itself in a unilateral loss of function of the laryngeal muscles and thus hoarseness, which may be the first symptom of lung cancer or an aortic aneurysm. Because of its course, which is dorsal to the thyroid capsule, it is not often damaged during thyroid surgery, which can also lead to unilateral loss of function of the laryngeal muscles and hoarseness. Bilateral injury to the recurrent laryngeal nerve can cause severe shortness of breath because the vocal cords cannot be opened wide enough.

#### Eleventh Cranial Nerve: Accessory Nerve

The accessory nerve (Fig. 9.12) only leads to motor fibres and innervates the trapezius muscle and the sterno-cleido-mastoid muscle. Its motor core forms an elongated cellular column that extends from the medulla oblongata to the cervical spinal cord at

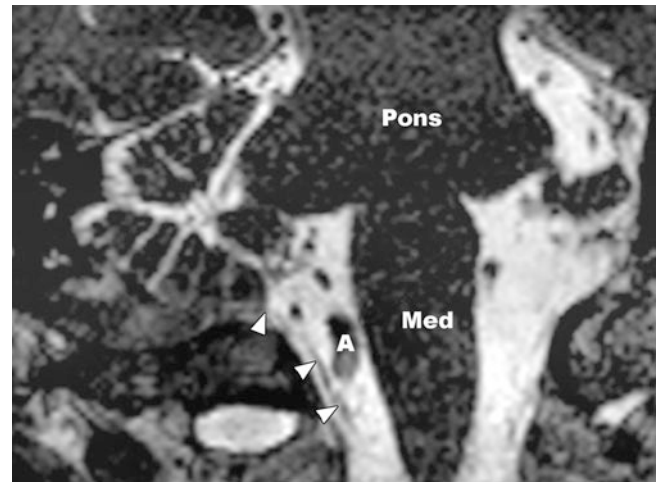


**Fig. 9.12** Accessory nerve (XI), MR cisternography. (From: Naidich et al. 2009). White arrows accessory nerve (XI), cisternal segments, A vertebral artery, Med medulla oblongata

the level of the fifth to seventh cervical vertebrae. The cranial accessory nerve consists of three to four fibre bundles that exit from the medulla oblongata immediately below the vagus nerve. The spinal radices consist of six to seven fibre bundles that emanate from the cervical cord and extend upwards in the spinal canal through the foramen magnum.

Owing to the innervation of the sterno-cleido-mastoid muscle, the accessory nerve provides an ipsilateral inclination of the head when the face simultaneously turns contra-laterally. The innervation of the trapezius muscle leads to a fixation of the scapula, an elevation of the shoulder, and an elevation of the arm above the horizontal. Damage leads to pronounced weakness when lifting the arm of the affected side above the horizontal and a weakness when raising the shoulder with a protruding shoulder blade (scapula alata).

#### Twelfth Cranial Nerve: Hypoglossal Nerve

The hypoglossal nerve (Fig. 9.13) is a purely motor nerve and accordingly has only a cranial nerve nucleus, the nucleus of the hypoglossal nerve. As the sole nerve before the olive, the nerve originates from the medulla oblongata, with multiple fibre bundles, and leaves the cranial cavity through the hypoglossal canal in the foramen magnum. It supplies the tongue and has greatest importance for speaking, eating, drinking, and swallowing. An injury manifests itself with a deviation of the tongue to the affected side when it is protruded. Histopathologically, it leads to a fatty degeneration of the tongue on the affected side.

**Medical Imaging.** On MRI, its course can be detected via thin-layer T1- and T2-weighted sequences.

### 9.1.3 Mid-brain

The mid-brain is adjacent to the caudal pons, cranial to the diencephalon and can be longitudinally divided into three layers.



**Fig. 9.13** Hypoglossal nerve (XII), MR cisternography. (From: Naidich et al. 2009). Black arrows hypoglossal nerve (XII), cisternal segments, white arrow with cross CSF, the twelfth surrounding cranial nerve, A vertebral artery, HC hypoglossal nerve canal, JT jugular tubercle, Med medulla oblongata, OC occipital condyle

From the front, the cerebral peduncles (crura cerebri) are visible, the tegmentum is anterior, and finally dorsally, the tectum that is visible from behind, the quadrigeminal plate. The quadrigeminal plate consists of two upper and two lower mounts (the superior and inferior colliculi). The mid-brain is crossed by the fluid-filled aqueduct, which connects the third and fourth ventricles.

### 9.1.4 Cerebral Peduncle

The cortico-spinal (pyramidal tracts), cortico-nuclear, and cortico-pontine tracts extend into the cerebral peduncle. In the mid-brain tectum, the superior optic reflexes switch in the colliculi through the emergence of saccades. The two inferior colliculi are an intermediate station of the auditory pathway. The substantia nigra, the red nucleus and the reticular formation are situated in the mesencephalic tegmentum. The red nucleus has important functions in the coordination of fine motor skills. The substantia nigra has an essential function during motion drive and in the initiation of appropriate reactions to sensory stimuli. Failure frequently leads to symptoms of Parkinson's disease. The reticular formation contains functional centres, such as the respiratory centre, the cardio-vascular centre, the vomiting centre, and the wake/sleep centre.

In the brain-stem and mid-brain, numerous optical reflexions (e.g. pupillary reflexes) in addition to the coordination and generation of horizontal and vertical eye movements are connected.

### 9.1.5 Cerebellum

The cerebellum is the most important and highest supervisory body for the coordination and fine-tuning of motion sequences. It can be divided into a vermis and two cerebellar hemispheres. The flocculo-nodular lobe can be found caudal to the cerebellar vermis. The surface of the cerebellum is characterised by numerous folia. Above the three cerebellar peduncles (superior, medial, and inferior cerebellar peduncles), which contain afferent and efferent pathways of the cerebellum, it is connected to the brain-stem (■ Fig. 9.14). The image of the arbor vitae originates in the sagittal section. It can be broken down into the cortex and medulla. In terms of functional and anatomical parameters, the cerebellum can be divided into **three parts**:

- **Vestibulo-cerebellum** receives the bulk of the afferents from the vestibular system and is represented by the flocculo-nodular lobe.
- **Spino-cerebellum** receives the most afferents from the spinal cord and is represented by the cerebellar vermis and the para-vermal zone.
- **Ponto-cerebellum** receives the most afferents via the pontine nuclei of the cerebellum and is represented by the two hemispheres.

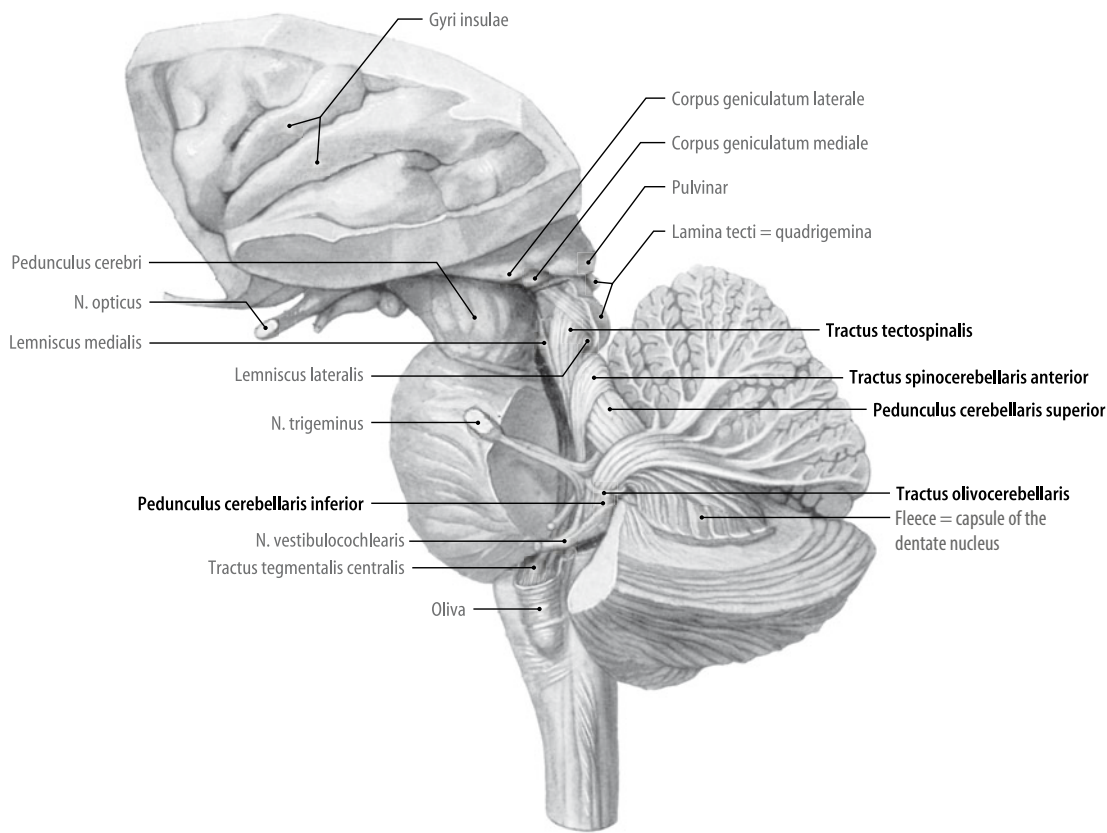
A failure of the cerebellum causes a variety of symptoms that can generally be described as cerebellar ataxia (lack of coordination of the loco-motor portions, vision stabilisation disorders and reduced muscle tone).

Median sagittal layers provide the best overview of the topographical relationship between the brain-stem and cerebellum. The basis pontis can be clearly differentiated from the mesencephalon of the medulla oblongata. In the mid-plane, the aqueduct separates the tegmentum from the mid-brain tectum, the quadrigeminal plate. The aqueduct joins with the fourth ventricle, which is upwardly and posteriorly separated from the superior medullary velum. The fourth ventricle extends downwards into the median aperture. The tip of the ventricular roof, the fastigium, points to the central white matter of the cerebellar vermis. From here, the white matter branches in a tree-like manner. Above, at the anterior ventricular roof, are the central lobe and the culmen, which together form the anterior lobe of the cerebellum. Separated by the fissure prima are the declive, folium, tuber, pyramis and uvula vermis in addition to portions of the posterior cerebellar lobe. The nodule lies in the posterior medullary velum and forms the cerebellar flocculo-nodular lobe with the flocculus of the cerebellar hemispheres.

### 9.1.6 Diencephalon

The diencephalon is bounded caudally from the mid-brain and rostrally and dorsally from the cerebrum. According to its topographical location in the embryonic phases, four sections can be distinguished:

- Epithalamus, which consists of the epiphysis, the habenula, and the pre-tectal area.



■ **Fig. 9.14** Cerebellum with projection fibres; cerebellar peduncles, fibre specimen, left lateral view. (From: Tillmann 2009)

- Thalamus, a large core complex, which is bounded by both sides of the third ventricle.
- Sub-thalamus, which consists of the sub-thalamic nucleus and parts of the pallidum.
- Hypothalamus, which consists of many smaller core areas that form the base of the third ventricle and extend downwards with the pituitary stalk to the posterior lobe of the pituitary gland.

The thalamus is a conglomerate of individual nuclei, which – with the exception of the olfactory nucleus – switch parts of the sensory pathways and direct them to the cerebrum. The hypothalamus contains many core areas for the vegetative and endocrine systems in addition to respiration, circulation, and fluid and food intake. In the epithalamus, vegetative and pupillary reflexes are switched.

### 9.1.7 Functional Pathways of the Cerebrum

The neo-cortex of the cerebrum can be divided into primary, secondary, and association cortices. The primary fields are the primary representation fields of sensory afferents (visual and auditory cortex) or the origin of descending motor pathways (motor cortex). Secondary fields are connected downstream (sensory) or upstream (motor) of the primary fields. The somato-motor system is mainly localised in the frontal lobe.

The pre-central gyrus, also known as the motor cortex, is located in front of the central sulcus and is the place of origin of

most of the pyramidal tracts (■ Fig. 9.2). It is somato-topically divided (homunculus) i.e. each section corresponds to the initiation of movement of certain body parts. Above the cortico-nuclear and cortico-spinal fibres, the motor cortex mainly initiates fine motor movements of the contra-lateral half of the body. Damage mainly causes distal paresis of the contra-lateral half of the body. The pre-motor cortex and the frontal eye field are located medially in front of the motor cortex. It can initiate direct movements, especially extra-pyramidal motor skills. The frontal eye field lies flat against the pre-motor cortex and is responsible for the initiation of voluntary eye movements.

In the inferior frontal gyrus, the so-called **Broca's speech centre** is located. It is responsible for the initiation of linguistic word and sentence structure. This centre is only formed unilaterally (usually in the dominant left hemisphere). Damage leads to so-called motor aphasia, whereby language acquisition is greatly impaired; language comprehension, however, is largely preserved. Functionally higher levels of psychological and mental performance are attributed to the pre-frontal cortex. Accordingly, injury can result in severe personality impairment.

#### ■ Parietal Lobes

The somato-sensory system is located in the parietal lobe. All protopathic pathways for pain, temperature and rough tactile sensation end in the spinal cord, with the spino-thalamic tract from the dorsal horn in the brain-stem from the spinal trigeminal nucleus. All these paths cross to the opposite side and extend to

the thalamus as a zone of the second neuron (ventral posterior nucleus). There, they are interconnected with the third neuron and directed to the somato-sensory cortex, the post-central gyrus. The disconnected and uncrossed epicritical tracts for fine tactile sensation and proprioception extend upwards towards the medulla oblongata with the primary neuron in the spinal cord, where they are connected to the cuneate and gracile nuclei. Together with the fibres of the principal sensory nucleus of the trigeminal nerve, they extend towards the junction on the opposite side of the thalamus and from there to connectivity on the tertiary neuron of the pathway to the post-central gyrus. Separated by the central sulcus, the dentate gyrus is situated behind the motor cortex and is the primary junction of the somato-sensory pathways.

**Damage** results in numbness in the corresponding areas. It is also somato-topically organised like the motor cortex. The secondary somato-sensory cortex is posterior to the post-central gyrus and is responsible for the interpretation of sensory information. A lesion leads to tactile agnosia, and items that are touched can no longer be recognised.

The angular gyrus wraps around the end of the superior temporal sulcus superior and is a central hub between the visual cortex and sensory speech centre in the secondary auditory cortex; injury results in the inability to read and write (alexia and agraphia). In the posterior parietal cortical cortex, spatial perception, orientation and movement in space are detected. Injuries often lead to spatial disorientation or apraxia.

#### ■ Occipital Lobe

The occipital lobe is the neocortical manifestation of the visual system. The visual pathway begins in the retina the ganglial cells of which and their axons form the optic nerve. This combines with the optic nerve, with the opposite side in the optic chiasm, where the fibres of the nasal retinal halves cross on the contra-lateral side. The optical tract that connects to the chiasm terminates in the lateral geniculate nucleus of the thalamus and continues from there as an optic radiation up to the primary visual cortex. The primary visual cortex (striate area) is located in the wall of the calcarine sulcus and forms the occipital pole of the brain. The visual cortex is responsible for the involuntary awareness of the visual stimuli of the contra-lateral side of the face of both eyes. A lesion of this area causes blindness in the area of the retina that projects into the damaged visual cortex area. In the secondary visual cortex and the superordinate visual association fields symbols and handwriting are recognised.

#### ■ Temporal Lobe

The auditory system is located in the temporal lobe. The auditory pathway begins in the cochlear nuclei in the medulla oblongata, from where the fibres cross to the opposite side, but extend upwards to the ipsilateral side. As a lateral lemniscus, the auditory pathway continues to the inferior colliculi from where it moves to the medial geniculate body of the thalamus. From there, the fibres extend as an auditory radiation to the primary auditory cortex in the temporal lobe.

**Primary auditory cortex** (transverse temporal gyrus) is hidden in the lateral sulcus. Here, tones and sounds but not language

or music are detected. A unilateral lesion of the primary auditory cortex results in hearing loss but not deafness.

**Secondary auditory cortex:** in the sensory speech centre (Wernicke's centre), which is located lateral to the primary auditory cortex in the superior temporal gyrus, speech is detected. Wernicke's speech centre is only formed in the dominant (usually left) hemisphere. Injury causes a loss of linguistic understanding with corresponding speech disturbances (sensory aphasia).

#### ■ CSF and Ventricular System

The cerebrospinal fluid (CSF), which acts as a liquid cushion, surrounds the brain and spinal cord. Its composition differs significantly from that of blood plasma. The total amount of CSF is approximately 150 ml. The intra-cranial CSF spaces are formed by the four ventricles, the basal cisterns and the sub-arachnoid spaces above the cerebral convexities (▣ Fig. 9.15). The two lateral ventricles are situated in the cerebral hemispheres and are divided into a frontal horn, a cella media, an occipital horn and a temporal horn. The transitional region between the temporal and occipital horns is also referred to as the antrum or trigone. Via the inter-ventricular foramen (foramen of Monro), the lateral ventricles communicate with the third ventricle. The third ventricle is situated in the median and is connected to the fourth ventricle via the aqueduct, which runs through the mid-brain. The fourth ventricle communicates with the outer CSF spaces through the laterally situated foramina of Luschka and the medio-dorsally situated foramen of Magendie (median aperture).

The production of CSF (about 500 ml per day) takes place in the choroid plexus, which can be found as specifically differentiated vesicular bundles in each ventricle. The reabsorption of CSF primarily occurs via Pacchioni's granulations, which correspond to projections of the sub-arachnoid space into the dural venous sinuses.

The CSF is formed in the lateral ventricle in the choroid plexus, passed via the foramen of Monro into the third ventricle, into the aqueduct of the mesencephalon, and then into the fourth ventricle and into the sub-arachnoid space via the foramina of Magendie and Luschka. As already mentioned, resorption into the venous system is carried out via Pacchioni's granulations. Movement of CSF is likely generated by pulsations of the choroid plexus in the alternation of systole and diastole.

On MRI, the flux of CSF can be represented with dynamic measurements.

In the case of **hydrocephalus** there is an imbalance among the formation, flow, and reabsorption of CSF (► Sect. 9.10). This leads to increases in the volume and pressure of the CSF and to a widening of the sub-arachnoid spaces. The increase leads to an increase in intra-cranial pressure. In infants and young children, hydrocephalus is apparent because of the increased head circumference and the emergence of enlarged fontanelles. In adults, increased intra-cranial pressure leads to symptoms such as restlessness, headache, nausea and vomiting. Later, memory disorders, increased fatigue, forgetfulness, double vision, unsteadiness and bladder disorders also occur. Hydrocephalus can be caused by excessive production of CSF, an obstruction to the flow of the CSF, or reduced resorption.

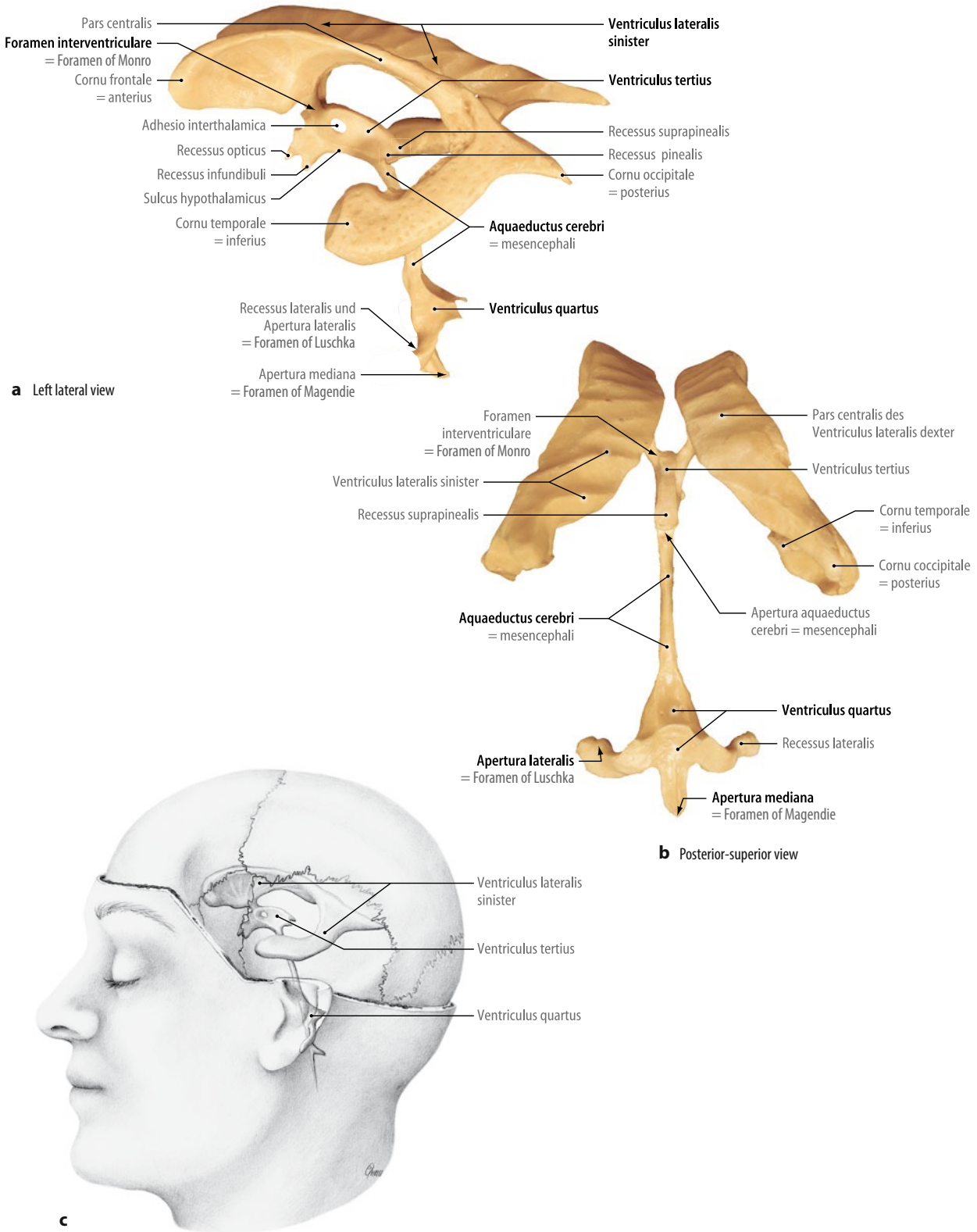


Fig. 9.15a–c CSF and the ventricular system. a, b Spout specimen. c Projection of the cerebral ventricles on the skull. (From: Tillmann 2009)

### 9.1.8 Blood Supply to the Brain

The brain is supplied with blood via four major extra-cranial arteries:

- Right and left internal carotid artery
- Right and left vertebral artery

Three arteries emit from the aortic arch, the brachio-cephalic artery, the left common carotid artery, and the left sub-clavian artery. These arteries are joined together at the base of the skull by a large circulatory anastomosis, the circle of Willis.

#### ■ Carotid Artery

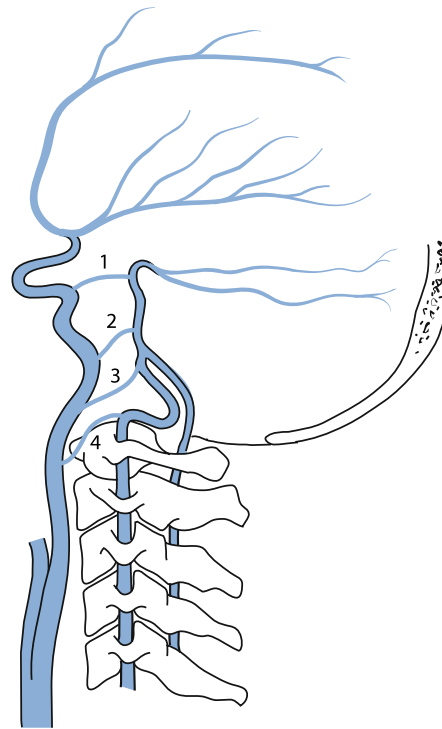
The carotid artery mostly divides into the external and internal carotid arteries at the level of the fourth to fifth or third to fourth cervical vertebrae. The internal carotid artery extends to the base of skull without branching off. It extends to the carotid canal of the petrous bone and enters into the cranial cavity via the foramen lacerum. In the cranial cavity, it directly enters the cavernous sinus and passes through this in an S-shaped manner, lateral to the pituitary gland. Afterwards, it proceeds forward into the sub-arachnoid space (chiasmatic cistern), emitting smaller branches until it reaches the level of the anterior perforated substance in the frontal lobe, where it divides into the anterior cerebral artery and the middle cerebral artery. In the course of the **internal carotid artery**, **four sections** are distinguished:

- Pars cervicalis (C1 segment): at the beginning up to the skull base
- Pars petrosa (C2 segment): in the pathway through the skull base
- Pars cavernosa (C3 segment): in the pathway through the cavernous sinus
- Pars cerebralis (C4 segment): after leaving the sinus cavernosus up to the division into the anterior and medial cerebral artery

The S-shaped curve in the pars cavernosa and at the beginning the **pars cervicalis** is also referred to as the carotid siphon.

In the **pars cerebralis** the internal carotid artery initially emits the ophthalmic artery, which supplies the eye and parts of the para-nasal sinuses. In the area of the medial canthus, the ophthalmic artery communicates with branches of the facial artery, which stems from the external carotid artery. In the case of stenosis of the internal carotid artery, collateral circulation can proceed via this anastomosis. As the next branch, the posterior communicating artery emits from the carotid artery. As part of the circle of Willis, it forms an anastomosis between the posterior and anterior cerebral circulation. In addition, before splitting, the carotid artery emits the superior and inferior pituitary arteries to form the pituitary gland, and the anterior choroidal artery.

The anterior choroidal artery is an important vessel. In addition to the choroid plexus of the lateral ventricle, it also primarily supplies the internal capsule, parts of the basal ganglia, the hippocampus, the amygdala, the thalamus and the substantia nigra. The supply in the internal carotid artery includes the complete



■ Fig. 9.16 Basilar carotid anastomoses, scheme. Persistent primitive connections between the basilar artery and the internal carotid artery. 1 primitive trigeminal artery, 2 acoustic artery, 3 primitive hypo-glossal artery, 4 pro-atlantal artery

frontal and parietal lobes, the largest part of the temporal lobe and the diencephalon, the eye, and the pituitary gland. The diameter of the section is generally between 3.5 and 5 mm. The ophthalmic artery has a diameter of about 0.7–1.4 mm and extends laterally and parallel to the lower surface of the optic nerve. In the orbital cavity, it crosses the optic nerve to divide into its terminal branches. The medial meningeal artery may also originate from the ophthalmic artery.

The posterior communicating artery usually shows considerable variations in calibre. Hypoplasia, aplasia and duplications are not uncommon. The vigorous posterior communicating artery gives the impression that the posterior cerebral artery arises directly from the internal carotid artery. It is designated as a foetal outflow of the posterior cerebral artery.

The anterior choroidal artery proceeds distally from the posterior communicating artery from the internal carotid artery. It has a lumen of approximately 0.5 mm in diameter.

#### ■ Basilar Carotid Anastomoses

Arteries that produce connections in the foetus between the carotid and basilar flow area are obliterated with regard to the extent to which they form vertebral arteries. First, the otic/acoustic artery disappears, followed by the hypo-glossal artery and finally the primitive trigeminal artery. Occasionally, some of these arteries may persist (■ Fig. 9.16). The primitive trigeminal artery is found with a frequency of 0.1–2%. The artery originates from the internal carotid artery after it is emitted from the carotid canal and extends dorsally in an arcuate or straight course to the upper portion of the basilar artery.

### ■ Primitive/Otic Acoustic Artery

This artery is very rare. It emits from the petrous segment of the internal carotid artery and extends into the internal auditory canal along with the facial and acoustic nerves.

### ■ Primitive Hypoglossal Artery

This is also relatively rare and originates from the cervical segment of the internal carotid artery at the level of the first and second cervical vertebrae, extends into the hypoglossal canal and joins with the lower portion of the basilar artery.


### ■ Pro-atlantal Artery

The persistent pro-atlantal artery is also very rare. It originates from the upper cervical portion of the internal carotid artery, passes through the foramen magnum into the internal skull, and joins with the vertebral artery. A persistent stapedia artery is also very rare; it does not belong to the basilar carotid anastomoses. It is a branch of the internal carotid artery, which forks off from the petrosal section, runs through the middle ear and becomes the meningeal artery.

### ■ External Carotid Artery

The external carotid artery supplies the facial skull, the scalp, most of the dura mater, and the upper pole of the thyroid lobe. After its origin from the common carotid artery, the external carotid usually proceeds antero-medially from the internal carotid artery. As a variant, it also has a postero-lateral or lateral course. The external carotid artery is about 7–8 cm long and can be divided into three sections:

- Lower cervical section
- Medial section in the region of the mandibular angle
- Terminal portion in the area of the parotid gland

The external carotid artery has numerous branches, which are shown in  Fig. 9.17.

**Superior Thyroid Artery.** It forks as a primary branch from the anterior wall of the external carotid artery, but it can also originate in 16% of cases in the common carotid artery.

**Lingual Artery.** The lingual artery is the secondary branch from the anterior wall of the external carotid artery. About 20% of the time, it forms a common trunk with the fascial artery. It forms a downwardly convex arc and emits the deep lingual artery and the sub-lingual artery. It supplies the tongue and pharynx.

**Facial Artery.** The third branch exhibits a tortuous upward course and extends via the maxillary branch to the labial angle and the medial canthus, where it terminates in the angular artery and anastomoses with the dorsal nasal artery, the terminal branch of the ophthalmic artery. With the terminal branches, the facial artery supplies the soft palate, the pharyngeal tonsils, and the sub-mandibular gland.

**Ascending Pharyngeal Artery.** The smallest branch of the external carotid artery is the ascending pharyngeal artery, which runs up-

wards from the posterior wall and branches out to the pharyngeal muscles. It has a meningeal branch, which supplies the dura of the clivus and the cerebello-pontine angle.


**Occipital Artery.** The occipital artery also originates from the posterior wall and anastomoses with branches of the superficial temporal artery, the posterior auricular artery and muscular branches of the vertebral artery. The posterior meningeal artery supplies the dura of the posterior cranial fossa.

**Posterior Auricular Artery.** The posterior auricular artery also originates from the posterior wall and supplies the pinna and the ear lobe in addition to the muscles in the mastoid area.

**Superficial Temporal Artery.** The superficial temporal artery is a terminal branch of the external carotid artery. Throughout their course, they cross the zygomatic process and supply large parts of the galea.

**Maxillary Artery.** The maxillary artery is the largest terminal branch, extending to the posterior section of the pterygo-palatine fossa and emitting numerous branches, including the middle meningeal artery, the accessory meningeal artery and the infra-orbital artery. The medial meningeal artery supplies the dura mater; it passes through the foramen spinosum into the cranial cavity. The infra-orbital artery extends through the infra-orbital canal and passes through the infra-orbital foramen to the cheeks, the lower eyelid, the upper lip, the lacrimal sac and the nose. It anastomoses with the terminal branches of the ophthalmic artery and may thus be involved in the occlusion of the internal carotid artery in the collateral system.

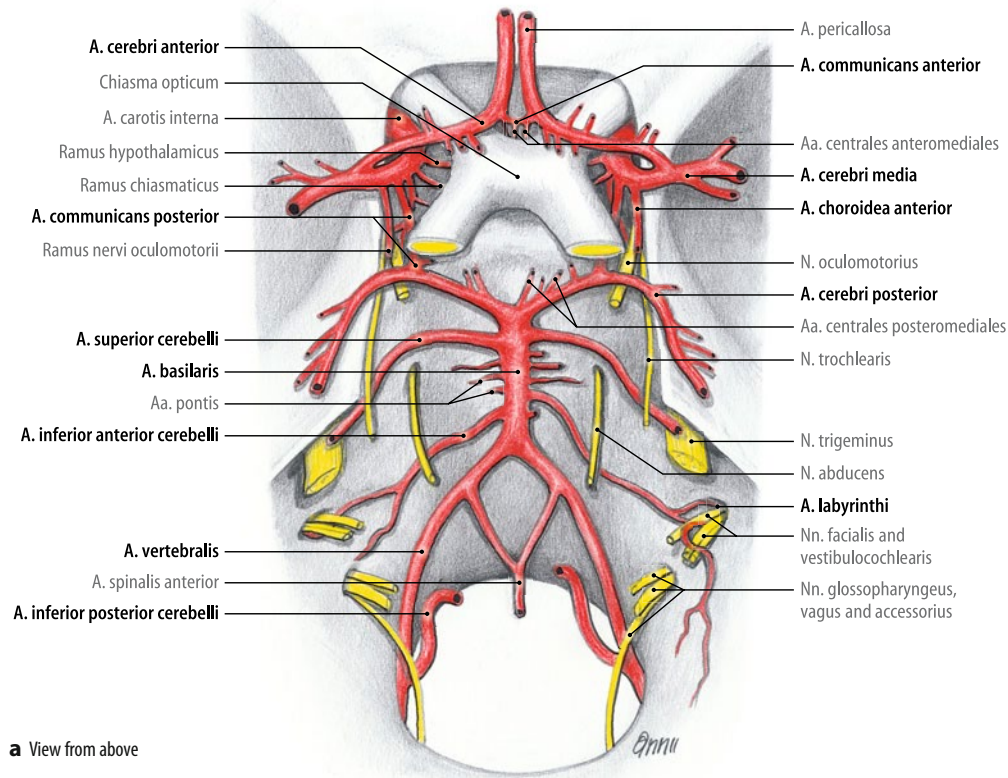
### ■ Vertebral Artery

The vertebral artery forks off as a branch of the sub-clavian artery and extends cranially into the costo-transverse foramen from the sixth to the second cervical spine. After passing through the costo-transverse foramen of the axis, it forms a laterally convex arc to reach the transverse perforation of the atlas. It extends backwards and winds its way around posterior to the lateral mass of the atlas. It has a strongly tortuous course; thus, it does not become overstretched with the wide range of motion in the upper cervical vertebrae. It then extends laterally into the medulla oblongata, through the foramen magnum, and into the cranial cavity. At the lower edge of the pons, it joins the vertebral artery of the opposite side to form the basilar artery ( Fig. 9.17).

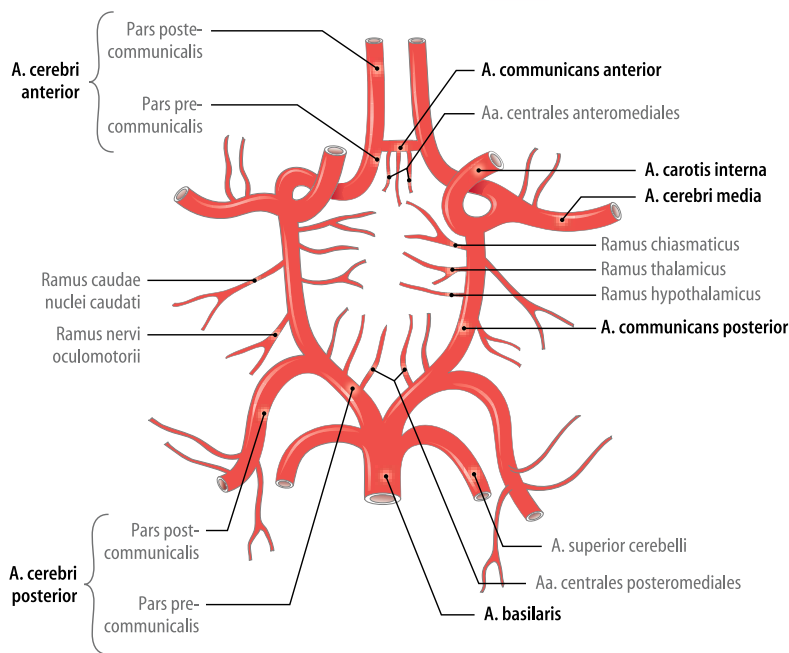
In the extra-cranial section, the vertebral artery forks off into muscular branches, which anastomose with the branches of the external carotid artery. Individual fine branches appear as meningeal branches in the spinal canal and anastomose with other spinal arteries. From the distal extra-cranial section, the arteries then branch off to the dura of the foramen magnum, the posterior cranial fossa and the tentorium (anterior and posterior meningeal branches).

**Anterior Spinal Artery.** The anterior spinal artery also originates from the vertebral artery shortly before the unification of the





**a** View from above



**b**

**Fig. 9.17a,b Cerebral arteries.** **a** Medial portion of the internal base of the skull with the arteries of the base of the brain and cranial nerves, viewed

from above. **b** Normal case of the cerebral arterial circle (circle of Willis). (From: Tillmann 2009)

so-called V4 segment. The anterior spinal artery first extends medially downwards and after about 2 cm, it joins with the opposite artery to form an unpaired mid-sized vessel at the face of the medulla.

**Posterior Inferior Cerebellar Artery.** The posterior inferior cerebellar artery (PICA) is a robust branch (Fig. 9.17) that originates from the vertebral artery at different heights. On about 20% of vertebral angiograms, no posterior inferior cerebellar artery can

be identified; the vascular supply is taken over by a robust anterior inferior cerebellar artery. The arterial pathway has many variants. It usually extends around the medulla backwards around the cerebellar tonsils. Infarctions of the PICA can cause Wallenberg's syndrome, an ischaemia of the dorso-lateral medulla oblongata. This causes pain and temperature loss with ipsilateral ataxia, vertigo and nystagmus, in addition to ipsilateral Horner's syndrome.

#### ■ Basilar Artery

The basilar artery (■ Fig. 9.17) extends into the medial plane along the pons. At the upper edge, it branches off into both cerebral posterior arteries. These are mostly responsible for the supply of the occipital lobe and partially responsible for the temporal lobe of each side. The basilar artery usually has a diameter of just under 4–4.5 mm. The basilar artery emits numerous small branches to the pons and medulla, which are not represented in angiography.

**Anterior Inferior Cerebellar Artery.** The inferior cerebellar artery anterior (AICA) is the first major branch of the basilar artery. It is quite variable in form and origin and has numerous variations. The AICA extends in the direction of the cerebello-pontine angle and can reach the internal auditory canal. It emits the labyrinthine artery, which supplies the inner ear and anterior portions of the cerebellum.

**Superior Cerebellar Artery.** The superior cerebellar artery originates from the basilar artery shortly before it splits into the posterior cerebral artery. It supplies parts of the mid-brain, the surface of the cerebellar hemispheres, and the upper vermal portions. The two superior cerebellar arteries are more constantly available than the remaining cerebellar arteries. Duplications in the main trunk are relatively common. In 28% of cases they are unilateral and in 8% of cases they are bilateral.

**Posterior Cerebral Artery.** The posterior cerebral arteries originally emit both phylogenetically and ontogenetically from the internal carotid artery, later connecting to the basilar artery. Anatomical studies revealed that in 10–30% of cases, the posterior cerebral artery directly emits from the internal carotid artery. The posterior cerebral arteries are emitted as paired terminal branches from the bifurcation of the basilar artery. Based on their coverage area, the branches of the posterior cerebral artery can be divided into cortical branches to form the occipital and temporal lobes, branches to the thalamus (the anterior and posterior anterior thalamo-perforating arteries), branches to the choroid plexus (medial and lateral posterior choroid arteries), and mesencephalic branches.

The **blood supply to the brain-stem** can be easily divided into three regions

- Vento-medial
- Vento-lateral
- Dorso-lateral

The ventro-medial portions of the brain-stem are directly supplied from small branches of the vertebral artery (medulla oblongata), the basilar artery (pons), or the posterior cerebral artery

(mesencephalon). In the area of the medulla oblongata, there is clear lateral separation in the supply because of both vertebral arteries. A unilateral circulatory disorder in the vertebral artery thereby results in isolated damage in one half of this brain-stem section. The ventro-lateral and dorso-lateral brain-stem portions are supplied by the short and long branches of the basilar artery or the cerebellar arteries and the posterior cerebral arteries.

#### ■ Circle of Willis

This is a vascular system that connects the anterior and posterior cerebral bloodstream via anastomosing arteries (■ Fig. 9.17). The right and left cerebral bloodstream are connected in this way. A posterior communicating artery is emitted from both the left and right internal carotid arteries. These form an anastomosis between the internal carotid artery and the two posterior cerebral arteries. The latter are in turn interconnected via a common origin from the basilar artery. Both anterior cerebral arteries are ultimately connected by the anterior communicating artery. Aneurysms are often found in the circle of Willis.

#### ■ Anterior Cerebral Artery

The anterior cerebral artery (■ Fig. 9.18) branches off from the internal carotid artery. It extends over the optic chiasm and draws away after emitting the anterior communicating artery to the inter-hemispheric gap. There, it proceeds forward around the genu of the corpus callosum to the dorsal side of the corpus callosum and divides into its two main branches, the peri-callosal artery and the callosomarginal artery. It gives off numerous branches and extends to the border of the parietal and occipital lobes. Before the separation of the anterior communicating artery, it is designated as the A1 segment (pars praecommunicalis); the subsequent portion is called the A2 segment (pars postcommunicalis).

The supply area of the anterior cerebral artery extends medially over the frontal and parietal lobes, the septum, and the basal anterior horn structures. It also reaches beyond the outer edge to the convexity of the cerebral hemisphere, where part of the frontal and parietal lobe is supplied. The anterior cerebral artery supplies a large part of the prefrontal and premotor cortex. The anterior limb of the internal capsule and the anterior part of the striatum are supplied via the recurrent artery of Heubner, which arises from the anterior cerebral artery after separation of the anterior communicating artery. Because cortico-pontine pathways also run through the anterior capsular limb, closure of this artery can lead to symptoms similar to a cerebellar failure, e.g. dysarthria. **Occlusion of the anterior cerebral artery** leads to paralysis of the contra-lateral side. In addition, severe personality changes can occur.

#### ■ Medial Cerebral Artery

As a terminal branch of the internal carotid artery, the medial cerebral artery (■ Fig. 9.18) is the strongest and thickest of the three major cerebral arteries. After branching from the internal carotid artery, the medial cerebral artery emits the central antero-lateral arteries (lenticulo-striate artery). It involves several perpendicularly branching arteries that pass through the anterior perforated substance in the brain and supply the striatum and globus palli-

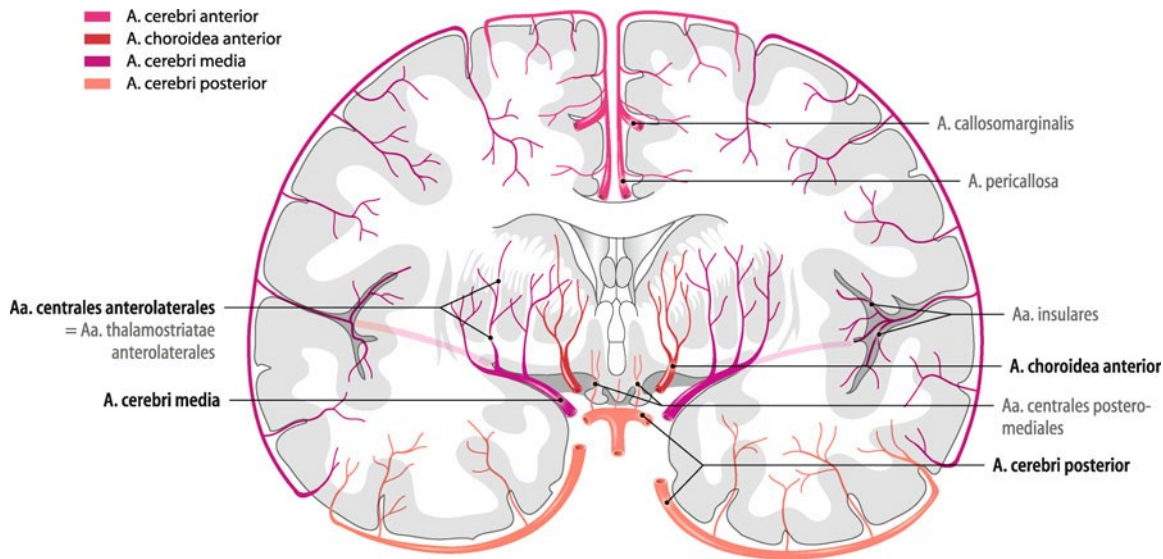


**Fig. 9.18 Anterior and medial cerebral artery.** Arterial supply of the cortex, basal ganglia and internal capsule; frontal section through the brain in the region of the striatum. (From: Tillmann 2009)

in addition to a portion of the internal capsule and thalamus. Angiographically, four sections of the medial cerebral artery can be distinguished:

- Pars sphenoidalis (M1 segment)
- Pars insularis (M2 segment)
- Pars opercularis (M3 segment)
- Pars terminalis (M4 segment)

The medial cerebral artery is most commonly affected by **ischemic events** in the case of atherosclerosis, embolism and vascular ruptures caused by high blood pressure. If the entire medial cerebral artery closed, this results in hemiplegia on the contralateral side. This is primarily attributable to insufficient supply to the internal capsular portions, which guide the cortico-fugal fibres, and insufficient supply to the motor cortex. In addition, unilateral numbness manifests on the contra-lateral side. Because the frontal eye field is supplied by the middle cerebral artery, there is a visual deviation to the ipsilateral side. If the dominant hemisphere is affected, global aphasia will occur because both language centres are affected. In addition, agraphia can often be manifested.

### 9.1.9 Cerebral Veins and Dural Venous Sinuses

#### ■ Cerebral Veins

The path of the cerebral veins is independent of the arteries (Fig. 9.19). Like almost all the cephalic veins, cerebral veins have no flaps. The delicate walls are free of muscle tissue and usually extremely thin. In the brain, superficial veins are distinguished from deep veins. The superficial veins flow directly into the dural venous sinuses, while the deep veins channel off into the great cerebral vein, which in turn flows into the straight sinus.

The **superficial veins** divert the blood from the outer 1–2 cm of the cerebrum. In these veins, a distinction can be made among

the upper veins, medial veins and lower veins. The upper veins (the superior cerebral veins) drain the blood of the upper, lateral and medial hemisphere, proceed to the sub-arachnoid cavity, and lead the blood directly into the superior sagittal sinus. From the brain surface, they must traverse the sub-arachnoid cavity and then pierce the arachnoid as so-called pontine veins. From the sub-dural cavity, they terminate in the venous sinus.

These veins can be injured following **mild cranio-cerebral trauma**, thereby resulting in extensive bleeding in the sub-dural cleft, known as **sub-dural haemorrhaging**.

The **medial veins** (superficial middle cerebral veins) lead the blood from the vicinity of the lateral sulcus directly into the sphenoparietal sinus.

The **inferior cerebral veins** accumulate blood from the region of the basal hemisphere and flow into the transverse sinus.

The **deep cerebral veins** join with the great cerebral vein and primarily drain the blood from the sub-cortical cerebral structures and the diencephalon. In the deep cerebral veins, two vessels can be highlighted:

- Basal Rosenthal vein
- Internal cerebral vein
- These join with all the other deep veins to form the unpaired **great cerebral vein**.

The basal vein is formed by the union of the anterior cerebral vein and the deep middle cerebral vein in the region of the anterior perforated substance. The **internal cerebral vein** arises in the region of the inter-ventricular foramen between the lateral ventricles and third ventricle by the union of three veins:

- Superior choroidal vein
- Vein of the septum pellucidum
- Superior thalamo-striate vein

The basal internal cerebral veins of both sides then unite to form the great cerebral vein, which joins with the straight sinus after a short, dorsally directed course.

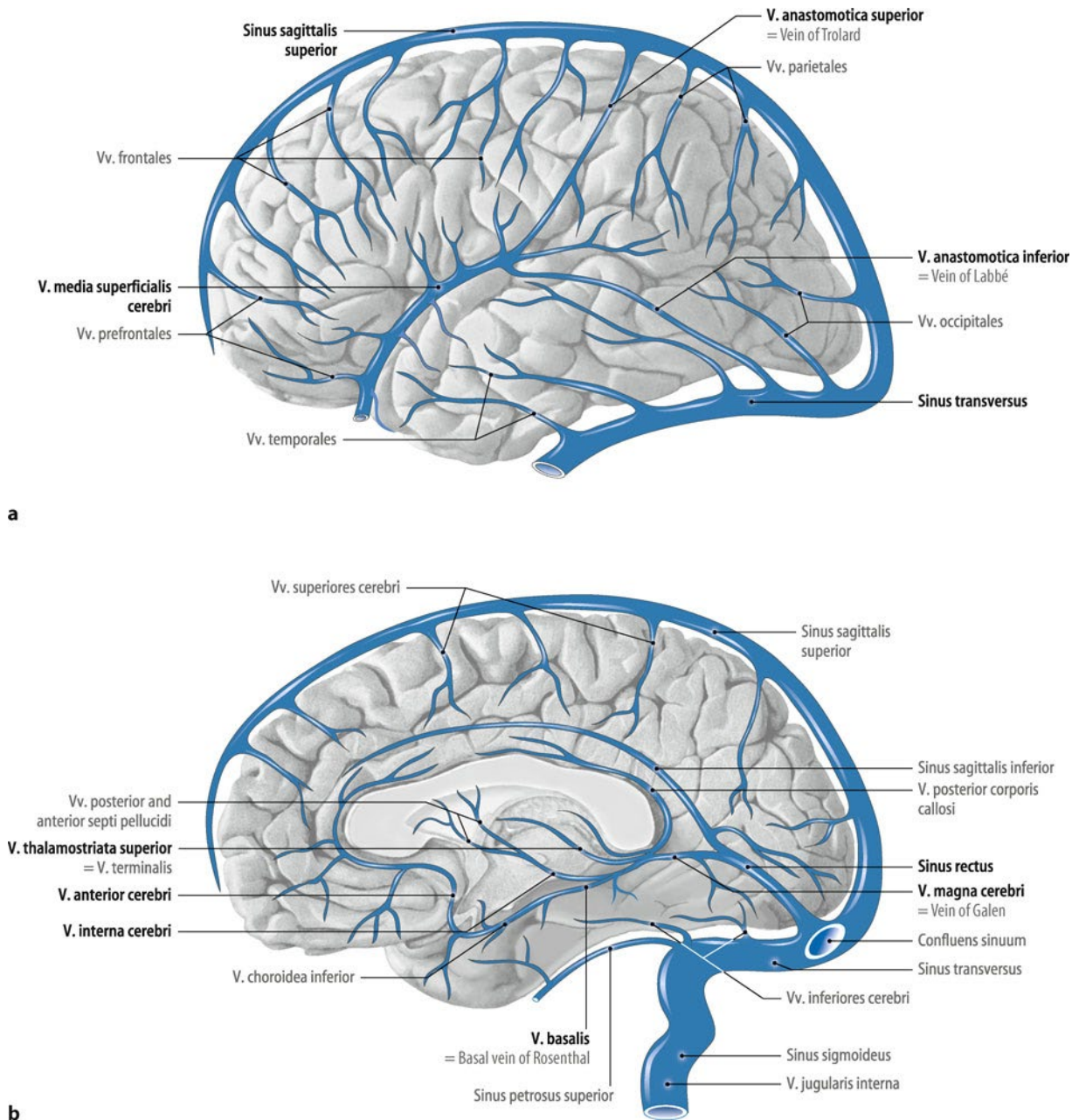


**Fig. 9.19a,b** Cerebral veins and dural venous sinuses. **a** Left hemisphere, lateral view. **b** Right hemisphere, medial view. (From: Tillmann 2009)

## ■ Sinus

The most important sinuses are the superior and inferior sagittal sinuses in the upper or lower edge of the cerebral falx, the straight sinus, the transverse sinus, and the sigmoidal sinus, which run along the occipital skull base, in addition to the cavernous sinus, which surrounds the pituitary gland and has special clinical significance. It receives venous tributaries from, among others, the superior ophthalmic vein of the eye, which anastomoses to the medial canthus with facial veins. The carotid artery and abducens nerve extend through the cavernous sinus; the ophthalmic nerve, the oculo-motor nerve, the trochlear nerve and the maxillary nerve proceed through its lateral wall. In the event of cavernous sinus lesions, such as fistulas, aneurysms, tumours and thrombosis, these pathways may become damaged.

## 9.2 Developmental Disorders and Malformations of the Brain

The imaging of the brain has been significantly improved by the introduction of cerebral MRI. The high soft tissue contrast and the arbitrary choice of the sectional image plane enable the visualisation of detailed structures of the nervous system, which had previously been reserved for anatomists and pathologists.

### 9.2.1 Embryogenesis of the Nervous System

The development of the nervous system during the embryonic period involves three key steps:

■ **Table 9.1** Schedule for the development of the human brain

Gestational age	Course of development	Malformation
0–18 days	Position of germ layer	Necrosis
19–21 days	Neural plate, neural folds, neural groove	Complete dysraphism
22–24 days	Optic vesicle	Hydrocephalus
24–28 days	Neural tube, closure of cranial and caudal neuropore	Anencephaly, encephalocele, spina bifida
Fourth week	Hind-brain, eye, medial longitudinal fissure	Holoprosencephaly
Fifth week	Olfactory lobes, cerebellum, ventral and dorsal roots, vascular system	Cerebellar hypoplasia, microcephaly, proliferation and migration disorders
Seventh week	Temporal lobe	
Eighth week	Choroid plexus	
Third month	Radiation of corpus callosum, island, corpus callosum, septum pellucidum, fornix, cerebellar upper vermis	Aplasia of the corpus callosum, vermis aplasia
Fourth month	Differentiation of the cortex, meninges, CSF circulation	
Fifth to sixth month	Delimitation of cerebral lobes, primary brain sulci, proliferation finished, mass increase in the cerebellum, foramina of the fourth ventricle, complete commissures	Disruption of cellular architecture, dystopia, disruption of myelination
Seventh to ninth month	Development of gyri and sulci, secondary and tertiary sulcation	Destructive changes
Sixth month to first year of life.	Neural migration, proliferation of glial cells, apoptosis and axosomatic dendritic connections, myelination	Disturbance of the cerebral and cerebellar micro-architecture

- Induction
- Neurulation
- Vesicle formation

**Induction.** Around the 17th embryonic day, after the three overlapping germ layers (endoderm, mesoderm and ectoderm) have developed in the embryo, the neuro-ectoderm is formed via the induction of the underlying mesoderm and the notochord in the ectoderm. (■ Table 9.1).

**Neurulation.** Early in the development of the embryo, at around the third week, nothing can be seen of the central nervous system except for a flat neural plate. Subsequently, at the edge, protuberances, the so-called neural folds, arise (■ Table 9.1). These ridges ultimately form the neural folds, which include the neural groove. Both ridges fuse together to form the neural tube (neurulation = constriction of the neural crest and neural tube from the ectoderm; ■ Fig. 10.7). The brain arises from the cranial section, and the spinal cord arises from the caudal section. The ventricular system develops from the cavity of the tube. Initially, the neural tube is open at the front and rear ends. On the 25th embryonic day, the front end closes followed by the rear end 2 days later.

Aberrations during neurulation lead to so-called **dysraphic disorders**. If the frontal cephalic end (rostral neuro-pore) fails to close, this will result in fatal anencephaly. If the rear end (caudal neuro-pore) fails to close, this will result in spina bifida. It is characterised by an incomplete closure of the vertebral arches and can have different degrees of severity and manifestations from occult spina bifida up to myelo-meningocele.

**Vesicle Formation.** Shortly after the closure of the neural tube, three small vesicles can be seen at the cranial end – the primary cerebral vesicles. These are referred to as:

- Prosencephalon (fore-brain)
- Mesencephalon (mid-brain)
- Rhombencephalon (hind-brain)

In addition, the neural tube bends in the cervical flexure and the cephalic flexure. In the fore-brain, both cerebral vesicles evert in the 5th week. They also form two small optic vesicles, which will become the optic cups. The lamina terminalis comes to rest between the two cerebral vesicles. Together, the terminal lamina and cerebral vesicles are called the telencephalon (end-brain). The remaining fore-brain is called the diencephalon (inter-brain). In the hind-brain the pontine flexure is formed by folding; the front portion of the rhombencephalon is now called the metencephalon. The cerebellum is later created from its top: the rear section is referred to as the myelencephalon.

**Development from the 6th Week.** At the end of the 6th week, the floor of the lateral ventricles begins to bulge, ultimately giving rise to the basal ganglia. The choroid plexus arises at the transition from the hemispheric wall to the diencephalon. Directly adjacent to this, the pallidum extends to the hippocampus. The development of the corpus callosum and of the commissures begins in the 7th week with a thickening of the dorsal portion of the terminal lamina. This thickened portion is called the lamina reuniens. The ventral portion of the lamina reuniens is called the meninx primitiva. The axons begin to cross over the median, which is likely mediated by chemical messengers, and form the

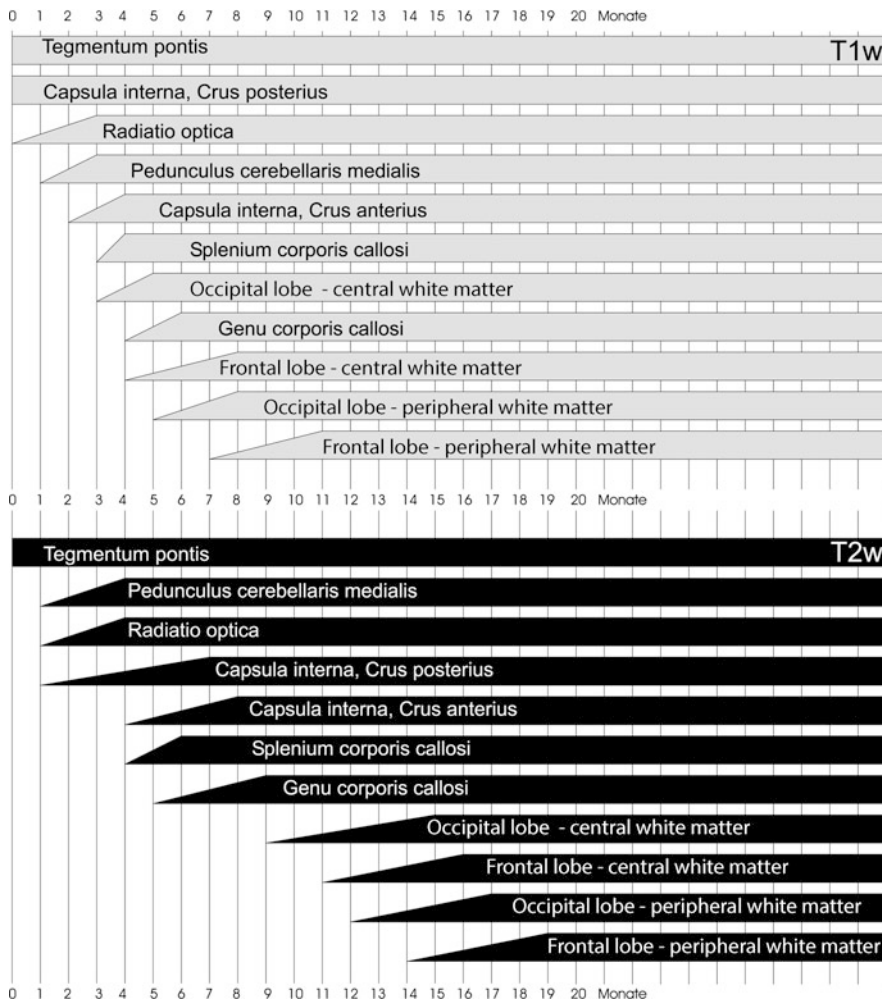


**Fig. 9.20** Myelination scheme according to Grodd. Schedule for normal myelination – details summarised from various publications. For 11 brain structures, the start and end points of the periods are schematically plotted, where T1-weighted (*light bars*) and T2-weighted (*dark bars*) myelination processes are recognisable (Fig. 9.21). (From: Reiser and Semmler 2002)

“bridge” between the hemispheres, the anterior commissure, the corpus callosum and the posterior commissure. First, the axons of the posterior portion of the genu cross, followed by the corpus and the anterior portion of the genu and finally the splenium and the rostrum of the corpus callosum. While the corpus callosum expands, the lamina terminalis, which gives rise to the septum pellucidum, becomes thinner.

The occipital pole of the **cerebrum** begins to develop at the end of 6th week, and the temporal pole at the beginning of the 8th week. At the beginning, the brain is smooth; **gyration** is completely absent. The first identifiable sulcus is the Sylvian fissure. In the 4th month, the brain looks like a figure eight. The cortical ribbon is still relatively thin. Between the 20th and the 22nd week, the cingulate gyrus and the parieto-occipital sulcus develop. Gyration proceeds in the portions with sensorimotor and visual functions. Around the actual birth date, the gyri and sulci have a form similar to that found in adults. However, the sulci are not as deeply pronounced as they are later. The **myelination** of the white matter does not begin until the 5th month of development. At birth, the medulla oblongata, the dorsal mid-brain, the upper and lower cerebellar peduncles, and the posterior peduncle of the internal capsule are usually myelinated.

The **diencephalon** is formed from the middle portion of the fore-brain. The thalamus and hypothalamus develop from the so-called alar plates of the diencephalon. The pituitary gland is

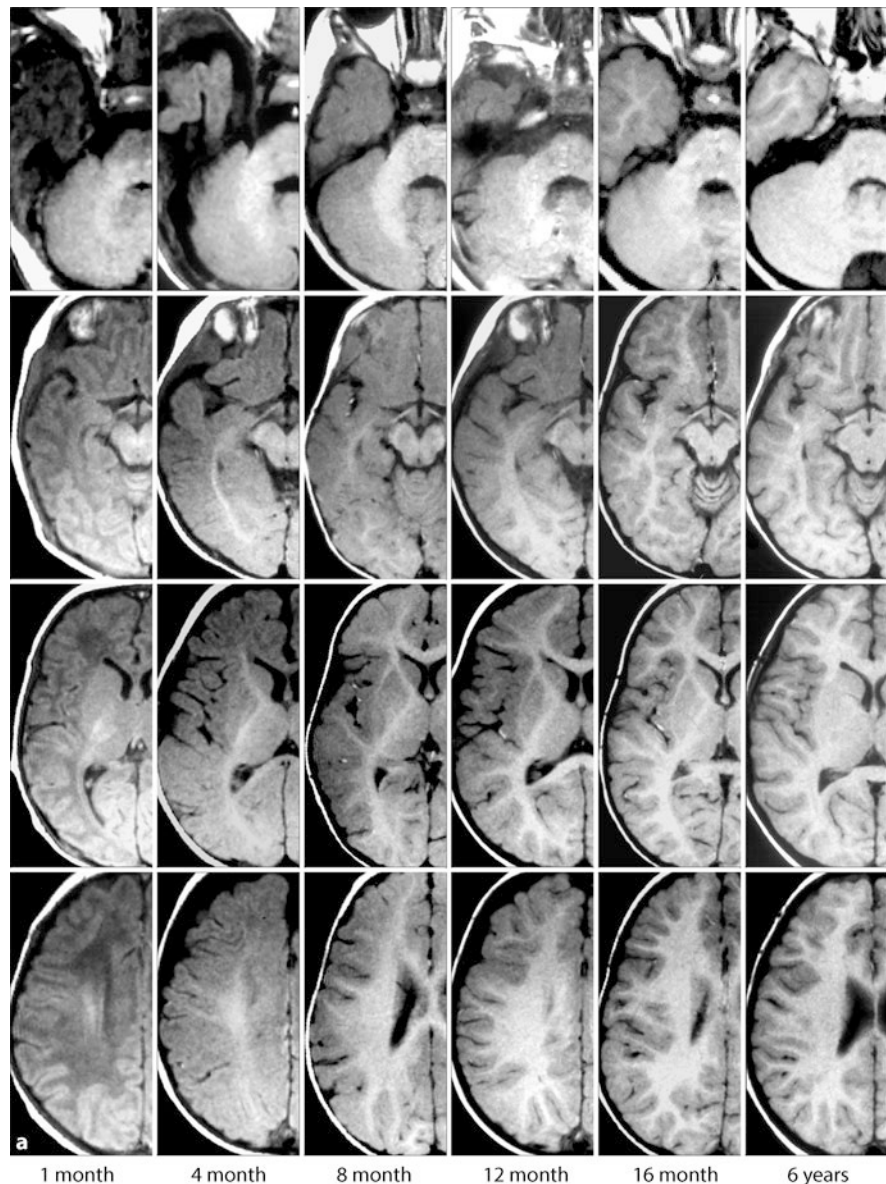
composed of part of the diencephalon. This later gives rise to the pituitary stalk and posterior pituitary lobe. The anterior pituitary arises from Rathke’s pouch, an ectodermal protuberance of stomodeum in front of the pharyngeal membrane. The roof of the pharyngeal pituitary and Rathke’s pouch cysts both derive from this.

From the basal plates of the **mesencephalon** arise the cerebral peduncle and various core groups that are important for the oculo-motor system. The red nucleus and substantia nigra develop adjacently to the quadrigeminal plate. The metencephalon develops from the front portion of the rhombencephalon, and the pons develops from the ventral portion of the metencephalon. The **cerebellum** is formed from the far side. During early cerebellar development, the two dorsal rhombic lips of the rhombencephalon approach each other and will ultimately form the cerebellar plate. In the 12th week, the cerebellar hemispheres and vermis can be distinguished. From the posterior portions of the rhombencephalon arises the myelencephalon from which medulla oblongata will ultimately develop.

### 9.2.2 Myelination of the Brain

**Medical Imaging.** Both T1- and T2-weighted spin-echo images have proven to be well suited to displaying normal brain matu-

**Fig. 9.21a,b Myelination.** **a** T1-weighted and **b** T2-weighted axial sectional images at the level of the fourth ventricle (*top row*), of the mesencephalon (*second row*), the basal ganglia (*third row*) and the semi-oval centre (*bottom row*) at six different ages ranging from 1 month to 6 years. (From: Reiser and Semmler 2002)



ration and myelination (■ Fig. 9.21). In addition, T1-weighted scans with the inversion-recovery sequence technique or turbo spin echo sequences can be used in T2-weighted imaging.

**Development.** With punctual birth, the posterior shank of the internal capsule, parts of the medulla oblongata, the dorsal mid-brain, and parts of the cerebral peduncles are myelinated. At the age of 4 months, the basilar part of the pons is myelinated, and the cerebellar peduncle also undergoes further myelination. Myelination can now additionally be identified in the cerebral peduncles.

At 4 months, the entire length of the posterior shank of the internal capsule appears to be myelinated; the mid-portion is depicted as being somewhat lighter. In addition, myelination of the anterior limb of the internal capsule and the splenium of the corpus callosum, but not the genu, can be proven. There is also significant myelination laterally adjacent to the temporal horn of the lateral ventricle. The myelination of the visual pathway proceeds posteriorly and medially so that the visual

cortex will soon be reached. On the T1-weighted sequences, in the semi-oval centre, the hyper-intensity of the medullary layer spreads parietally and frontally from the central sulcus (■ Figs. 9.20, 9.21).

At 2 years of age the basilar part of the pons is largely myelinated. Beyond that, only the foliae cerebelli and the middle cerebellar peduncles are myelinated. At the age of 24 months, on the T2-weighted sequences the corpus callosum and internal capsule can be recognised with reduced signal. The thalamus also exhibits different compartments, which can be detected into adolescence. In the temporal lobe, all gyri have been myelinated. However, myelination of the rostral cortex has not yet been achieved. In the occipital lobe, the medullary/cortical margin is now sharply delineated throughout because all gyri have been myelinated. At 2 years of age, the entire medullary layer is well matured and fills the frontal lobe up to the periphery. However, in the other regions of the cerebrum, the cortex still appears to be relatively thick. In a 2-year-old child, the semi-oval centre is largely homogeneous and hypointense on T2-weighted sequences with good demarca-

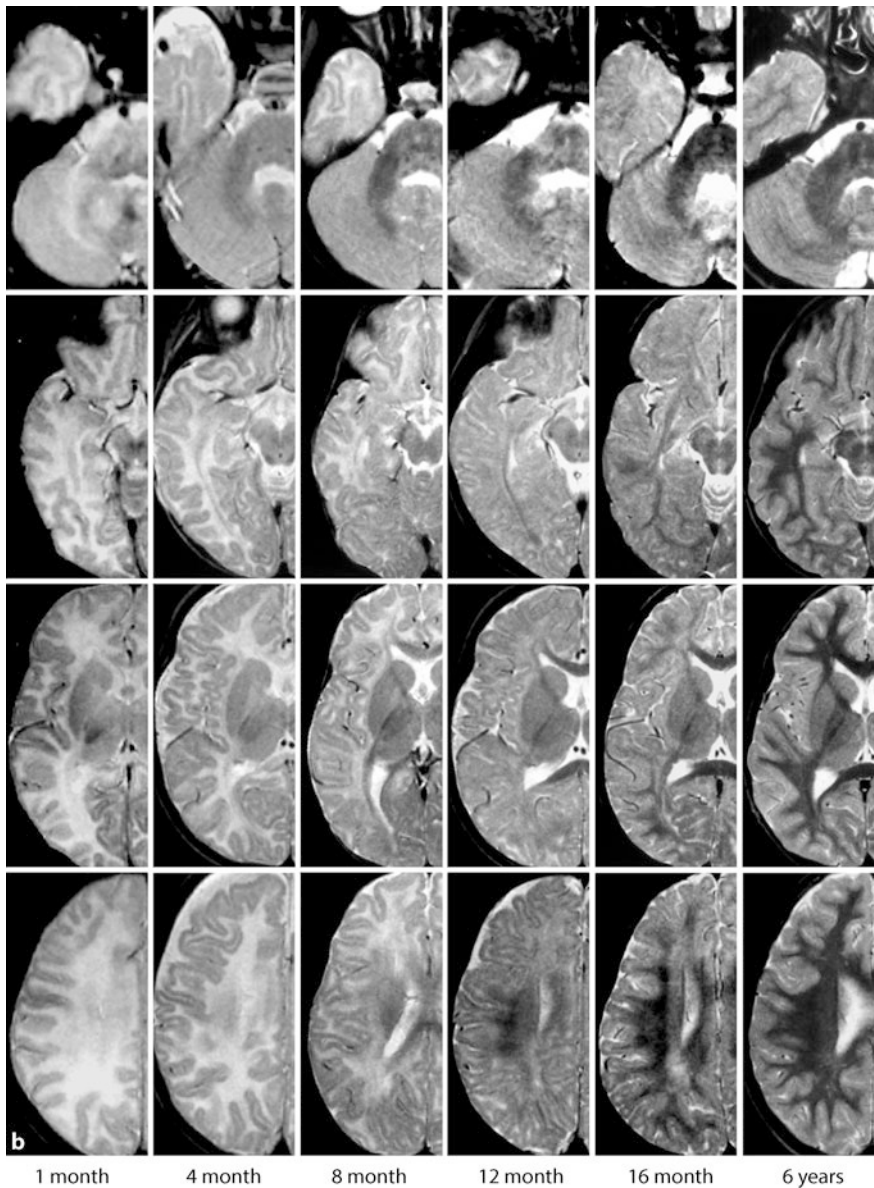


**Fig. 9.21b Myelination.** a T1-weighted and b T2-weighted axial sectional images at the level of the fourth ventricle (*top row*), of the mesencephalon (*second row*), the basal ganglia (*third row*) and the semi-oval centre (*bottom row*) at six different ages ranging from 1 month to 6 years. (From: Reiser and Semmler 2002)

tion of the medullary/cortical margin. Excluded from this is the aforementioned area dorso-lateral to the posterior horns of the lateral ventricles.

### 9.2.3 Neural Tube Defects

Neural tube closing defects are the most common malformations of the nervous system and generally occur at the rostral or caudal end (■ Fig. 10.7). This results in anencephaly, cranio-rachischisis, meningo-myelocele, or spina bifida occulta.

#### ■ Anencephaly

In anencephaly, the cerebrum is fully or partially aplastic, the skull cap is missing, and the facial skeleton is usually normal in shape. If the mid-brain and pons are flattened, the cerebellum, hypothalamus, and neuro-hypophysis fail to develop. Extra-cranial malformations occur only occasionally, but endocrine changes are frequent. Clinically, abnormal patterns of movement

of the foetus appear on ultrasound, the lack of cranial development provides early pre-natal diagnosis, which results in termination of the pregnancy.

#### ■ Cephaloceles

If the closure defect only affects a limited region of the skull, this results in local protrusions, which are located in the median line and usually covered by intact skin. They contain only the meninges (cranial meningocele), parts of the brain (meningo-encephalocele), or the ventricular system (encephalocystocele).

Encephaloceles occur in **different locations**. Occipital and fronto-ethmoidal encephaloceles are most frequently observed, each lying in the median. However, parietal, occipito-cervical, temporal, frontal, spheno-maxillary, nasopharyngeal and lateral locations have been described. There are clear differences in the geographical distribution. Occipital encephaloceles occur most frequently in Central Europe; fronto-ethmoidal cephaloceles are more frequently observed in South East Asia.



In the case of Meckel's syndrome, they are combined with other anomalies (hexadactyly and cystic changes of the internal organs).

### ■ ■ Occipital and Parietal Cephaloceles

Occipital encephaloceles are already present at birth and occur between the foramen magnum and the lambdoid suture. Within the cephaloceles, the brain is usually dysplastic. A female predominance and an association with neural tube disorders (approximately 7% myelo-meningocele and 3% diastemato-myelia) are apparent. Parietal cephaloceles display a cranial defect between the lambdoid suture and bregma. They are also associated with anomalies of the median.

### ■ ■ Fronto-ethmoidal Cephaloceles

Fronto-ethmoidal cephaloceles often display late clinical signs, usually the obstruction of nasal breathing. Occasionally, however, facial dysmorphism may arise. According to their location, fronto-ethmoidal encephaloceles can be divided into:

- Naso-frontal encephaloceles
- Naso-orbital encephaloceles
- Naso-ethmoidal encephaloceles

**Medical Imaging.** In the case of fronto-ethmoidal encephaloceles, T1- and T2-weighted sequences should be performed in all spatial planes to depict the defect (■ Fig. 9.22). Thin-layer CT scans should also be prepared in order to detect the osseous defect. It must be observed that up to the 2nd year of life, the osseous frontal skull is not yet fully formed.

### ■ ■ Atretic Cephaloceles

Atretic cephaloceles include portions of the dura mater and connective tissue. They are most commonly found in the occipital region. Atretic parietal cephaloceles are often associated with other malformations. An atretic cephalocele is present if only a long narrow channel traverses the osseous structures of the skull. Within this channel are portions of the dura mater and connective tissue. On MRI, thin-slice T1- and T2-weighted sequences or volume sequences should be performed. Furthermore, CT images may be helpful for depicting osseous defects.

### ■ ■ Spina Bifida

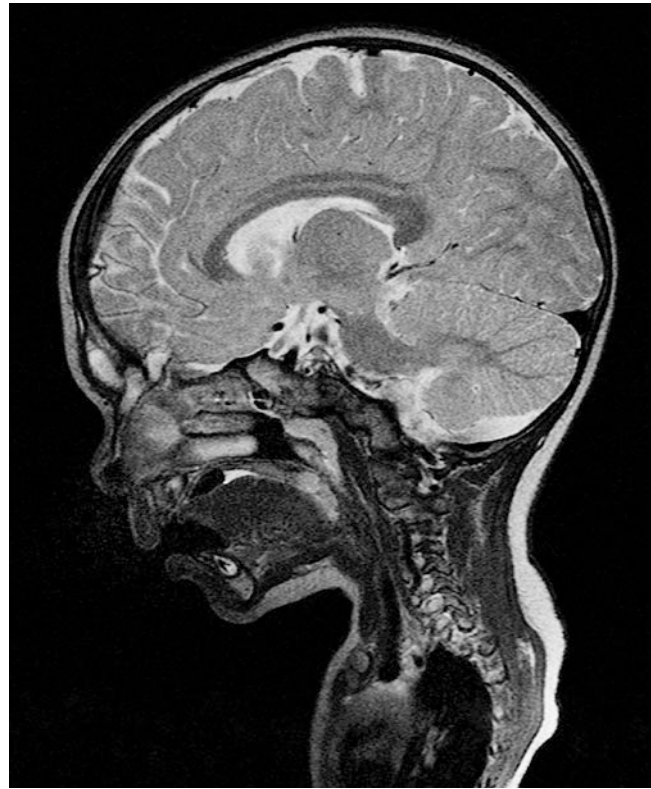
Dysraphic disorders in the area of the spine and spinal cord may occur in varying degrees of severity depending on the genesis. The disturbances will be more thoroughly discussed in the chapter on the spinal column (► Chap. 10).

## 9.2.4 Anomalies of the Medial Structures

In the case of the pathogenetic relationship of dysraphia and holoprosencephaly, anomalies of the median can be found, either in combination with other malformations or in isolation.

### ■ Agenesis of the Corpus Callosum

A partial or complete absence of the great commissure may remain clinically undetected. The investigation of isolated functions is difficult because too many other abnormalities are present.



■ Fig. 9.22 Frontal encephaloceles. On the sagittal T2-weighted sequences, an osseous gap appears at the base of the frontal skull and re-enters the cerebral parenchyma

Because the development of the corpus callosum occurs during a critical period of brain development, this error is often **associated with various syndromes (overview)**. A corpus callosum anomaly is relatively frequently associated with **Chiari syndrome** (type II Chiari malformation). In addition to agenesis/dysplasia of the corpus callosum, a depression of the cerebellar tonsils, a beak-shaped configuration of the tectum, a compression and flattening of the fourth ventricle and the pons, and kinking of the medulla oblongata may occur. Agenesis/dysplasia of the corpus callosum is often associated with **Dandy-Walker syndrome**. These examples show an enlargement of the posterior fossa with hypoplasia or aplasia of the vermis and cystic enlargement of the fourth ventricle.

### Syndromes Associated with Agenesis of the Corpus Callosum

- Type II Chiari malformation
- Dandy-Walker malformation
- Aicardi syndrome
- Morning glory syndrome
- Apert syndrome
- Rubinstein-Taybi syndrome
- Cogan's syndrome

Development of the corpus callosum takes place in the 7th week of embryogenesis and is accompanied by thickening of the dorsal

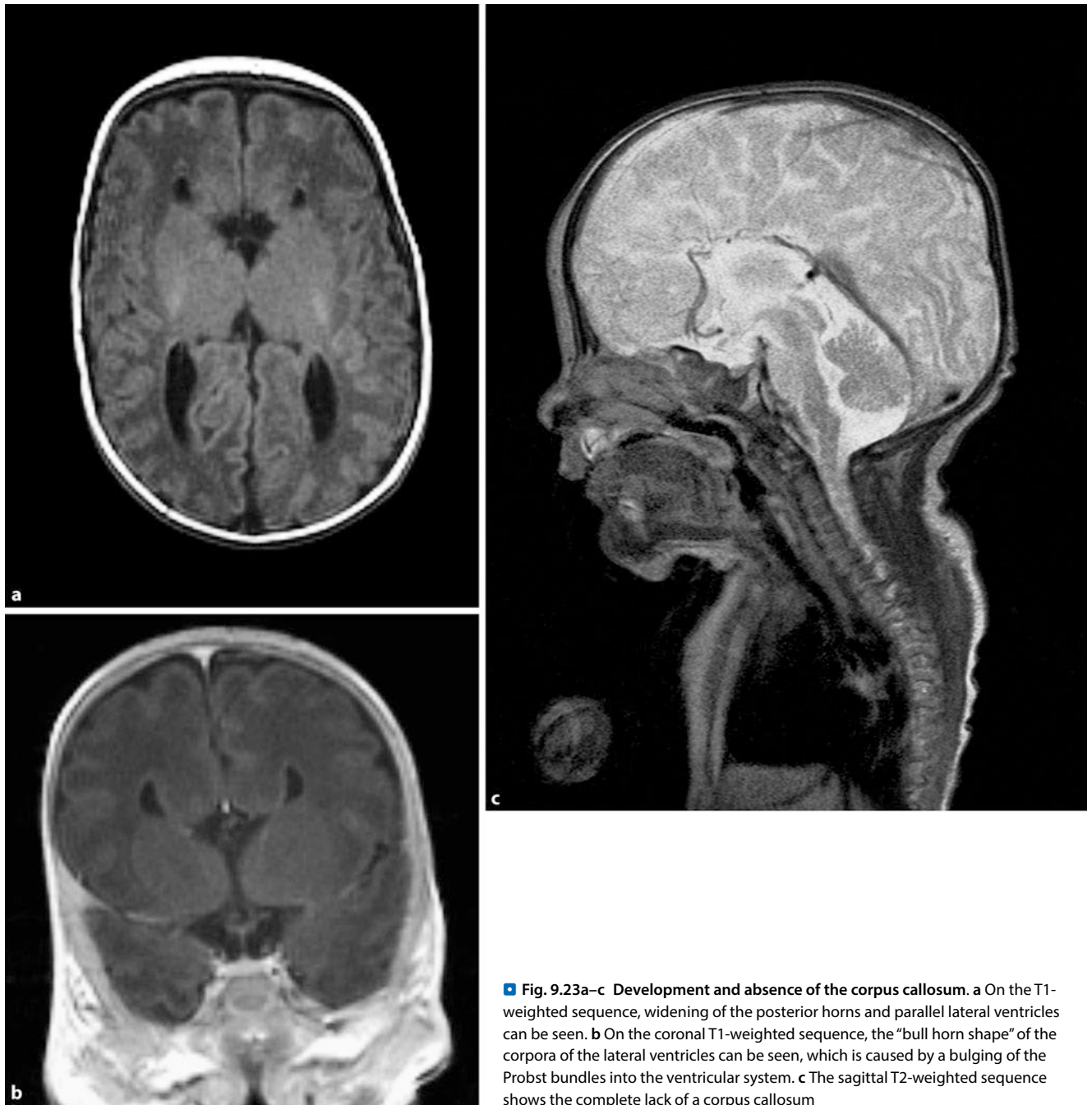


**Fig. 9.23a–c** Development and absence of the corpus callosum. **a** On the T1-weighted sequence, widening of the posterior horns and parallel lateral ventricles can be seen. **b** On the coronal T1-weighted sequence, the “bull horn shape” of the corpora of the lateral ventricles can be seen, which is caused by a bulging of the Probst bundles into the ventricular system. **c** The sagittal T2-weighted sequence shows the complete lack of a corpus callosum

portion of the terminal lamina. This thickened portion is called the lamina reuniens (▶ Sect. 9.2.1). The overall development of the corpus callosum takes place between the 7th and 20th week. Possible causes are primary system disorders in the case of autosomal recessive or sex-linked inherited mutations, multifactorial origin, combinations with certain brain malformations, secondary consequences of vascular disorders, inflammation, teratogens (e.g. alcohol), or hydrocephalus. The anomaly may remain asymptomatic, be accompanied by various disorders (developmental delay, cerebral palsy, seizures), or occur in the context of syndromes (overview, e.g. Aicardi syndrome in girls with chorio-retinopathy, hemi-hypertrophy, and salaam spasms). The structural changes can be depicted and quantitatively recorded on MRI (■ Fig. 9.23).

**!** A differentiation between system failure and secondary damage of the corpus callosum are important because system failures have completely different aetiologies from secondary damage.

Contrary to the system failures of the corpus callosum, which occur in the context of hypo- or agenesis, **secondary damage** can result in lesions to or thinning of the corpus callosum. A common cause of a secondary thinning in the peri-isthmic area is **peri-ventricular leukomalacia (PVL)** (■ Fig. 9.24). A PVL is caused by hypoxic-ischaemic injury to the germinal matrix zone. In premature infants, this is particularly highly metabolically active and thereby leads to a common pattern of damage. The decay



■ **Fig. 9.24a,b** Peri-ventricular leukomalacia (PVL). **a** On the T2-weighted axial sequences, a significant rarefaction of the white matter with irregular ventricular wall formation is revealed. The now 7-year-old patient is a former premature infant from the 24th week of pregnancy with known grade II peri-ventricular haemorrhaging. **b** Even on the fluid-attenuated inversion recovery (FLAIR) sequences, the rarefaction of the peri-ventricular white matter with irregularities in the ventricular wall is revealed

of the intersecting paths results in peri-isthmic thinning of the corpus callosum, which may be so pronounced that it appears as a complete defect in this area. Other secondary damage can have the following causes:

- Leukodystrophies
- Infarctions
- Autoimmune diseases, such as encephalomyelitis disseminata

**Medical Imaging.** Within the corpus callosum are densely packed fibres, which are important for the stability and shape of the lateral ventricle. A typical sign of corpus callosal agenesis or pituitary agenesis is in the axial slice orientation of a **widening of the lateral ventricles** with an emphasis on the posterior horns. This characteristic configuration is also referred to as **colpocephaly**. In the area of the anterior horns, the widening is less pronounced, because the caudate nucleus and lenticular nucleus additionally contribute to shaping. Another distinguishing sign of a missing corpus callosum on axial and coronal slice orientation is a “**bull-horn shape**” of the corpora of the lateral ventricles (■ Fig. 9.23). This configuration results from a lateral indentation of the medial ventricle by the so-called Probst bundles, which arise during embryonic or foetal development in the case of a deficiency of the corpus callosum.

#### ■ Abnormalities of the Septum Pellucidum

During development, cavities in the septum pellucidum usually appear. They usually disappear after birth, but may have a connection with the remaining sub-arachnoid space as the fifth and sixth ventricles (cavum septum pellucidum, cavum vergae and cavum velum interpositum). Cysts with space-occupying effects are rare. An agenesis of the septum pellucidum is observed in combination with corpus callosum aplasia or holoprosencephaly. Cerebral seizures and other neurological disorders are generally an indication for the examination; any connection generally remains unexplained.

#### ■ Septo-optic Dysplasia

In the case of septo-optic dysplasia (de Morsier syndrome), the absence of the septum pellucidum, hypoplasia of the optic nerve (possible disturbance) and various endocrine disorders (disturbance of the hypothalamic–pituitary axis) can be found. In the new-born, hypotension, convulsions, hypoglycaemia and jaundice, and later vision problems, developmental delays and seizures, are observed.

**Medical Imaging.** If the septum pellucidum is absent in a child, septo-optic dysplasia should be investigated. For this purpose, it is advisable to carry out thin-slice MRI of the front portions of the visual pathway (■ Fig. 9.25).

#### ■ Corpus Callosum Abnormalities with Intra-cranial Lipomas

Intra-cranial lipomas are likely false differentiations of the meninx primitiva, undifferentiated mesenchyme that surrounds the brain during embryonic development.

About 30% of all intra-cranial lipomas occur in the area of the corpus callosum (■ Fig. 9.26). If a corpus callosal lipoma appears in the front section of the corpus callosum, it is usually associated with an abnormality of the corpus callosum. Lipomas in the back section of the corpus callosum often accompany normal formation of the corpus callosum. Lipomas associated with the corpus callosum may calcify and then present on X-ray images. They are often associated with other abnormalities of the median, e.g. cleft lips, jaws, or palates.

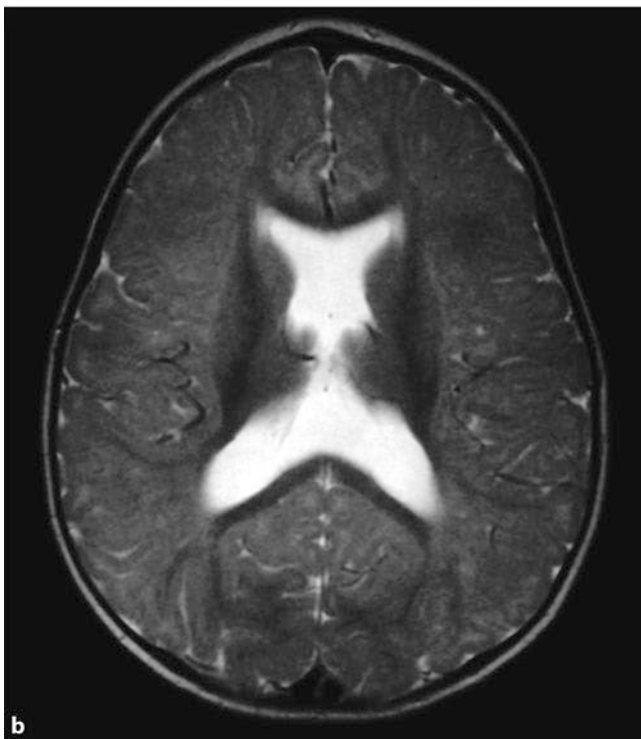
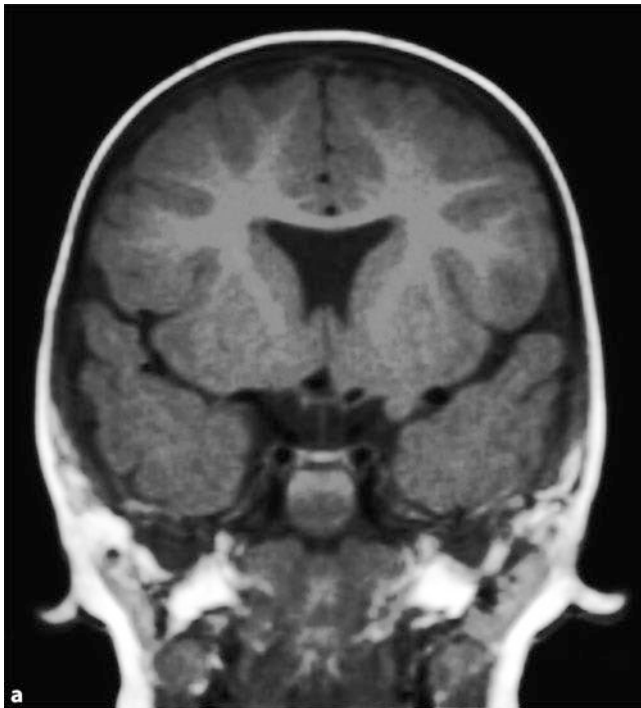


**Fig. 9.25a,b** Septo-optic dysplasia. **a** On the coronal T1-weighted sequence, hypoplasia of the optic chiasm and optical nerves in addition to a missing septum pellucidum. **b** T2-weighted imaging: missing septum pellucidum

**Medical Imaging.** On CT, the corpus callosal lipoma displays fat-isodense (negative) density values. Nodular and lumpy calcifications may occasionally occur. On MRI, the lipomas are depicted as fat-isointense on all sequences, i.e. on T1-weighted sequences, they are strongly hyperintense. A sequence with a fat saturation pulse can help with the differentiation.

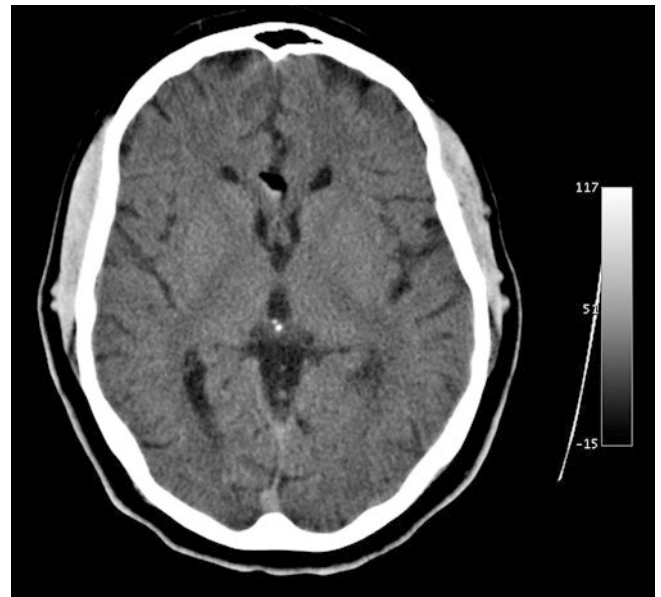


**Fig. 9.26** Corpus callosal lipoma. On CT, the corpus callosal lipoma is depicted as an area of hypo-density with fat-equivalent Hounsfield units (negative values)

#### ■ Corpus Callosal Anomalies with Inter-hemispheric Cysts

Corpus callosal malformations are often associated with inter-hemispheric cysts. Inter-hemispheric cysts may be clinically silent, but are also conspicuous with epilepsy. The inter-hemispheric cysts are divided into three groups:

- **Type 1:** a single large cyst that is connected to the lateral or third ventricle
- **Type 2:** additional disturbances of cortical development, such as poly-microgyria, pachygyria, migration disorders, or schizencephaly. The cysts are septate and not connected to the ventricular system
- **Type 3:** cysts with complex internal structures with asymmetric sub-space. Owing to the different composition of the cyst contents, the signal of the cysts can vary from the signal of the CSF if there is no direct communication with the ventricular system.

### 9.2.5 Disturbances in Cortical Development

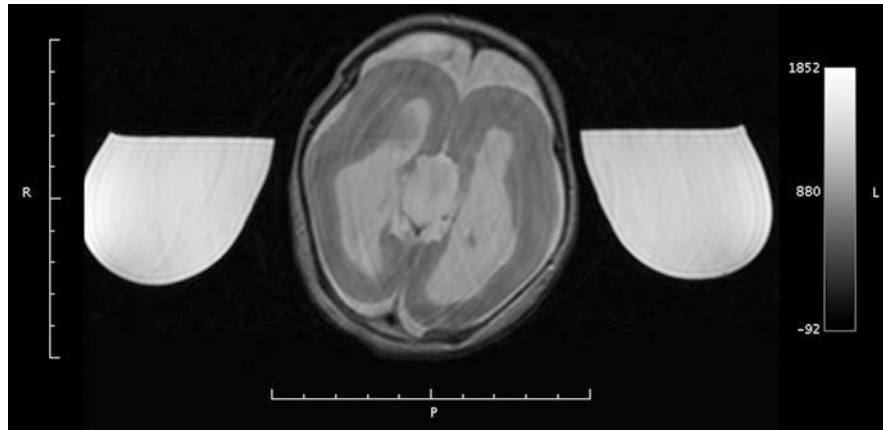
Various abnormalities in the differentiation of the cortex, usually the result of a migration disorder, impair the formation of gyri and sulci in the second half of pregnancy. Disorders in neuronal and glial proliferation can occur:

- Generalised disturbance of cortical development (micro-lissencephaly)
- Focal or multi-focal disorder (in phakomatoses, isolated, neoplastic)

**Disorders of Neuronal Migration.** The following should be distinguished:

- **Generalised** classical lissencephaly (type 1; agyria/pachygyria spectrum), linked to chromosome 17 (Miller-Dieker syndrome, isolated) bonded to X-chromosome (lissenceph-

**Fig. 9.27 Lissencephaly.** Pronounced gyration disturbance in this 2-week-old infant on axial T2-weighted sequences. This involves a particularly severe form in which the formation of the Sylvian fissure is also missing (group 5 micro-lissencephaly)



aly, sub-cortical heterotopia), cobblestone lissencephaly (type 2) in congenital Fukuyama muscular dystrophy, in the case of Walker–Warburg Syndrome, muscle eye brain disease as heterotopia (sub-ependymal, sub-cortical and cortical).

- **Focal and multi-focal:** focal agyria or pachygyria (partial lissencephaly), focal or multi-focal heterotopia with abnormality of the organisation of the cortex (e.g. Aicardi syndrome, paroxysmal diseases).

**Disorders of the Organisation of the Cortex.** The following should be distinguished:

- Generalised poly-microgyria
- Focal or multi-focal polymicrogyria/schizencephaly

#### ■ Lissencephaly

A largely smooth surface of the brain is found in lissencephaly (agyria; **Fig. 9.27**). Pachygyria leads to some weakly pronounced, coarse gyri. The cortex is relatively thick; its neurons are irregularly arranged in only four layers. The white matter appears narrow, the ventricular system is usually extended.

According to morphology and genetics, **various forms** of lissencephaly can be distinguished. A gene (LES 1) was shown to be responsible. It is related to platelet-activating factor (PAF), which is important for the differentiation of the cortex. The gene is located on chromosome 17p13.3.

The group of micro-lissencephalies can be divided into five different sub-groups, which differ clinically and on MRI (**Table 9.2**).

In **lissencephaly syndrome** (Miller–Dieker), in addition to autosomal inheritance, a micro-deletion is observed in the region of the short arm of chromosome 17. In addition to the brain malformation, there are further anomalies: high forehead, prominent occiput, slanting palpebral fissures, anteverted nostrils, corneal opacity, abnormally shaped ears, micrognathia, hirsutism, poly- and syndactyly, Simian crease, and heart defects. Affected children show little developmental progress. In addition to growth retardation and recurrent infections, they have cerebral seizures in the case of hypsarrhythmia. Microcephaly is observed in utero. MRI should provide a diagnosis.

#### ■ Poly-microgyria

The proliferation of the gyri gives the brain a cauliflower-like appearance. The changes are often localised (poikilogyria, e.g. in dysgenetic areas; **Fig. 9.28**). The differentiation of the cortex is altered, the white matter is hypo-plastic. Impaired neuroblastoma migration results in movement disorders, mental retardation and seizures.

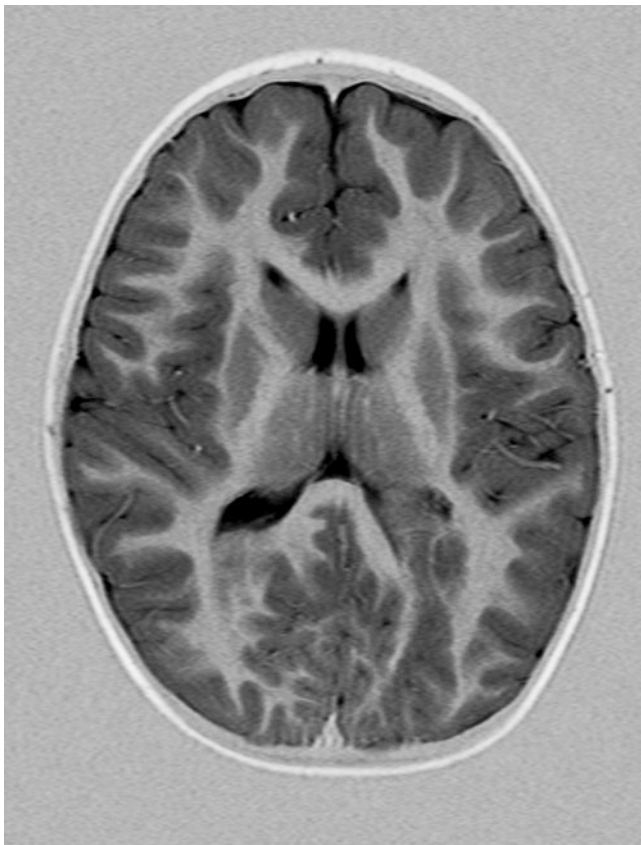
#### ■ Hemimegalencephaly

Hemimegalencephaly is a complex and relatively uncommon disorder of neuronal proliferation, migration, and organisation. This is a hamartomatous change in one hemisphere that can affect the entire hemisphere or part of it. Hemimegalencephaly may be associated with hemihypertrophy of the body, but can also occur in isolation.

**Medical Imaging.** It is usually an enlargement of a hemisphere or part of the hemisphere. The cortex is usually dysplastic: there is often pachygyria or agyria in the affected area.

**Table 9.2** Grouping of the micro-lissencephalies

Group classification	Characteristic presentation
Group 1	Uncomplicated pregnancy and birth, microcephaly with a few broad gyri, cortex itself is not dysplastic
Group 2	Complicated birth, microcephaly with a few broad gyri, cortex itself is not dysplastic, often delays in myelination
Group 3	Uncomplicated pregnancy and birth, fewer and broader gyri than in groups 1 and 2, often associated with heterotopia and arachnoid cysts
Group 4	Pre-natal problems, often poly-hydramnios, jejunal atresia and arthrogyriposis multiplex
Group 5	Most severe form, massive microcephaly, maximum of five gyri per hemisphere, cortex with thinned appearance



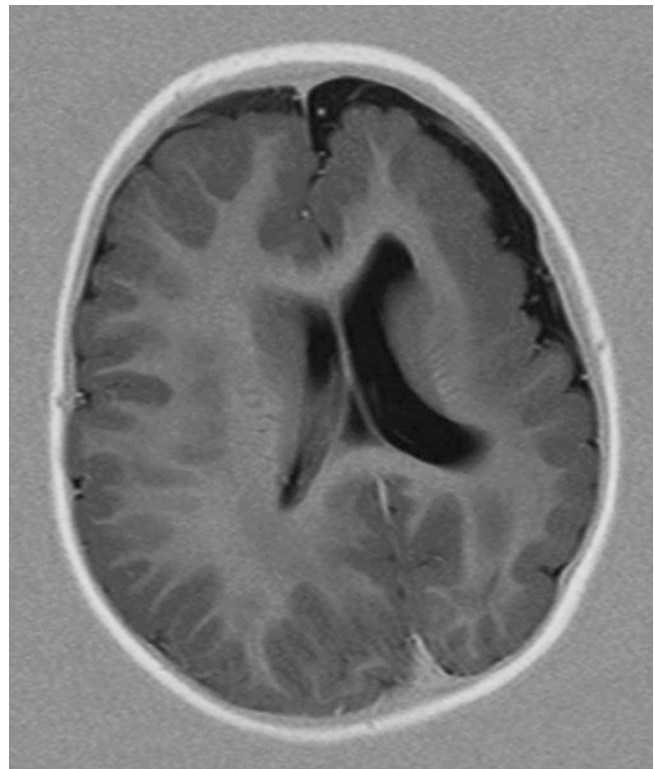
■ **Fig. 9.28 Poly-microgyria.** Occipitally, the small and smallest gyri appear on the axial T1-weighted imaging

#### ■ Cortical Dysplasia

With the help of MRI **circumscribed differential aberrations of the cerebral cortex** (abnormalities of cortical development) can be detected (■ Fig. 9.29), which can be responsible not only for cerebral seizures (approximately 25% in the case of partial seizures), but also for development and performance deficits. Because of the morphology, different forms are differentiated (focal or laminar dysplasias, heterotopias). In addition to the cortex, medullary structures are also affected; neuronal proliferation and cortical organisation can be affected. With improved diagnostics, such anomalies are more frequently detected so that the causes of many cryptogenic epilepsies or developmental abnormalities can be clarified.

Focal cortical dysplasia with and without balloon cells can be distinguished from each other. Histopathologically, it is possible to distinguish between dysplasia of the cortex architecture with ectopic neurons in the white matter, and dysplasia of the cyto-architecture of the cortex with enlarged neurons and Taylor dysplasia, in which dysmorphic neurons and balloon cells are present.

In the case of trans-hemispheric cortical dysplasia, dysplastic cells are found along the entire length between the sub-ependymal germinal matrix zone and the cortex. Histology reveals atypical neurons and glial cells. The histological findings correspond to those of tuberous sclerosis, which is why focal trans-hemispheric, cortical dysplasia is sometimes also referred to as an abortive form of tuberous sclerosis.



■ **Fig. 9.29 Cortical dysplasia, heterotopia.** On the axial T1-weighted inversion-recovery recording, a band-like signal change in the medulla layer appears in addition to a thickening of the cortex and a gyration disturbance with simultaneous cystic enlargement of the lateral ventricle

**Medical imaging.** The MRI reveals dysplasia, which extends from the sub-ependymal ventricular surface to the cortex and usually has a linear or funicular configuration. The adjacent cortex is generally also dysplastic. Compared with the surrounding white matter on T2-weighted sequences and fluid-attenuated inversion recovery (FLAIR) images, the dysplasia is hyper-intense. The transition between the grey and white matter appears blurred.

#### ■ Cobblestone Lissencephaly

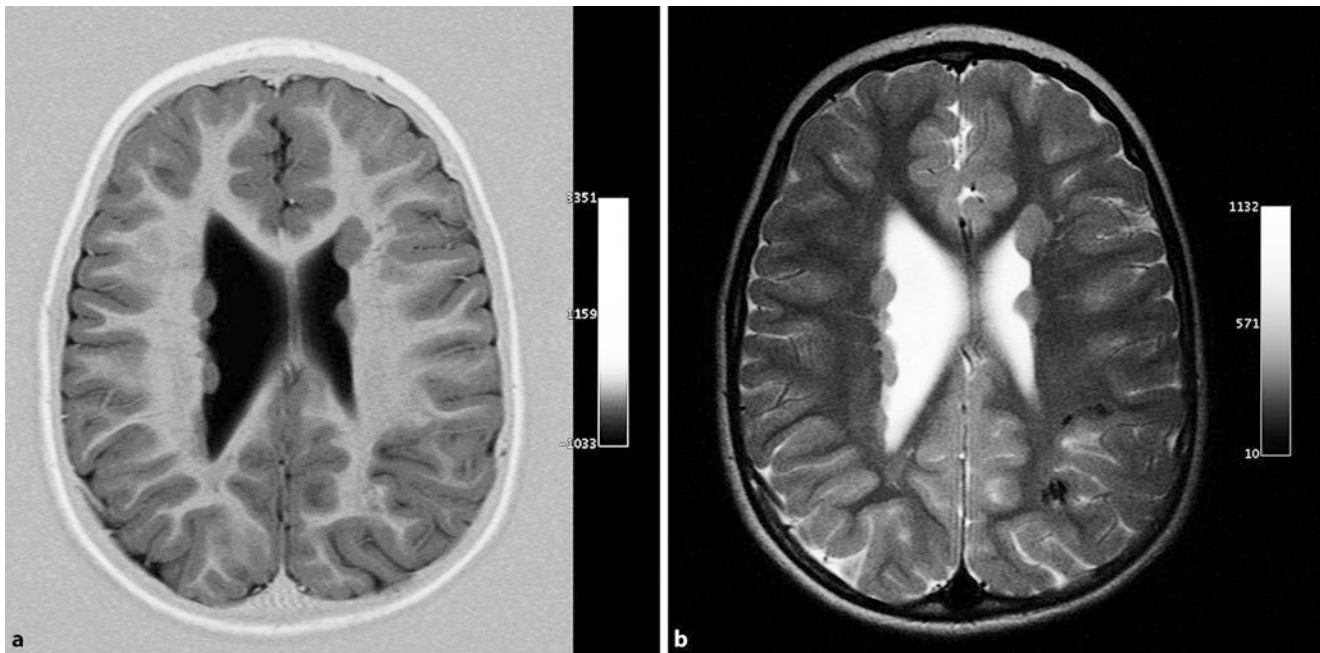
Cobblestone lissencephaly is associated with congenital muscular dystrophy. The absence of certain proteins leads to a migration disorder. This group of diseases includes Walker–Warburg syndrome, Fukuyama congenital muscular dystrophy and muscle–eye–brain disease.

#### ■ Heterotopia

##### ■ Sub-ependymal and Focal–Sub-cortical Heterotopia

Heterotopia is the classic disorder of neuronal migration. This involves scattered grey matter; because of an arrest of neural migration on their way from the sub-ependymal germinal matrix zone, the neurons remain on the surface of the brain. A distinction is made between sub-ependymal and focal–sub-cortical heterotopia:

- In sub-ependymal heterotopia, the neurons remain directly in the germinal matrix zone
- In focal–sub-cortical heterotopia, the neurons can be found between the ventricular surface and the cortex



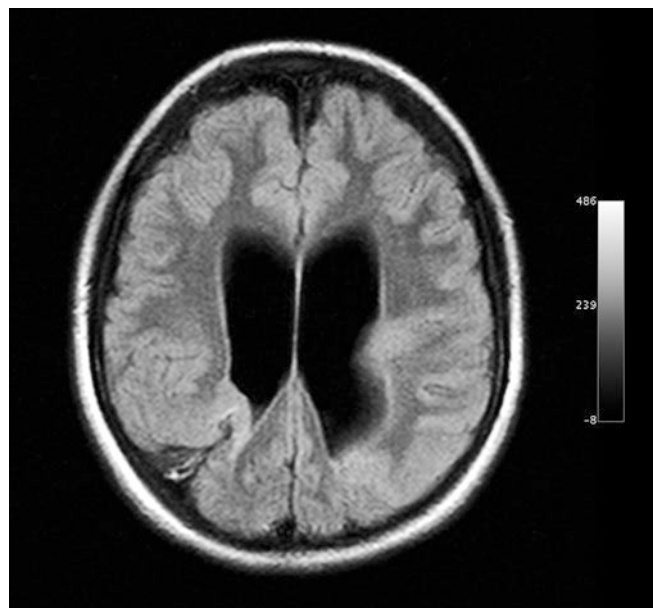
■ Fig. 9.30a,b Sub-ependymal heterotopia. In all weightings (a T1-weighting with the inversion-recovery technique b T2-weighting) nodular, sub-ependymal heterotopia of grey matter appears, iso-intense to the cortex

► A third form, the so-called ribbon-like heterotopia, in which the grey matter is sessile and ribbon-like within the white matter, has recently been counted among the lissencephalies

**Clinically,** patients with heterotopia often display epileptic seizures and developmental delay. Heterotopia is often associated with other malformations, e.g. cortical dysplasias, pachygyria and poly-microgyria. A sub-set of sub-ependymal heterotopia displays an X-linked or autosomal recessive inheritance. The most important differential diagnosis with sub-ependymal heterotopia is tuberous sclerosis. In the case of focal-sub-cortical heterotopia, neurons have migrated towards the cortex surface, but remain within the white matter. It may occur singly or multiply. The corresponding cortical ribbon is usually dysplastic or thinned.

**Medical Imaging.** Sub-ependymal heterotopia is directly periventricular, adjacent to the ventricular ependyma (■ Fig. 9.30). On all sequences, sub-ependymal nodular heterotopia is depicted as isointense signalling in the grey matter.

With regard to differential diagnosis, they are distinguished from tubers in tuberous sclerosis. Focal sub-cortical heterotopia is directly sub-cortical, within the white matter. It may occur singly or multiply. Focal sub-cortical heterotopias are frequently associated with other congenital malformations of the brain. The overlying cortex is often dysplastic. The ribbon-like heterotopias are included in the lissencephaly complex.



■ Fig. 9.31 Schizencephaly. The axial FLAIR images reveal a right parieto-occipital cleft that connects the inner and outer sub-arachnoid cavities. The entire length of the cleft is lined with grey matter

### 9.2.6 Schizencephaly, Porencephaly, Hemi-atrophy

**Structural defects in the hemispheres** are a result of a developmental disorder or vascular occlusion. In the case of schizencephaly the symmetrical poria is predominantly situated parieto-temporally (■ Fig. 9.31). They range from the cortex to the ventricle and are surrounded by poly-microgyria. Seizures may occur. Schizencephaly may remain unnoticed.

### ■ Schizencephaly

The cleft formations are divided into so-called open- and closed-end clefts (**open- and closed-lip schizencephaly**). In open-lip schizencephaly, the ventricular system directly communicates with the outer sub-arachnoid cavities via the cleft. In the case of closed-lip schizencephaly, clefts lined with grey matter touch each other.

The MRI reveals that in schizencephaly, the cleft formation is lined in grey matter. However, the adjacent cortical structures show dysplasia. Closed-lip schizencephaly is often recognised by a focal extension of the lateral ventricular wall towards the cleft. The various forms of schizencephaly are often associated with an absence of the septum pellucidum.

### ■ Porencephaly

Porencephaly (■ Fig. 9.32) refers to a lesion that has occurred as a result of circulatory disorders (vascular anomalies, embolism, and thrombosis) in utero and has led to a parenchymal decay. These pori are irregularly arranged. Depending on their development, they mainly display irregular wells, especially in the FLAIR sequences.

### ■ Hemi-atrophy

The lesion of an entire half of the brain (cerebral hemi-atrophy) is mostly due to prenatal circulatory disorders. It results in cranial asymmetries, spastic hemiplegia with growth retardation and frequent cerebral seizures in addition to learning and performance difficulties.

## 9.2.7 Holoprosencephaly

In close relation to the pre-chordal mesoderm, developmental disorders of the fore-brain (between the 4th and 6th gestational weeks) also lead to **facial anomalies**:

- Cyclopia
- Ethmocephaly with hypo-telorism
- Median cleft lip, jaw and palate

The causes are heterogeneous; monogenic inheritance may occur (autosomal recessive and dominant or a chromosome aberration of trisomy D, deletion of 18t and 13q), but exogenous factors must also be taken into consideration (viral infection, maternal diabetes and dioxin). There are several **forms of holoprosencephaly**:

- Alobar holoprosencephaly
- Semi-lobar holoprosencephaly
- Lobar holoprosencephaly

**Alobar holoprosencephaly** is the most severe disorder. Life expectancy is significantly reduced; affected children are often stillborn. In the case of alobar holoprosencephaly, there is no differentiation between the hemispheres. A holoventricle, which merges into a large, dorsally located cyst, can be found. The lateral ventricles are not separated.

In the **semi-lobar holoprosencephaly** the hemispheres are typically fused in the anterior region. The splenium of the corpus



■ Fig. 9.32 Porencephaly. Right frontal defect following partial infarction in the area supplied by the middle cerebral artery (T2-weighted sequence)

callosum is found in the posterior region; it is missing in the anterior region. The extent of the absence of the corpus callosum collides with the severity of the clinical disorder. Semi-lobar holoprosencephaly is the only congenital disorder in which the anterior portions of the corpus callosum are missing; the posterior portions, however, are present.

The **lobar form** of holoprosencephaly involves the absence of the septum pellucidum. The anterior horns of the lateral ventricles are usually created rudimentarily, the third ventricle is properly developed. To some extent, transitions to septo-optic dysplasia are blurred.

## 9.2.8 Developmental Disorders of the Cerebellum and Brain Stem

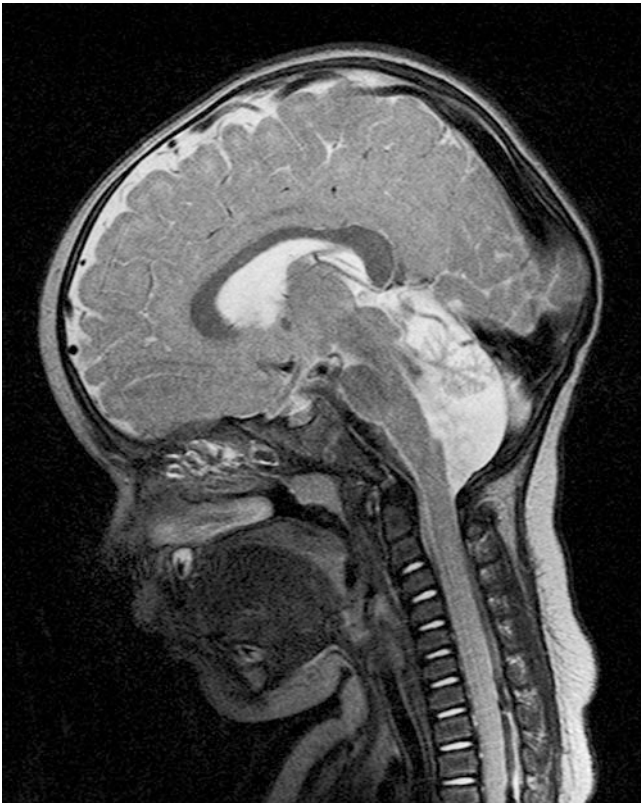
### ■ Cerebellar Agenesis and Hypoplasia

The cerebellum is rarely completely absent. There are usually developmental disorders of individual parts, the hemispheres, or medially situated structures (cerebellar vermis). With MRI, the posterior fossa can be well depicted, and anomalies can be distinguished from variants (enlargement of the cisterna magna).

Clinically, the symptoms are often very mild, even when findings are pronounced, which indicates the good compensatory capacity of the cerebellar system.

Hypoplasia of a cerebellar hemisphere is associated with a prenatal lesion or a malformation in the contra-lateral hemisphere. Various anomalies of the cerebellum are familiar and lead to non-progressive heredo-ataxia. A progressive cerebellar atrophy is typical of congenital disorder of glycosylation (CDG) syndrome (■ Fig. 9.33).





■ Fig. 9.33 Congenital disorder of glycosylation (CDG) syndrome. On the sagittal T2-weighted sequences, the typical cerebellar hypoplasia of this rare metabolic disease can be seen

#### ■ Chiari Anomalies

In the context of a dysraphic disorder, changes in the cerebellum and brain-stem with delocalisation and deformation may occur and are often accompanied by occlusive hydrocephalus.

In the case of **type I Chiari malformation**, symmetric or asymmetric displacements of the cerebellar tonsils into the foramen magnum can be seen (■ Fig. 9.34). The cause is usually hypoplasia of the posterior fossa. Additional malformations, such as block vertebrae and cranio-vertebral abnormalities, can be found. The **clinical symptoms** may be relatively non-specific. In addition to headaches, compression of the caudal cranial nerves may occur. Disturbances in the circulation of CSF may also arise. In patients with Chiari malformation, the entire neural axis should always be investigated (syringo-hydromyelia).

**Medical Imaging.** To evaluate a Chiari malformation, sagittal thin-slice scans should be performed. The cerebellar tonsils should not be more than 5 mm below a line connecting the basion and opisthion.

In the case of a **type II Chiari malformation** (■ Fig. 9.35), parts of the cerebellar vermis may shift to the spinal canal. In addition, this malformation is associated with spina bifida and myelomeningocele. The small posterior fossa results in the steep position of the tentorium. At the junction of the medulla oblongata to the cervical spinal cord, a bayonet-shaped bend (kinking) of the brain-stem is formed. The cerebellar hemispheres wrap around the brain-stem and can be detected in the foramen magnum. The



■ Fig. 9.34 Chiari I malformation. Depression of the cerebellar tonsils and hypoplasia of the posterior fossa (sagittal T2-weighting)

fourth ventricle is narrow and compressed. The quadrigeminal plate may often change its shape (beaking). This can lead to cranial nerve disorders and autonomic dysregulation.

Pressure changes in the cranial fossa often lead to a disturbance in CSF circulation, which manifests as a non-communicating hydrocephalus.

A type II Chiari malformation is often associated with supratentorial malformations (corpus callosal agenesis, hypogenesis). The cerebral falx is often not fully formed, thus resulting in a mesh of sulci and gyri of the two hemispheres (interdigitations). The gyri of the medial occipital lobe are often too numerous and too delicate (stenogyria).

In the case of a **type III Chiari malformation**, there is an extra-cranial shift of the cerebellum into a sub-occipital-cervical rupture; the signs encountered in a **type IV malformation** resemble those of cerebellar hypoplasia.

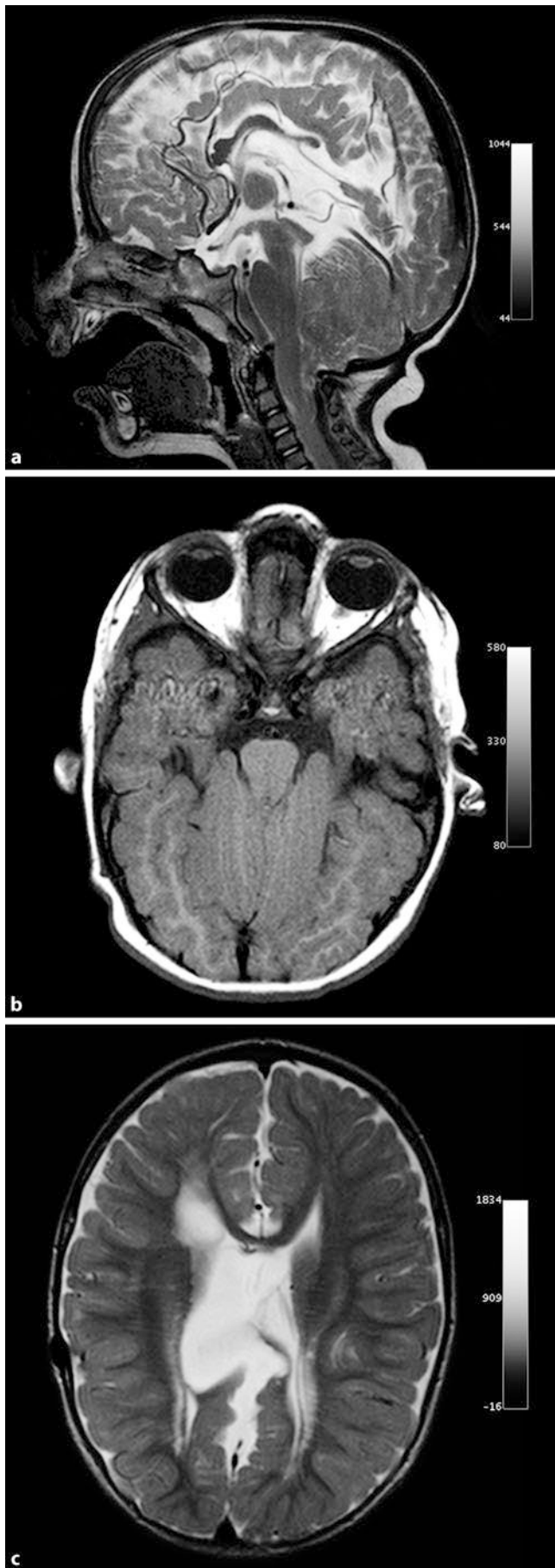
❗ **An important differential diagnosis of Chiari malformation is CSF hypotension syndrome in the case of a leakage.**

#### ■ Dandy-Walker Syndrome

The hallmark for the syndrome is partial or complete vermian agenesis, which is why the roof of the fourth ventricle is defective and cystically modified (ventriculocoele). The posterior cranial fossa can thus be greatly expanded; the tentorium and the torcula are high (■ Fig. 9.36). Even if the apertures of the fourth ventricle are not closed, hydrocephalus is usually caused by a developmental disorder of the sub-arachnoid cavity. Additional cerebral malformations may occur. **Clinical symptoms** include projecting occipital scales, cranial nerve disorder, nystagmus and truncal ataxia in addition to spastic symptoms.

Generally, **three groups** can be distinguished:

- Dandy-Walker malformation
- Dandy-Walker variants
- Mega cisterna magna



The transitions among these groups are fluid and not always clearly separable. In the Dandy–Walker variant, there is a reduction in the volume of the vermis with concurrent cystic dilatation of the fourth ventricle. However, the posterior fossa is not enlarged.

Mega cisterna magna involves enlargement of the posterior fossa without evidence of a cystic malformation of the fourth ventricle. Only the cisterna magna is enlarged and cystically expanded. The fourth ventricle and the cerebellar vermis are not pathologically altered in these disorders.

#### ■ Joubert Syndrome

This is a complete or partial vermian agenesis without cystic expansion of the fourth ventricle. Joubert syndrome may entail an autosomal recessive mode of inheritance. It is accompanied by attacks of hyperpnoea, abnormal eye movements (opsoclonus), ataxia and mental retardation.

**Medical Imaging.** On MRI, the axial layers reveal vermian hypoplasia and the resulting directly overlapping cerebellar hemispheres in the caudal portion. By configuring the frail mid-brain and cerebellar peduncle, the fourth ventricle has a bat-like configuration.

#### ■ Rhombencephalic Synapsis

In the case of rhombencephalic synapsis, the two hemispheres of the cerebellum are not completely separated from each other (■ Fig. 9.37). The vermis is often completely missing. In addition, there are usually other malformations, such as a missing septum pellucidum or cortical abnormalities.

### 9.2.9 Arachnoid Cysts

#### ■ Definition

Arachnoid cysts are fluid-filled cavities in the meninges or below the arachnoids (sub-arachnoid cysts) (■ Fig. 9.38). They may be associated with structural changes of adjacent brain areas and are connected with the CSF system. True congenital arachnoid cysts are surrounded by two layers of the arachnoid.

The walls of sub-arachnoid cysts also contain components of the pia mater and neural tissue. A distinction must be made among intra-cerebral cysts, pori and cystic tumours.

#### ■ Epidemiology, Aetiology

In autopsy studies, arachnoid cysts are found in 1 in 1,000 cases. As a congenital abnormality, arachnoid cysts probably arise in the first weeks of pregnancy. In some cases, a familial occurrence is observed. As acquired abnormalities, arachnoid cysts may be the result of inflammation, trauma, or bleeding.

←  
 ■ Fig. 9.35a–c Type II Chiari malformation. a Deep approach of the tentorium in the case of a small posterior cranial fossa, depression of the cerebellar tonsils on the T2-weighted image. b On the axial T1-weighted images, the cerebellar tonsils laterally encompass the brain-stem. c Additional supratentorial malformation with corpus callosal dysplasia. The spinal meningocele, which also belongs to the Chiari malformation, is not depicted

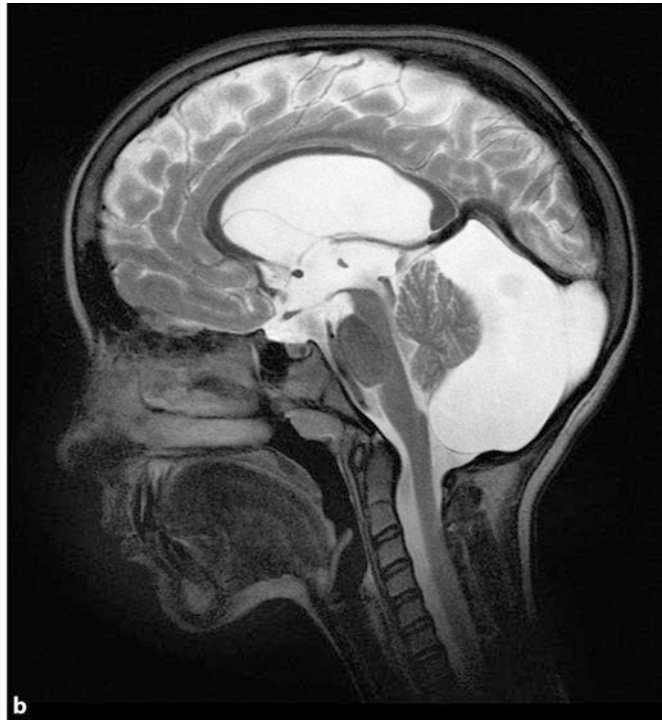
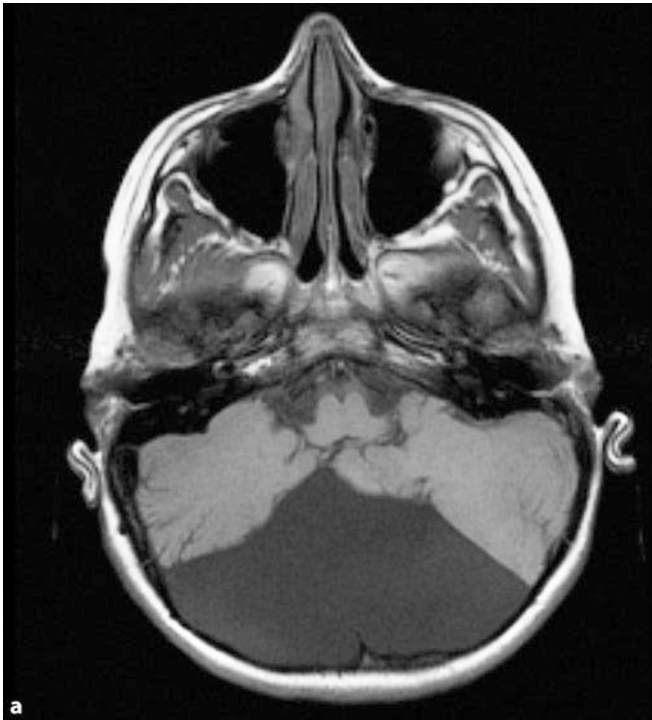


**Fig. 9.36a,b** Dandy–Walker malformation. **a** Cystic malformation of the posterior cranial fossa with upright confluence of sinuses on the axial T1-

weighted sequences. **b** In addition, hypogenesis of the cerebellar vermis is shown on the sagittal T2-weighted image

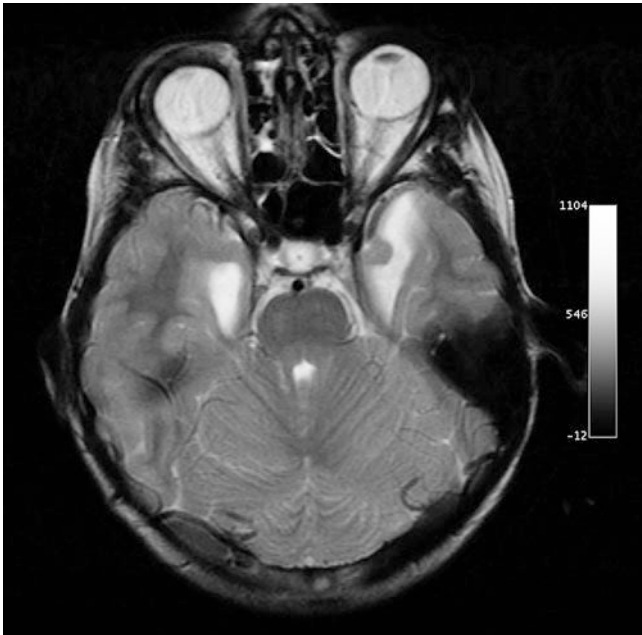


**Fig. 9.37** Rhombencephalic synapsis. On the axial T2-weighted sequence, this fusion of the two cerebellar hemispheres can be clearly recognised.

The cells of the cyst wall can secrete liquid, which can lead to an increase in size if a connection to the sub-arachnoid cavity is missing.

#### ■ ■ Symptoms

Arachnoid cysts remain clinically asymptomatic and are often an incidental finding. Occasionally, they may cause symptoms such as CSF circulation disorders with headache, papilloedema,

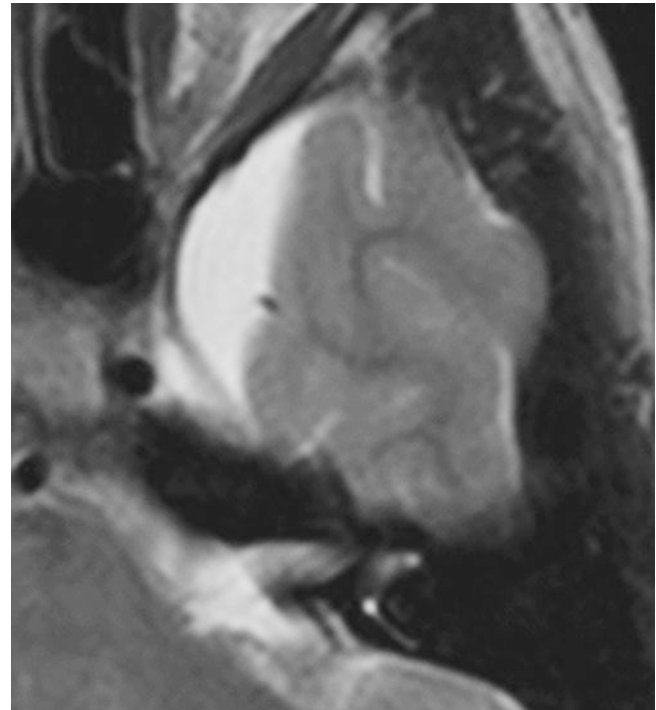


**Fig. 9.38** Arachnoid cysts. Temporo-mesially located mass isointense to CSF, which is typical of an arachnoid cyst

vomiting and character change. In infants, accelerated cranial growth will usually occur.

#### ■ ■ Medical Imaging

On CT and MRI, arachnoid cysts are usually easy to recognise. In the case of superficially located arachnoid cysts, there is often

a thinning of the cranial vault. Cystic tumours, schizencephalies, sub-dural haematoma (SDH), Dandy–Walker syndrome, and a large cisterna magna should all be differentiated via differential diagnosis.

Arachnoid cysts are mainly situated in the inter-hemispheric fissure, temporally, in the basal cisterns, or in the posterior fossa.

### 9.2.10 Neuro-cutaneous Syndromes (Phakomatoses)

Neuro-cutaneous syndromes or phakomatoses refer to a heterogeneous group of genetic diseases that are characterised by dysplasia and in particular neuro-ectodermal tissue. In recent years, the underlying genetic defects could be clarified for a number of these diseases. This results in an enhanced pathogenic understanding and prospects for new therapeutic approaches. In addition to the diseases listed here, the neuro-cutaneous syndromes include a number of rare disorders that are beyond the scope of this book. These can be found in special textbooks.

#### ■ Type I Neurofibromatosis

##### ■ ■ Definition, Epidemiology

Autosomal-dominant type I neurofibromatosis (NF-I), also referred to as peripheral neurofibromatosis von Recklinghausen's disease, occurs with a frequency of approximately 0.3 in 1,000. There are no regional or sex differences. It is one of the most common hereditary diseases. The spectrum and severity of the findings typical of the disease are extremely variable and not predictable in individual cases. This can complicate the consultation and care of affected patients.

##### ■ ■ Aetiology

The disease is caused by a mutation of the *NF-I* gene, which was identified in 1990 and localised to chromosome 17q11.2. Half of the cases of NF-I can be traced to spontaneous mutations. This encodes a tumour suppressor protein, which has multiple influences on cell proliferation and differentiation.

##### ■ ■ Symptoms

The characteristic feature of NF-I are circumscribed, café-au-lait-like hyperpigmentation of the skin with a diameter of 0.5 to 5 cm. These **café-au-lait spots** can be detected in almost 100% of affected patients during the first presentation. Café-au-lait spots may occur even without the context of NF-I; however, more than six of these benign lesions likely indicates neurofibromatosis. The patches may already be present at birth and increase in size and number during childhood. In 40% of patients, a freckle-like pigmentation occurs in the armpits and groin.

**Neurofibromas** are benign tumours of the peripheral nerve connective tissue that develop in almost all NF-I patients throughout the course of their lives. There are two main forms of differences:

- Plexiform neurofibromas, extending from major visceral nerve fibres, they can lead to the displacement of adjacent organs and significant cosmetic disfigurement. This type of tumour is highly specific to NF-I and occurs congenitally

or in infancy and early childhood. In about 5% of cases, neurofibrosarcomas develop from plexiform neurofibromas and malignant schwannomas.

- Dermal neurofibromatoma, on the other hand, are rarely diagnosed before the age of 5 and are small, tumours that frequently occur in large numbers. They arise from the terminal branches of the cutaneous nerves.

The most frequent intra-cerebral tumours are **optic gliomas**, which mostly occur in early childhood and in approximately 15% of all NF-I patients. Bilateral occurrence is almost exclusively observed in association with NF-I; in approximately 70% of cases, unilateral optic gliomas are associated with NF-I. These tumours do not usually cause any clinical symptoms. Because optic gliomas rarely show a progressive course and spontaneous regression has been described in some cases, no specific treatment is necessary in the case of asymptomatic tumours.

The pathognomonic findings of NF-I include the so-called **Lisch nodules**. These are iris haematomas that have a diameter of 1–2 mm. Lisch nodules increase in number with increasing age and are found in 100% of adult patients with NF-I.

**Primary bone lesions** are another feature of NF-I. Scoliosis is found in 10% of patients and typically starts between the ages of 6 and 10. Additional characteristic bone defects are sphenoid wing dysplasia, congenital pseudo-arthritis of the tibia, and early childhood curvature of the long bones. Other frequent findings include short stature, macrocephaly, cerebral seizures and frequently occurring circulatory disorders that arise because of circumscribed cellular hyper-proliferation on the vascular wall.

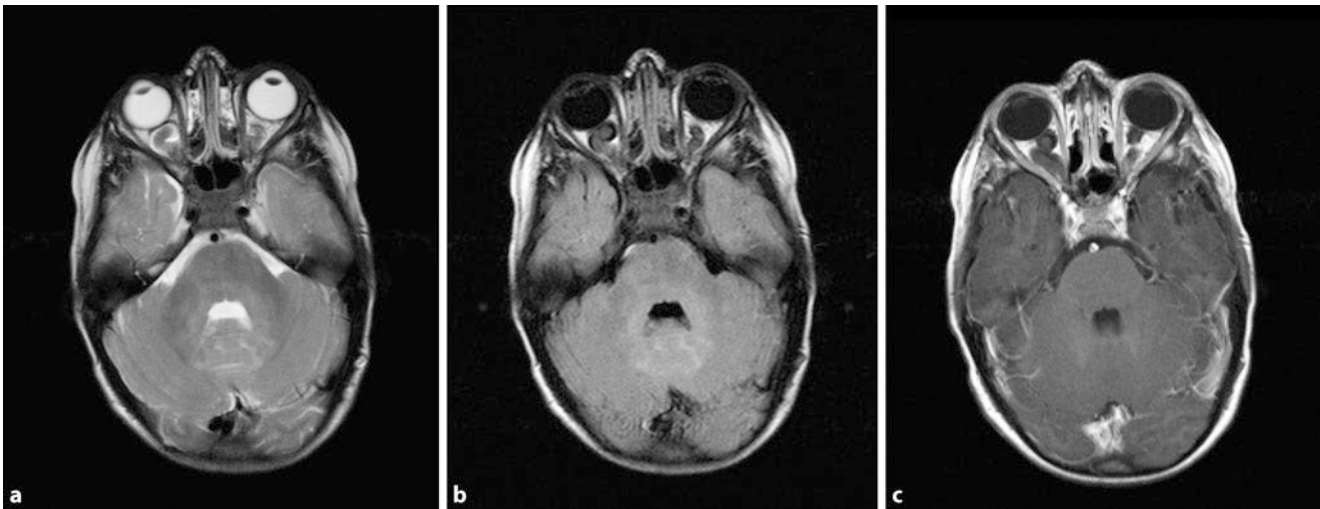
On **MRI findings** of the parenchyma of NF-I patients, focal hyper-intensities are frequently revealed in the basal ganglia, brain-stem and cerebellum, which most closely corresponds to myelin vacuolation (■ Figs. 9.39, 9.40). These transient findings are more frequently found in children aged under 15. In older adults, they are only found in 30% of cases.

##### ■ ■ Diagnosis

A diagnosis can be made if at least two of the following internationally defined NF-I diagnostic criteria are met.

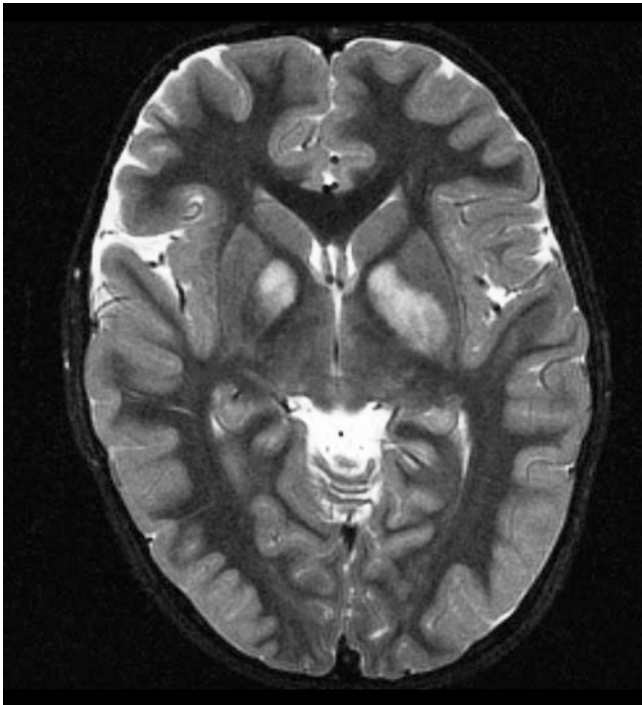
#### NF-I Diagnostic Criteria

- Six or more café-au-lait spots with a diameter more than 5 mm in pre-pubertal patients and greater than 15 mm in post-pubertal patients
- Two or more neurofibromas of any type or at least one plexiform neurofibroma
- Freckle-like pigmentation of the armpits or groin
- Optic nerve glioma
- Lisch nodules (iris hamartomas)
- Typical bone lesions, such as sphenoid wing dysplasia or curvature of the long bones with or without pseudo-arthritis
- A first-degree relative (parent, sibling or child) with a diagnosis of NF-I based on the above criteria



■ **Fig. 9.39a–c** Type I neurofibromatosis (NF-I). **a, b** On the T2-weighted and FLAIR images, there are signal increases at the typical location for the fourth ventricle, which are consistent with myelin vacuolation. In addition, thickened

and elongated optic nerves appear with extended neural sheathes. **c** On the T1-weighted image, after the administration of contrast agent, no pathological contrast enhancement can be seen



■ **Fig. 9.40** Myelin vacuolation. Typical myelin vacuolation in the basal ganglia in a patient with NF-I

### ■ ■ Medical Imaging

In patients with a clinical suspicion of a type I neurofibromatosis, T2- and T1-weighted sequences, a FLAIR sequence of the entire neuro-cranium, and a FLAIR sequence of the anterior visual pathway should be performed. In addition, T1-weighted images should be carried out before and after the administration of contrast agent. The orientation should be customised to the shape of the optic nerve and optic chiasm.

In **children** with type I neurofibromatosis, the T2-weighted and FLAIR sequences often reveal multiple, relatively low in-

creases in signal intensity in the medulla. On the T1-weighted sequences, these lesions do not usually appear. For these medullary lesions, the term **myelin vacuoles** is frequently used, although this is not actually correct from a histopathological perspective. These are probably small areas with dysplasia of the myelin. In adults, this myelin vacuolation is only found in approximately 30% of cases. They likely have no clinical relevance.

In children with type I neurofibromatosis, various types of **tumours** frequently arise, especially gliomas of the anterior visual pathway (▶ Sect. 9.4). Histopathologically, these optic gliomas are pilocytic astrocytomas (WHO grade I). However, highly malignant gliomas of the anterior visual pathway may occur. After the administration of contrast agent, the optic glioma often shows pronounced enhancement, especially in the area of the optic nerve and the chiasma and, in some cases, also the optic tracts.

In addition to the optic gliomas, intra-cerebral astrocytomas frequently occur. They can be of any histological grade; WHO grade I pilocytic astrocytomas, however, are particularly widespread (■ Fig. 9.83). In patients with NF-I, these astrocytomas mainly occur in the area of the pons, the medulla oblongata, and the mid-brain, but also in the region of the cerebellar hemispheres.

Because frequent **vascular changes** occur, a depiction of the intra- and extra-cranial vessels should be obtained via MRI.

Fibrous dysplasia, especially at the sphenoid bone, also occur frequently and may lead to a pressure effect on the orbital cavity with resultant proptosis or optic atrophy.

The typical characteristic of NF-I is the presence of **neurofibromas**. These are tumours of the nerve sheath. On MRI of the neural axis, neurofibromas are usually revealed intra- or paraspinally. These can be nodular tumours of the cauda equina or be situated intra-foraminally. Intra-foraminal neurofibromas can lead to an expansion of the affected neuroforamen. If this neurofibroma reaches intra- and extra-spinally, this results in an hourglass configuration.

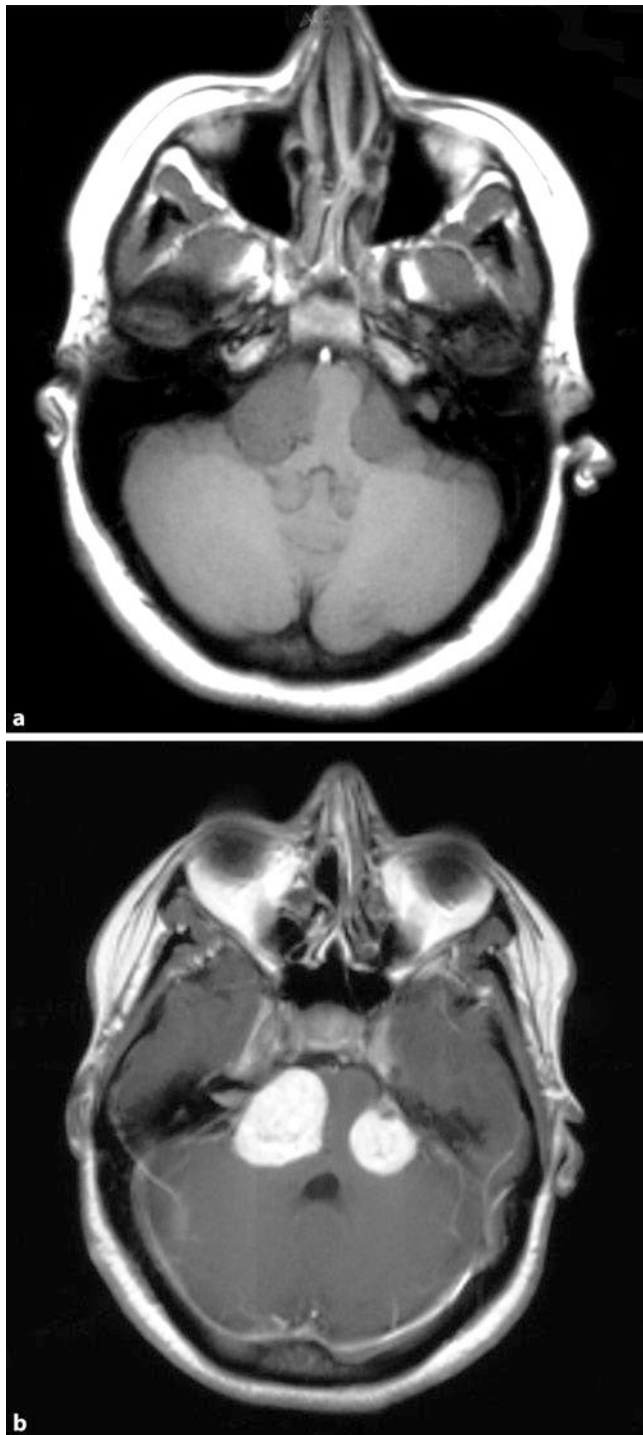


**Fig. 9.41 a,b** Type II neurofibromatosis (NF-II). Bilateral vestibular schwannoma as a typical example of NF-II. **a** T1-weighted image before the administration of contrast agent. **b** T1-weighted image after the administration of contrast agent with strong enhancement

On MRI T1-weighted sequences, the neurofibromas appear hyper-intense. On the T2-weighted sequences, their signal intensity is variable. After the intra-venous administration of contrast agent, there is usually a significant enhancement of the neurofibromas. Particularly in a paravertebral location, fat-suppressed T1-weighted sequences can be helpful following the administration of contrast agents.

▶ Unlike neurofibromas, *neurosarcomas* are usually larger and often blurred. The internal structure is often heterogeneous, but there is no reliable criterion that can provide a reliable differentiation of a neurofibroma from a neurofibrosarcoma. If in doubt, surgical removal or biopsy should be performed.

**Plexiform neurofibromas** consist of simple neurofibromas. They usually spread diffusely along a nerve; as a rule, the original nerve can no longer be distinguished. They grow locally and aggressively, but do not metastasise. On MRI, they usually appear as flat-growing infiltrative space-occupying lesions. On the T1-weighted sequences, they are slightly hyper-intense; after the administration of contrast agent, there is focal, heterogeneous enhancement. On the T2-weighted sequences, they appear relatively hyper-intense.

Neurofibromatosis-I frequently results in **spinal malformations**. Dysplasia of the vertebral body often appears, which can lead to scoliosis, usually involving dextroscoliosis.

Patients with NF-I additionally show dural ectasia and lateral meningoceles.

#### ■ Type II Neurofibromatosis

##### ■ ■ Definition, Epidemiology, Aetiology

Type II neurofibromatosis (NF-II) – or central neurofibromatosis – differs clinically and genetically from NF-I. It occurs with an incidence of approximately 1 in 30,000 and is therefore much less common than NF-I. Here, a mutation of the *NF II* gene could also be localised to chromosome 22 q11.2. The mutation is autosomal-dominantly inherited. In half of the cases, it can be traced to a spontaneous mutation. The altered protein is involved in the control of cell shape, cell motility, and cell-to-cell communication.

##### ■ ■ Symptoms

NF II is a disease of adolescents and young adults; only 10% of patients display symptoms before the age of 10. The clinical variability is not nearly as large as it is for NF-I. The typical finding, which affects more than 80% of patients, is **bilateral tumours in the eighth cranial nerve** (■ Figs. 9.41, 9.86). These tumours consist almost exclusively of Schwann cells, which extend from the vestibular portion of the nerve. The term **vestibular schwannoma** is therefore preferable to the previously designated term, acoustic neuroma, which is still frequently used.

##### ■ ■ Symptoms

The vestibular schwannomas manifest as progressive hearing loss or deafness in addition to vertigo and tinnitus. If the facial and trigeminal nerves are impaired, muscle weakness and sensory loss can occur in the facial area.

In NF-II, schwannomas may occur in other nerves or the spinal roots. If sub-cutaneous peripheral nerves are affected, these schwannomas can look clinically like dermal neurofibromas in the case of NF-I.

Approximately 40% of patients exhibit **meningiomas** in the course of the disease, which can also occur multiple times. In addition, an accumulation of various other intra-cranial tumours

can be observed. Café-au-lait spots appear more frequently in NF-II than in the general population. However, the occurrence of more than six of these hyper-pigmentations is rare in the case of NF-II.

**Posterior sub-capsular cataracts** can be found in nearly half of the patients. They usually appear as early as childhood and may be crucial to the diagnosis. Hamartomas of the retina are also frequently observed in NF-II.

### ■ ■ Diagnosis

Clinical criteria that can be used to make a diagnosis are listed below.

#### NF-II Diagnostic Criteria

A diagnosis of NF-II may be made if the criteria for points I or point II are met:

- I. CT or MRI evidence of bilateral tumours of the eighth cranial nerve or
- II. A first-degree relative with a confirmed diagnosis of NF-II and either
  - a) A unilateral tumour of the eighth cranial nerve or
  - b) two of the following findings:
    - Neurofibroma
    - Meningioma
    - Glioma
    - Schwannoma
    - Juvenile posterior sub-capsular cataract

On suspicion of NF II, a thorough ophthalmological and ear, nose and throat (ENT) examination in addition to a cranial MRI should be performed. The children of affected parents should be examined physically, neurologically and ophthalmologically at yearly intervals. Annual audiometric examinations are recommended between the ages of 10 and 30. However, a normal cranial MRI at the age of 30 years makes a diagnosis of NF-II very unlikely.

**Medical Imaging.** In NF-II, T2-weighted and FLAIR sequences through the entire neuro-cranium should be performed in addition to axial T1-weighted sequences before and after the administration of contrast agent and axial thin-slice sequences through the cerebello-pontine angle. If there is a suspicion of small intra-meatally located vestibular schwannoma, additional T2-weighted sequences or a CISS sequence may be helpful.

In the case of a NF-II, intra-cranial tumours are indistinguishable from spontaneously occurring tumours. The combination of the tumours suggests a diagnosis of NF-II. In bilateral vestibular schwannomas, the diagnosis of NF-II should be made, even without the presence of other tumours. The existence of other tumours should nevertheless still be considered. The entire neuraxis should therefore be investigated because intra-spinal and para-spinal schwannomas may occur.

### ■ ■ Tuberos Sclerosis

#### ■ ■ Definition, Epidemiology

Tuberous sclerosis was previously called Bourneville–Pringle disease and more recently, tuberous sclerosis complex (TSC). Along with the neurofibromatosis, this disease belongs to the most common neuro-cutaneous syndromes. Tuberous sclerosis has an incidence of 1 in 20,000. In half the cases, an autosomal dominant mode of inheritance can be detected. The cases of the TSC disease can be attributed to new mutations. So far, two different gene loci have been identified: the TSC 1 gene on chromosome 9q34 and the TSC 2 gene on chromosome 16p13.3.

#### ■ ■ Symptoms

In addition to seizures and psychomotor retardation, hypopigmented patches of skin (white spots) may occur. They vary in size from a few millimetres to approximately 5 cm. In approximately 90% of cases these areas of hypopigmentation can occur as early as infancy. Facial angiofibromas usually occur before the age of three or four. These are small, symmetrical telangiectatic papules above the cheeks, naso-labial folds and chin. They represent hamartomatous malformations of the facial skin and were formerly referred to as adenoma sebaceum.

Sub- and peri-ungual fibromas are also among the characteristic findings. These disorders occur as gliomatous retinal tumours and cardiac rhabdomyomas. Renal involvement in the form of angiomyolipoma or renal cysts is also significant.

#### ■ ■ Diagnosis

The combination of a cerebral seizure disorder with macular hypopigmentation of the skin should suggest the presence of tuberous sclerosis. The diagnosis includes a dermatological and ophthalmological examination in addition to the implementation of a cranial MRI (■ Fig. 9.42). In these patients, FLAIR and T1- and T2-weighted axial sequences should be carried out. For the assessment of sub-ependymal tubers of the lateral wall of the ventricles, it is helpful to run coronary T1-weighted sequences before and after the administration of contrast agent.

Focal dysplasia of the cerebral cortex, the so-called **tuber**, is pathognomonic for the disease. This involves hard and noticeable white lesions ranging from a few millimetres to a few centimetres in diameter. They are histologically characterised by the loss of normal cortical architecture, nerve cell death and astrogliosis. Similar glial nodules are found sub-ependymally in the lateral walls of the lateral ventricles. The number of tubers that can be detected via MRI seem to correlate with the severity of the disease. Malignant transformation of individual tubers has also been described.

On the T1-weighted sequences, tubers present as hypo-intense. On the T2-weighted and FLAIR sequences, they present as hyper-intense in the myelinated white matter. Tubers can also lie heterotopically to the cortical ribbon. Sub-ependymal nodules, small focal hamartomas in sub-ependymal position, appear as small nodular protrusions, which present as hypo-intensity on the T2-weighted sequences and slight hyperintensity on the T2-weighted sequence compared with the not yet myelinated white matter. With increasing age, sub-ependymal nodules tend to calcify; these calcifications often appear lumpy on CT and give rise to signal loss or void on the T2- and T2\*-weighted sequences.

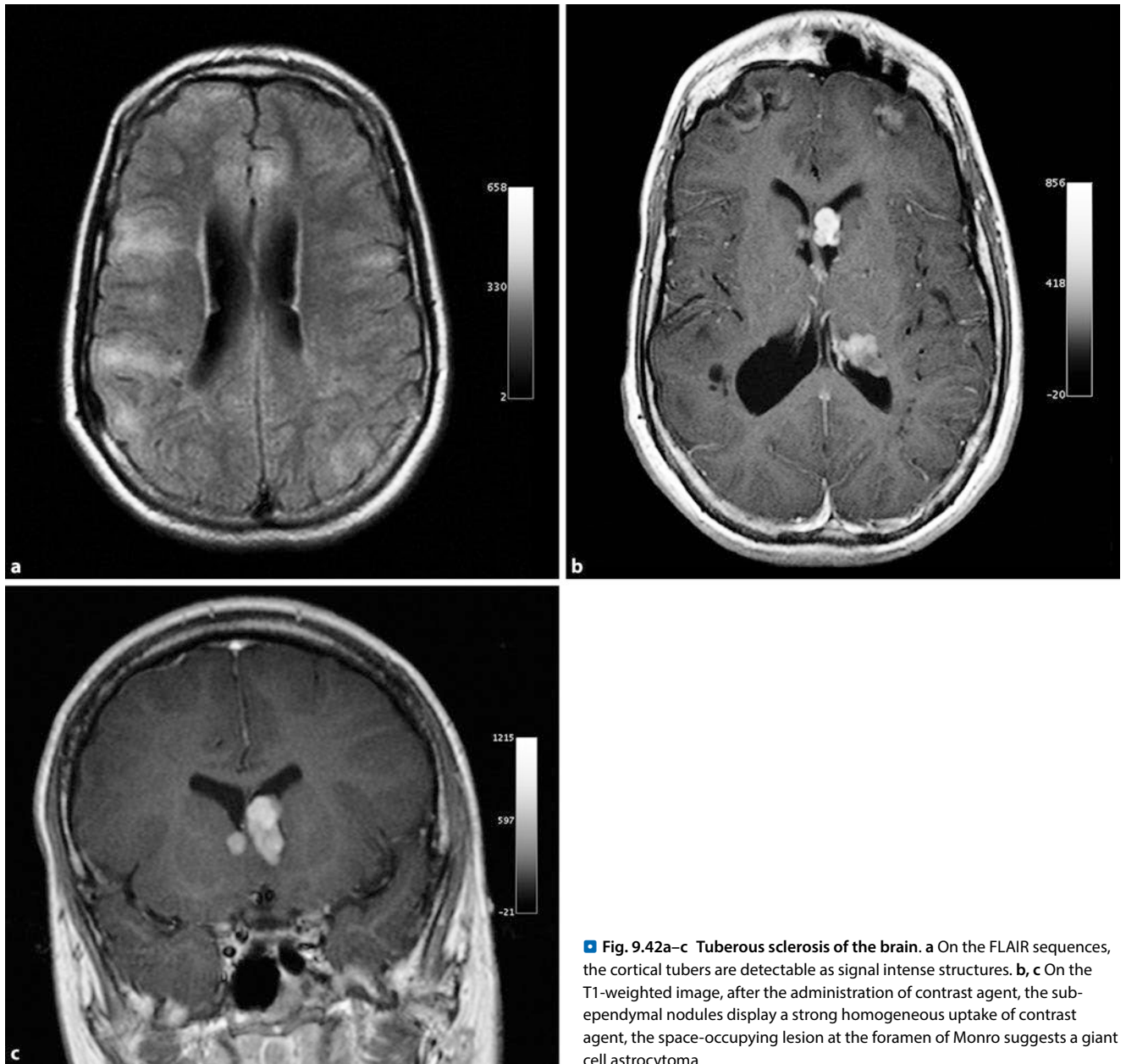


**Fig. 9.42a–c Tuberosclerosis of the brain.** **a** On the FLAIR sequences, the cortical tubers are detectable as signal intense structures. **b, c** On the T1-weighted image, after the administration of contrast agent, the subependymal nodules display a strong homogeneous uptake of contrast agent, the space-occupying lesion at the foramen of Monro suggests a giant cell astrocytoma

➤ **The most important differential diagnosis of sub-ependymal tubers is sub-ependymal heterotopia. On all sequences, heterotopia always displays iso-intense signal behaviour in the grey matter. Sub-ependymal nodules are not iso-intense to cortex on T2-weighted sequences.**

**Giant cell astrocytoma** arises when a sub-ependymal nodule indicates a clear growth trend in tuberosclerosis. Giant cell astrocytoma occurs in 10% of patients (■ Fig. 9.42). They are mostly situated in the area of the foramen of Monro and can lead to displacement of the foramen with a consequent pooling of CSF in the affected lateral ventricle. Giant cell astrocytoma generally displays displaced and non-invasive growth. In rare cases, however, degeneration to a higher-grade astrocytomas has been described. Giant cell astrocytomas exhibit marked enhancement after the administration of contrast agent. However, the uptake of

contrast agent is not a criterion for differentiation from uncomplicated sub-ependymal nodules. For the evaluation, particular attention should be paid to a size progression of a sub-ependymal hamartoma. However, as the preferred localisation of giant cell astrocytoma, the foramen of Monro should also be given special consideration. A sub-ependymal mass with a diameter greater than 12 mm and significant contrast enhancement is suggestive of a giant cell astrocytoma.

#### ■ **Sturge–Weber Syndrome** ■ **Definition, Epidemiology, Aetiology**

The syndrome is named after the British physicians William A. Sturge and Frederick Parkes Weber and is a meningo-facial angiomatosis with cerebral calcifications. The congenital disease usually occurs sporadically at a frequency of approximately 1 in 50,000. Some familial cases have also been reported; however,



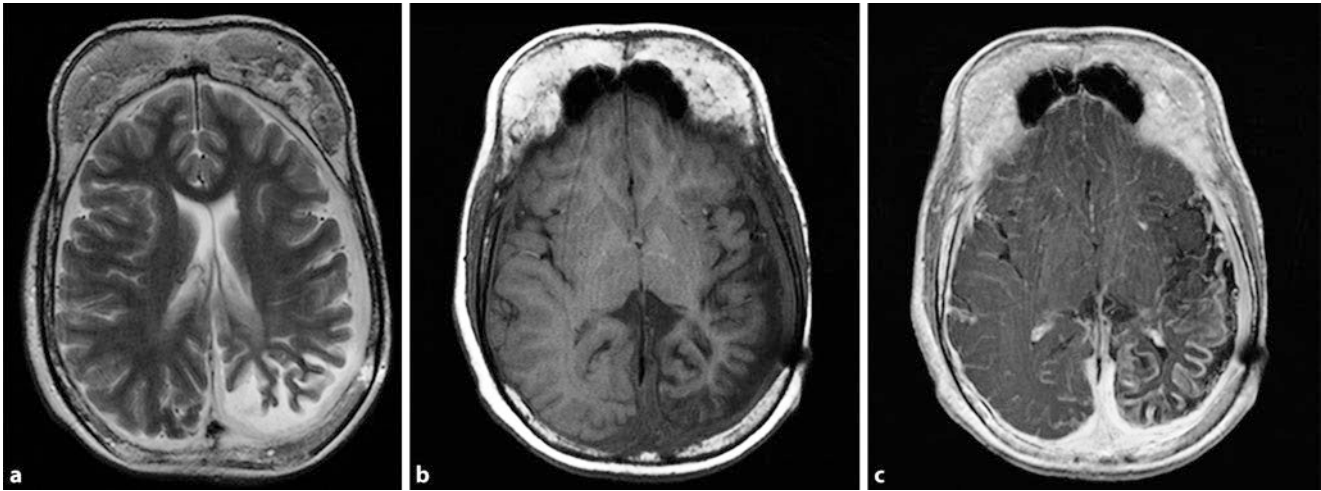


**Fig. 9.43a–c Sturge–Weber syndrome.** a The axial T2-weighted sequences and the T1-weighted sequences **b** before and **c** after the administration

of contrast agent reveal the extended pial angioma with adjacent cortical atrophy and distinct cortical enhancement with contrast agent

the mode of inheritance and the underlying genetic defect are unknown.

#### ■ ■ Symptoms

Typical for this disease is a naevus flammeus, ectasia of the superficial dermal vessels. It is suspected to be caused by a local loss of autonomous vascular innervation. The key changes are explained by embryonic venous vascular malformation of the cortex, which leads to hypoxic damage to the cortex on the one hand and the compensatory formation of lepto-meningeal vascular ectasia on the other. The anatomical proximity of the visual cortex, ocular system and cerebrum in the early embryonic period can explain the frequent co-occurrence of ocular and cerebral involvement.

The naevus flammeus usually occurs in the innervation area of the trigeminal nerve and is already present at birth. The expansion of the naevus is different, but always touches the area of the frontal branch of the trigeminal nerve. Likewise, the mucous membranes of the mouth, larynx, or pharynx may be also affected. An angiomatous change in the choroid is also frequently encountered and can lead to the development of glaucoma.

Seizures occur in approximately 80% of patients with Sturge–Weber syndrome. These usually begin in the first year of life and are thought to result from cerebral changes. Up to two thirds of patients exhibit mental retardation. Depending on the extent and localisation of cerebral participation, neurological disorders such as spastic hemiparesis and sensory deficits may occur in the further course.

#### ■ ■ Diagnostics

In the vast majority of cases, a naevus flammeus is an isolated anomaly. However, if the forehead and upper eyelid are also affected, Sturge–Weber syndrome should be considered, especially if seizures occur simultaneously.

**Medical Imaging.** In addition to an MRI examination, EEG and ophthalmological examinations should be performed. On MRI (■ Fig. 9.43), T2\*-weighted-sequences should be run in addition to T2-weighted, FLAIR and T1-weighted images before and after

the administration of contrast agent. On these sequences, the aforementioned calcifications appear as narrow, linear areas of hypointensity in the vicinity of the cortical ribbon. On the unenhanced sequences, there is often a magnification of the ipsilateral choroid plexus. In infants with an incompletely myelinated medulla, on the unenhanced T2-weighted sequences, an area of relative hypointensity often appears in the vicinity of the medullary layer, which is directly adjacent to the angioma. On MRI T2-weighted sequences, pial angiomas generally appear as areas of hypointensity. After the administration of contrast agent, a linear and sometimes planar enhancement can be seen.

The cerebral calcifications, usually calcified cortex and sub-cortical medulla, are best seen on T2-weighted sequences or CT. Most reveal an atrophy in the affected area. A hypo-atrophy of the choroid plexus occurs laterally to the angioma and often displays a stronger enhancement. This is explained by an increased return via the choroid plexus. Choroid angiomas can be detected via enhancement of contrast agent at the anterior wall of the bulb. In these patients, pneumosinus dilatans (i.e. an above-normal continuous expansion of the frontal sinus) can often be observed. The cranial vault adjoining the angioma often also exhibits thickening.

## 9.3 Vascular Diseases

### 9.3.1 Intra-cerebral Vascular Malformations

Intra-cerebral vascular malformations include:

- Abnormalities of the vein of Galen
- Arterio-venous malformations (AVM)
- Cavernomas
- Dural arterio-venous fistulas
- Capillary telangiectasias
- Venous system variants, developmental venous anomalies (DVA)

Although some familial vascular malformations are described, the vast majority occur spontaneously.

### ■ Classification of Vascular Malformations in the Different Age Groups

The various vascular malformations can be symptomatic at different ages. The timing and type of therapy depend inter alia on the age of the patients. In this section, patients are divided into the following age groups:

- Foetal period
- Neonatal period (up to 30 days)
- Children up to 2 years
- Older children up to the age of 18
- Adults

#### ■ ■ Foetal Period

In the foetal period, precautionary ultrasound examinations increasingly reveal cerebral lesions or cysts in addition to vascular malformations such as malformations to the vein of Galen and dural sinus. This often appears as a macrocrania on ultrasound or foetal MR examinations.

Macrocrania can be demonstrated in both a vein of Galen malformation (VGAM) and in a dural sinus malformation (DSM). Proof of encephalomalacia has a significant impact on the diagnosis and prognosis, regardless of the type of AVM. Cardiomegaly is also associated with a poorer prognosis.

#### ■ ■ Neonatal Period

At this age, there is a fundamental difference between a vein of Galen malformation and other AVMs, especially pial AVMs.

Early-onset neurological symptoms in **vein of Galen malformations** usually indicate a poor prognosis. Further treatment depends on the extent of the neurological symptoms. If no therapy is initiated, a vein of Galen malformation leads to multi-organ failure and extended cerebral lesions within days or weeks. In the case of a vein of Galen malformation, seizures often indicate ischaemic brain lesions. Vein of Galen malformations usually rapidly lead to heart failure because the dural veins provide no resistance. However, on the other hand, this protects the brain from a retrograde venous congestion.

In pial AVMs, seizures are a first indication of venous ischaemia or focal haemorrhaging. In these patients, prompt treatment should be carried out in order to prevent further damage to the cerebral parenchyma. In vein of Galen malformations, haemorrhaging rarely occurs in this age group.

#### ■ ■ Children up to 2 Years

In this age group, the venous system is not yet fully formed. Pachioni's granulations are also not yet fully developed; it is even believed that increased pressure results in delayed maturation. First signs of water retention manifest as **macrocrania without ventriculomegaly**. Clinical consequences are usually neurocognitive delays without direct correlation with the degree of increase in head circumference. If the expansion of the sutures and enlargement of the head circumference is too low compared with the intra-cranial pressure increase, this leads to a transependymal resorption of CSF.

In pial AVMs, pial or sub-arachnoid venous congestion often arises; in vein of Galen malformations, this occurs quite late – if at all. In the case of AVMs, this local venous stasis leads to

ischaemia, which may manifest as seizures and haemorrhaging. Diffuse venous congestion by a constriction of venous outflow conditions can also lead to direct damage to the cerebral parenchyma. Adequate treatment can stop the progression of these symptoms.

#### ■ ■ Children up to 18 Years

In this age group, cardiac symptoms are very rare. Vascular malformations are usually only symptomatic when it comes to compression of the mesencephalon and the aqueduct with a consecutive hydrocephalus. Venous thrombosis can occur as part of the “high-flow angiopathy” phenomenon.

#### ■ ■ Adults

In the case of atypically located bleeding in young adults, vascular malformation must always be considered as the cause, and adequate diagnostic measures must be carried out.

#### ■ Vein of Galen Malformations

Vein of Galen malformations are relatively rare. These involve congenital connections between the intra-cranial arteries, usually the thalamo-perforating artery, the choroidal arteries, and the anterior cerebral artery to the vein of Galen or with primitive mid-line veins. Vein of Galen malformations can directly represent fistula connections or a number of smaller connections. The cause of these abnormal connections is unknown. In some cases, a venous abnormality with a missing straight sinus and a persistent falcine or occipital sinus has been observed. Intra-uterine thrombosis of the straight sinus with recanalisation is therefore considered to be the cause. It could be shown that the dilated venous structure involves the persistent prosencephalic vein of Markowski. In addition, an association with certain cardiovascular abnormalities, usually with a co-arcuation of the aortic arch and atrial septal defects could be demonstrated.

There are **two large groups of** vein of Galen malformations:

- Choroidal malformations
- Mural malformations

**Choroidal Malformations.** About 90% of vein of Galen malformations are choroidal malformations. This involves an arteriovenous connection between the front wall of the prosencephalic vein, which is supplied by a number of choroidal, pericallosal and thalamo-perforating vessels. New-borns typically display cardiomegaly with symptoms of heart failure. Choroidal malformations have a very poor prognosis and often a fatal outcome if not treated adequately.

**Mural Malformation.** Mural malformation is characterised by a few (usually between one and four) vigorously strong connections of the prosencephalic veins, which are fed from the posterior choroidal artery. Patients with a mural malformation of the vein of Galen show delayed development, hydrocephalus and seizures. However, there are only mild or no signs of heart failure. The vascular malformations can be approached with an endovascular treatment, i.e. with occlusion of the anastomoses. Mural malformations frequently have a good outcome with a low rate of morbidity.

### ■ ■ Symptoms

According to the clinical symptoms, three categories can be formed:

1. New-borns with heart failure and intra-cranial noises
2. New-borns with hydrocephalus and/or seizures
3. Older children or young adults

The patients of group 1 typically have choroidal malformations, while the patients in groups 2 and 3 will usually display mural malformations of the vein of Galen.

### ■ ■ Medical Imaging

Because of the **pre-natal ultrasound examinations** usually performed, many vein of Galen malformations are diagnosed in utero. On the prenatal ultrasound, a large hypoechoic mass appears, which has a very strong flow in the Doppler investigation. If such a diagnosis is made, an interventional neuroradiologist who is familiar with the disease image should be consulted immediately. If the new-born displays signs of heart failure that cannot be dealt with medication, they should be treated immediately after birth or within the first few days of life. On the post-natal ultrasound investigations, a vein of Galen malformation shows a hypoechoic to low echogenic structure in the median, which may sometimes shift the front portion of the third ventricle.

► **It is important to detect continuity with the straight sinus.**

**Doppler studies** provide information about the flow velocity of the AVM. On CT, the varix node presents as unenhanced iso- to hyper-density in the cerebral parenchyma. A certain hyper-density can be found in the case of thrombosis within the malformation. The cerebral parenchyma often displays density losses that are caused by secondary ischaemia or the onset of encephalomalacia. On the other hand, hyper-dense areas could indicate haemorrhaging or dystrophic calcifications in the parenchyma. The effects of a brain injury should be carefully analysed. Before the therapy, the parents should be informed of possible neurodevelopmental delays.

On **MRI** the malformation usually appears hypo-intense because of the signal loss caused by the rapid flow in the AVM (■ Fig. 9.44). The afferent vessels may be detected as thin hypointensity, which leads to the varix node.

On the T1-weighted sequences, acute thromboses within the AVM are iso-intense to the cerebral parenchyma. On the T2-weighted sequences, they are hypo-intense. On the T1- and T2-weighted sequences, sub-acute thromboses display an increase in signal. At this age, lesions of the cerebral parenchyma can be difficult to prove on T2-weighted sequences. T1-weighted sequences are more suitable for this purpose.

### ■ ■ Treatment

If possible, heart failure should be treated before treatment of the AVM. It has been found that new-borns with heart failure have a mortality rate of up to 90%. Afterwards, interventional neuro-radiological treatment should be carried out with the aim of closing the fistulae. Alternatively, there is the possibility of surgical ligation of the short-circuit connections – however, this

has led to somewhat poorer results. The vein of Galen malformation can be treated interventionally/neuroradiologically via a trans-arterial or trans-venous aditus. In up to 100% of cases, the definitive curative treatment is possible with the less frequently occurring type of mural vein of Galen malformations.

### ■ Cavernomas

#### ■ ■ Definition, Epidemiology, Aetiology

Cavernous malformations or cavernomas (formerly cavernous haemangiomas) typically show a sinusoidal, spherical aspect of the vessels. Cavernomas occur in approximately 0.5–1% of the population. A genetic pre-disposition is assumed. Multiple cavernomas are frequently encountered. In these cases, they are associated with a familial pre-disposition. The genetic defect is located on chromosome 7q. In cases of familial occurrence, multiple cavernomas occur in 50% of cases, whereas in sporadic cases, the incidence of multiple cavernomas is 13%.

#### ■ ■ Pathology, Histology

Patho-anatomically, cavernomas involve livid blue, bulging cavities that are lined with endothelia. Various old, partly hyalinised thrombi are also frequently seen in specimens. No cerebral tissue is found between the cavity tissue, and the surrounding cerebral parenchyma often displays gliosis. Cavernomas have a very slow circulation; arterio-venous shunts are normally not found. The incoming arteries and draining veins, therefore, have a normal size. Venous malformations and capillary telangiectasia are often found in addition to cavernomas. This results in the assumption that a venous hypertension of obstructed effluent veins of the malformation causes the corresponding changes in the venous vessels.

#### ■ ■ Symptoms

The clinical appearance is highly variable. Approximately 10–20% of patients are asymptomatic, the cavernoma is only randomly discovered. Approximately 30–50% of patients have seizures, although it is unclear whether the haemosiderin margin depicts the epileptogenic focus as recurrent haemorrhaging. Most cavernomas are, however, only symptomatic in the third to fourth decades of life. Approximately 20% of patients with a cavernoma suffer from intra-cranial haemorrhaging. In the pre-natal period, the incidence of haemorrhaging is estimated to be 0.25–0.7%, which is significantly lower than in the case of AVM.

#### ■ ■ Medical Imaging

On **CT**, if they are not masked by fresh haemorrhaging, cavernomas appear as heterogeneous round foci that accumulate little contrast medium and often have stippled calcifications. The highest sensitivity in the detection of cavernomas is afforded by **MRI**. The signal behaviour of the lesion is determined by the mixture of blood at different decomposition levels and flow rates, intrinsic calcifications and reactive changes in the adjacent parenchyma. On T1- and T2-weighted sequences, most cavernomas are hyperintense at the centre and hypo-intense at the margins, with a rim containing haemosiderin. The centre of the cavernomas may exhibit heterogeneous signal behaviour, which is mainly because of the different flow conditions and the degree of calcification and thrombosis.

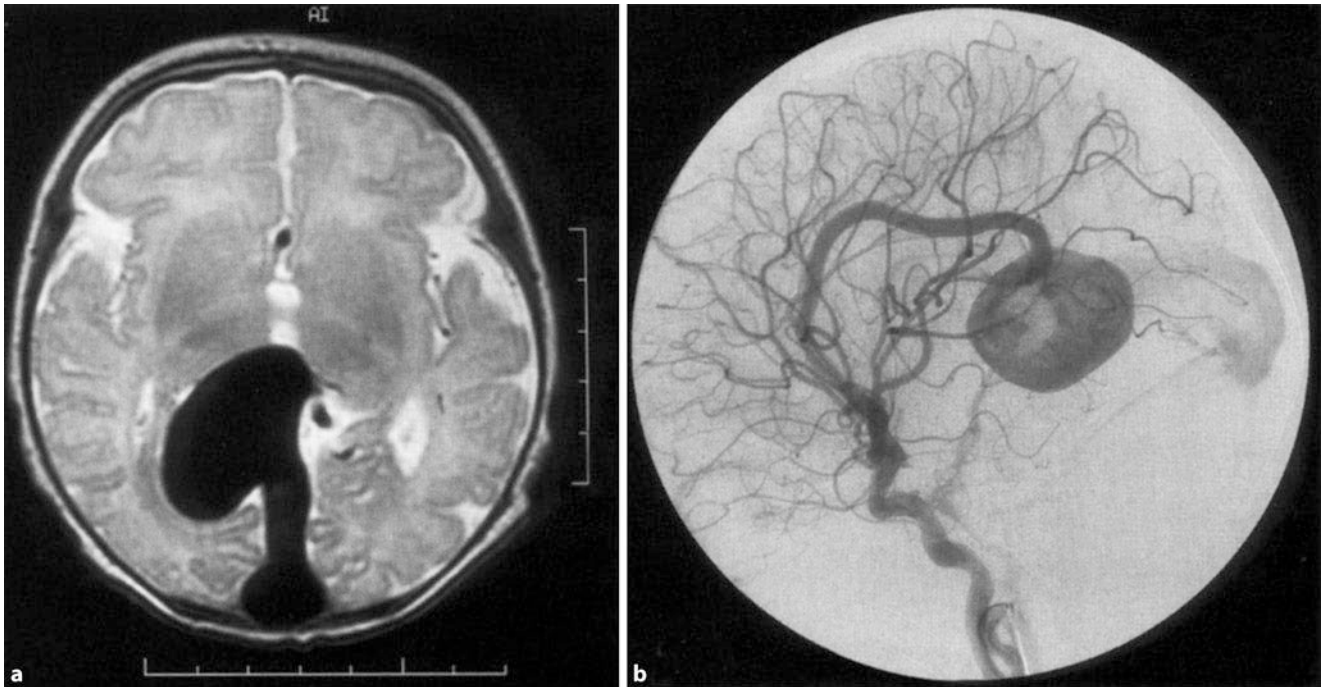


**Fig. 9.44a,b Vein of Galen malformation.** A 13-month-old infant with a suspected vein of Galen malformation. **a** On the T2-weighted images, a hypo-intense area corresponding to a signal void is presented in projection to the superior sagittal sinus. The remaining cerebral parenchyma

corresponds to age. **b** Lateral projection of digital subtraction angiography (DSA) depicts the massively expanded posterior choroidal artery and the fistula connection in the venous pouch. (From: *Radiologe* 2003, 43:936, Fig. 1 b, d)

The presence of other small cavernomas can be assessed with gradient echo sequences, which are very sensitive to haemosiderin and calcifications (■ Fig. 9.45). In some cases, difficult differential diagnosis of thrombosed aneurysm, an older haematoma, or haemorrhaging in the tumour may be difficult. About 20% of the lesions identifiable on MRI exhibit an associated vascular malformation, AVM, or often a DVA. Because this may affect the treatment, it is recommended that patients who have suffered cavernous haemorrhaging undergo pre-operative angiography. On the angiography itself, the cavernomas are not detectable, which can be used as a diagnostic criterion.

### Cavernous Haemangioma

- Sinusoidal pathological condition, spherical aspect of endothelial line, dilated vessels; no normal brain parenchyma within the lesion; haemorrhaging detectable at different ages
- Localisation: 80% supra-tentorial, but can occur in any localisation, 50–80% multiple
- Incidence: in the normal population, this is approximately 0.5–1%, a genetic predisposition is assumed, multiple cavernomas are frequently encountered and are then associated with a familial predisposition. The genetic defect is located on chromosome 7q
- Clinical symptoms: seizures, focal neurological deficits, headaches
- Risk of haemorrhaging: 0.25–0.7%/year and cavernoma

### ■ ■ Treatment

Superficially located cavernomas can be operated on with a low rate of mortality and morbidity. Surgery is normally only advised if there are uncontrollable seizures emanating from the cavernoma or if there has been recurrent haemorrhaging. Asymptomatic cavernomas without evidence of haemorrhaging do not have to be treated.

### ■ Capillary Telangiectasias

#### ■ ■ Definition

Capillary telangiectasias are probably variants of a capillary malformation and are mainly localised in the brain-stem. This is a collection of dilated capillaries that are separated by normal brain parenchyma. Haemorrhaging is generally rare and usually only found by chance during autopsies.

#### ■ ■ Medical Imaging

On CT, capillary telangiectasias are usually not visible. On MRI, increased signal intensity appears on T2-weighted sequences. On T1-weighted sequences, capillary telangiectasias are usually iso- or hypointense. After the administration of contrast agent, a dull, sometimes finely flecked area of contrast enhancement can typically be seen. On gradient echo sequences, there is often marked hypo-intensity, probably because of the slow flow with deoxygenated blood in the vessels. The combination of poor detectability on the turbo spin-echo sequences and clearer visibility on the gradient-echo sequence in addition to the increase in contrast agent is typical of capillary telangiectasia (■ Fig. 9.46).

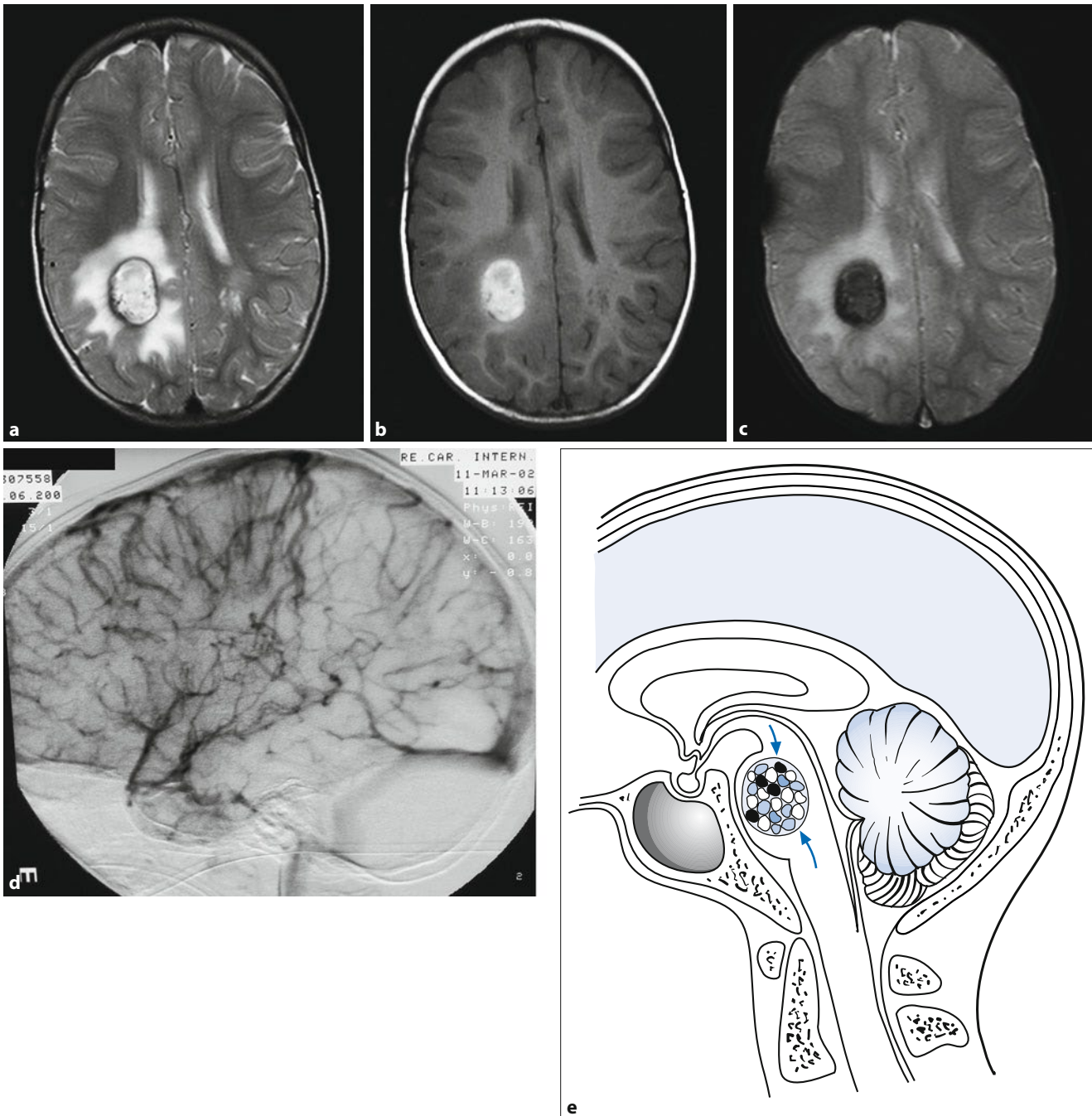


**Fig. 9.45a–e Cavernoma.** **a** On the T2-weighted sequences a space-occupying lesion with peri-focal finger-shaped oedema appears above the right trigone. The lesion has a hypo-intense rim and is heterogeneously hyper-intense in the centre. **b** On the T1-weighted sequences, before the administration of contrast agent, the portions of the space-occupying lesion that were hyperintense on the T2-weighted sequences also appear hyper-intense with

a T1 shortening. After the administration of contrast agent (not shown) there is no significant additional enhancement. **c** On the T2<sup>w</sup>-weighted sequences, the lesion is predominantly depicted as hypo-intense with slightly hyper-intense peri-focal oedema. **d** DSA. **e** Schematic representation of a cavernoma in the area of the pons with multiple enclosed blood break-down products. The *arrows* indicate the hemosiderin/ferritin rim

➤ **Capillary telangiectasias are likely harmless incidental findings. The rare reports of inter-cerebral haemorrhaging are likely attributable to associated cavernomas.**

#### Capillary Telangiectasias

- Pathology: collection of dilated capillaries, which are separated by normal brain parenchyma
- Localisation: particularly in the pons, cerebellum and spinal cord, but can occur anywhere
- Risk of haemorrhaging: very low if any at all

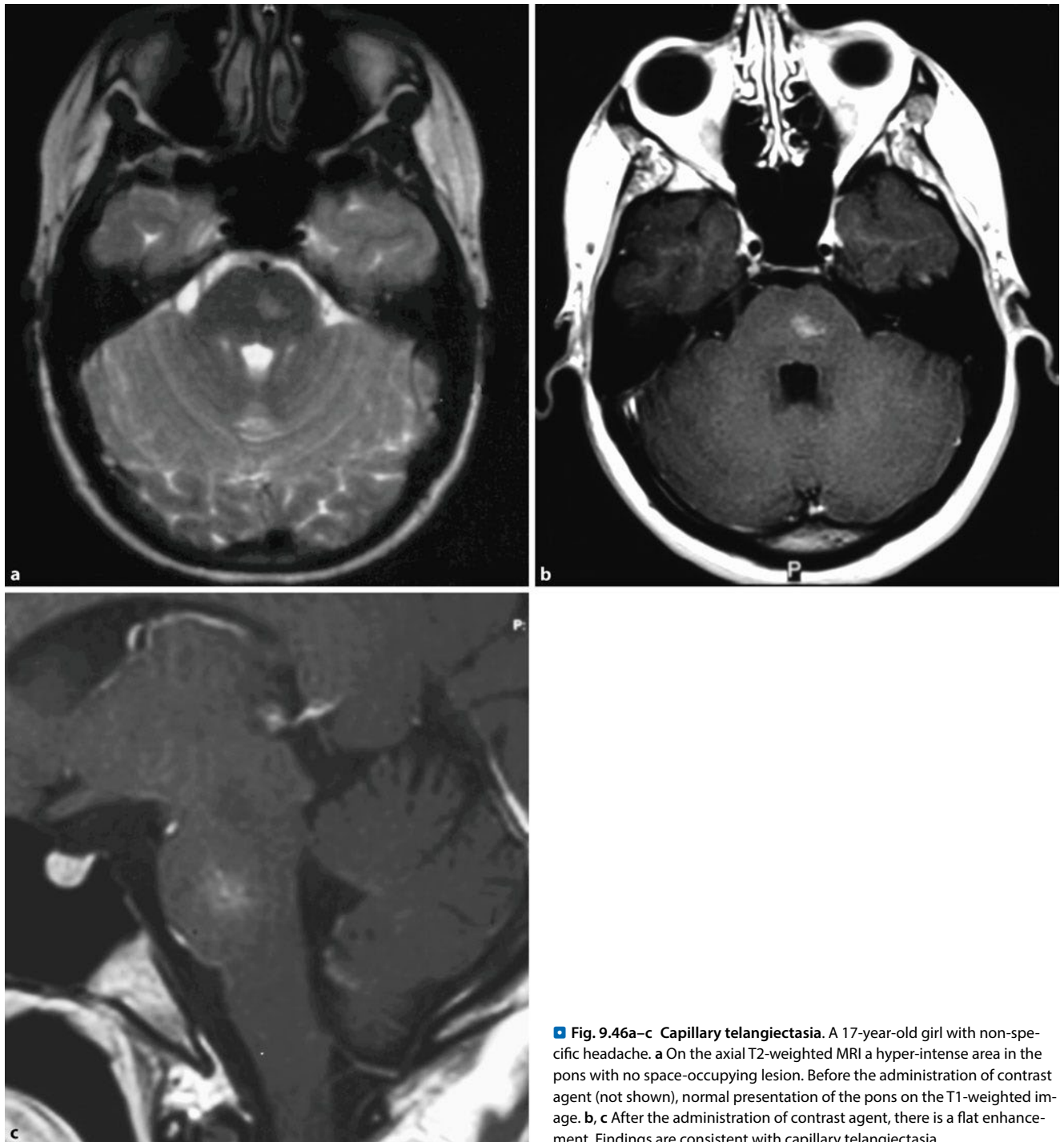


**Fig. 9.46a–c Capillary telangiectasia.** A 17-year-old girl with non-specific headache. **a** On the axial T2-weighted MRI a hyper-intense area in the pons with no space-occupying lesion. Before the administration of contrast agent (not shown), normal presentation of the pons on the T1-weighted image. **b, c** After the administration of contrast agent, there is a flat enhancement. Findings are consistent with capillary telangiectasia

### ■ Developmental Venous Anomalies

#### ■ Definition, Aetiology

Like capillary telangiectasia, venous malformations, formerly known as venous angioma, are regarded not as true malformations, but rather as system variants. Macroscopically, there are expanded Medusa-like venules, which drain into a trans-cerebral coronary sinus (■ Fig. 9.47). Histologically, this involves primary dysplasia of the capillary and the small veins or the consequence of embryonically formed bypasses that are later closed. The interposed cerebral parenchyma between the vascular structures is

normal, although the vessels are often neither veins nor arteries. This is more of a non-pathological variant of venous drainage in the white matter. Therefore, instead of venous angiomas, the term DVA is now used (■ Figs. 9.48, 9.49).

Congenital venous anomalies tend to be found in the frontal brain and cerebellum. The developmental venous anomaly (DVA) consists of radially arranged, dilated collector veins that are surrounded by normal brain parenchyma. These collector veins, also known as a Medusa head, drain into an enlarged vein. An arterio-venous shunt is normally not detectable.

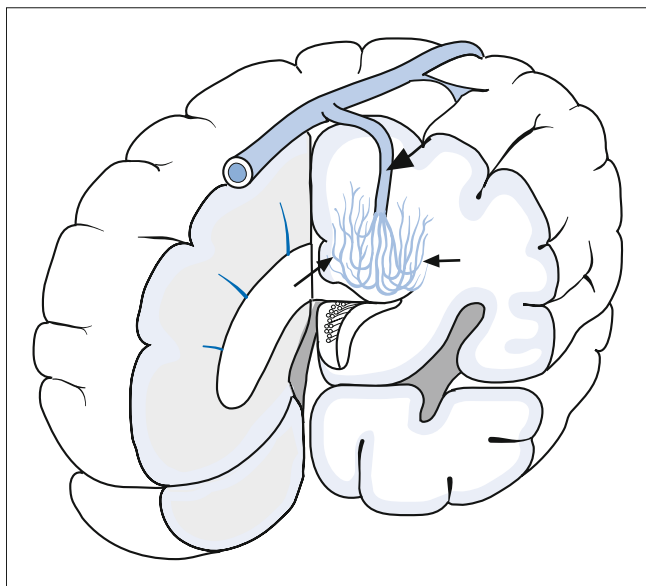


**Fig. 9.47 Developmental venous anomaly (DVA), schematic representation.** Numerous enlarged medullary veins (*small arrows*) deep within the white matter unite near the ventricle to form an increased trans-cortical collector vein (*large arrow*). This vein then leads to the superior sagittal sinus

#### ■ Epidemiology

In autopsy studies, at 1.5%, the incidence of congenital venous anomalies is approximately three to four times higher than that of AVMs.

#### ■ Symptoms

In general, a DVA is an incidental finding and does not clearly correlate with the clinical symptoms that led to the investigation. This is particularly true for patients suffering from headaches. The risk of bleeding for intra-cerebral and sub-arachnoid haemorrhaging is generally 0.22% per year. There is a strikingly high coincidence of congenital venous anomalies with cavernomas. The haemorrhaging tends to stem from the cavernoma and not from the DVA.

#### Developmental Venous Anomaly (DVA)

- Pathology should not be regarded as genuine malformations, but rather as a system variant. The venous malformation consists of a radially arranged, dilated collector vein that is surrounded by normal cerebral parenchyma.
- Localisation: the preferred location of the DVA is the frontal cortex and cerebellum.
- Clinical symptoms: mostly asymptomatic.
- Imaging: On the unenhanced CT, the draining collector vein of the DVA is often not visible. Only on contrast-enhanced CT can the extended Medusa-like venules be seen next to the trans-cerebral vein. No space-occupying lesion and no peri-focal oedema are seen. On MRI, the vascular structures are detectable as typical signal voids. On T1-weighted images, after the administration of contrast agent, the collector veins and enlarged venules appear hyper-intense.

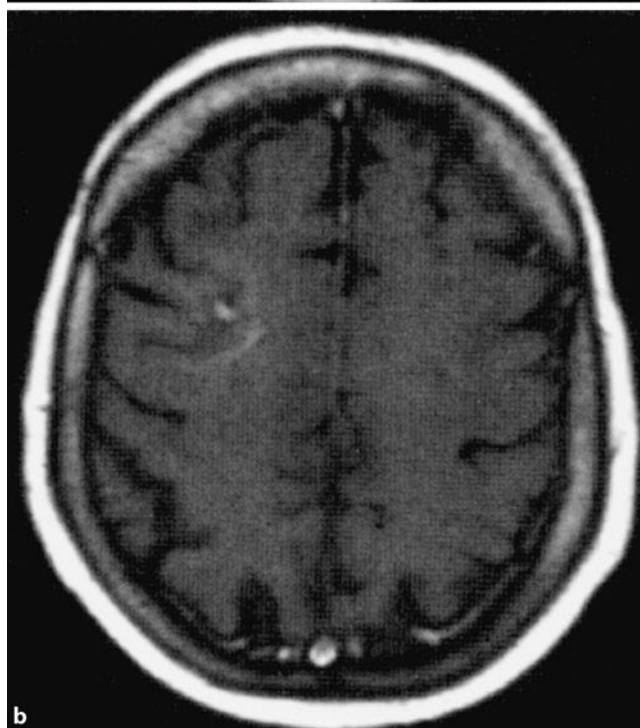
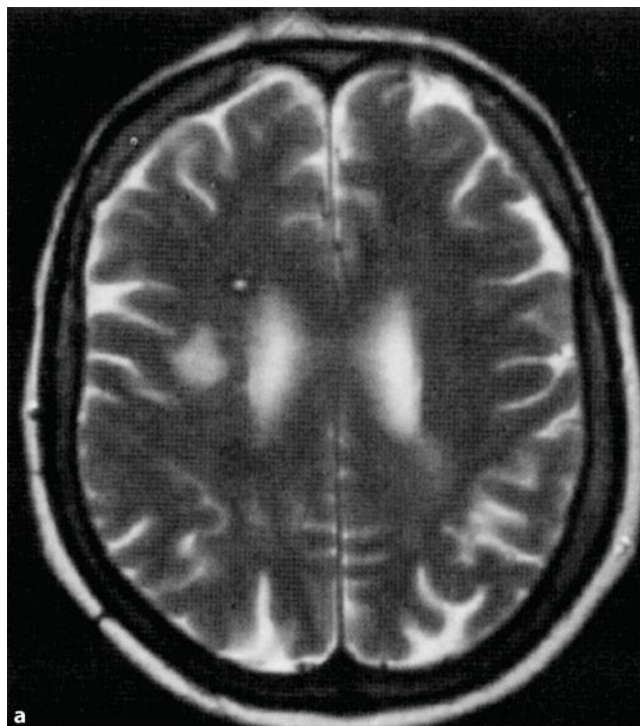


**Fig. 9.48a,b DVA.** **a** The T2-weighted sequence from a 16-year-old girl presents a hyper-intense area in the right semi-oval centre as an incidental finding. **b** On the T1-weighted sequences, after the administration of contrast agent, an enhanced vessel can be detected (DVA). (From: *Radiologe* 2003 43.940, Fig. 4 a, b)

#### ■ Medical Imaging

On unenhanced CT, DVA is often not apparent. Often, the Medusa-like extended venules can only be seen next to the trans-cerebral veins on contrast-enhanced CT. Neither a space-occupying lesion nor a peri-focal oedema is detectable. On MRI, the vascu-

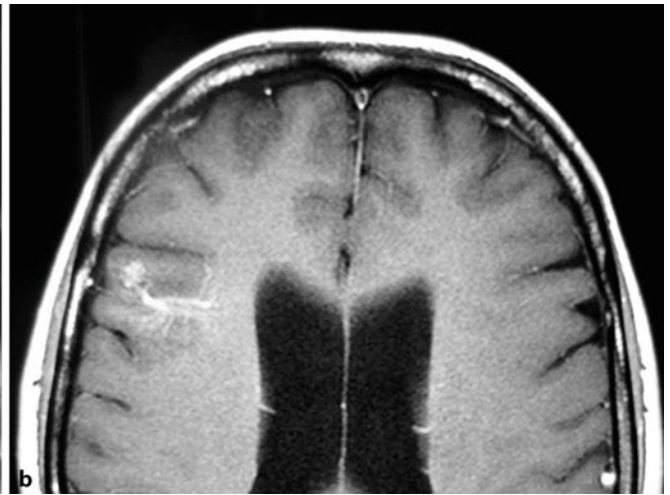
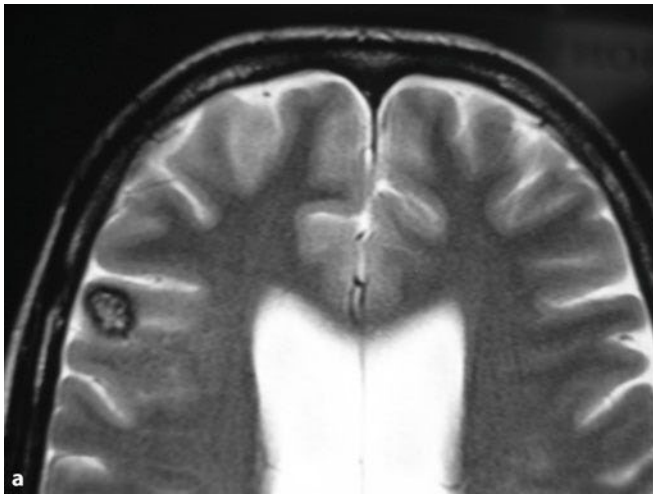


**Fig. 9.49a,b DVA and cavernoma.** A 15-year-old patient with a lesion in the right trigone. **a** On the T2-weighted sequences, there is a hypointense rim with hypo-, almost cerebral iso-intense centre with only a slight space-occupying effect on the surrounding cerebral parenchyma.

**b** On the T1-weighted sequences, after the administration of contrast agent, there is moderately strong hyper-intensity that most closely corresponds to small calcifications or blood in the methaemoglobin stage. There is also a DVA

lar structures are detectable as a typical signal void. On the T1-weighted sequences, after the administration of contrast agent, the coronary sinus and enlarged venules appear hyper-intense.

**Angiographically,** one or more pathologically enlarged, intra-cerebral veins appear in the venous phase. These drain the blood into a coronary sinus to the outside of the pontine and to the inner cerebral veins. Only on MRI can the cavernomas associated with the congenital venous anomaly be reliably identified. Digital subtraction angiography (DSA) is not indicated for typical CT or MRI findings. However, if haemorrhaging is indicated, the patient should undergo angiography so that an additional arterio-venous vascular malformation is not overlooked. An indication for surgery to treat DVA is only given if there is also an arterio-venous vascular malformation or a cavernoma (Fig. 9.49, overview).

#### Arterio-venous Malformations

The incidence of AVMs is about 2 in 100,000. This is characterised by the direct communication between arteries and veins. After classical divisions, there is no distinction between dural and pial AVMs. Both are summarised as angioma, whereby the aetiological and pathogenic difference between the two diseases is not taken into account (Figs. 9.50, 9.51).

#### Pial Arterio-venous Malformations

Histologically, AVMs consist of arteries, veins and interposed, primitively formed vessels. As a rule, normal capillaries are lacking. This is probably the reason for the increased tendency towards haemorrhaging because the drainage veins are directly exposed to the arterial pressure. As a result of venous hypertension, venous and arterial aneurysms and stenoses frequently form in the drainage veins.

**Epidemiology, Pathogenesis and Symptoms** Approximately 50% of AVMs manifest clinically as **haemorrhaging** that occurs intra-cerebrally (63%), sub-arachnoidally (32%), or purely intra-

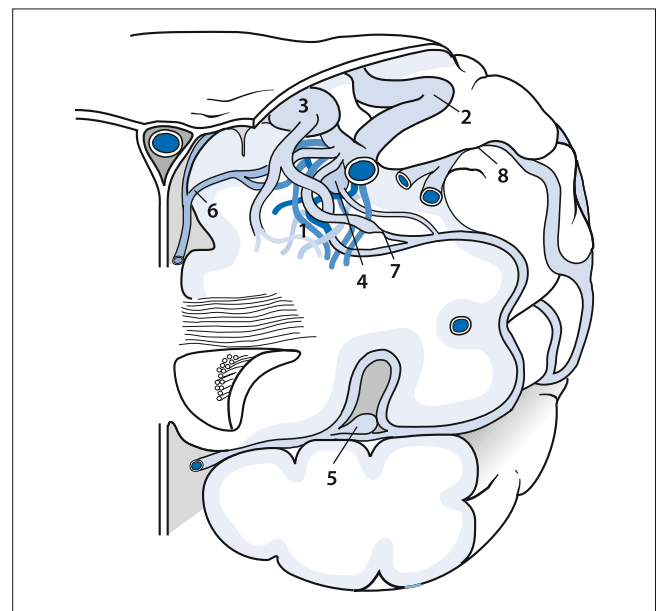


**Fig. 9.50 Angioma, schematic representation.** The cone-shaped structure of the arterio-venous malformation (AVM) consists of arteries and veins, the base is situated on the cerebral surface, the tip points in the direction of the lateral ventricle. 1 AVM nidus, 2 increased cortical draining veins, 3 varicose vein, 4 aneurysm within the nidus, 5 aneurysm at the bifurcation of the middle cerebral artery, 6 large feeder of the anterior cerebral artery and media, 7 vasculopathy with focal stenoses of the feeder arteries, 8 vasculopathic changes in the draining vein

ventriculary (6%). A quarter to two thirds of all patients with AVMs suffer from epileptic seizures. Arterio-venous malformations have an annual risk of bleeding of approximately 2–4%. The incidence of bleeding depends on the size, location and venous drainage situation. The annual cumulative probability of angioma patients suffering fatal intra-cerebral haemorrhaging or haemorrhaging associated with significant deficits is 2.7%. Haemorrhaging is often the first symptom of AVM (> 50%). This is often



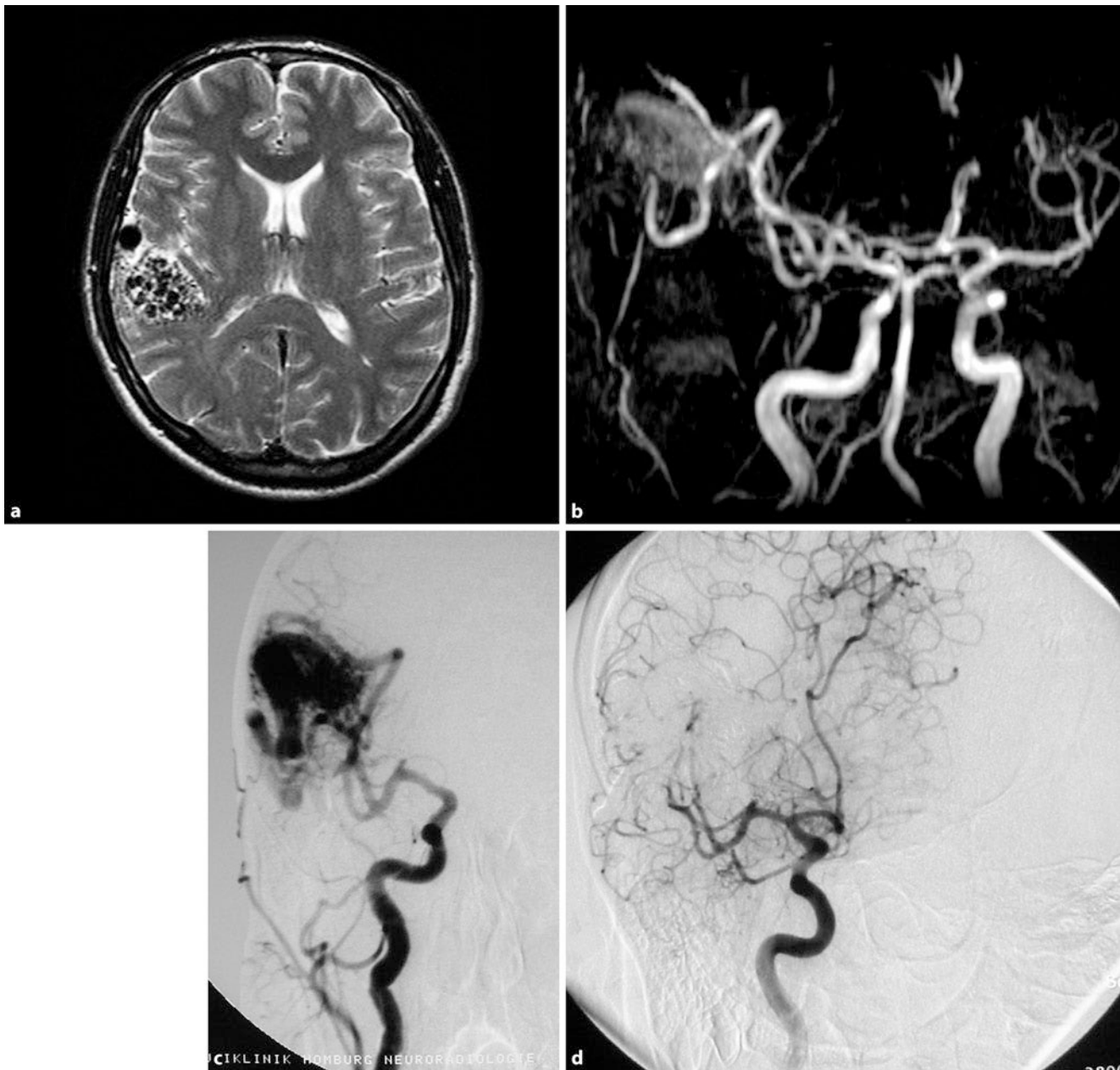


**Fig. 9.51a–d Angioma.** **a** On the T2-weighted sequences, heterogeneous structure appears temporally on the right with a hypo-intense garland-like structure corresponding to the large vessels and draining veins. No oedema and no space-occupying lesion are detectable. **b** On MR angiography (time-of-flight, TOF), the right middle cerebral artery is rather strongly depicted. Two larger afferent branches lead to this AVM. **c** On the subsequently per-

formed DSA (antero-posterior projection) a strong middle cerebral artery and two strong medial branches leading to the angioma nidus can be observed. The venous drainage is carried out via the cortical veins. **d** Condition after liquid embolysate (Onyx). Antero-posteriorly, no afferent vessels and no early draining vein can be detected. The angioma is completely closed

situated in brain areas that are rarely affected by hypertensive haemorrhaging.

The mortality rate of the initial haemorrhaging of an AVM is given as 10%; the morbidity rate is 30–50%. Mortality and morbidity continue with each case of haemorrhaging. Arterio-venous malformations are the cause of up to 40% of spontaneous intra-cranial haemorrhaging in younger patients. Superficial malformations can haemorrhage into the sub-arachnoid space; deeper malformations can cause intra-ventricular haemorrhaging. Symptomatic vasospasms and re-haemorrhaging can occur

if the haemorrhaging was caused by a flow-associated aneurysm. The risk of re-haemorrhaging of an AVM is higher in children than in adults. In children younger than 15 years, AVMs are the most common cause of spontaneous intra-cranial haemorrhaging. They account for approximately 20% of all childhood strokes.

With increasing age, AVMs may increase in size and display progressive dilatation of the afferent arteries and draining veins. Because of the high shunt volume, hypo-perfusion of the still normal brain parenchyma may occur with resulting gliosis and

atrophy – this is referred to as a **steal phenomenon**. Similar to the classic saccular aneurysms at the circle of Willis, the rapid flow in the afferent arteries can also lead to arterial aneurysms. The high pressure, the shear forces and the turbulent flow can lead to stenosis or occlusion of the draining veins, especially at the junction sites in the dural sinus. Proximal to the venous stenoses, so-called varicose veins or venous aneurysms can occur and lead to haemorrhaging. Arterio-venous malformations can also lead to space-occupying lesions.

In addition to the aforementioned haemorrhaging, AVMs are characterised by **seizures**, headaches, progressive neurological deficits, or hydrocephalus. Approximately 20% of patients display symptoms before the age of 20. Seizures occur in about 70% of patients with AVMs; half of these patients exhibit a generalised seizure. The most common are seizures in AVMs that occur in the cerebral cortex: the cause of these seizures is often a gliosis after previous haemorrhaging or a so-called vascular steal phenomenon with subsequent ischaemia.

Chronically occurring **headaches** can likewise occur with AVMs and are probably caused by hypertrophied dural vessels. Headaches mainly occur in peripheral arteriovenous malformations, which led to stenoses or occlusions of the afferent cerebral vessels. Arterio-venous malformations in the occipital region are most frequently associated with migraine attacks with visual symptoms.

**Progressive neurological symptoms** occur in a small percentage of children with AVMs, especially if the malformation is very large and situated close to the cortex. In these cases, the so-called vascular steal phenomenon is considered to be a cause. Another cause of neurological deficits is venous hypertension. This can be so pronounced that it results in malabsorption of CSF with a consequent hydrocephalus owing to the high venous pressure.

**Medical Imaging** **Unenhanced CT** can provide a first indication, especially if calcifications, focal atrophy, or tubular hypo-dense structures corresponding to vessels are detectable. Linear or stippled compressions and irregular parenchymal hypo-densities are often the only evidence of an AVM. After the intra-venous administration of contrast medium, there is a strong density increase in the vessels, and the dilated drainage veins can clearly be seen. During the acute stage of intra-cerebral haemorrhaging, an AVM can be masked by the bleeding.

On **MRI**, apart from the consequences of previous haemorrhaging (haemosiderin), a gliosis and a signal void through the vascular convolutions can be seen. As with the dural fistula, this involves vascular malformations with rapid flow. The rapidly flowing blood in the draining vessels appears as an area of predominantly punctate structures that are devoid of signal.

On **MR angiography**, possibly the time-of-flight (TOF) technique or contrast-enhanced MR angiography, the nidus and the afferent arteries or draining veins can also be clearly detected.

➤ **Despite CT, MRI and MRA, intra-arterial DSA (as pan-angiography) is essential in the diagnosis of AVMs. The afferent vessels, haemodynamics and drainage can currently only be detected via angiography.**

A commonly used classification of angioma, which takes into account the therapeutic risk of the individual patient, is the **classification of AVMs** according to Spetzler and Martin (Table 9.3). The angiomas are distinguished by the size of the AVM, the localisation and the venous drainage (overview). Cerebral AVMs are wholly or mostly supplied by cerebral arteries. Aneurysms are often detected on the afferent angioma vessels. Intra-nidal aneurysms are mostly depicted by intra-arterial DSA.

**Treatment** The decision to treat a symptomatic AVM must take into consideration the natural course of the disease in addition to the risks and benefits of the treatment. The main therapeutic treatment approaches can be divided into three categories:

- Surgical excision
- Radiosurgery
- Endovascular embolisation of AVMs

A combination of these techniques is often performed (see below). By improving the microsurgical operating techniques, large and complex malformations can also be treated with relatively low morbidity and mortality. The complete excision or suppression of the nidus of the malformation is the goal of any treatment. The radio-surgery produces hypoplastic changes in the vascular wall of the AVM. Complete occlusion of an AVM can mainly be achieved in a nidus that is < 3 cm. The main drawback of the radio-surgical technique is that there is still a risk of haemorrhaging during the first 1–2 years after stereotactic irradiation. To largely avoid radiation-induced damage to the surrounding cerebral parenchyma, usually only stereotactic one-time irradiation with a linear accelerator or a gamma knife is performed.

Endovascular techniques have become established as the third treatment modality. The complete angiographic obliteration of a large AVM is often not possible. Smaller AVMs can be completely closed – even endovascularly. Often, a combined treatment is carried out. The deep, surgically inaccessible, afferent vessels of AVMs are thereby embolised to subsequently facilitate the surgical extirpation. This pre-operative embolisation can reduce the size and the pressure within the nidus and thus facilitate operational excision and minimise intra-operative blood loss.

Table 9.3 Grading system for pial arterio-venous malformations (AVMs) by Spetzler and Martin

Size of the AVM	
Small (< 3 cm)	1
Medium (3–6 cm)	2
Large (> 6 cm)	3
Affected brain region	
Not eloquent	0
Eloquent	1
Pattern of venous drainage	
Only superficial veins	0
Deep venous system	1

### Pial Arterio-venous Malformations

- Pathology: congenital (multiple in the case of Wyburn–Mason and Rendu–Osler–Weber syndromes); dilated arteries and veins without a capillary bed, usually gliotic cerebral parenchyma. Flow-induced aneurysms are detectable in approximately 10–12% of cases.
- Localisation: 85% supratentorially, 15% infratentorially.
- Clinical symptoms: bleeding risk 2–3% per year; seizures in approximately 25% of cases.

### ■ ■ Dural Arterio-venous Fistulas

A dural arterio-venous fistula (DAVF) refers to a direct arterio-venous shunt within the dura (■ Fig. 9.52). These exist between dural arteries or the lepto-meningeal branches of pial arteries and a dural sinus or dural or lepto-meningeal vein.

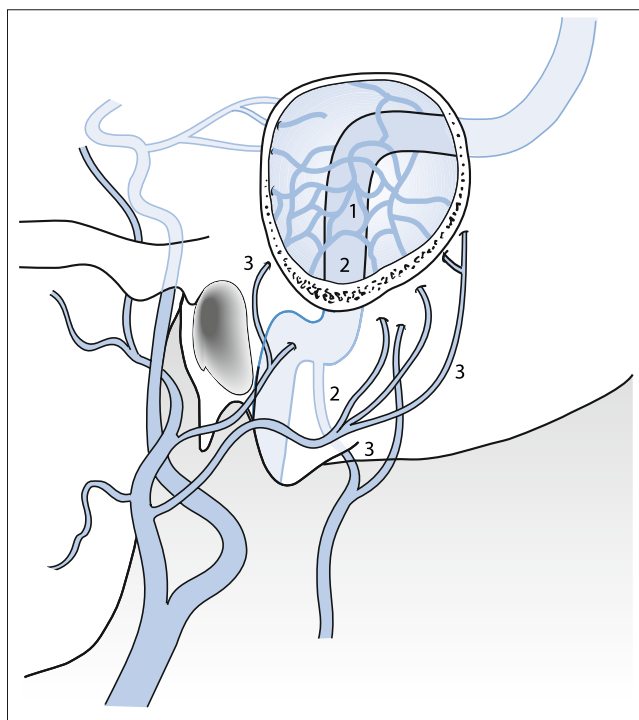
#### Classification of Dural Arterio-venous Malformations According to Djindjian

- Type I: direct drainage into a dural sinus with normal flow direction
- Type II: normal drainage as in type I, but with reflux into a pontine vein.
- Type III: direct drainage into a pontine vein.
- Type IV: drainage into a venous pouch, which can also be space-occupying

**Aetiology, Symptoms** In dural arterio-venous fistulas in adults and children, a broad spectrum of clinical symptoms is displayed, which depends on the location and size in addition to venous drainage or the arterio-venous shunt. There is some controversy surrounding the causes of dural arterio-venous fistulas. Some fistulas in the area of the transverse sinus and sigmoid are acquired and a consequence of dural sinus thrombosis. Several genetic factors that lead to a hyper-coagulable state are associated with a cumulative occurrence of dural arterio-venous fistulas in various locations. Congenital dural arterio-venous fistulas rarely occur in children. These congenital fistulas often display a greater arterio-venous connection and an increased flow compared with the acquired dural arterio-venous fistulas in adults. The cause of congenital dural malformations is unknown.

In paediatrics, dural malformations are usually already diagnosed in the new-born. They often show symptoms similar to vein of Galen malformations, including macrocephaly, heart failure, vascular noise, increased intra-cranial pressure and haemorrhage, and dilated veins in the head region. The combination of macrocephaly, expanded scalp veins and heart failure should raise the suspicion of an intra-cranial vascular malformation.

**Intra-cranial haemorrhaging** is the most serious complication of a dural arterio-venous fistula. The haemorrhaging can occur intra-cerebrally, sub-durally, or sub-arachnoidally. In the case of sub-cortical, aetiologically unclear intra-cerebral haemor-



■ Fig. 9.52 Dural arterio-venous fistula, schematic representation. 1 The dural arterio-venous fistula is formed by a network of dural arteries and veins on the wall of the transverse sinus and sigmoid, 2 the dotted line indicates the closed lumen of the sinus, 3 blood flows (feeder) of the fistula also come from the occipital, retro-auricular and vertebral arteries

rhaging, sub-arachnoid haemorrhaging without evidence of aneurysm, or acute SDH without adequate trauma, a dural arterio-venous fistula should also be considered.

The bleeding tendency of dural arterio-venous fistulas mainly depends on the venous drainage. The individual assessment of the risk of haemorrhaging and thus the indication for therapeutic measures is decisively influenced by its angiogram. To better estimate the risk of haemorrhaging, the dural arterio-venous fistula is angiographically classified.

Intra-cerebral haemorrhaging occurs most frequently in the case of dural arterio-venous fistulas with cortical venous drainage. The bleeding incidence of this type of drainage is over 40%. The bleeding incidence may be even higher because some of the patients have a history of headaches resulting from micro-haemorrhaging. The risk of haemorrhaging can also be assessed based on the localisation of the dural arteriovenous fistula. Those in the anterior cranial fossa, however, usually display venous drainage through pontine veins into the superior sagittal sinus or the cavernous sinus and thus carry a significantly higher risk of haemorrhaging (84%).

Dural arterio-venous fistulas cause **symptoms that are not caused by haemorrhaging significantly more frequently than AVMs**. The turbulent flow in the draining vein and the nidus is often due to pulse-synchronous tinnitus, especially if the drainage is located in the immediate vicinity of the temporal bone. Cranial nerve deficits have also been described, which are presumably caused by a steal mechanism of the vasa vasorum of the corresponding nerves from the dural arteries. Papilloedema is

often an expression of increased pressure in the venous system. Ophthalmoplegic symptoms may also occur as local findings in the fistula of the cavernous sinus. Even more rarely, dural arterio-venous fistulas can lead to a cerebral pseudotumour or acute visual deterioration.

**Medical Imaging** The diagnosis of dural arterio-venous fistula is only possible with intra-arterial DSA because this shows the arterial inflow, the precise location and position, and the venous outflow. On CT and MRI, extended drainage veins may sometimes be identified. However, a distinction between pial and dural AVMs is often not possible here. In the case of a carotid–cavernous fistula, CT and MRI often show exophthalmos at the site of the lesion in addition to the easily identifiable, dilated ophthalmic vein. If there is also a postero-basal venous flow, a dural arterio-venous fistula is barely detectable on the conventional turbo spin echo sequences.

Large dural fistulas of the base of the skull close to the sinus can often not be detected by CT and are also problematic on MRI diagnostics. In patients with pronounced arterialisation in the sinus, there may be signal loss due to the rapid flow. This is most easily detected in the dural sinuses of the cavernous sinus. If the shunt exceptionally leads to the superficial veins of the brain, the CT and MRI images appear like those from pial AVMs.

➤ **Dural arterio-venous fistulas of the transverse sinus frequently accompany sinus thrombosis. The detection of transverse sinus thrombosis may thus be a decisive indication of dural arterio-venous fistulas.**

**Treatment** Cerebral pan-angiography is required to plan an endovascular approach. This can be done either trans-arterially or trans-venously. Surgical therapy is used less frequently. There has recently been evidence that radiotherapy of the fistula leads to good results.

## ■ Intra-cranial Aneurysms

### ■ Aetiology

Intra-cranial aneurysms do not indicate any congenital diseases. It is assumed that a combination of certain factors is responsible for the development of an aneurysm, particularly the saccular type (■ Fig. 9.53). It has now been demonstrated that hypertension, smoking and contraceptives promote the formation of an aneurysm. It usually takes 15 years for an aneurysm to form. On the other hand, there are many diseases in which cumulative aneurysms frequently occur because of a weakness in the vascular wall. These factors probably play an important role in the aetiology of childhood aneurysms. The increased incidence of aneurysms with infectious and traumatic origin in children implies that the vessels are more susceptible than in adults. On the other hand, it must be assumed that the vessels in children favour “healing” of aneurysms more than in adults because there are numerous reports of spontaneous thrombosis in the case of childhood aneurysms.

The **childhood aneurysms** deviate somewhat from aneurysms in adulthood:

- A preponderance of boys in a 3:1 ratio
- A higher incidence of unusual localisation, e.g. with about 15% in the posterior circulation, frequent peripheral occurrence
- Predilection of the carotid bifurcation (31–54%)
- Frequent occurrence of large and giant aneurysms (20%)
- Lower incidence of multiple aneurysms (2%)
- Lower rate of morbidity
- Higher incidence of traumatic and infectious aneurysms
- Higher incidence of spontaneous thrombosis

These differences become smaller with increasing age.

### ■ Epidemiology

The incidence of intra-cranial aneurysms in the general population varies between different countries and continents; it is 4.9% in North America, Europe and Japan, but only 0.2% in some Middle Eastern countries.

Paediatric intra-cranial aneurysms account for <5% of all intra-cranial aneurysms. There are no data available on incidentally discovered aneurysms in autopsy studies in children. There is a higher incidence of intra-cranial aneurysms in adult women, which is inversely related to childhood aneurysms: this reflects an increased incidence in males in a ratio of 3:1, especially in children <8 years (see above). In the group of 10- to 20-year-olds, the ratio is still 1.2:1. The ratio is reversed in the 5th decade of life; slightly more women than men are affected. The proportion of women continues to increase with increasing age.

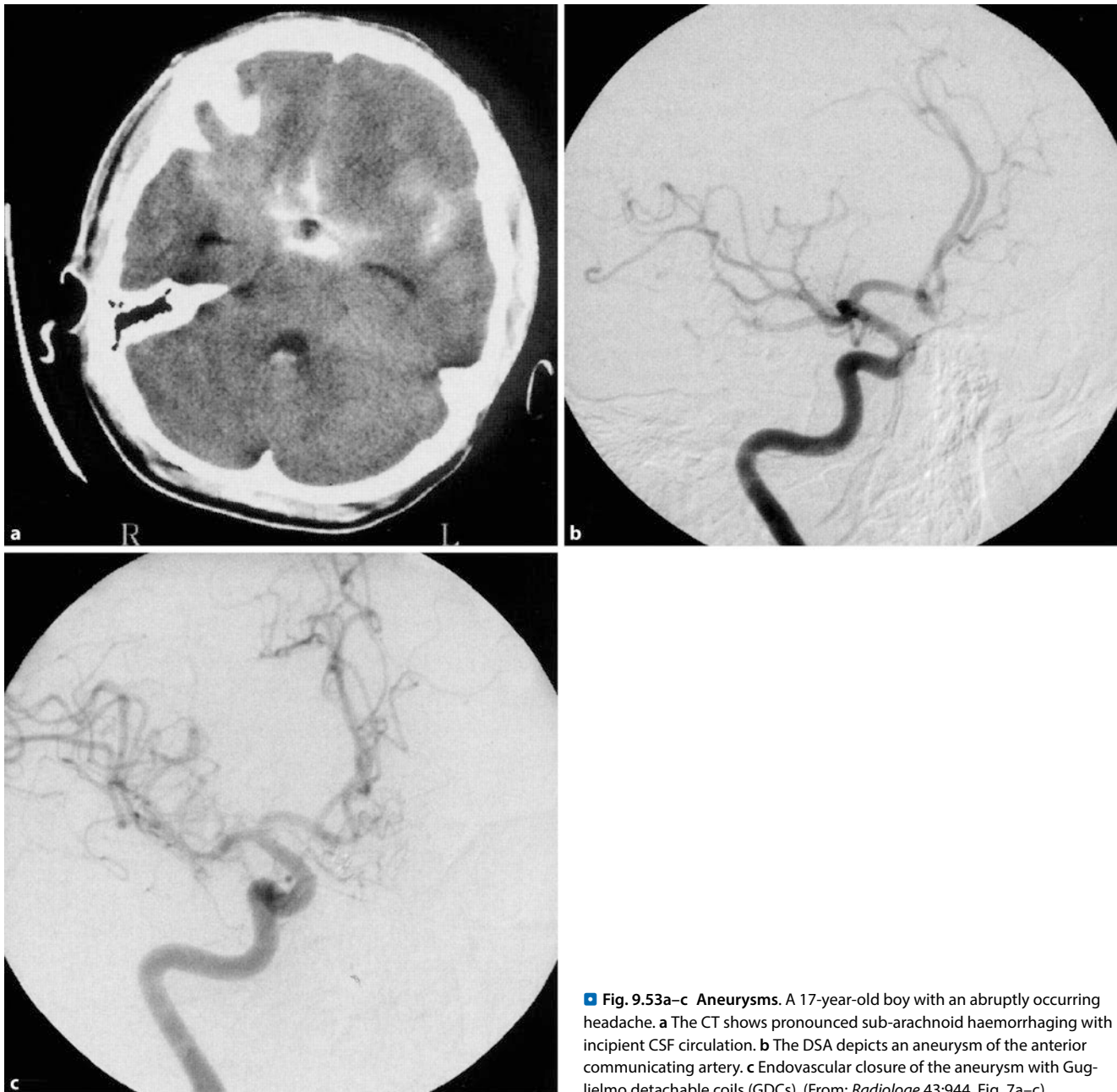
### ■ Pathogenesis

It is assumed that in children, approximately 75% of the aneurysms are saccular. They most commonly occur at vascular junctions. Common sites of **saccular aneurysms in adults** include the bifurcation of the anterior communicating artery with the anterior cerebral artery, the bifurcation of the posterior communicating artery with the internal carotid artery, and the bifurcation of the middle cerebral artery. They mainly occur at the base of the skull.

Furthermore, saccular aneurysms occur at the basilar head and at the bifurcation of the basilar artery with the superior cerebellar or the anterior–inferior cerebellar artery. In 85% of cases, the aneurysms occur in the circle of Willis. Ten to thirty per cent of adult patients have multiple aneurysms; in 10–20% there is another aneurysm at the identical site on the contra-lateral side.

**An aneurysm** usually arises from the formation of a neck and an aneurysm sac. The width of the neck and the size of the aneurysm sac are crucial for further therapeutic planning. The internal elastic lamina disappears in the region of the aneurysm neck, and the media thins. At the rupture site, which often occurs in the area of the aneurysm sac, the wall thins to <0.3 mm, and the tear is often not longer than 0.5 mm. It is not possible to predict which aneurysms will result in haemorrhaging. However, several studies indicate that aneurysms >7 mm have a higher probability of rupturing.

In patients younger than 20 years, **traumatic aneurysms** often occur. They account for approximately 5–15% of paediatric aneurysms. The spontaneous healing tendency of these traumatic



■ **Fig. 9.53a–c Aneurysms.** A 17-year-old boy with an abruptly occurring headache. **a** The CT shows pronounced sub-arachnoid haemorrhaging with incipient CSF circulation. **b** The DSA depicts an aneurysm of the anterior communicating artery. **c** Endovascular closure of the aneurysm with Guglielmo detachable coils (GDCs). (From: *Radiologe* 43:944, Fig. 7a–c)

aneurysms is estimated to be up to 20%. Approximately 40% of traumatic aneurysms occur in the area of the anterior cerebral artery, 35% are found in the large vessels at the base of the skull, and about 25% occur distally in the periphery. Approximately 3–4 weeks after the traumatic event, most of the children experience intra-cranial haemorrhaging. Approximately 70% suffer from a closed cranio-cerebral trauma, and approximately 16% suffered from a gunshot wound. In some cases, aneurysms have apparently been caused by birth trauma. **Post-traumatic aneurysms** are often so-called false or aneurysms with a rupture of the wall. Here, the aneurysm is covered only by the surrounding parenchyma.

#### ■ **Special Form: Giant Aneurysms and Infectious Aneurysms**

**Giant aneurysms** (>25 mm in diameter; ■ **Fig. 9.54**) seem to be based on a special form of wall weakness. They are about four times more common in children than in adults. In children <5 years, the proportion of giant aneurysms is estimated to be up to 20%. In some cases, incidence rates of up to nearly 50% have been reported. The incidence of dissociating aneurysms with a traumatic or spontaneous origin is probably greatly underestimated because vascular narrowing distally or proximally to the aneurysm of the carrier vessel is not recognised.

Flow-induced aneurysms generally do not occur in the paediatric age group, not even in the case of very high arterio-venous shunts.

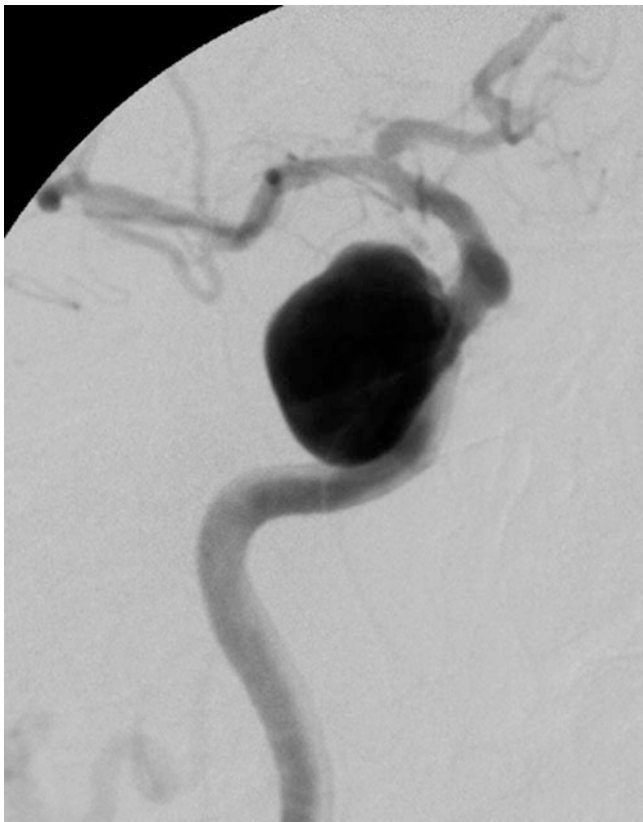


**Fig. 9.54 Giant aneurysms** A 26-year-old patient with paresis of the ocular muscle. In the petrous segment of the internal carotid, a laterally directed aneurysm, approximately 18×25 mm, was detected (paralytic aneurysm)

**Infectious aneurysms** account for approximately 5–15% of all paediatric aneurysms. The most common cause is infection with staphylococci, streptococci and various gram-negative bacteria. Infectious aneurysms often occur in the context of endocarditis or in connection with congenital or rheumatic heart disease. There are also some reports of intra-cranial aneurysms in the case of human immunodeficiency virus (HIV) infection. Here, mostly fusiform aneurysms will be found. These often seem to occur in the course of an opportunistic infection. Infectious aneurysms develop within a short time and often display symptoms of ischaemic infarcts caused by arteritis. Intra-cranial haemorrhaging rarely occurs.

Even in the case of **systemic diseases**, e.g. collagenous diseases, aneurysms may occur. Aneurysms in childhood have been described in connection with Ehlers–Danlos syndrome, Klippel–Trenaunay–Weber syndrome, hereditary haemorrhagic telangiectasia, tuberous sclerosis, Moyamoya syndrome, aortic stenosis and fibromuscular dysplasia.

**!** As mentioned above, multiple aneurysms are only observed in approximately 2% of all children. In infectious aneurysms, however, a multiplicity is reported in approximately 15% of cases. In adults, multiple aneurysms occur in up to 15% of cases; it is therefore necessary to depict all cerebral vessels on pan-angiography or on MR or CT angiography.

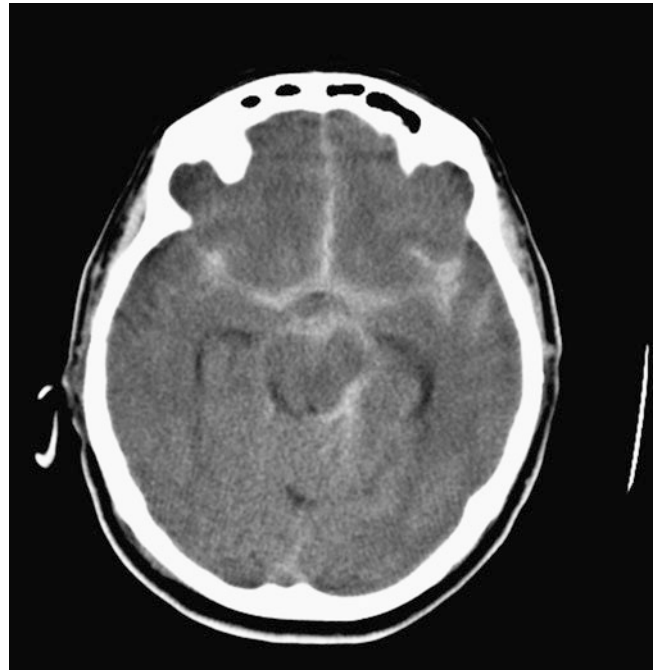


**Fig. 9.55 Sub-arachnoid haemorrhaging.** On CT, typical basal blood distribution can be seen in the case of pronounced sub-arachnoid haemorrhaging

#### ■ ■ Symptoms

The rupture of an intra-cranial aneurysm is the most common cause of **sub-arachnoid haemorrhaging** (■ Fig. 9.55). In 82% of cases in infants and children younger than 5 years, intra-cranial aneurysm haemorrhaging is indicated as a cause of sub-arachnoid haemorrhaging. The incidence decreases with increasing age and is only about 45% in children older than 5 years. Between 10 and 20 years of age, the cause of sub-arachnoid haemorrhaging is an intra-cranial aneurysm (approximately 40% of cases) or an AVM (just over 30% of cases). However, there are great differences between different population groups. In the Asian population, there are significantly fewer intra-cranial aneurysms. There are only a few reports of sub-arachnoid haemorrhaging in new-borns. In these cases, clinical symptoms include seizures, intra-cranial brain pressure and hemiparesis. In older children and adults, sub-arachnoid haemorrhage typically manifests with the sudden onset of headache, which is usually described by the patient as a “headache like no other”. Common associated symptoms include nausea, vomiting, neck pain and impaired consciousness.

The classification of the clinical status is based on the **classification of Hunt and Hess** (■ Table 9.4). The prognosis depends on the severity of the initial clinical symptoms. Grade 0 often refers to asymptomatic, incidentally detected aneurysms. However, the diagnosis is not always so “classical”. There are patients who do indeed complain of severe headache in which the pain intensity gradually increases because of meningeal irritation. In this situation, misdiagnosis may be more frequent, e.g. an initial manifestation of a migraine or tension headache. Especially in children, the existence of a sub-arachnoid haemorrhage is usually not initially considered. In older children, the symptoms are

**Table 9.4** Classification of sub-arachnoid haemorrhaging according to Hunt and Hess

Degree	Findings
0	Asymptomatic aneurysms
I	Slight headache and neck stiffness, no focal neurology
II	Moderate to severe headache, neck stiffness, no neurological failures except for cranial nerve symptoms
III	Dizziness, confusion and/or slight neurological deficits
IV	Sopor, moderate to severe neurological deficits such as hemiplegia, autonomic disorders
V	Coma, symptoms of decerebration

similar to those in adults. Most consist of a sudden headache. In addition, there may be a brief loss of consciousness and a stiff neck. In approximately 10% of patients, there are bilateral symptoms in the pyramidal tract. In one third of cases, a rupture occurs after physical exertion.

Regardless of the location of the aneurysm, the headaches are almost always diffuse. In the case of an aneurysm rupture with pronounced sub-arachnoid haemorrhaging, the intra-cranial pressure approaches the arterial pressure and the cerebral perfusion pressure falls. This is probably the explanation for the sudden transient loss of consciousness that occurs in approximately 45% of cases. This may be preceded by thunderclap headache, but most patients only complain of headaches after they have regained consciousness. If a sudden headache is associated with vomiting, acute sub-arachnoid haemorrhaging should always be suspected.

Although the absence of focal neurological symptoms is a characteristic of aneurysm haemorrhaging, these can still occur – and not only through direct nerve compression due to pressure of the enlarged aneurysm (paralytic aneurysm; [Fig. 9.56](#)).

Some factors may indicate the presence and **localisation of an unruptured aneurysm**. For example, an aneurysm in the region of the splitting of the internal carotid artery and the posterior communicating artery can lead to paralysis of the oculomotor nerve. This should especially be considered in the case of pupillary expansion, a loss of light reflex, or focal pain above and behind the eye. Paralysis of the abducens nerve may indicate an aneurysm in the cavernous sinus. Visual field loss may occur in the case of a supraclinoid carotid aneurysm. Occipital pain may indicate a PICA or AICA aneurysm. An expanding media aneurysm can lead to pain in and behind the eye in addition to the lower temporal area.

### Medical Imaging

The aim of radiological investigation is to determine whether sub-arachnoid haemorrhaging has actually occurred. If radiology cannot provide evidence of sub-arachnoid haemorrhaging, lumbar puncture absolutely must be implemented if this is clinically suspected. If blood is found in the CSF, it is imperative to locate the origin of haemorrhaging.

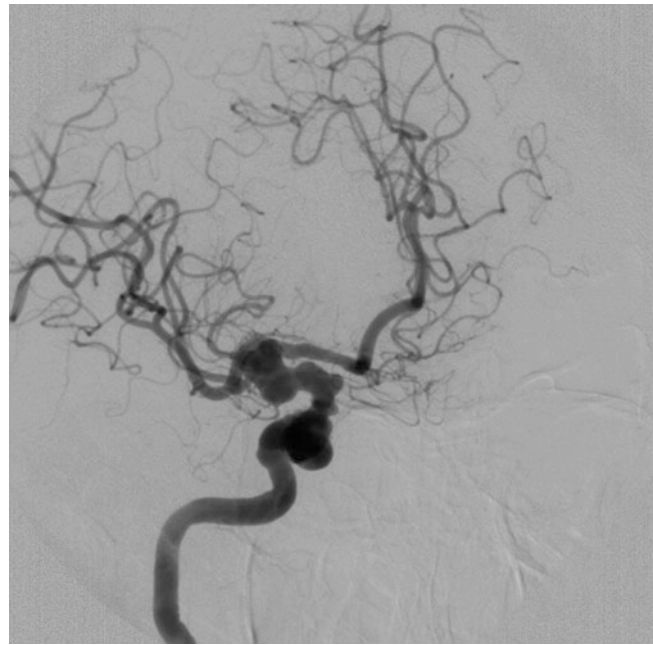


**Fig. 9.56** Paralytic aneurysm. Fusiform enlargement of the carotid sections leads to paralysis of the caudal cranial nerves: paralytic aneurysm

**Computed Tomography.** If sub-arachnoid haemorrhaging is suspected, CT is the method of choice because of the high sensitivity (85–100%) within the first 3 days following the haemorrhaging ([Fig. 9.57](#)). On CT, the blood distribution does not always indicate the location of the aneurysm. Based on the blood distribution, multiple aneurysms can imply ruptured aneurysms, which must then be treated immediately. If the haemorrhaging dates back a few days, the sensitivity of CT is severely decreased; after 14 days, it is down to about 50%. In the case of a low amount of blood in the sub-arachnoid space, the blood can be resorbed after a few days.

**CT Angiography.** Computed tomographic angiography of intracranial vessels can be quickly performed with modern multi-slice scanners, which afford excellent image quality ([Fig. 9.58](#)). For the detection of an aneurysm with a diameter less than 3 mm, CT angiography is inferior to DSA. Even with aneurysms close to the base of the skull, there are still diagnostic problems. However, CT angiography can be employed as an adjunct to DSA. In a prospective study of 134 consecutive patients, in 21 patients, no aneurysm was found on the DSA. In 5 of these patients, a small aneurysm of the anterior communicating artery and in one case, an aneurysm of the middle cerebral artery could be detected with CT angiography. In treatment planning, CT angiography can be helpful for the planning of elective surgery, especially in the case of large and morphologically complex aneurysms. Thus, in thrombosed and calcified aneurysms, the perfused residual lumen can be better depicted.

**Magnetic Resonance Imaging.** For many years, MRI was less capable of detecting acute haemorrhaging than CT. For intracerebral haematoma, good “haemorrhaging sensitive” sequences are now available. Consequently, MRI can at least be considered



**Fig. 9.57 Haemorrhaging in the case of aneurysm, CT.** In this patient, the typical basal blood distribution in the sub-arachnoid space can be seen, in addition to frontal intra-parenchymal haemorrhaging, which is indicative of an aneurysm of the anterior communicating artery

an equivalent methodology. Because the radiological diagnosis of stroke is increasingly performed using MRI, it was important to create specific MR protocols that ensure that sub-arachnoid haemorrhaging – which can clinically resemble a stroke – is not overlooked. If a stroke is suspected, an MR protocol should include a FLAIR sequence and possibly a proton density (PD)-weighted sequence so that sub-arachnoid haemorrhaging can be detected.

In the acute phase, the MRI is still not the method of choice for the detection of sub-arachnoid haemorrhaging. In addition to the higher costs, this is because of the longer examination time compared with CT and the more costly monitoring during the MRI examination of patients with diminished awareness. In the sub-acute phase of sub-arachnoid haemorrhaging, MRI is superior to CT because the increased concentration of protein in the CSF combined with para-magnetic effects of blood degradation products can locally lead to characteristic MR changes (■ Fig. 9.59).

**MR Angiography.** Like CT angiography, MR angiography allows the reliable depiction of complexly formed larger aneurysms before treatment. However, it currently only plays a minor role in the acute situation for aneurysm detection. However, unlike DSA, CTA and MRA can be used to detect thrombosed aneurysmic portions.

In the **after-care of closed aneurysms**, MR angiography, especially TOF MR angiography, contrast-enhanced MR angiography and T1-weighted sequences **play an important** role. MR angiography source images combined with 3D reconstructions are highly sensitive when it comes to the detection of recurrent an-

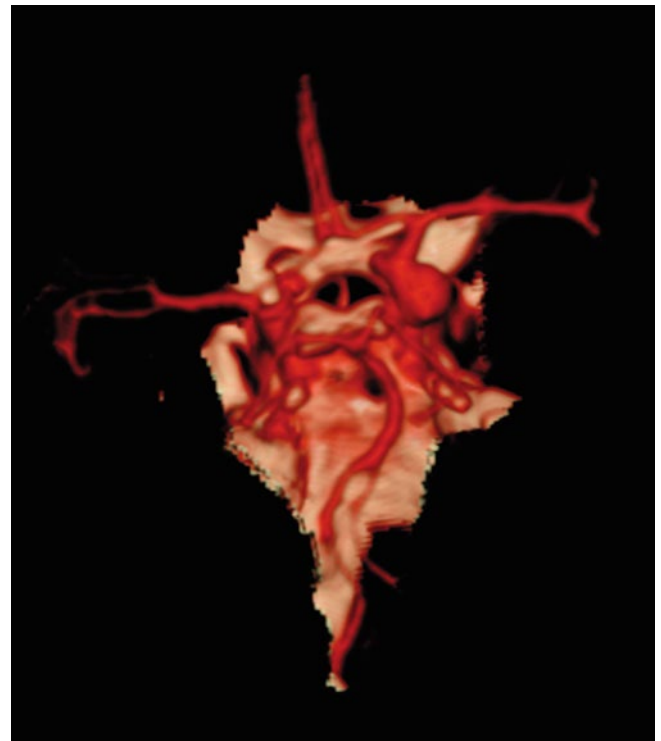


**Fig. 9.58 Sub-arachnoid haemorrhaging.** Detection of an aneurysm in the end section of the left internal carotid artery

eurysms. Although the platinum coils used to close an aneurysm can cause artefacts owing to the “signal quenching” of adjacent structures, the aneurysmic vessel can often still be sufficiently evaluated. Contrast-enhanced MRA is even better suited to this. Even small, residually perfused aneurysmic portions can be detected. The platinum coils do not provide a contra-indication for an MR examination. If anything, MRI is an integral part of the follow-up of endovascular aneurysms supplied with platinum spirals.

#### ■ ■ Complications of Sub-arachnoid Haemorrhage

**Recurrent Haemorrhaging.** Depending on the size and especially the localisation of a ruptured aneurysm, in up to 40–50% of cases, early re-haemorrhaging occurs. It is therefore crucial to disconnect the aneurysm from the blood circulation as soon as possible. Patients who survive recurrent haemorrhaging have a worse prognosis than patients without re-haemorrhaging. This is probably partly because re-haemorrhaging results in adhesions of the sub-arachnoid space, which tend to lead to intra-cerebral haemorrhaging. The risk of re-haemorrhaging is very high within the first days (1.5% per hour for the first 6h), which is why aneurysms should be treated as quickly as possible.

**Hydrocephalus.** Because of an acute malabsorption or acute outflow obstruction of the CSF by intra-ventricular blood clots, acute hydrocephalus can occur. This situation is often the reason for the primarily poor level of consciousness of the patients. In the further course of the disease, hydrocephalus persists in about 25–30% of patients, who then require permanent ventricular drainage via the insertion of a shunt.





■ **Fig. 9.59** Sub-arachnoid haemorrhaging with peri-mesencephalic blood. The temporal horns are emphasised, thus indicating incipient hydrocephalic pooling

**Vasospasm.** In addition to the re-haemorrhaging of a non-treated aneurysm, vasospasm is feared after sub-arachnoid haemorrhage. Around 4–14 days after the haemorrhaging, because of the appearance of blood in the sub-arachnoid space, vasospasm of the larger, but also the smaller intra-cranial arteries occurs for pathophysiologically unclear reasons. The cause of the vasospasm is likely blood break-down products or released mediator substances. The vasospasm can lead to significant circulatory disorders, with neurological deficits to multi-infarct syndrome, resulting in death. The narrowing of the vessels is not limited to the aneurysm-carrying vessel; generalised narrowing can also be observed. Narrowing can even manifest in the vessels of the other hemisphere or infratentorially. Persistent neurological deficits caused by a vasospastic cerebral infarction occur in approximately 20% of patients with sub-arachnoid haemorrhaging (■ Fig. 9.60).

**Nowadays,** the vasospasm is usually **diagnosed** by repeated transcranial Doppler studies. A DSA is only necessary if the Doppler ultrasound does not sufficiently explain the clinical deterioration of the patient or if endovascular spasmolysis should be performed in the case of a clinically symptomatic vasospasm detected by Doppler ultrasound. Transluminal angioplasty is suitable for spasms in the distal internal carotid artery and if necessary for spasms of the proximal portions of the middle cerebral artery (M1 segment). In the posterior cerebral circulation, angioplasty can be used to treat spasms of the vertebral and basilar arteries. If the patient has generalised vasospasm involving the distal vessel segments, the intra-arterial administration of nimodipine, a calcium antagonist, can be attempted. The disadvantage here is the short efficacy of the drug; the treatment must be applied several times in some patients.

## ■ ■ Treatment

The principle of aneurysm treatment involves disconnecting the aneurysm from the bloodstream. This can be done through a surgical procedure – aneurysm clipping – or by an endovascular occlusion with platinum or Guglielmo detachable coils (GDC). Early treatment is preferred to prevent re-haemorrhaging. In general, an interdisciplinary team, consisting of neurosurgeons and radiologists should be consulted regarding the treatment of an aneurysm.

The data from the International Subarachnoid Aneurysm Trial (ISAT) showed that in patients with ruptured aneurysms, endovascular treatment resulted in a better clinical outcome. This controlled prospective study on the risk of treatment of ruptured aneurysms was prematurely stopped after 2,143 of the 2,500 planned patients had been enrolled because, compared with the operated patients, endovascular treatment resulted in a 6.9% decrease in the absolute risk of treatment. **Endovascular treatment** should therefore be initially considered as the first option (see below).

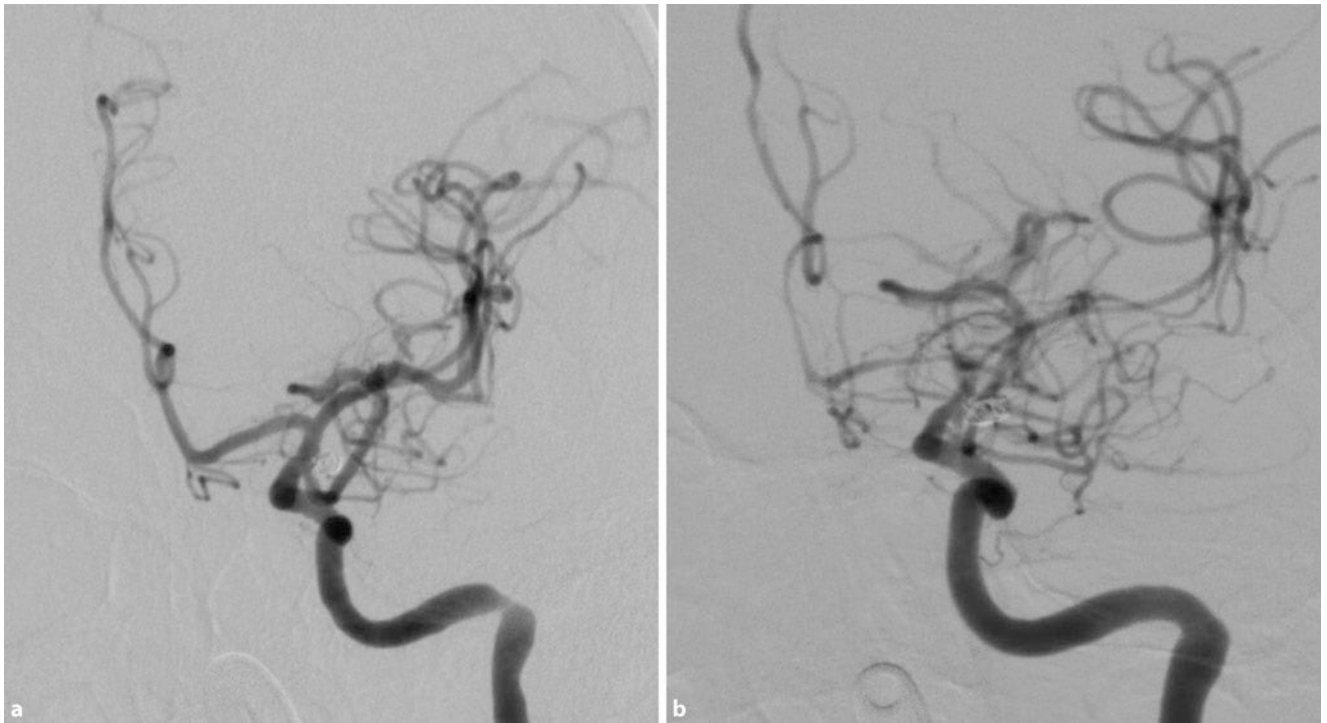
However, **surgery is indicated** if a space-occupying intraparenchymal haematoma is present. Such a haematoma should be surgically removed. As a rule, the aneurysm can be clipped via the same aditus. For aneurysms in which the regional vascular anatomy cannot be clearly shown or in which arteries cannot be revealed, surgery is also the method of choice. This situation is more common in aneurysms at the bifurcation of the middle cerebral artery.

Aneurysms in the posterior circulation are preferably treated endovascularly because of the proximity to the brain stem, the difficult surgical access along the cranial nerves, and the numerous, functionally important perforating arteries from the basilar artery. The results of endovascular treatment are so convincingly positive that a randomised trial is no longer ethically justifiable.

The assumption that vasospasms can be prevented by intra-operative rinsing of the sub-arachnoid cavity with saline and recombinant tissue plasminogen activator (rTPA) to remove sub-arachnoid blood has yet to be confirmed. A comparative study has even shown that in the group of patients treated with coiling, vasospasms occurred less frequently than in the surgically treated group.

After Krayenbühl and Yasargil introduced the microscope during neurovascular operations in 1967/1968, the open treatment of intra-cranial aneurysms has significantly improved, both in terms of clinical outcome and efficiency. In some cases, the additional implementation of an endoscope can provide important information about the configuration of the neck of the aneurysm and the regional vascular anatomy, thereby minimising tissue retraction. In any case, cranial trepanation – albeit not as widespread as 50 years ago – is required to precisely place the clip on the neck of the aneurysm and thereby safely eliminate vascular outpouching from the blood circulation.

However, after clipping of an aneurysm, there may also be residual aneurysmal portions and **recurrent aneurysms**. The rate of recurrent aneurysms is not yet sufficiently known because post-operative angiography is rarely performed. In previous studies, a rate of up to 13% can be specified. In patients with sub-arachnoid haemorrhaging, clinical outcome, procedural morbidity and



■ Fig. 9.60a,b Vasospasm in the case of sub-arachnoid haemorrhaging

mortality are difficult to separate from disease-related complications. A meta-analysis of 2,460 patients with 2,568 non-ruptured, clipped aneurysms revealed a procedural morbidity with 10.9% permanent deficits and a procedural mortality of 2.6%. A higher morbidity was reported for larger aneurysms in the posterior circulation.

**Endovascular Treatment** The development of soft electrolytic detachable platinum coils by Guglielmo (GDC) led to a breakthrough in the endovascular treatment of intra-cranial aneurysms. Using this technique, it is possible to co-axially manoeuvre a specially marked micro-catheter through the guide catheter into each aneurysm immediately after diagnostic angiography. Depending on the size and shape of the aneurysm, a specially designed and selected platinum coil is placed in the aneurysm using the micro-catheter. This coil consists of several components. The most important is a detachment point, the so-called breaking point, which is activated by switching on a DC so that the coil can be electrolytically detached from the insertion wire. A helpful and new development is that the coil can be removed from the aneurysm at any time before it is detached. This is particularly important if the coil is too large or too small and partially extends into the carrier vessel. Few aneurysms can be completely closed with just one coil; in most cases, two or more coils are necessary. The treatment is terminated once the control angiography no longer shows filling of the aneurysm (■ Fig. 9.61). When using conventional platinum coils, a maximum of 30–40% of the lumen of the aneurysm is covered by material.

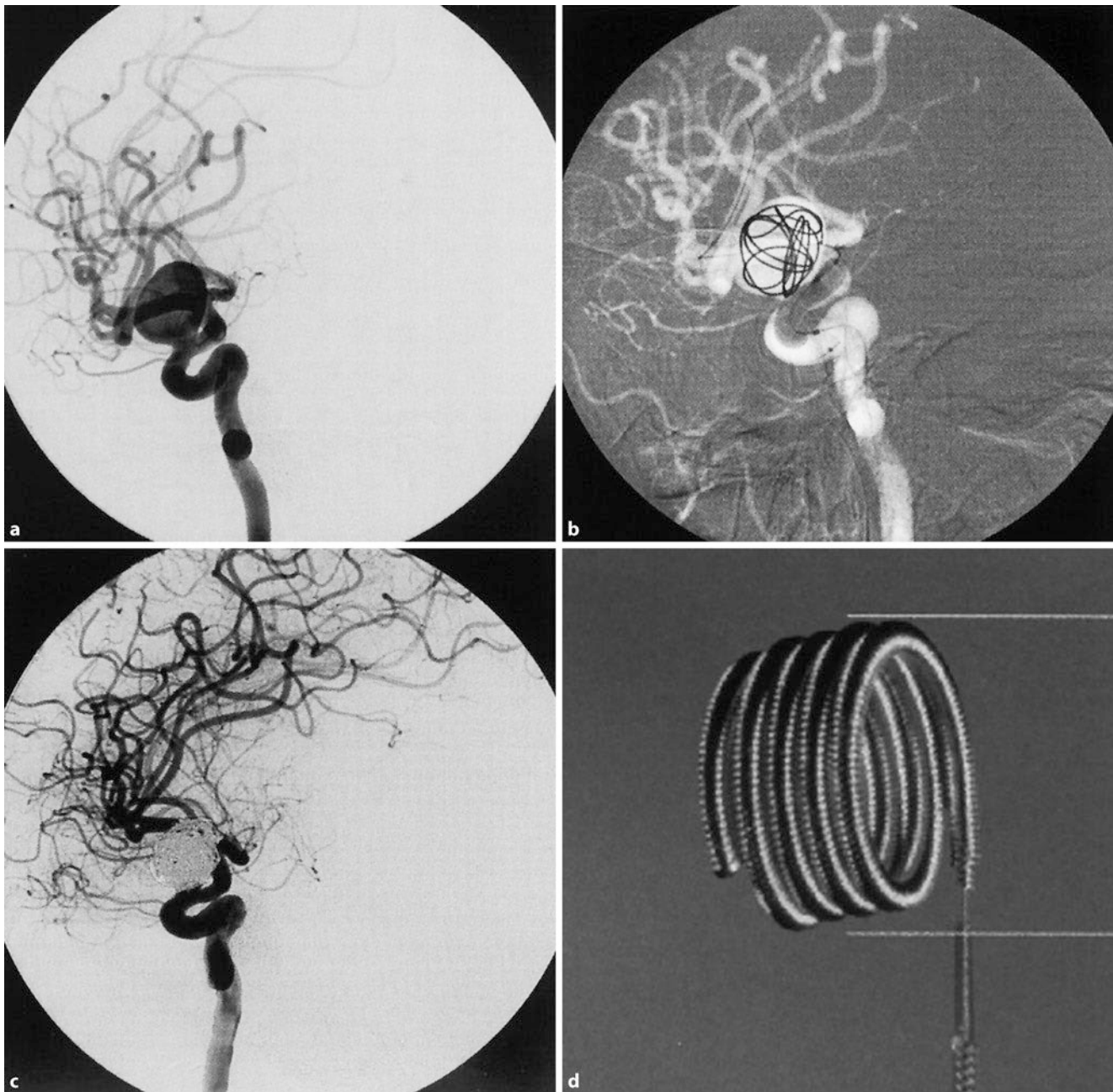
A **disadvantage of endovascular treatment** is that a relatively high rate of recanalisation of the aneurysm is expected. This mainly concerns large aneurysms that are greater than 25 mm in diameter. However, coated platinum coils are now available,

which should minimise the rate of recanalisation. The first results in the application of this novel coated spiral are encouraging. Fluid embolisation (Onyx), which is introduced into the lumen of the aneurysm with the help of a balloon catheter, results in an improved rate of occlusion. In the carrier vessel, the balloon catheter is inflated at the level of the neck of the aneurysm until the liquid is cured. This process is repeated until the aneurysm is completely filled with liquid embolysate.

Although endovascular treatment is “minimally invasive”, it is not without complications. The main **complications** are thrombo-embolic events. Distal vessel occlusions or thrombi that are released from the catheter or aneurysm can appear. However, heparinisation can significantly reduce the rate of thrombo-embolic complications. In 2–3% of cases, an aneurysm rupture occurs during treatment. However, this situation can almost always be controlled by the further introduction of platinum coils into the aneurysm.

Broad-based aneurysms were previously difficult to treat endovascularly. Using intra-cranial stents that are placed on the wide neck of the aneurysm in the carrier vessel, the prolapse of the coil loop in the supporting vessel can be prevented. Alternatively, soft balloons can also be used – the remodelling technique.

**Clinical Outcome of Endovascular Treatment.** With the endovascular procedure, procedural morbidity (3.7%) and mortality (1%) are significantly lower than with neurosurgical clipping. In the prospective, randomised ISAT study, a better clinical outcome was observed in patients treated with platinum coils. Neuro-psychological deficits that do not play a role in the standard evaluation (e.g. with the Glasgow Outcome Scale) are also significantly lower in the case of endovascular treatment. But the decisive factors for the outcome of patients with sub-arachnoid



■ Fig. 9.61a–d Coiling of an aneurysm. a Before, b during and c after coiling. d Platinum coil

haemorrhaging are the severity of the initial haemorrhaging and the quality of intensive care treatment of the complications.

So far, the risk of recurrent haemorrhaging after treating an aneurysm with platinum coils does not appear to be relevantly increased. Nevertheless, patients who received endovascular treatment should undergo follow-up angiography, TOF or contrast-enhanced MR angiography, or a multi-slice CT angiography after 6 months and 1 year to rule out a recanalisation of the aneurysm. If the follow-up examination reveals a recurrence, renewed endovascular treatment may be required. Depending on the findings of the second follow-up, subsequent follow-up examinations can be performed at longer intervals. Because of the thrombogenic materials that are used for the treatment of an aneurysm, increased thrombo-embolic events may occur. In

many clinics, a dose of aspirin (100–300 mg) is recommended for 3–6 months following endovascular treatment.

### 9.3.2 Stroke

- Stroke in Adults: Basics
- Definition, Aetiology

The symptoms of stroke subsume a number of different disorders. Most commonly, the stroke is caused by cerebral ischaemia (70–80%) or intra-cerebral haemorrhaging (approximately 15–20%). In addition to sub-arachnoid haemorrhaging (2–5%), tumours, inflammations and epileptic seizures cause a stroke. This leads to sudden, sub-acute, focal neurological symptoms, which de-



**Fig. 9.62** Lacunar infarct in the thalamus. A 75-year-old patient with newly occurring hemiparesis. 48 h after the onset of clinical symptomatology, the CT reveals a lacunar lesion in the right thalamus

pend on the affected brain region. Accurate differentiation, e.g. between intra-cerebral haemorrhaging and ischaemia is often clinically impossible; here, the cause is determined via imaging.

The stroke, acute circulatory disorder of the brain, is not a uniform disease; it can have many causes. **Microcirculatory disturbances** account for about 30–35% of all cerebral infarcts. They manifest as acute lacunar infarcts (■ Fig. 9.62) and chronically in sub-cortical arterio-sclerotic encephalopathy (SAE) (■ Fig. 9.63). The most important risk factor is hypertension. **Macrocirculation disorders** that lead to territorial (■ Fig. 9.64) or haemodynamic infarcts (■ Fig. 9.65), are the cause of an additional 45–60%. They are often caused by cardiac embolism in the case of absolute ar-

rhythmia, heart valve replacement or an open oval foramen, and arterio-arterial embolism at the base of arterio-sclerotic vascular changes such as carotid stenosis in addition to local thromboses such as atherosclerosis, arteritis, or coagulation disorders. The combination of micro- and macro-circulation disorders is responsible for 10–20% of cerebral infarcts. Another 10% cannot be reliably classified.

In the last 10 years, the treatment possibilities for stroke have substantially increased, mainly through the establishment of stroke unit treatment and the introduction of fibrinolysis. Although treatment methods are as diverse as the causes of strokes, there are important principles for ischaemic cerebral infarcts, which will be discussed below.

## ■ Ischaemic Stroke

### ■ Epidemiology

Depending on geographic division, strokes can be expected at a rate of 700 in 100,000 per year. Currently, the highest incidences can be found in the Eastern European countries, while lower rates can be found in the Western European countries, Scandinavia and North America. Approximately 80–85% of patients in the acute phase survive the first stroke. Of these patients, 8–15% suffer from a second stroke in the first year. Here, the risk is highest in the first few weeks and decreases with increasing time. Patients with multiple vascular risk factors or those with concomitant coronary artery disease or peripheral arterial disease are particularly vulnerable. In the case of transient ischaemic attacks, patients with cerebral symptoms are more vulnerable than those with retinal symptoms (amaurosis fugax). Patients older than 60 with symptoms of paralysis or speech disorders lasting longer than 10 min are also at risk. The greatest risk is in the first 3 days after a transient ischaemic attack.

### ■ Course and Prognosis

Approximately 15% of patients with an **ischaemic insult** die within the first 3 months. Through improvements in the treatment concept, approximately 40% of patients can be expected

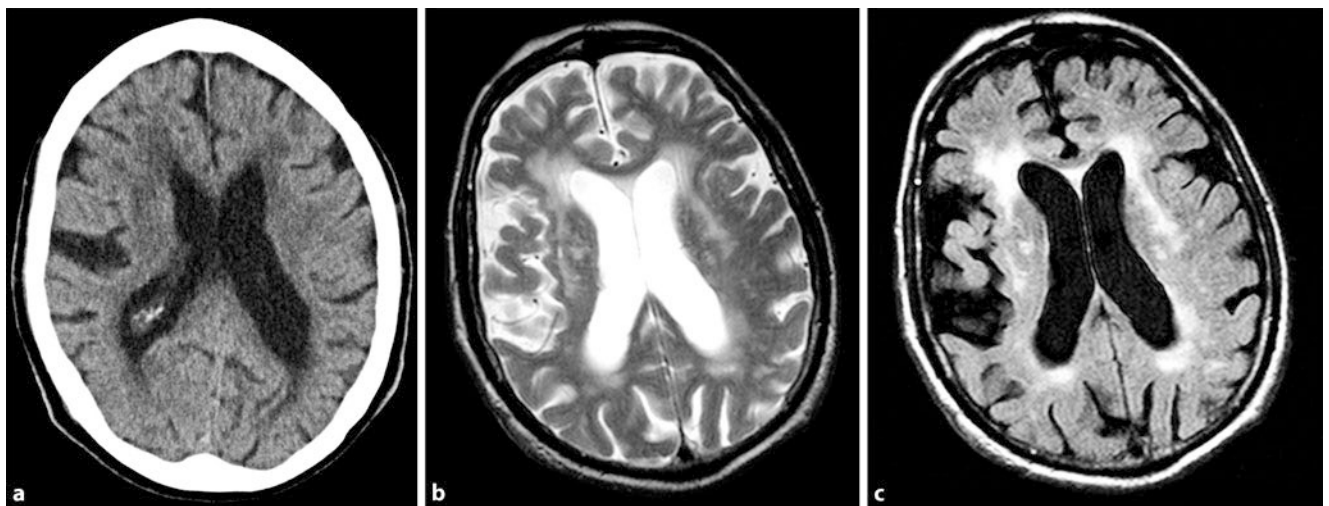
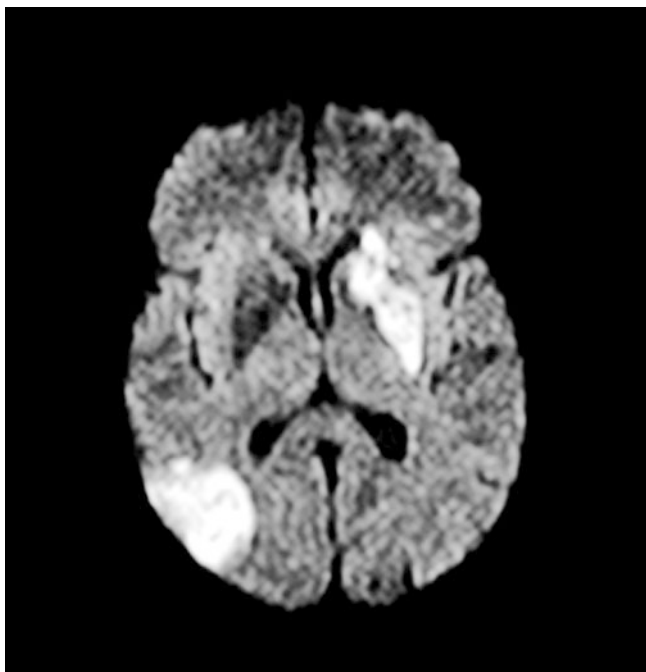
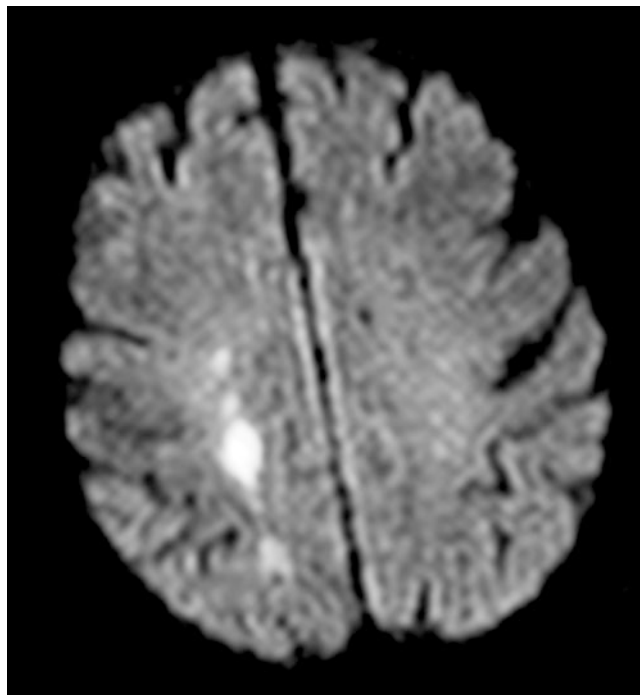


**Fig. 9.63a–c** Sub-cortical arterio-sclerotic encephalopathy (SAE). An 82-year-old patient with long-standing hypertension. a On the axial CT images, confluent hypo-density, mainly in the frontal-parietal white matter and less

pronounced in the peri-ventricular white matter. In addition, there is significant expansion of the inner and outer CSF spaces. On the b T2-weighted and c FLAIR sequences the diffuse changes in white matter are depicted as hyper-intensity.



■ **Fig. 9.64 Territorial infarct.** On the diffusion-weighted sequence, a signal increase in the left basal ganglia area and in the right posterior median distribution area, consistent with fresh ischaemia, most likely of cardio-embolic aetiology



■ **Fig. 9.65 Haemodynamic infarct.** Increased signal intensity on the diffusion-weighted sequence, matches fresh ischaemia in a 72-year-old patient with upstream filiform right internal carotid artery stenosis

to lead an unobstructed life following the first stroke. The risk profile for cerebral ischaemia is relatively well known; the greatest risk factor is arterial hypertension. The consistent treatment of hypertension with both primary and secondary prevention reduces the risk of stroke. The risk of ischaemic stroke increases with age, particularly in the case of atrial fibrillation, left ventricular insufficiency, or diabetes mellitus. Men are more likely to be affected than women. The second largest risk factor is nicotine abuse. Known risk factors also include alcohol, obesity and hyperlipidaemia.

The **treatment of risk factors** includes:

- Consistent treatment of arterial hypertension
- Treatment of diabetes mellitus
- In patients with focal cerebral ischaemia and coronary heart disease, statins should be used independently of the baseline values of LDL cholesterol.

#### ■ ■ **Diagnosis, Treatment**

Each acute stroke is an emergency. Briefing must therefore be done in a stroke unit (SU). An SU is a treatment unit in which the necessary diagnosis, treatment, and the corresponding monitoring is carried out around the clock by a specialised medical and nursing team under the constant guidance of a neurologist. The continuous 24-h availability includes cerebral CT (CCT) or MRI, Doppler/duplex ultrasound, trans-thoracic or trans-oesophageal echo-cardiography, an internist with cardiac competence, intensive medical treatment options, the rapid availability of a neuro-surgical department, clinical and instrument-based monitoring, and the possibility of fibrinolysis. Participation in recognised external quality assurance is mandatory.

For the prognosis of the patients, it is crucial that they be brought to a hospital specialising in coronary heart disease as quickly as possible. The **pre-hospitalisation measures** serve to confirm the diagnosis and the vital parameters. If crossed neurological symptoms indicate acute brain-stem infarction or if the patient demonstrates severely impaired consciousness, he or she should be admitted to a supra-regional stroke unit that has the capability of performing direct angiography for the indication of fibrinolysis. Apart from the neurological symptoms, the monitoring includes the vital parameters, i.e. respiration, blood pressure, cardiac output and blood sugar (■ Table 9.5). It must be noted that in the acute phase, blood pressure of up to 220/120 mmHg is tolerated and no schematic reduction of blood pressure occurs. The patient's prognosis will otherwise worsen (see below). For exactly this reason, it is important to ensure unhindered breathing with high O<sub>2</sub> and low CO<sub>2</sub>.

Acute basic therapy is as follows:

- High O<sub>2</sub> and respiratory rate
- Low blood sugar and body temperature
- Infection prophylaxis

**Respiration** The airway must be kept clear, so that an optimal peripheral oxygen saturation of greater 95% can be achieved, possibly via continuous administration of oxygen by a nasal tube (2–4l/min). Equally important are optimal pCO<sub>2</sub> values of 35–40 mmHg. Indications for mechanical ventilation are:

- pO<sub>2</sub> < 50 mmHg
- pCO<sub>2</sub> > 55 mmHg
- Respiratory exhaustion
- Severe vigilance disorder
- Brain-stem lesion with increased risk of aspiration

**Table 9.5** Treatment of stroke in the prehospital phase

Treatment options for vital signs	
Hypoxaemia	4 l of O <sub>2</sub> via a naso-gastric tube
Respiratory rate < 220/120 mmHg	No reduction in respiratory rate
Respiratory rate > 220/120 mmHg	Slow reduction in respiratory rate
Hypotension and/or dehydration	Fluid substitution (i.v. Ringer's solution)
Hypoglycaemia < 80 mg %	Glucose 40% 30 ml i.v.
Hyperglycaemia 160 mg %	2 IE short-acting insulin as a bolus
Hyperglycaemia 200 mg %	4 IU short-acting insulin as a bolus
Heart failure, relevant cardiac arrhythmia	See further reading
Seizure	Clonazepam 1–2 mg i.v.
Aspiration risk	Gastric tube
Body temperature	Therapy for fever > 37.5°C

**Blood Pressure** Because of a central regulatory mechanism, within the first three days, 75–80% of all stroke patients exhibit increased blood pressure values (with or without reversal of the circadian rhythm), which normalise within 1 week or decrease to hypertension-related values. In one third of stroke patients, it could be demonstrated that high blood pressure values of up to 230 mmHg could reduce clinical deterioration during the first 3 days. In patients with existing hypertension, target values of

180 mmHg systolic and 100–105 mmHg diastolic are recommended. In previously normotensive patients, values between 160–180 mmHg systolic and 90–100 mmHg diastolic should be striven for.

**Blood Sugar** Elevated blood sugar levels lead to cerebral oedema (via a lactic acidosis), increased intra-cranial pressure, and a deteriorating prognosis of the patient. With diffusion- and perfusion-weighted MRI, it could be demonstrated that in the case of equivalently sized penumbra at the beginning of the cerebral infarct, the final infarct volume in normoglycaemic patients was smaller than in the hyper-glycaemic patients. Blood glucose values between 100 and 150 mg/dl are therefore desirable.

**Body Temperature** Increased body temperatures negatively affect the morbidity and mortality of stroke patients. The prophylaxis of infections, especially pneumonia and urinary tract infection, remains at the forefront. Physical measures, such as storage and physiotherapy, are important in addition to the timely detection of stroke-induced aspiration and prevention via the early implementation of a stomach tube or PEG. Efficient anti-pyretic therapy is recommended from values of 37.5°C.

**Intra-cranial Pressure** The treatment of increased intra-cranial pressure (ICP) and cerebral oedema occurs via graduated measures. An ICP greater than 20 mmHg requires treatment. Basic treatments include normoglycaemia, normothermia and normocapnia in addition to sufficient oxygenation and sedation. Moderately elevated blood pressure values should be tolerated.

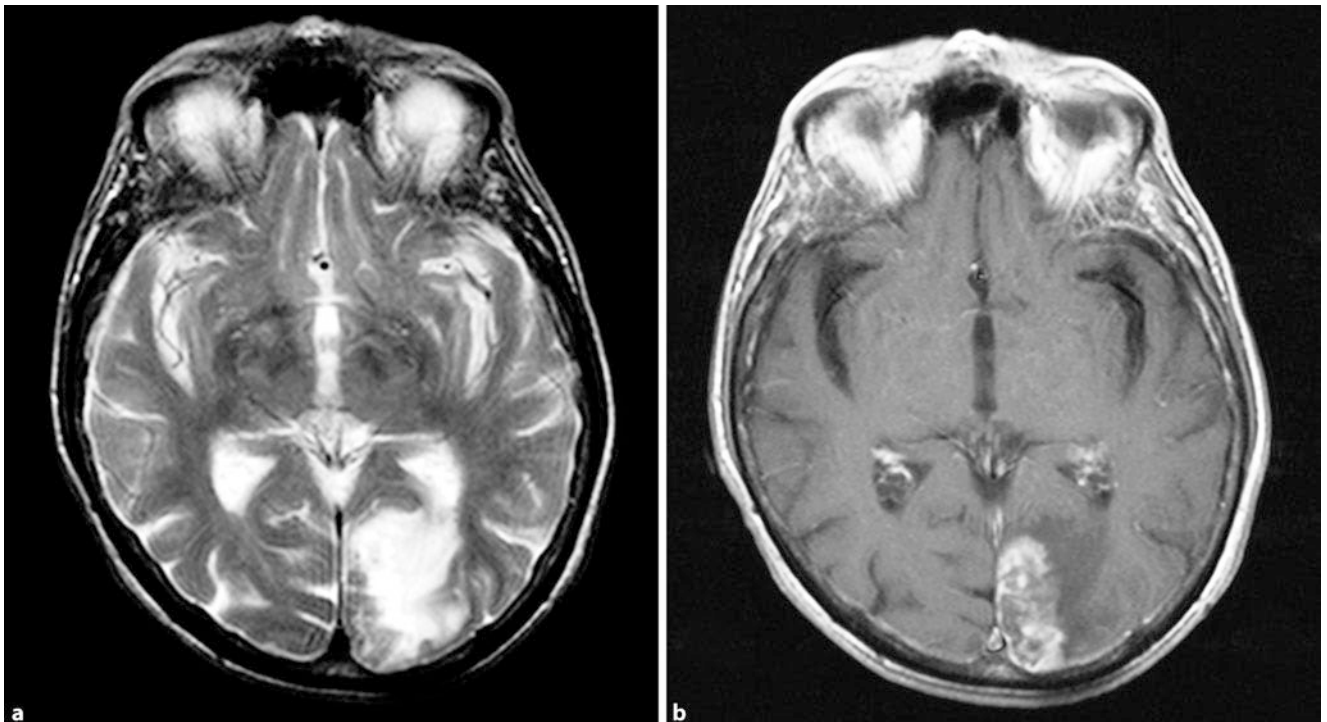


**Fig. 9.66a,b** Blood flow after ischaemia, haemorrhagic transformation. **a** The axial T2-weighted image reveals a posterior infarct: a 78-year-old patient

who has had hemi-anopia for 7 days. **b** On the T1-weighted image, irregular hyperintensity corresponding to blood in the methaemoglobin stage

In any case, the blood pressure must be reduced before the ICP. Otherwise, the cerebral perfusion pressure may drop to critical levels.

**Decompressive Craniectomy** According to some studies, hemi-craniectomy (■ Fig. 9.67) decreases the mortality from 80 to 40% in large, space-occupying malignant media infarcts. A malignant media infarct should be expected if more than two thirds of the territory are affected, especially when dealing with younger patients. The trepanation should be sufficiently large and have a diameter of 12–14 cm.

In **cerebellar infarcts**, CSF obstruction and local compression of the brain-stem may occur in individual cases despite the intra-cranial pressure treatment. In the case of an increasingly severe vigilance disorder, they are an indication for external ventricular drainage and surgical decompression via sub-occipital trepanation. In comatose patients, intervention can reduce mortality from 80 to 30%. Pre-requisites are increasing hydrocephalus detected via CCT or MRI or compression of the fourth ventricles and the basal cisterns.

**Hypothermia** There is much evidence of the neuro-protective effect of hypothermia, However, because of the potentially serious complications, this is still an experimental approach and should only be taken by clinics with suitable experience.

**Fibrinolysis** Intra-venous fibrinolysis with rtPA in the anterior cerebral distribution is the treatment with the highest degree of evidence and the highest effectivity. It is more than twice as efficient at reducing death and disability in a cerebral infarct than in a myocardial infarct. The success of the fibrinolysis depends on the earliest possible recanalisation of the vessel and the lowest possible rate of severe intra-cerebral haemorrhaging into the remaining infarcted area. The clinically relevant intra-cerebral haemorrhaging should not be confused with the relatively frequent haemorrhagic transformation of ischaemic tissue, which does not usually lead to clinical deterioration. There are therefore limitations to the indication for lysis that mainly concern the therapeutic time window and the severity of the clinical symptoms. In Germany, fibrinolysis with rtPA for the treatment of ischaemic cerebral infarction is permitted within 3 h of the event (■ Fig. 9.68). Within this time window, the shorter the span between the onset of symptoms and the start of treatment (symptom to needle time), the greater the effectiveness. The “number needed to treat” is therefore only half as high if the lysis is performed within 1.5 h (4) instead of 3 h (9).

**Study Data.** In Germany, fibrinolysis must be carried out by a trusted team led by an experienced neurologist, and further treatment in an SU must be ensured. According to a meta-analysis of the National Institute of Neurological Disorders and Stroke (NINDS) study, the admission of patients older than 80 years is not justified. The meta-analysis has further shown that all types of infarction regardless of gender, medical history and clinical status benefit from fibrinolysis. Because of the increased risk of haemorrhaging with large infarcts, it is only sensible in medium



■ Fig. 9.67 Hemi-craniectomy. Large trepanation in malignant infarct to relieve pressure

neurological deficits, which correspond to NIH Stroke Scale values between 4 and 26.

After experience from the **European rtPA trials**, early CCT-based infarct signs in more than 33% of the media distribution area are usually regarded as a contra-indication because the risk of severe intra-cerebral haemorrhaging otherwise appears to be too large. However, this concept is also not supported by the conclusive North American NINDS study because after a post-hoc analysis, early CCT-based ischaemic signs in less than 33% of the distribution area were neither decisive for the success of lysis nor for the complications. Patients who displayed earlier symptoms of ischaemia in the CCT benefited particularly well from the lysis. It therefore makes sense to replace this criterion with the finding after mismatch concept (see below). Pre-requisites, contra-indications, and implementation must therefore be individually orientated to each case. Vascular imaging is not required. It is, however, useful for assessing the course provided that it does not delay the start of treatment. Successful recanalisation is more likely in the case of a distal vessel occlusion than in a proximal vessel occlusion. However, a proximal carotid occlusion or a distal carotid T occlusion are not contra-indications for an i.v. lysis. A pre-requisite for success is the presence of a penumbra (see below). The RtPA dose is 0.9 mg/kg body weight (up to 90 mg).

**PWI–DWI Mismatch.** In the 3- to 6-h window, fibrinolysis is also effective, but to a much lesser extent unless there is still a large Diffusion-weighted imaging and perfusion-weighted imaging (PWI–DWI) mismatch in the patient. Because the effectiveness of the lysis is dependent on the presence of a penumbra regard-

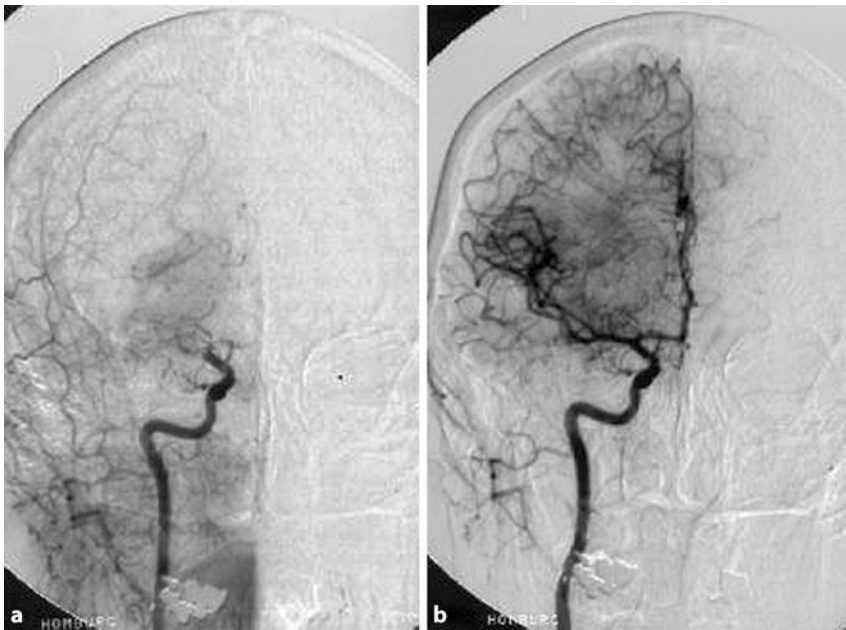


**Fig. 9.68a,b Medialysis.** **a** On angiography, the closure of the middle cerebral artery is depicted. **b** After thrombolysis, the complete reopening of the occluded vessel

less of the time window, the diagnostic option to depict this as a perfusion–diffusion mismatch on MRI or CT (PWI–DWI mismatch) should be used more frequently (■ Fig. 9.69). The PWI MRI shows the area in which the blood flow is disturbed. The DWI image depicts the infarct. The blood flow is so strongly decreased that the structure metabolism has collapsed and irreversible tissue damage has occurred. The difference, i.e. the mismatch, between PWI and DWI corresponds to the **penumbra**, the area in which the reduced blood flow has led to a loss of function, but still no structure destruction and which should still be saved by the lysis. Patients with a relevant PWI–DWI mismatch are thus suitable candidates for a successful lysis, regardless of the time window. Even in this non-approved time window, this investigation is a pre-requisite to conducting intra-venous lysis as part of an individual treatment experiment and corresponding study protocol in experienced centres.

**Intra-arterial Thrombolysis in the Anterior Circulation Area** Intra-arterial catheter lysis with pro-urokinase, which has not yet been approved, is safe and effective within a window of up to 6 h. It leads to a higher and more rapid recanalisation rate and offers the opportunity to mechanically break up the clot, thus further improving the chances of recanalisation. However, it is bound to a correspondingly specialised and available team in addition to highly complex apparatus. The pre-requisite for this is the presence of a PWI–DWI mismatch. Urokinase or rtPA was previously used as a fibrinolytic agent.

The **bridging method** combines the intra-venous and intra-arterial applications. To avoid losing time up to the angiography, a part of the rtPA dose or a thrombolytic agent (e.g. abciximab) is administered directly as a bolus after the decision to lyse.

The remaining fibrinolytic agent is then administered intra-arterially via the catheter as a local lysis. According to the pilot study, a higher recanalisation rate and a better outcome were achieved compared with systemic lysis alone.

In pilot studies, **mechanical extraction of the thrombus** has also proven to be promising; using a variety of mechanical systems, the thrombus can be removed from the vessel with a relatively high recanalisation rate (sometimes up to 90%).

#### Procedure for intra-venous thrombolysis with rtPA in the Anterior Cerebral Circulation

Prerequisites:

- Exclusion of intra-cranial bleeding on CCT/MRI
- Time interval between onset of symptoms and start of thrombolysis is less than 3 h (see text for details)
- Medium neurological deficit (NIH Stroke Scale between four and twenty-six.)
- PWI–DWI mismatch

Contraindications:

- Intra-cerebral haemorrhaging
- Early symptoms of infarct on the CCT (hypo-density of the supply region of the middle cerebral artery: more than one third)
- Fixed head and/or gaze deviation with hemiplegia or more than somnolent consciousness disturbance as symptoms of a very large infarct

For further information, see technical information

Implementation:

- rtPA 0.9 mg/kg body weight, 10% as an i.v. bolus; maximum 90 mg
- Rest in 40 ml of 0.9% NaCl i.v. continuously over 1 h
- Heparin or anti-platelet drugs no earlier than 24 h

**Thrombolysis in the Case of Basilar Thrombosis** Circulatory disorders in the case of basilar artery occlusion or partial thrombosis are life-threatening and lead to 50% mortality. Immediate diagnosis and treatment in a national SU are required. For mid-



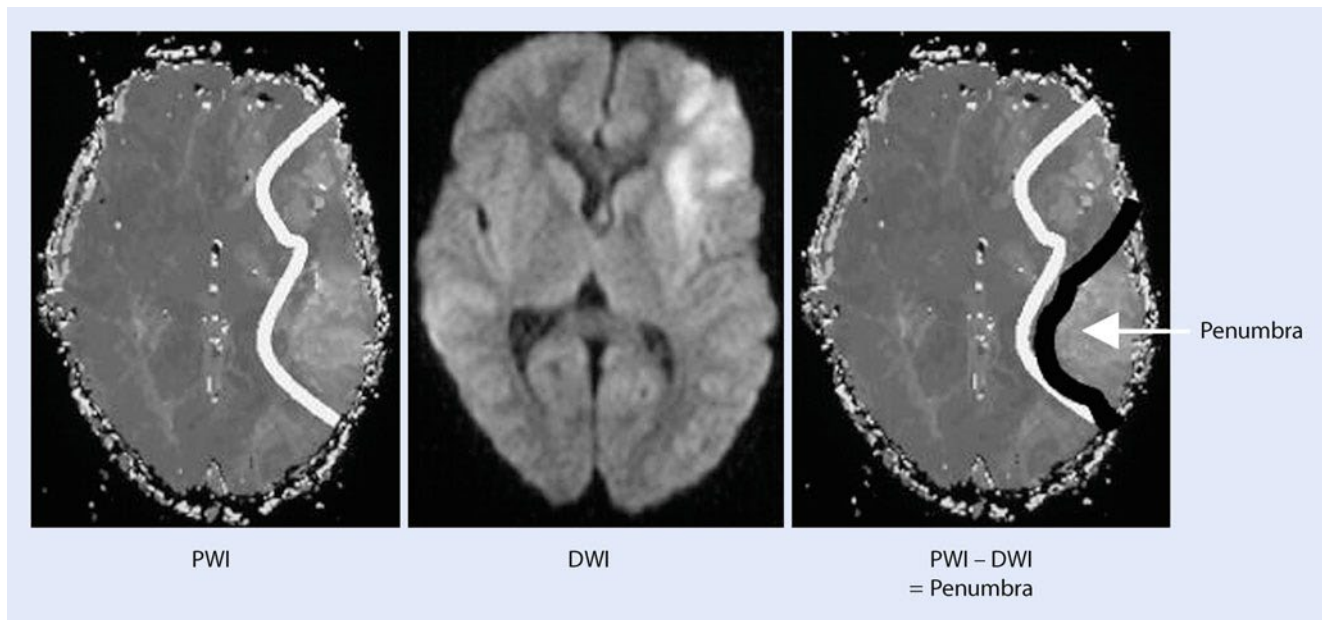


**Fig. 9.69 PWI–DWI mismatch.** Fresh ischaemia in accordance with the hyper-intensity of the diffusion-weighted image (*DWI*). The perfusion deficit in the perfusion-weighted imaging (*PWI*) is significantly larger; this mismatch

corresponds to the tissue at risk. It is postulated that this area might be saved by therapy, a thrombolysis, before infarction

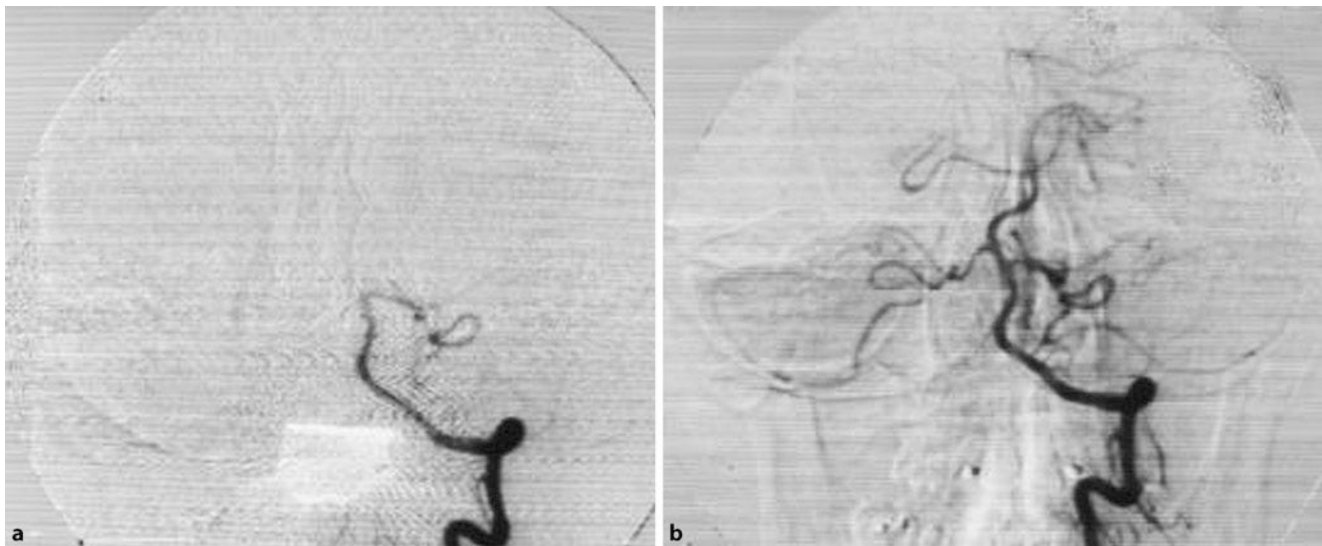


**Fig. 9.70a,b Basilar thrombosis and lysis.** On DSA, occlusion of the middle portion of the basilar artery can be seen. After 1.0 million units of urokinase,

the basilar artery is once again completely recanalised. The right posterior cerebral artery extends directly from the right internal carotid artery

grade and severe neurological symptoms, intra-arterial catheter thrombolysis is indicated with or without the bridging method (■ Fig. 9.70).

There are not enough studies to be able to recommend the time frame of implementation or the thrombolytic agent to be used. Compared with lysis in the anterior circulation, the time window is significantly larger (less than 12 h, in some cases up to 24 h). Key exclusion criteria are immobile dilated pupils, coma for 2–4 h and fresh infarcts in the vertebra-basilar distribution area depicted as hypo-density in CCT. In specialised centres, the lysis is performed with urokinase (up to 1.5 million IU) or rtPA (70–90 mg fractionated). With the double-shot procedure, the

intra-arterial rtPA fibrinolysis is combined with the subsequent intra-venous administration of a GP IIa/IIIb inhibitor such as abciximab.

**Early Secondary Prophylaxis** Early secondary prophylaxis should prevent reinfarction in the acute phase. The following options are available:

1. Platelet inhibitors: the effectiveness of an early treatment with acetyl-salicylic acid as a reinfarction prophylaxis has been proven in various studies. It is not especially high, but is generally recommended in the guidelines. The dosage ranges from 100 to 300 mg ASA/day.

2. Early anticoagulation with heparin for cardio-embolic infarcts: until recently, full heparinisation was used quite frequently in some clinics. This is now almost only used in the case of cardio-embolic aetiology and dissection. The basis of this approach is the confirmed studies.

Phenprocoumon therapy is the most effective reinfarction prophylaxis (risk reduction of 75%) in the secondary prophylaxis of cardio-embolic cerebral infarcts outside the acute phase. However, the risk of re-embolism was highest immediately after the acute stroke. Nevertheless, in various studies, the prophylactic effect of early partial thromboplastin time (PTT)-active complete heparinisation could not be unequivocally demonstrated. The increased rate of intra-cerebral haemorrhaging and the resulting clinical deterioration cancelled out the benefits of the reduced rate of recurrence. Surprisingly enough, in North America, there is still a great discrepancy between the lack of literature and daily practice. Nearly 90% of cardio-embolic infarcts are still completely heparinised. In summary, however, in view of the unsatisfactory scientific findings, there is no evidence-based foundation for early anti-coagulation with heparin; thus, it is at best considered when it is certain that there is a high risk of recurrence.

3. Early anti-coagulation with heparin in the case of carotid artery dissection: the incidence of dissection as a cause of cerebral infarct is considerably high at 3 in 100,000 per year. It mainly affects younger patients. In patients under 45 years of age, it causes 15% of cases of cerebral infarcts. It is often associated with typical pain in the neck. The angiography is characterised by a flame-like narrowing of the vessel. Here, there is also no experimentally proven evidence for complete heparinisation. However, because of the high rate of re-infarction and frequently achieved recanalisation, a two- to three-fold increase in PTT is recommended in many guidelines. Vascular surgery or an alternative interventional stent implantation only comes into question in the case of high-grade stenoses and accompanying infarcts, especially those that are haemodynamic. It included phenprocoumon therapy with an international normalised ratio (INR) of 2.0–3.0 over months. The vascular findings for the exclusion of a stenosis or pseudo-aneurysm are then clarified by angiography or Doppler ultrasound. In the case of normal vascular conditions, drug therapy is stopped. In the case of persisting embolism-prone vascular changes, an anti-platelet agent is used. A pseudo-aneurysm does not justify permanent anti-coagulation.

4. Other measures:

- The importance of early mobilisation in the SU was confirmed in Scandinavian studies
- Pneumonia, decubitus and thrombo-prophylaxis with low-dose heparinisation also rate highly
- Health training to combat the risk factors (e.g. smoking, hypertension, diabetes mellitus, obesity, physical inactivity and hyperlipidaemia) must begin at a person's sick bed.
- Depending on the degree of severity and type of neurological deficits, including neuro-psychological defects, 35% of patients undergo rehabilitative treatment.

- Consistent secondary prophylaxis with anti-platelet agents reduces the risk of reinfarction by up to 30%. Hypertension treatment reduces the risk by 50%. Phenprocoumon therapy in the case of cardiac embolisms caused by absolute arrhythmia reduces the risk by 75%.
- Approximately 10% of patients develop symptomatic epilepsy, and 50% develop depression, which delays the regaining of independence and integration into daily life as a result of social withdrawal.

## ■ Intra-cerebral Haemorrhaging

### ■ Aetiology

The clinical presentation of intra-cerebral haemorrhage is varied and ranges from the severe, acute onset of headache with or without neurological deficits to sub-acute courses without pain symptoms. Approximately 15% of impact seizures can be traced to intra-cerebral haemorrhaging, and approximately 2–5% can be traced to sub-arachnoid haemorrhaging.

### ■ Epidemiology, Aetiology

The annual incidence of intra-cerebral haemorrhaging is 10–15 in 100,000. Men and women are equally affected.

Causes of spontaneous, non-traumatic intra-cerebral haemorrhaging are:

- Hypertension (in more than 60% of cases)
- Alcoholism (approximately 10%)
- Amyloid angiopathy or vascular malformations (approximately 10%)
- Rare blood diseases and coagulation disorders, tumours, venous thrombosis and intoxication

Non-traumatic cerebral haemorrhages most occur often in the fifth to seventh decade of life, especially in connection with arterial hypertension, which leads to vascular changes such as hyalinosis and micro-aneurysms. The risk of suffering from intra-cerebral haemorrhaging increases markedly with age. In patients up to 45 years of age, sub-arachnoid haemorrhaging is more common than intra-cerebral haemorrhaging. Intra-cerebral haemorrhaging predominates thereafter. In younger patients, aneurysms of the cerebral arteries and AVMs (► Sect. 9.3.1), rare brain tumours, blood clotting disorders, inflammation, and venous sinus thrombosis should be considered as causes.

### ■ Prognosis

The mortality of intra-cerebral haemorrhaging, which depends heavily on the size and location, is between 30 and 50%. The greater the haemorrhaging, the worse the prognosis: if the blood haemorrhaging volume exceeds 100 ml, mortality increases to 90%. An early coma in addition to bleeding in the thalamus and brain-stem also provide a worse prognosis. Other unfavourable prognostic factors include an invasion of the haemorrhaging into the ventricular system or the sub-arachnoid space.

### ■ Medical Imaging

Diagnostic imaging is primarily used to distinguish between cerebral ischaemia and intra-cerebral haemorrhaging or sub-

■ **Table 9.6** Signal characteristics of intra-cerebral haemorrhaging on spin echo (SE) sequences

Biochemical form	Time	T2	T1
Oxyhaemoglobin	> 24 h	Hyper-intense	Hypo-intense to iso-intense
Deoxyhaemoglobin	Several hours to days	Hypo-intense	Hypo-intense to iso-intense
Methaemoglobin – Intra-cellular – Extra-cellular	– > 3 days – > 7 days to months	– Hypointense – Hyperintense	– Hyperintense – Hyperintense
Ferritin/haemosiderin	> 14 days	Hypo-intense	Hypo-intense to iso-intense

arachnoid haemorrhaging and thus forms the pre-requisite for continuing specific treatment. The exact location and extent of intra-cerebral haemorrhaging or sub-arachnoid haemorrhaging can be clearly and reliably observed with CT. Sub-acute and chronic haemorrhaging, however, are more reliably diagnosed with MRI. Until now, MRI was not considered to be particularly sensitive in the early diagnosis of intra-cerebral haemorrhaging. However, recent studies show that MRI is highly capable of clearly depicting intra-cerebral haemorrhaging in the acute phase if the appropriate MR sequences are used (■ Table 9.6). Based on the different signalling on the various MR sequences, the age of the haemorrhaging can be inferred.

In the differential diagnosis of intra-cerebral haemorrhaging, the following questions arise:

- Are there known risk factors such as hypertension or alcoholism?
- Does the individual suffer from existing coagulation disorders or are coagulation agents such as phenprocoumon, heparin, fibrinolytics or contraceptives taken?
- Does the individual suffer from a malignant primary disease, endocarditis, or collagenosis?
- Is there evidence of a recently suffered ischaemic infarction?

### ■ ■ Types of Haemorrhaging

**Hypertensive Haemorrhaging of the basal ganglia** (■ Fig. 9.71) is viewed as the classic hypertensive mass haemorrhaging. The basal ganglia are supplied by perforating arteries, which have thinner walls than cortical arteries of the same diameter. Chronic hypertension leads to vascular wall changes with fibrinoid necrosis, sub-intimal lipohyalinosis with adipose deposits, and the formation of micro-aneurysms. In the case of reduced vaso-reactivity, an additional increase in blood pressure can no longer be compensated for and lead to so-called **haemorrhaging per rhexis**. The hypertensive mass haemorrhaging is typically located in:

- Basal ganglia (approximately 40%)
- Sub-cortical white matter (approximately 25%)
- Thalamus (approximately 20%)
- Cerebellum (approximately 10%)
- Pons (approximately 5%)

Especially in the case of thalamic haemorrhaging and medial haemorrhaging of the basal ganglia, the haemorrhaging can invade the ventricular system. Purely intra-ventricular haem-



■ **Fig. 9.71** Haemorrhaging of the basal ganglia. On the CT of this 58-year-old patient, hyper-density can be observed in the lateral basal ganglia; this is the typical image of lateral hypertensive haemorrhaging in the basal ganglia

orrhaging rarely occurs. A complication of intra-ventricular haemorrhaging is the formation of a disturbance in CSF circulation caused by displacement of the aqueduct, which in turn is caused by coagulated blood or the adhesion of Pacchioni's granulations.

**Haemorrhaging in Amyloid Angiopathies** Atypical intra-cerebral haemorrhaging in patients over 70 years, so-called **lobar haemorrhaging** (■ Fig. 9.72) is frequently the result of amyloid angiopathy. It mostly appears parietally or occipitally and less frequently temporally. Haemorrhaging near the cortex can lead to involvement of the sub-arachnoid. Lobar haemorrhaging in younger patients should always lead to the suspicion of a vascular malformation (e.g. a dural fistula, an AVM, or an atypically located aneurysm).



**Fig. 9.72** Haemorrhage in the case of amyloid angiopathy. Left parieto-occipital haemorrhaging in an 84-year-old woman, allegedly in the case of angiopathy. (From *Radiologie* 1999;39:828–838, p. 830, Fig. 2)

▶ **Bleeding at the base of an amyloid angiopathy can only be ascertained histologically, but is assumed to be likely if there is a medical history of relapsing haemorrhaging in the sub-cortical white matter of elderly patients without hypertension.**

**Haemorrhaging After Taking Anti-coagulant and Thrombolytic Substances** The annual risk of suffering intra-cerebral haemorrhaging whilst undergoing phenprocoumon therapy is 0.5–1%. Approximately 5% of all intra-cerebral haemorrhaging occurs whilst undergoing therapy with warfarin or heparin. Only one third of patients present with an overdose. The intra-cerebral haemorrhages are often very large and are usually found sub-cortically in the medullary layer. Fluid levels are detectable within the haematoma in addition to hypo-dense areas suggestive of hyper-acute haemorrhaging. Secondary intra-cerebral haemorrhaging resulting from the use of anti-coagulants and thrombolysis is divided into:

- Clinically silent haemorrhagic transformation
- Parenchymal haemorrhaging

A haemorrhagic transformation occurs in approximately 60–70% of patients with embolic cerebral infarcts. A parenchymal haemorrhage after infarction almost always leads to clinical deterioration. The risk of intra-cerebral haemorrhaging following thrombolytic therapy of a myocardial infarct is between

0.5 and 2%. In approximately 6–15% of cases, thrombolysis in cerebral ischaemia leads to intra-cerebral parenchymal haemorrhaging.

**Intra-cerebral Haemorrhaging in Blood Disorders** In blood disorders, particularly leukaemia, intra-cerebral haemorrhaging may occur. There are no criteria to distinguish haemorrhaging caused by leukaemia from other intra-cerebral haematomas.

**Sinus and Cerebral Venous Thrombosis** This can lead to congestive haemorrhaging with haemorrhagic infarcts in the catchment area of the closed veins (see below). However, expansive intra-cerebral or sub-dural haemorrhaging caused by the rupture of venous collaterals may also occur. If the superior sagittal sinus closes, bilateral haemorrhaging often occurs in the sub-cortical white matter of the cerebral hemispheres.

**Haemorrhaging Tumours** This may be the first manifestation of a cerebral tumour or can result in the deterioration of an existing neurological deficit. These are usually the brain's own malignant tumours or metastases. Metastases of malignant melanomas in addition to bronchial carcinomas, renal carcinomas, mammary carcinomas, thyroid carcinomas, and choriocarcinomas bleed particularly often. Metastases more frequently lead to sub-cortical haemorrhaging, while glioblastomas often cause more deeply situated haemorrhaging. Of the brain's own tumours, glioblastomas and oligodendrogliomas bleed most frequently. However, almost any intra-cerebral tumour can haemorrhage. The incidence of haemorrhagic tumours is 1–15%. Relatively early extensive oedema in addition to a heterogeneous and irregularly shaped hyper-density suggest a haemorrhagic tumour. After the administration of contrast agent, there is often additional disturbance of the blood–brain barrier. The underlying tumour is usually first detected during follow-up examinations if the haemorrhaging is largely absorbed.

▶ **A reliable distinction between a haemorrhagic tumour and spontaneous intra-cerebral haemorrhaging is usually not possible. On MRI, an incomplete haemosiderin ring rather suggests a haemorrhagic tumour, while multiple haemorrhaging and the absence of oedema tend to suggest primary intra-cerebral haemorrhaging.**

**Haemorrhaging in the Case of Vascular Malformations** Vascular malformations can be further divided into (see above):

- AAVMs (■ Fig. 9.73)
- Dural arterio-venous fistulas
- Aneurysms
- Cavernomas
- Capillary telangiectasias

After hypertension, cerebral vascular malformations are the second most common cause of non-traumatic intra-cranial haemorrhaging.

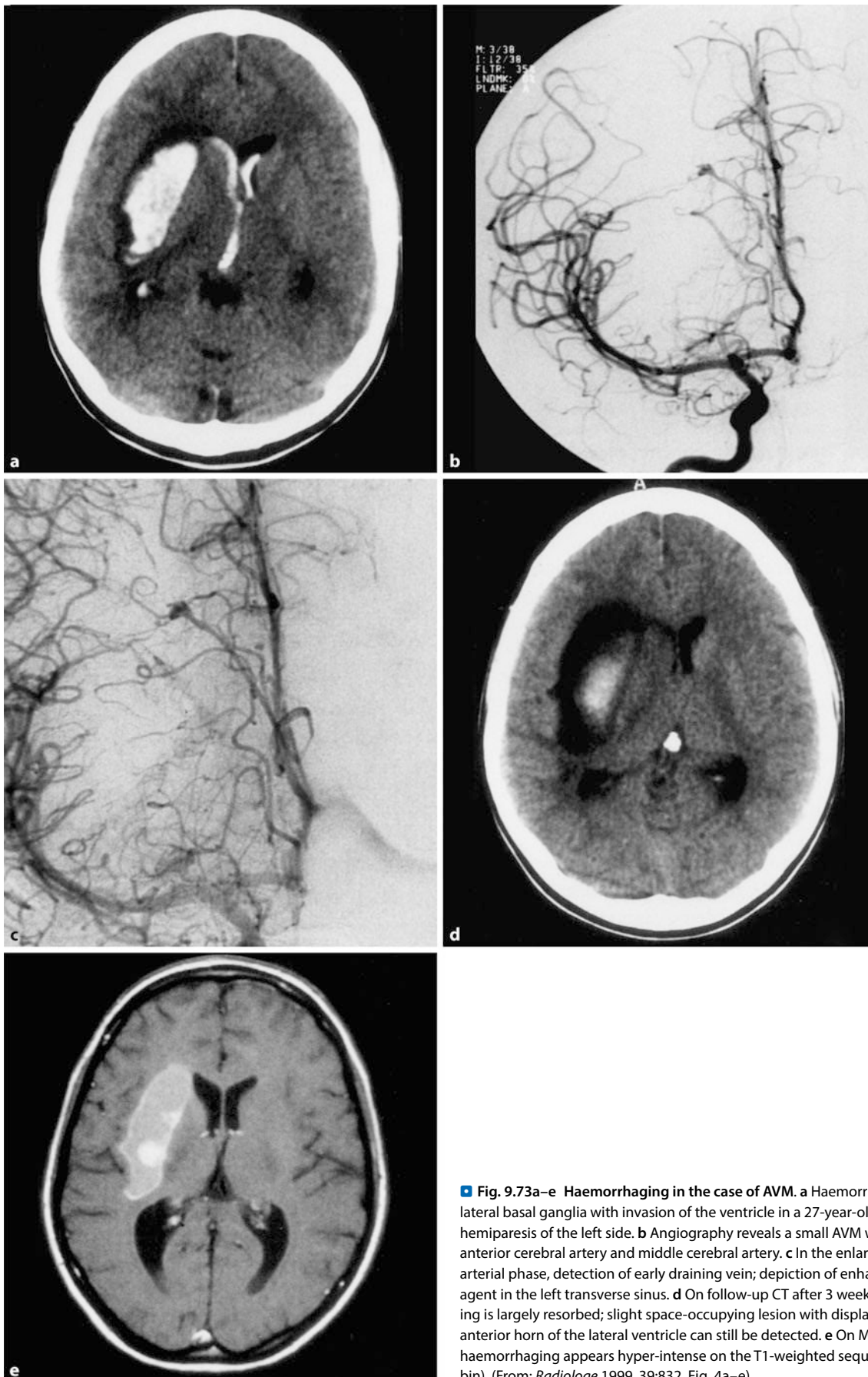


**Fig. 9.73a–e Haemorrhaging in the case of AVM.** **a** Haemorrhaging of the right lateral basal ganglia with invasion of the ventricle in a 27-year-old patient with acute hemiparesis of the left side. **b** Angiography reveals a small AVM with supply from the anterior cerebral artery and middle cerebral artery. **c** In the enlargement in the late arterial phase, detection of early draining vein; depiction of enhancement of contrast agent in the left transverse sinus. **d** On follow-up CT after 3 weeks, the haemorrhaging is largely resorbed; slight space-occupying lesion with displacement of the right anterior horn of the lateral ventricle can still be detected. **e** On MRI, after 4 weeks, the haemorrhaging appears hyper-intense on the T1-weighted sequences (methaemoglobin). (From: *Radiologie* 1999, 39:832, Fig. 4a–e)

### ■ ■ Therapy and Course

Spontaneous supra-tentorial haematomas are usually treated conservatively unless an improvement in the clinical condition is anticipated; in the case of imminent brain-stem compression, removal of the haematoma can make a lot of sense. If occlusive hydrocephalus develops, external CSF drainage can be configured. The introduction of a catheter into the haematoma for spontaneous emptying and the instillation of fibrinolytic agents are still at the experimental stage and cannot yet be conclusively assessed. If the cause of bleeding remains unresolved, further diagnostic measures should be taken.

❗ **Later in the course, a pronounced oedema develops around the intra-cerebral haemorrhage. At this stage, after the administration of contrast agent, the haemorrhaging can be confused with a tumour or an abscess.**

The haemorrhaging slowly degrades over days and weeks. A small, slit-shaped defect can still often be seen and sometimes even larger cystic lesions.

### ■ ■ Stroke in Childhood

Approximately 3% of all strokes occur in childhood; among young adults, the incidence of stroke is even rarer. In childhood, cerebral infarcts usually have a different aetiology compared with that of adults. Sinus vein thrombosis is a condition that is often not diagnosed in time. The symptoms, causes, diagnosis and treatment are presented.

### ■ ■ Epidemiology

Vascular occlusive diseases are rare in childhood and vary among different ethnic groups. In the US, the annual incidence of ischaemic and haemorrhagic strokes in children is 2.5 in 100,000. That of ischaemic stroke is estimated to be 1.2 in 100,000. These data refer to patients younger than 15 years and include periventricular leukomalacia. The distribution of stroke reveals a constant incidence from the second year of life. However, during the neonatal and infant stages, the incidence is much higher.

### ■ ■ Symptoms

Ischaemia can even occur in utero. The clinical symptoms are sometimes first seen days or weeks after birth depending on the extent and localisation of the infarct. In neonates with acute stroke, seizures often occur. Focal neurological deficits are less common. The neurological deficits usually become clinically apparent later on, often over the coming months and years. Infants and school children often react to an acute stroke with a preference for one hand or one side of the body (■ Table 9.7). The exact timing of stroke in young children cannot often be accurately determined. The clinical symptoms may include fever, seizures and coma. In older children, there is typically an acute focal neurological deficit, usually hemiparesis, with or without accompanying seizures. The neurological symptoms usually improve within a short time.

Seizures, fever, headache and altered consciousness may occur. However, in older children, this is less frequent than in the neonatal and infant stages.

■ **Table 9.7** Acute cerebral ischaemia in childhood

Clinical manifestation	(%)
Hemiplegia	76
Unconsciousness	35
Aphasia	18
Seizures	17
Locked-in syndrome	6
Ataxia	3
Double vision	3

### ■ ■ Aetiology

To clarify the aetiology, CT, MRI, conventional angiography, blood count, serum electrolytes, inflammatory markers (C-reactive protein, erythrocyte sedimentation rate), coagulation parameters, trans-oesophageal echocardiogram, electro-encephalogram, 24-hour echo-cardiography, blood lipids, lactate, protein C, protein S and anti-phospholipid anti-bodies in addition to urine and CSF examinations should be performed. Antibody titres for varicella zoster virus, cytomegalovirus (CMV), type 1 herpes simplex virus and the measles virus should also be performed in serum and CSF.

The cause of an ischaemic stroke in childhood varies significantly from the underlying causes in adulthood (■ Figs. 9.74–9.76). In the majority of cases (about 80%), a specific aetiology can be found for the stroke (■ Table 9.8). The most common cause of stroke in childhood is a **congenital heart disease**. Embolisms from the heart or from the periphery via a right–left shunt are the most common causes of ischaemic stroke. The most common congenital cardiac diseases are tetralogy of Fallot and transposition of the large vessels. Embolisms from prosthetic heart valves are also an important source of cerebral ischaemia. Mitral valve prolapse, however, is not thought to lead to an increased risk of stroke in childhood.

In embolisms resulting from congenital heart diseases, children older than 2 years are more likely to have a cerebral abscess than cerebral ischaemia. In children with congenital heart disease, common accompanying symptoms include polycythaemia and an increased blood viscosity, which is also considered to be a cause of the frequent occurrence of cerebral sinus venous thromboses. A trans-oesophageal ultrasound can and should be performed, even for smaller children, to discover a thrombus or open foramen ovale with paradoxical embolism. Infections such as bacterial or viral meningitis may be the cause of inflammatory arteritis, which can lead to an acute ischaemic stroke. A stroke has been described as a rare complication in children with HIV infection (approximately 1% of the affected children). In children affected by HIV, autopsies revealed participation of the vessels in about 10–30% of cases.

**Haematological Disorders and Coagulopathy** Sickle cell anaemia is the most common coagulopathy associated with cerebrovascular complications. Approximately 25% of these patients develop cerebrovascular complications; 80% of these are younger

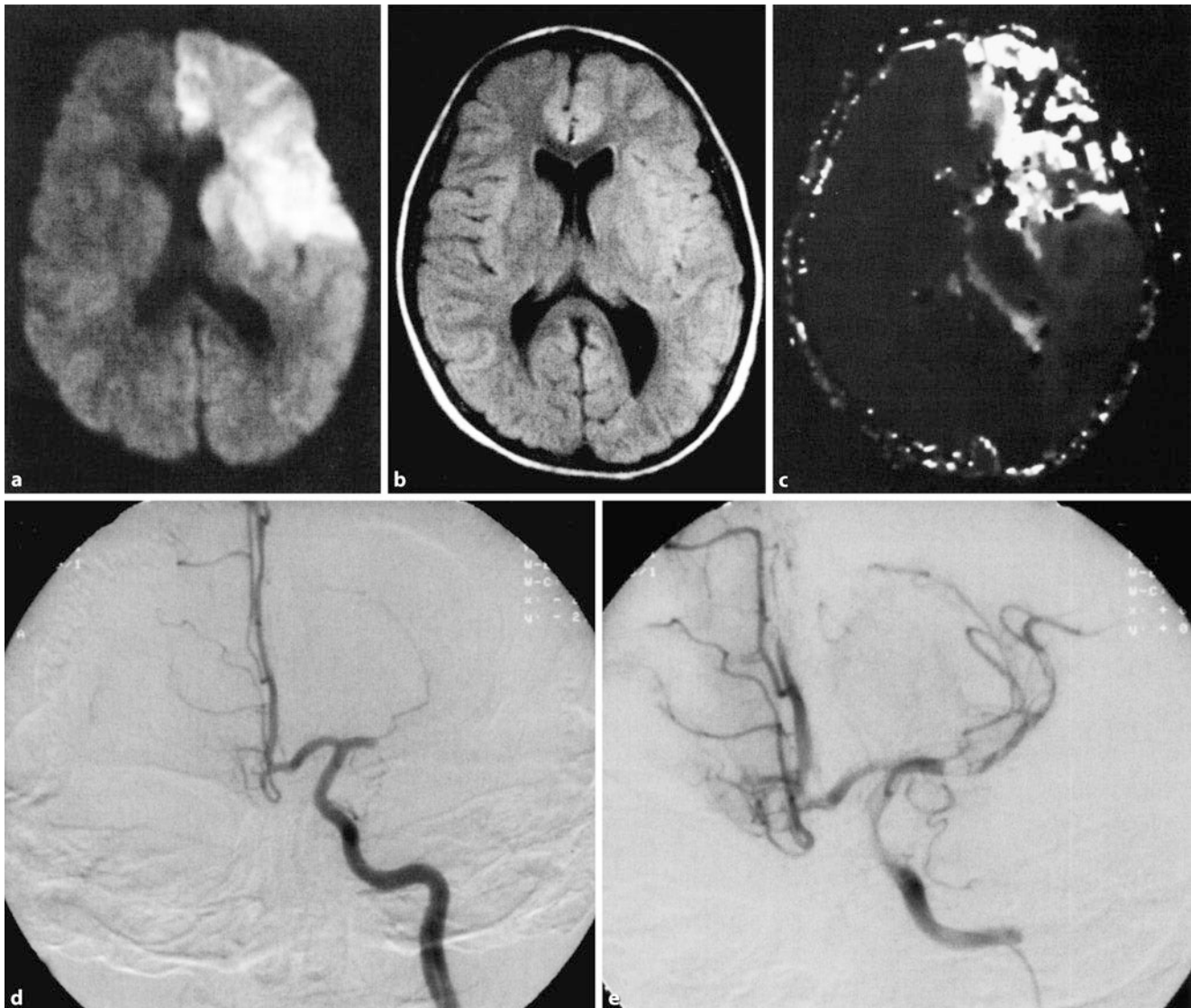


**Fig. 9.74a–e Stroke in childhood.** A 5-year-old girl with a known trisomy 21. Four hours before the MRI, the child suffered aphasia and right-sided hemiparesis. **a** Diffusion-weighted sequences with hyper-intense left frontal areas in the supply area of the middle cerebral artery and anterior cerebral artery. **b** On the FLAIR sequence, no pathological signal change has been revealed yet. **c** On the perfusion-weighted sequence, there is a clear disturbance in perfusion of the left frontal area. The size and expansion of the area

suggests disturbed diffusion weighting. **d** Despite this mismatch, an arterial DSA was performed, which revealed a complete occlusion of the middle cerebral artery. **e** An immediately performed, intra-arterial thrombolysis only revealed a partial canalisation of individual media branches; a thrombus still remained in the main stem of the media. (From: *Radiologe* 2003; 43:952, Fig. 2a–e)

than 15 years. A stroke usually occurs in the context of an acute thrombotic crisis. The occlusion of large and small blood vessels by the sickle-shaped erythrocytes leads to local disturbances in circulation. Focal or generalised seizures occur in about 70% of these patients. If angiography must be performed, the risk should be minimised by good hydration and adequate transfusion.

There are also several congenital bleeding disorders that can lead to thrombosis or a stroke. In children, protein C, protein S, anti-thrombin III, and dysfibrinogenaemia should be investigated. Various anti-phospholipid antibodies including the lupus anti-coagulant, can also lead to disturbed coagulation and cerebral infarcts in childhood. These anti-phospholipid are auto-antibodies against phospholipids; they are increasingly detect-

able in systemic lupus erythematosus and other auto-immune diseases. Their pathogenetic role in acute stroke has not yet been fully clarified.

**Metabolic Disorders Homocystinuria** is based on a defect in cystathionine synthase (chromosome 21q22–3). It is one of the metabolic disorders that predispose to arterial and venous thrombosis with cerebral infarcts. Infarcts may often occur, before the other consequences of this disease (e.g. dislocation of the lenses, a developmental delay, and Marfanoid habitus) become evident. **Fabry disease**, caused by a deficiency of  $\alpha$ -galactosidase, also leads to cerebral infarcts. The infarcts tend to be of the lacunar type and occur more frequently in early adulthood. In Fabry disease, globotriaosylceramide is deposited in many organs, such

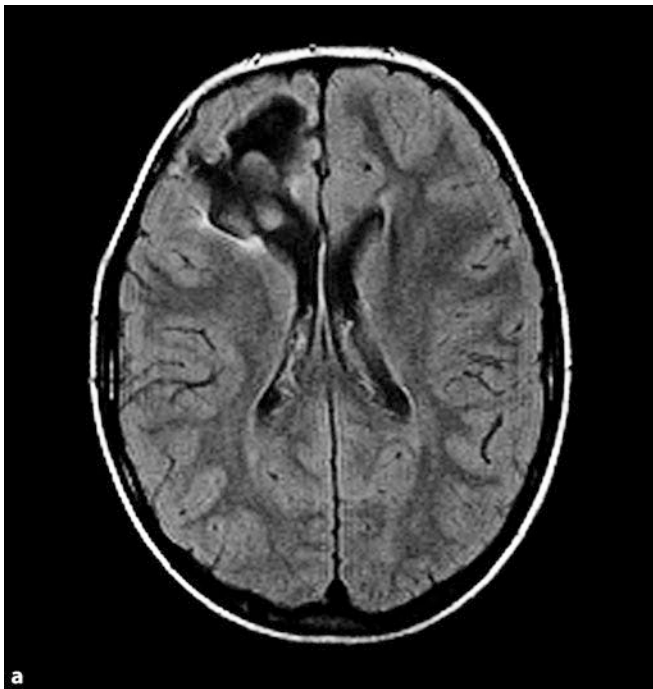


**Fig. 9.75a,b** Stroke in childhood A 13-year-old patient with a known right frontal peri-partum infarct. **a** On the FLAIR images, the defect is iso-intense to CSF; a small zone of gliosis can only be seen at the dorsal edge. The anterior

horn of the right lateral ventricle is consequently extended. **b** On the coronal T1-weighted images, the defect is also iso-intense to CSF. The cortex adjacent to the injured site has thinned



**Fig. 9.76a,b** Vasculitis in childhood. A 10-year-old patient with headaches persisting for months and dizziness symptoms (no pathological signal deviations on T2-weighted images). **a** The coronal FLAIR images also show no pathological signal changes. **b** However, the MR angiography performed using the TOF technique reveals a distinct change of diameter in the middle cerebral artery as an indication of bilateral vasculitis of the middle cerebral arteries. (From: *Radiologie* 2003; 43:953, Fig. 3 b, c)

as the kidneys, heart, nervous system and blood vessels. **Mitochondrial myopathy** with encephalopathy, lactic acidosis and stroke-like episodes (► Sect. 9.8, Metabolic Diseases) can also occur in childhood with headaches, seizures, hemiparesis and cortical blindness.

Acute, **regressive cerebral arteriopathy** is characterised by transient acute angiitis of the vascular walls. In a series by Sebiri, it was identified as the cause of a stroke in about 26% of cases. A frequent cause of this cerebral arteriopathy is infectious diseases such as a varicella zoster infection or other viral meningo-



**Table 9.8** Aetiology of ischaemic and haemorrhagic stroke in childhood (according to Lo et al. (2009, S. 194))

Pathology	Trigger	Percentage
Ischaemic stroke	Congenital heart disease	9.6
	Head trauma	9.5
	Meningitis, encephalitis	8.7
	Sepsis	8.5
	Sickle cell anaemia	7.8
	Coagulopathy	6.2
	Arrhythmia	6.1
	Hypertension	5.4
	Autoimmune diseases	4.6
	Purpura	4.4
	Moyamoya	2.6
	Cerebral tumours	2.4
	Leukaemias	2.4
	Migraine	2.4
Cardiac arrest	2.4	
Haemorrhagic stroke	Congenital heart disease	13.6
	Arteriovenous malformations	13.5
	Sepsis	9.4
	Arrhythmia	9.0
	Coagulopathy	7.7
	Hypertension	6.1
	Purpura	6.0
	Cerebral tumour	5.6
	Meningitis, encephalitis	3.8
	Leukaemia (including ALL)	2.9
	Cardiac arrest	2.9
	Head trauma	2.9
	Autoimmune diseases	2.6
	ALL	2.1
Sickle cell anaemia	1.5	

encephalitis. In this type of arteriopathy, the pathological process only occurs transiently, which can also be demonstrated angiographically. In the acute phase, segmental narrowing of the basal arteries, especially the middle cerebral artery can be observed. This often regresses within weeks to months. Angiography cannot directly demonstrate these inflammatory vascular diseases. However, focal or segmental stenoses are not typical of an embolic or thrombotic process, but rather suggest a change in the vascular wall. Dissections, which can also occur intra-cranially, must also be considered in the differential diagnosis. The mean age at dissection was 12 years older in a series by Lasjaunias et al. In addition, there was usually a medical history of neurotrauma.

In dissections, vascular irregularities were mostly detectable in the supra- and infra-clinoid segment of the internal carotid artery, but not focally or multi-focally in the area of the anterior and middle cerebral artery and media.

*ALL* acute lymphoblastic leukaemia

A temporal correlation between an ischaemic stroke in young patients and **infectious diseases** (tonsillitis, cervical lymphadenopathy [varicella zoster infection; Epstein–Barr virus, EBV]) has been described in several studies. In the series by Sebiri, in 5 children, varicella infection was present before acute cerebral ischaemia

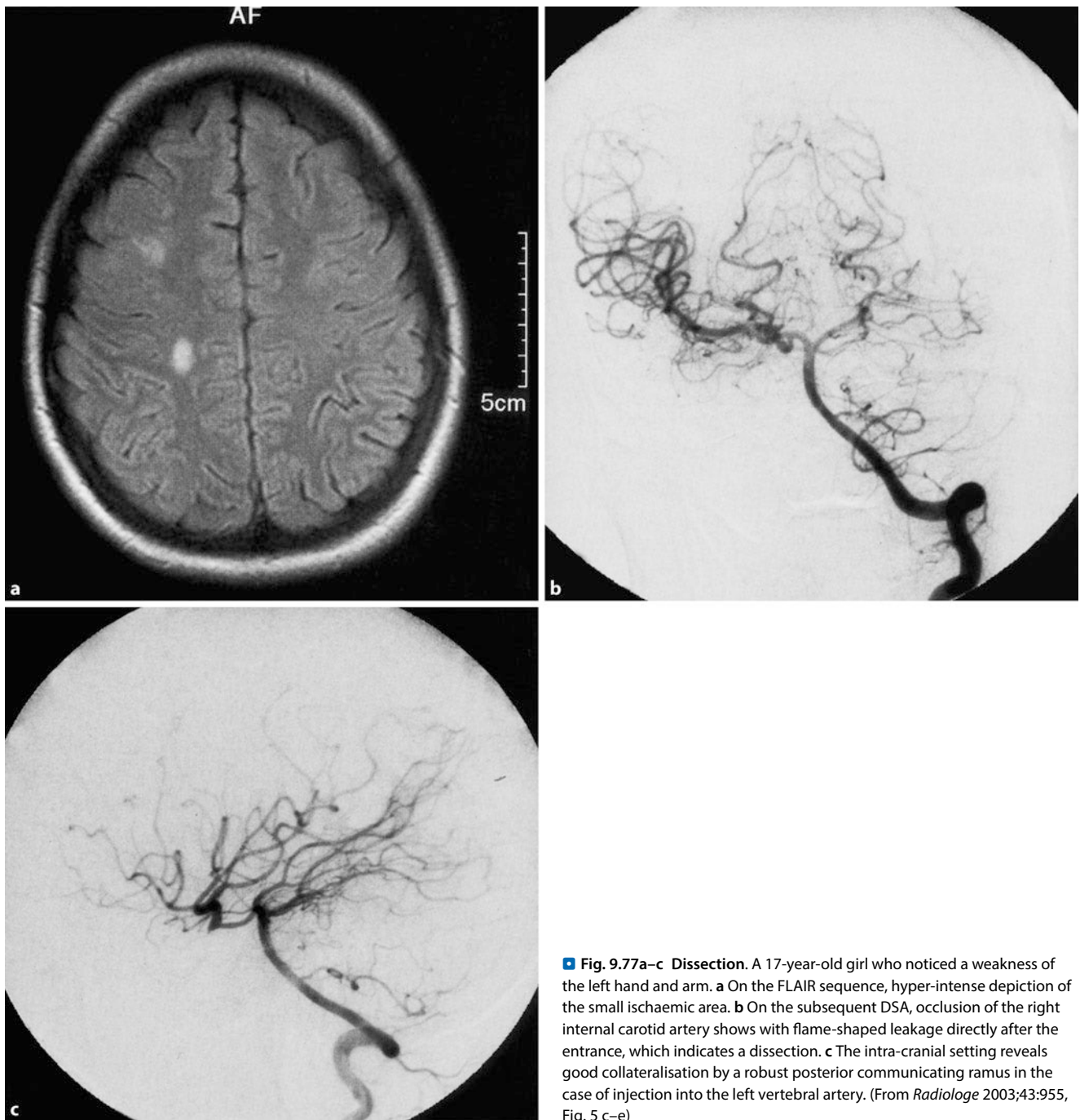
**Vasculopathy** Non-infectious vascular diseases, such as periarteritis nodosa and systemic lupus erythematosus, occur much less frequently in children than in adults. The same applies to fibro-muscular dysplasia, which is rarely associated with a heart attack in children. **Moyamoya disease** is a primary vascular disease characterised by progressive stenosis and occlusions, especially the supra-clinoid portion of the internal carotid artery (see ▶ Sect. 9.3.3, Rare Causes of Vascular Disease). The adjacent segments of the middle and anterior cerebral artery are often involved. The body reacts by forming an abnormal vascular network, the so-called **Rete mirabile** or Moyamoya in Japanese, to compensate for the vascular occlusions.

The most common symptoms of childhood are multiple, transient ischaemia, sometimes with lasting clinical symptoms. In children younger than 6 years, seizures frequently occur as symptoms of acute ischaemia. The disease may stabilise at a certain level. However, a progressive course with increasing motor-driven deficits and intellectual deterioration is more frequent.

In children with various slowly-progressing “large vessel vasculopathies”, so-called Moyamoya-like images with the formation of collateral circulation can occur. However, the symmetry, the trans-dural angiogenesis, and the absence of lepto-meningeal collaterals in addition to the normal appearance of the vessels of the posterior fossa and the role of ventriculostriate vessels differentiate this disease from a true Moyamoya disease (see below, ▶ Fig. 9.78).

**Takayasu’s disease** is form of arteritis that mainly affects the aorta and the supra-aortic vessels. It is accompanied by missing pulses and vascular noises. An acute stroke occurs in approximately 5–10% of these patients. The disease usually affects young women between 15 and 20 years, but has also been described in younger children.

**Trauma** Intra-cerebral traumas or injuries in the neck region can cause an acute stroke (▶ Sects. 9.5 and 9.3.3). These injuries can necessitate a dissection of the carotid or vertebral arteries with the consecutive formation of thrombosis or an embolism. Sometimes, the neurological symptoms only first appear hours or even days after the accident. It can also lead to a progressive deterioration of the clinical symptoms. Dissections may also occur spontaneously (▶ Fig. 9.77). Horner’s syndrome should always draw attention to participation of the ipsilateral internal carotid artery.



■ **Fig. 9.77a–c Dissection.** A 17-year-old girl who noticed a weakness of the left hand and arm. **a** On the FLAIR sequence, hyper-intense depiction of the small ischaemic area. **b** On the subsequent DSA, occlusion of the right internal carotid artery shows with flame-shaped leakage directly after the entrance, which indicates a dissection. **c** The intra-cranial setting reveals good collateralisation by a robust posterior communicating ramus in the case of injection into the left vertebral artery. (From *Radiologe* 2003;43:955, Fig. 5 c–e)

**Vascular Changes after Radiotherapy** A radiogenically induced vascular occlusion is a rare cause of stroke in children and usually occurs more than 6 months or even years after the radiotherapeutic treatment of intra-cranial tumours.

#### ■ ■ Medical Imaging

**Computed tomography** is still considered to be the method of choice for differentiating between intra-cerebral haemorrhaging and acute ischaemia. Using multi-line technology, the unenhanced diagnostics can now be combined with CT angiography in excellent quality and with perfusion imaging.

However, in cases of suspected acute, early intra-cerebral ischaemia **MRI** provides better options. In particular, diffusion-

weighted MR sequences, which are increasingly used in clinical routine, can depict the full extent of the ischaemic area within the first few hours (■ Table 9.9). With CT, this is usually only possible after about 12 h. MR angiography, especially the TOF technique for intra-cranial vessels and contrast-enhanced MR angiography in the area of the cervical vessels, is the most suitable technique for the detection of vascular pathological conditions.

**Digital subtraction angiography** is still the standard for the detection of minute vascular lesions, especially vasculitic changes in the vascular walls. DSA is also a component of endovascular interventional treatment options.

■ **Table 9.9** Stroke protocol

MR sequence	TR (ms)	TE (ms)	Layer thickness (mm)	Acquisition time (min)
T2-weighted sequence	4,010	108	6	2:14
Diffusion-weighted sequence	3,800	120	6	0:11
Perfusion-weighted sequence	1,550	30	5.0	1:36
MRA, TOF	21	3.24	0.94	5:44
FLAIR	7,400	119	6.0	2:13
				TI 2,300 mg

*MRA* magnetic resonance angiography, *TOF* time-of-flight, *FLAIR* fluid-attenuated inversion recovery

### ■ ■ Outcome and Prognosis

The prognosis for children with acute cerebral ischaemia is generally considered to be more favourable than in adults, although only a few studies have proven this. Studies describe a survival rate of 85% in children with acute cerebral ischaemia. However, a residual deficit was detected in 75–100% of patients. Almost all children with a stroke in the neonatal period exhibited a mental and physical developmental delay. As already mentioned, in cases of childhood cerebral ischaemia, seizures occur at the beginning of a stroke. This is probably also of prognostic importance because 60% of children younger than 3 years who experienced a seizure at the beginning of cerebral ischaemia display developmental disorders. Of these, 75% continue to suffer from seizures. In children with a stroke who had no seizure at the start, only 20% experience development delays, and less than 10% continue to suffer from seizures. Because seizures are more frequent in children younger than three to four years, younger patients probably have a worse long-term prognosis for their further development.

Movement disorders are also likely to be an under-represented long-term consequence in children with infarcts of the basal ganglia.

The risk of recurrent stroke in children is considered to be low; the repetition rate is estimated to be approximately 20%.

### 9.3.3 Rare Causes of Vascular Diseases

#### ■ Moyamoya Disease

##### ■ ■ Definition

Moyamoya disease is an idiopathic cerebrovascular disease that is characterised by a spontaneous, slowly-progressing stenosis of the distal internal carotid artery and the proximal arteries of the circle of Willis with secondary formation of a dense network of collateral vessels. The collateral network mainly consists of the lenticulo-striate and choroid arteries.

##### ■ ■ Epidemiology

The disease, which was first described in Japan in the 1960s, is more common in Asia. In Japanese, the term “Moyamoya” refers to fog or smoke and was used to describe the characteristic angiographic appearance of the pathological collateral vessels. In Japan, the disease occurs with an incidence of 0.35%, with 400

new manifestations annually. There, it is recognised as the most common cause of stroke in childhood. In the rest of the world, the manifestation is much lower. Moyamoya disease can appear both in childhood and in adulthood, although with differing clinical manifestations. There is a predominance of the female sex.

##### ■ ■ Aetiology

The aetiology of this disease remains unclear. Because of the increased incidence in Japan and Korea in addition to the familial occurrence in Japan, it has been suggested that genetic components might be involved. A genetic modification has been revealed in the chromosomal loci 3p24.2–26 and 6.

##### ■ ■ Clinical Picture

The clinical presentation of Moyamoya disease is different in childhood and adulthood. In the first decade of life, there is an increased incidence of the disease. **Children** often present with transient ischaemic attacks (TIA). Cerebral ischaemia may manifest as reversible motor deficits, sensory or visual disturbances and recurrent hemiparesis. Headaches and seizures also occur in some patients. Intra-cerebral haemorrhaging rarely occurs in children. Several reports show that in children with symptomatic Moyamoya disease, there may be a reduction in the intelligence quotient (IQ). This reduction depends on the duration of symptoms and stabilises after approximately 10 years. Some studies indicate an improvement in IQ following surgical intervention. A hypothalamic–pituitary dysfunction in children has also been reported.

Unlike children, in adults the disease manifests as intra-cranial haemorrhaging. Factors that may lead to haemorrhaging include hypertension in addition to pseudo- and micro-aneurysms. Any type of intra-cranial bleeding may occur. One study revealed haemorrhaging of the basal ganglia in 40% of cases, intra-ventricular haemorrhaging in 30%, thalamic haemorrhaging with ventricular invasion in 15% and sub-cortical haemorrhaging in 5%. Recurrent haemorrhaging can occur long after the first episode. Mortality rises after the first recurrence of haemorrhaging; the prognosis is generally poor. Although rare, chronic headaches, recurrent TIA, and neuro-psychological changes may occur.

##### ■ ■ Medical Imaging

Computed tomography in addition to conventional MRI and MR angiography (■ Fig. 9.78) are very helpful not only for the diag-

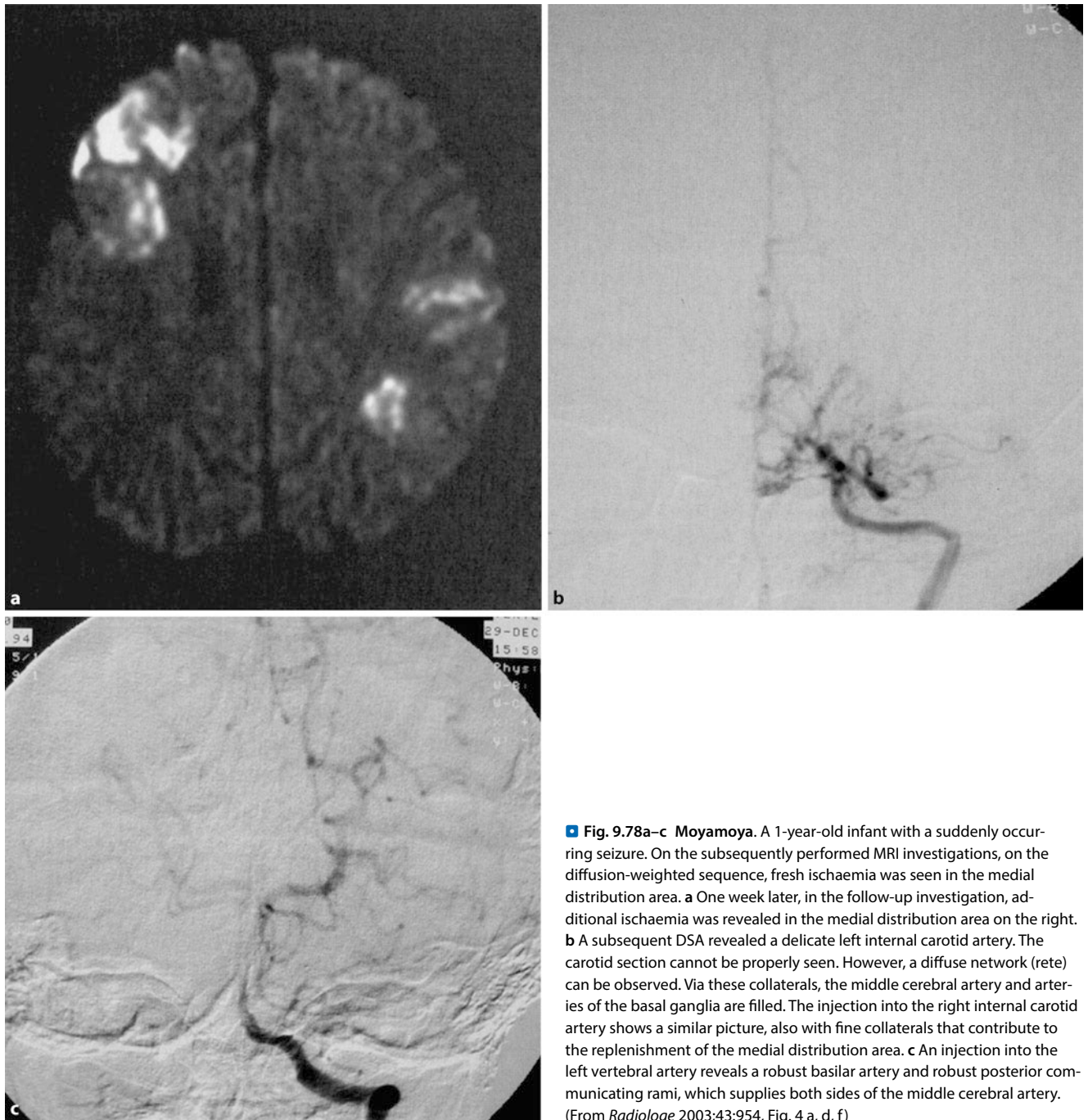


**Fig. 9.78a-c Moyamoya.** A 1-year-old infant with a suddenly occurring seizure. On the subsequently performed MRI investigations, on the diffusion-weighted sequence, fresh ischaemia was seen in the medial distribution area. **a** One week later, in the follow-up investigation, additional ischaemia was revealed in the medial distribution area on the right. **b** A subsequent DSA revealed a delicate left internal carotid artery. The carotid section cannot be properly seen. However, a diffuse network (rete) can be observed. Via these collaterals, the middle cerebral artery and arteries of the basal ganglia are filled. The injection into the right internal carotid artery shows a similar picture, also with fine collaterals that contribute to the replenishment of the medial distribution area. **c** An injection into the left vertebral artery reveals a robust basilar artery and robust posterior communicating rami, which supplies both sides of the middle cerebral artery. (From *Radiologie* 2003;43:954, Fig. 4 a, d, f)

nosis of Moyamoya disease, but also for pre-operative assessment and post-operative follow-up.

**Computed Tomography.** On cranial CT, the initial diagnosis may reveal hypo-dense focal areas, which suggest infarcts. Signs of brain atrophy, which are often emphasised frontally, can also be detected. CT is useful in the diagnosis of intra-cranial haemorrhaging, which is mostly localised in the vicinity of the lateral ventricles. On contrast-enhanced CT, “points” with an affinity to the contrast agent can be seen in the area of the basal ganglia. These correspond to large vessels of the collateral network (lenticulo-striate arteries).

**Magnetic Resonance Imaging.** The findings of Moyamoya disease on MRI are well documented. A variety of pulse sequences, including FLAIR, DWI sequences, perfusion-weighted sequences, and contrast-enhanced sequences are available in addition to MR angiography. Compared with CT, MRI can sensitively depict ischaemic areas. On the T2-weighted sequences, the infarct areas appear cortically and in the white matter as signal-enhanced regions. The collateral vessels can be depicted as a hypo-intense “network” in the basal cisterns or as hypo-intense “points” in the basal ganglia. As on CT, a frontal reduction in cerebral volume may be detectable. For the depiction of cortical infarcts, FLAIR sequences are more sensitive than T2-weighted sequences because of the suppression of the fluid signal. On the contrast-enhanced

T1-weighted sequences, the collateral vessels in the basal ganglia and basal cisterns have an affinity to the contrast agent. In the cortical sulci, a **lepto-meningeal enhancement is revealed**, which is designated as an “ivy sign”. This lepto-meningeal enhancement most closely corresponds to fine anastomoses. This enhancement is found to be smaller after effective bypass surgery. On the FLAIR sequences, the “ivy sign” appears as a hyper-intense cortical sulcus. For the differentiation of acute and older ischaemic events, **DWI** can be particularly helpful. On DWI, fresh infarcts are detectable as signal-enhanced areas. The perfusion-weighted sequences reveal the relatively low perfusion of the white matter in the anterior distribution area compared with the perfusion of the posterior distribution area. It is valuable for distinguishing infarction risk areas in addition to demonstrating the post-operative improvement in perfusion. MR angiography shows a high-grade stenosis of both distal internal carotid arteries in addition to the proximal arteries of the circle of Willis.

**Cerebral Angiography.** The implementation of cerebral angiography is necessary for the diagnosis and planning of treatment. An angiographic characteristic of the disease is bilateral **supraclinoid stenosis of the internal carotid artery**. The extent of the changes is not necessarily symmetrical. This progressive stenosis, which ultimately leads to an occlusion, results in the development of a collateral network in the basal ganglia, thalamus and hypothalamus and possibly the mesencephalon via the lenticulo-striate arteries, the anterior choroidal artery and the posterior communicating artery and their lateral branches in addition to via collateral pathways of the external carotid artery to the distribution area of the internal carotid artery distal to the circle of Willis. Over time, these collaterals extend and form a dense network. In the later stages of the disease, stenosis also appears in the area of the circle of Willis, which leads to new collateral networks, e.g. lepto-meningeal or trans-dural anastomoses.

#### Classification of Moyamoya Disease

Based on a **classification of angiographic findings** according to Suzuki, the disease is divided into six stages:

- Stage I: isolated stenosis of the terminal carotid tract.
- Stage II: occurrence of a fine collateral plexus and extension of the distal cerebral arteries.
- Stage III: full development of the collateral plexus (Moyamoya) with reduced display of the anterior cerebral artery and middle cerebral artery.
- Stage IV: the basal vascular network gradually disappears and is replaced by a coarser plexus. The stenosis of the terminal carotid tract expands and overlaps the basal cerebral arteries. A trans-dural collateral circulation appears, which may lead to development of an orbital and ethmoidal Moyamoya. The middle cerebral artery, anterior cerebral artery and peri-callosal artery are only thin and poorly depicted.
- Stage V: the basal Moyamoya is only sparsely developed, and the anterior cerebral artery and middle cerebral artery are hardly recognisable. The intra-cerebral anastomoses of

the posterior cerebral artery and the trans-dural collateral pathways strengthen.

- Stage VI: the vascularisation of the anterior, peri-callosal, and medial distribution areas now only takes place via external branches and the vertebral–basilar distribution area.

#### ■ ■ Treatment

The only effective treatment for Moyamoya disease involves **surgical revascularisation** of the under-perfused parenchyma. A number of operational techniques are applied to create a collateralisation. In the surgical procedures, either direct revascularisation (e.g. the bypass between the superficial temporal artery and the middle cerebral artery) is strived for or indirect revascularisation, such as encephalo-duro-arterio-synangiosis (EDAS) or pial synangiosis, is performed. In general, indirect revascularisation is preferred in the treatment of children. In successful cases, the frequency of TIA is reduced, thus avoiding new infarcts.

#### ■ Venous Sinus Thrombosis

##### ■ ■ Epidemiology

Venous sinus thromboses are less common in children than in adults. In children, the incidence is 0.07 in 100,000. In adults, it is estimated to be 0.25–0.5 in 100,000. The actual number of dural sinus vein thromboses in the paediatric patient population is not precisely known, but they are probably still more common than previously thought.

##### ■ ■ Aetiology

In new-borns, it is assumed that a haemorrhagic infarction of the thalamus is caused by thrombosis of the central veins and the straight sinus, e.g. through dehydration. In infancy and childhood, in a large majority of the cases, a sinus vein thrombosis is based on a purulent focal infection in the head region (otitis media, mastoiditis, sinusitis, tonsillitis, meningitis). The clinical picture is determined by the localisation and the extent of venous occlusion. For example, mastoiditis can lead to thrombosis in the transverse and sigmoid sinuses. In addition, there is a relationship between a dural sinus vein thrombosis and generalised infections (e.g. a common cold) in addition to trauma and dehydration.

Intra-cranial arterio-venous bypasses such as a vein of Galen malformation or dural arterio-venous shunt can also lead to sinus and venous thrombosis. In the case of malignant diseases such as leukaemia, sinus vein thromboses can occur. The same is true for vasculopathy, which is considered to be a predisposing factor (■ Fig. 9.79)

Even in children with congenital coagulopathy, such as anti-thrombin defects or protein C or protein S defects, venous sinus thrombosis frequently occurs – but this is usually only the case later in childhood. A defect in the factor V gene is associated with activated protein C (APC) resistance and also frequently leads to venous sinus thrombosis. In the plasma of up to 50% of patients, APC resistance with an individual or family history of venous sinus thrombosis was found. Approximately 5% of the healthy population show an APC resistance, which is associated

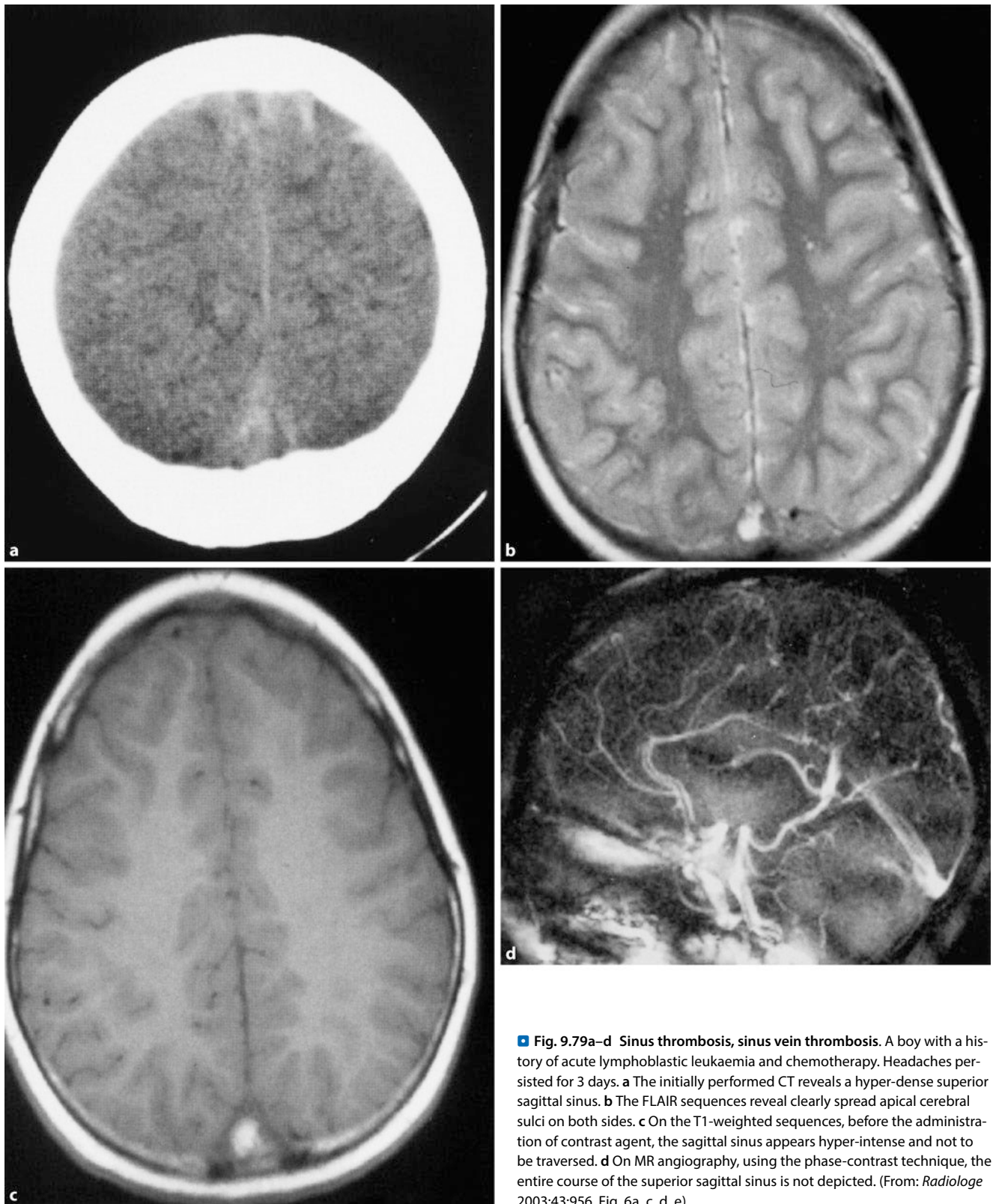


**Fig. 9.79a–d Sinus thrombosis, sinus vein thrombosis.** A boy with a history of acute lymphoblastic leukaemia and chemotherapy. Headaches persisted for 3 days. **a** The initially performed CT reveals a hyper-dense superior sagittal sinus. **b** The FLAIR sequences reveal clearly spread apical cerebral sulci on both sides. **c** On the T1-weighted sequences, before the administration of contrast agent, the sagittal sinus appears hyper-intense and not to be traversed. **d** On MR angiography, using the phase-contrast technique, the entire course of the superior sagittal sinus is not depicted. (From: *Radiologie* 2003;43:956, Fig. 6a, c, d, e)

with a seven-fold increased risk of deep vein thrombosis. APC resistance is the most common genetic, autosomal dominant risk factor for the development of thrombosis. APC resistance poses a 10-fold higher risk than all known genetic risk factors for thrombosis combined (protein C, protein S, anti-thrombin deficiency).

Homozygous carriers even have a 50- to 100-fold increased risk of developing thrombosis.

Haematological disorders such as polycythaemia or congenital heart diseases are also associated with an increased risk of cerebral venous sinus thrombosis. Central venous catheters are

the most common cause of iatrogenic venous thrombosis, in particular those of the jugular vein.

### ■ ■ Symptoms

The clinical features of venous sinus thrombosis are determined by the localisation and extent of the venous occlusion. As long as the circulation of a thrombotic vessel remains open in the case of sinus thrombosis, only general symptoms (e.g. fever, headache, vomiting and increased intra-cranial pressure) arise. The diagnosis is often made late or not at all, especially if the patients have only mild or unusual clinical symptoms. If there is a gradual development of dural venous sinus thrombosis, children often show signs of chronic obstruction with macrocrania and expanded facial veins.

Occlusion of the transverse sinus is known to be one of the causes of benign intra-cranial hypertension. Focal symptoms are caused by a localised oedema and haemorrhaging. The clinical presentation mainly depends on the location of the closure in addition to the anatomical conditions. Left lateral thrombosis can lead to congestion in the temporal lobe and aphasia. In advanced cases, posterior temporal lobe herniation and an arterial infarction of the middle cerebral artery may arise.

During the spread of thrombosis, cerebral symptoms occur in the cerebral veins. These findings can often suggest encephalitis. Headache and disturbance of consciousness are mainly caused by an increase in intra-cranial pressure. In older children and in adults, the initial symptoms of cerebral pseudotumour are usually headaches, which are associated with nausea and vomiting. In younger children, cerebral pseudotumours usually manifest clinically as somnolence or apathy. In asymptomatic patients, papilloedema is often discovered by chance. Ataxia and dizziness in addition to neck and shoulder pain may also occur as early symptoms.

A unilateral proptosis with peri-orbital oedema and an ipsilateral paralysis of the ocular nerves and the first two trigeminal branches may develop in the case of thrombosis of the cavernous sinus. A thrombosis of the transverse sinus with or without mastoiditis often develops in otitis media. The prognosis is considered to be relatively favourable as long as the thrombo-phlebitis remains localised.

The clinical outcome will degrade if the inflammatory process spreads to the superior sagittal sinus.

In the neonatal period, dural venous sinus thrombosis is rarely documented. In new-borns, it manifests as seizures in approximately 88% of cases. Further follow-up of these patients reveals that a good clinical outcome can be expected in almost all cases. Peri-natal asphyxia is detected in only a very few cases.

### ➤ A venous sinus thrombosis is thus an important and often unrecognised cause of cerebral seizures during the neo-natal period.

In the absence of peri-natal asphyxia, normal neurological development can generally be expected. The risk of developing further seizures is regarded as quite low. A thrombosis of the central veins can lead to thalamic haemorrhaging, while a lateral sigmoid sinus thrombosis tends to lead to benign cerebral pseudo-tumours.

### ■ ■ Medical Imaging, Diagnosis

**Computed Tomography.** On unenhanced CT, cerebral venous sinus thrombosis often manifests as a circumscribed area of hypodensity in the corresponding venous sinuses. In addition, there is focal brain swelling, sometimes with haemorrhagic transformations in the sense of venous infarctions. On CT, it is possible to make a distinction between direct and indirect signs. The direct signs reveal the intra-luminal thrombus in a dural sinus or a pial vein. The indirect signs are an expression of a thrombosis caused by venous congestion of the cerebral parenchyma. Although they should raise the suspicion of a cerebral venous circulatory disorder, they must be distinguished from other differential diagnoses.

**Direct signs** include:

- Hyper-dense sinus on unenhanced CT (■ Fig. 9.79)
- “Cord sign” – a pontine vein on unenhanced CT
- “Empty-triangle-sign” of the sinus on contrast-enhanced CT

On CT, freshly thrombosed blood is hyper-dense, while a 1- to 2-week-old blood clot is hypo-dense. In the case of a fresh thrombus in the sinus lumen, a hyperdense sinus should be expected on unenhanced CT. In the case of a thrombosed pontine vein, a hyper-dense “cord sign” should be expected. At a later time point, in the case of an iso-dense or hyper-dense thrombus, the sinus thrombosis is directly detectable as the “empty-triangle sign” after the administration of a contrast agent.

**Indirect signs** include global cerebral oedema and focal oedema in addition to uni- or multi-locular congested haemorrhaging. The assessment of indirect signs must take into account the clinical and radiological **differential diagnosis**. If the focal oedema is of venous origin, it is to be expected that the form and extent correspond to non-typical arterial vascular territories. From a differential diagnostic perspective, this should be distinguished from multi-focal lesions in vasculitis and posterior encephalopathy. Other differential diagnostic considerations include infarcts or other disorders associated with cerebral haemorrhaging. At the beginning of the CT clarification, unenhanced CT should always be performed. With contrast-enhanced CT angiography, the exact localisation of the thrombus can usually be detected.

**Magnetic Resonance Imaging.** On MRI, acute and sub-acute venous sinus thromboses are usually directly detectable in addition to the facultative oedematous and haemorrhagic changes of the cerebral parenchyma emanating from vascular occlusion. Here, it is highly important to consider the diagnosis because it requires an adequate examination protocol (see below). Thrombosed cerebral sinuses exhibit typical time-dependent changes in their signal intensities, which, in the first few weeks, have a course similar to that of intra-cerebral haematomas. However, haemosiderin defects do not occur in the venous sinus. The signal pattern of the intra-luminal thrombus can allow the age to be inferred. In ■ Table 9.10 the corresponding stages and signal characteristics of sinus thrombosis are listed.

In the case of a **fresh sinus thrombosis** the otherwise typical flow-related signal voids are missing from the T1-weighted-images. Between the first and fifth days, the venous sinuses appear strongly hypo-intense on the T2-weighted sequences. At this

**Table 9.10** Stages and signal characteristics of sinus thrombosis

Stage I	Acute thrombosis	First to fifth day	T1-weighted image: iso-intense T2-weighted image: strongly hypo-intense
Stage II	Sub-acute thrombosis	Up to the 15th day	T1-weighted image: hyper-intense T2-weighted image: hyper-intense
Stage III		16 days to 3 months	T1-weighted image: heterogeneous, hyper-, iso-, hypo-intense T2-weighted image: heterogeneous, hyper-, iso-, hypo-intense
Stage IV		Over 3 months	T1- and T2-weighted images: normalisation with flow-induced signal loss or iso-densely organised thrombus

early stage, because of the minor changes, venous sinus thrombosis can often be overlooked and interpreted as a normal finding. If there is clinical suspicion of sinus thrombosis, flow-sensitive gradient-echo sequences or phase-contrast MR angiography should be conducted.

In the **sub-acute phase**, there is hyper-intensity on T1-weighted sequences. This finding must be distinguished from flow-related increases in signal intensity.

At the **later stage**, from the third to fourth week, the signal is heterogeneous as an expression of organisational and recanalisation procedures. It results in organisation of the thrombus, which is iso-intense, or recanalisation of the vessel with the recurrence of flow-related signal voids.

The reliable assessment of suspected venous sinus thrombosis by MRI requires a corresponding **examination protocol**. In addition to axial and coronal turbo spin echo sequences, this should also include phase-contrast angiography and possibly contrast enhanced MR angiography to depict the venous sinuses.

➤ **With the possibility of CT angiography and MR angiography in addition to the implementation of flow-sensitive gradient echo sequences, dural sinus thrombosis can be almost invariably ascertained without the use of invasive catheter angiography. Rare problems involving contrast agents, e.g. Pacchioni's granulations, can lead to misjudgements. In this case, CT angiography or catheter angiography should be performed for clarification.**

**Cerebrospinal Fluid.** In the case of venous sinus thrombosis, CSF findings are extremely variable. Most consistently, there is an increase in protein content. The cell count is usually moderately increased, but often normal. In the case of a haemorrhagic infarction, xanthochromia or admixture of blood may result.

#### ■ ■ Disease Progression

The clinical course of venous sinus thrombosis is difficult to predict. In children, a spontaneous, favourable outcome can be observed, especially in focal thrombosis with minimal clinical symptoms because children usually tolerate changes in blood flow better than adults. The prognosis of spontaneous dural sinus venous thrombosis is therefore usually more favourable in children than in adults. An exception to this is new-borns and infants.

#### ■ ■ Treatment

Usually, dural venous sinus thrombosis is treated **with anti-coagulants**. There have been and still are indications that heparin may provoke haemorrhaging in haemorrhagic areas. Because an untreated venous sinus thrombosis can lead to a serious disease, heparin is nevertheless used. It could be shown that it leads to a significant improvement in the prognosis. The benefit of local fibrinolytic treatment is controversial. If necessary, a large-scale trepanation can additionally be considered. Following anti-coagulation with heparin, oral anti-coagulation with phenprocoumon should continue for 6 months. In the case of septic thrombosis, antibiotics and adjuvant anti-convulsive treatment are self-evident.

#### ■ Vascular Dissection

##### ■ ■ Epidemiology, Aetiology

Dissections mainly occur in patients younger than 45 years (■ Figs. 9.77, 9.80). Often, a history of trauma, sometimes only “trivial traumas”, can be elicited. If no cause can be detected, this is referred to as “spontaneous” dissection. Pre-disposing conditions for dissection are fibro-muscular dysplasia, Ehler–Danlos syndrome, other elastin- or collagen-related disorders, and inflammation.

##### ■ ■ Medical Imaging

**Digital Subtraction Angiography.** A dissection can be unambiguously detected on DSA; a flame-shaped leakage of the contrast agent appears in the closed vessel (■ Fig. 9.80). At the sub-acute and later stages, often only irregularities of the vascular wall, stenosis, or pseudo-aneurysmal widening at the base of the skull can be identified. Intra-cranial dissections, which can lead to sub-arachnoid haemorrhaging, rarely occur.

**MRI and MR Angiography.** On MRI, dissections can generally be clearly demonstrated. On the axial slices, the eccentric narrowing of the vessels by the intra-mural haematoma usually leads to increases in signal. Hyper-intense intra-mural haematoma can be seen, especially on fat-suppressed T1-weighted sequences in coronary sectioning. On MR angiography, mural haematoma may go undetected if only TOF angiography and MIP reconstruction are performed.

##### ■ Fibromuscular Dysplasia

The mean age of diagnosis is about 50 years. Young women in particular are affected. The disease mainly affects the internal



■ **Fig. 9.80a,b Dissection.** **a** On DSA, there a vascular occlusion of the internal carotid artery with flame-shaped leakage of the vascular stump. **b** On the axial T2-weighted image through the neck, the mural haematoma in the internal carotid artery can be seen as a crescent-shaped signal increase



carotid and the renal arteries; the vertebral arteries are less frequently affected. Vascular changes are characterised by constrictions and expansions and have a beaded appearance. Usually, only DSA can provide an unambiguous diagnosis (■ Fig. 9.81).

❗ **In younger women without vascular risk factors, the possibility of fibro-muscular dysplasia should always be considered in the case of infarcts, TIAs, or unexplained cerebral embolism.**

### ■ Vasculitis

#### ■ Epidemiology, Classification, Symptoms

Isolated vasculitis of the CNS is extremely rare. Vasculitis can be divided into primary and secondary vasculitis of which the vast majority can manifest in various organ systems, including the CNS. Isolated CNS vasculitis is limited to the CNS. In this case, as with other forms of vasculitis, headaches, encephalopathy, focal deficits, and seizures are prominent. A criterion of isolated CNS vasculitis is the clinical and laboratory exclusion of other forms of vasculitis or other organ systems.

#### ■ Medical Imaging

Multiple changes in the calibre of intra-cranial arteries in cerebral angiography and multiple, small lesions that take up contrast agent in cerebral MRI are findings typical of vasculitis, which can also be found in the case of other vasculitides (■ Fig. 9.76). The only proof is meningeal or cerebral parenchymal biopsy. Accurate diagnosis is required, especially with a background of immunosuppression with steroids and cyclophosphamide. MRI is more sensitive than CCT for detecting multiple small lesions in the cerebral parenchyma that occur with vasculitis. A normal MRI largely excludes the possibility of intra-cranial vasculitis, regardless of whether it involves a systemic or an isolated CNS vasculitis.



■ **Fig. 9.81 Fibro-muscular dysplasia.** DSA of the left communicating carotid artery. In the lateral projection, bifurcation and an irregularity of the wall of the internal carotid artery are typical representations of fibro-muscular dysplasia

#### Classification of Vasculitis

##### Primary Vasculitis

- Large vessels:
  - Giant cell arteritis
  - Takayasu's arteritis
  - Isolated angiitis of the CNS

- Mid-sized vessels:
    - Poly-arteritis nodosa
    - Kawasaki
  - Small vessels:
    - Churg–Strauss syndrome
    - Wegener’s granulomatosis
    - Microscopic polyangiitis
- Secondary Vasculitis
- Rheumatic diseases:
    - Systemic lupus erythematosus
    - Mixed connective tissue disease
    - Rheumatoid arthritis
    - Sjögren’s syndrome
  - CNS infections:
    - Viruses
    - Bacteria
    - Fungi
    - Parasites
  - Other:
    - Medication
    - Neoplasia
    - Inflammatory bowel disease.
    - Sarcoidosis

## ■ CADASIL Syndrome

### ■ Clinic and Aetiology

CADASIL stands for “cerebral autosomal dominant arteriopathy with sub-cortical infarcts and leuko-encephalopathy.” In middle adulthood, incipient cerebral blood flow disorders and the development of sub-cortical dementia with spastic quadriplegia and pseudo-bulbar palsy are prominent. In addition, migraine headaches and psychiatric disorders also frequently occur.

In 1993, with the help of a large French family, the gene defect responsible was localised to the short arm of chromosome 19 (26). Meanwhile, in Europe more than 100 families with this disease have become known.

### ■ Symptoms

Clinically, patients present with signs of sub-cortical dementia, which include drive disorder and emotional flattening, reduced attention span, perseveration and reduced active memory performance. Migraine-like headaches are common and an important early symptom of the disease.

### ■ Diagnosis, Medical Imaging

In addition to clinical symptoms and a positive family history, MRI findings are essential for the diagnosis. The T2-weighted images reveal diffuse, predominantly peri-ventricular confluent hyper-intensities, which later touch the entire medullary layer, in addition to circumscribed, lacunar infarcts with a predilection for the basal ganglia, the internal capsule, the thalamus and the brain-stem. The cortex is usually not affected. In advanced cases, it sharply contrasts with the pronounced changes of the medullary layer. Infra-tentorial lesions are rare. Territorial infarcts are not part of the clinical picture.

Because the genetic effect of CADASIL has now been identified, direct DNA diagnostics will soon be available.

## 9.4 Intra-cranial Tumours

### 9.4.1 Basics

#### ■ Primary Brain Tumours

##### ■ Epidemiology

Each year in Germany, 3,700 men and 3,400 women develop tumourous growths of the nervous system. This corresponds to an annual incidence of between 6 and 7 per 100,000. Thirty per cent of tumours in women and more than 50% of the tumours in men occur before the age of 60; 10% of these manifest in childhood.

The age distribution of brain tumours shows a first peak incidence in childhood (3–9 years) and a second peak between 55 and 65 years of age. The histology and localisation of brain tumours of children differ from those of adults. In children, medulloblastoma and low-grade astrocytomas are the most frequent, while malignant gliomas and meningiomas are prevalent in adults. Men often suffer from gliomas, while women suffer more frequently from meningiomas.

Childhood brain tumours account for approximately 15–20% of all primary brain tumours. Tumours of the CNS are the second most common paediatric tumours after leukaemic diseases. Infra- and supra-tentorial tumours occur with almost equal frequency. There are, however, differences with regard to the age of the disease; supra-tentorial tumours are more common in the first 2–3 years of life, while infra-tentorial tumours reach their peak at between 4 and 10 years of age. From the 10th year of life, infra-tentorial and supra-tentorial tumours occur with almost equal frequency.

In the US, the annual incidence of primary intra-cranial tumours is about 11.5 in 100,000. Among these tumours, 52% are gliomas, 24% are meningiomas, 8% are pituitary adenomas, 6.5% are schwannomas and 4% are primary CNS lymphomas. The remaining 5.5% of primary intra-cranial tumours involve very rare tumours.

##### ■ Symptoms

The symptoms of intra-cranial tumours strongly depend on the time of life. In infancy, symptoms include an increase in head circumference, nausea, vomiting and lethargy. Older children often show symptoms similar to adults: in addition to general symptoms (headaches, seizures, or visual disturbances), local or neurological deficits and nerve paralysis, ataxia and hemiparesis may occur.

Tumours of the pituitary region in the area of the hypothalamus frequently reflect their endocrine dysfunction with symptoms such as diabetes insipidus, growth retardation, or precocious puberty.

**Indications for neuroradiological diagnosis** on suspicion or for the exclusion of a brain tumour include:

- Persistent headaches (lasting longer than 6 months) that do not respond to medical treatment
- Headaches associated with neurological symptoms

- Persistent headaches with no family history, e.g. migraines
- Persistent headaches that accompany episodes of confusion, disorientation and vomiting
- Headaches that occur in children whilst sleeping or immediately after waking up
- Headaches in children with syndromes that are associated with an increased rate of brain tumours (e.g. neurofibromatosis or other phakomatoses)

### ■ ■ Medical Imaging

**Characteristics of Intra-cerebral Tumours.** On CT or MRI, space-occupying lesions are typically seen in normal parenchyma because of their **deviating density or signal intensity**. Furthermore, there may be a mass effect, which leads to a shift in the brain structures or a pathological enhancement following the administration of contrast agent. In the healthy CNS, contrast agent enhancement is seen only in the region of the pituitary gland, pituitary stalk and its place of origin from the hypothalamus, in addition to the pineal gland and the choroid plexus. Compared with the rest of the brain tissue, tumours show up as hypo-dense on unenhanced CT. On T1-weighted MRI sequences, they appear hypo-intense to the myelinated white matter. On T2-weighted images, they are hyper-intense.

The incidence of **haemorrhaging, necrosis, calcification**, and the behaviour of contrast agents can even vary among tumours of similar histological classification and even more for tumours of a different cell type. All tumours display a mass effect. In cases of a relatively slow-growing, peripheral tumour, the **mass effect** leads to expansion or erosion of the cranium.

In faster-growing, more centrally located tumours, displacement is involved. This can lead to the **herniation of cerebral tissue**. Supra-tentorial lesions usually cause a herniation caudally through the tentorial incisure, and infra-tentorial lesions can lead to cranial herniation.

Trans-tentorial herniation usually leads to pressure on the mid-brain with subsequent disturbances in eye movement and pupillary response. A tentorial herniation may also result in a compression of the posterior cerebral arteries between the mid-brain and tentorium with subsequent unilateral or bilateral ischaemia in the area supplied by these arteries. The herniation of the cerebellar tonsils through the foramen magnum can occur in both supra-tentorial and infra-tentorial space-occupying lesions. The tonsillar herniation, which is readily depicted via MRI, can lead to respiratory failure.

As soon as a space-occupying lesion is detected, it must be decided whether it is situated **intra-parenchymally or extra-parenchymally**. In other words: does the space-occupying lesion come from the cerebral parenchyma or from extra-parenchymal structures such as the meninges, the choroid plexus, or the sub-arachnoid cavity?

**Intra-parenchymal lesions** compress the cisterns and sulci, infiltrate the surrounding cerebral parenchyma and can cause significant oedema.

**Extra-parenchymal lesions** typically shift the brain structures instead infiltrating them. The brain is pushed away from the bone and the dura mater, which leads to an extended cistern. A well-definable gap divides the extra-parenchymal space-occu-

pying lesion of the brain. There are normally few or no signs of peri-focal oedema.

Other characteristics that indicate an extra-parenchymal tumour include a low mass effect compared with the size of the tumour, an expansion of the mass above the median without involvement of the cerebral commissure, and relatively bland clinical symptoms. Of course there are exceptions. For example, an intra-parenchymal space-occupying lesion with slow growth may result in only a small mass effect. However, based on the above rules, it is generally possible to distinguish between intra- and extra-parenchymal growth.

**Differential Diagnosis.** After it has been determined that the space-occupying mass is situated intra-parenchymally, it must be decided if it does indeed involve neoplasia. **Infections and ischaemia** may resemble neoplasia and should at least be briefly considered in the differential diagnosis. Cerebral abscesses are intra-parenchymal lesions, which are characterised by rapid growth and marginal enhancement. Tumours typically grow slowly and show more irregular, marginal enhancement. The diagnosis as ischaemia is based on the localisation in a vascular distribution area and the involvement of both grey and white matter. Tumours and infections occur typically in the white matter or at the cortico-medullary border. However, there are tumours that are primarily located in the cortex, which have symptoms resembling acute infarction. If the differential diagnosis is difficult because of the imaging and clinical criteria, a follow-up examination should take place before biopsy. If the structural changes involve an infarct, this results in an enhancement within 5 days, and the space-occupying effect will have decreased by the end of the first week. An abscess growing rapidly, and the marginal, contrast agent-related ring becomes more evident. Tumours will change only slightly, if at all, within 7 days.

The **diagnostic imaging** is based on cranial and spinal CT and MRI. Pre-operative angiography is performed in accordance with the operating surgeon. In the case of brain tumours that tend to metastasise in the CSF (e.g. medulloblastomas, ependymomas), the primary diagnosis includes spinal MRI and CSF examination. A disturbance in CSF circulation may result in a deterioration of neurological status because of the pressure relief associated with the lumbar puncture.

Even if the primary diagnosis of an intra-cranial tumour usually proceeds via means of CT, MRI should be performed as a pre-operative evaluation because the multi-planar layers afford a more precise investigation of the tumour and its relationship to surrounding structures. Particularly in the area of the posterior fossa, an evaluation based on the osseous artefacts on the CT is often limited. MRI is more sensitive for investigating tumour proliferation along the sub-arachnoid cavity.

➤ **In children, MRI should be performed at the beginning of the diagnosis because of the exposure to radiation. In small children, adequate sedation is required to prevent motion artefacts.**

**Computed Tomography.** The imaging should be performed without and after contrast enhancement in axial slices. If a tumour in

the posterior fossa is involved, coronal images (either directly or reformatted) are helpful for depicting the relationship between the tumour to the tentorium and the foramen magnum. Even small lesions close to the dura or the bone can be more easily found. Reformatted sagittal images are mainly helpful in centrally located tumours, e.g. on the third ventricle.

**Magnetic Resonance Imaging.** The standard sequences best consist of a sagittal T1-weighted sequence, and axial T2-weighted spin echo (SE), or fast spin echo (FSE) images. The sequences should have a layer thickness of 5 mm or less throughout the entire brain. In addition, T1-weighted images of either coronal or axial sections through the tumour can better assess the magnitude and relationship to the surrounding structures. After the administration of contrast agent, the slice orientation of the pre-contrast examination should be adjusted.

In general, the brain-stem, supra-sellar space, and space-occupying lesions of the third and fourth ventricles are best represented in sagittal or coronal slice orientation. Space-occupying lesions in the cerebral hemispheres and cerebellum can best be assessed in the axial and coronal slice orientations.

The amount of contrast agent is 0.1 mg/kg body weight and is administered as an i.v. bolus immediately before the investigation.

**! The time of contrast agent administration should be as uniform as possible because a delay may result in increased diffusion into the extra-cellular space, which leads to a larger enhanced area. Differences in the time interval can thus lead to the incorrect assessment of tumour size.**

**Flow compensation techniques** (peripheral or cardiac gating) are useful for tumours in the posterior fossa because a partial misregistration of contrast agent may obscure areas of blood flow. In particular, if the T1 relaxation time has been reduced by paramagnetic contrast agents, flowing blood may lead to artefacts. These artefacts are especially problematic in the posterior fossa. High doses of contrast agent may increase the number of artefacts. Flow compensation techniques (either by gradient pulses or gated recordings) are therefore important following the administration of contrast agent. A delay of 15–30 min following the administration of the contrast agent can reduce the appearance of artefacts because the intra-vascular contrast is reduced.

However, in clinical routine, this is hardly an acceptable delay.

**CT Versus MRI.** Contrary to popular assumption, CT is often more accurate than MRI when it comes to the assignment of tumours. Before the administration of contrast agents, small round cell tumours such as medulloblastoma or germinoma are iso-dense or hypo-dense compared with the rest of the brain parenchyma. In children, astrocytomas are usually hypo-dense. Thus, a supra-sellar germinoma can be distinguished from a supra-sellar astrocytoma, and a medulloblastoma can be distinguished from a cerebellar astrocytoma. On MRI, this is more difficult. Calcifications, which occur in the case of craniopharyngioma and teratoma, are easier to detect via CT. The additional anatomical

information provided by MRI predominates over the more limited pre-operative, histological classification.

**Post-operative Control.** The post-operative “follow-up” usually involves unenhanced and contrast-enhanced CT or better MRI within 72 h. Following the immediate post-operative period, the initial imaging should include T1- and T2-weighted axial sequences before the administration of contrast agent in addition to T1-weighted images after the administration of contrast agent. The unenhanced images are required to distinguish between post-operative haemorrhaging and residual tumours. An enhancement along the resection margin can be observed within 24 h after tumour resection. The degree of enhancement rapidly increases in the post-operative phase. Early imaging (within the first 72 h) should therefore be performed in order to determine the extent of resection. In the course of further investigations, the surgery-related enhancement at the surgical margin decreases after 6 weeks and should no longer be detectable after 12 months. After the administration of contrast agent, meningeal and parenchymal enhancement is almost always present on post-operative MRI. A dural enhancement of a different thickness is usually smooth and often persists for several years in the cerebral convexities and along the tentorium. In the case of a nodular meningeal enhancement, sub-arachnoid tumour growth should be suspected.

#### ■ ■ Histology

The classification, including the grading of intra-cerebral tumours, is still based on histogenic findings. The 1993 revision of the WHO classification of brain tumours, also resulted in a change in the grading of astrocytic gliomas. In addition, the atypical meningioma was introduced. For the prognostic assessment and for therapeutic decisions, an unequivocal assignment is important, which can ultimately only proceed via histopathology. With a mean survival of 15 months, the prognosis of glioblastoma (grade IV astrocytoma) is still relatively poor.

The histological classification of the WHO considers the cyto-genetic origin of brain tumours and up to four different grades of malignancy (WHO grades I–IV). Symptoms of brain tumours mostly include personality changes, focal neurological disturbances, signs of intra-cranial pressure, or cerebro-organic seizures. Malignant brain tumours occasionally metastasise in the CSF and lead to spinal and radicular symptoms, as is also the case with primary spinal tumours. Systemic metastases of primary intra-cranial tumours are rare.

#### ■ ■ Treatment

As a rule, **complete resection** of the tumours is strived for. If germinoma or lymphoma is suspected, or in the case of tumour localisation in functionally critical regions, stereotactic or neuro-navigational biopsies are taken to confirm the diagnosis. Then, depending on the histological findings, radiotherapy, chemotherapy, or a combination will be initiated. It may also be preferable to wait. The complete resection of a WHO grade I tumour is curative.

In neurinomas, especially acoustic neuromas up to 2 cm in diameter, one-stage or fractional **radiotherapy** is an alternative

to surgery, especially in the case of an increased risk of surgery. Fractionated irradiation is also considered in larger neurinomas. Post-operative irradiation is an established therapy in the higher grade gliomas WHO (grade III and IV) in addition to in the case of medulloblastoma and germ cell tumours of the CNS. Surgery and radiotherapy cure more than 50% of medulloblastomas. Germinomas are usually exclusively cured by irradiation. In the case of macroscopically incompletely resected low-grade gliomas (WHO grade II) and macroscopically completely removed malignant meningiomas, radiation therapy is somewhat controversial.

Compared with irradiation, **chemotherapy** plays a minor role in the treatment of the primary brain, but is nevertheless effective at treating some tumours. In the case of anaplastic gliomas and glioblastomas, temozolomide has an effect in primary and relapse therapy and competes with protocols based on nitrosourea, e.g. vincristine (PCV). Children with medulloblastomas seem to benefit from chemotherapy. In recent years, chemotherapy has also been proven effective for malignant germ cell tumours of the central nervous system. For primary non-Hodgkin's lymphomas of the CNS, methotrexate-based chemotherapy is now the standard first-line therapy.

- **Brain Metastases**
- ■ **Epidemiology**

Approximately 10–20% of all **systemic tumour disease** involves **metastasis in the nervous system**. The risk is 20–50% for malignant melanoma and small cell bronchial carcinoma and 10–30% for non-small cell bronchial carcinoma, breast cancer and renal cell carcinoma. There are mainly cerebral intra-parenchymal or spinal epidural metastases.

- ■ **Symptoms**

Brain metastases display symptoms of focal neurological disorders, intra-cranial pressure, or cerebro-organic seizures, while epidural metastases display symptoms of cross-sectional syndromes.

- ■ **Medical Imaging**

The diagnostics include MRI as the method of choice or CT with and without contrast agent. To distinguish between the presence of single or multiple metastases, MRI is essential. Approximately 5% of breast cancer patients, 10% of patients with lung cancer, 5–15% of patients with melanoma and non-Hodgkin lymphoma patients, and 5–15% of patients (despite CNS prophylaxis) with acute lymphoblastic leukaemia (ALL) develop **neoplastic meningitis**. Up to two thirds of these patients simultaneously exhibit intra-parenchymal metastases. In addition to the symptoms occurring in brain metastases, neoplastic meningitis involves cerebral nerve and radicular disorders. Using CT or MRI, neoplastic meningitis can be proven via the uptake of contrast agent in lesions of the sub-arachnoid cavity, but should nevertheless be confirmed via the detection of tumour cells in the CSF.

- ■ **Prognosis**

Cerebral or spinal manifestations usually occur in advanced primary disease. Even with adequate therapy, one can only expect a mean survival time of 3–6 months. The 1-year survival rate is

10–20%. In patients with solitary metastases or isolated leptomeningeal infiltration, e.g. in breast cancer, multi-year survival is occasionally possible.

### 9.4.2 Infra-tentorial Tumours

In childhood, the most common tumours of the posterior fossa are medulloblastoma, astrocytomas of the cerebellum and brain-stem, atypical teratomas, rhabdoid tumours and ependymomas. Although medulloblastomas, ependymomas, atypical teratomas and rhabdoid tumours often appear to grow intra-ventricularly, it is in fact intra-parenchymal tumours that proliferate in the fourth ventricle. Brain-stem tumours have recently been divided into different groups.

The differential diagnostic considerations of infra-tentorial brain tumours in childhood and adulthood are summarised in the overview.

#### Differential Diagnosis of Infra-tentorial Tumours in Children and Adults in Order of Decreasing Frequency

Children:

- Cerebellar astrocytoma
- Medulloblastoma
- Brain-stem glioma
- Ependymoma

Adults:

- Schwannoma
- Meningioma
- Epidermoid
- Metastasis

- **Medulloblastoma (Primitive Neuro-ectodermal Tumour of the Posterior Fossa)**

- ■ **Definition, Epidemiology**

Medulloblastomas are highly malignant tumours that are composed of primitive, undifferentiated, small round cells. These undifferentiated cells were described by Bede and Cushing as medulloblasts, which led to the term “medulloblastoma”.

After cerebellar astrocytomas, medulloblastomas are the second most frequent infra-tentorial tumours in childhood. They account for about 15–20% of all intra-cranial tumours in childhood and 30–40% of tumours of the posterior cranial fossa. Boys are two to four times more likely to be affected than girls. Approximately 40% of medulloblastomas occur within the first 5 years of life; 75% occur within the first 10 years. However, medulloblastomas can also occur in adulthood; they account for approximately 0.5–1% of adult brain tumours.

In rare cases, medulloblastomas are located near the surface of the cerebellar hemispheres. Histologically, these tumours are often desmoplastic and frequently occur in adults. They are also genetically indistinguishable from the classical type. As they probably originate from the external granule cell layer of the cerebellar cortex, they are mostly found on the surface and have a close relationship with the dura or infiltrate them early.

### ■ ■ Clinical Symptoms, Localisation

After the onset of the clinical symptoms of a medulloblastoma, diagnosis usually occurs within 4 weeks. The most common clinical symptoms include nausea, vomiting and headaches. In addition to general intra-cranial pressure, nausea and vomiting can also be explained by an outgrowth of the tumour in the area postrema, which is generally considered the “vomiting centre”

Within the first year of life, a rapid growth in head circumference is often observed if the cranial sutures are not completely closed. Medulloblastomas of the first 3 years of life are different from those of older children especially because of the more frequent hydrocephalus, a higher tumour stage and a higher incidence of CSF dissemination, which are even evident in the early stages of diagnosis. The prognosis is therefore also dependent on the age of the patient.

In older children and young adults, truncal and static ataxia are often leading symptoms. Should paraparesis or symptoms of the cauda equina occur, spinal dissemination of CSF must be assumed. This is considered a poor prognostic factor. In the case of known or proven medulloblastoma in the posterior fossa, the entire neuraxis must then be investigated via MRI.

In childhood, two thirds of medulloblastomas occur in the vermis, in adolescents and adults, they are located more frequently in the cerebellar hemispheres. The tumour often forms a well-defined space-occupying lesion in the vermis, which expands the space between the cerebellar tonsils. It impacts the roof of the fourth ventricle, resulting in a partial or complete shift of the CSF circulation with consecutive occlusive hydrocephalus. Overgrowth can occur dorsally in the cisterna magna and caudally in the foramen magnum. The medulloblastoma may occasionally infiltrate the cerebello-pontine angle through the foramina of Luschka. An outgrowth into the brain-stem can be seen in approximately one third of patients. A lepto-meningeal dissemination via the CSF occurs very frequently; in the literature, it is reported in up to 100% of cases. Supra-tentorial dissemination most frequently occurs in the Sylvian fissure, the basal cisterns and the posterior fossa. On T1-weighted sequences, after the administration of contrast agent, lepto-meningeal tumour dissemination can be depicted as a hyper-intense structure that traces the sulci and cisterns. A frosting-like coating of the brain-stem can also be seen.

A retrograde dissemination may also occur via the aqueduct in the third ventricle and in the lateral ventricles. From there, intra-parenchymal outgrowth of the tumour may occur. Spinal drop metastases are detected in up to 40% of cases. Systemic metastasis is rare and usually only occurs in the case of tumour recurrence. The skeleton is frequently affected, followed by the lymph nodes and lungs.

### ■ ■ Diagnosis/Medical Imaging

**Histology.** Histologically, more than half of medulloblastomas are of the classic undifferentiated type. In 25% of cases, this is a so-called desmoplastic medulloblastoma, which commonly occurs in the second decade of life and in the cerebellar hemispheres. Approximately 20–25% show a glial or neuronal differentiation within the tumour, thereby resulting in a poorer overall prognosis.

**Computed Tomography.** On the CT, the typical medulloblastoma appears as a relatively circumscribed hyper-dense mass in the cerebellar vermis, which usually shows homogeneous enhancement after the administration of contrast agent. This primary hyper-density arises because of the high number of small-cell medulloblastomas. The tumour is often surrounded by a hypo-dense rim, which is oedema. Calcifications and cysts may occur. The fourth ventricle is usually pushed anteriorly and is sometimes no longer delineated. Because of the space-occupying lesion in the posterior fossa, incipient disturbances of the CSF circulation can frequently be observed, with enlargement of the temporal horns and the third ventricle. Hydrocephalus is seen in about 95% of patients at the time of imaging.

In general, cysts and calcifications rarely occur in medulloblastomas. However, several studies showed up to 60% atypical CT appearances with calcifications in up to 40% of cases and cysts or necrosis and tumour components without enhancement in up to 50% of cases.

➤ **A differential diagnosis is the astrocytoma, which is usually hypo-dense in the surrounding cerebral parenchyma on unenhanced CT. The hyper-density on the unenhanced CT is the best criterion for distinguishing them from other tumours of the posterior cranial fossa.**

**Magnetic Resonance Imaging.** On MRI, the medulloblastoma is variable and non-specific (■ Fig. 9.82). The tumour location and patient age are the most important factors contributing to a correct diagnosis. On sagittal slices, the starting point of the classic medulloblastoma of the cerebellar vermis is easy to recognise because a ventral slit-shaped lamella of CSF separates the tumour from the base of the fourth ventricle. Occlusive hydrocephalus is the result of CSF circulation disturbance from the posterior fossa. On T1-weighted imaging, the medulloblastoma is depicted as a hypo-intense space-occupying lesion. After the administration of contrast medium, a homogeneous, partly heterogeneous area of enhancement appears. In 5–10% of cases, medulloblastomas do not display enhancement after the administration of contrast agent. There is, however, weak or strong uptake of the contrast agent by the tumour. On T2-weighted sequences, the tumour is hyper-intense to iso-intense in grey matter. The signal behaviour depends on the cell density and the free water within the tumour. A high cell count and low water content within the tumour lead to lower hyperintensity on T2-weighted image sequences. On the T2-weighted images, the medulloblastoma is often clearly more hypo-intense than a pilocytic astrocytoma.

On unenhanced images, a **lepto-meningeal spread of the tumour** into the CSF spaces is difficult to detect. Therefore, if a medulloblastoma is suspected, pre-operative examination of the entire neuraxis must be performed before and after the administration of contrast agent. Medulloblastomas have often already metastasised in the CSF by the time of diagnosis. In one study, 17% of medulloblastomas exhibited CSF dissemination at the time of diagnosis. CSF metastases are usually nodular and partly laminar. They occur can either cranially or spinally. Meningeal and epidural metastases are variable in their contrast agent behaviour and may have a different behaviour from the primary

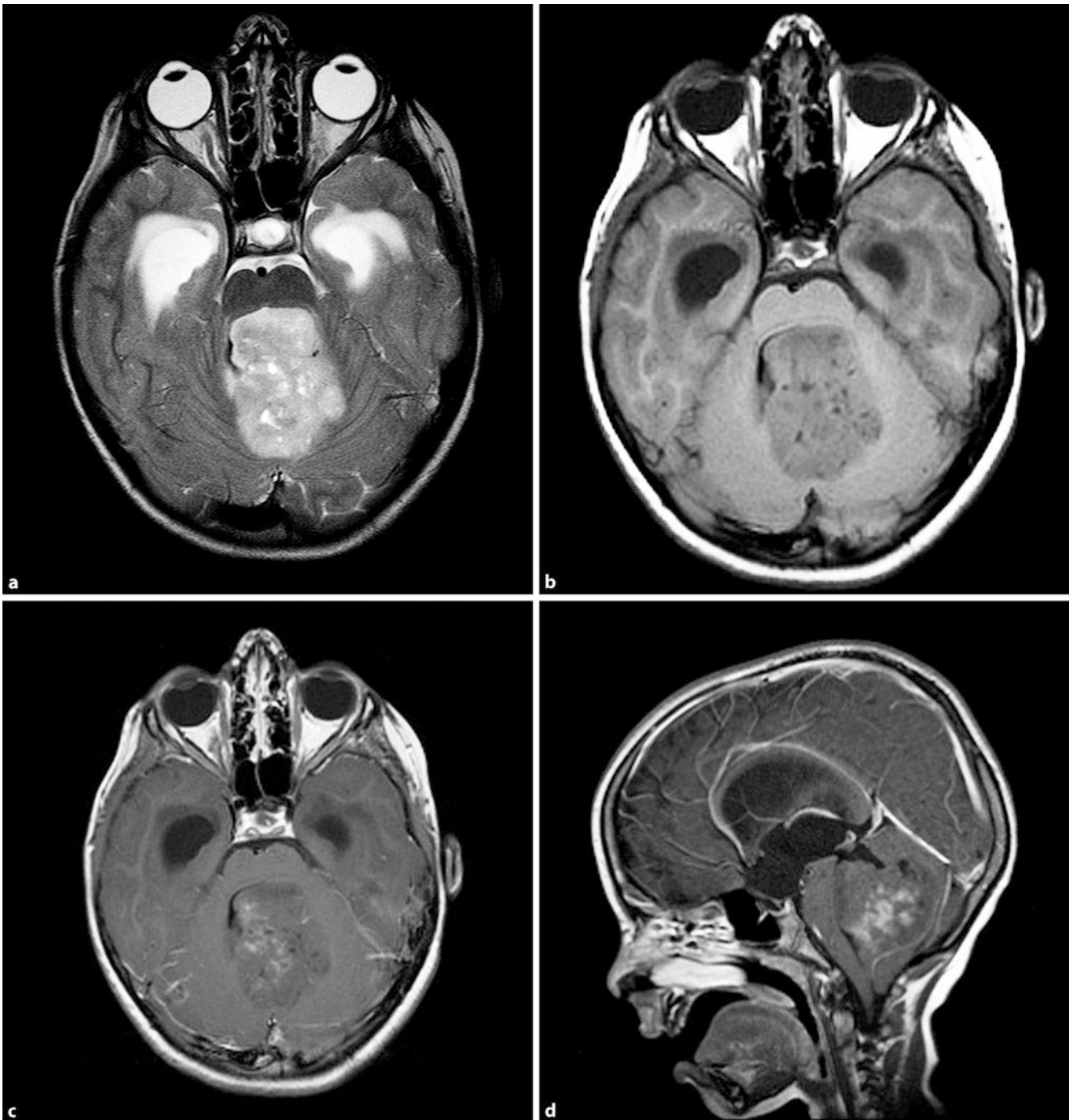


**Fig. 9.82a–d Medulloblastoma.** A 3-year-old girl with fasting vomiting persisting for 3 weeks. **a** On the T2-weighted images, compared with the grey matter, there is a hyper-intense space-occupying lesion in the fourth ventricle with compression of the brain-stem and incipient CSF circulation disturbance (widening of the temporal horns). **b, c** Before and after the administration

of contrast agent, the axial T1-weighted sequences reveal a hypo-intense space-occupying lesion with moderate uptake of contrast agent. **d** On the sagittal recording, the expansion of the tumour and the exit from the roof of the fourth ventricle can be seen

tumour. CSF dissemination is frequently seen in the infundibular recess of the third ventricle, which can sometimes only be seen by means of a non-physiological thickening of the pituitary stalk.

#### ■ Cerebellar Astrocytomas

##### ■ Definition, Epidemiology, Classification

Astrocytomas are the most common brain tumours in childhood and account for approximately 40–50% of primary intra-cranial

neoplasms. Approximately 60% of all astrocytomas in childhood are localised infra-tentorially, 40% are found in the cerebellum, and approximately 20% are found in the brain-stem.

Most cerebellar astrocytomas in childhood are of a special histological type, the so-called **juvenile pilocytic astrocytoma**. These astrocytomas are considered a separate tumour entity and classified as a grade I tumour according to the WHO criteria. The name derives from the characteristic hair-like extensions of

the tumour cells. Juvenile pilocytic astrocytomas are the most common benign astrocytic tumour of the CNS. These are well-defined, low-grade tumours, which frequently appear in the area of third and fourth ventricles. They account for approximately 30% of all gliomas in children and adolescents and approximately 5–10% of all gliomas. They are therefore the most common tumour in this age group.

Juvenile pilocytic astrocytomas occur with equal frequency in boys and girls. Most experience these tumours within the first 10 years of life. Blastic astrocytomas, which account for approximately 25% of cerebellar astrocytomas, tend to occur in older children, usually in the first half of the second decade of life.

**Malignant infra-tentorial astrocytomas** and glioblastomas (grade IV astrocytoma) can occur – albeit rarely – in childhood and adolescence.

### ■ ■ Symptoms, Prognosis

In patients with cerebellar astrocytomas, the clinical symptoms are often morning sickness and headaches that persist for weeks and months. Cerebellar symptoms such as ataxia or dysidiadochokinesia can occur and may provide clues to the location of the tumour within the cerebellum. Patients with juvenile pilocytic astrocytoma have a very good prognosis, with a survival rate of 90% after 25 years; this is especially true for cystic juvenile pilocytic astrocytomas. In solid cerebellar astrocytomas, the survival rate after 25 years is reported to be 40%. A malignant transformation of a benign cerebellar astrocytoma is very unusual.

### ■ ■ Treatment

Complete resection of a pilocytic astrocytoma is generally regarded as a curative intervention. Under good conditions and inoperability, stereotactic irradiation can be carried out.

### ■ ■ Medical Imaging

Most cerebellar astrocytomas in childhood occur in the median and propagate in the cerebellar hemisphere. Spreading into the cerebellar hemispheres alone occurs in about 15% of cases. Cerebellar astrocytomas can be cystic, solid, or solid with necrotic central portions (■ Fig. 9.83). A cystic lesion often appears with a tumour nodule within the cyst wall. The cyst wall mostly consists of compressed cerebral parenchyma. Cystic pilocytic astrocytomas with mural tumour nodules account for approximately 50% of cerebellar astrocytomas. The remaining 40–45% usually consist of a solid tumour with a cystic portion or a central necrotic portion.

In approximately 20% of cerebellar astrocytomas, calcifications are found in the histology. Tumour haemorrhaging rarely occurs. At the time of diagnosis, the tumour usually has a diameter of approximately 5 cm. If the tumour extends into the fourth ventricle, it must be distinguished from a medulloblastoma or ependymoma.

In contrast to the pilocytic astrocytomas at the chiasma and hypothalamus, most **cerebellar astrocytomas** are at least partially cystic. The cerebellar astrocytoma typically appears as a large, predominantly cystic mass in the cerebellar vermis or in the cerebellar hemisphere. The solid portion of the tumour usually appears iso-dense to hypo-dense to the surrounding white

matter. However, higher grade tumours can also appear iso-dense or hyper-dense. After administration of the contrast medium, irregular enhancement often appears on the CT. Half of the tumours display a heterogeneous pattern.

**Pilocytic astrocytomas** (WHO grade I) generally exhibit strong homogeneous enhancement of the solid tumour portions. If a large cyst with mural tumour nodules appears, this results in homogeneous enhancement after the administration of contrast agent. If there is no tumour enhancement, it is usually not a pilocytic astrocytoma. On CT, the cyst wall may easily appear to be slightly hyper-dense, but normally has no enhancement. Enhancement of the cyst wall is usually an argument in favour of pilocytic astrocytoma and against haemangioblastoma (Lindau tumour), which can lead to difficulties in the differential diagnosis of older adolescents and young adults.

On **MRI** cerebellar astrocytomas have a variable appearance. Solid and cystic portions can be clearly distinguished. On T1-weighted sequences, the solid portions are usually hypo-intense to the surrounding cerebral parenchyma; on T2-weighted sequences they are usually hyper-intense. However, higher grade tumours may also display a lower signal intensity on T2-weighted sequences, and some may even resemble a medulloblastoma. After the administration of a para-magnetic contrast agent, the solid portions of the tumour usually display similar contrast behaviour to that of CT.

► **Rare anaplastic pilocytic astrocytomas can behave clinically as malignant tumours. Despite the low malignancy, in approximately 5% of all pilocytic astrocytomas, either primary or secondary lepto-meningeal dissemination is observed. The detection of lepto-meningeal dissemination, therefore, does not exclude the diagnosis of low-grade astrocytoma.**

### ■ Ependymomas

#### ■ ■ Localisation, Epidemiology

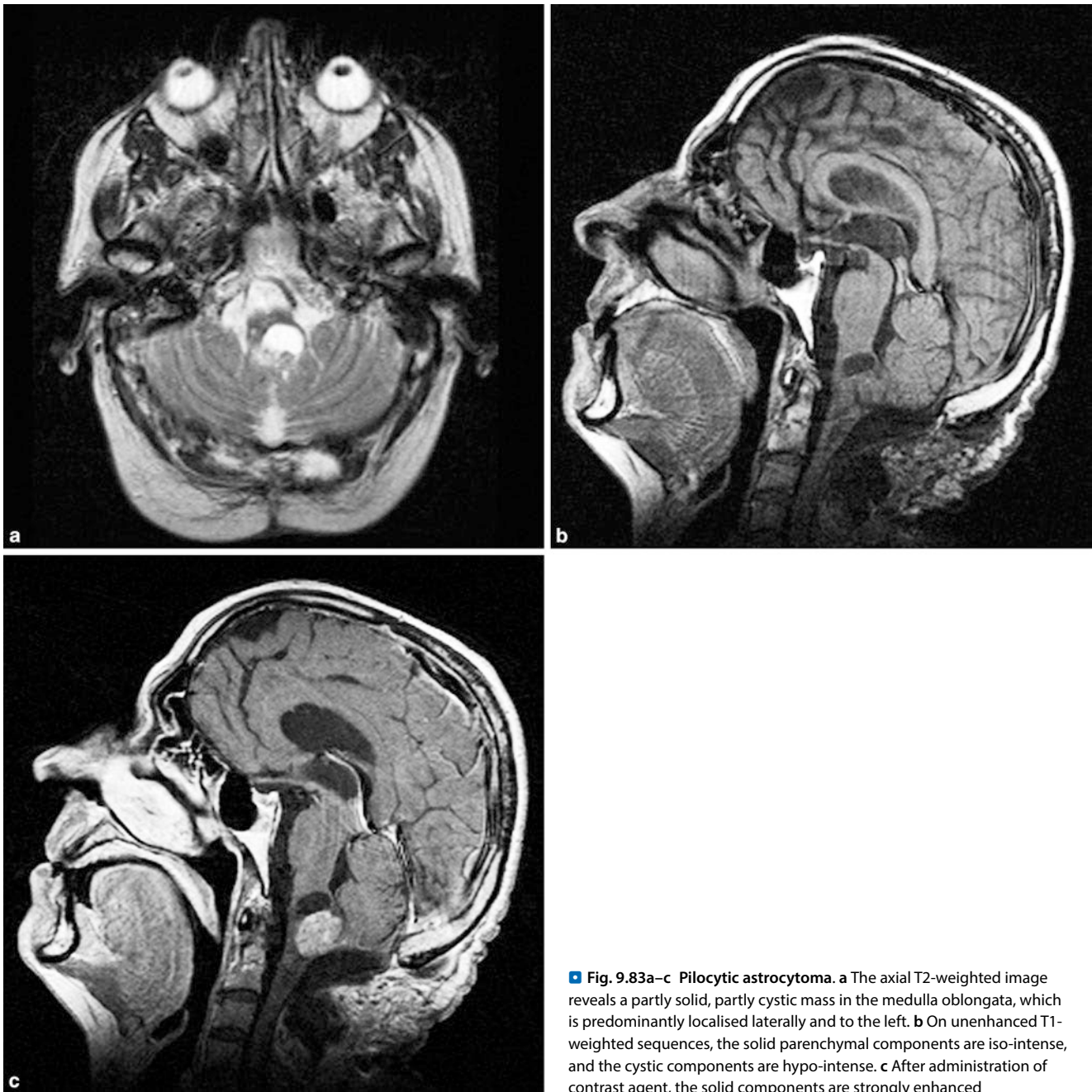
Ependymomas account for approximately 8–9% of primary brain tumours in children and 8–15% of infra-tentorial tumours. In childhood infra-tentorial ependymomas are more common (70%) than supra-tentorial ependymomas (30%). Intra-cranial ependymomas occur more frequently than intra-spinal ependymomas. These are slightly more frequent in boys than in girls.

Ependymomas of the posterior fossa show two peak ages: the first between 1 and 5 years of age and the second between the 30th and 40th years of life.

#### ■ ■ Symptoms

In patients with an ependymoma of the posterior fossa, there is often a long medical history. The delay in diagnosis mostly resulted from a lack of pronounced clinical symptoms. At diagnosis, the children often suffer from nausea and vomiting, which can usually be traced to the accompanying hydrocephalus and intra-cranial pressure increase caused by the shifting of the fourth ventricle, which occurs in approximately 90% of patients. Other symptoms include torticollis and ataxia in addition to lesions of the caudal cranial nerves.





■ **Fig. 9.83a–c Pilocytic astrocytoma.** **a** The axial T2-weighted image reveals a partly solid, partly cystic mass in the medulla oblongata, which is predominantly localised laterally and to the left. **b** On unenhanced T1-weighted sequences, the solid parenchymal components are iso-intense, and the cystic components are hypo-intense. **c** After administration of contrast agent, the solid components are strongly enhanced

#### ■ ■ Localisation, Histology

Ependymomas originate from differentiated ependymal cells from the floor and roof of the fourth ventricle; they grow in the lateral recess of the fourth ventricle and in the foramina of Luschka (■ Fig. 9.84). Supra-tentorially, they emit from the ependyma of the lateral ventricle (foramen of Monro or trigone) or the third ventricle. They either intra-ventricularly or are situated para-ventricularly in the medulla of the cerebrum.

Approximately 50% grow through the foramina of Luschka into the cerebello-pontine angle. In some cases, ependymomas also occur in the cerebello-pontine angle without detection of a tumour in the fourth ventricle or the lateral recess. In this case, it must be assumed that the tumour originates from minimal cell

nests in the cerebello-pontine angle. Ependymomas that occur in the cerebello-pontine angle have a relatively poor prognosis.

Sub-arachnoid spreading of ependymomas via the CSF occurs in approximately 10–12% of cases, mostly in higher grade tumours. In the case of sub-arachnoid spreading, anaplastic ependymoma must be assumed.

Most ependymomas are solid. Calcifications can be histologically detected in up to 50% of cases; cysts can be detected in approximately 20% of cases. Ependymomas can spread along the sub-arachnoid cavity and enclose the vessels and nerves. They can also infiltrate through the ventricular wall into the adjacent brain parenchyma. This so-called **plastic growth** of ependymomas is irregular and adjusted to the shape of the fourth ventricle.

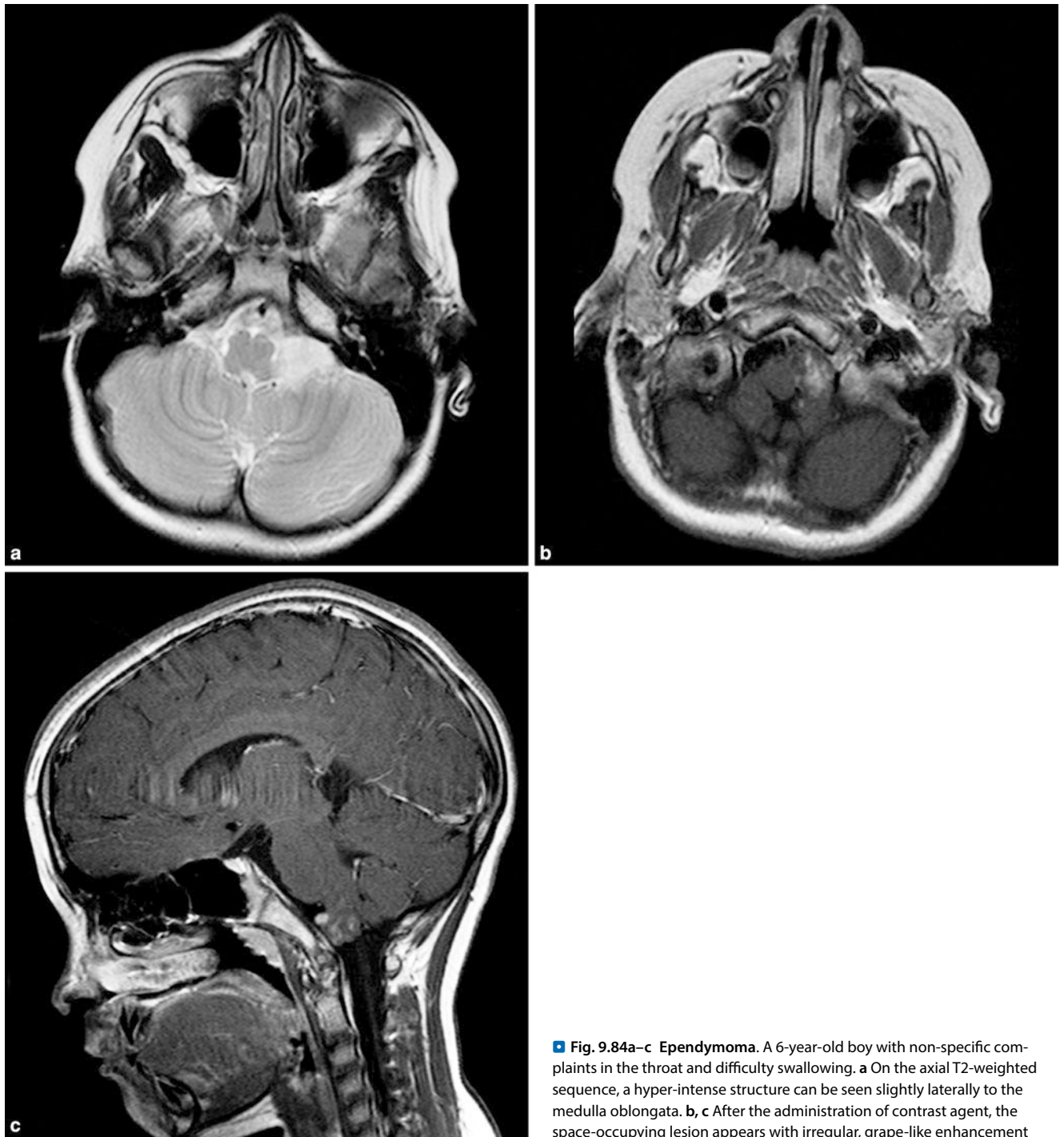


**Fig. 9.84a–c Ependymoma.** A 6-year-old boy with non-specific complaints in the throat and difficulty swallowing. **a** On the axial T2-weighted sequence, a hyper-intense structure can be seen slightly laterally to the medulla oblongata. **b, c** After the administration of contrast agent, the space-occupying lesion appears with irregular, grape-like enhancement

As a result, complete removal of the tumour is often very difficult, and the recurrence rate is correspondingly high.

#### ■ ■ Medical Imaging

**Computed Tomography.** On CT, infra-tentorial ependymomas are usually depicted as iso-dense to hyper-dense space-occupying lesions of the fourth ventricle, partly with punctate calcifications and small cysts. Larger clumpy calcifications are rarely detected. Intra-tumoural haemorrhaging can be seen in approximately 10% of the patients. After the administration of contrast agent, moderately strong contrast enhancement can usually be observed.

The spread of the tumour through the foramen of Luschka into the cerebello-pontine angle cistern supports the diagnosis of ependymoma.

**Magnetic Resonance Imaging.** On MRI T1-weighted sequences, the ependymoma usually appears slightly hypo-intense to surrounding cerebral parenchyma. There are sometimes small areas that appear strongly hypo-intense and most closely correspond to small cystic or regressive modifications. On the T2-weighted sequences, the lesion usually appears iso-intense to the grey matter. The cystic or necrotic areas appear strongly hyper-intense.

Sometimes, fluid levels can be detected within the cystic changes. Ependymomas exhibit a stronger and more regular uptake of the contrast agent than do medulloblastomas. The enhancement in the cyst wall results in a grape-like image, which is especially characteristic of ependymomas (■ Fig. 9.84). From a differential diagnostic perspective, medulloblastomas often cannot be reliably distinguished from ependymomas. Dissemination into the sub-arachnoid cavity is rather rare in ependymomas.

#### MR spectroscopy in medulloblastomas, cerebellar astrocytomas and ependymomas

In general, a proton spectrum of the cerebral tumour reveals increased choline peaks and decreased N-acetyl aspartate (NAA) peaks. The normal spectrum of the cerebellum in childhood has a NAA–choline ratio of  $1.49 \pm 0.36$  and creatine–choline ratio of  $1.3 \pm 0.23$ . Medulloblastomas have a NAA–choline ratio of  $0.17 \pm 0.09$  and a creatine–choline ratio of  $0.32 \pm 0.19$ . Moderate astrocytomas and ependymomas typically display values similar to those of medulloblastoma and the normal cerebellum. Spectral MR microscopy can therefore be helpful in distinguishing medulloblastoma from astrocytomas and ependymomas. However, the choline and NAA values of brain tumours vary greatly. For example, pilocytic astrocytomas, which are generally regarded as benign brain tumours, have very high choline levels, high lactate levels and low NAA values (NAA–choline ratio of 0.29, creatine–choline ratio of 0.29). Such values are usually seen in “high-grade tumours”. However, inflammatory lesions may show spectra similar to malignant tumours.

#### ■ Acoustic Neuroma

##### ■ Definition, Epidemiology, Medical Imaging

This is a benign swelling of Schwann cells and almost always affects the vestibular portion of the acoustic vestibular nerve. With an annual incidence of 1.3 in 100,000 inhabitants, it is integral in the spectrum of neuroradiology.

##### ■ Aetiology

Occurrence of bilateral acoustic neuroma is pathognomonic for type II neurofibromatosis. A genetic defect on chromosome 22 with inactivation of the *NF-II* tumour suppressor gene is responsible for the disease (■ Fig. 9.41). In more than half of the patients, however, it is a new mutation. Approximately 25% exhibit a mosaic formation. In these patients, a deviating and milder clinical course can be observed.

##### ■ Symptoms

Patients usually develop slow hearing loss, tinnitus, dizziness or vertigo.

Facial paralysis also frequently occurs in addition to pain that extends to the ear and brain-stem symptoms in the case of very extensive tumours. The pathophysiology of hearing deterioration has not yet been clarified. This is not only based on a degeneration of the auditory nerve, but also on degenerative changes in the inner ear.

#### ■ Pathogenesis and Imaging

The growth mostly begins in the internal auditory canal and in later stages reaches the cerebello-pontine angle (■ Fig. 9.85). In the process, the internal acoustic meatus is frequently widened. In the case of lower tumour expression, only a thickening of the modiolus may appear on MRI. The tumour tissue exhibits homogeneous uptake of the contrast agent, but may also feature cystic components. Most of the intra-canalicular portion grows posteriorly because the facial nerve is an anterior border.

From a differential diagnostic perspective, the extremely rare cavernous haemangioma must also be considered in the case of small tumours in the internal acoustic meatus.

#### ■ Histology

Histologically, the acoustic neuroma is divided into Antoni A type and Antoni B type, depending on the different reticulin fibre network surrounding the tumour cells. Antoni A type tumour areas are rich in cells; the cells are arranged in parallel. There is a so-called fascicular pattern (school of fish or palisade-shaped pattern). Antoni B type tumour areas have few cells and are regressively modified. The tumour cells are situated in a microscopically loosened reticulin fibre network. Fatty deposits can occasionally be found within the tumour. In the case of type B acoustic neuroma, facial palsy and vestibular symptoms develop significantly more frequently than in type A.

#### ■ Atypical Teratomas and Rhabdoid Tumours

##### ■ Definition, Characteristics

In the last 7–15 years, it has been found that some tumours that were classified as medulloblastomas behave completely differently. These so-called atypical teratomas or rhabdoid tumours occur at a younger age than the medulloblastomas. The mean age at diagnosis is 16 months, while the mean age at the diagnosis of a medulloblastoma is 6 years.

Because the atypical teratoma/rhabdoid tumours do not respond to standard therapy, it is important to differentiate them from the medulloblastomas. One result of this lack of response of medulloblastomas to common chemotherapy is that patients with atypical teratomas/rhabdoid tumours usually die within 1 year of diagnosis.

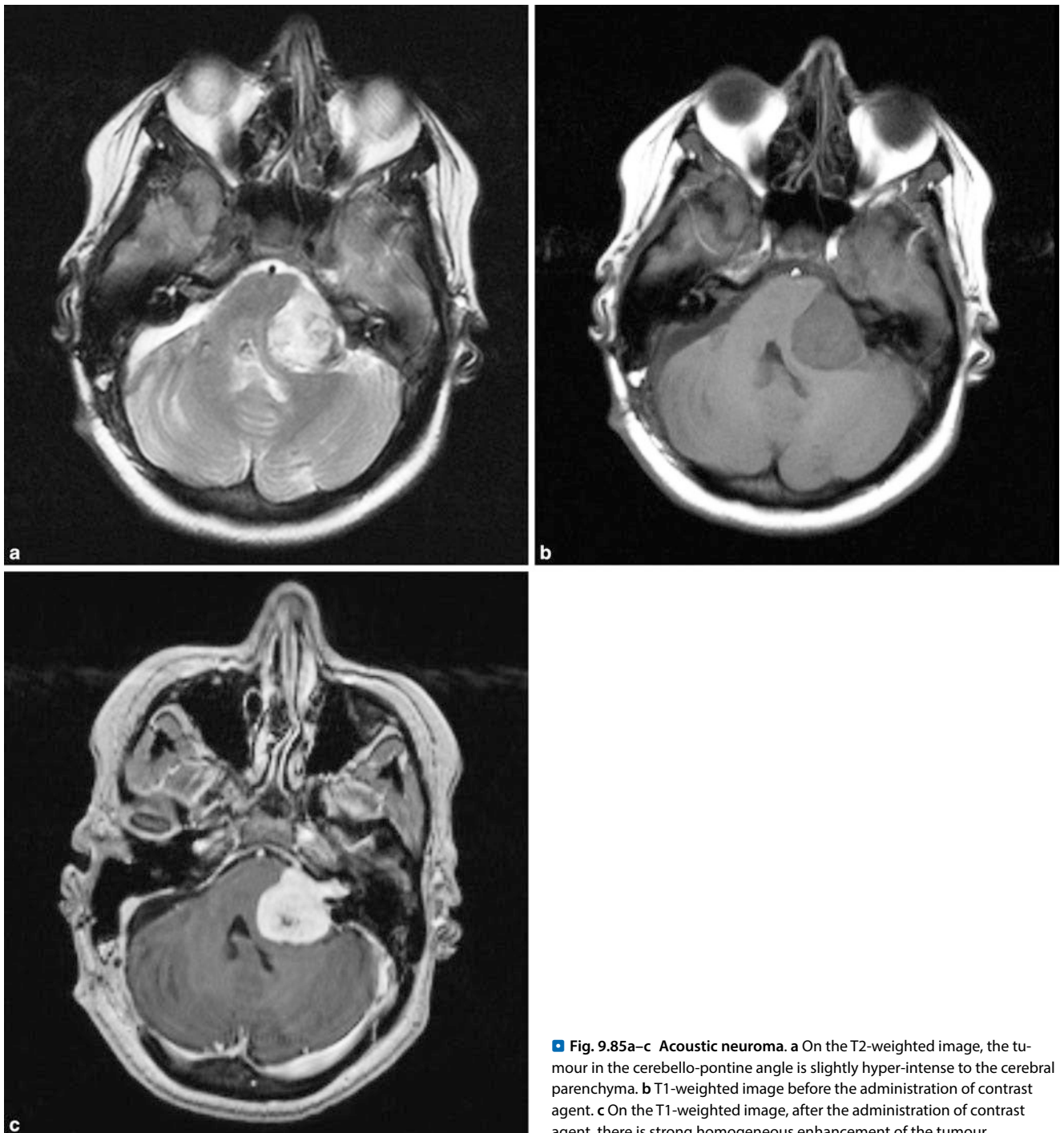
##### ■ Diagnosis

Atypical teratomas/rhabdoid tumours can be distinguished from medulloblastoma using microscopic and histological techniques. Most of these tumours occur in the cerebellum (about 60%), but can also occur in the cerebral hemispheres (20%), in the pineal region and the hypothalamus. These tumours cannot be differentiated from the medulloblastomas and ependymomas in the posterior fossa via imaging. Supra-tentorially, they can be distinguished from neither ependymomas nor primitive neuroectodermal tumours.

#### ■ Haemangioblastomas

##### ■ Definition, Epidemiology

Haemangioblastomas are relatively rare, benign tumours of vascular origin with a frequency of 1–2.5% of all intra-cranial neoplasms. Most haemangioblastomas are diagnosed in young



■ Fig. 9.85a–c Acoustic neuroma. a On the T2-weighted image, the tumour in the cerebello-pontine angle is slightly hyper-intense to the cerebral parenchyma. b T1-weighted image before the administration of contrast agent. c On the T1-weighted image, after the administration of contrast agent, there is strong homogeneous enhancement of the tumour

and middle adulthood. Males are affected slightly more often than women. Approximately 10% of haemangioblastomas occur along with retinal angiomas, a constellation referred to as **Hippel–Lindau disease**. Patients with Hippel–Lindau disease often display multiple haemangioblastomas of the CNS; multiple cysts or tumours often involve the pancreas, kidneys, liver and lungs. Rhabdomyomas can occur in the heart. Patients with haemangioblastoma sometimes show erythrocythaemia, which is thought to arise from increased erythropoietin secretion of the tumour.

#### ■ ■ Localisation

Haemangioblastomas usually occur in the cerebellar hemisphere. If the tumour grows in the medulla, it is often accompanied by a syringomyelia. Haemangioblastomas of the brain-stem or the cerebral hemispheres are less common. As they normally exit from the surface of the brain, the tumours always have a connection to the pial surface. Haemangioblastomas are usually well-circumscribed, soft, cystic tumours with mural tumour nodules.

However, 30–40% of haemangioblastomas only display solid portions.

### ■ ■ Medical Imaging

**Computed Tomography.** On CT, haemangioblastomas usually appear as cystic or solid space-occupying lesions in the posterior fossa. The solid portion of the tumour usually displays strong, homogeneous contrast enhancement. However, small solid portions of the tumour cannot always be detected by CT.

**Angiography.** A haemangioblastoma can be confirmed by angiography because the solid tumour node has typical perfused vascular structures or an extended tumour blush ■ Fig. 9.86.

**Magnetic Resonance Imaging.** On MRI, T1-weighted sequences usually reveal a cystic space-occupying lesion with parietal, slightly hyper-intense nodes. On the T1-weighted sequences, these can often indicate “flow voids,” which result from the strong vascularisation. After the administration of contrast agent, there is a strong homogeneous enhancement. In all patients with suspected Hippel–Lindau disease, the entire neuraxis should be investigated by means of MRI.

### ■ Brain-stem Tumours

#### ■ ■ Epidemiology, Classification

Brain-stem gliomas account for approximately 15% of all tumours of the CNS in children and approximately 20–30% of infra-tentorial brain tumours. Boys and girls are equally affected, and the peak age of these tumours is between the 3rd and 10th year of life. Brain-stem tumours should not be considered as a single entity, but instead are divided into at least four categories:

- Medullary tumours
- Pontine tumours
- Mesencephalic tumours
- NF-I tumours

Within each of these categories, the tumours can be differentiated into **focal and diffuse tumours**.

**MRI** is the method of choice for detecting brain-stem tumours. This main advantage is that unlike CT, no artefacts occur because of the osseous structures of the base of the skull. Another advantage is the multiplanar sectioning. In the case of suspected brain stem tumours, sagittal and axial T2-weighted sequences in addition to FLAIR sequences are applied.

**Diffuse tumours** tend to cause the affected parenchyma to increase moderately, without exhibiting focal exophytic tumour portions. The tumour margins are generally poorly delineated and involve more than 50% of the brain stem in an axial slice orientation at the level of maximum extension. There is normally little to no enhancement of contrast agent.

**Focal neoplasias** are well-circumscribed tumours and usually involve less than 50% of the brain-stem in the axial expansion. Focal tumours often show enhancement and generally have a more favourable prognosis than diffuse tumours.

### ■ ■ Symptoms, Medical Imaging

**Medullary Tumours** The medulla oblongata is rarely affected by brain-stem tumours. Patients typically present with signs of intra-cranial pressure in the brain. In addition, failures of the

caudal cranial nerves can be observed. In the advanced stage, hemiparesis or tetraparesis may occur. Within this tumour entity, focal, dorsally growing exophytic tumours can be distinguished from the more diffusely growing tumours. The diffuse medullary tumours display more infiltrative growth and may spread rostrally into the pons and caudally towards the intra-medullary area. Diffuse medullary tumours have a very poor prognosis compared with the more focally exophytic medullary tumours. Focal medullary tumours often occur in NF-I. Histologically, this often involves pilocytic astrocytomas.

**Medical Imaging.** As with pilocytic astrocytomas of other localisations, the signal of the T2-weighted sequence is usually clearly hyper-intense. The T1-weighted image reveals blurred, limited enhancement. Although these tumours appear to be infiltrative on MRI, they are nevertheless operable. A biopsy should be avoided in favour of a resection, the radicality of which is first decided intra-operatively.

**Pontine Tumours** Pontine tumours are the most frequent manifestation of brain-stem gliomas. Their most common symptoms are multiple cranial nerve deficits combined with pyramidal symptoms and cerebellar dysfunction, usually ataxia and nystagmus. Smaller tumours often initially exhibit isolated cranial nerve deficits. Hydrocephalus and increased intra-cranial pressure are rather rare. The prognosis greatly depends on the localisation and extent of the tumour. The overall prognosis for patients is poor; despite optimal therapy, the five-year survival rate is approximately 10%. Again, these rare focal, exophytic tumours that frequently proliferate into the ventricle exhibit a better prognosis with a five-year survival rate of up to 73%.



■ Fig. 9.86 Haemangioblastoma. DSA of the vertebral artery: clear tumour blush of the haemangioblastoma

**Medical Imaging.** Diffuse pontine tumours appear as hypodense tumours in CT. In MRI, in they appear hypointense in T1-weighted sequences and hyperintense in T2-weighted sequences. In the axial and sagittal expansion, the pons exhibits an increase in size, the fourth ventricle is ventrally bulged in a convex arc and narrowed. The diffuse pontine tumours usually show no pathological uptake following the intra-venous administration of the contrast agent (■ Fig. 9.87). Focal pontine tumours are very rare and only represent approximately 10% of all pontine tumours. By definition, these tumours are seen in less than 50% of the axial orientations of the pons. After the administration of contrast agent, these tumours typically display heterogeneous enhancement.

**Mesencephalic Tumours** The mid-brain is the second most common site of this tumour entity. Again, focal tumours can be differentiated from diffuse tumours. Unlike the pons, focal tumours are more common here than diffuse tumours. Patients with diffuse brain-stem gliomas typically complain of blurred or double vision, which is often acute. Focal tumours usually cause headaches, vomiting, diplopia, and hemiparesis. Parinaud's syndrome may also occur. Hydrocephalus often appears at tectal tumour sites.

**Medical Imaging.** The accurate diagnosis and extent of these tumours in the mid-brain is important for the further procedure because focal brain-stem tumours can be surgically treated. On the other hand, diffuse tumours are irradiated. Diffuse brain-stem tumours usually exhibit a minimal space-occupying effect. Following the administration of contrast agent, they generally exhibit low enhancement. In the case of focal cerebral tumours, haemorrhaging and cystic modifications occur in approximately 25% of cases. The tumour may expand superiorly into the thalamus or inferiorly into the pons. After the administration of contrast agent, focal mesencephalic tumours can display annular enhancement. Tumours of the quadrigeminal plate, so-called tectal gliomas, are usually benign and are only symptomatically treated by treating the accompanying hydrocephalus. Most of these tectal gliomas show no growth.

**Brain-stem Tumours in NF-I** In patients with NF-I, brain-stem tumours are more common (■ Fig. 9.88). In this case, the most common tumour localisation is the medulla (68–82%). Although brain-stem gliomas in patients with NF-I cannot be distinguished from those without NF-I, they often display a very different clinical behaviour. Many of these patients are asymptomatic, the tumours are discovered by chance. The most striking difference is the tumour growth. The follow-up study revealed that the radiographic progression of brain-stem glioma was detectable in only 32–42% of patients with NF-I; a clinical progression was only detected in 14–18% of patients. Spontaneous remission of these tumours has even been reported in individual cases. Patients with NF-I are therefore recommended to wait and undergo follow-up examinations.

#### ■ ■ Differential Diagnosis of Brain-stem Tumours

The most important differential diagnosis is encephalitis (viral or autoimmune encephalitic). Another important differential diagnostic aspect is the dysmyelination, e.g. in NF-I in addition to Langerhans cell histiocytosis, hamartomas, haematoma, vascular malformations and tuberculomas. Given the excellent soft tissue contrast and good differentiation of blood and blood degradation products, astrocytomas can easily be distinguished from vascular malformation and sub-acute haemorrhaging on MRI. However, in some cases, it may be difficult to differentiate encephalitis or a tuberculoma from a brain-stem tumour based on a single investigation. Follow-up examinations, laboratory tests, the lumbar puncture and clinical examination enable a correct diagnosis.

### 9.4.3 Supra-tentorial Tumours

In children younger than 2 years and older than 10 years, supra-tentorial tumours are more common than infra-tentorial tumours (■ Table 9.11).

#### ■ Tumours of the Hemispheres

During childhood, tumours of the astrocytoma series are most frequently found in the cerebral hemispheres. In new-born infants, however, other tumour entities should be considered, especially teratoma. In older children, an atypical teratoid/rhabdoid tumour (AT/RT), ependymoma and primary neuro-ectodermal tumours (PNETs) should all be considered in the differential diagnosis. In particular, the diagnosis should consider PNETs if solid portions of the tumour appear hyper-dense on CT and display signal behaviour similar to the grey matter on MRI. In children with a long history of seizures, ganglioma and a dysembryoblastic neuro-epithelial tumour (DNET) should be considered.

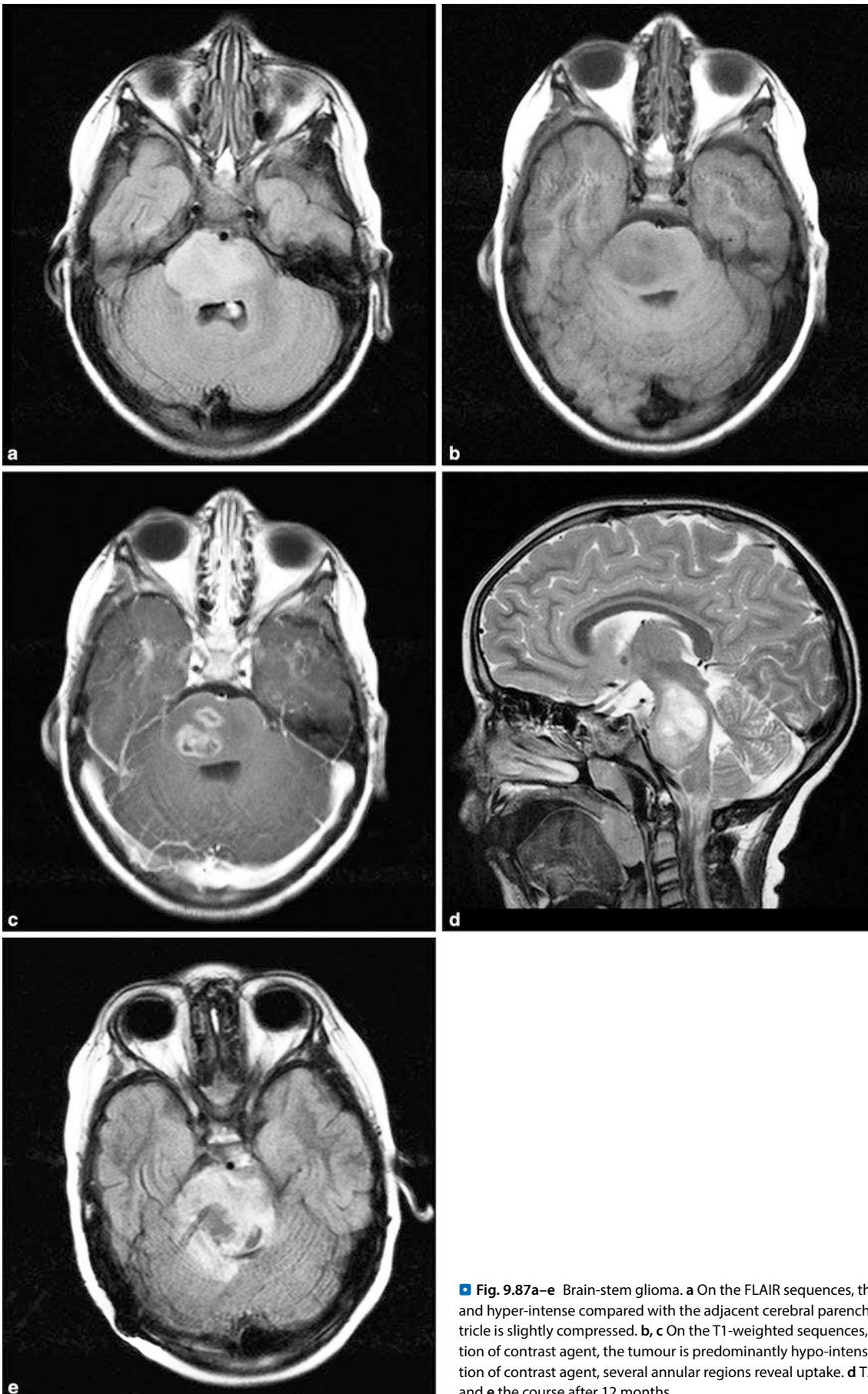
**Histology.** The classification, including the grading of intra-cerebral tumours, is still based on the histopathological findings (**overview**). In the 1993 revision of the WHO classification of brain tumours, an amendment was made to the grading of astrocytic gliomas. In addition, the atypical meningioma was introduced.

#### Grading of tumours according to the WHO

- Grade I: cell-poor tumour without mitosis and necrosis, no vascular proliferations
- Grade II: increased cell number, no mitosis
- Grade III: increased cell density, polymorphisms, nuclear atypia, mitotic figures, no vascular proliferations
- Grade IV: cell-rich and polymorphic tumour with numerous atypical mitoses, necrosis, vascular proliferations

#### ■ Tumours of the Astrocytoma Series

**Definition, Epidemiology, Localisation** Astrocytomas originate from astrocytes. They account for approximately 10% of all brain tumours. Astrocytomas mainly proliferate in the frontal and tem-



■ **Fig. 9.87a–e** Brain-stem glioma. **a** On the FLAIR sequences, the pons is distended and hyper-intense compared with the adjacent cerebral parenchyma. The fourth ventricle is slightly compressed. **b, c** On the T1-weighted sequences, before the administration of contrast agent, the tumour is predominantly hypo-intense. After the administration of contrast agent, several annular regions reveal uptake. **d** T2-weighted uptake and **e** the course after 12 months

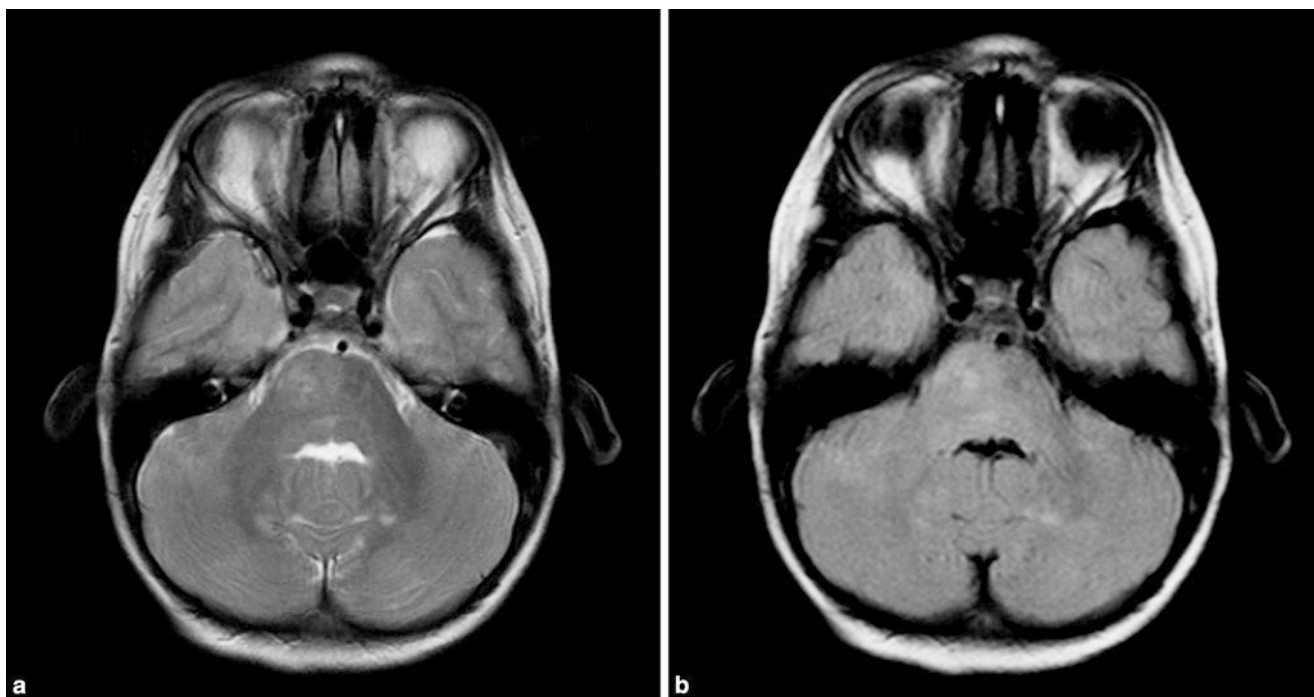


**Fig. 9.88a,b Hamartoma with NF-I.** A 16-year-old patient with known NF-I. In the right paramedian pons, situated anteriorly, there is a moder-

ate increase in signal intensity on the a axial T2-weighted and b FLAIR sequences

**Table 9.11** Characteristic findings in supra-tentorial tumours in children

Tumour	Typical findings/characteristics
Astrocytoma	The most frequent tumour Appearance varies with tumour grade
Giant cell tumour	Near the foramen of Monro
Ependymoma	Peri-trigonal, heterogeneous
PNET	Young children Heterogeneous, solid portions, intensity like grey matter
DNET	Cortical location Strongly hyper-intense on T2-weighted images
Teratoid/rhabdoid tumours	Cortical location Hyperintense on T2-weighted images
Neuronal-glia tumours	Cortical location Calcifications, cysts

*PNET* primary neuro-ectodermal tumour, *DNET* dysembryoblastic neuro-epithelial tumour

poral lobes. In children younger than 10, they are typically localised in the pons. According to the degree of anaplasia, four grades of malignancy can be distinguished (Table 9.12). Astrocytomas of the cerebral hemispheres account for approximately 30% of the supra-tentorial brain tumours in childhood. In most series, a slight predominance in men has been proven. All paediatric age groups are affected. There is a peak age between the 7th and 8th years of life.

**Symptoms** The clinical symptoms mainly depend on the location of the tumour. In addition to seizures, focal neurological deficits and signs of increased intra-cranial pressure, general symptoms such as headaches, vomiting and nausea occur. Seizures mainly occur if the tumour has a frontal or temporal–cortical location.

**Pathology** The astrocytomas occurring in the cerebral hemispheres are similar to those in the cerebellum. They may be solid, solid with necrotic portions, or cystic with parietal tumour nodules. Most astrocytomas are low-grade astrocytomas, although glioblastomas can occur during childhood. However, they have a slightly better prognosis than in adults.

Juvenile pilocytic astrocytomas (grade I) are rarely located in the hemispheres and often occur in the cerebellum. This tumour entity is mainly present in the white matter and often infiltrates the basal ganglia and the thalamus. Often, more than one lobe is infiltrated.

At the time of diagnosis, these astrocytomas can sometimes be quite large. Astrocytomas in childhood, even with low histological grading, can occur multi-centrally. This is mostly because of the spread of sub-arachnoid or intra-ventricular tumours. This multicentricity is mainly found when the primary tumour is located in the hypothalamus.

#### Grade I Astrocytoma

Pilocytic astrocytomas predominantly occur in childhood and early adulthood and account for approximately 5% of all brain tumours. Grade I astrocytomas frequently occur in association with NF-I, especially in the optical chiasma, the hypothalamus, the brain-stem, and the cerebellum (Fig. 9.89).



■ **Table 9.12** Malignancy grade of astrocytoma

Malignancy grade	Description	WHO grade
Grade I astrocytoma	Corresponds to the juvenile pilocytic astrocytoma	WHO grade I
Grade II astrocytoma	Corresponds to fibrillary/diffuse astrocytoma	WHO grade II
Grade III astrocytoma	Corresponds to anaplastic astrocytoma	WHO grade III
Grade IV astrocytoma	Corresponds to glioblastoma multiforme	WHO grade IV

### ■ ■ Grades II and III Astrocytoma

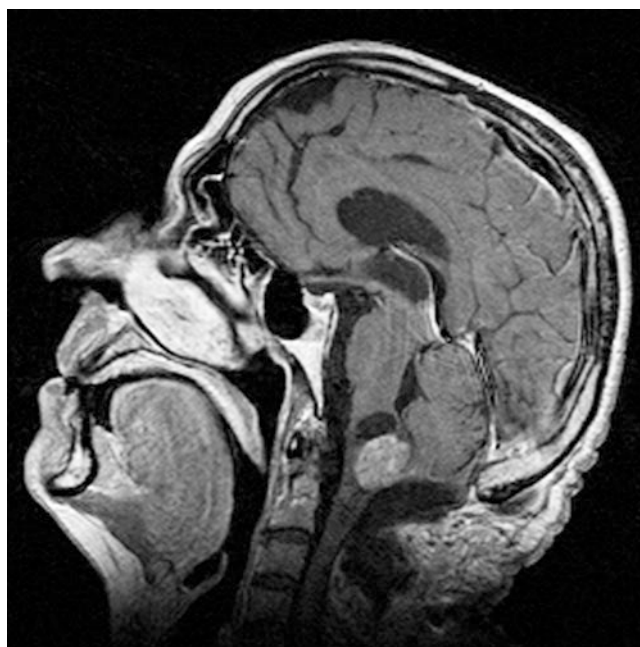
**Definition** Because there is no significant difference in the survival rate, grade II and III astrocytomas can be combined with “**low-grade gliomas**” and compared with “**high-grade gliomas**”, the glioblastomas. In low-grade astrocytomas, the average survival time is about 5 years.

**Medical Imaging** On imaging, grade II astrocytomas can be differentiated from grade III anaplastic astrocytoma because of the lack of contrast agent uptake (■ Figs. 9.90, 9.91). Grade II astrocytomas demonstrate slow and infiltrative growth and are poorly delineated compared with healthy brain tissue. The shape of the brain is not changed, i.e. no mass-occupying lesion can be demonstrated.

On CT grade II astrocytomas appear as circumscribed zones of reduced density. Distinction from the peri-focal oedema surrounding the tumour is usually not possible. The indirect symptoms of a mass-occupying lesion are discrete or even absent. Intra-venous contrast agent is not enriched. Occasionally, distinction of infarcts is difficult. The typical wedge shape and the increasing demarcation of the infarcts on follow-up examinations are differential diagnostic criteria.

On MRI, grade II astrocytoma has a lower signal intensity on T1-weighted sequences and appears hyper-intense on T2-weighted and FLAIR sequences. Again, there is typically a lack of clear enhancement after the administration of contrast agent. There is little or no peri-focal oedema. In individual cases, cystic degeneration and/or haemorrhaging may occur. The diffusion-weighted imaging can also distinguish between an acute myocardial infarct and a tumour.

➤ **The diagnosis of grade II astrocytoma is considered probable in the case of all well-delineated, intra-axial lesions, which display a hyper-intense signal on T2-weighted sequences and do not show uptake of contrast agent on the T1-weighted images. However, the final tumour classification is not based on imaging, but rather on histology.**



■ **Fig. 9.89 Grade I astrocytoma.** Astrocytoma with strong contrast agent uptake on the sagittal T1-weighted images at the base of the fourth ventricle

### Differential Diagnosis of Grade II Astrocytoma

- Oligodendroglioma: this is often calcified. However, approximately 20% of grade II astrocytomas also exhibit calcifications.
- Grade III astrocytoma: a more infiltrative growth is typically seen, usually with peri-focal oedema and the uptake of contrast agent.
- Ganglioglioma: here, cysts and calcifications are often detectable, and the tumour is usually situated in the temporal lobe.
- Arachnoid cyst: extra-axial position, liquor-isointense signal on all MRI sequences.

### ■ Grade III Astrocytoma

**Definition** Anaplastic astrocytomas are tumours with higher cell density, polymorphisms, haemorrhaging, minor necrosis, and pathological vessels. The transition to grade IV astrocytoma (glioblastoma) is fluid and often difficult to determine.

**Medical Imaging** On CT and MRI, grade III astrocytomas are highly variable and show solid and cystic components in addition to partial necrosis. On the T1-weighted images, they are hypointense. On the T2-weighted sequences, they are hyperintense. They also show contrast enhancement (■ Fig. 9.91). To avoid confusion with haemorrhaging, an unenhanced T1-weighted sequence should always be performed.

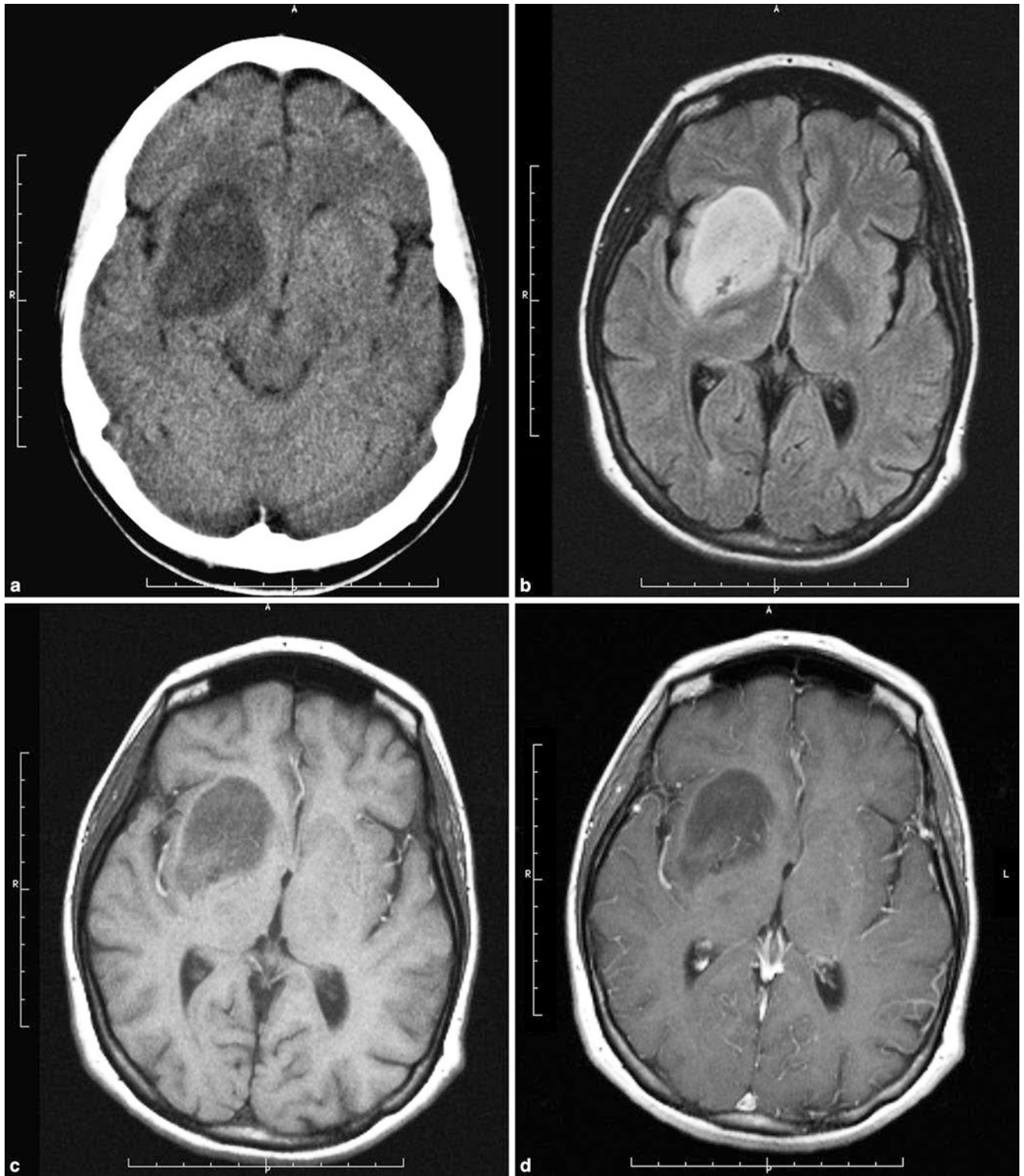


**Fig. 9.90a–d Grade II astrocytoma.** **a** In this 14-year-old boy, a heterogeneous, hyper-dense, smooth-edged, space-occupying lesion appears right parietally on CT. **b** On the FLAIR images, the tumour is hyper-intense with a relatively smooth border. There is no significant space-occupying lesion and

no significant environmental response. **c, d** On the T1-weighted sequences **c** before and **d** after administration of contrast agent the tumour is hypointense without enhancement

#### ■ Grade IV Astrocytoma/Glioblastoma

**Epidemiology, Localisation** Glioblastomas are the most common primary brain tumours. In adulthood, they occur twice as frequently as the other astrocytomas. Histologically, they show necro-

sis, vascular proliferation, cellularity and nuclear polymorphisms. They stand out because of rapid infiltrative growth and are mainly localised in the medulla and in the basal ganglia of the cerebrum.

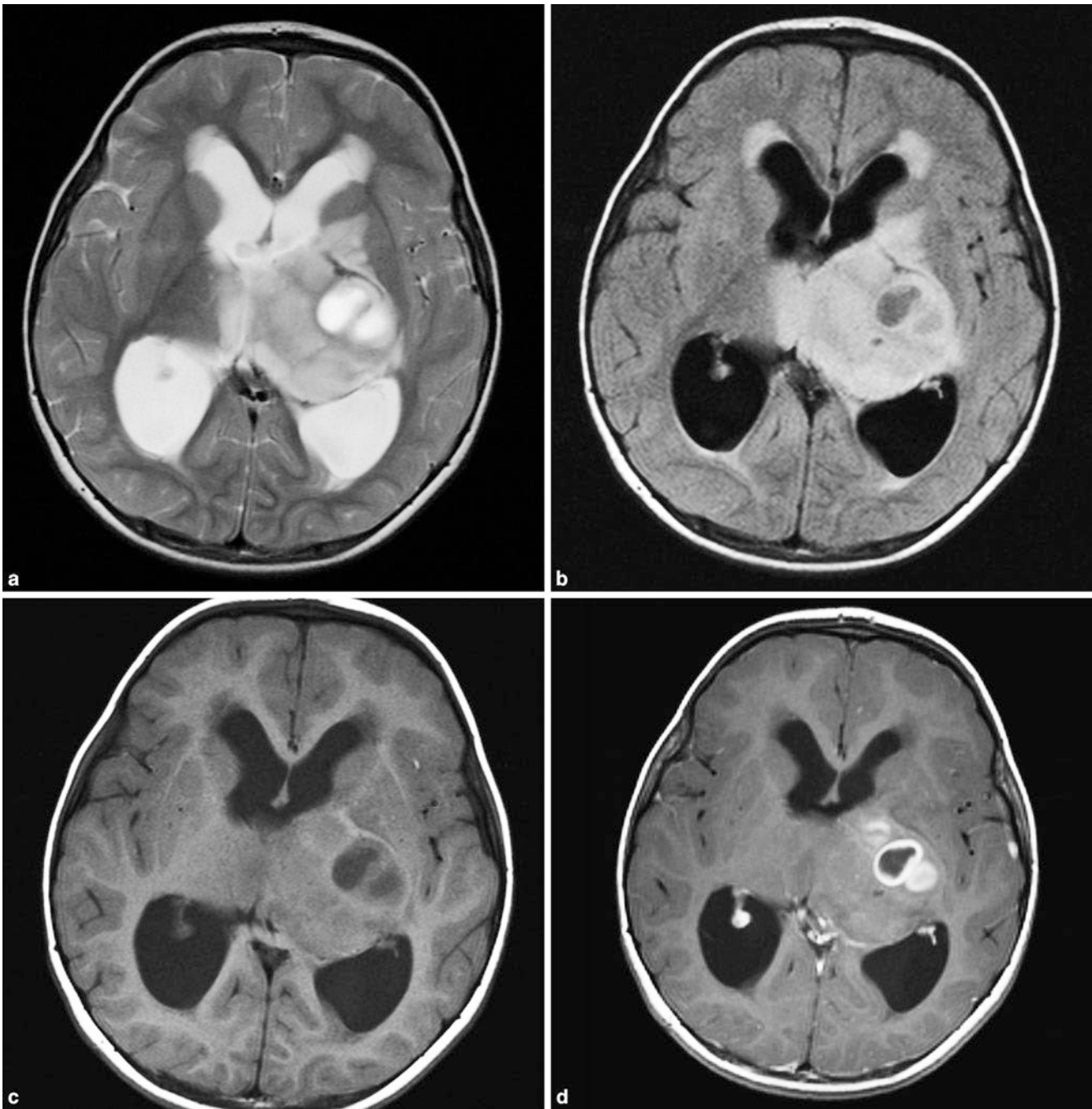


**Fig. 9.91a–d** Grade III anaplastic astrocytoma. **a, b** On the axial T2-weighted and FLAIR images, a partly hyper-intense, slightly iso-intense to the grey matter, space-occupying lesion is revealed in the thalamus and the left basal ganglia. **c** On the T1-weighted sequences, this space-occupying lesion

is predominantly hypo-intense. **d** After administration of contrast agent in the axial sectioning, there is a partly flat, partly annular enhancement of contrast agent. Histological examination revealed a grade III anaplastic astrocytoma

Occasionally, the corpus callosum is penetrated, thus resulting in growth in both hemispheres (butterfly glioblastoma). Glioblastomas can also occur multi-centrally. The peak incidence is between the fourth and sixth decades of life, although glioblastomas can occur at any age.

The medical history is usually only a few weeks to a few months. In children, glioblastomas occur as a second malignancy after acute leukaemias and other brain tumours (especially medulloblastomas) as a result of cranial irradiation.

**Medical Imaging** Regarding CT, a space-occupying lesion appears on the unenhanced scan, usually with mixed density. There are often necrotic zones and rarely cysts and haemorrhaging. There is usually extended peri-focal oedema with clear signs of the indirect space-occupying lesion. There is almost always contrast enhancement. The highly vascular tumourous tissue appears as a garland-shaped ring-wall lesion or, more rarely, as nodes, while the necrotic areas do not take up contrast agent. Calcifications are rare. The high vascularity can simulate an arterio-venous malformation.

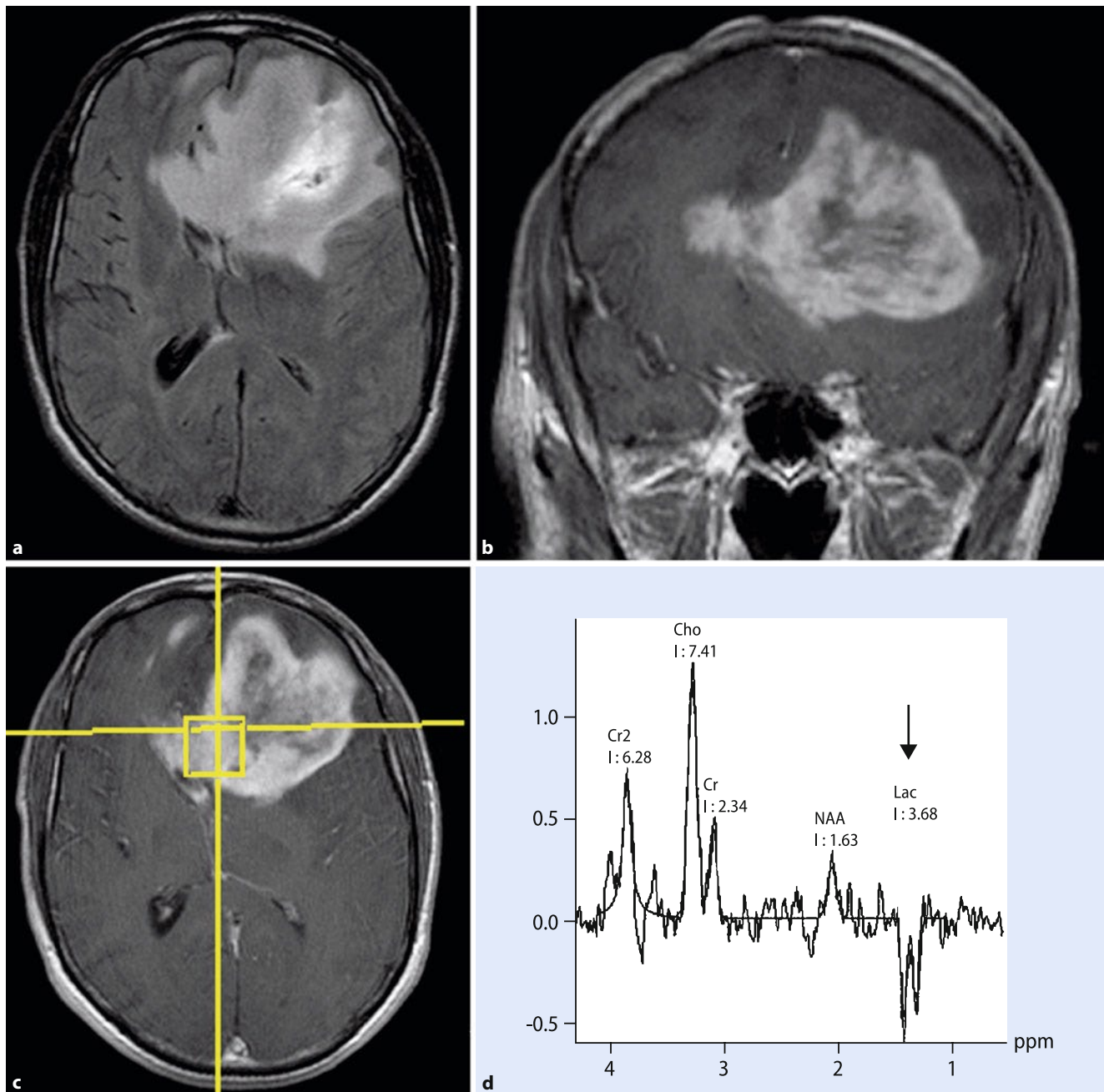


**Fig. 9.92a–d Glioblastoma.** a–c A 43-year-old patient with a frontal glioblastoma. a On the FLAIR sequence a large, left frontal, space-occupying lesion spreading across the corpus callosum to the opposite side and shift of the median, strong heterogeneous absorption after administration of

contrast agent. d Tumour spectrum: TE = 135 ms, increase in choline (*Cho*), decrease in creatine (*Cr*) and N-acetyl aspartate (*NAA*), *Cho*–*Cr* (3.1) and *Cho*–*NAA* (4.54) ratios strongly increased, consistent with a high-grade tumour (arrow: lactate peak, *Lac*). (From: *Radiologie* 2007;47:523, Fig. 4a–d)

The MRI also reflects the heterogeneity of the glioblastoma (Figs. 9.92, 9.93). The T1-weighted sequences reveal a poorly margined tumour signal with necrosis or cysts and a thick, irregular wall. This results in a significant, but heterogeneous enhancement. Because glioblastomas are highly vascular, clear flow voids and haemorrhaging of different ages can often be seen. The T2-weighted sequences frequently reveal the heterogeneous space-occupying lesion with central necrosis and haemorrhaging of different ages. Pronounced peri-focal oedema is typical. However, anaplastic cells can also be detected outside the T2 changes. The contrast medium is also well suited to demonstrat-

ing lepto-meningeal metastases, recurrences, or a multi-centric growth.

#### ■ Giant Cell Tumours

**Definition, Epidemiology, Symptoms** The name giant cell tumour is used for tumours that are usually associated with tuberous sclerosis (Sect. 9.2). These tumours occur in 5–15% of patients with tuberous sclerosis. If a giant cell tumour detected, it should therefore be specifically examined for phakomatosis. The prognosis for patients with giant cell tumours and tuberous sclerosis is better than for patients with giant cell components

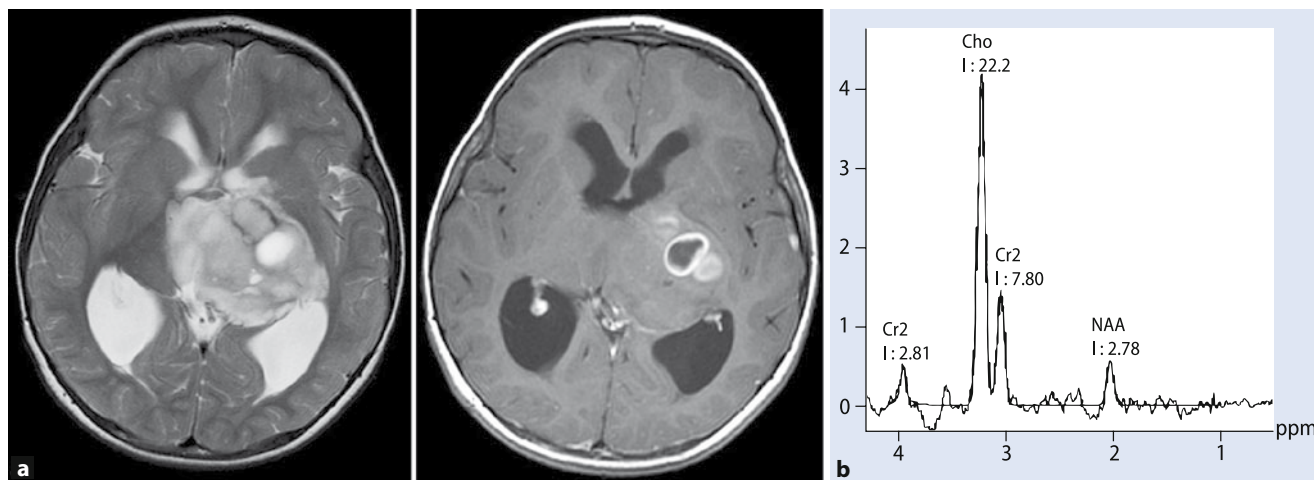


**Fig. 9.93a,b** Highly malignant glioma in a 4-year-old girl. **a** Tumour spectrum. **b** TE = 135 ms, marked increase in Cho, strong decrease of NAA as

a sign of the degree of malignancy of the lesion, strongly increased Cho–NAA ratio (7.98). (From: *Radiologe* 2007;47:524, Fig. 5a,b)

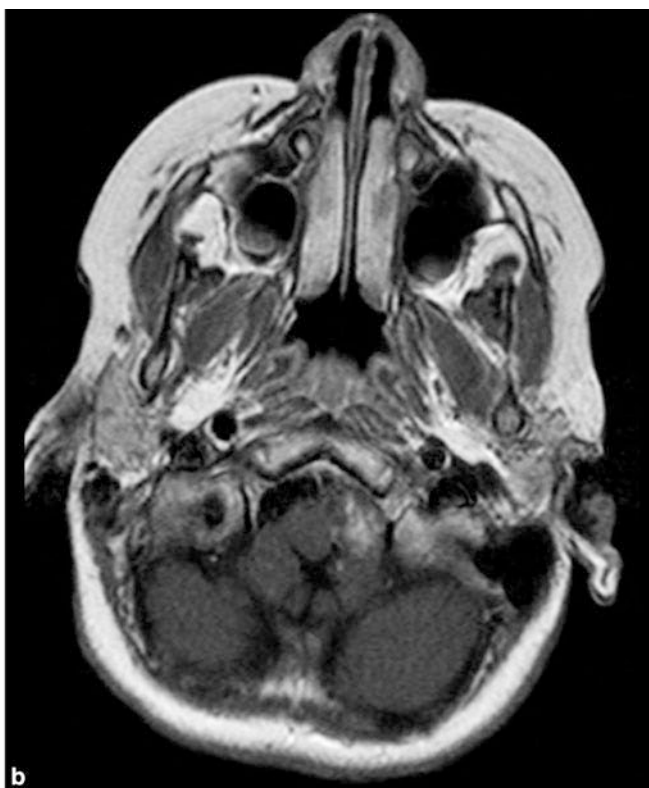
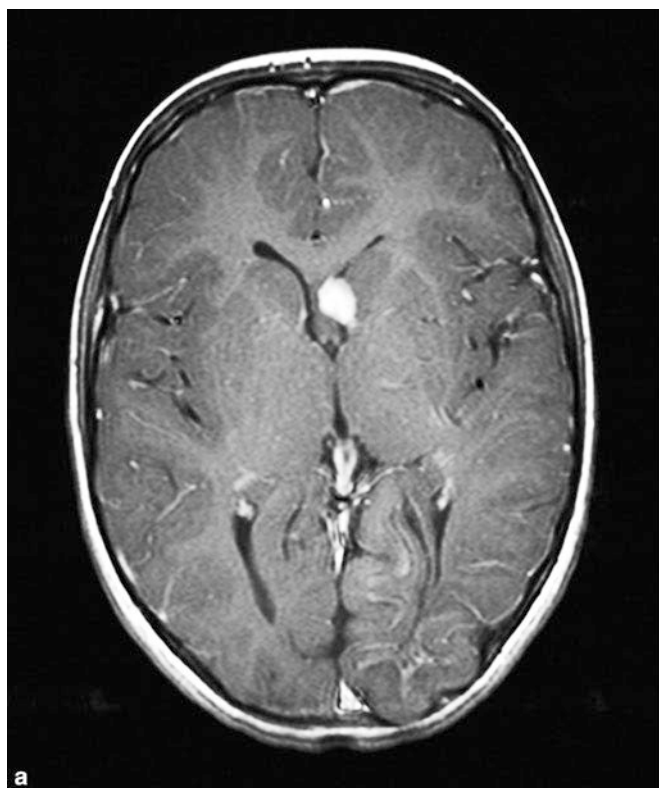


**Fig. 9.94a,b** Giant cell astrocytoma. On the T1-weighted sequences, there is homogeneous enhancement of the giant cell astrocytoma at the entrance

of the foramen magnum after the administration of contrast agent. This localisation may lead to an acute disruption of CSF circulation

in normal astrocytomas. Boys and girls are equally affected. The tumour can be diagnosed at any age, peak incidence is between the 5th and the 10th year of life. The clinical symptoms can usually be traced to hydrocephalus. In rare cases, the tumour can become malignant and infiltrate the surrounding cerebral parenchyma.

**Pathology** Giant cell tumours originate on the wall of the lateral ventricle near the foramen of Monro, and their obstruction can lead to hydrocephalus (Fig. 9.94). They probably originate

from sub-ependymal hamartomas and are to be regarded as part of the tuberous sclerosis complex. In general, the giant cell astrocytomas are sharply delimited. Focal calcifications are rarely encountered. Anaplasia is also infrequent.

**Diagnostic Medical Imaging** The characteristic appearance of giant cell astrocytoma on CT is a hypodense to iso-dense, well-demarcated round lesion in the region of the foramen of Monro in addition to hydrocephalus. These sub-ependymal space-occupying lesions may indicate calcification diseases. After the

administration of contrast agent, giant cell astrocytomas show marked homogeneous enhancement.

On **MRI**, the circumscribed, round space-occupying lesions in the foramina of Monro are well depicted. On the T1-weighted sequences, they usually appear hypointense. On T2-weighted sequences, they are usually hyper-intense. After the administration of contrast agent, there is strong homogeneous enhancement. In addition to the sub-ependymal tubers, patients with tuberous sclerosis complex often exhibit multiple cortical hamartomas. On the T2-weighted sequences in particular, these cortical hamartomas are depicted as hyper-intense, ill-defined increases in signal.

**!** **Giant cell tumours usually exhibit slow growth. However, if a rapid increase in the growth of a giant cell astrocytoma is discovered on follow-up imaging, malignancy should be considered.**

#### ■ ■ Pleomorphic Xantho-astrocytoma

Another rare form of astrocytoma is the pleomorphic xantho-astrocytoma. They usually appear at the cortico-medullary border, are temporally localised, and often have cysts. On the T1-weighted images, minor enhancement occurs after the administration of contrast agent. These tumours mainly occur in childhood and early adulthood.

#### ■ Oligodendrogliomas

##### ■ ■ Epidemiology, Localisation

Oligodendrogliomas represent about 7% of all brain tumours. They occur frequently between the age of 35 and 55 years are slightly more predominant in men. In children, oligodendrogliomas are extremely rare. They constitute only about 1% of all paediatric brain tumours.

Oligodendrogliomas mainly occur supra-tentorially and rarely infra-tentorially or intra-ventricularly. They are mainly localised in the cerebral hemispheres, especially in the frontal and temporal lobes. Only the oligodendrogliomas of the thalamus can also be found in younger patients.

##### ■ ■ Symptoms

Affected individuals often have epileptic seizures. Other clinical symptoms include headaches, visual field defects and paresis. The tumour grows very slowly; it often takes years between the onset of symptoms and diagnosis.

##### ■ ■ Classification, Histology

The tumours derived from oligodendrocytes display diffuse and infiltrative growth. The prognosis depends on the histological grade of the tumour. A combination with astrocytic portions, referred to as oligo-astrocytoma (mixed tumour), frequently occurs. The WHO distinguishes between tumours of grades II and III. Histologically, calcifications occur in up to 90% of cases, often in the marginal parts of the tumour. Other regressive changes occur with haemorrhaging and cysts. Grade III oligodendrogliomas exhibit enhanced cellular polymorphisms with elements of giant cells, which are analogous to the astrocytomas.

The distinction between grades II and III can only be ensured via histology. A clear differentiation from astrocytomas is often not possible.

#### ■ ■ Medical Imaging

On **CT**, the characteristic calcifications, which occur in more than 50% of cases, are well detected (■ Fig. 9.95). After the administration of contrast agent, there is frequently heterogeneous enhancement. Cystic changes or haemorrhaging may also occur. Calcifications and haemorrhaging in addition to a superficial layer tend to suggest an oligodendroglioma. These calcifications are usually surrounded by hyper-dense tumour areas. They are occasionally also iso-dense. Thus, the true extent of the tumour cannot be seen. Like the astrocytomas, the oligodendrogliomas are poorly delineated against peri-focal oedema. Oligodendrogliomas with a low malignancy (grade II) rarely take up contrast agent. Anaplastic oligodendrogliomas (grade III) are rare; their tissue density is mixed hypo-dense, iso-dense and hyper-dense. They often exhibit cystic areas, but rarely intra-tumourous haemorrhaging. There is usually slight peri-focal oedema. In 50% of anaplastic oligodendrogliomas, there is a stained-diffuse or annular enhancement of contrast agent.

On **MRI**, oligodendrogliomas also show a relatively colourful picture. With gradient-echo sequences, calcification effects and haemorrhaging can be well demonstrated. With conventional spin-echo sequences and fast spin-echo sequences, calcifications cannot be depicted with great sensitivity. On the T1-weighted sequences, with unenhanced images, they rarely show primary hyper-intense areas corresponding to either haemorrhaging at the methaemoglobin stage or calcifications. After the administration of contrast agent, there is heterogeneous enhancement. The uptake of contrast agent does not always equate with a grade III oligodendroglioma. On the T1-weighted images, the tumours range from iso-intense to slightly hypo-intense. On the T2-weighted images, they are depicted as homogeneously signal intense, often with minor peri-focal oedema. Anaplastic grade III oligodendrogliomas have a stronger signal decrease on the T1-weighted sequences; these tumours usually take up contrast agents. Meningiomas can be successfully distinguished because they show marked enhancement after the administration of contrast agent. Astrocytomas rarely show calcifications. Ependymomas cannot always be clearly delineated from astrocytomas.

**➤ The diagnosis of an oligodendroglioma is mainly based on the presence of calcifications, cysts, minor oedema and heterogeneous contrast enhancement.**

#### ■ Neural Tumours

Neural tumours are derived from nerve cells. With an incidence of 0.4% of all brain tumours, they are comparably rare. In approximately 80% of cases they occur in patients younger than 30. In principle, neural tumours can occur anywhere in the brain, but predominate in the medial temporal lobe.

This tumour entity also typically has a long history, often with seizures that persist for years. Except for neuroblastoma, which corresponds to a grade IV tumour, most of the tumours can be

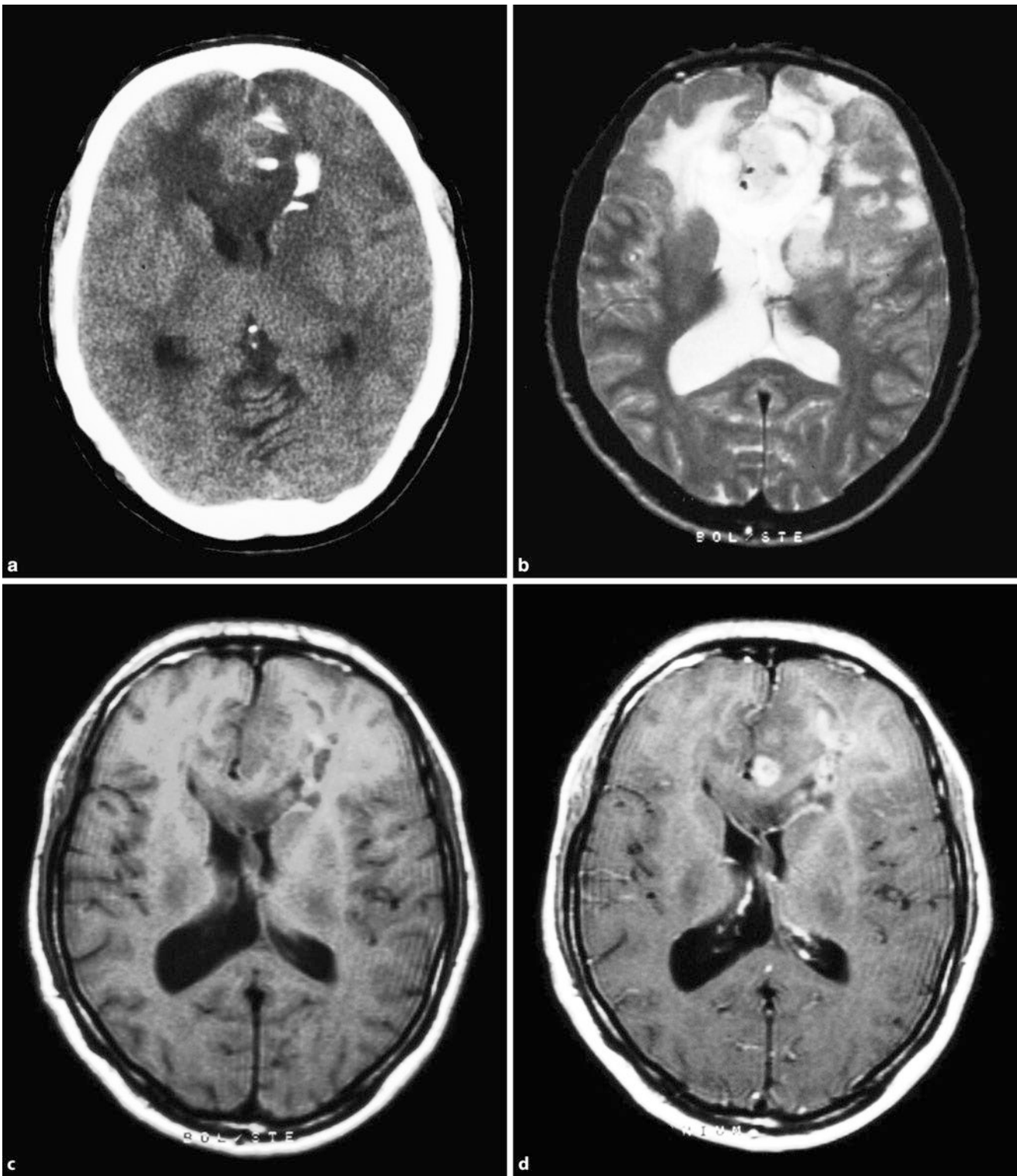


**Fig. 9.95a–d Oligodendroglioma.** **a** On CT, striking clumpy calcifications left frontally with oedema especially in the front corpus callosal genu. Moderate compression of the anterior horn of the left lateral ventricle. **b** On the T2-weighted sequence, the extent of oedema is much more apparent. The calcifications are depicted as hypo-intense. **c** On the T1-weighted sequences,

before the administration of contrast agent, a space-occupying lesion and a hyper-intense left frontal area appear. These most closely correspond to calcification. **d** After the administration of gadolinium, there is nodular enhancement in the front corpus callosal genu. (From: *Radiologie* 2003;43:992, Fig. 5a–d)

designated as WHO grade I tumours. Neural tumours are classified as follows:

- Ganglioglioma, gangliocytoma, infantile desmoplastic
- Ganglioglioma
- Central neurocytoma
- Neuroblastoma

#### ■ ■ Gangliogliomas

Gangliogliomas are the most common mixed-glial, neural tumours of the CNS. At 0.4–1.3% of all brain tumours, the incidence is very low. In the paediatric patient population, they occur much more frequently, with an incidence of up to 7.6%. Clinically, gangliogliomas are usually characterised by epileptic seizures. They are usually localised in the temporal lobe, although they can occur at any other site of the CNS, including the brainstem and spinal cord (■ Fig. 9.96).

**Infantile Desmoplastic Ganglioglioma** Infantile desmoplastic ganglioglioma is a rare, embryonal tumour that is characterised by macrocephaly and/or complex focal seizures in infancy.

**Medical Imaging.** A large, predominantly cystic tumour appears in the cerebral hemispheres. The infiltration of several lobes is not uncommon; in this case, the frontal and parietal lobes are affected. A solid tumour component can often be identified on the periphery. This solid tumour component often infiltrates the lepto-meninges and can thus simulate an extra-parenchymal tumour. A curative treatment can be achieved by complete resectioning of the tumour.

On CT, the solid portion of the tumour is iso-dense to hyperdense compared with the grey matter. On T1- and T2-weighted MRI sequences, it is iso-intense to the cortex. This tumour component exhibits strong enhancement following the administration of the contrast agent. As a rule, the cystic wall of the tumour does not exhibit an uptake of contrast agent.

In the case of desmoplastic juvenile ganglioglioma, imaging is important because it affords an unambiguous diagnosis in conjunction with histology. In addition to astroglial and neuronal tumour cells, these tumours often contain components from small, mitotically active cells, which can be misinterpreted as malignant neoplasms. Infantile desmoplastic gangliogliomas differ from cystic astrocytomas based on the peripheral localisation and the relative hyper-density on CT in addition to the T2 contraction of the solid parts of the tumour compared with the hypo-intensity and relative T2 prolongation of astrocytomas. In the differential diagnosis, the following also come into consideration: high-grade astrocytomas, PNETs and ependymomas. If the lepto-meningeal tumour component is extensive, a meningioma or a meningosarcoma must also be considered.

**Central Neurocytoma** Central neurocytoma is an intra-ventricular, neural tumour, which occurs in adulthood and has a relatively good prognosis. It is usually localised in the anterior sections of the lateral ventricles around the foramen of Monro; the highest incidence is in young adults with an average age of approximately 30 years. The tumour is overgrown

with the ependyma of the ventricle and often exhibits intraventricular bulging. Histologically, this is a cell-rich tumour with low mitotic activity. Immunohistochemistry can be used to prove neuronal differentiation via the detection of synaptic membrane protein, synaptophysin. Focal calcifications are detectable (■ Fig. 9.97).

**Clinical** symptoms of intracranial pressure predominate as a result of the shifted foramen of Monro. Even with incomplete resection, a permanent cure may be achieved.

#### ■ Supra-tentorial Ependymomas

##### ■ ■ Epidemiology

In childhood, supra-tentorial ependymomas account for 20–40% of the ependymomas. They are more common in boys than in girls, with a peak incidence between the 1st and 5th years of life. They are less frequent in adults.

##### ■ ■ Symptoms

The clinical symptoms mainly depend on the location of the tumour. Intra-cranial pressure and focal seizures are the most frequent clinical manifestations of supra-tentorial ependymomas.

##### ■ ■ Histology, Localisation

Histologically, supra-tentorial ependymomas do not differ from infra-tentorial ependymomas (see above). In almost half of the cases, small foci of calcification can be detected. Cystic areas also frequently occur, particularly in the case of tumorous lesions.

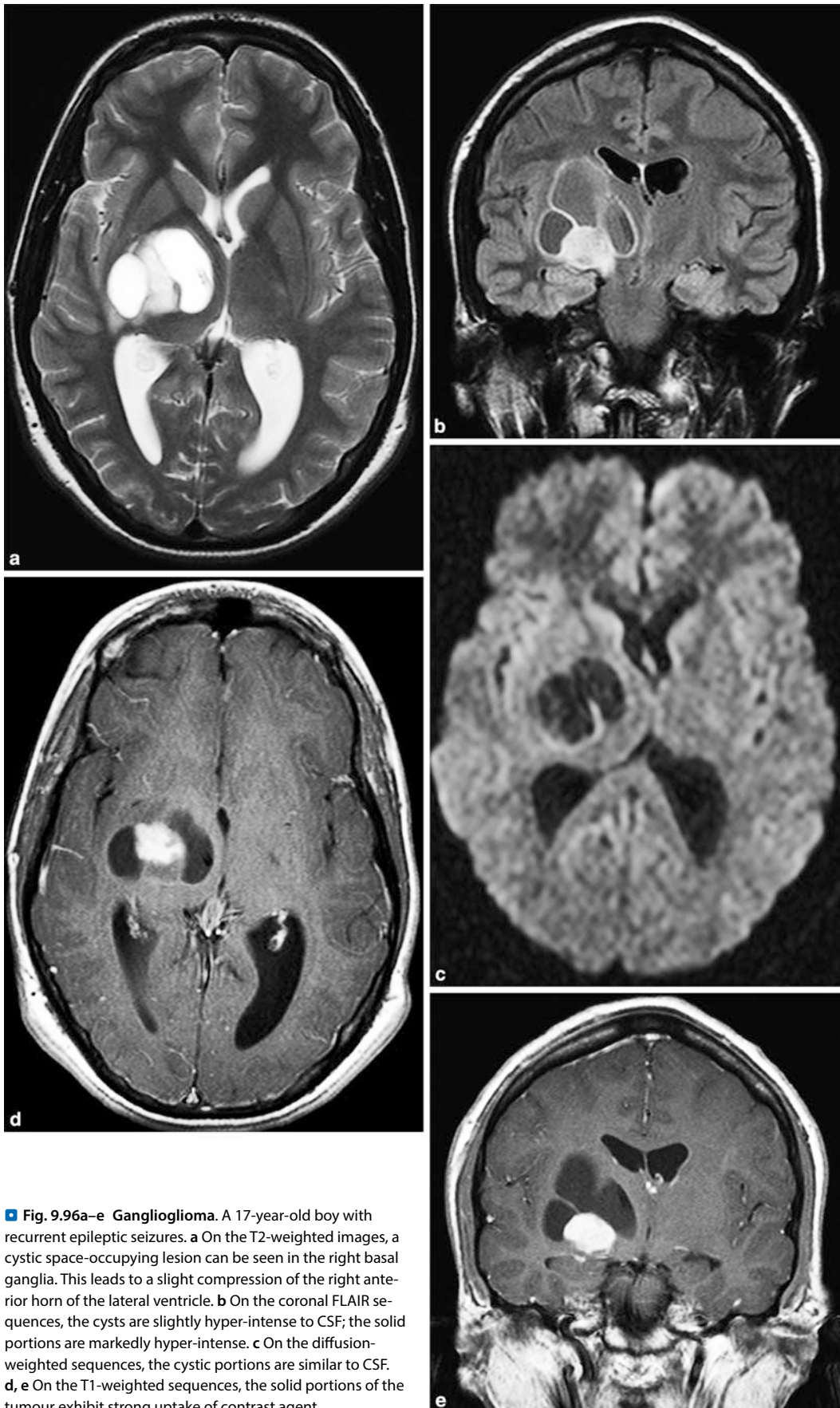
The tumours are usually very extensive at diagnosis, probably because of their frequent localisation in the frontal lobe. They are less frequent in the parietal and temporo-parietal regions. Unlike the infra-tentorial ependymomas, supra-tentorial ependymomas are generally not found intra-ventricularly. Accordingly, metastatic spread of the tumour through the sub-arachnoid cavities is rare.

##### ■ ■ Medical Imaging

Supra-tentorial ependymomas exhibit a variable appearance on CT and MRI. They are usually well demarcated and appear iso-dense to hyper-dense on unenhanced CT. Calcifications and cystic portions are commonly found. After the administration of contrast agent, the solid tumour portions mainly exhibit variable enhancement. A diagnosis of an ependymoma should be considered if an iso-dense frontal or parietal, juxta-ventricular space-occupying lesion with calcifications, cysts and homogeneous enhancement is encountered.

On MRI, there is heterogeneous signalling on all sequences. This heterogeneity results from the intra-tumoural calcifications, cysts and occasional haemorrhaging, which displays a mixed signal intensity in all sequences. However, supra-tentorial ependymomas may also appear homogeneous on MRI and cannot be distinguished from low-grade astrocytomas. In rare cases, an annular uptake of contrast agent can occur with extensive perifocal oedema. This tumour can then not be distinguished from a high-grade astrocytoma or a primitive neuro-ectodermal tumour (■ Fig. 9.98).





**■ Fig. 9.96a–e** Ganglioglioma. A 17-year-old boy with recurrent epileptic seizures. **a** On the T2-weighted images, a cystic space-occupying lesion can be seen in the right basal ganglia. This leads to a slight compression of the right anterior horn of the lateral ventricle. **b** On the coronal FLAIR sequences, the cysts are slightly hyper-intense to CSF; the solid portions are markedly hyper-intense. **c** On the diffusion-weighted sequences, the cystic portions are similar to CSF. **d, e** On the T1-weighted sequences, the solid portions of the tumour exhibit strong uptake of contrast agent

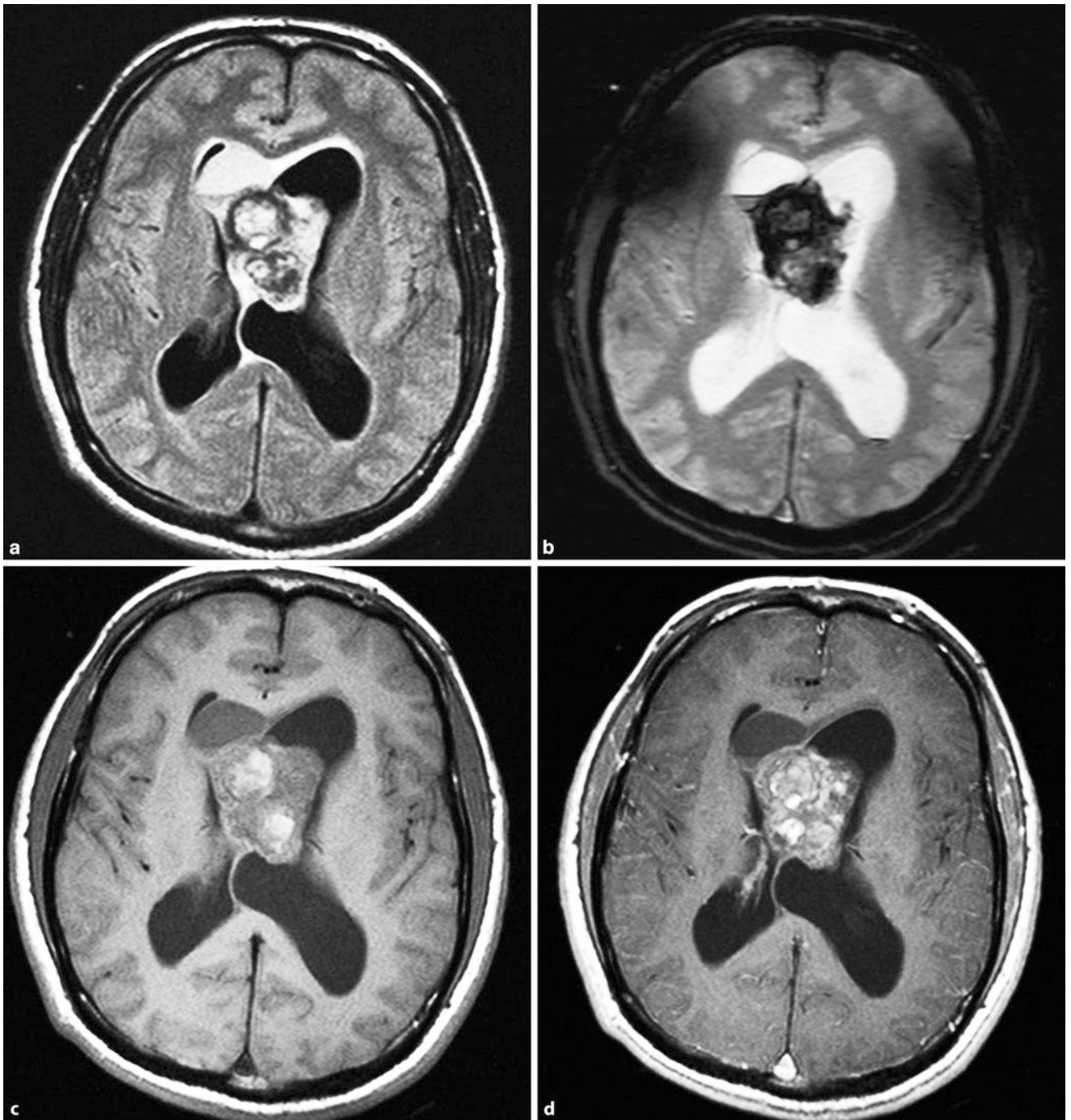
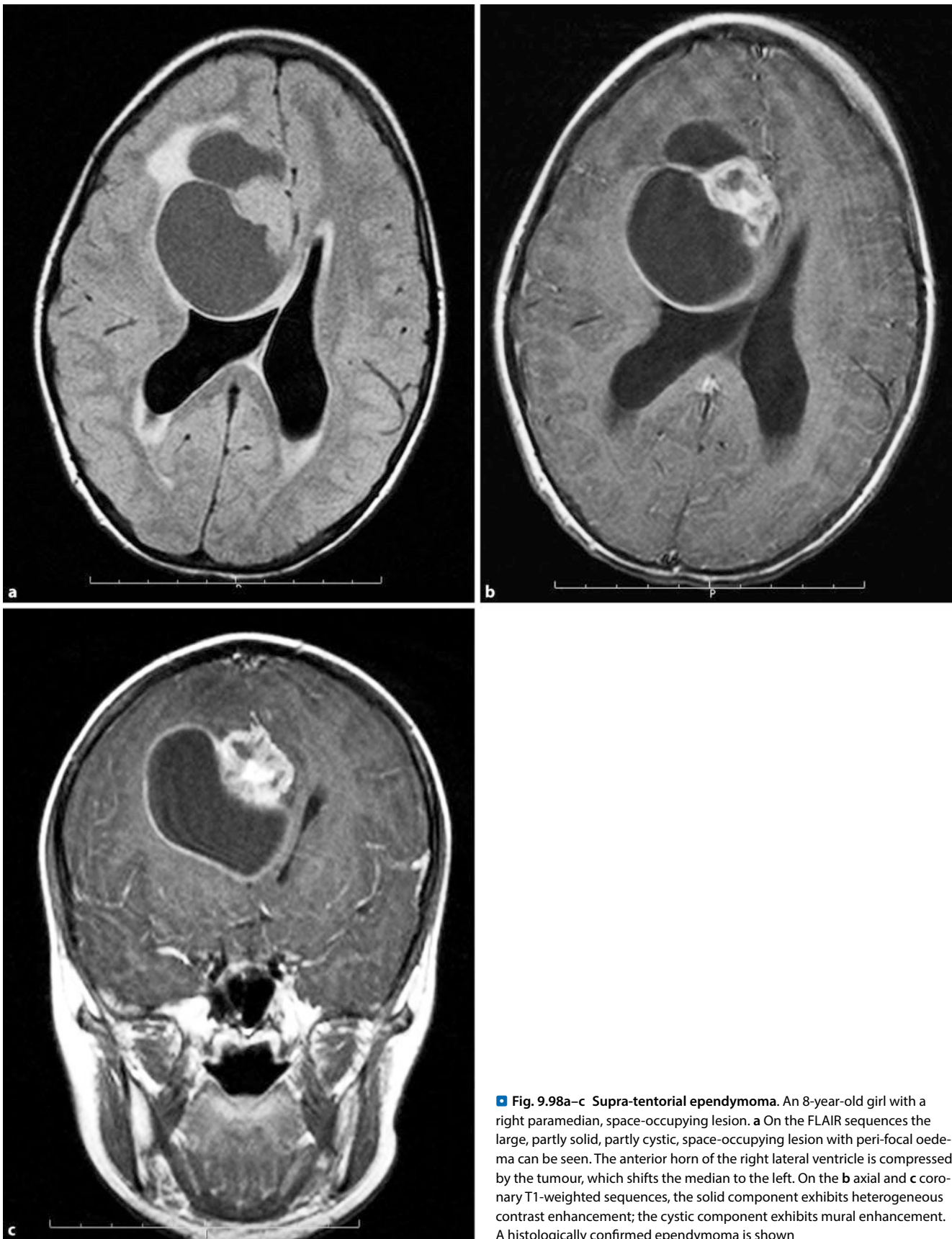


**Fig. 9.97a–d Neurocytoma.** **a** On the FLAIR sequence, there is an irregular, centrally located space-occupying lesion that has led to a disturbance of CSF circulation with hydrocephalic back-up as a result of the blockage of the foramen of Monro. The solid portion of the tumour appears with a heterogeneous signal. **b** On the T2\* sequences, there is marked hypo-intensity of the

tumour, which most likely corresponds to calcification. **c** On the T1-weighted sequences, before the administration of contrast agent, the tumour is sometimes depicted unenhanced with hyper-intense portions that correspond to calcifications. DD: minor haemorrhaging at the methaemoglobin stage. **d** Poor enhancement after the administration of the contrast agent

**Differential Diagnosis.** Supra-tentorial ependymomas are mainly found in young children. If MRI reveals a heterogeneous tumour near the median, especially in the 1st year of life, a teratoma should be considered in the differential diagnosis. If the tumour is neither located near the median nor extra-ventricularly, ependymoma, primitive neuro-ectodermal tumours

and atypical teratoid/rhabdoid tumours should be included in the differential diagnostic considerations, especially if the child is between 1 and 5 years of age. If a heterogeneous intra-ventricular tumour is detected, it must be considered as a colloid plexus carcinoma.



**■ Fig. 9.98a–c** Supra-tentorial ependymoma. An 8-year-old girl with a right paramedian, space-occupying lesion. **a** On the FLAIR sequences the large, partly solid, partly cystic, space-occupying lesion with peri-focal oedema can be seen. The anterior horn of the right lateral ventricle is compressed by the tumour, which shifts the median to the left. On the **b** axial and **c** coronary T1-weighted sequences, the solid component exhibits heterogeneous contrast enhancement; the cystic component exhibits mural enhancement. A histologically confirmed ependymoma is shown

## ■ Primitive Neuro-ectodermal Tumours

### ■ ■ Definition, Epidemiology

Primitive neuro-ectodermal tumours (PNETs) were first defined by Hard and Earl as tumours that exist as undifferentiated cells in 90–95% of cases. Even if a differentiation of glial or neuronal cells can be found within the tumour mass, this tumour can be distinguished from other tumours based on the high proportion of undifferentiated cells. PNETs are histologically related to medulloblastoma, pineoblastoma, atypical teratoid/rhabdoid tumours and peripheral neuroblastomas. At a rate of less than 5%, supra-tentorial neoplasms occur relatively infrequently in children. Although they have also been described in young adults up to the middle of the 20th year of life, they are mainly observed in children younger than 5 years. A sex predilection has not been verified.

### ■ ■ Symptoms

From a clinical perspective, patients mostly attract attention because of macrocephalus and signs of cerebral pressure or seizures.

### ■ ■ Pathology

Primitive neuro-ectodermal tumours are mainly found in the deep white matter and are usually quite large by the time they are diagnosed. In general, they have sharp boundaries, even though histologically, the tumour spreads past the borders detected in imaging studies. Necrotic areas and calcifications are found in half of the tumours. Metastases via the sub-arachnoid cavity and in the lungs, liver and bone marrow have been described.

### ■ ■ Medical Imaging

On unenhanced CT, the solid portions of the neuro-ectodermal tumour exhibit hyper-density to the surrounding cerebral parenchyma, probably because of the high cell density. Cysts and calcifications are often detectable, and haemorrhaging is seen in approximately 10% of cases. After the administration of contrast agent, enhancement can always be seen, sometimes heterogeneously. Sometimes there is annular enhancement because of the cysts and necrotic portions of the tumour.

On MRI, the primitive neuro-ectodermal tumour appears as a large, well-defined mass, which is localised in the cerebral hemispheres or the lateral ventricles (■ Fig. 9.99). Like ependymomas, they can display a rather variable picture, which is caused by the various solid portions, cysts and necrotic areas in addition to calcification and haemorrhaging. As on CT, after the administration of contrast agent, there is strong heterogeneous enhancement with necrotic areas and tumourous cysts.

► If MRI reveals a large space-occupying lesion with a variable appearance and heterogeneous enhancement in a child younger than 5 years, a primitive neuro-ectodermal tumour, ependymoma, or atypical teratoid/rhabdoid tumour should be considered in the differential diagnosis.

## ■ Atypical Teratoid/Rhabdoid Tumour

### ■ ■ Definition, Localisation

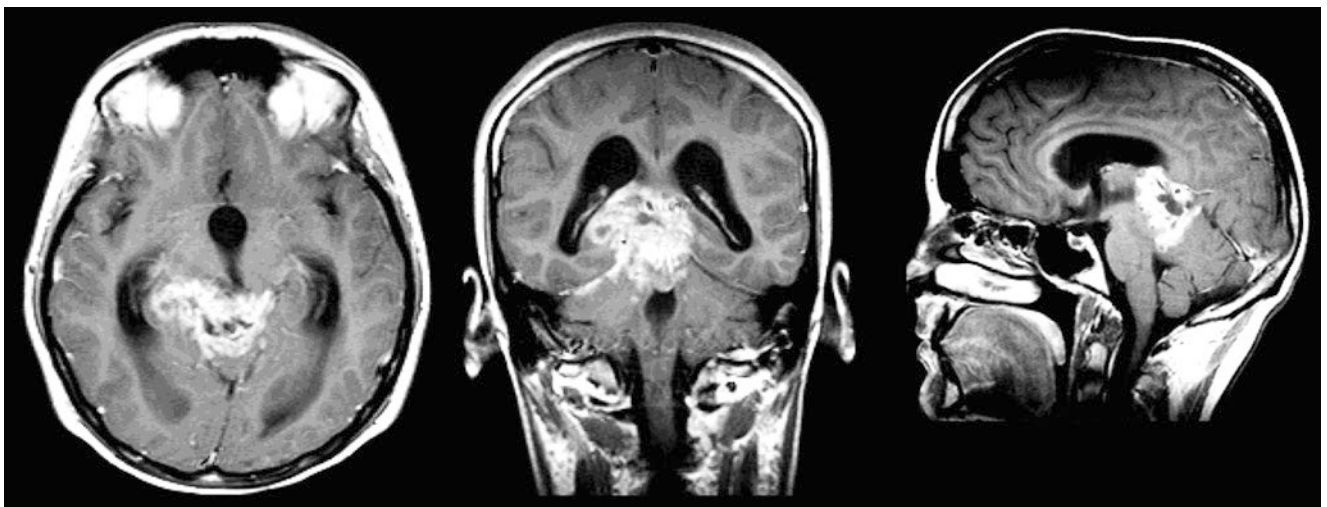
Malignant rhabdoid tumours are neoplasms of unknown histogenesis. The name is derived from their histologically rhabdoid appearance, although this entity does not belong to the group of rhabdomyosarcomas. Rhabdoid tumours are rarely found in the cerebral parenchyma; they usually appear as malignant neoplasms of the kidney. Most cases of cerebral rhabdoid tumours are described in the first years of life.

### ■ ■ Symptoms and Prognosis

Clinically, patients display symptoms of nausea, blurred vision and lethargy. The prognosis is very poor; the mean survival time is slightly over 1 year.

### ■ ■ Pathology

Most are solid tumours with necrotic portions. Histologically, they exhibit round to ovoid cells with eccentric nuclei and prominent, eosinophilic cytoplasm and hyaline inclusions. From a molecular genetic perspective, a deletion in the *IN11* gene on chromosome 22 in the tumour is conclusive. Otherwise, these can only be found in plexus carcinomas.



■ Fig. 9.99 PNET. MRI of a PNET in the pineal region, findings at the time of diagnosis. (From: *Radiologe* 2003;43:994, Fig. 6a)

### ■ ■ Medical Imaging

For diagnosis, there is often a very large solid tumour with necrotic portions and a diameter greater than 5 cm. The solid portions of the tumour are iso-dense to hyper-dense to the grey matter on CT and iso-intense to the grey matter on MRI. After the administration of contrast agent, the solid portions of the tumour display heterogeneous enhancement. On imaging, the tumour cannot be differentiated from ependymoma or PNET.

### ■ Dysembryoplastic Neuro-epithelial Tumour

#### ■ ■ Definition, Symptoms

Dysembryoplastic neuro-epithelial tumours (DNETs) are benign lesions of the cerebral cortex that usually clinically manifest as complex partial seizures in childhood and adolescence. Other focal neurological signs are very rare. The best diagnostic criteria suggesting a dysembryoplastic neuro-epithelial tumour are:

- Complex partial seizures that occur before the age of 20
- No neurological or cognitive deficits
- Cortical space-occupying lesion

In extremely rare cases, the tumour can also occur in the deeper region of the hemispheres, e.g. in the caudate head.

#### ■ ■ Pathology

Approximately 60% of DNETs are found in the temporal lobe, 30% are found in the frontal lobe, and less than 10% are found in the parietal lobe, occipital lobe, deep core areas, brain-stem and cerebellum. There are solid tumours that often have cystic or micro-cystic portions. Sometimes, these tumours are found in addition to cortical dysplasia. This indicates that they are either a cellular malformation or a maldevelopment of the cells during the second trimester of pregnancy.

➤ It is likely that some of the tumours previously histologically classified as gangliogliomas or mixed oligo-astrocytomas would now be classified as DNETs.

### ■ ■ Medical Imaging

On imaging, they sometimes display a highly variable appearance. Despite this variable appearance, all DNETs are well-circumscribed, lobulated, cortically situated space-occupying lesions that appear hypo-dense to the white matter on unenhanced CT. On MRI T2-weighted sequences, they display a signal increase. On the T1-weighted sequences, they appear hypo-intense (■ Fig. 9.100). In approximately 30–40% of cases, cystic or micro-cystic tumour portions are visible. Calcification effects can be detected in up to 30% of the tumours. Because these lesions are primarily cortical and thus located superficially, DNETs often show an extension of the tabula interna of the cranial vault. A sub-cortical propagation is seen in approximately 30% of the cases. Contrast enhancement is only detectable in 20–40% of cases and tends to be diffuse and streaky.

➤ The diagnosis of a DNET should be considered if a space-occupying lesion is primarily located cortically and is depicted as hyper-intense on T2-weighted se-

quences and if the patient has a long history of seizures alongside otherwise normal neurological findings

(■ Fig. 9.100).

## 9.4.4 Extra-parenchymal Tumours

Extra-parenchymal lesions typically shift brain structures instead of infiltrating them. The brain is pushed away from the bone, or dura, which may lead to additional cisterns. A well-definable space divides the extra-parenchymal mass-occupying lesion from the brain. There is usually little to no peri-focal oedema.

Intra-parenchymal lesions, however, compress the cisterns and sulci. They often infiltrate the surrounding cerebral parenchyma and may cause significant oedema.

All **characteristics** that indicate an extra-parenchymal tumour include:

- A small mass effect compared with the size of the tumour
- A spread of the space-occupying lesion above the median without any involvement of the cerebral commissure
- Relatively bland clinical symptoms

The **differentiation between extra-axial and intra-axial is of interest** for the diagnosis of type and for surgical planning. The most important extra-axial tumours are meningioma and neurinoma in addition to sub-arachnoid, dermoid and epidermoid cysts. The latter can also be located intra-axially.

### ■ Meningiomas

#### ■ ■ Definition, Epidemiology

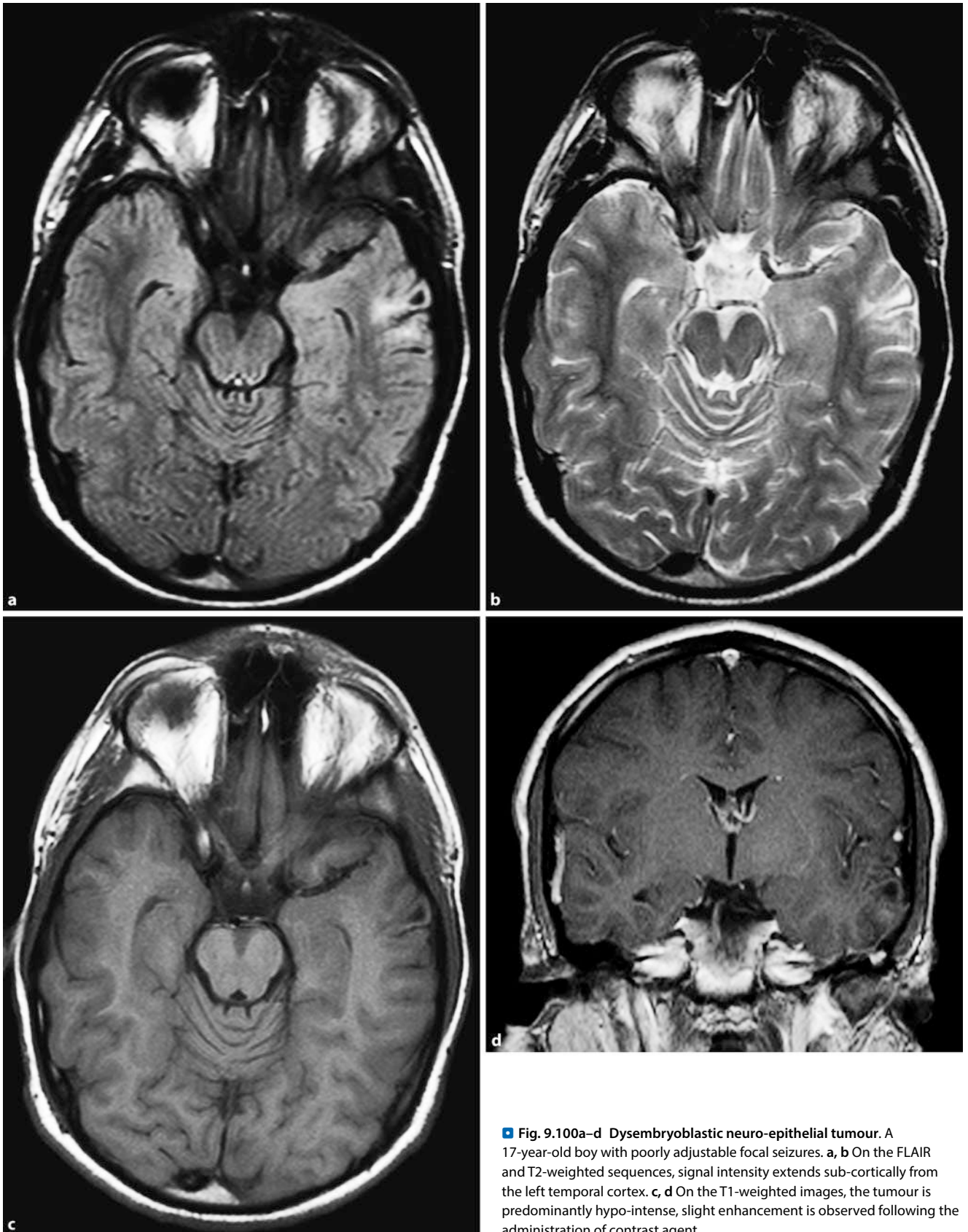
After astrocytic tumours, meningiomas are the most frequent tumour entity. They are the most common primary non-glial intra-cranial tumours. These are extra-axial neoplasms, which account for 15–20% of primary intra-cranial neoplasms. The peak incidence is in the fifth decade of life. In children and adolescents, meningiomas are rare. Women are affected more often than men.

#### ■ ■ Pathogenesis, Localisation

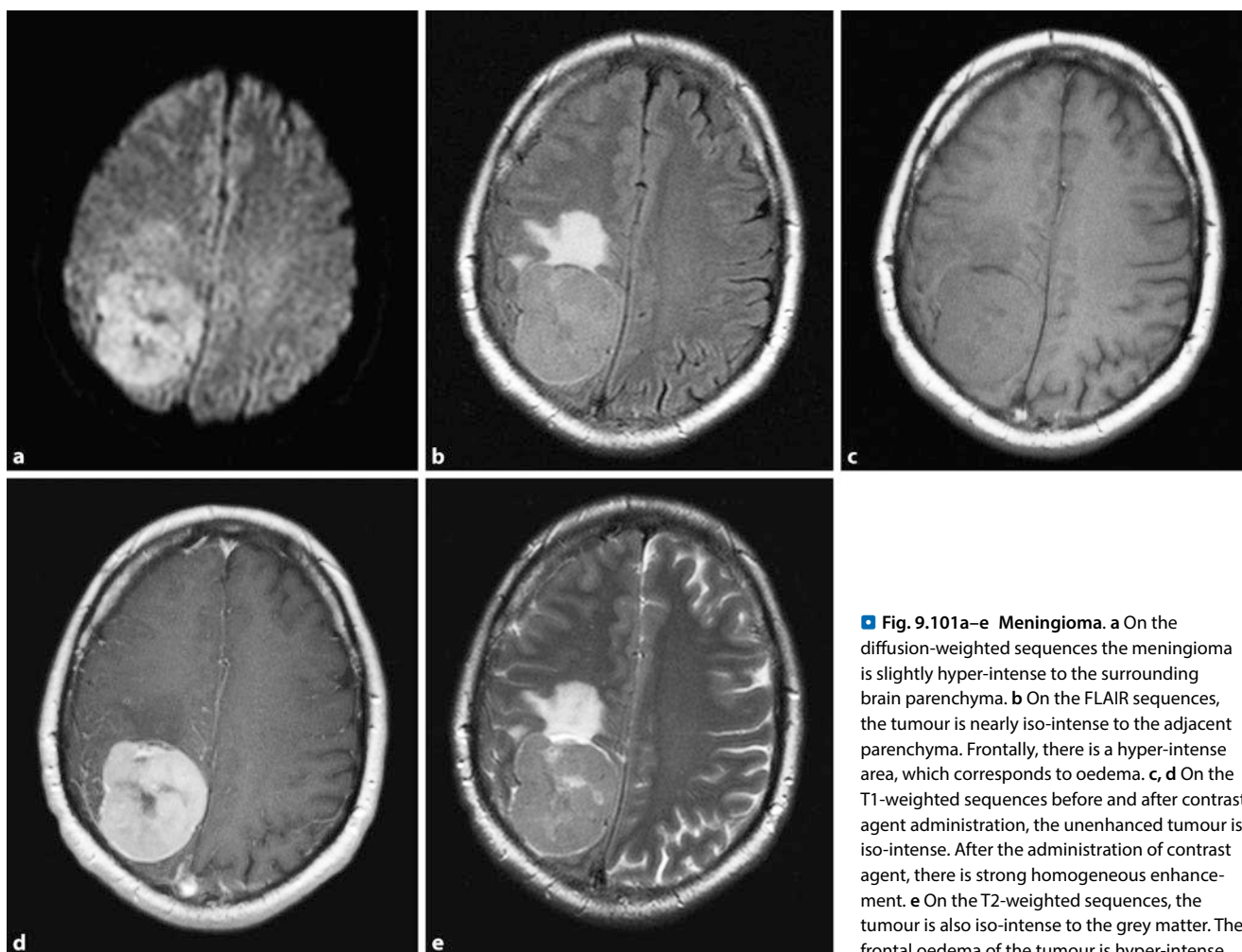
Most meningiomas arise from arachnoid cells of the inner dura and therefore grow inwards towards the brain, where they form an intra-dural mass. They are usually benign. However, they are atypical or aggressive in 6% of cases and malignant in 1–2%. They are typically **localised** parasagittally at the falx, the convexity, the entire base of the skull, the cerebellum and the tentorium. In 90% of cases, they are situated supra-tentorially. Patients with breast cancer have a higher incidence of meningiomas.

### ■ ■ Medical Imaging

On **unenhanced X-ray photography** hyperostosis of the cranial vault appears at the sites of attachment, and there is an extension of the meningeal vascular channels. On **CT**, they are usually hyper-dense; more rarely they are homogeneously iso-dense. There is also partial calcification. They have a mid-grade peri-focal oedema. After the administration of contrast agent, there is pronounced homogeneous enhancement with sharp delineation of the tumours and their relationship to the meninges.



■ Fig. 9.100a–d Dysembryoplastic neuro-epithelial tumour. A 17-year-old boy with poorly adjustable focal seizures. **a, b** On the FLAIR and T2-weighted sequences, signal intensity extends sub-cortically from the left temporal cortex. **c, d** On the T1-weighted images, the tumour is predominantly hypo-intense, slight enhancement is observed following the administration of contrast agent



■ **Fig. 9.101a–e Meningioma.** **a** On the diffusion-weighted sequences the meningioma is slightly hyper-intense to the surrounding brain parenchyma. **b** On the FLAIR sequences, the tumour is nearly iso-intense to the adjacent parenchyma. Frontally, there is a hyper-intense area, which corresponds to oedema. **c, d** On the T1-weighted sequences before and after contrast agent administration, the unenhanced tumour is iso-intense. After the administration of contrast agent, there is strong homogeneous enhancement. **e** On the T2-weighted sequences, the tumour is also iso-intense to the grey matter. The frontal oedema of the tumour is hyper-intense

On MRI the meningiomas are iso-intense to hypo-intense on T1-weighted images, and iso-intense to hyper-intense on T2-weighted images. The well-defined extra-axial space-occupying lesion shifts the cortex inward. After contrast agent administration, there is strong homogeneous enhancement (■ Figs. 9.101, 9.102); a “dural-tail” sign (thickening and marked enhancement of the adjacent dura) is common, but non-specific. Because the meningiomas often appear iso-intense compared with the grey matter on all sequences, they can easily be overlooked without contrast agent.

Meningiomas can rapidly grow “en plaque”, line the inner skull, and infiltrate the bone and the dura. Calcified meningiomas are rarely malignant. Even in the absence of NF-II, in 16% of cases multiple meningiomas can occur; thus, lesions must be actively sought. In less than 1% of cases, meningiomas arise **extra-durally**. Sites of origin can include the intra-diploid cavity, the external cranial vault, the skin and para-nasal sinuses in addition to the parotid and para-pharyngeal cavities. On imaging, benign, atypical, and **malignant meningiomas** often appear to be identical, although malignant tumours frequently display perifocal oedema and cerebral infestation.

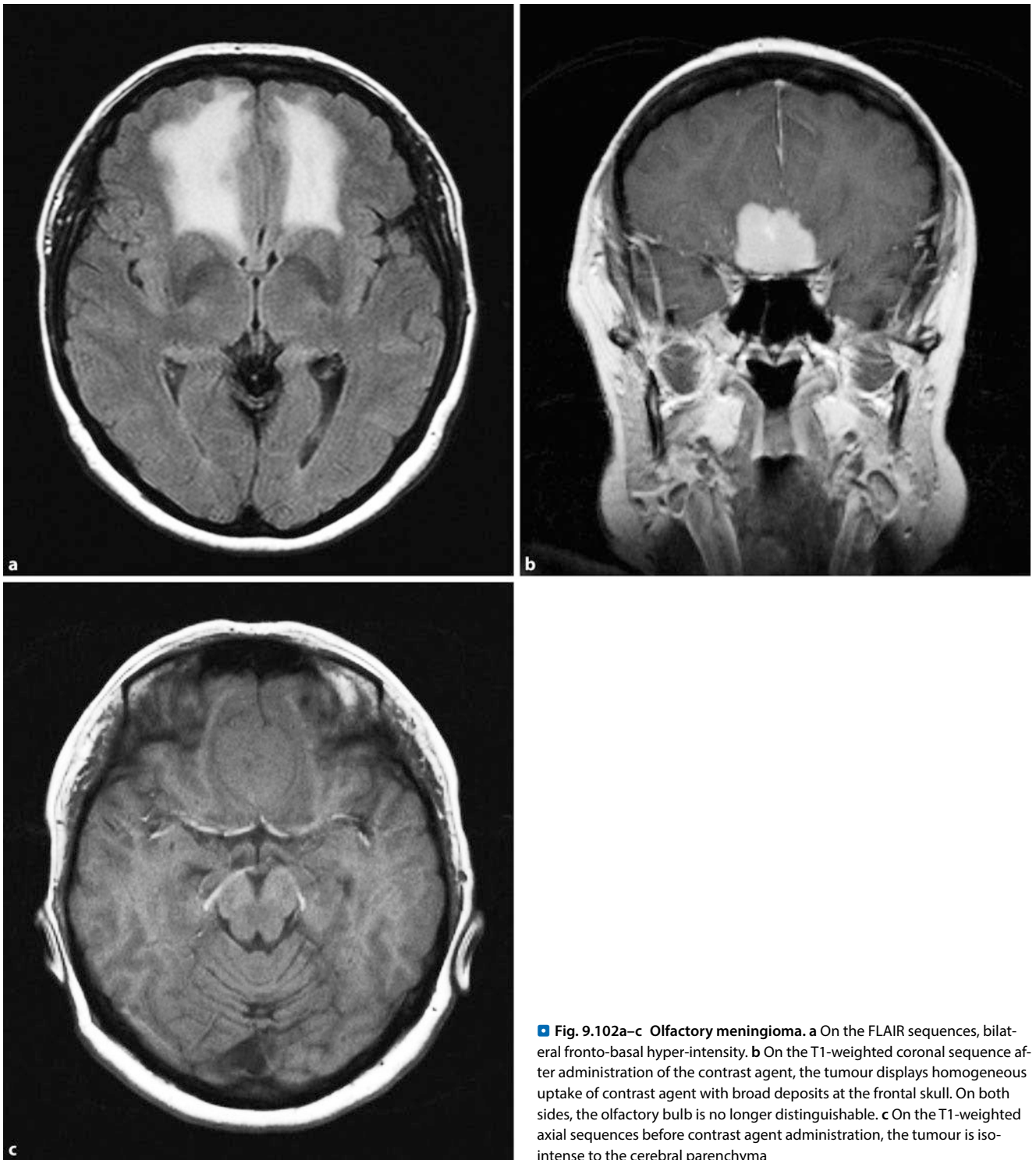
In 15% of meningiomas, there can be atypical imaging with heterogeneous enhancement, cysts, haemorrhaging and/or fatty degeneration.

Like extra-axial tumours of meningeal origin, meningiomas exhibit a typical vascular supply via the meningeal arteries. In intra-ventricular meningiomas, they are supplied by choroidal arteries. On **angiography**, the representation of the external carotid artery, especially the middle meningeal artery is necessary. In principle, branches of the internal carotid artery can also be involved in the supply to the meningioma, particularly from the central portions of the tumour. Therefore, during angiographic presentation, selective probing of the external and internal carotid artery is necessary.

#### ■ **Neuromas** ■ **Definition, Pathology**

Neuromas, or **schwannomas**, are tumours that arise from Schwann cells. They form in the myelin sheaths around the axons of nerve fibres. Neuromas account for approximately 8% of primary brain tumours. They arise more frequently in adults. In children, they account for approximately 2% of the tumours in the posterior fossa. If a schwannoma is diagnosed in a child, the presence of NF-II should be considered. A search for other schwannomas and meningiomas should be included.

Schwannomas preferentially occur at locations where oligodendroglial cells bypass Schwann cells. Schwannomas of the acoustic nerve are common in the internal acoustic meatus or in the cerebello-pontine angle.



■ **Fig. 9.102a–c Olfactory meningioma.** **a** On the FLAIR sequences, bilateral fronto-basal hyper-intensity. **b** On the T1-weighted coronal sequence after administration of the contrast agent, the tumour displays homogeneous uptake of contrast agent with broad deposits at the frontal skull. On both sides, the olfactory bulb is no longer distinguishable. **c** On the T1-weighted axial sequences before contrast agent administration, the tumour is iso-intense to the cerebral parenchyma

### ■ ■ Symptoms

Schwannomas are tumours of the nerve sheathes and not the nerve cells. Patients often exhibit neuropathy because the tumours exert pressure onto the nerve cells because of their size. If a schwannoma of the acoustic nerve proliferates in the cerebello-pontine angle, it usually only causes symptoms if surrounding neural structures are affected by the pressure. There are frequently signs of brain-stem compression or hydrocephalus due to compression of the aqueduct of the fourth ventricle. Neuromas

most commonly infest the eighth cranial nerve, followed by the fifth, ninth and tenth. Other intra-cranial schwannomas are extremely rare.

### ■ ■ Medical Imaging

On CT the schwannoma is hypo-dense to iso-dense, sometimes with calcifications. Central necrosis may occur in large tumours. After the administration of contrast agent, there is typically homogeneous enhancement. If the schwannoma proliferates within



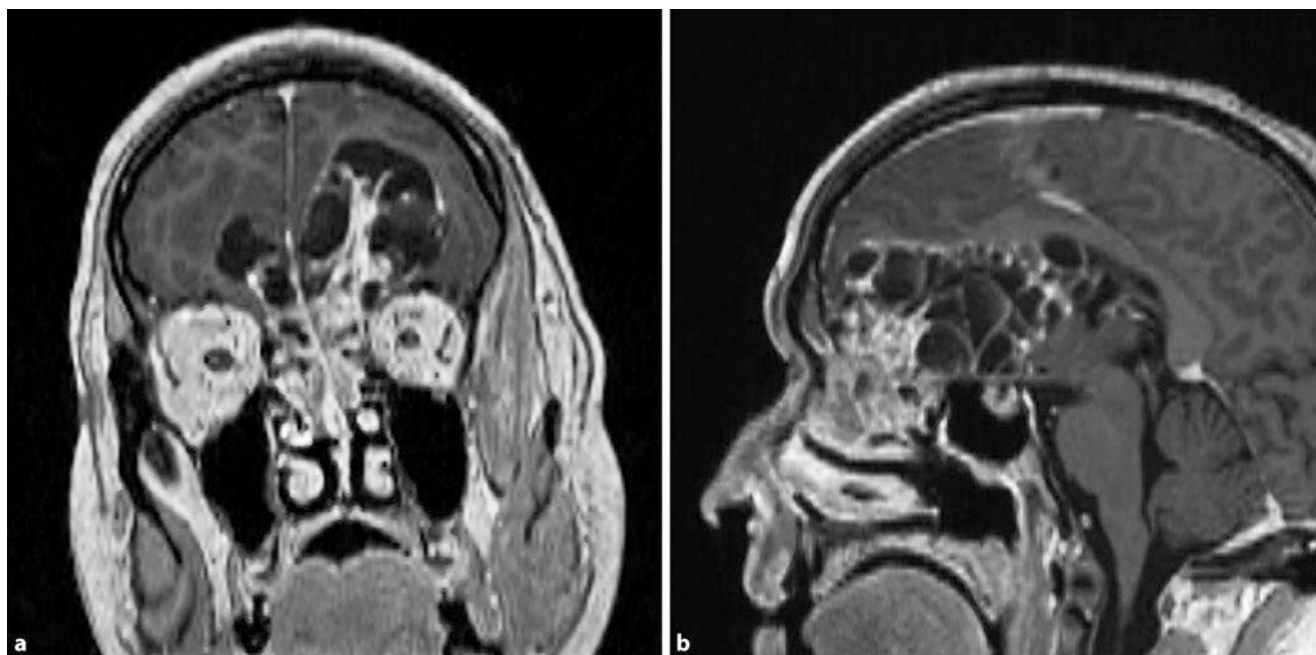


**Fig. 9.103a,b Aesthesioneuroblastoma.** **a** On the T1-weighted coronal sequences, the solid portions of the tumour appear hyper-intense following the administration of contrast agent. In addition, there are frontal cystic tumour areas on both sides. The tumour has infiltrated the sinuses. **b** On the sagittal

T1-weighted sequences, after the administration of contrast agent, the tumour completely extends dorsally from the sinuses to the third ventricle with cysts and solid tumour portions

the internal acoustic meatus, there is widening of the lacrimal duct within the temporal bone.

On MRI, schwannomas have a prolonged T1 and T2 relaxation time. Large schwannomas often show a heterogeneous signal with areas of high and low signalling on the T2-weighted sequences. These hypointense areas are often caused by intratubular haemorrhaging. The thickened cranial nerves are detected because of the enlarged neural foramina, e.g. the oval foramen and the foramen rotundum in the case of trigeminal schwannoma and the internal acoustic meatus in the case of acoustic schwannoma. After the intra-venous administration of contrast medium, there is strong, mostly homogeneous enhancement.

**Aesthesioneuroblastoma** An aesthesioneuroblastoma is a tumour originating from the olfactory epithelium (■ Fig. 9.103).

#### 9.4.5 Malformation and Germ Cell Tumours

Classification of malformation and germ cell tumours:

- Epidermoid cysts/epidermoid
- Colloid cysts
- Arachnoid cysts
- Hamartomas
- Lipomas
- Germ cell tumours

This involves tumours in which an abnormality of organ differentiation is the basis of scattered cells that have not developed further. Epidermoids, dermoids and teratomas are relatively benign malformation tumours. They originate in the embryonic

epidermal cisterns. They grow slowly, but can achieve a considerable magnitude. Typical sites include the cerebello-pontine angle, the para-sellar region, the pineal region, and the ventricle. Dermoids and epidermoids probably originate from congenital, intra-cranially remaining cells as a result of incomplete separation of the neuro-ectoderm from the ectoderm during closure of the neural tube. Epidermoids are more common than dermoids.

##### ■ Epidermoids

##### ■ ■ Definition, Epidemiology, Pathology

Epidermoid cysts consist of a conglomerate of horny scales, which is surrounded by an epidermal capsule. They account for 0.2–1% of intra-cranial tumours. Because of their slow growth, they are mainly found in adulthood.

##### ■ ■ Localisation, Symptoms

In 40% of cases, the intra-cranial epidermoids occur in the area of the cerebello-pontine angle. They account for 5% of all tumours of the cerebello-pontine angle. The next most common sites are the pineal region, the supra-sellar region and the medial cranial fossa. Epidermoids in the supra-sellar and pineal regions usually become noticeable because of hydrocephalus, while epidermoids of the medial cranial fossa often display symptoms of chemical meningitis caused by the spread of the tumour into the sub-arachnoid cavity.

##### ■ ■ Medical Imaging

On CT, epidermoids appear as hypodense, lobulated space-occupying lesions with typical localisation. The density values are similar to those of a cyst. Calcifications are occasionally

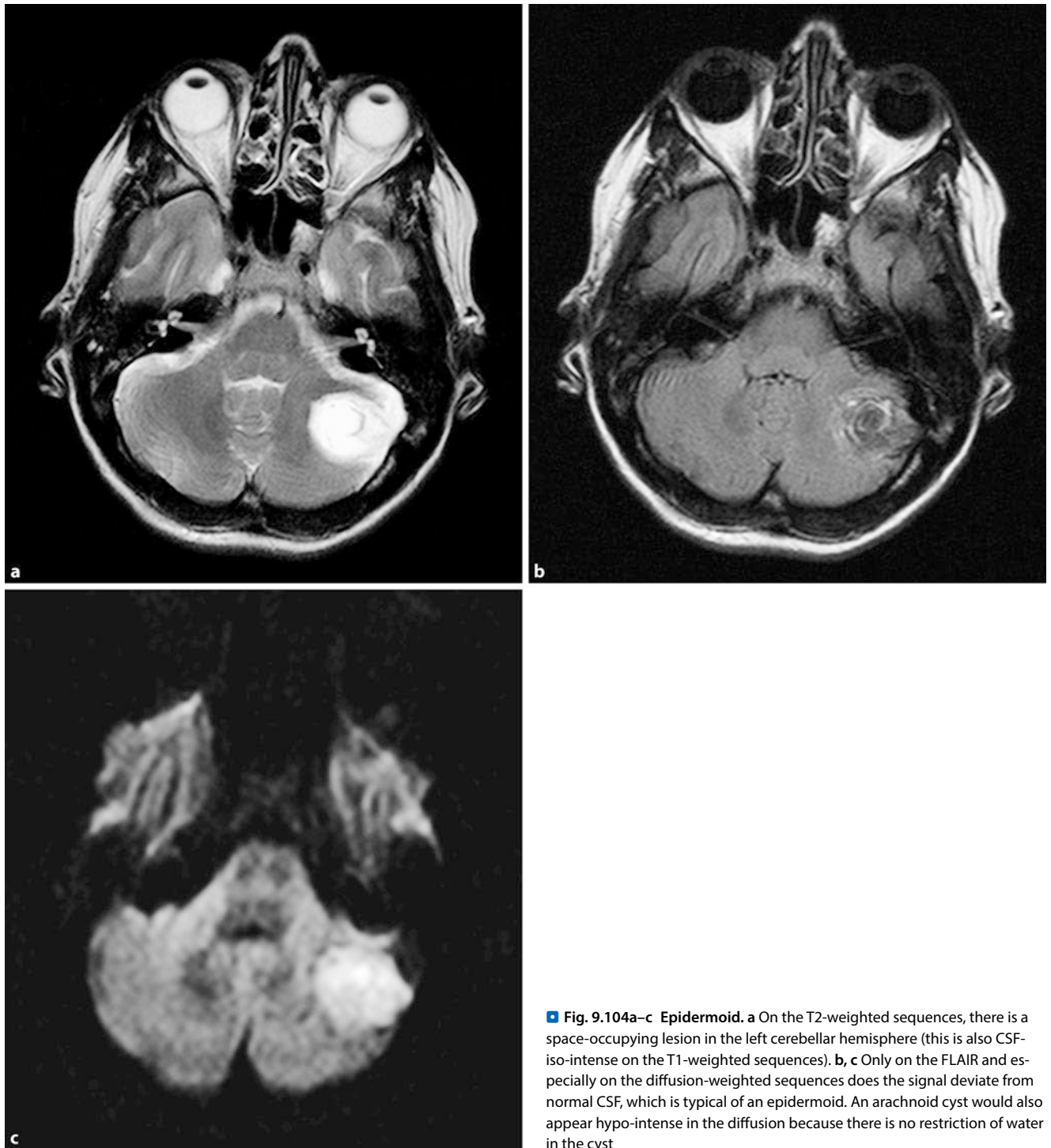


**Fig. 9.104a–c Epidermoid.** **a** On the T2-weighted sequences, there is a space-occupying lesion in the left cerebellar hemisphere (this is also CSF-iso-intense on the T1-weighted sequences). **b, c** Only on the FLAIR and especially on the diffusion-weighted sequences does the signal deviate from normal CSF, which is typical of an epidermoid. An arachnoid cyst would also appear hypo-intense in the diffusion because there is no restriction of water in the cyst

found in the surrounding capsule portions. In 25% of cases peripheral calcifications are found in epidermoids. Because the density values are similar to those of CSF, an identification of these extra-axial space-occupying lesions often proves to be difficult. On the unenhanced CT images, only the displacement of the surrounding brain structures can provide evidence of an extra-axial space-occupying lesion. Intra-theal administration of contrast agent is one way of better delineating these tumours on CT.

Today, there are modern **MR techniques and sequences** that can afford a reliable diagnosis of epidermoids. At the forefront are the so-called FLAIR and diffusion-weighted sequences (Fig. 9.104). On FLAIR sequences, there is no complete suppression of CSF; the epidermoids appear hyper-intense. The situation is similar on diffusion-weighted sequences; the CSF normally appears hyper-intense because of its high diffusion. On the conventional T1- and T2-weighted sequences, the signal resembles that of CSF. It is also very difficult to diagnose an epi-

dermoid using conventional sequences. An epidermoid growing in the basal cisterns can be identified based on the expansion of the cistern and the often characteristic lobulated appearance of the space-occupying lesion.

As an alternative to FLAIR and diffusion-weighted sequences, magnetised transfer techniques can be implemented to reveal the solid matrix of the tumour in front of and next to the surrounding free water. Epidermoids can thus display a T1 shortening with a hyper-intense signal. In this case, a differentiation from dermoids or lipomas can be difficult. Here, a T1-weighted-sequence with fat saturation can additionally help because the fat is suppressed in the case of lipomas and dermoids, while epidermoids continue to display a hyper-intense signal. Every now and then, after the administration of contrast agent, epidermoids display a narrow, contrast-enhanced rim, which likely corresponds to an inflammatory reaction at the periphery of the tumour.

#### ■ Dermoids

##### ■ ■ Definition, Localisation

In dermoids, fat, calcifications, sweat glands and hair are found in the cyst in addition to the epidermal portion. In teratomas, cartilaginous, osseous and endodermal portions can also be found. Intra-cranially, dermoids are less frequent than epidermoids. However, they are more frequent in the spinal canal. Intra-cranially, they can usually be found in the posterior fossa too, either within the vermis or in the area of the fourth ventricle. In the spinal canal, they usually appear in the lumbosacral transition region, either extra- or intra-medullary. Approximately, 20% of dermoids are associated with a dermal sinus.

##### ■ ■ Symptoms

Symptoms of intra-spinal dermoids occur mainly in the first two decades of life. Intra-cranial dermoids reach their age peak in the third decade of life. Symptoms result from displacement of CSF circulation, chemical meningitis, spread of the cyst contents into the sub-arachnoid cavity, or – if a dermal sinus is present – by an infection or an abscess within the sinus or the dermoid.

##### ■ ■ Medical Imaging

On CT, dermoid with negative Hounsfield units appear (■ Fig. 9.105). They are extra-axial space-occupying lesions, which are usually located in the median. After the administration of contrast agent, there is usually no enhancement. There are, however, exceptions in the case of an infection. If a dermoid or epidermoid is detected in the median, the occipital region of the skull base and naso-frontal region should be investigated to exclude a dermal sinus. In the case of intra-spinal localisation, the posterior elements of the vertebral arches should be accurately investigated to exclude a dermal sinus here. During infection, the dermoid cysts display the typical appearance of an abscess with an annular uptake of contrast agent.

On MRI, the dermoid appears hyper-intense on T1-weighted sequences and moderately hyper-intense on T2-weighted sequences. For differentiation (e.g. haemorrhaging), fat-suppressed sequences can be run (■ Fig. 9.105). Dermoid cysts are typically less lobulated than lipomas and displace vessels and nerves. In

lipomas, however, the vessels and nerves are embedded within the space-occupying lesion.

#### ■ Teratomas

##### ■ ■ Definition, Localisation

Intra-cranial teratomas are rare and only account for approximately 0.5% of intra-cranial tumours. In children younger than 15 years, they are responsible for 2% of intra-cranial tumours. Intra-cranial teratomas occur more frequently in boys than in girls, especially teratomas of the pineal region. The clinical symptoms mainly depend on the localisation of the tumour. As with other tumours of the median a hydrocephalus is often found. Teratomas are most frequently found in the pineal and parapineal region, followed the region of the third ventricle and the posterior fossa. They occur less frequently spinally than intra-cranially. However, they may occur at any spinal level and are often associated with spina bifida occulta.

##### ■ ■ Pathology

Most teratomas are well circumscribed and benign, but sometimes they contain primitive cells and are highly malignant with a poor prognosis. Some release their biochemical markers (e.g.  $\alpha$ -fetoprotein, chorionic gonadotropin, and  $\beta$ -HCG), which can be detected in the CSF and serum. The tumours have both solid and cystic portions and often exhibit calcifications.

##### ■ ■ Medical Imaging

On CT and MRI, teratomas appear as well-circumscribed, heterogeneous lesions, which are often localised in the median. With CT, they can be relatively reliably diagnosed when either fatty deposits and calcifications occur within the space-occupying lesion. Teratomas with a homogeneous appearance are more often malignant and often indistinguishable from other intrinsic brain tumours. Malignant teratomas are often accompanied by marked vasogenic oedema and an irregular appearance and are less sharply demarcated from the surrounding parenchyma. Malignant teratomas frequently consist of less cysts and calcifications than benign teratomas. A lack of contrast agent uptake tends to suggest a low-grade tumour. However, the presence of contrast agent uptake does not always suggest a malignant tumour.

### 9.4.6 Other Rare Tumours of the Posterior Cranial Fossa and Base of the Skull

#### ■ Langerhans Cell Histiocytosis

##### ■ ■ Definition

Langerhans cell histiocytosis, formerly known as histiocytosis X, involves an endothelial tumour, which occurs rarely in the CNS. If an osteolytic lesion infiltrates the base of the skull, the orbital, or the cranio-facial region, Langerhans cell histiocytosis should be considered as the cause (► Chap. 38).

##### ■ ■ Symptoms

In the case of Langerhans cell histiocytosis, the leading clinical symptom is often diabetes insipidus due to participation of

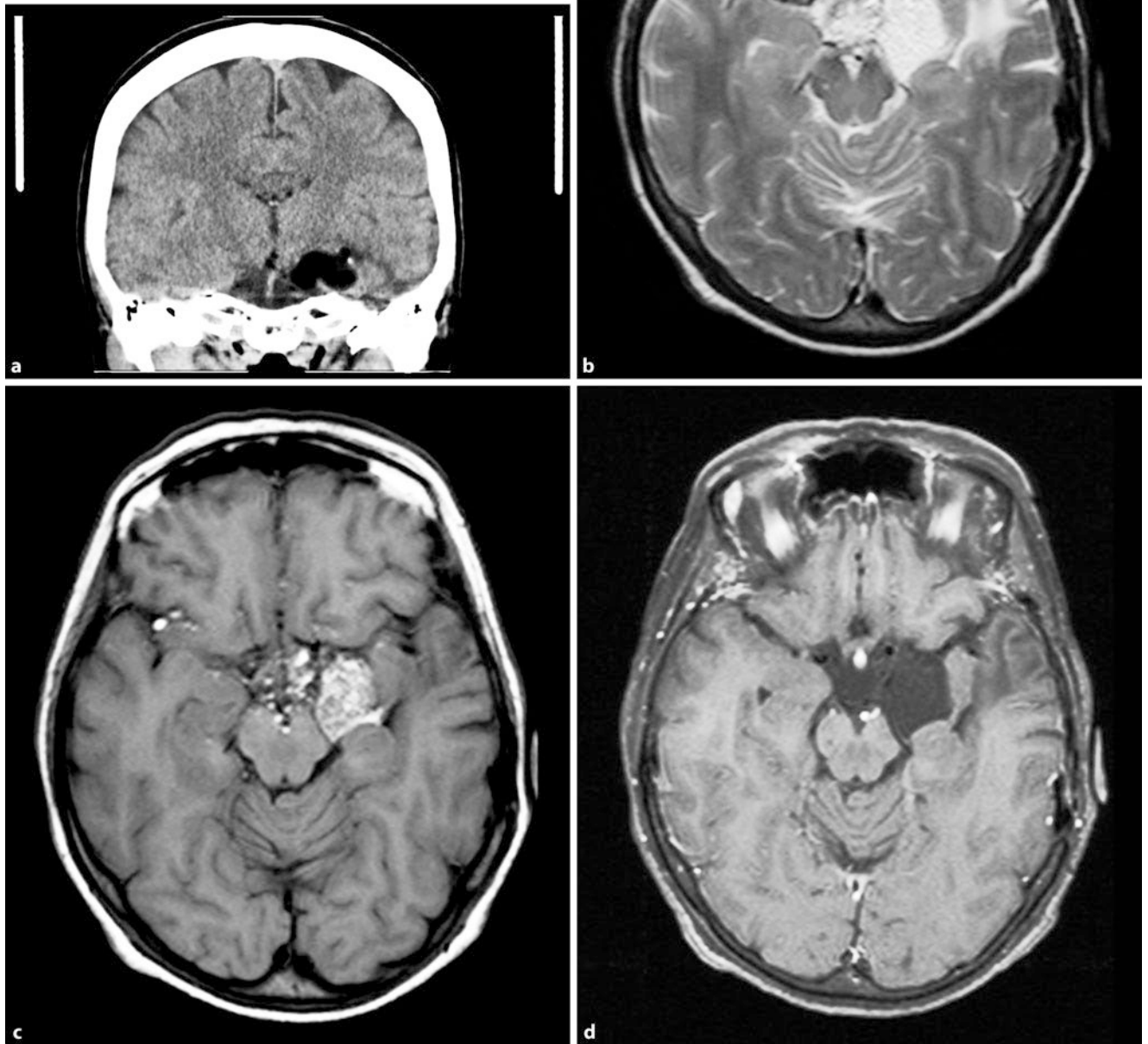


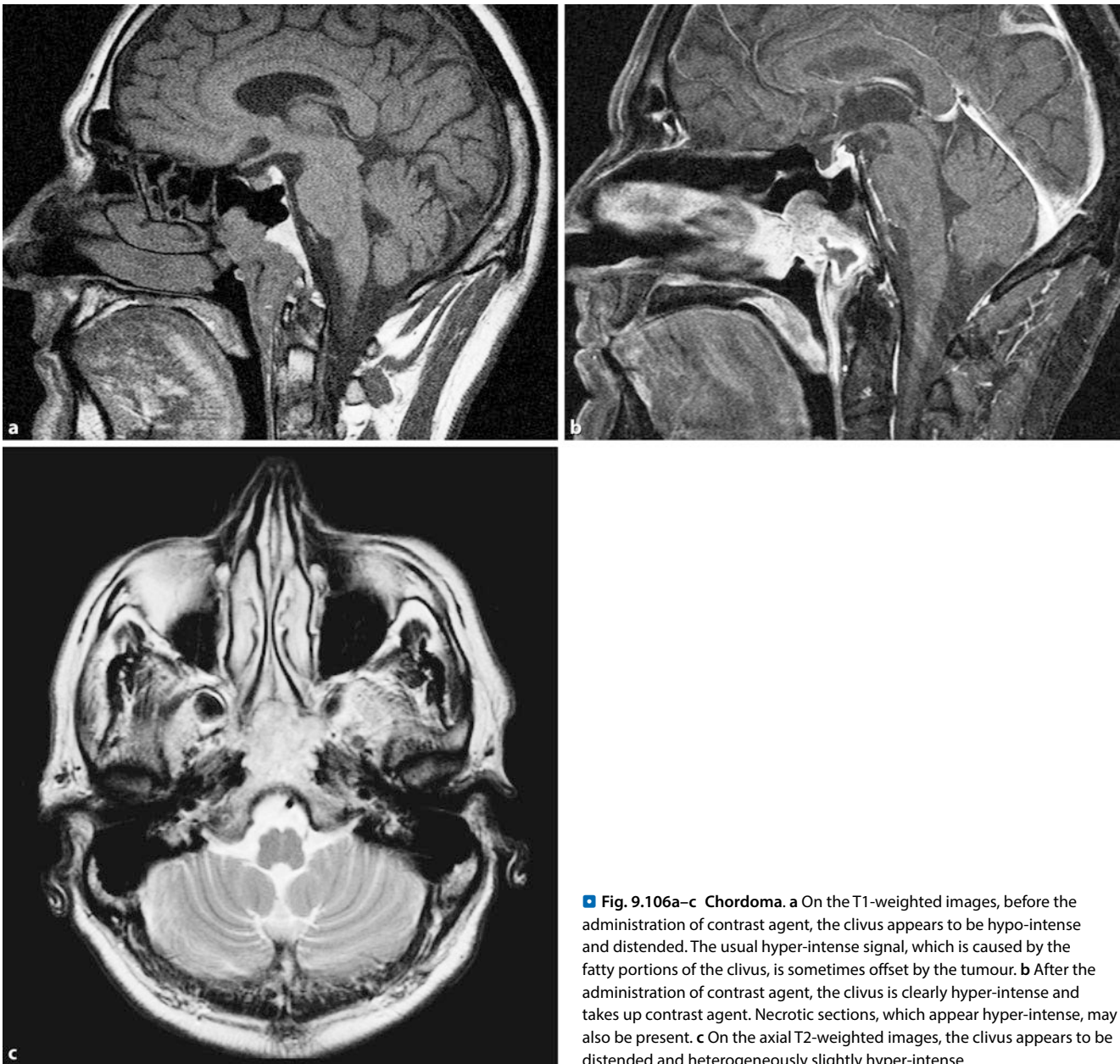
**Fig. 9.105a–d** Dermoid cysts. **a** On CT left fronto-basal hypo-dense formation, density values correspond to fatty deposits. **b** Hyper-intensity on the T2-weighted sequences. **c** On the T1-weighted sequences, hyper-intense

imposition of the space-occupying lesion. **d** After fat suppression, the space-occupying lesion appears as signal reduction on the T1-weighted sequence, which is consistent with a dermoid cyst

the pituitary stalk. Other patients may exhibit a palpable space-occupying lesion at the base of the skull along with proptosis or cerebral/cerebellar symptoms. In this case, the mass grows intra-cranially.

#### ■ ■ Medical Imaging

On the imaging, a well-circumscribed space-occupying lesion can often be found within the skull, the orbital, or the base of the skull. On CT, the space-occupying lesion often ap-



■ **Fig. 9.106a–c Chordoma.** **a** On the T1-weighted images, before the administration of contrast agent, the clivus appears to be hypo-intense and distended. The usual hyper-intense signal, which is caused by the fatty portions of the clivus, is sometimes offset by the tumour. **b** After the administration of contrast agent, the clivus is clearly hyper-intense and takes up contrast agent. Necrotic sections, which appear hyper-intense, may also be present. **c** On the axial T2-weighted images, the clivus appears to be distended and heterogeneously slightly hyper-intense

pears sharply circumscribed and is usually situated temporally. Following the administration of contrast agent, there is often homogeneous enhancement. On MRI, the lesion appears as a sharply defined, soft-tissue space-occupying lesion with signal behaviour similar to that of muscle tissue. Following the administration of contrast agent, there is strong enhancement. In such cases, Langerhans cell histiocytosis can occur in the cerebellum or in the cerebral hemispheres. The neurological symptoms then depend on the corresponding localisation of the space-occupying lesion. On imaging, these tumours are highly variable. A prolonged T1 and T2 time is often seen, especially in the brain-stem and medullary corpus of the cerebellum.

Calcifications may also be detected on CT, especially in the cerebellum.

## ■ Chordoma

### ■ ■ Definition, Epidemiology, Localisation

Chordomas are benign, slow-growing, and locally infiltrating tumours. They rarely occur in childhood; only a few dozen cases have been reported in the literature. Unlike adults, in whom the chordoma usually occurs sacally, in childhood and adolescence, chordoma usually manifests at the base of the skull.

The most common site is the sphenoid-occipital synchondrosis. As a rule, clival chordomas usually exhibit extensive destruction of the sphenoid bone (■ Fig. 9.106). They frequently proliferate in the sphenoid sinus and nasopharynx and rarely in the ethmoidal region.

### ■ ■ Symptoms, Medical Imaging

Patients with chordoma often exhibit cranial nerve failures with diplopia and tongue weakness, which indicates that the tumour

has spread into the neural foramina of the skull base. Headaches, pyramidal tract symptoms, and increased intra-cranial pressure may also occur. If the tumour disseminates into the nasopharynx, a differentiation of primary naso-pharyngeal tumours, which secondarily spread into the clivus, is often impossible. However, the presence of spicules and a tumour with only slight enhancement on CT tends to indicate a chordoma. On MRI, chordoma appears as a large, intra-osseous space-occupying lesion, which often proliferates in the pre-pontine cistern, the sphenoid sinus, the medial cranial fossa, and the naso-pharynx. The brainstem may also be forced back. Chordomas typically have a prolonged T1 and T2 relaxation time.

**On the other hand, chondroid chordoma**, a histological variant with a significantly better prognosis, displays a lower T2 time reduction.

After the administration of contrast agent, chordomas exhibit variable enhancement. However, most chordomas exhibit little to no uptake of contrast agent.

### ■ Chondrosarcomas

#### ■ ■ Definition, Localisation, Epidemiology

Chondrosarcomas very rarely occur at the base of the skull. Chondrosarcomas are malignant cartilage tumours that arise in synchondroses or via the secondary malignisation of benign cartilaginous tumours. Only about 10% of chondrosarcomas show up in the paediatric patient population. Most of these tumours occur only in the middle decades of life. The most common sites are the petro-occipital, sphenobasilar and sphenothmoidal synchondroses.

#### ■ ■ Medical Imaging

On MRI and CT, chondrosarcomas are extremely heterogeneous. The non-osseous portions have long T1 and T2 relaxation times and heterogeneous enhancement after the administration of contrast agent. Because these tumours are often situated next to fatty bone marrow in the infra-temporal fossa, fat-suppressed sequences should be carried out following the administration of contrast agent. On imaging, chondrosarcomas are indistinguishable from chordomas.

### ■ Neuroblastoma

#### ■ ■ Definition, Localisation

In neuroblastomas, involvement of the brain parenchyma is extremely rare and only occurs in about 1% of cases. Sometimes neuroblastomas may arise from sympathetic fibres in the upper cervical region or at the base of the skull (■ Fig. 9.107).

#### ■ ■ Medical Imaging

These primary neuroblastomas appear as homogeneous, extra-parenchymal space-occupying lesions, which take up contrast agent and are usually localised in the cerebello-pontine angle. If the tumour has infiltrated the cranial vault, it appears as an infiltrative space-occupying lesion, which takes up contrast agent and raises the periosteum from the bone. The identification of a space-occupying lesion with periosteal elevation is important for the diagnosis of a metastatic tumour of the base of the skull because in children, the normal bone contains

haematopoietic bone marrow, which also still accumulates contrast agent.

! **When they infiltrate the skull, Ewing's sarcoma, leukemic infiltrates and neuroblastoma have a similar appearance on CT and MRI.**

### ■ Aneurysmal Bone Cysts

#### ■ ■ Definition, Localisation

Only 2–6% of aneurysmal bone cysts occur in the skull area. They are usually located orbitally and occipitally. It is important to diagnose these lesions pre-operatively because embolisation can minimise intra-operative blood loss.

#### ■ ■ Medical Imaging

**Plain X-rays** show an expansive lesion in the skull bone with the typical appearance.

On CT, aneurysmal bone cysts appear as a multi-lobulated mass with a thin peripheral osseous portion. The aneurysmal bone cyst is an osteolytic lesion of the bone, which consists of blood-filled cavities of different sizes. These are divided by connective tissue and contain osseous or osteoid trabeculae and osteoclastic giant cells. From a differential diagnostic perspective, the aneurysmal bone cyst must be distinguished from a juvenile bone cyst and a giant cell tumour (telangiectatic osteosarcoma). In most cases, there are no adverse symptoms; they are discovered by chance, e.g. in the case of pathological fracture. On the T2-weighted MR sequences, the aneurysmal bone cyst often shows a fluid level with hyper-intense portions.

### ■ Tumours of the Pineal Region

**Definition, Classification** Tumours of the pineal region are generally very rare with an incidence of less than 1% of all intracranial tumours. Clinically, these tumours are characterised by three main symptoms:

- Hydrocephalus caused by aqueduct stenosis
- Parinaud's syndrome, caused by compression in the tectum (upward ocular muscle movement disorders, pupillary light reflex disorder with preserved accommodation, lack of convergence reaction)
- Endocrinological changes caused by supra-sellar tumour growth (general precocious puberty in boys with nuclear tumours)

Pineal tumours can be **divided into two large groups**: germ cell tumours and tumours of the pineal parenchyma.

A whole series of tumours of the pineal region (e.g. astrocytomas or glioblastomas) propagate in the pineal body with the corresponding clinical symptoms.

**Medical Imaging** Pineal cysts are often incidental findings. Thanks to advances in MRI, the diagnosis of tumours in the pineal region has been significantly improved. It is sometimes possible to distinguish between benign and malignant pineal tumours and to clarify whether there is outgrowth of the tumours in the pineal body. On imaging, tumours of the pineal region often exhibit typical characteristics and can therefore often be specified.

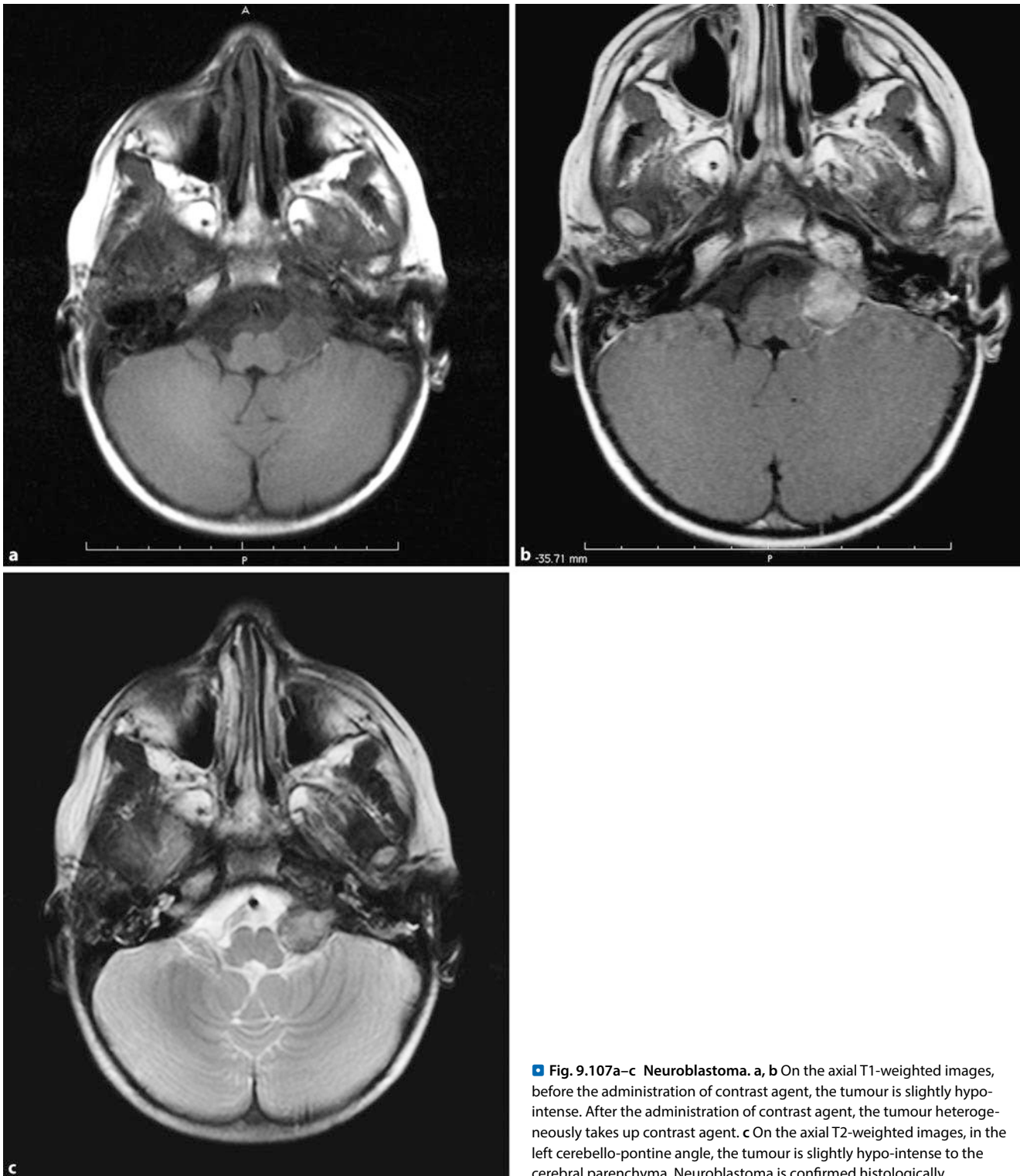


**Fig. 9.107a–c Neuroblastoma.** a, b On the axial T1-weighted images, before the administration of contrast agent, the tumour is slightly hypointense. After the administration of contrast agent, the tumour heterogeneously takes up contrast agent. c On the axial T2-weighted images, in the left cerebello-pontine angle, the tumour is slightly hypo-intense to the cerebral parenchyma. Neuroblastoma is confirmed histologically

The responsiveness of certain pineal tumours to radiotherapy was previously used to confirm the diagnosis. Today, MRI with intra-venous administration of contrast agent is the method of choice for diagnosing tumours of the pineal region and is also used for planning treatment.

The surgical approach depends on the size of the space-occupying lesions of the pineal body and their precise localisation, especially in relation to the tentorium. The infra-tentorial

aditus is usually preferred unless a larger supra-tentorial portion is available. For the radiologist, this entails describing the exact size and localisation of the tumour and possibly delineating whether the tumour originates from the parenchyma of the pineal or extends into the pineal body from the outside. The medical history of the patient is also quite helpful in the differential diagnosis.

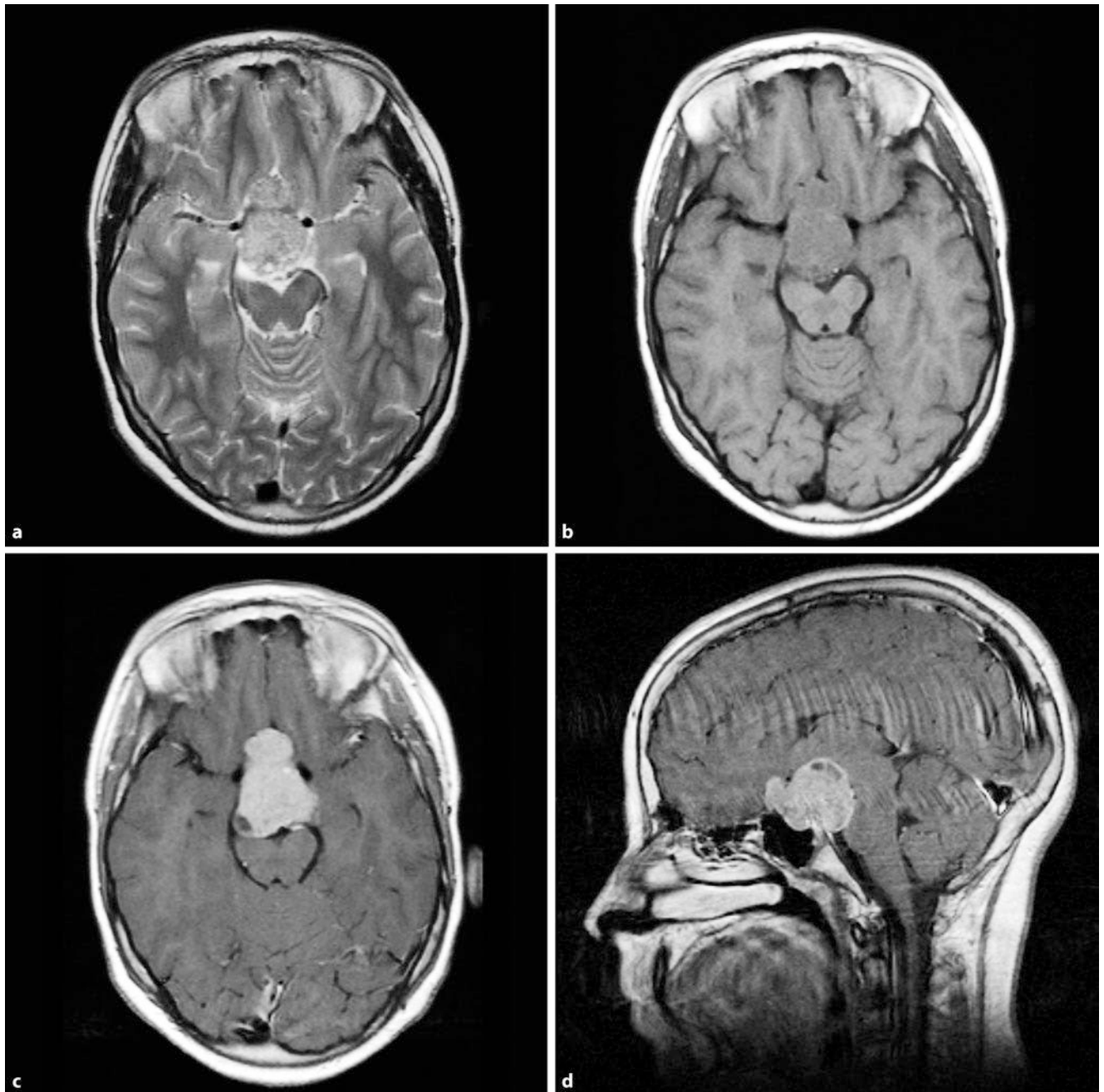


**Fig. 9.108a–d** Germinoma. Supra-sellar space-occupying lesion in the region of the infundibular recess of the third ventricle. **a** On the T2-weighted sequences, the histologically confirmed germinoma reveals heterogeneous

intermediate and **b** on unenhanced T1-weighted sequences iso-intense signal behaviour compared with the white matter. **c, d** After the administration of contrast agent, there is largely homogeneous enhancement.

### ■ Germ Cell Tumours

**Definition, Classification, Localisation** The most common pineal tumours are derived from germ cells. The family of germ cell tumours include germinoma in addition to the non-malignant, non-germinating germ cell tumour, including embryonic carcinoma, colloid carcinoma, yolk sac carcinoma, mixed types, and finally teratoma. Germ cell tumours of the central nervous system usually arise in the median, most commonly in the pineal region, followed by the supra-sellar region and the fourth ventricle. Laterally situated basal germ cell tumours are

slightly more common and have mostly been reported in Asian patients.

**Symptoms** Germinomas are the most common germ cell tumours and also the most common mass-occupying lesion of the pineal region (■ Fig. 9.108). These tumours have a long clinical history with endocrine disorders, mainly growth disorders and diabetes insipidus. Less frequently, they lead to hydrocephalus or Parinaud's syndrome. They may also present as a precocious puberty in boys. Germinomas of the pineal region have their



peak incidence in adolescence, and most patients are clinically symptomatic within the first three decades of life. Over 90% of patients are men. Studies have also demonstrated an increased incidence in Japan. The tumours show frequent dissemination in the sub-arachnoid cavity and infiltration of the surrounding cerebral parenchyma. They are generally highly radio-sensitive and have a high overall survival rate in the case of disseminated metastases. Intra-tumoural haemorrhaging is common.

The second most common germ cell tumour of the pineal gland is the **teratoma**. These tumours exhibit great variability in their histological grading and accordingly display variable growth and different clinical courses. Teratoma occurs earlier than germinoma and is most frequently encountered in the first 10 years of life. Because these lesions can be derived from all three germinal zones, they contain hair, teeth, bones and fat. Cystic changes and haemorrhaging can almost always be detected.

Embryonic carcinomas, yolk sac tumours, chorionic carcinomas and mixed germ cell tumours are rare and have a poor prognosis because of their high malignancy. These lesions often display haemorrhaging. A diagnosis can sometimes be made without biopsy if increased human chorionic gonadotropin or  $\alpha$ -fetoprotein can be detected in the serum or CSF. The survival rate can be improved by combined radiotherapy and chemotherapy.

**Medical Imaging** **Germinomas of the pineal gland** are well-defined, relatively homogeneous lesions, which cannot be distinguished from the pineal gland. On T2-weighted sequences, they often exhibit iso-intensity to the grey matter. Intra-tumoural haemorrhaging is encountered more frequently in pineal gland tumours. There is often concurrent oedema in the adjacent cerebral parenchyma. Spread into the sub-arachnoid cavity is also frequently encountered. Germinomas and their metastases display clear, homogeneous enhancement after the administration of contrast agent. Germinomas of the pineal gland region usually do not contain calcifications or cystic changes. This does not, however, apply to germinomas in the region of the basal ganglia.

On MRI, **teratomas of the pineal gland region** are heterogeneous (e.g. intra-tumoural haemorrhaging, fatty and cystic portions) because of their different types of tissue. Teratomas often display extensive calcification or osseous changes. In teratomas, enhancement is quite variable following the administration of contrast agent. In the differential diagnosis, rhabdoid tumours or high-grade astrocytomas should also be considered.

#### ■ ■ Pineal Cell Tumours

Pineal cell tumours, pineoblastomas (WHO grade IV) and pineocytomas (WHO grade II) are encountered less frequently than germinomas or teratomas. These lesions show no gender predilection. The tumours originate from neuro-epithelial cells of the pineal gland. Here, various graduations are encountered within a pineal cell tumour (WHO grades II and III). The pineoblastomas and pineocytomas may contain melanin.

**Pineoblastomas** usually occur in childhood, are rich in cells, and infiltrate the surrounding cerebral parenchyma (■ Fig. 9.109). They often exhibit focal haemorrhaging and regressive changes. Histologically, the tumours resemble medul-

loblastomas and other primitive, undifferentiated neoplasms. Pineoblastomas spread early in the sub-arachnoid cavity. In children with pineoblastomas, the prognosis is worse than in children with medulloblastomas. A rare variant of pineoblastoma is “bilateral retinoblastoma”. This term is used in patients with bilateral retinoblastomas and pineoblastoma. It involves an inheritable syndrome. In patients with bilateral retinoblastomas, it is imperative to examine the pineal body.

**Pineocytomas** are commonly found in middle-aged and older adults. These tumours are well-circumscribed lesions that usually do not infiltrate the surrounding cerebral parenchyma. Pineocytomas are less rich in cells than pineoblastomas. These tumours tend to include solid mass-occupying lesions. Cystic lesions are less frequent. Therefore, the detection of a cystic pineal gland space-occupying lesion should be more indicative of a simple pineal cyst than this form of tumour. Pineocytomas display a more benign course. However, more aggressive variants with shorter survival rates occur in the case of less differentiated forms of tumour.

**Differential Diagnosis.** The specific diagnosis and histopathological typing of pineal cell tumours is often not possible using imaging alone. Above all, it is important to distinguish a pineal gland neoplasm from a pineal gland cyst (see below). On MRI, pineal gland neoplasms appear as lobulated solid tumours that exhibit a strong uptake of contrast agent. In most cases, cystic lesions should be described as pineal gland cysts. The signal intensity can vary. On T2-weighted spin-echo sequences, pineoblastomas usually display iso-intense behaviour compared with grey matter.

More primitive tumours display atypical signal behaviour. On MRI, it is often difficult to differentiate between germinomas of the pineal region and pineoblastomas. Pineocytomas have a higher signal on T2-weighted sequences. Both pineoblastomas and pineocytomas can calcify; intra-tumoural calcifications occur more frequently in pineocytomas.

#### ■ ■ Pineal Gland Cysts

**Definition, Epidemiology, Symptoms** Pineal gland cysts are common findings and are detected in up to 40% of routine autopsies. Since the introduction of MRI, these incidental, non-neoplastic glial lesions have been more frequently diagnosed. Even large pineal gland cysts with compression of the dorsal mid-brain remain generally asymptomatic. Haemorrhaging into the cyst may also occur. In rare cases, the space-occupying lesion of the pineal cyst can lead to aqueduct stenosis with secondary hydrocephalus.

**Medical Imaging** On MRI, the diagnosis of a pineal gland cyst is based more on the morphology and less on the signal intensity. Pineal gland cysts are round and well demarcated. They can be relatively small and situated within the parenchyma of the pineal gland, but may also fill the entire pineal body. On the T1- and T2-weighted sequences, most pineal gland cysts display iso-intense signal behaviour to CSF (■ Fig. 9.110), but they may also exhibit hypo-intensity. This relative hypo-intensity of the cyst fluid can have different causes including a higher protein content or older haemorrhaging. Pineal gland cysts usually do

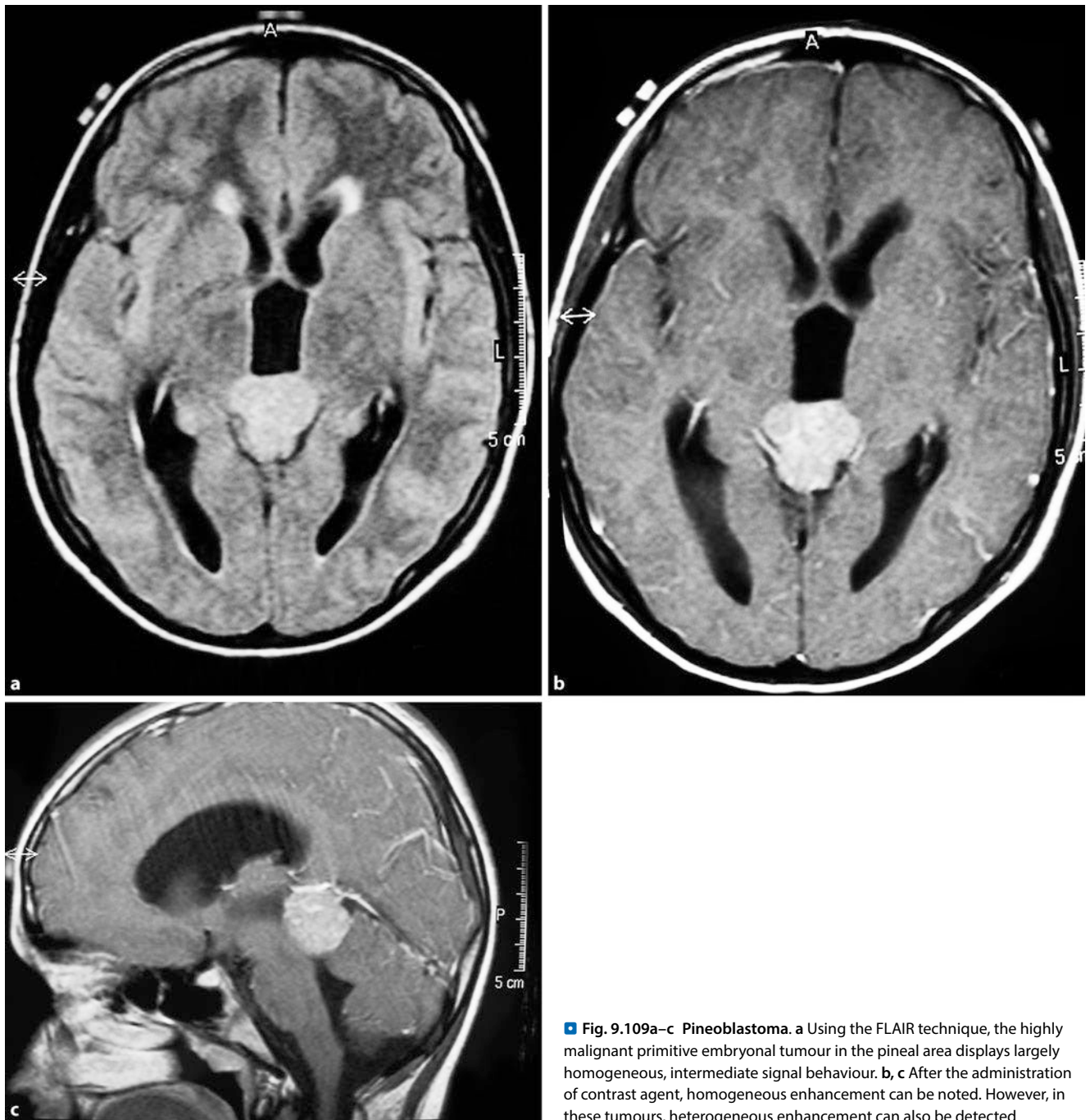


**Fig. 9.109a–c Pineoblastoma.** **a** Using the FLAIR technique, the highly malignant primitive embryonal tumour in the pineal area displays largely homogeneous, intermediate signal behaviour. **b, c** After the administration of contrast agent, homogeneous enhancement can be noted. However, in these tumours, heterogeneous enhancement can also be detected

not exhibit enhancement after the administration of contrast agent. There can still be marked enhancement in the surrounding tissue of the pineal gland because there is no blood–brain barrier in the pineal capillaries.

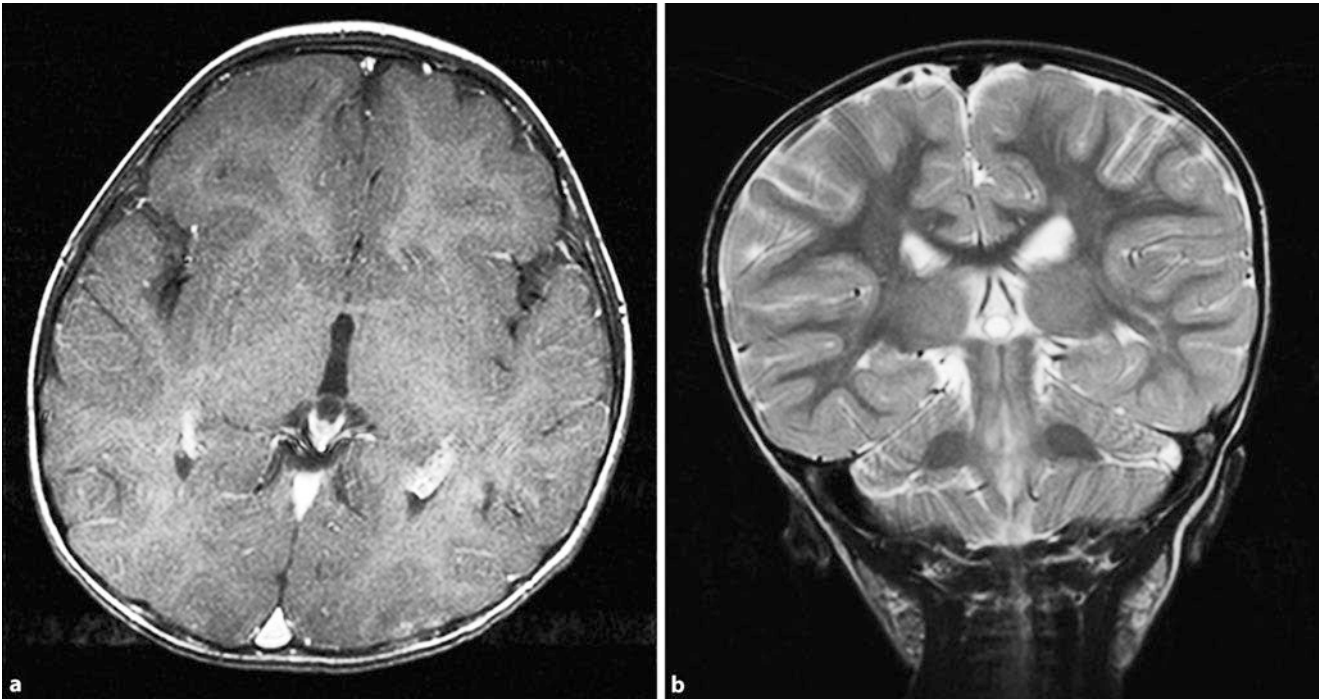
- **Colloid Cysts**
- **Definition, Epidemiology, Pathology**

Colloid cysts are rare, benign, epithelium-lined cysts in the anterior portion of the third ventricle. It was assumed that these lesions originated from the primitive neuro-epithelium. However, recent studies reveal that they originate from the endoderm.

Colloid cysts are the most common neuro-epithelial cysts. They can occur in the area of the choroid plexus, the lateral ven-

tricles, or in the sub-arachnoid cavity. In rare cases, they can even be found in the cerebral parenchyma.

It is estimated that colloid cysts account for approximately 2% of all glial neoplasms. Colloid cysts can be differentiated from other neuro-epithelial cysts based on their location and composition. Colloid cysts contain dense mucoid material in addition to older blood components such as haemosiderin, macrophages, and cholesterol crystals. They can also contain various ions, e.g. sodium, magnesium, calcium, copper, aluminium, iron and phosphate. Some of these ions display paramagnetic behaviour on MRI. Other cysts contain clear serous fluid, similar to CSF, and accordingly only exhibit a slight deviation to CSF on the different MR sequences.



■ **Fig. 9.110a,b Pineal gland cyst.** **a** On the axial T1-weighted sequences, after administration of contrast agent, a small CSF-iso-intense cystic structure in the pineal body appears that leads veins filled with contrast agent around

this lesion. **b** On the coronal T2-weighted sequences, the cystic formation appears in the pineal body

#### ■ ■ Symptoms

Colloid cysts become symptomatic if they occlude the foramina of Monro and lead to hydrocephalus. This can be intermittent, but also permanent. The clinical symptoms of the mostly young and middle-aged patients are headaches, sudden paralysis of the lower limbs, incontinence and personality disorders or dementia. The clinical symptoms can be traced to the localisation of the colloidal cysts or the position in the front upper portion of the third ventricle between the fornices.

#### ■ ■ Medical Imaging

The diagnosis of a colloid cyst is essentially based on localisation and morphology (■ Fig. 9.111). Several other pathological processes can occur in the same region, including neoplasms of the choroid plexus, meningiomas, gliomas and granulomas. Colloid cysts usually exhibit highly variable signal intensity on MRI. On the T2-weighted sequences, they usually exhibit a marked hyper-intensity, although colloid cysts that are hypo-intense and iso-intense to the CSF have been described. On T1-weighted sequences, they also usually exhibit a hyper-intensity. However, hypo-intense colloid cysts have also been described. This signalling spectrum is mainly based on the concentration of paramagnetic substances, free water and mucoid material in the cysts. A thin wall can almost always be distinguished. After the intra-venous administration of contrast agent, the wall of the colloid system can reveal enrichment, although solid enhancement indicates a different diagnosis.

#### ■ Primary Lymphomas

##### ■ ■ Definition, Epidemiology, Localisation

The term malignant lymphoma includes tumours of the lymphoreticular system and includes the following entities:

- Reticulum cell sarcoma
- Adventitial sarcoma
- Plasmacytoma
- Hypothalamic granuloma (histiocytosis)
- Hodgkin's lymphoma

Secondary tumours should be distinguished from the primary malignant lymphomas, whereby leukaemic infiltrates of the brain can also occur. Tumours of grade III or IV are found.

**Primary lymphomas of the CNS** are rare and account for only 1% of all primary brain tumours, although there has been a 10-fold increase in their occurrence in the last two decades. This increase is not only caused by patients with HIV infection, but also by the increasing number of immunosuppressed patients. The cause of primary CNS lymphoma remains unclear because the CNS does not have endocrine lymphatic tissue or lymphatic drainage. There are essentially groups of patients with an increased risk of developing a primary CNS lymphoma:

- Organ transplant patients
- Patients with congenital immunodeficiency
- Patients with HIV infection and other systemic illnesses that are associated with an immune deficiency

The peak incidence in patients without HIV infection is the sixth decade of life. Approximately 90% of primary CNS lymphomas are of the non-Hodgkin's type. If a non-Hodgkin's lymphoma has infiltrated the brain parenchyma, this is usually the result of

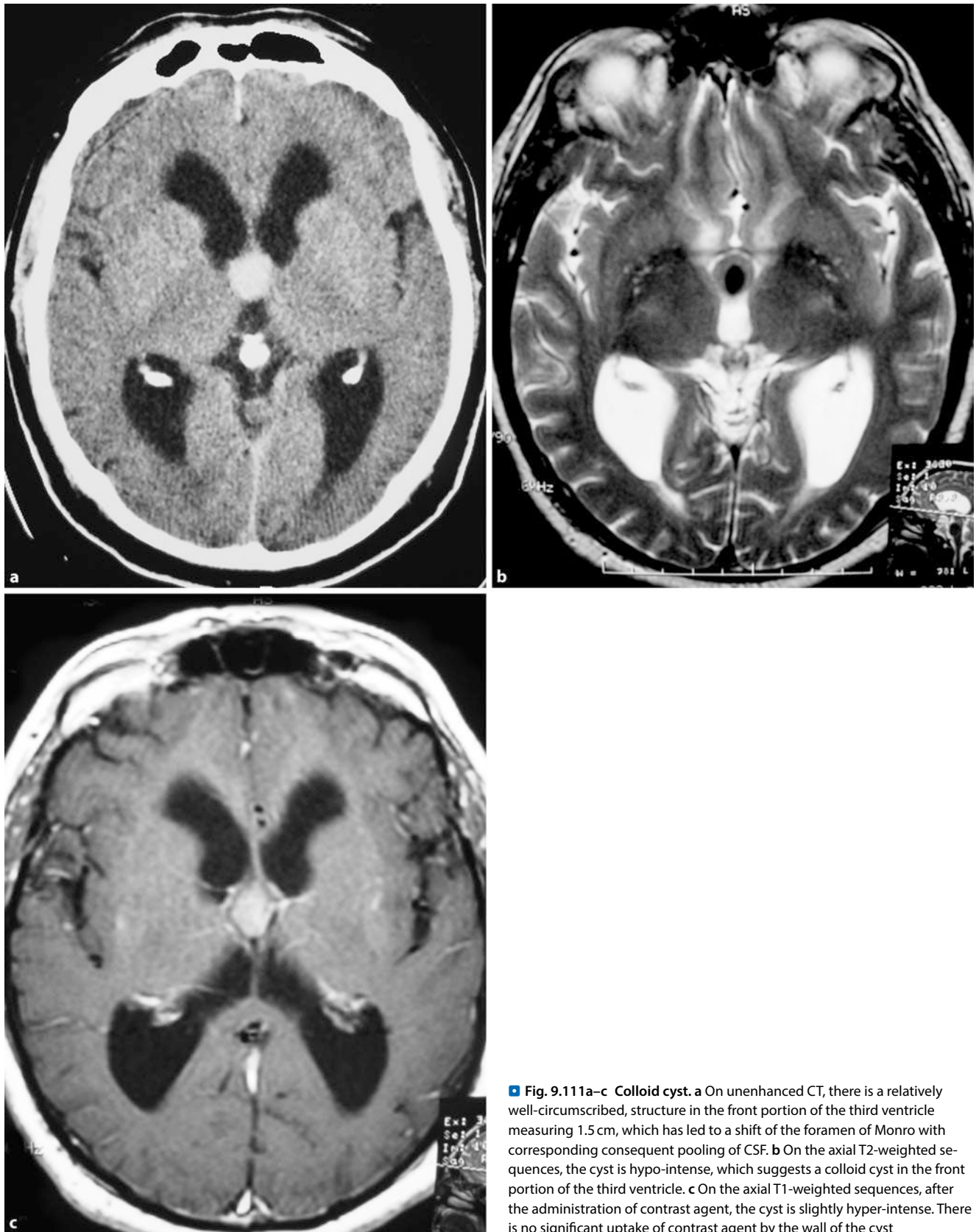


**Fig. 9.111a-c Colloid cyst.** **a** On unenhanced CT, there is a relatively well-circumscribed, structure in the front portion of the third ventricle measuring 1.5 cm, which has led to a shift of the foramen of Monro with corresponding consequent pooling of CSF. **b** On the axial T2-weighted sequences, the cyst is hypo-intense, which suggests a colloid cyst in the front portion of the third ventricle. **c** On the axial T1-weighted sequences, after the administration of contrast agent, the cyst is slightly hyper-intense. There is no significant uptake of contrast agent by the wall of the cyst

a systemic disease or a dural proliferation. Focal intra-cerebral lesions are usually the first signs of a primary CNS lymphoma.

Spread into the sub-arachnoid space is extremely rare. In 75–85% of cases, the tumour is found supratentorially. A multifocality is frequent and is detected in almost half of all cases. Intra-cranial metastases from systemic lymphomas are either lepto-meningeal in origin or located within the dura.

#### ■ ■ Prognosis

After radiotherapy, 60% of patients with primary CNS lymphoma achieved complete remission with a mean survival time of more than 12 months. Patients with a solitary lesion have longer survival rates than patients with multiple lesions.

#### ■ ■ Medical Imaging

On **CT**, unenhanced lymphomas mainly appear as homogeneously iso-dense to slightly hypo-dense space-occupying lesions with peri-focal oedema. After the administration of contrast agent, there is significant enhancement, which results in good delineation of the tumour. The clinical and CT results resemble those of rapidly growing gliomas, metastases and occasionally meningiomas (if the tumours are close to the cortex).

On **MRI**, the tumours mostly appear as an intense signal on T2-weighted sequences. In some cases, however, there can also be signal attenuation, which reflects the paramagnetic effect of the tumour cells. On the scans, the tumours are relatively sharply demarcated. The administration of contrast agent results in typical homogeneous enhancement (■ Fig. 9.112). The focal tumours are often surrounded by extended peri-focal oedema, which is better delineated through the administration of contrast agent. It is often the case that diffusely growing lymphomas exhibit neither peri-focal oedema nor enrichment of contrast agent. On T2-weighted sequences, an iso-intensity to hypo-intensity compared with the grey matter is mainly due to the high cell density in the tumour.

➤ **It is characterised by high sensitivity to radiation and the effect of cortisone administration, which had also been used for differential diagnosis. A steroid may show a dramatic effect; cortisone should therefore be administered before biopsy.**

In HIV-infected patients, administration of contrast agent often results in annular enhancement. As a rule, these patients also have extended peri-focal oedema. Lepto-meningeal delocalisation can go undiagnosed on CT. However, this can be detected on MRI following the intra-venous administration of contrast agent.

#### ■ Arachnoid Cysts

##### ■ ■ Definition, Epidemiology, Localisation

Arachnoid cysts are often first diagnosed in adulthood. These closed cavities between the arachnoid and pia mater appear as a congenital malformation. They are predominantly situated in the basal and inter-hemispheric cisterns. They are frequently also found in the Sylvian fissure and the temporal fossa (■ Fig. 9.38). Combinations with temporal lobe polygenesis are possible. The

cysts are filled with fluid and grow slowly. Arachnoid cysts account for approximately 1% of all non-traumatic, intra-cranial space-occupying lesions. They occur in all age groups. However, 75% of cases are in children. They are more frequently detected in men than in women (3:1).

#### ■ ■ Medical Imaging

▶ Sect. 9.2.9.

#### ■ Hamartomas

##### ■ ■ Definition, Localisation

Histologically, these malformation tumours are composed of gliosis-like tissue. They are typically localised in the temporal lobes. Psycho-motor seizures can occur as early as childhood. They mostly do not show signs of space-occupying lesions. Another typical localisation is in front of the pituitary stalk and behind the mammillary bodies. Hamartomas in this region are congenital, non-neoplastic heterotopias; they are composed of neural tissue. These rare lesions are primarily found in men.

##### ■ ■ Symptoms

The hamartoma is typically pedunculated and attached in the area of the cavity between the pituitary stalk and mammillary bodies (tuber cinereum). Larger lesions may be associated with Pallister–Hall syndrome. Here, weight anomalies, polydactyly, imperforate anus and hypothalamic hamartomas can occur. For the two main clinical symptoms, precocious puberty and seizures, in addition to the characteristic gelastic seizure (laughing fit), a hamartoma should be considered. Delayed neural development and hyperactivity are associated with lesions greater than 1 cm in size.

#### ■ ■ Medical Imaging

The lesions range from a few millimetres in size to 4 cm and exhibit enhancement neither on CT nor on MRI (■ Fig. 9.88). On **CT**, they appear as rounded, iso-dense space-occupying lesions to the remaining cerebral tissue. These rarely appear in the supra-sellar/inter-peduncular cisterns with cystic components in the axial layers. There is no haemorrhaging, and calcification rarely appears.

On **MRI**, hamartomas appear iso-intense to the grey matter on T1-weighted sequences. On T2-weighted sequences, they are iso-intense or hyper-intense. For the purposes of diagnosis, MRI is significantly more sensitive and specific than CT. Sagittal sequences should be acquired on both T1- and T2-weighted images. The base of the third ventricle should be smoothly delimited from the infundibulum up to the mammillary bodies. For each nodular irregularity, a hamartoma should be suspected.

Small lesions are easily overlooked. Thin-slice sequencing is therefore decisive (T1- and T2-weighted volumetric sequences, e.g. magnetisation-prepared rapid gradient-echo, MP-RAGE, true fast imaging with steady state precession, True-FISP, and a coronary, high-resolution, SE phase, T2-weighted sequence with a thickness of 2–3 mm). This should be performed in every child with precocious puberty or gelastic seizures because these lesions can otherwise hardly be detected on the imaging.

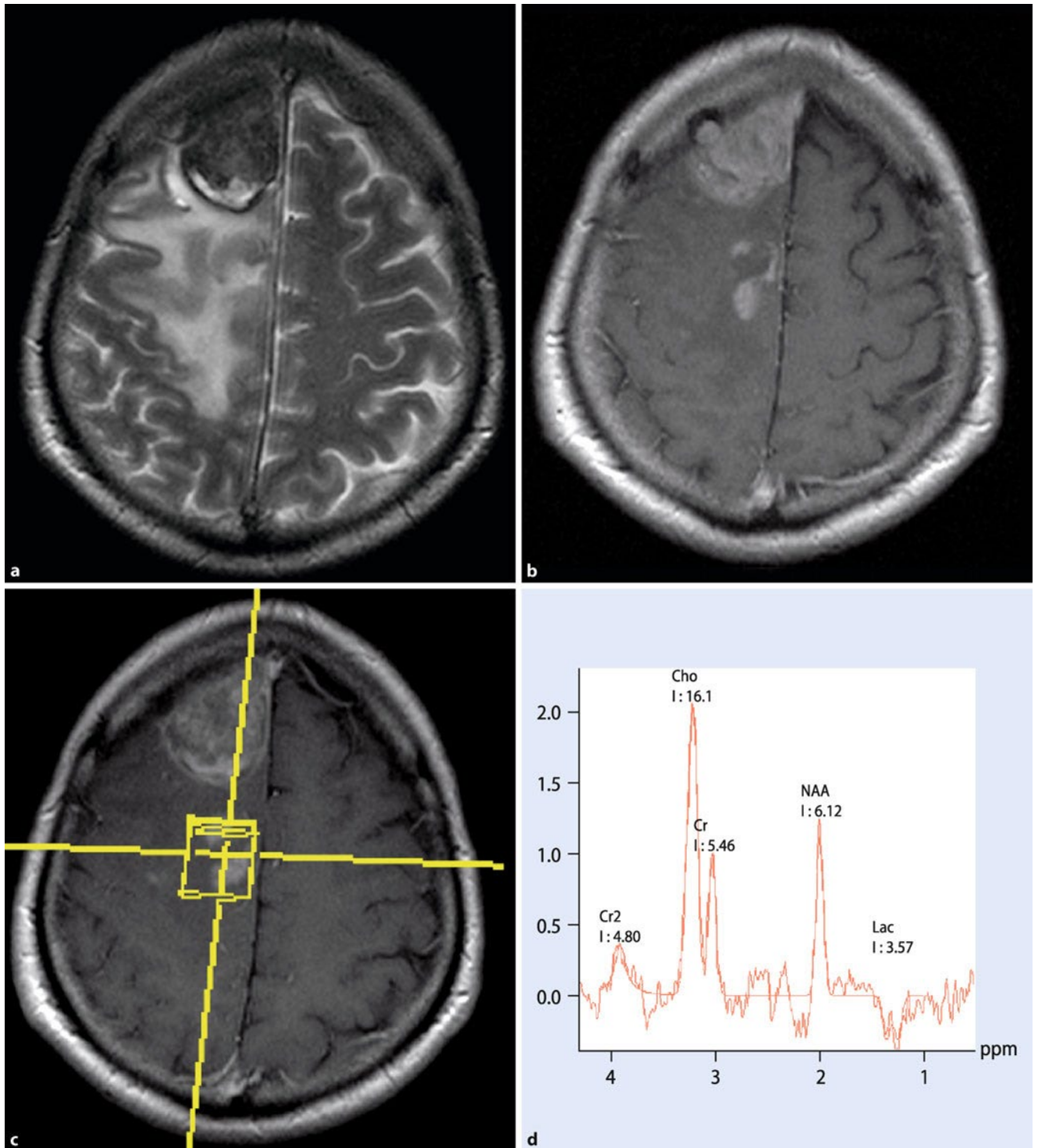


**Fig. 9.112 Lymphoma.** A 50-year-old patient with cerebral lymphoma. **a** T2 sequence, right frontal lesion with large peri-focal oedema; the haemorrhaging portion of the tumour is hypo-intense. **b** T1 sequence after the administration of contrast agent, para-sagittal focus with uptake of contrast agent. **c** Localisation of the spectroscopic measurement in the parasagittal

focus to avoid artefacts caused by blood on the large frontal lesion. **d** Despite the small lesion and involvement of normal cerebral tissue in the measurement, there is a significant increase in Cho and degradation of NAA in the tumour spectrum (TE = 135 ms), lactate peak detectable. (From: *Radiology* 2007;47:525, Fig. 7a–d)

### ■ Lipoma

#### ■ ■ Aetiology

Lipomas of the CNS are malformations and not neoplasms. Sub-arachnoid lipomas are caused by congenital malformations of the lepto-meninges. In the case of incomplete absorption of the meninx primitiva in the embryonic stage, these cells can differentiate into adipose tissue.

#### ■ ■ Medical Imaging

On **CT**, the lipomas can be recognised as sharply contoured, homogeneous, hypo-dense foci (less than  $-100$  HU). They occasionally have a calcified, hyper-dense rim.

On **MRI** there is typical signal behaviour with clear signal intensity on T1-weighted sequences and lower signal intensity on T2-weighted sequences. Aside from the areas of calcification, the signal behaviour resembles that of sub-cutaneous fat. The decisive factor is a loss of signal on fat-suppressed images (■ Fig. 9.113). Neurovascular structures, which extend over the space-occupying mass, are frequently seen. The diagnosis can be confirmed via fat saturation or by chemical shift artefacts, which are best confirmed on proton density-weighted sequences.

Fat within the cavity of the petrous bone can be mistaken for a lipoma of the internal auditory canal.

If a T1-weighted sequence is run only after the administration of contrast agent, a lipoma can be confused with an enhanced lesion such as an acoustic neuroma (■ Fig. 9.85). If the bandwidth is increased, the chemical shift is less pronounced.

Nerves such as the eighth cranial nerve and blood vessels extend over and through the lesion and can be injured in the attempted resection.

### ■ Plexus Tumours

#### ■ ■ Epidemiology, Classification

Plexus tumours are rare and account for only about 0.5% of all brain tumours. In children and adolescents, they mainly occur in the lateral ventricles. In adults, they mainly occur in the third and fourth ventricles. Plexus tumours originate from the choroid plexus. **Plexus papillomas** (■ Fig. 9.114), benign WHO grade I tumours (which mainly occur in children), can be differentiated from **plexus carcinomas** (grades III and IV). Anaplastic plexus carcinoma can often not be differentiated from the benign variant, plexus papilloma.

#### ■ ■ Medical Imaging

On **CT**, the tumours are usually iso- to slightly hypo-dense with strong contrast enhancement. On **MRI**, on T1-weighted sequences, they are often iso-intense to the grey matter. On T2-weighted sequences, they are hyper-intense. The tumour is usually relatively well defined and has a moderate oedema and strong enhancement of contrast agent. Clinically, there are often signs of increased intra-cranial pressure, which is usually caused by blockage of the CSF circulation and rarely by hyper-secretion caused by the tumour.

## 9.4.7 Tumours of the Sellar Region

### ■ Pituitary Gland

#### ■ ■ Anatomy

The pituitary gland, which is approximately the size of a cherry stone, is embedded in a small group of bones of the cranial base, the sella turcica, under the mid-brain. It secretes various hormones into the blood. The hypothalamus, part of the mid-brain, affects the action of the pituitary gland by distributing transmitter hormones, and is connected via the pituitary stalk. Thus, this system plays a central role in linking the nervous system with hormonal balance.

The pituitary gland is composed of two parts:

#### ■ **Anterior lobe of the pituitary gland** (adenohypophysis) produces the following hormones:

- Growth hormone (somatotropin – GH), prolactin
- Sex hormones (gonadotropins – luteinising hormone/ follicle-stimulating hormone, LH/FSH)
- Adrenocorticotrophic hormone (ACTH)
- Thyroid-stimulating hormone (TSH)

#### ■ **Posterior lobe of the pituitary gland** (neurohypophysis) distributes the following hormones:

- Anti-diuretic hormone (ADH, arginine vasopressin, AVH)
- Oxytocin

The endocrine gland is connected to the hypothalamus via the pituitary stalk (infundibulum).

**Anatomy of the Sellar Region.** Anatomically speaking, the pituitary gland is situated in a bony depression of the sphenoid bone, the so-called Turkish saddle (sella turcica). The sella is adjacent to the sphenoid sinus. On both sides, the structure is adjacent to the cavernous sinus, in which the internal carotid artery is located, and extends through some cranial nerves, namely the oculo-motor, trochlear and abducens nerves. Portions of the trigeminal nerve (first and second branches) are also located in the cavernous sinus. To the rear, the pituitary gland borders the pre-pontine cistern. Above the pituitary gland is the supra-sellar cistern in which the pituitary stalk and the chiasm are located. Further rostral to this is the hypothalamus as a part of the mid-brain. The pituitary gland itself is divided into an anterior and posterior lobe (see above).

#### ■ ■ Epidemiology

Approximately 10–15% of verified intra-cranial tumours are pituitary tumours. The tumours of the pituitary region are mostly benign. Most arise from cells of the anterior lobe of the pituitary gland and are referred to as pituitary adenomas.

#### ■ ■ Classification, Symptoms

It is possible to distinguish between endocrine and non-endocrine tumours. Micro-adenomas with a diameter up to 10 mm are distinguished from those with a diameter greater than 10 mm (■ Figs. 9.115, 9.116). A rarer group of tumours of the pituitary are the craniopharyngiomas, which arise from cell nests of the so-called Rathke's pouch. They produce no hormones themselves

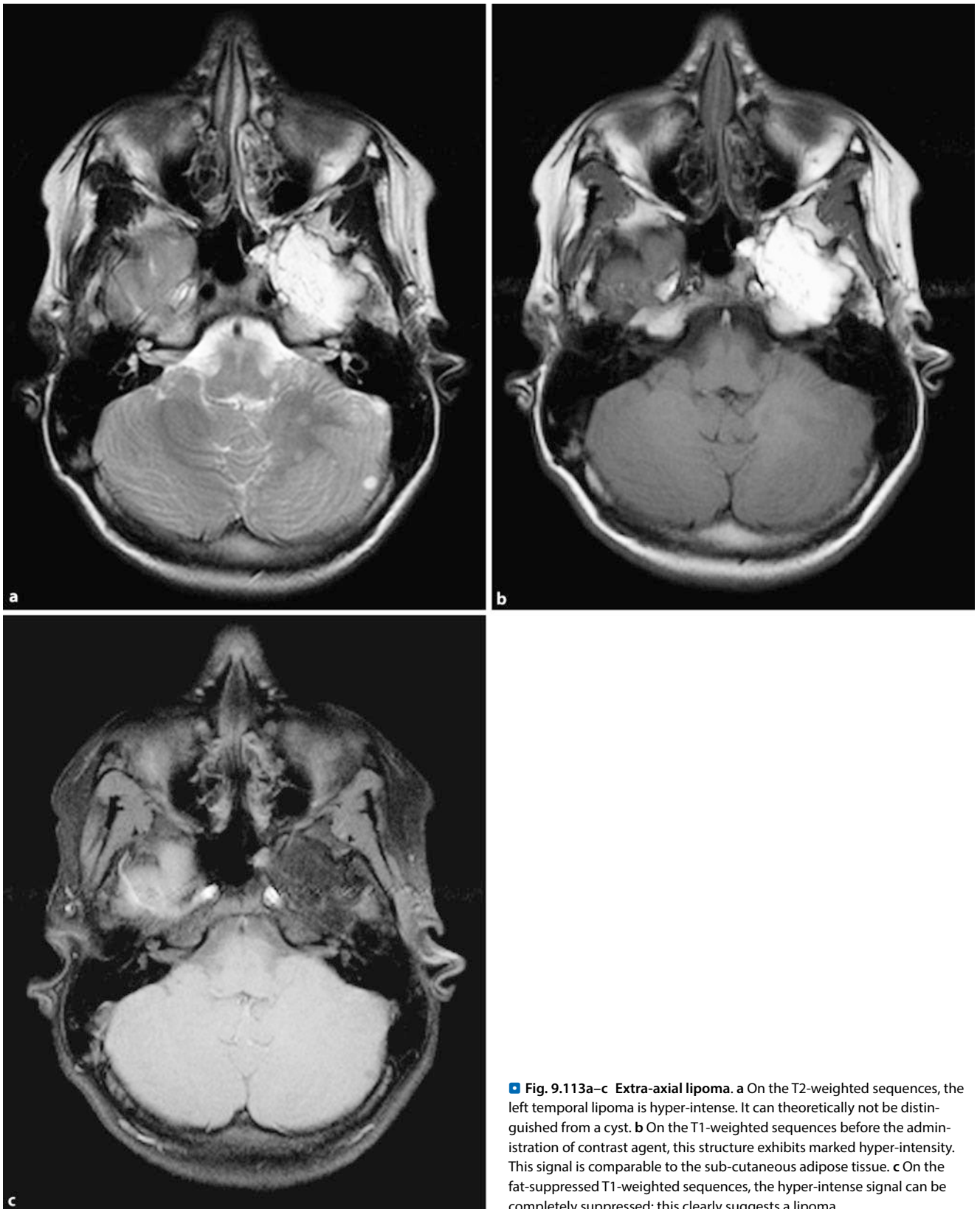


**Fig. 9.113a–c Extra-axial lipoma.** **a** On the T2-weighted sequences, the left temporal lipoma is hyper-intense. It can theoretically not be distinguished from a cyst. **b** On the T1-weighted sequences before the administration of contrast agent, this structure exhibits marked hyper-intensity. This signal is comparable to the sub-cutaneous adipose tissue. **c** On the fat-suppressed T1-weighted sequences, the hyper-intense signal can be completely suppressed; this clearly suggests a lipoma



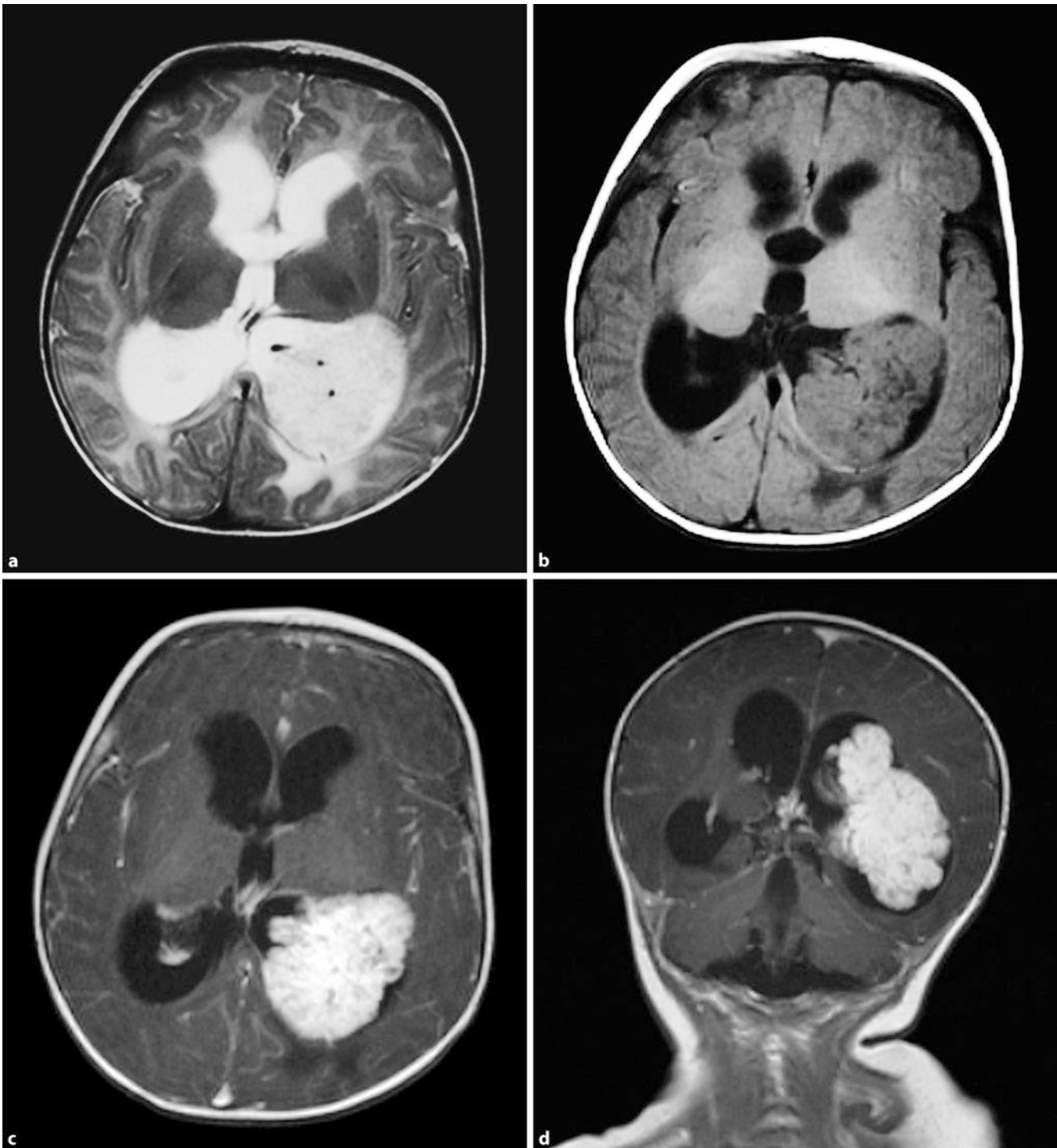


**Fig. 9.114a–d Choroid+ plexus papilloma.** **a** In this 7-year-old boy, widening and a signal increase in the left posterior horn can be seen on the T2-weighted sequences. **b** T1-weighted sequence before the administration of contrast agent. **c, d** After the administration of contrast agent, there is

strong homogeneous axial and coronal enhancement at the medial edge of the dorsal horn, which clearly appears to be expanded, and the clear and homogeneous uptake of contrast agent by the plexus papilloma

and stand out because of blurred vision and reduced function of the pituitary gland.

Other tumours of the pituitary region can lead to reduced pituitary (hypopituitarism) in addition to hyper-secretion syndrome (acromegaly, Cushing's syndrome) because of a prolactinoma or TSH-secreting adenoma. Immediately above the pituitary is the optic chiasm, which can lead to impairment of vision

in the case of tumours of the pituitary region. Most involve a deterioration of the lateral visual field of both eyes (bi-temporal hemi-anopia).

#### ■ ■ Diagnosis

Endocrine disorders are usually diagnosed via endocrinological investigations in the blood. The method of choice is MRI of the

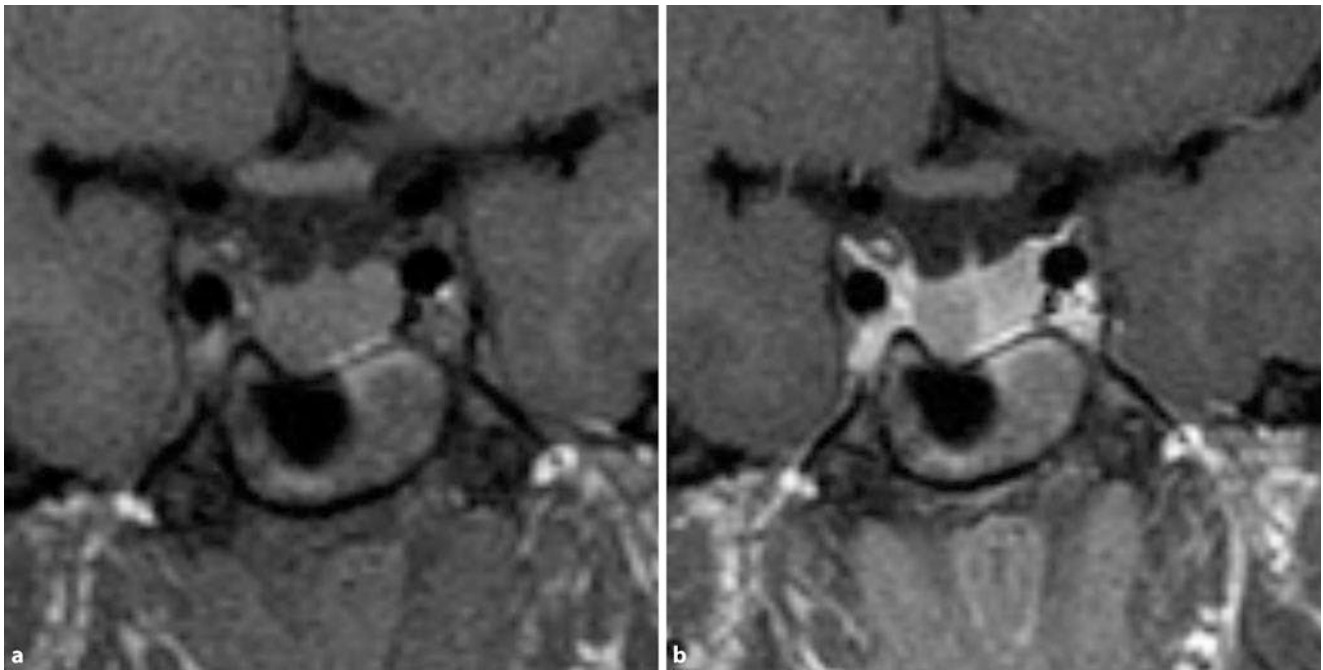


**Fig. 9.115a,b Micro-adenoma.** **a** On the coronal T1-weighted sequences, before the administration of contrast agent, depiction of the pituitary gland and the pituitary stalk, which is shifted slightly to the left. The pituitary gland appears with a nearly cerebral iso-intense signal. **b** After the administration

of contrast agent, there is normal enhancement of the left pituitary tissue. Hypointensity in the right half of the pituitary gland is detectable, which corresponds to a micro-adenoma (From: *Radiologe* 2009, Tumoren der Sellaregion)

pituitary region in thin-slice coronal and sagittal orientation using the T1-weighted technique before and after the administration of contrast agent.

#### Space-occupying Processes in the Area of the Pituitary Gland and Hypothalamus

- Pituitary adenoma
- Craniopharyngioma
- Meningioma
- Germinoma
- Glioma
- Metastases, especially in breast, lung, renal cell and prostate cancer
- Lymphomas
- Granulomatous diseases (sarcoidosis, tuberculosis (▶ Sect. 9.6), histiocytosis)
- Chordoma
- Rathke's pouch cyst
- Epidermoid cysts
- Aneurysms

#### ■ Pituitary Adenomas

##### ■ Definition, Epidemiology, Classification

Pituitary adenomas are rare benign tumours that arise from cells of the anterior lobe of the pituitary gland. The annual incidence of clinical, self-manifesting adenoma is approximately 30–40 in 1,000,000.

Non-endocrine adenomas (approximately 40% of all pituitary adenomas) are distinguished from hormone-secreting adenomas,

which include prolactinoma (about 30%), GH-secreting adenoma (about 20%), and ACTH-producing adenoma (approximately 5%).

Rarely, TSH or LH/FSH is secreted. Pituitary carcinomas are rare. They can also produce hormones (prolactin, GH, ACTH).

**Other disorders such as** a disturbance in pituitary function, the so-called empty sella syndrome, the condition after cranial irradiation, traumatic hypopituitarism, various forms of hypophysitis, Sheehan's disease, and congenital hypothalamic or pituitary disorders in hormone formation should be differentiated from pituitary adenomas.

➤ **Because of the low incidence and prevalence of pituitary diseases, they are often only first diagnosed years after the onset of clinical symptoms.**

##### ■ Disease Progression

Untreated or inadequately treated pituitary adenomas lead to increased morbidity and mortality. In the case of acromegaly, there is an increased risk of cardio-vascular problems and malignoma among others. Inadequate treatment can promote prolactinoma, infertility, and osteoporosis. Long-term hypopituitarism is likewise associated with increased morbidity and mortality in addition to a restriction of performance, well-being and quality of life.

##### ■ Symptoms

The main symptoms of patients with pituitary adenomas are as follows:

- Overproduction of hormones in secreting adenomas
- Loss of pituitary functions
- Space-occupying lesion of the adenoma

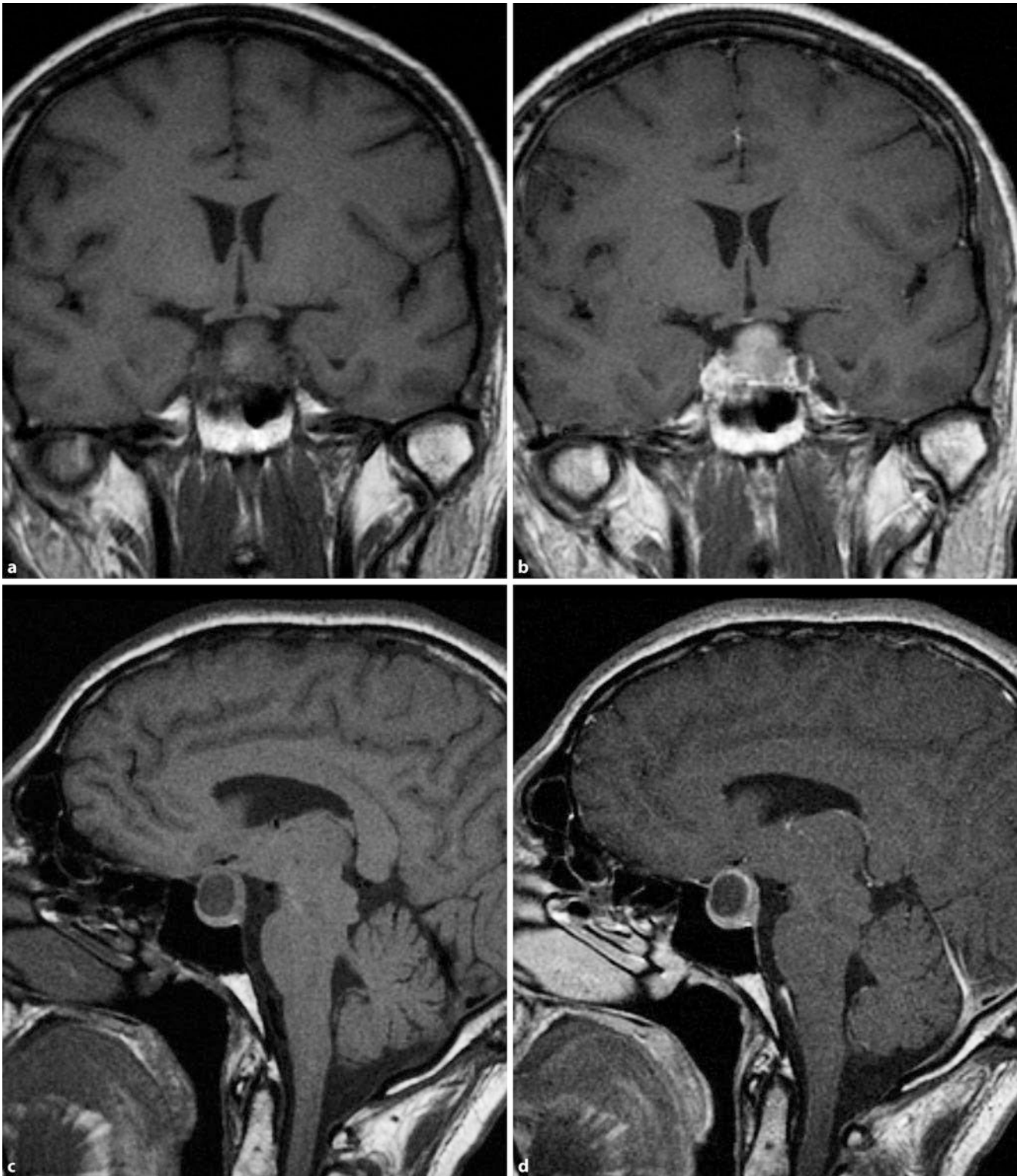


**Fig. 9.116a–d Macro-adenoma.** **a** On the coronal T1-weighted images, macro-adenoma with extension to the optic chiasm can be seen. **b** After the administration of contrast agent, homogeneous enhancement can be seen. The macro-adenoma extends to the left cavernous sinus. **c, d** On the sagittal

T1-weighted sequences before (**c**) and after (**d**) the administration of contrast agent, a cyst in the macro-adenoma is revealed as an expression of regressive changes (From: *Radiologe* 2009, Tumoren der Sellaregion)

Patients with pituitary adenomas often display non-specific symptoms. In the case of acromegaly, symptoms in the region of the mandible, carpal tunnel syndrome, or sleep apnoea syndrome can be the ground-breaking symptoms. In patients with a pro-

lactinoma or with hypopituitarism, symptoms include menstrual disorders, amenorrhoea, libido and potency disorders, or infertility. Patients with Cushing's disease display psychiatric symptoms such as depression, anxiety, or even euphoria.

In large adenomas with chiasmal syndrome, limitations of the visual field and visual impairment predominate. In women with a macro-adenoma, the guiding symptom is amenorrhoea.

## ■ ■ Diagnosis

**Basic Endocrine Diagnostics.** In the case of suspected pituitary disease with over- or under-production of hormones, the basic laboratory programme includes the differential determination of cortisol, TSH, FT4, GH, EGF-1, LH, FSH, testosterone/oestradiol and prolactin. The assessment of the hormone values and the test results is carried out by an experienced endocrinologist.

- **Prolactinoma:** if there is clinical suspicion of a prolactinoma, the level of prolactin must be determined. The reference values are less than 25 ng/ml for women and less than 15 ng/ml for men. A concentration greater than 200 ng/ml is almost conclusive of a prolactinoma. In these cases, MRI must always be included in the diagnosis.
- **Acromegaly:** if there is clinical suspicion of acromegaly, an oral glucose tolerance test (oGTT/GH suppression test) should be performed in fasting patients with a commercially available oral solution containing 75 g of glucose.
- **Cushing's disease:** if there is clinical suspicion of Cushing's syndrome, an ACTH test should be performed. A value of less than 200 ng/ml of cortisol in serum essentially rules out Cushing's syndrome. In the case of small ACTH-producing pituitary adenomas, a suppression of less than 80 ng/ml may rarely occur. In cases of doubt, the free cortisol and hourly urine output can be determined.

**Insufficiency of the Anterior Lobe of the Pituitary Gland.** If clinical symptoms indicate the failure of one or more pituitary functions, endocrinological function tests should be conducted. In each individual case, the decision to pursue extensive diagnostic tests for hypopituitarism should be made by a specialist. In addition, an MRI of the pituitary region should be performed.

**Incidentally Discovered Pituitary Adenoma (Incidentaloma).** In autopsy studies, micro-adenomas were found in up to 27% of the pituitary glands examined. These did not clinically manifest during life. On the MRI of the skull with non-endocrinological indications, pituitary adenomas are also detected in about 10–20% of cases. In macro-adenomas, hormone activity should be clarified and pituitary function should be monitored via the appropriate endocrine stimulation tests. Because the issue of surgical indication often arises, these patients should always be presented to a specialist early on. In the case of micro-adenomas, exclusion of hormone activity is a focus. If there are clinical indications, further diagnostic measures are not required. As a rule, hypopituitarism does not occur in the case of micro-adenomas. To exclude an increase in size, regular MRI check-ups should be performed.

**Medical Imaging.** Magnetic resonance imaging is the most important method for the investigation of the pituitary region. The indication, implementation, evaluation, and assessment should be carried out according to the current quality assurance guidelines of the Federal Medical Association. Accordingly, MRI of

the sellar region should provide a complete, symmetrical, and artefact-free depiction of the sella and supra-sellar cistern with coronary, sagittal, and – if necessary – also axial slices.

The investigation should enable differentiation of adenohypophysis and neurohypophysis. The pituitary stalk, the infundibulum, the chiasma, and the cavernous sinus (including internal structures) must be clearly demarcated from one other. CT is only useful if bone erosions or calcifications should be detected, or MRI cannot be performed.

### ➤ Imaging should only be performed if:

- Endocrinological diagnostics have demonstrated a dysfunction of the pituitary gland and/or
- There are symptoms that indicate a space-occupying lesion in the sellar region

Because pituitary adenomas can lead to typical visual field defects due to compression of the optic chiasm or the optic tract, an ophthalmological examination should always be performed.

## ■ ■ Treatment

The therapeutic approach should be decided upon after consulting endocrinologists and neurosurgeons. If symptoms of a space-occupying effect of the adenoma (e.g. visual field defects and headaches) predominate, the patient should be immediately referred to a specialist.

! In the case of severe acute-onset headaches, the possibility of a tumour apoplexy should be considered. In this case, immediate admission is required because of the risk of blindness.

In the case of pituitary disease, early-stage collaboration with endocrinologists, neurosurgeons and radiotherapists is always recommended to ensure adequate treatment.

## ■ Craniopharyngioma

### ■ ■ Definition, Epidemiology

Craniopharyngiomas are benign, slow-growing tumours that arise in the region of the sella turcica if cellular debris of the adjoining cranio-pharyngeal canal suddenly multiply during embryonal development. Craniopharyngiomas occur in both children and adults and account for 3–5% of intra-cranial tumours in adults and 5–10% in children. In children craniopharyngiomas account for approximately 50% of all tumours of the pituitary region. Women and men are equally affected. The age distribution is 5–10 and 40–60 years.

In children and adolescents, an adamantine histological type with cysts usually forms. In adulthood, the tumour is usually diagnosed with a peak incidence at 50–75 years and is usually of the papillary type histologically.

### ■ ■ Symptoms

The clinical picture at diagnosis often involves non-specific symptoms of increased intra-cranial pressure, such as headaches and morning fasting and vomiting. Additional clinical symptoms include visual disturbances and endocrine deficits. Endocrine

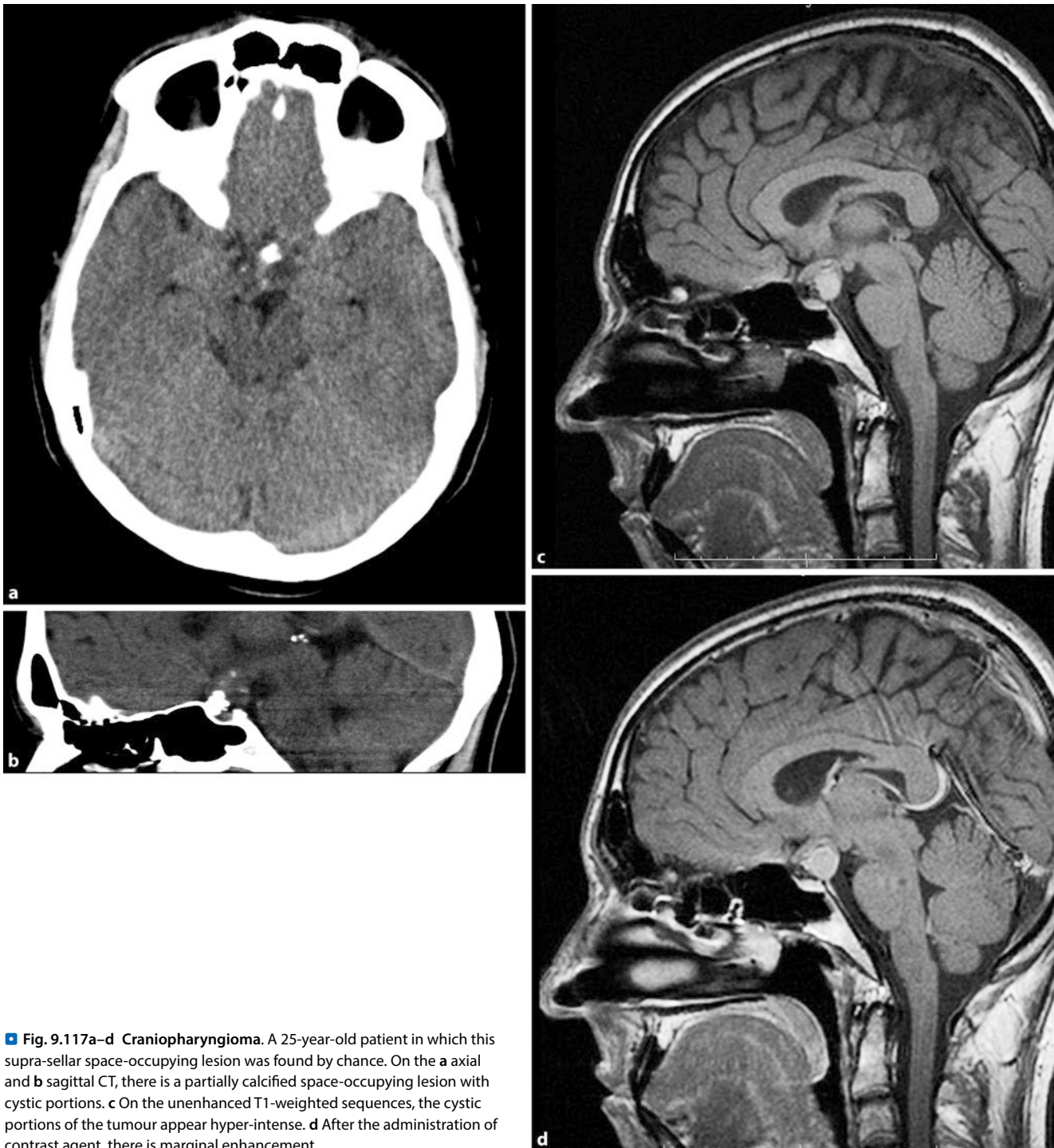


**Fig. 9.117a–d Craniopharyngioma.** A 25-year-old patient in which this supra-sellar space-occupying lesion was found by chance. On the **a** axial and **b** sagittal CT, there is a partially calcified space-occupying lesion with cystic portions. **c** On the unenhanced T1-weighted sequences, the cystic portions of the tumour appear hyper-intense. **d** After the administration of contrast agent, there is marginal enhancement

deficits affect the hypothalamic/pituitary axes with regard to growth hormone (GH) in addition to adrenocorticotrophic hormone (ACTH) and thyroid-stimulating hormone (TSH). Pre-operatively, 17% of affected patients suffer from diabetes insipidus neurohormonalis.

► **The combination of guiding symptoms, which includes headaches, visual disturbance, growth failure and polydipsia/polyuria, should prompt the suspicion of a craniopharyngioma during differential diagnosis.**

#### ■ ■ Medical Imaging

Both on the CT and the MRI, craniopharyngiomas are mostly cystic tumours that appear in the intra- and/or peri-sellar region (► Fig. 9.117). The CT can better detect calcifications, which are present in about 90% of tumours.

On MRI, craniopharyngiomas have a highly variable signal intensity, which depends on the protein content of the cysts. Solid portions of the tumour and cyst membranes appear iso-intense on a T1-weighted image and often have a slightly heterogeneous structure. The most common localisation is supra-sellar with an

intra-sellar portion. In approximately 20% of cases, the craniopharyngioma is localised exclusively supra-sellarly. In approximately 5% of the cases, it is localised exclusively intra-sellarly. The combination of solid, cystic and calcified tumour portions indicates the diagnosis of tumour type.

#### ■ ■ Treatment

A complete microscopic resection whilst preserving the optical and hypothalamic/pituitary function is the treatment of choice in the case of favourable localisation. In the case of unfavourable localisation, this treatment option is controversial and should be weighed against a planned limited resection followed by radiation therapy. After sub-total resection followed by radiation, the rate of progression is approximately 21%.

#### ■ Less Common Tumours

**Meningioma.** Although they account for 15% of all intra-cranial tumours, only about 10% of meningiomas occur in the sellar region. Supra- and para-sellar meningiomas are thus the third most common tumour of this region. The meningioma of the sellar tubercle is a classic supra-sellar tumour. It often leads to vision problems. Compression of the pituitary stalk with hyperprolactinaemia is often the only hormone disorder. Cavernous sinus meningiomas lead to diplopia, proptosis, oculo-motor disturbances and hypoesthesia in the area supplied by the trigeminal nerve. Optic nerve sheath meningiomas often lead to progressive visual loss.

**Rathke's Pouch Cysts.** The clinical and radiological appearances of Rathke's pouch cysts resemble those of craniopharyngioma. Histologically, they are difficult to distinguish from the craniopharyngioma and the colloid cyst. They are composed of epithelial cells with a single-layer, cubic cyst wall, which is situated in a basement membrane.

**Colloid Cysts.** Colloid cysts contain colloid-like material and have no wall. They often cause endocrinological deficits.

**Arachnoid Cysts.** Arachnoid cysts frequently cause headaches, visual disturbances and hypopituitarism (■ Fig. 9.38). On MRI, only CSF is displayed; this can be easily confused with an "empty sella". An arachnoid cyst is a cyst with a thickened membrane, which can lead to compression of the optic chiasm and the sella. In the case of an "empty sella", only the sub-arachnoid cavity is extended and bulges without increased pressure in the sella. Primary and secondary "empty sella" syndromes are distinguished from one other. An incompletely formed sellar diaphragm is typical in the case of a primary "empty sella" syndrome.

**Other Tumours in this Region.** Other tumourous changes can occur around the pituitary gland/sella. These become evident as a result of hormonal and ocular disorders. In addition to the meningiomas, these include:

- Bone tumours, such as chordomas
- Cystic/aberrant tumours such as craniopharyngiomas
- Rathke's cysts
- Epidermoid

- Metastases from other parts of the body
- Inflammatory changes (hypophysitis)
- Sarcoidosis (■ Fig. 9.148)
- Germ cell tumours
- Germinomas (■ Fig. 9.108)

### 9.4.8 Metastases

#### ■ Extra-axial Intra-cranial Metastases

Extra-axial intra-cranial metastases are often found during clinical routine. In an autopsy study of patients with extra-cranial tumours and intra-cranial metastases, solitary dural metastases were found in only 18%. Mammary carcinoma most commonly undergoes dural metastasis, followed by lymphoma, prostatic carcinoma and neuroblastoma.

Metastases can have a histological structure similar to that of the primary tumour or can be more anaplastic. Depending on the tumour type, necrotic inclusions and haemorrhaging can occur. There is usually an extensive peri-focal oedema, which far surpasses the size and the space-occupying effect of the tumour. The incidence of brain metastases in relation to the total number of brain tumours varies between 5 and 40% depending on whether statistics are drawn from neuro-surgical clinics or pathological institutes.

On CT, the metastases appear as small, round zones with varying signal behaviour. There is extensive peri-focal oedema. After the administration of a contrast agent, there is strong enhancement. In rare cases, the metastases are large with central necroses, which can complicate the differentiation from glioblastoma. Some metastases, particularly in melanoma, are prone to tumour haemorrhaging and can thus be misdiagnosed as cerebral haemorrhaging. The accumulation a smaller region of contrast agent within a broad zone of oedema suggests cerebral metastasis. Meningeal metastases generally remain undetected after the administration of contrast agent. They are sometimes only revealed in the case of consecutive hydrocephalus. The signal intensity on MRI is usually not specific. On T1-weighted images, metastases are slightly hypointense to the cortex. On T2-weighted images, they are hyper-intense.

**Lepto-meningeal metastases** are often not seen on contrast-enhanced CT, especially in the case of leukaemia or lymphoma. An MR examination without contrast agent is not suitable for this tumour entity. The administration of contrast agent increases the sensitivity when detecting lepto-meningeal metastases. Lepto-meningeal tumour infiltration cannot usually be distinguished from other diffuse meningeal diseases, such as infectious meningitis.

Although MRI is currently the most sensitive method, subependymal/ependymal tumour metastases show no contrast enhancement and may thus be overlooked. The diagnosis of lepto-meningeal metastasis must often be supported by other findings, such as CSF or symptoms. On CT and even MRI, hydrocephalus in a patient with a known extra-cranial malignoma can indicate a diagnosis of lepto-meningeal carcinomatosis. Therefore, further diagnostic tests should be performed, with investigation of the CSF.

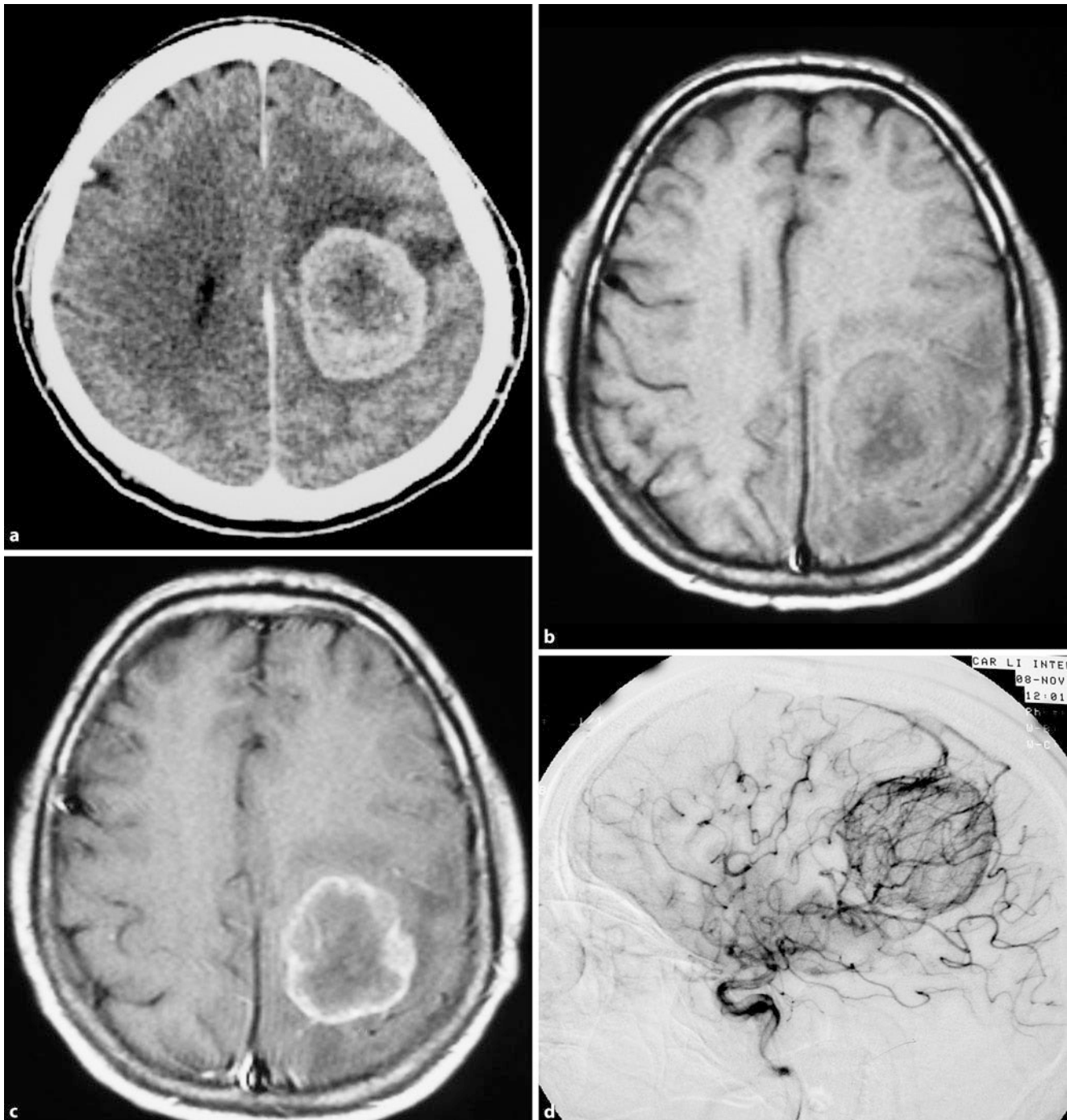


**Fig. 9.118a–d** Parenchymal metastasis. Histologically confirmed metastasis of an adenocarcinoma. **a** On the axial CT, after the administration of contrast agent, a strong marginal uptake of the left frontal and central space-occupying lesion is revealed. **b** On the unenhanced T1-weighted sequences, the space-occupying lesion largely appears iso-intense to the

cerebral parenchyma with a central hypo-intense portion, which matches central necrosis. **c** Annular enhancement after the administration of a contrast agent. **d** Late arterial phase in the selective view of left absorption contrast imaging with evidence of the strong vascularisation of the space-occupying lesion

### ■ Intra-parenchymal Metastases

Twenty-five per cent of all lesions in the CNS are metastases. The most frequent are:

- Bronchial carcinomas
- Mammary carcinomas
- Renal cell carcinomas
- Carcinomas of the gastro-intestinal tract
- Melanomas

Metastases can occur anywhere in the brain, but are usually localised at the cortico-medullary boundary. Eighty per cent of all cerebral metastases are supra-tentorial, 20% infra-tentorial. In approximately 70% of cases, multiple metastases are detectable. Metastases can also occur extra-axially and infect the meninges and the bone. Characteristic features are the presence of multiple space-occupying lesions in addition to a sub-cortical location. Depending on their primary tumour, the cell metastases may be either cell-rich or cell-poor and display calcification and haemorrhaging. Their size can also be quite variable. After the administration of a contrast agent, most metastases display ring-shaped or homogeneous enhancement.

Magnetic resonance imaging can detect metastases more sensitively than CT. It is regarded as the method of choice for the detection of the smallest metastases in addition to the detection of carcinomatous meningitis. A double dose of contrast medium, provided that this is feasible, results in better visibility of the metastases; alternatively, waiting time can be increased to approximately 20–30 min.

Even very small metastases often have significant oedema. The cortex and corpus callosum are usually spared. Haemorrhaging in the metastases mainly occurs in renal cell carcinomas and in melanomas. Because of their melanin content, melanomas are often hyper-intense on the unenhanced T1-weighted MRI. Also in this case, unenhanced studies should be performed first.

Examples are: parenchymal metastases (■ Fig. 9.118) in addition to lepto-meningeal and dural metastases (■ Fig. 9.119) – in the proper sense, the latter are located in extra-axial tumours.

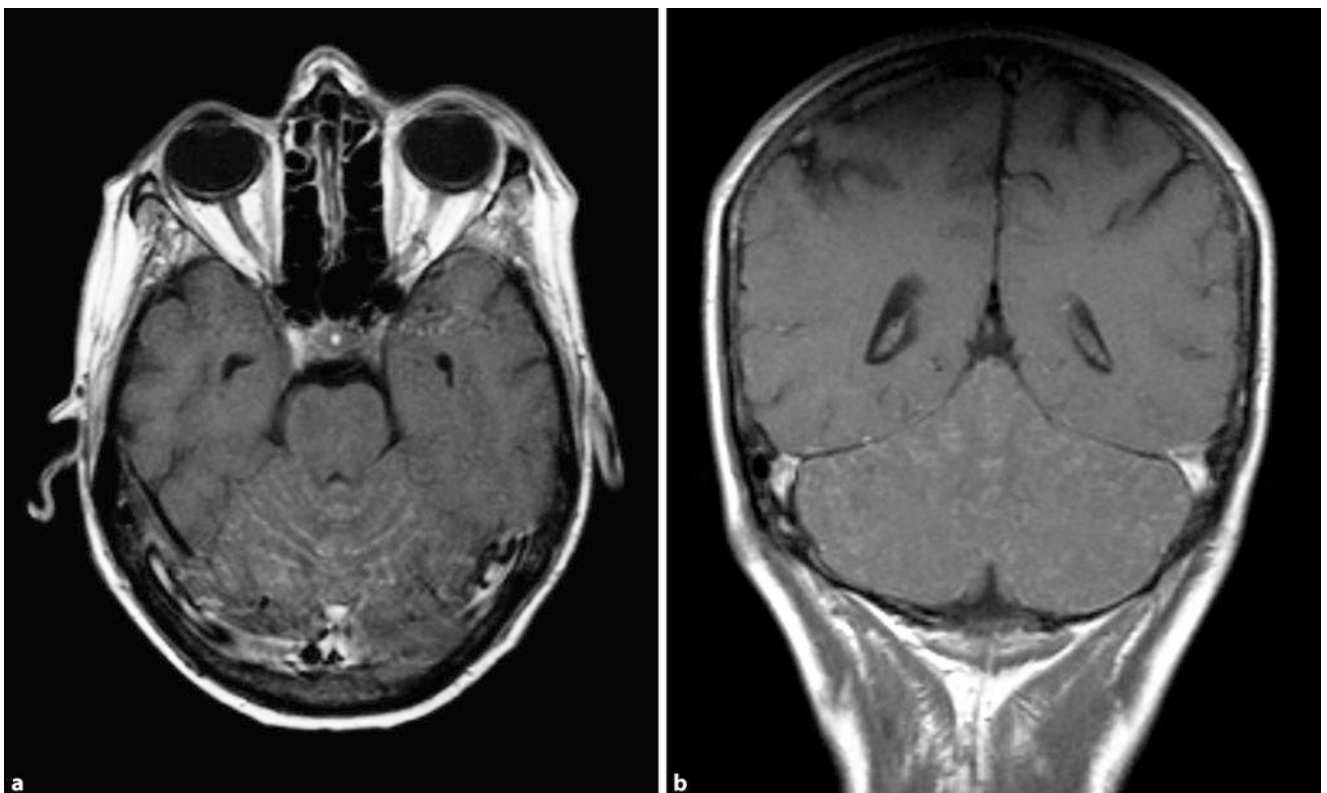
## 9.5 Cranio-cerebral Trauma

### 9.5.1 Basics

Cranio-cerebral traumas occur at a frequency of about 200–300 per 100,000. Children younger than 15 years account for about 25% of these. Injuries caused by accidents are among the most common causes of death in children and young adults; in about half of all fatal accidental injury, intra-cranial injury plays a leading role.

#### ■ Classification of Intra-cranial Trauma

In the English-speaking world, the severity of intra-cranial injury is classified according to the Glasgow Coma Scale. The clinical criteria are assessed using this. Points are given for the ability of the patients to open their eyes in addition to linguistic and motor response. The total score ranges from 3 (non-reactive patients) to 15 points (normal). A score of 3–8 is referred to as



■ Fig. 9.119a,b Lepto-meningeal metastasis. On the a axial and b coronary T1-weighted sequences, after the administration of contrast agent, there is

strong lepto-meningeal enhancement infra-tentorially and an icing-like lining that corresponds to the sulci



a severe intra-cranial injury, 9–12 points as moderately severe, and 13–15 points as a minor intra-cranial injury. In patients who are not initially unconscious, this is referred to as concussion. Depending on whether the dura mater is injured, it is possible to differentiate between a closed and an open intra-cranial injury.

Consequences of trauma can be divided into primary and secondary lesions. Primary lesions can occur at the moment of trauma, either by direct action or indirectly by shear forces. Secondary lesions occur as a complication of further proceedings.

#### ■ Peculiarities in Children

In comparison to those of adult patients, childhood intra-cranial injuries reveal significant differences in the mechanism of injury, the intra-cranial effects, the trauma, and the course. Traumas not only refer to accidents but also to birth trauma, and especially child abuse (see below).

In children, there are some anatomical peculiarities, especially in the first weeks and years. They have a soft elastic skull and open fontanelles. Severe trauma may lead to short-term deformities, but not always to fractures. Compared with adults, children have a higher cerebral water content and incomplete myelination, which result in greater plasticity of the infant brain. The highly flexible spine with limp ligaments and weakly toned cervical muscles in combination with the disproportionately large head allow considerable movement thereof with strain on the cranial vault, the meningeal structures, the vessels and the brain so that acceleration/deceleration trauma (shear injury and brain swelling) may occur, even in the case of relatively mild trauma.

Particularly in the first 2 years of life (i.e. infancy), significantly larger outer sub-arachnoid cavities allow for more extensive movements of the brain compared with older children. In fontanelles that are still open, intra-cranial space-occupying lesions can manifest late, despite their considerable size. Because the child's brain is still developing, and the vessels in the child react more sensitively, children strongly tend to exhibit general cerebral swelling. These factors are most significant in the first 2 years of life.

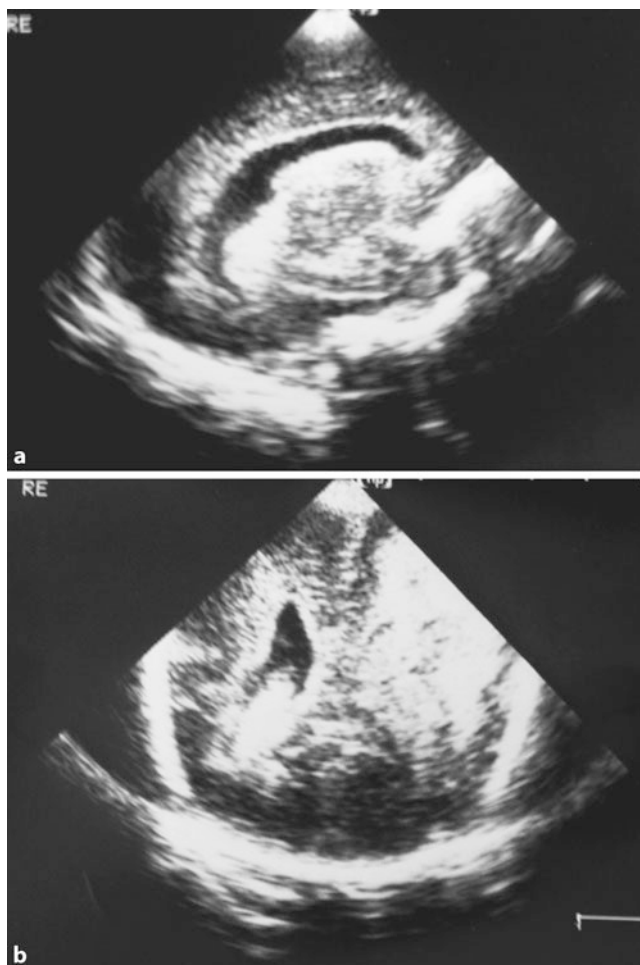
Between the 2nd and 8th years of life, the brain and fontanelles mature, the sutures begin to close and the body proportions change in favour of the body trunk. From about the 10th to 12th years of life, the cranial vault and brain respond to trauma like adults.

#### ■ Imaging Methods

First, a brief overview of the imaging procedures for typical **childhood intra-cranial traumas** should be given. Childhood traumatic brain injury can be divided into:

- Birth trauma
- Accidental trauma
- Non-accidental trauma (► Sect. 9.5.5)

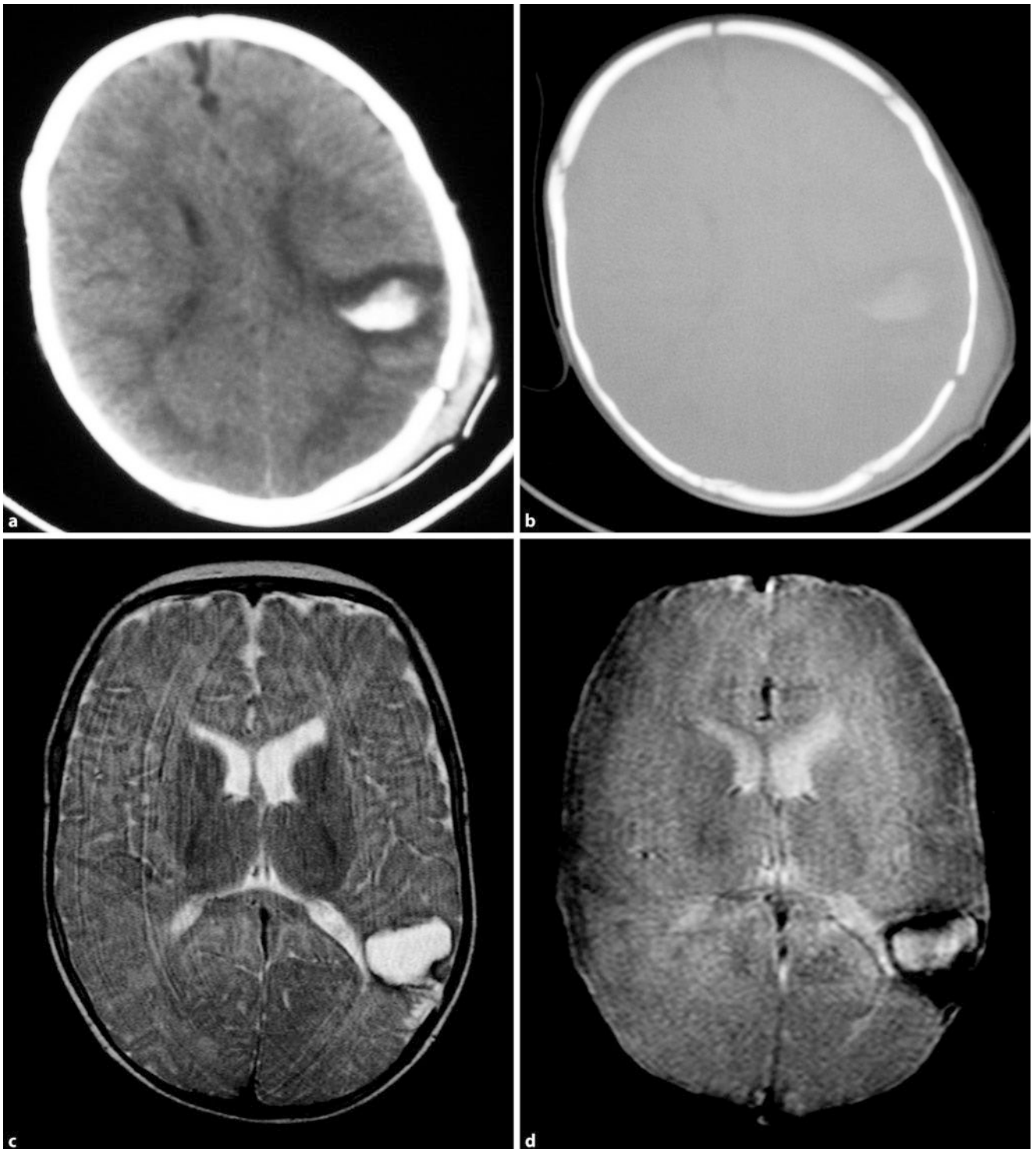
Birth trauma describes traumatic–mechanical damage that can occur during birth. Although asphyxia is sometimes also considered a birth trauma, it is not discussed at length in this chapter. Accidental trauma describes trauma resulting from accidents. Non-accidental trauma refers to child abuse (see below, ► Fig. 9.141).



■ Fig. 9.120a,b Ultrasound, cranio-cerebral trauma. a Ultrasound of a 14-day-old infant with intra-parenchymal haemorrhaging with ventricular collapse. b The right lateral ventricle is filled with blood

**Ultrasound.** The ultrasound is the method of choice for diagnosing neonates (► Fig. 9.120). Epidural and SDH can be readily detected. However, the assessment of the posterior cranial fossa is often difficult. Even small SDHs in the area of convexity can cause difficulties. In the case of corresponding symptoms or the deterioration of findings and normal ultrasound results, a CT or MRI must nevertheless be performed. Ultrasound is ideal suited for monitoring the progress of small, conservatively treated, epidural or sub-dural haemorrhaging. Fractures to the cranial vault and impression fractures are also well represented with ultrasound.

**Computed Tomography.** If the fontanelles are closed, CT is the method of choice for the evaluation of acute cranio-cerebral trauma (► Fig. 9.121). The layers parallel to the orbito-meatal line should be investigated, with a slice thickness of 4–5 mm from the foramen magnum to the cranial vault. The documentation must take place in the soft-tissue window and, after reconstruction, in a high-resolution kernel in the bone window. The topogram should also be documented because fractures parallel to the stratification can go undetected and may be detected on the topogram.



■ **Fig. 9.121a–d CT, MRI, traumatic brain injury.** A 10-month-old infant with slightly reduced movement of the right side. **a, b** On CT, left parietal intra-parenchymal haemorrhaging and a fracture of the cranial vault can be seen. **c** On T2-weighted MRI performed 2 days later, there is a hyper-intense

left parietal parenchymal defect with a hypo-intense rim. **d** On the T2\*-weighted sequences, the blood flow (especially at edge) is hypo-intense with centrally hyper-intense portions

**Radiography.** In a child, the X-ray examination of the skull at two levels is an investigation that is unnecessary and is **superfluous to further proceedings**. Especially with young children, it is not often possible to obtain a good projection because these patients are restless and less willing to be X-rayed. In addition, recordings of the juvenile skull are often overexposed. The non-dislocated

fracture has no therapeutic consequence (■ Fig. 9.122). There may, however, be intra-cranial haemorrhaging, which requires treatment. A normal X-ray finding does not exclude an intra-cranial injury.

A study of 9,269 children with only minor trauma revealed that on unenhanced X-rays, a detectable fracture only has a low pre-



■ Fig. 9.122a,b Plain radiography, cranio-cerebral trauma. a, b Antero-posterior and lateral survey radiographs of the skull showing multiple radiolucent lines that correspond to fractures. In the case of intra-cranial injury, survey radiographs are generally not indicated; the exception: suspected child abuse

dictive value for intra-cranial injury. In the last 30 years, numerous publications have deemed the survey radiographs to have little value. In addition, several studies reported that fractures are only found in about 2–3% of all survey radiographs. Particularly

in children, simple linear fractures without neurological symptoms are rarely associated with intra-cranial injuries. The clinical symptoms are decisive for organising a CT and not the suspicion of a simple fracture of the cranial vault.

In cases of suspected child abuse a survey radiograph is indicated because fractures are recognised for a long time and can possibly detect multiple incidences of trauma.

! There should be strict indications for X-ray examination. In the infant 35% of the red bone marrow is found in the face and cranium. This is reduced to 16% in a 5-year-old child. In addition, there is also pressure on the lens of the eye.

**Magnetic Resonance Imaging.** Magnetic resonance imaging is currently of **no value** in the **acute phase** of the treatment of patients with intra-cranial injury. This is justified by the longer examination time compared with CT in addition to the poor observability of the patient during the MRI. Particularly with haemodynamically unstable poly-trauma patients, the longer examination times are not acceptable. In addition, the availability is not always guaranteed in emergency conditions. Computed tomography also offers the advantage that the thorax, abdomen, and spine can now be examined within a short time of the injury without repositioning the patient.

In the **sub-acute phase** of patients with intra-cranial injury, MRI is becoming increasingly **more important**; injuries that are only indirectly or not at all visible on CT can be depicted on MRI. These include diffuse axonal shear injuries (shear injuries with and without petechial haemorrhaging, contusions of the brainstem and the corpus callosum), which occur particularly often in children. In the acute phase, these changes have no causal or therapeutic consequences. They must be clarified according to the general stabilisation of the patient.

An MRI investigation is indicated if the CT findings cannot adequately explain the neurological condition of the patient and if there is a large discrepancy between a normal CT and massive neurological symptoms. As a rule, axial, coronary, and sagittal T2 or FLAIR-weighted sequences should be carried out to depict the injury. T2\*-weighted gradient-echo sequences are used to detect haemorrhagic lesions in addition to contusions and shear injuries. The diffusion-weighted sequence can depict incipient infarcts in the case of vascular injuries. A contrast agent is only necessary to clarify inflammatory complications, e.g. a post-traumatic abscess following open intra-cranial injury. ■ Table 9.13 shows an MRI protocol in patients with cranio-cerebral trauma.

### 9.5.2 Birth Trauma and Other Fractures in Children

During birth, intra-cranial bleeding in addition to injury to the extra-cranial soft tissues can be observed. Intra-cranial haemorrhaging can arise spontaneously or as a result of peri-natal trauma, asphyxia, bleeding into infarcts, infections and coagulation disorders. Prenatally, it is not uncommon to see smaller SDHs, which are not clinically expressed, found by chance or

■ **Table 9.13** MRI examination protocol

Sequence	Weighting	Slice thickness (mm)	Orientation
SE	T1	4	Axial/coronal
TSE	T2	4	Axial
TSE	T2	3	Sagittal
GRE	T2*	5	Coronal/axial
FLAIR	T2	4	Coronal
SE-EPI	Diffusion	6	Axial/sagittal

*SE spin echo, TSE turbo spin echo, GRE gradient echo, EPI echo planar*

in the context of another investigation. In rare cases, a vascular malformation may be the cause of haemorrhaging. The particular subject matter of neonatal brain injury (hypoxic–ischaemic lesion) is described in the section on developmental disorders and malformations (► Sect. 9.2.4).

#### ■ Caput Succedaneum

A caput succedaneum corresponds to haemorrhaging with oedema in the Galea and is a **clinically irrelevant incidental finding** (■ Fig. 9.123). It is usually not limited to the sutures. Sub-galeal haematoma involves haemorrhaging into the loose connective tissue that connects the galea with the periosteum and can reach a considerable size. The bleeding may exceed the sutures, but calcification does not normally occur. Such is the extent of the haemorrhaging that it may also necessitate a transfusion.

**Cephalic Haematoma** A cephalic haematoma is a sub-periosteal haemorrhage that is limited by the sutures (■ Fig. 9.124). This also involves a **clinically irrelevant finding**, which requires no further radiological investigation. In rare cases, cephalic haematomas may calcify. They most frequently occur after long births. They can still increase in size after the birth. Cephalic haematomas generally regress, however, although this can take several months.

#### ■ Medical Imaging

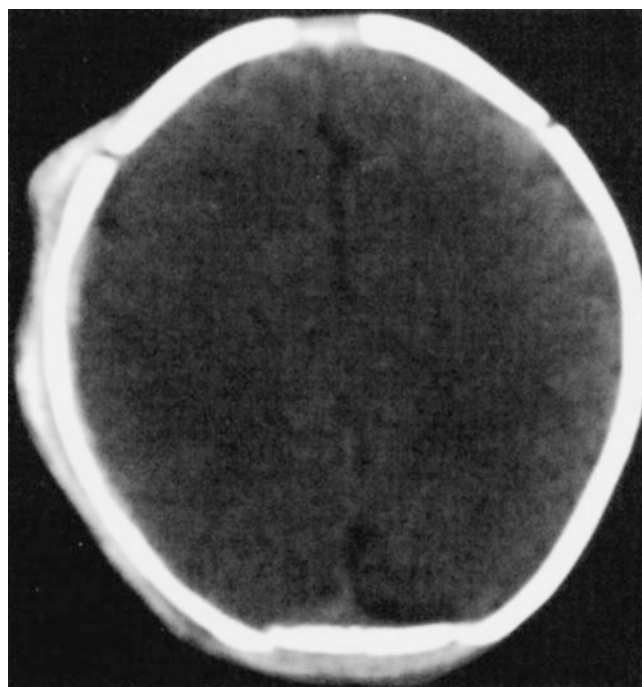
On the MRI or CT, they appear as crescent-shaped masses in the region of the outer cranial vault. Depending on the age of the haemorrhage, the cephalic haematomas appear as iso-intense (with fresh haemorrhage) or hyper-intense (methaemoglobin stage) on the T1-weighted sequence (■ Table 9.14).

#### ■ Cranial and Depressed Fractures

Linear cranial fractures or a ping-pong fracture can appear during the birth as the head passes through the pelvis (see below). In particular, depressed fractures can be caused by the use of mechanical aids.

#### ■ Sub-dural Haematomas

Not infrequently, narrow SDH may occur during birth. This does not often manifest clinically and may only be detected by coin-



■ **Fig. 9.123** Caput succedaneum. A 24-hour-old infant after spontaneous vaginal delivery: Caput succedaneum with oedema and haemorrhage in the galea and a narrow sub-dural haematoma (SDH) in the right fronto-parietal region. (From *Radiologie* 2003;43:968, Fig. 1)

idence. They frequently occur in difficult births and when mechanical aids are used. However, in spontaneous vaginal birth, in up to 30% of cases, SDHs can be observed in new-borns, usually as an incidental finding.

**The cause** is the bending and compression of the cranial skeleton, which then leads to pulled muscles at the dura, the falx, the tentorium and the bridging veins, which may cause venous haemorrhaging. This comes about because the sutures have not yet closed and the skull is relatively “soft”. The haematoma may be located above a hemisphere, on the tentorium, or in the inter-hemispheric fissure (■ Fig. 9.125).

**Infra-tentorial SDHs** also occur via occipital osteodiaschisis. However, they are rare and only require treatment when a compression syndrome of the brain-stem is clinically manifested.

**Medical Imaging.** On CT, the haematomas appear as typically hyper-dense, crescent-shaped masses in the area of the hemispheres.

! **Because SDHs are the most frequent lesions after child abuse, a detailed birth history is necessary to be able to assess the aetiology of a SDH.**

#### ■ Intra-parenchymal Haemorrhage

Intra-parenchymal haemorrhage may occur either focally or multi-focally at any gestational age. The preferred localisation is the peri-ventricular white matter with development of a peri-ventricular leukomalacia. In most cases, haemorrhages in the thalamus are uni-lateral; there is usually an intrusion in the ven-

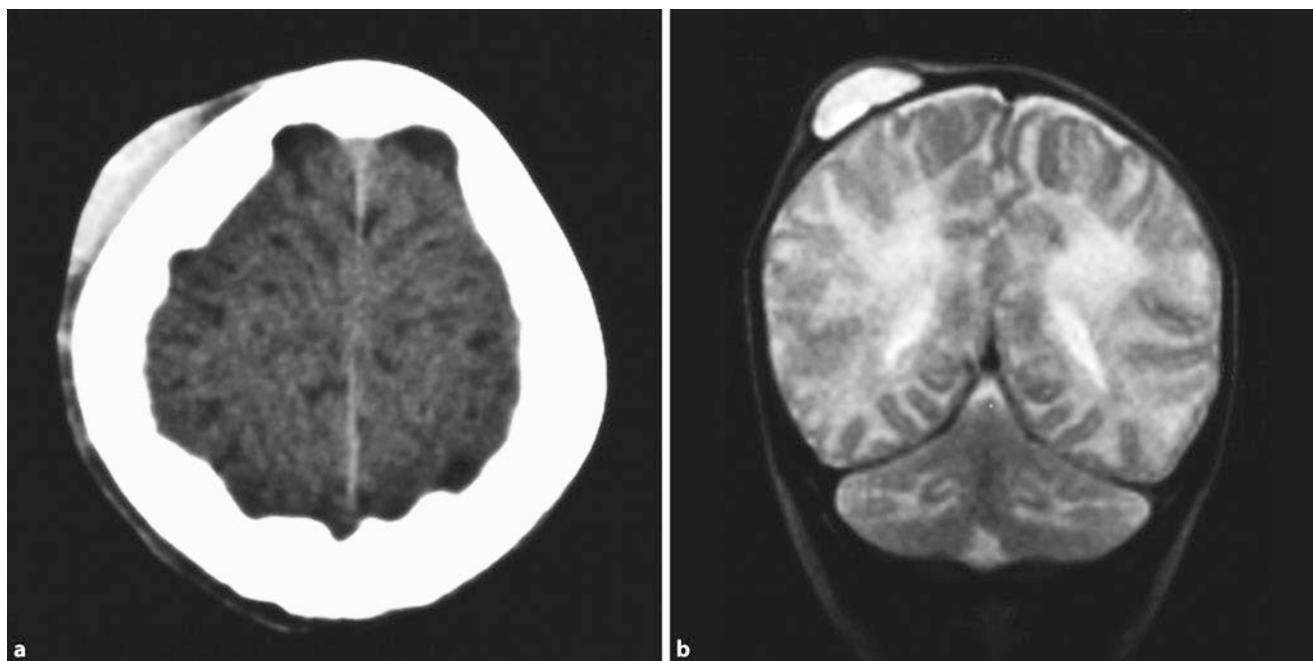


**Fig. 9.124a,b** cephalic haematoma. a, b Evidence of right parietal cephalic haematoma in the case of birth with mechanical aids (a: CT), haematoma

as s fresh hyper-intense lesion on b the T2-weighted sequence

tricular system (Fig. 9.126). Haemorrhage into the root ganglia is also possible.

**!** In the case of peri-partum intra-cranial bleeding, a follow-up should be performed to be able to detect developing hydrocephalus in time. After a traumatic birth, injury to the cervical spine and brachial plexus should always be considered.

#### Accidental Trauma

Severe accidental trauma is rare in infants up to about two years, the vast majority of cases presenting to the emergency department are trivial traumas. The most common causes are falls, e.g. from the changing table. In this age group, a severe traumatic brain injury must therefore evoke suspicion of child abuse if there is no clear medical history with a credible massive trauma.

**>** From a radiological perspective, in childhood, many injuries such as contusions, traumatic sub-arachnoid haemorrhage, and herniation syndrome are similar to those seen in adulthood.

#### Cranial Fractures

In two thirds of patients with severe intracranial injuries, there are cranial fractures. According to their shape, it is possible to distinguish linear fractures, comminuted fractures, depressed fractures and perforated fractures (shot and stab wounds). In the case of a compression fracture, the intra-cranial radiological shift of bone fragments does not necessarily have to correspond to the maximum displacement at the time of trauma. Depressed fractures should be revised if the depth of penetration of the fragments is greater than the thickness of the cranial vault.

**Table 9.14** MR appearance of the intra-cerebral haemorrhage

Stage (time interval)	T1-weighted SE	T2-weighted SE
Hyper-acute (first hours)	Iso-intensity	Hyper-intensity
Acute (2 days)	Iso-intensity	Hypo-intense centre with high signal edge
Sub-acute (2 days to 2 weeks)	Hyper-intensity	Hyper-intensity

#### Cranial Fractures

Cranial fractures are usually frontal or parietal. They appear as a radiolucent line without a sclerotic rim. The gap is spindle-shaped and thus wider in the middle than at the beginning and end of the fracture line. Without dislocation, spontaneous healing occurs within approximately 6 months. In older children, the healing takes about 1 year; in adults, it takes about 2–3 years.

**>** An important difference between neonates or infants and older children is that the middle meningeal artery is not yet embedded in the temporal cranial vault. Therefore, in infants up to 2 years, epidural haematomas occur only rarely.

**During birth, depressed fractures** can result from pressure on the cranial vault in the pelvic area with the use of mechanical aids, maltreatment, or accidental trauma (Figs. 9.127, 9.128). On the MRI or CT, a contusional injury of the cortex below the fracture or an extra-axial haematoma can be sufficiently well depicted. Survey radiographs are not sufficient for this.

If fissures appear in the dura, extra-cranial herniation of the cerebral membrane can occur owing to fracturing. The interposi-

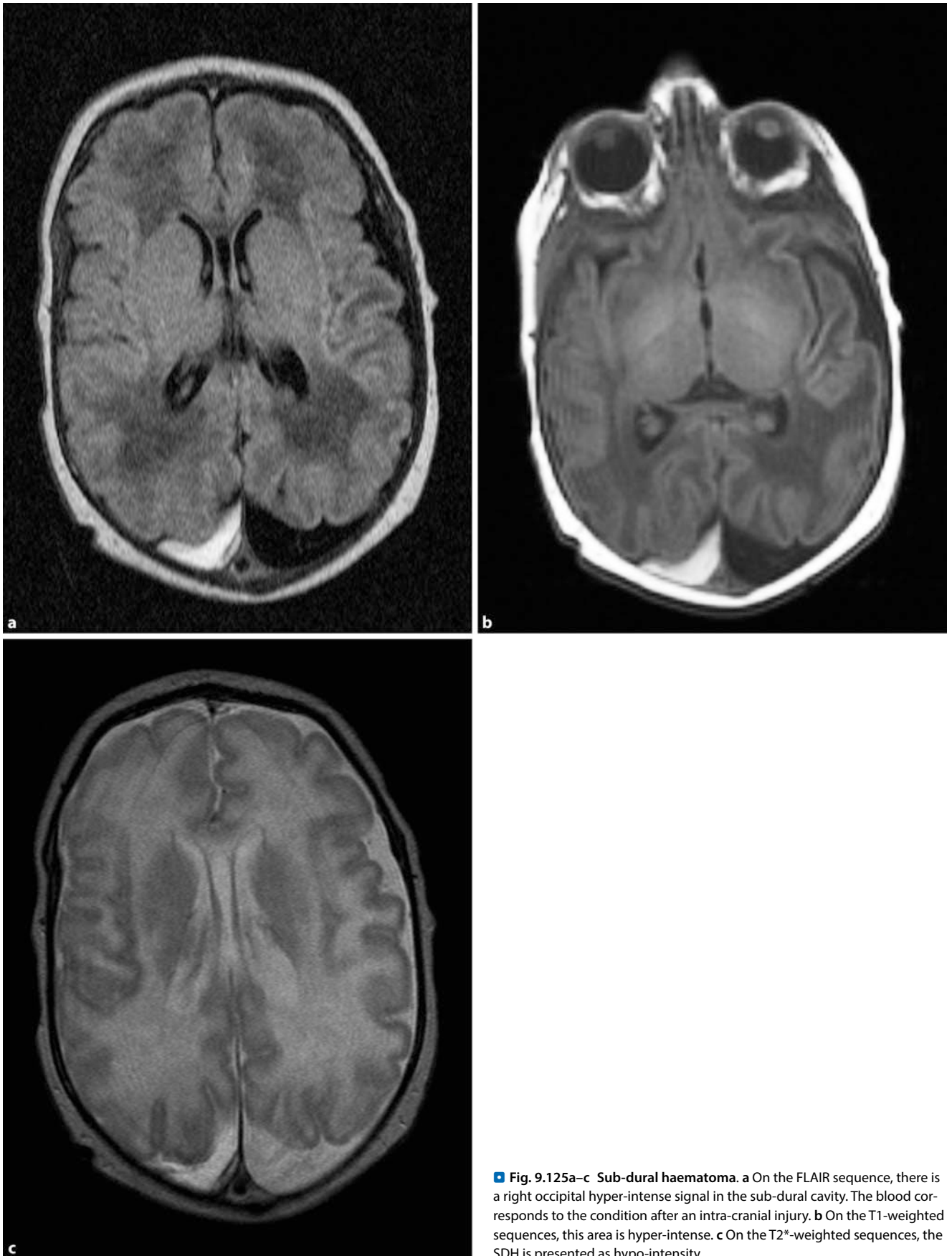


**Fig. 9.125a–c Sub-dural haematoma.** a On the FLAIR sequence, there is a right occipital hyper-intense signal in the sub-dural cavity. The blood corresponds to the condition after an intra-cranial injury. b On the T1-weighted sequences, this area is hyper-intense. c On the T2\*-weighted sequences, the SDH is presented as hypo-intensity

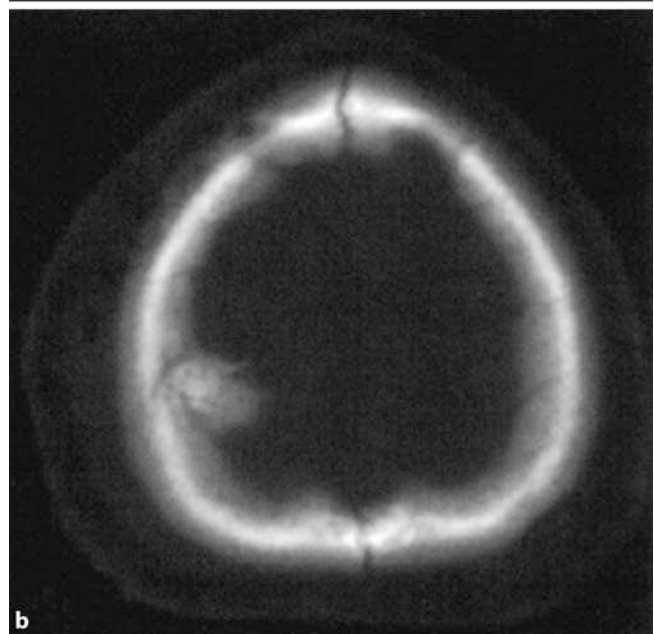
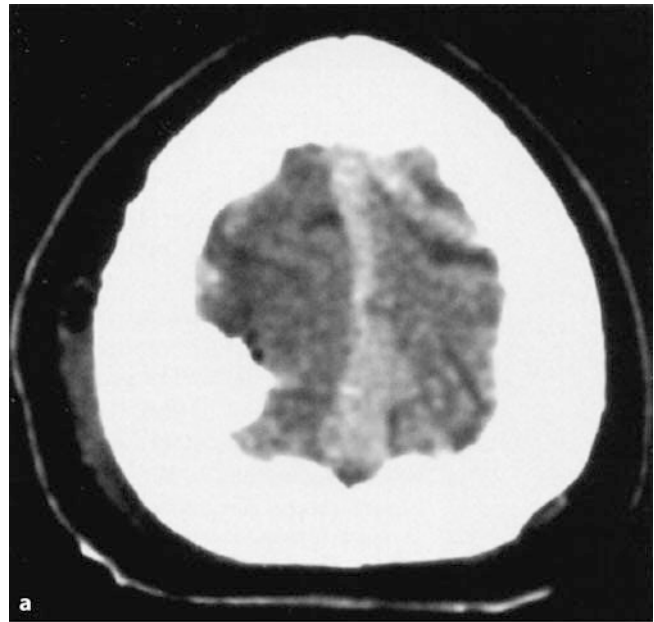


■ **Fig. 9.126 Intra-parenchymal haemorrhage.** Axial CT of a new-born that attracted attention because of feeding difficulties. Thalamic haemorrhage with low peri-focal oedema, invasion into the ventricular system, supply with two external ventricular drains. (From: *Radiologe* 2003; 43:968, Fig. 3)

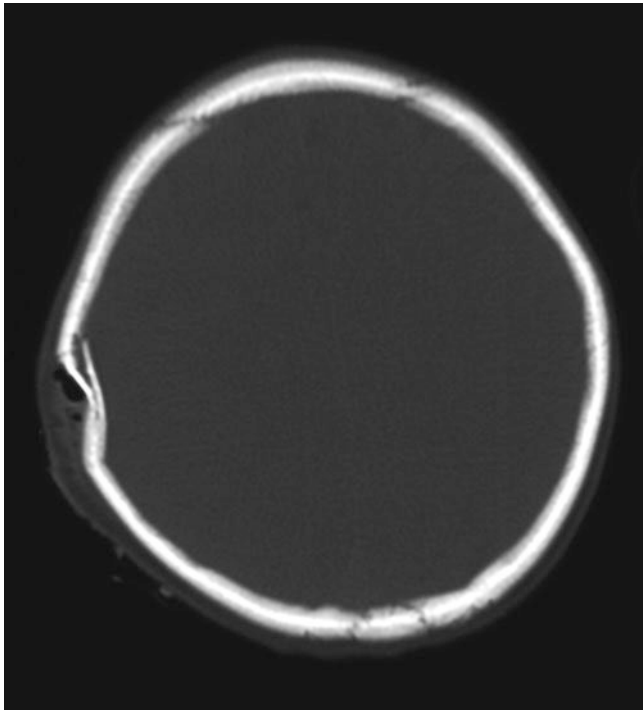
tion of the dura in a fracture gap prevents bone regeneration, and CSF pulsations lead to an increase in the width of the fracture gap. This process is designated as a **growing fracture** or **post-traumatic lepto-meningeal cyst** (■ Fig. 9.129). These cysts are very rare and occur in 0.6% of all fractures. Approximately 90% of patients are less than 3 years old. On survey radiographs, a widening of the fracture gap with sclerotic edges appears. On CT and MRI, the cyst may be filled with CSF.

Only in new-borns is the phenomenon of **ping-pong fracture** observed. This involves circumscribed areas of the cranial vault, which arch intra-cranially and spontaneously assume a regular form because of the plasticity of the bone.

**Traumatic separation of sutures** rarely occurs after the age of 30. The separation of sutures most commonly affects the lambdoid suture, which closes late (■ Fig. 9.130). A width of 2 mm is still considered normal; from a width of 3 mm, a separation of the sutures can be assumed.



■ **Fig. 9.127a–c Cranial fracture, depressed fracture.** An 8-year-old boy who fell from a tree whilst playing. **a** CT: depressed fracture without evidence of intra- or extra-axial haemorrhage. **b** Presentation in the bone window: significant intra-cranial fragment. **c** Blurred compression in the lateral projection, slight translucency of the cranial vault apical to the compaction. (From: *Radiologist* 2003; 43:972, Fig. 8 a–d)



■ Fig. 9.128 Depressed fracture. On the CT with bone window settings, intra-cranial indentation of the fragment can clearly be seen

### 9.5.3 Other Consequences of Trauma

In both children and adults, **these include** contusions, traumatic sub-arachnoid haemorrhaging, cranial nerve injury and open trauma with pneumatocephalus in addition to rhinoliquorrhoea, vascular injury, or skull base fractures and herniation syndrome. The aetiology and the radiological signs of these injuries are identical in both age groups.

#### ■ Epidural Haematomas

#### ■ Epidemiology

Epidural haematoma can be found in about 5% of all traumatic brain injuries. The most common cause is a cranial fracture, which is typically temporo-parietal. The fracture results in injury of the middle meningeal artery or its branches or injury of the venous vessels (medial meningeal artery, venous sinuses, or diploic veins). The extra-dural accumulation of blood often leads to a biconvex mass. The spread of the haematoma is almost always limited by the sutures of the skull because the dura firmly adheres to the bone. To differentiate sub-dural hematoma, the boundary of the cranial sutures is more reliable than the bi-convex form.

Epidural haematomas are rare in young children; the incidence increases with age and reaches a maximum in adulthood.

#### ■ Pathology

In extra-axial haematomas, the time course of haemoglobin degradation can significantly deviate from that observed in intra-axial haematomas. This is partially because of the increased partial oxygen pressure in the extra-axial compartment in addition to the dilution of the blood by CSF. Multi-

lateral bleeding can cause heterogeneous signals (adjacent light and dark areas).

#### ■ Aetiology

In infants epidural haematomas are usually caused by venous haemorrhage owing to tears of dural veins or haemorrhage after fractures. They are a manifestation of acts of violence to the skull (■ Fig. 9.131). Only in older children and adolescents is an injury of the medial meningeal artery the leading cause. This can be explained by the fact that with increasing age, the artery is embedded in a vascular groove of the tabula interna of the cranial vault and is particularly vulnerable in this region in the case of cranial fractures.

#### ■ Symptoms, Medical Imaging

Clinical symptoms develop more slowly in children than in adults. The typical unconsciousness is more infrequent. In children, the prognosis is much better than in adults. The diagnosis is identical for infants, children and adults.

**Medical Imaging.** An epidural haematoma appears as a lens-shaped, hyper-dense mass, which does not usually exceed the sutures (■ Figs. 9.131, 9.132).

#### ■ Sub-dural Haematomas

#### ■ Epidemiology

Sub-dural haematomas (SDH) are found in 10–20% of all cranio-cerebral traumas. In children, the consistency of the unmyelinated brain leads to increased distortion during the trauma with distension and strain of the veins. Unlike adults, 80–85% of the cases of haematoma in infants are bilateral and fronto-parietal.

#### ■ Aetiology

Most SDH are the result of an acceleration, deceleration, or rotational trauma. They are most frequently caused by injury to the bridging veins that run from the surface of the brain along the dura to the venous sinus. They are the most vulnerable in their sub-dural section. Direct injury to the sinus (e.g. in penetrating trauma can result in both epidural and sub-dural bleeding. Severe intra-cranial injury usually results in a SDH. This is often accompanied by severe intra-parenchymal injuries, which contribute to the poor prognosis of the patient.

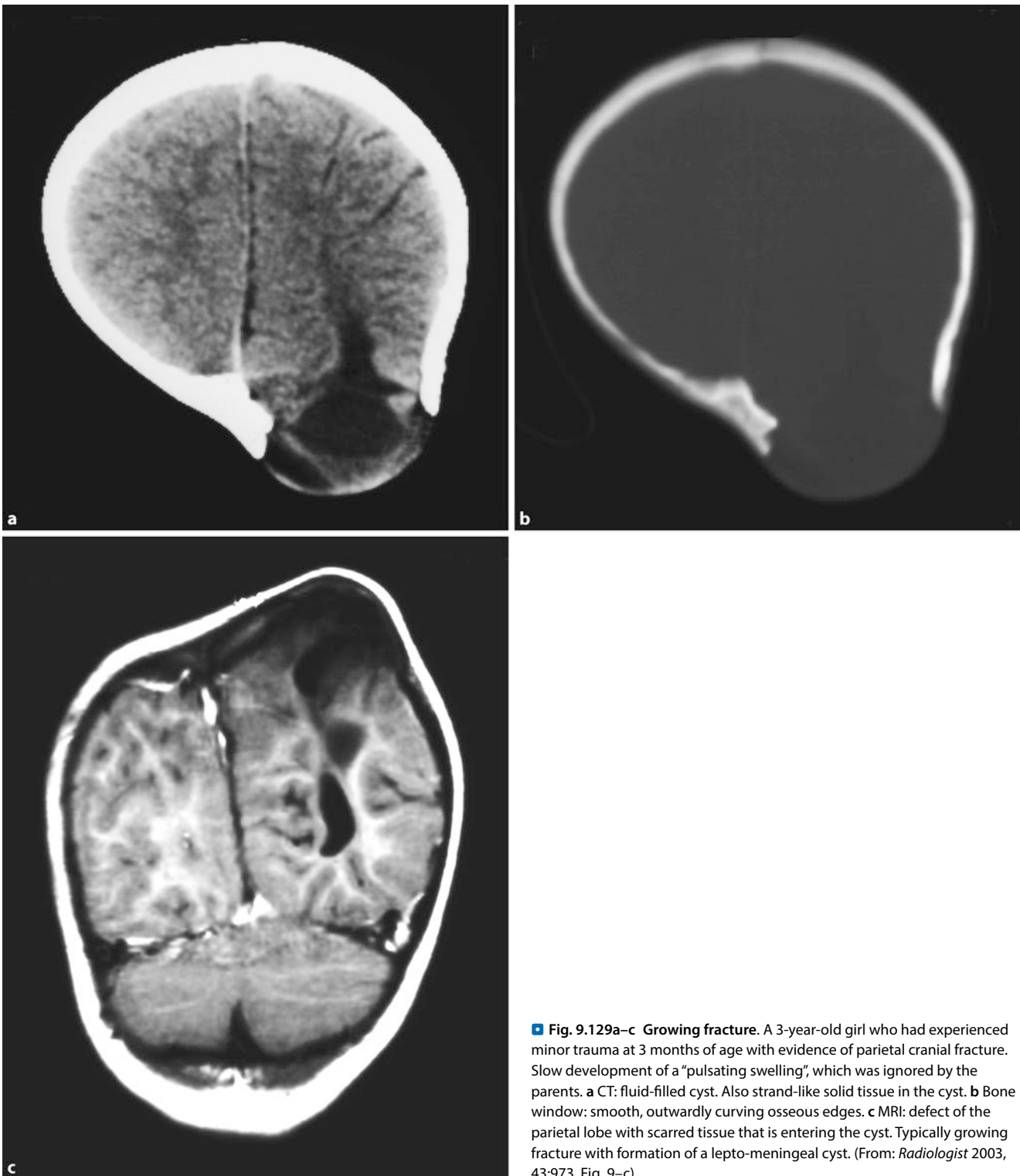
SDH are typical for children and older adults. They are caused by a rupture of the cortical veins.

A **laceration of the falx cerebri** can lead to a supra-tentorial, SDH. The falx usually lacerates relatively close to the tentorium. The bleeding often originates in the superior sagittal sinus. The resulting supra-tentorial, SDH is often located dorsally in the inter-hemispheric gap.

A **laceration of the bridging veins** also leads to a supra-tentorial, SDH. However, this is located above a hemisphere and exhibits the typical crescent-shaped, convex–concave configuration of a SDH. Unlike SDH in older children, SDH in new-borns is usually unilateral. In addition, sub-arachnoid haemorrhaging can even be observed.

A **laceration of the tentorium** usually leads to laceration of the vein of Galen or to a rupture of the small infra-tentorial veins.





■ **Fig. 9.129a–c Growing fracture.** A 3-year-old girl who had experienced minor trauma at 3 months of age with evidence of parietal cranial fracture. Slow development of a “pulsating swelling”, which was ignored by the parents. **a** CT: fluid-filled cyst. Also strand-like solid tissue in the cyst. **b** Bone window: smooth, outwardly curving osseous edges. **c** MRI: defect of the parietal lobe with scarred tissue that is entering the cyst. Typically growing fracture with formation of a lepto-meningeal cyst. (From: *Radiologist* 2003, 43:973, Fig. 9–c)

If the vein of Galen is affected, extensive infra-tentorial haemorrhaging usually occurs. For each major sub-dural haemorrhage, a disturbance in the CSF circulation can occur, with formation of hydrocephalus.

In the case of a **occipital diastase**, which is generally rare, dehiscence of the occipital scales of the cranial vault occurs during birth. This can lead to a laceration of the venous sinuses and thereby an infra-tentorial, SDH.

#### ■ **Symptoms**

Clinically, seizures, lethargy and an increase in head circumference may arise. In older children, hemiplegic symptoms may occur; distinct acute SDH may result in herniation.

#### ■ **Medical Imaging**

**The imaging** is identical in children and adults. A crescent-shaped mass appears, which may exceed the sutures. On the CT,

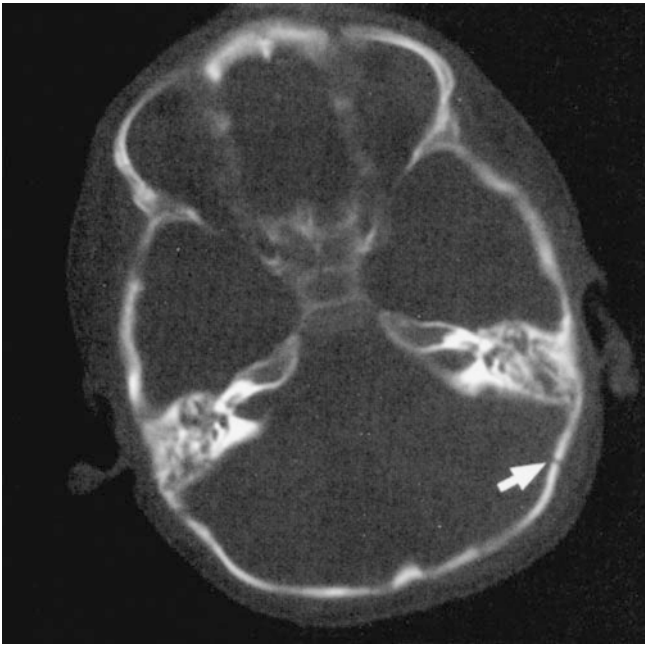


**Fig. 9.130 Separation of sutures.** A 5-year-old boy after a fall on the back of the head. Bone window: left lambdoid suture (*arrow*) significantly expanded, the right not distinguishable. (From: *Radiologe* 2003;43:974, Fig. 10)

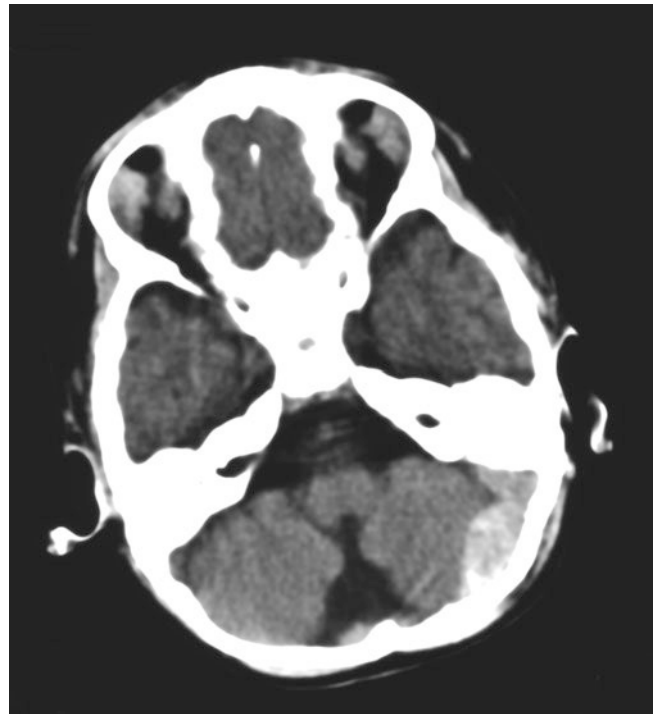


**Fig. 9.131 Epidural haemorrhage.** Soft-tissue window: a recognisable epidural haematoma with low mass effect is indicative of separation of the lambdoid suture with the formation of a fracture haematoma. (From: *Radiologe* 2003; 43:974, Fig. 10)

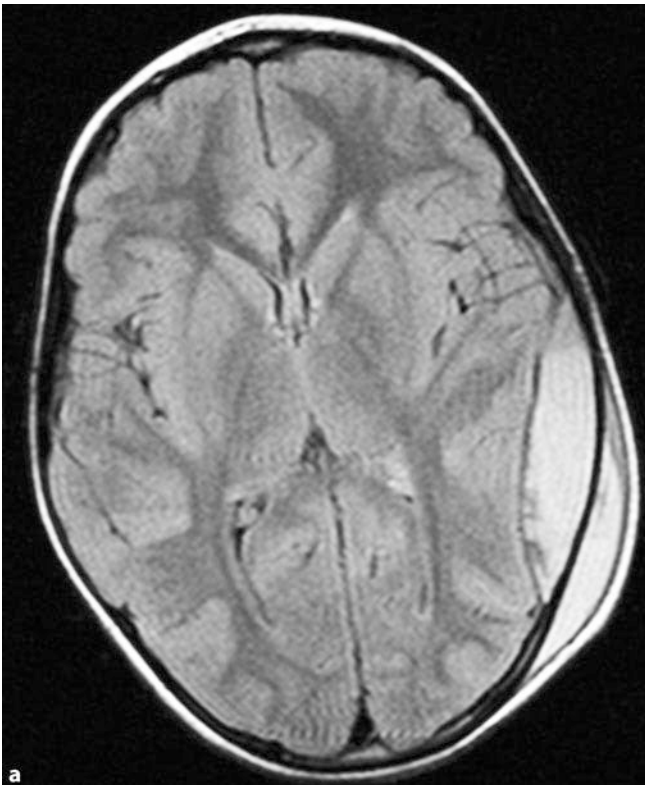
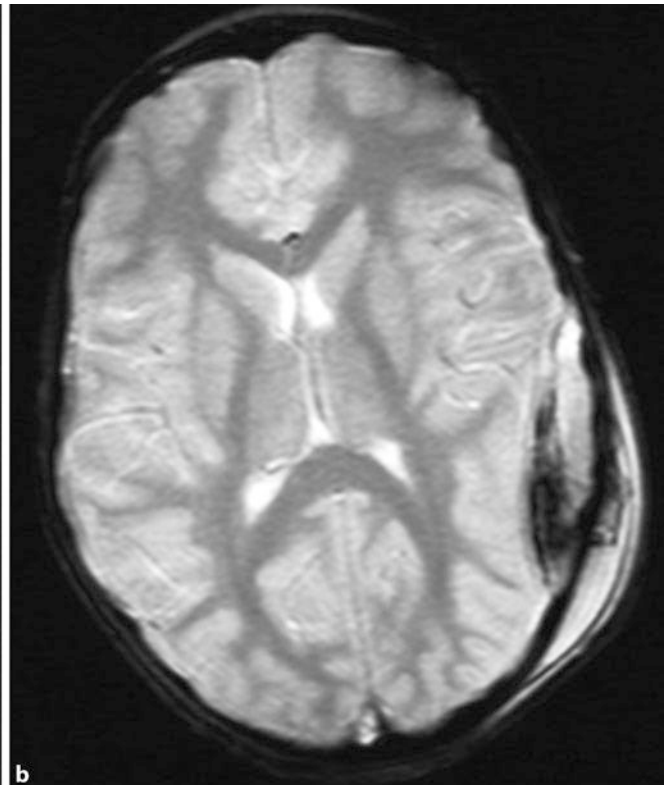
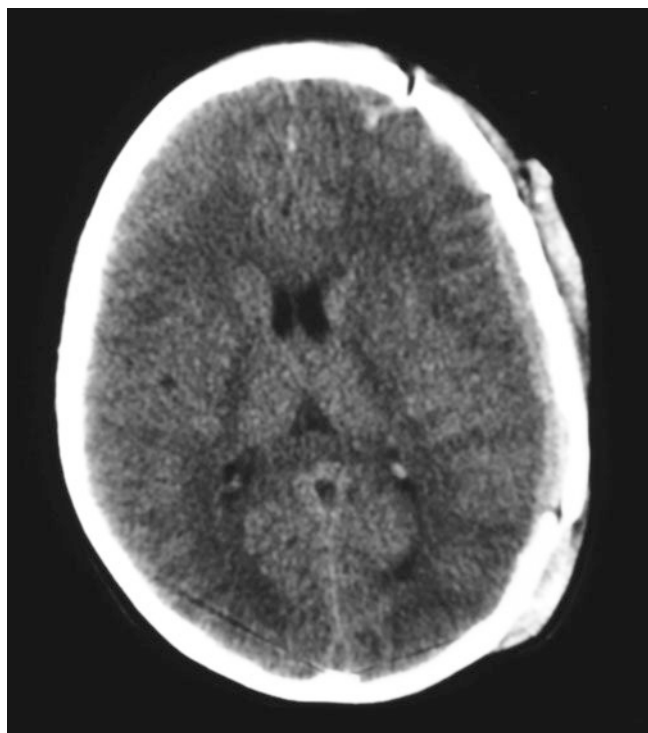


**Fig. 9.132a,b Epidural haemorrhage.** Typical bi-convex epidural left temporal haematoma with associated galeal haematoma. **a** On the FLAIR sequence it is represented as hyper-intense haemorrhaging. **b** On the T2\*-



weighted sequence, the typical decreased signal can be observed for blood degradation products



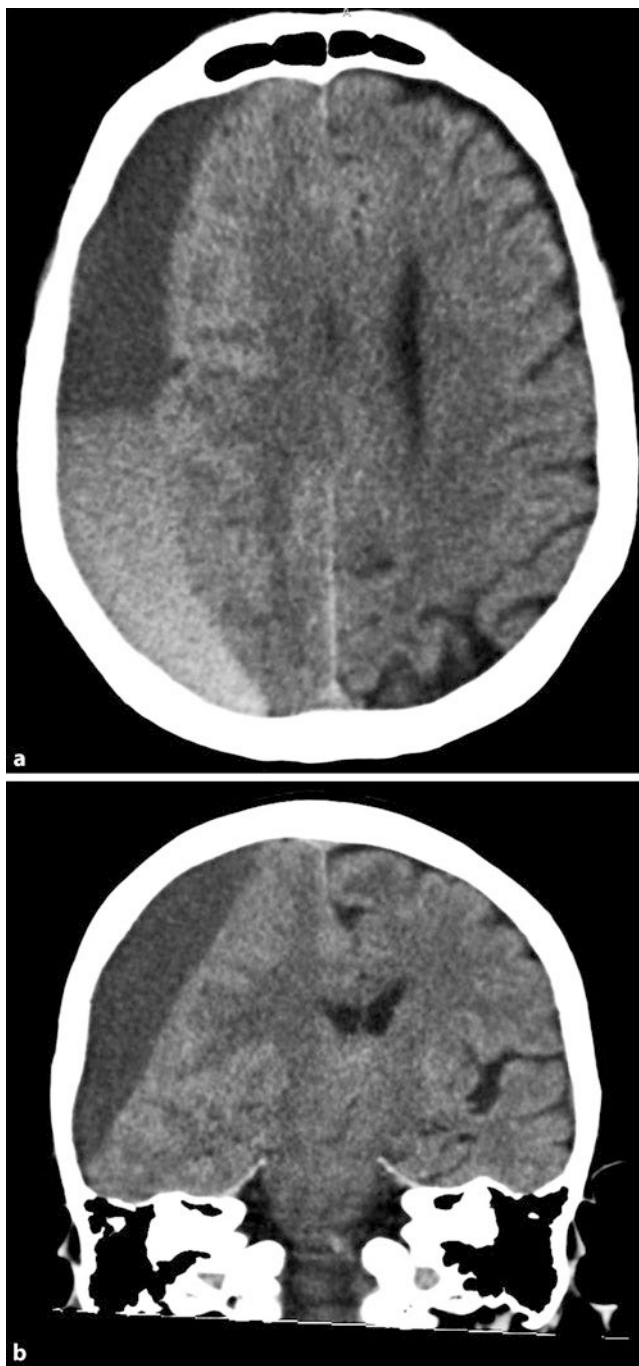
■ **Fig. 9.133 Sub-dural haemorrhaging.** CT: left fronto-parietal SDH, right frontal traumatic sub-arachnoid haemorrhaging, frontal and parietal cranial fracture

a fresh hyper-dense SDH is clearly seen (■ Fig. 9.133). On the MRI, the signal intensity depends on the age of the haemorrhage. In acute SDH, the haemorrhaging on the T2-weighted sequences is hypo-intense. On the T1-weighted sequences, it is iso-intense to the cerebral parenchyma.

As an **acute phase**, the span is said to be a few hours to a few days. This signal intensity is caused by deoxyhaemoglobin. In the **further course**, deoxyhaemoglobin is converted into methaemoglobin. This leads to marked hyper-intensity on the T1-weighted sequences. Conversion to methaemoglobin takes place at the periphery of the haematoma. Only later will the centre of the haemorrhage also become hyper-intense. Because the conversion of deoxyhaemoglobin to methaemoglobin depends on the partial oxygen pressure and this is increased in sub-dural and epidural haematomas compared with intra-cerebral haemorrhage, there is a slightly different time course of the signal changes. Unlike intra-parenchymal haemorrhaging, sub-dural haemorrhaging is completely resorbed relatively quickly, usually within 3 weeks, without the later detection of haemosiderin and ferritin. If the haemorrhaging is completely resorbed, sub-dural, CSF-iso-intense fluid accumulation is observed.

#### ■ **Chronic Sub-dural Haematomas** ■■ **Epidemiology, Aetiology, Clinical**

Chronic SDH predominantly occur in elderly patients. Even trivial traumas may be sufficient. Days or weeks later, patients often display symptoms of focal neurological deficits, impaired consciousness, or headaches. Chronic SDH may even occur in infants and young children.



■ **Fig. 9.134a,b Chronic sub-dural hematoma.** a, b Typical right hemispheric concave-convex haematoma with sedimentation of fresh blood units

#### ■ **Medical Imaging**

On CT, the chronic SDH are usually hypo-dense and occasionally also iso-dense. Haemorrhaging at different times can lead to mixed density values (■ Fig. 9.134). To be able to demonstrate an iso-dense chronic SDH, it is often helpful to use contrast agents during CT or to perform an MRI. A distinct membrane formation with the uptake of contrast agent is sometimes detectable. Untreated chronic SDH may also partially calcify. On MRI, chronic SDH are predominantly signal-intense on both T1- and T2-weighted images. However, the haematomas often show het-

erogeneous signal behaviour with septa and blood degradation products at different ages.

#### ■ “Talk and Die” Syndrome

Especially after minor trauma, both adult and juvenile patients who are barely responsive and admitted without focal neurology pose a particular problem. In the case of primary comatose or ventilated and therefore non-assessable patients in addition to in patients with clear neurological deficits, a CT examination is always performed.

#### ■ ■ Clinical Course

In the case of alert and apparently unremarkable patients, the clinical course determines whether a CT is required. In the case of a secondary deterioration, intra-cranial haematoma is generally feared to be the cause.

In **childhood**, the development of cerebral swelling poses a particular problem. A generalised cerebral swelling occurs about twice as frequently in children as in adults. In larger series from the 1970s, about 5% of all children who died of a head injury were alert and responsive upon admission to the hospital. Approximately 75% of these children died within 48h of admission. In the case of children who were admitted in an alert and responsive (talk and die) condition with secondary deterioration, pathological studies revealed a generalised brain swelling with only minor evidence of brain injury. There was an obliteration of the sub-arachnoid spaces with venous congestion. Diffuse cerebral swelling may therefore be the cause of secondary deterioration. The formation of intra-cranial haemorrhaging is also possible but less frequent.

With timely treatment, these children have a good prognosis. The syndrome is probably caused by vaso-dilatation and hyperaemia with an increase in the intra-cranial blood volume.

This behaves differently in **adult patients**: a secondary deterioration is almost always caused by an intra-cranial haematoma.

❗ In order to detect a secondary deterioration, monitoring should be performed after minor trauma to recognise the clinical signs of increased intra-cranial pressure symptoms (e.g. nausea, vomiting and drowsiness) in time.

#### ■ ■ Medical Imaging

The CT reveals a frail ventricle and narrowing of the apical cistern. In particular, the peri-mesencephalic cisterns, which are normally always visible, even in the infant, are often no longer distinguishable. The medulla appear to be markedly hypo-dense (■ Fig. 9.135). In individual cases, it can be difficult to detect cerebral oedema as such.

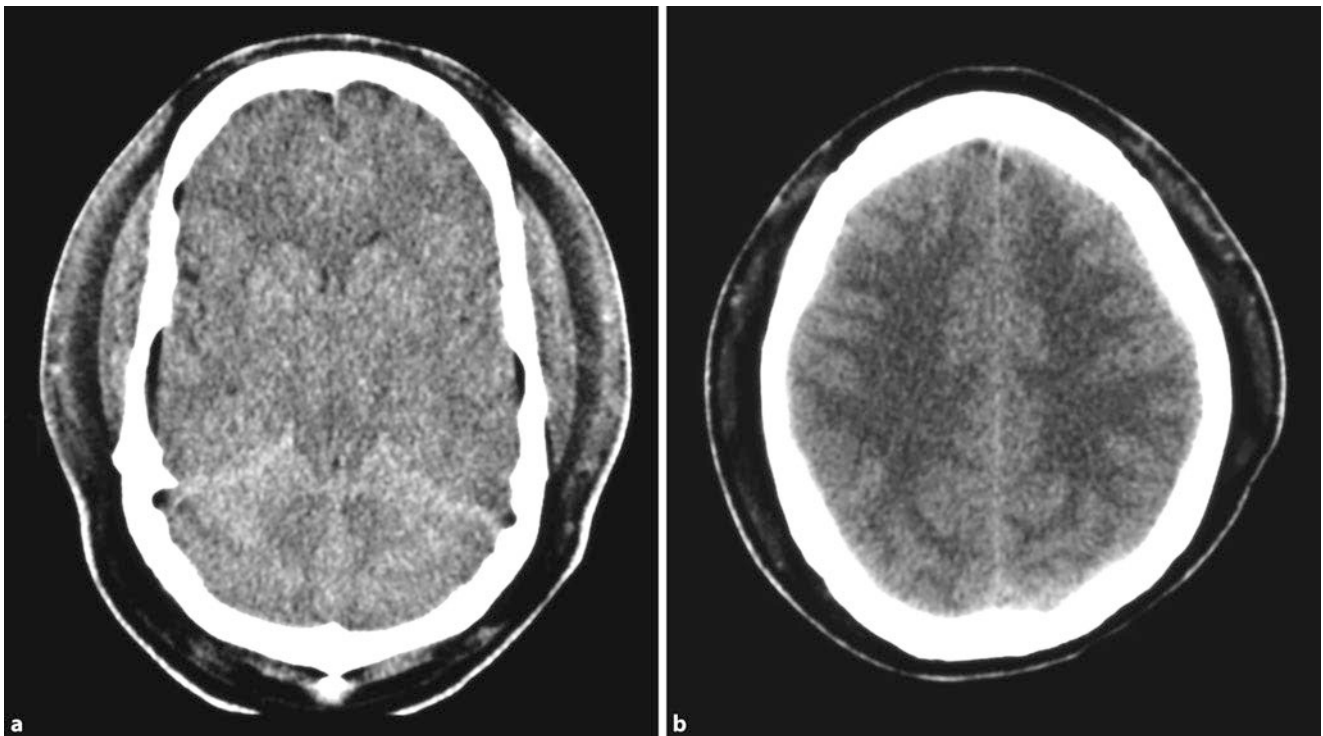
#### ■ Sub-dural Hygroma

##### ■ ■ Definition, Aetiology

Sub-dural hygromas are sub-dural accumulations of fluid that behave like CSF on imaging. They are referred to as hygromas. They can arise at the moment of trauma and are caused by a partial laceration of the arachnoid or by the resorption of an SDH.

##### ■ ■ Medical Imaging

It is often difficult to distinguish sub-dural hygroma from chronic SDH. This is more feasible on MRI than on CT, possibly because



■ Fig. 9.135a,b Diffuse swelling after trauma. Peri-mesencephalic cisterns are not seen at the level of the tentorial incisura, only implied delineation of the anterior horns, above the cella media, the medullary layer is markedly

hypodense, the outer sub-arachnoid cavities not distinguishable, no intraparenchymal injury or extra-axial haematomas, severe soft tissue swelling, findings consistent with diffuse cerebral oedema

the sub-dural hygromas behave in a CSF-iso-intense manner in all sequences. On the other hand, chronic SDH often have a higher protein content, which leads to a signal increase on T1- and T2-weighted sequences. From a differential diagnostic perspective, arachnoid cysts should be distinguished from this. It is often difficult to distinguish sub-dural hygroma from enlargement of the sub-arachnoid spaces caused by cortical atrophy. A space-occupying aspect is indicative of a hygroma. Moreover, in the case of hygroma, cerebral bridging veins are displaced to the surface of the brain. In the case of an extension of the sub-arachnoid space, the veins running through the sub-arachnoid space are often readily detected on T1- and T2-weighted sequences.

### ■ Shearing Injuries, Diffuse Axonal Injury, Brain-stem Contusions

#### ■ ■ Pathogenesis

**Shearing injuries** resulting from acceleration/deceleration trauma with rotational form. Because the incompletely myelinated juvenile brain is more plastic and less stiff than a completely myelinated brain, shear injuries are a common type of childhood injury. They manifest on the border of the grey and white matter, in the corpus callosum, the basal ganglia and in the brain-stem (■ Fig. 9.136). Shear forces not only act on the cerebral parenchyma, but also on vessels, which results in haemorrhaging in the basal ganglia and infarction due to the rupture of small arteries.

#### ■ ■ Clinical and Medical Imaging

The symptoms of these patients often present without a fixed form. As a rule, this involves traumas (e.g. motor vehicle accidents). At the scene of the accident, the patients are primarily comatose and do not spontaneously regain consciousness; they are intubated by the para-medics and ventilated whilst they are transported to the hospital. Directly after the trauma, the initial CT examination often reveals very discrete or no noticeable findings. There is initially a small amount of blood in the posterior horns of the lateral ventricle, minor petechial haemorrhaging at the border of the grey and white matter, which is a few millimetres in diameter, and implied minor haemorrhaging in the inter-peduncular cisterns. On the first control CT, these changes are often very pronounced about 6h after the trauma. In addition, cerebral swelling with extortion can manifest, especially in the peri-mesencephalic cisterns. On short-term controls, these small haemorrhages can indicate rapid resorption.

On CT, non-haemorrhagic lesions are virtually untraceable. Probably only about 20% of the lesions have haemorrhaged. In particular, injuries of the corpus callosum and the brain-stem are only visible on MRI (■ Fig. 9.137). However, MRI likely does not depict all lesions.

In the area of the **brain-stem** it is possible to distinguish between **primary and secondary lesions**. The primary injury is caused by a shear injury with diffuse axonal injury; the lesions are localised to the dorso-lateral mid-brain and upper pons. The ventral parts of the pons and the medulla are also affected. Because these injuries are often not haemorrhagic, they are often only visible via MRI. Secondary contusions are caused by herniation syndrome, among other things. The lesions are typically ventral and ventro-lateral in the mid-brain and in the pons.

In general, the primary and secondary changes are summarised as **brain-stem contusions**. Childhood injuries are identical to those seen in adulthood. In individual cases, it can be difficult to distinguish between primary and secondary brain-stem contusions.

**Parenchymal haemorrhaging** can be caused by contusional haemorrhaging or by shear injuries. Contusional haemorrhaging can often be observed in the area of primary impact of the cranial vault and in the opposite cerebral area through the impact of the soft part of the contra-lateral skull (contrecoup). This is referred to as a coup and contracoup lesion. Contusional haemorrhaging frequently increases in size within the first 48h of the trauma. At the initial site of trauma, a cranial fracture – especially a cranial fracture with a compression fracture – can occur. On CT, there is acute contusional haemorrhaging. Like all acute to sub-acute intra-cranial haemorrhaging, it is hyper-dense with a surrounding hypo-dense rim, which corresponds to an oedema. On the MRI, the signal intensity of the haemorrhage proceeds according to the well-known stages. If the haemorrhaging has completely degraded, CSF-iso-intense parenchymal defects and glial scars remain.

### ■ Traumatic Sub-arachnoid Haemorrhaging

#### ■ ■ Epidemiology, Aetiology

In moderate or severe traumatic brain injury, traumatic sub-arachnoid haemorrhaging is a common finding. This often occurs alongside cerebral contusions or shear injuries. Patients with traumatic sub-arachnoid haemorrhaging have a significantly worse prognosis than patients with injuries of the same degree of severity who do not have sub-arachnoid haemorrhaging.

#### ■ ■ Medical Imaging

Here, there is no difference between sub-arachnoid haemorrhaging caused by aneurysm and that caused by trauma. If the medical history is not clear, the patient must undergo vascular diagnosis to rule out aneurysmatic haemorrhaging. In the case of traumatic sub-arachnoid haemorrhaging, however, blood distribution is more focally localised. Blood is found in the cortical sulci of a contusional area or below an SDH. Involvement of the basal cisterns is atypical and rather suggests aneurysmal haemorrhaging.

On the CT, hyper-dense areas can be found in the sub-arachnoid CSF spaces.

On MRI, a FLAIR sequence can prove the presence of blood in the CSF spaces. Traumatic sub-arachnoid haemorrhaging often occurs as a side effect of severe cranio-cerebral trauma. ■ Figure 9.138 shows traumatic sub-arachnoid haemorrhaging on the CT compared with a non-traumatic one.

### ■ Vascular Injuries

#### ■ ■ Epidemiology, Aetiology

Traumatic vascular injuries in the context of cranio-cerebral traumas are rare (■ Fig. 9.139). Injury of the carotid artery in the cervical region may be caused by direct trauma (e.g. strangulation), perforating trauma, or also stretching. In the case of fractures, vascular avulsion and dissections may occur at the base of the skull. In the case of fractures, penetrating injuries, and over-stretching, the vertebral artery is compromised in its course through the foramina of the transverse process. Severe trauma

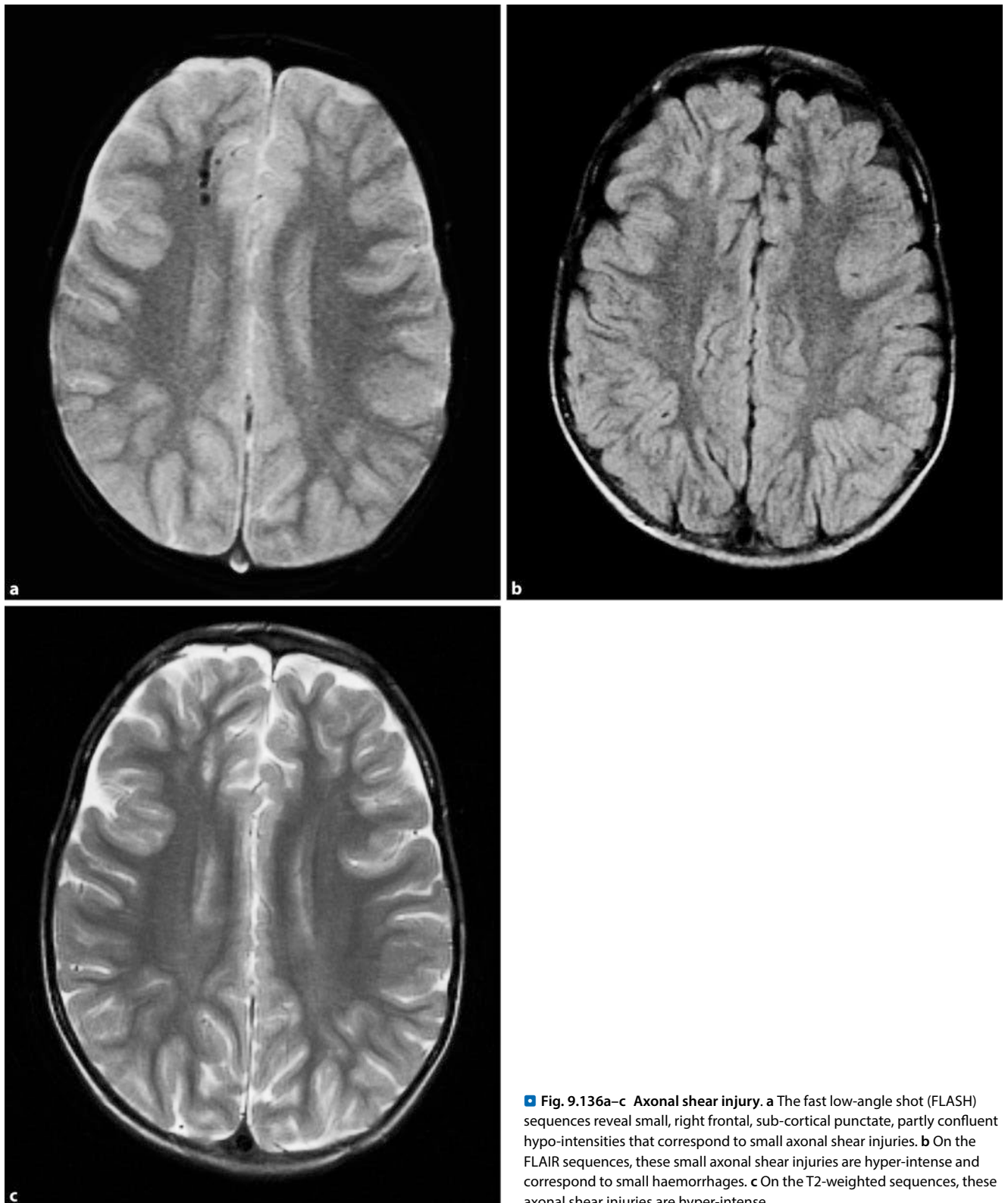


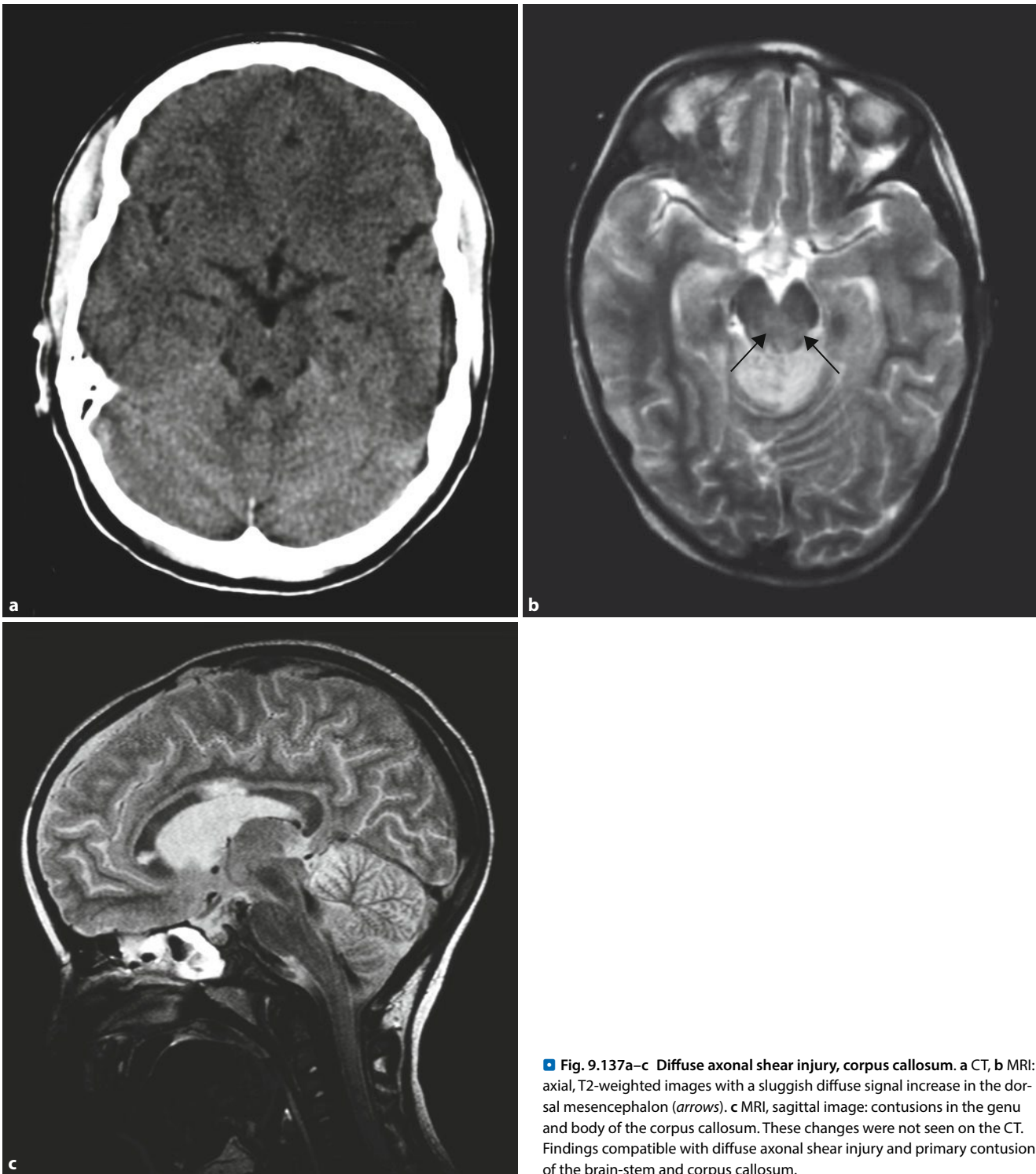
**Fig. 9.136a–c Axonal shear injury.** **a** The fast low-angle shot (FLASH) sequences reveal small, right frontal, sub-cortical punctate, partly confluent hypo-intensities that correspond to small axonal shear injuries. **b** On the FLAIR sequences, these small axonal shear injuries are hyper-intense and correspond to small haemorrhages. **c** On the T2-weighted sequences, these axonal shear injuries are hyper-intense

does not always have to be present; even chiropractic measures can lead to dissection.

#### ■ ■ Symptoms, Medical Imaging, Therapy

While vascular avulsions quickly become noticeable as a result of haemorrhaging and infarction, dissections can initially remain

asymptomatic and therefore go undetected. They only manifest through the outflow of thrombi with the occurrence of infarctions. Dissections of the carotid artery may be visible in the case of Horner's syndrome. If the vertebral artery is dissected, blood supply to the spinal cord can also be affected.



■ Fig. 9.137a–c Diffuse axonal shear injury, corpus callosum. a CT, b MRI: axial, T2-weighted images with a sluggish diffuse signal increase in the dorsal mesencephalon (arrows). c MRI, sagittal image: contusions in the genu and body of the corpus callosum. These changes were not seen on the CT. Findings compatible with diffuse axonal shear injury and primary contusion of the brain-stem and corpus callosum.

Dissections can be detected by means of **DSA** and **ultrasound**. On MRI T1-weighted sequences with fat suppression are applied; the intra-mural haematoma can thus be detected. On MR angiography, vascular occlusion can also be detected. **CT angiography** can also contribute to this.

Wall injury of the internal carotid artery in the region of the cavernous sinus can also lead to a carotid–sinus cavernous fistula. This fistula can become noticeable through proptosis, chemosis, and a pulse-synchronous noise in the case of auscultation in the

temple region. On sectional imaging, the asymmetrical representation of the ophthalmic vein, with marked ectasia of the affected side, is sometimes the only indication of such an injury. A Doppler investigation and DSA must then be performed.

The **preferred treatment** is embolisation with a fistula.

➤ **Patients who have suffered a penetrating trauma, especially gunshot wounds to the head, should be subjected to DSA because in approximately 12% of all cases, trau-**

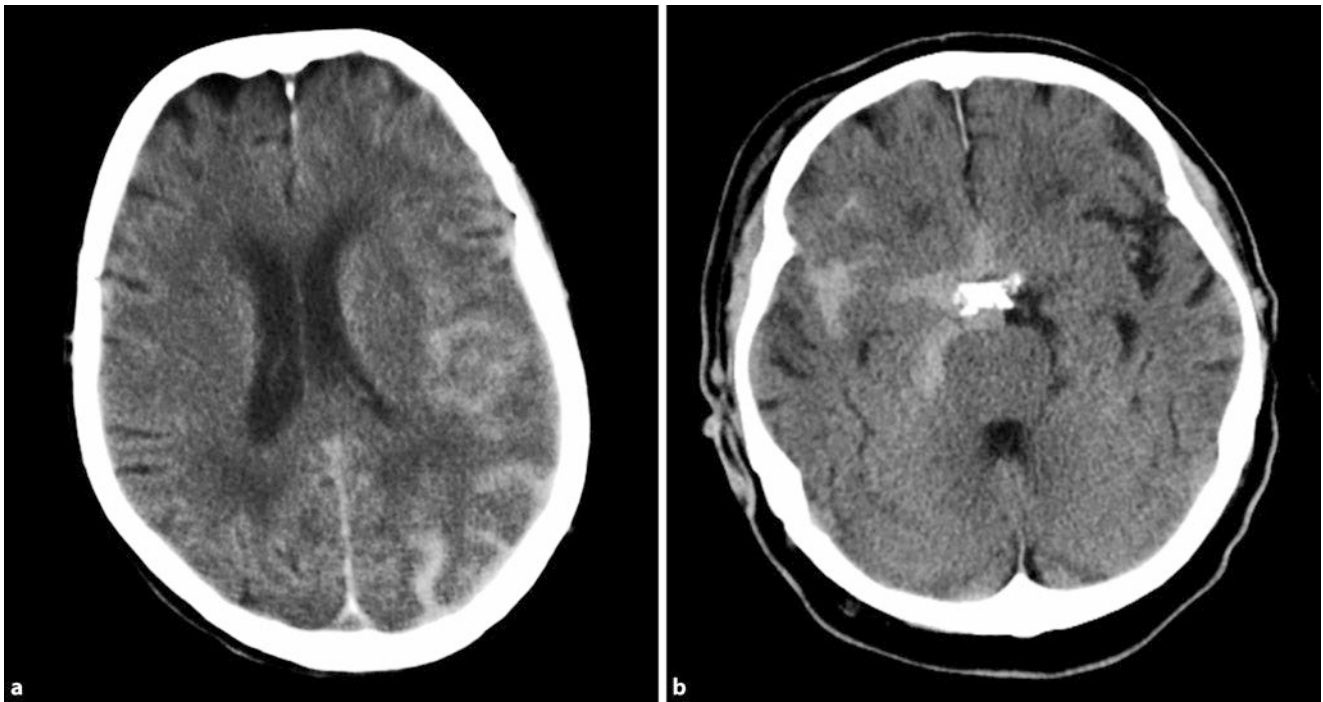


**Fig. 9.138a,b** Traumatic sub-arachnoid haemorrhaging. Unenhanced CT. **a** Evidence of blood in the left temporo-occipital sulci. **b** Less than traumatic

sub-arachnoid haemorrhaging in the right Sylvian fissure with expansion into the basal cisterns. (From: *Radiologist* 2008; 43:509, Fig. 4a, b)

**matic aneurysms and fistulas can form in these patients as a result of direct vascular injury. The investigation should be completed within 14 days of the trauma.**

#### ■ Intra-ventricular Haemorrhaging

##### ■ Epidemiology, Aetiology

Intra-ventricular haemorrhaging is noted in only about 1–5% of all patients with traumatic brain injury and almost always associated with other primary intra-axial injuries. In almost every case, intra-ventricular haemorrhaging indicates the presence of severe cranio-cerebral trauma (■ Fig. 9.140). The prognosis is correspondingly poor.

A rupture of sub-ependymal veins, shear injuries and haemorrhaging in peri-ventricular areas of the brain with intrusion into the ventricular system can lead to intra-ventricular haemorrhaging (in comparison, ■ Fig. 9.73 shows spontaneous intra-ventricular haemorrhaging). On CT, haemorrhaging appears as hyper-dense blood accumulation in the ventricles; air–fluid levels are possible. It should be noted that tamponading the lateral ventricle, the aqueduct, or the fourth ventricle can result in obstructed CSF flow. In this case, the implantation of a ventricular catheter may be necessary. Acute hydrocephalus, however, is rarely observed.

#### ■ Medical Imaging

In a patient with intra-ventricular haemorrhaging, shear injury with contusion of the brain-stem and the corpus callosum should always be ruled out by means of MRI. Approximately 60% of all contusions of the corpus callosum and 50% of all diffuse axonal shear injuries are accompanied by ventricular haemorrhaging.

#### ■ Cranial Nerve Injury

Damage to the cranial nerves with corresponding deficits may be caused by two mechanisms in the context of a brain-stem injury:

- Through direct damage to the nerves
- By damage to the core region of a nerve

In general, cranial nerve palsies may occur in fractures in the area of the bony canals (e.g. optical and facial canal) or in fractures at the base of the skull (e.g. nerves of the ocular muscles in the cavernous sinus or olfactory nerve in a fracture of the lamina cribrosa). In the case of herniation syndromes, the trochlear nerve can be compressed against the free edge of the tentorium, thereby becoming damaged.

### 9.5.4 Secondary Consequences of Trauma

Primary injuries often involve typical secondary consequences of trauma. These include:

- Focal or generalised cerebral oedema
- Herniation syndrome
- Secondary cerebral infarction or haemorrhaging
- Infections

As an ambient reaction, contusions, shear injuries, or ischaemic areas often manifest as focal oedema. Generalised swelling occurs in about 10–20% of all cases of severe cranio-cerebral traumas. If they lead to a considerable increase in intra-cranial pressure, the mortality rate rises to 50%. Generalised cerebral oedema can also occur without visible intra-cranial injuries (e.g. as a result of cerebral hypoxia in the context of an accident). Generalised brain



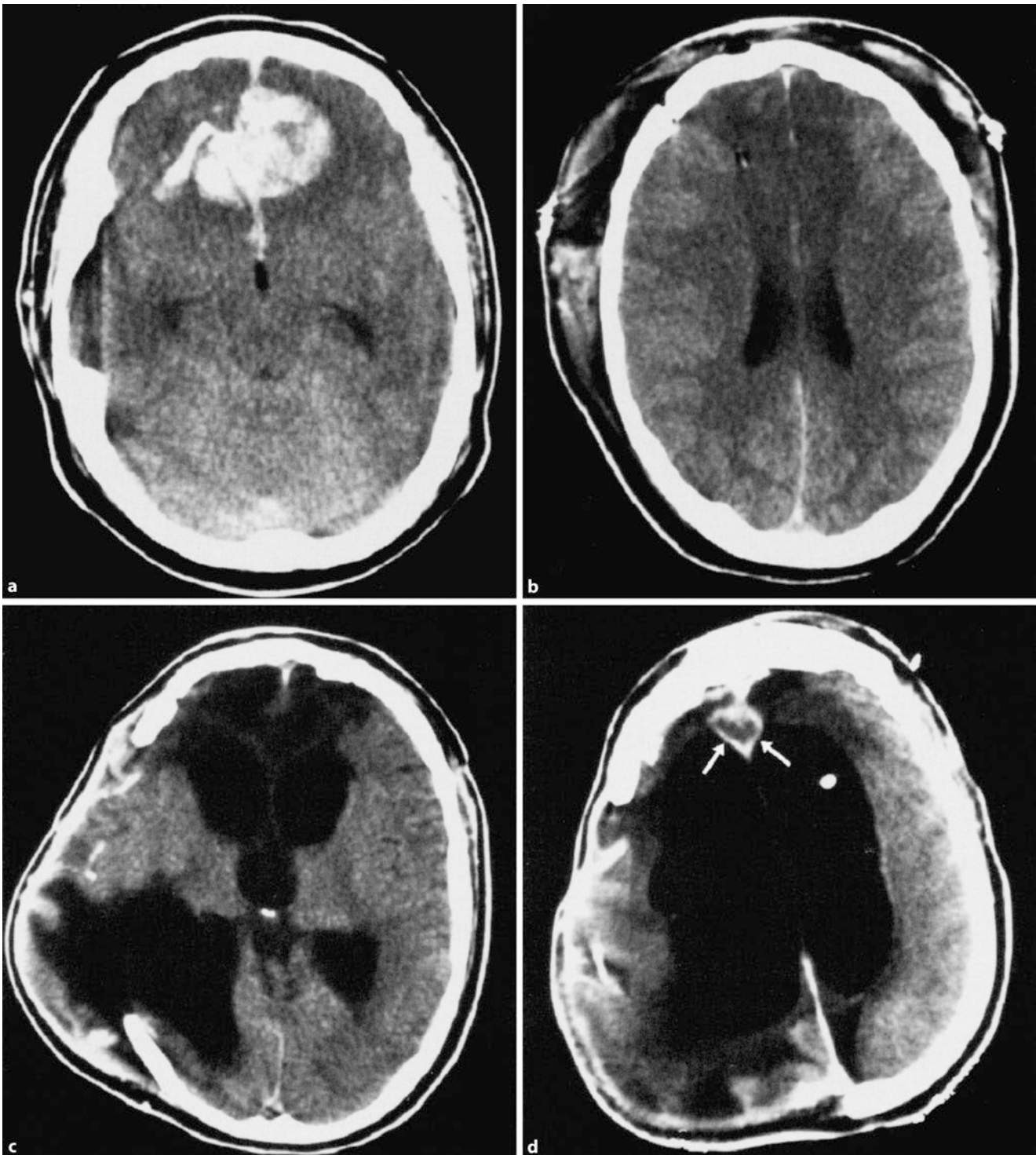
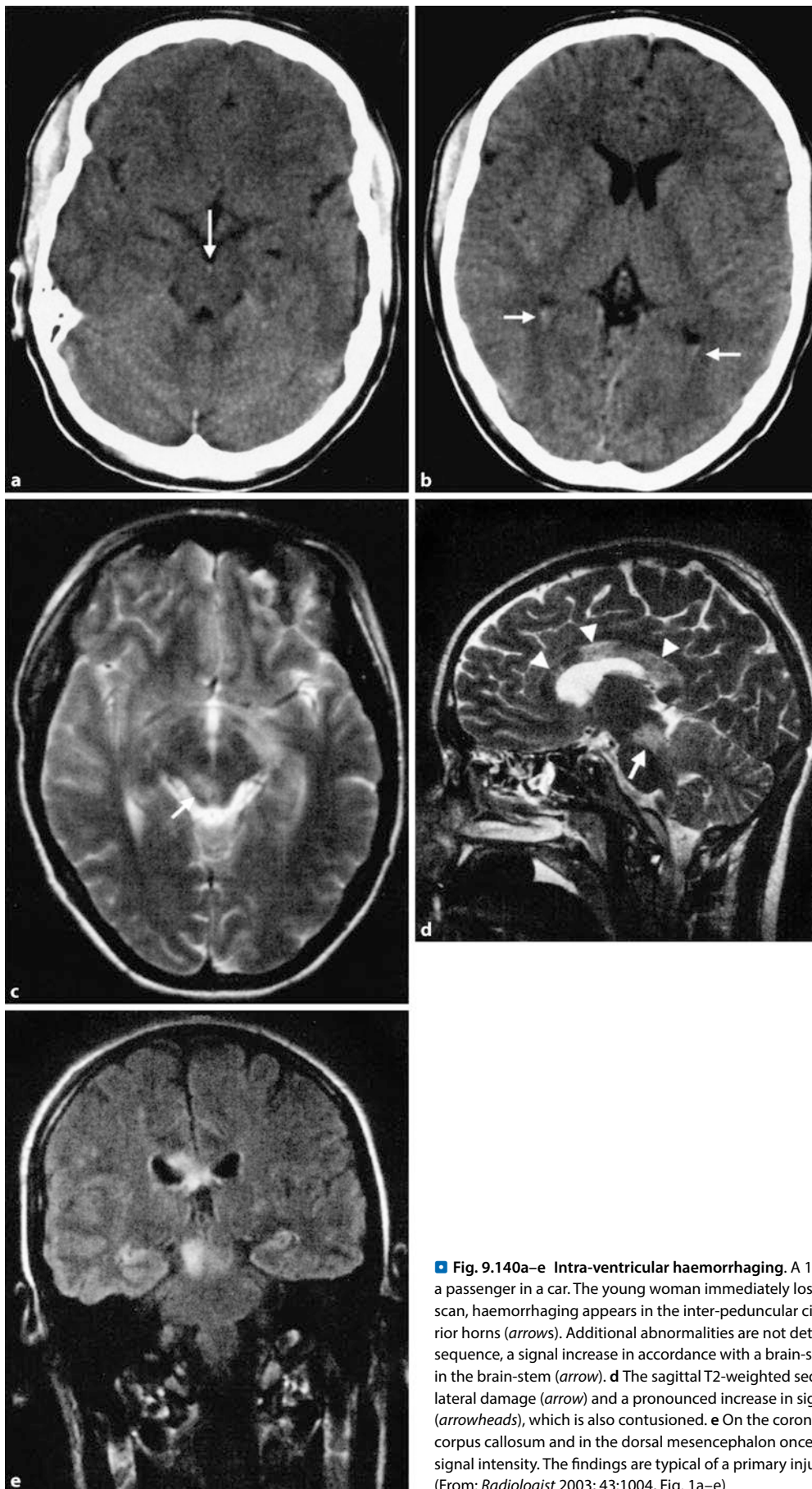


**Fig. 9.139a–d Traumatic vascular injury.** a Penetrating trauma to the skull base with the formation of bilateral fronto-basal haemorrhaging. b Intra-operatively: bilaterally lacerated anterior cerebral artery resulting in bilateral infarcts. c In the further course, formation of a post-traumatic hydrocephalus and post-malacic defects in the anterior distribution area on

both sides. d In the course of clinical deterioration in condition and fever: after the administration of a contrast agent, marginal fronto-basal lesions (arrows) corresponding to an abscess are visible. (From: *Radiologe* 2003; 43:1012, Fig. 8a–d)



**■ Fig. 9.140a–e Intra-ventricular haemorrhaging.** A 19-year-old woman had an accident as a passenger in a car. The young woman immediately lost consciousness. **a, b** On the initial CT scan, haemorrhaging appears in the inter-peduncular cistern (*arrow*). Blood in both posterior horns (*arrows*). Additional abnormalities are not detectable. **c** On the axial T2-weighted sequence, a signal increase in accordance with a brain-stem contusion appears dorso-laterally in the brain-stem (*arrow*). **d** The sagittal T2-weighted sequence once again reveals the dorso-lateral damage (*arrow*) and a pronounced increase in signal intensity of the corpus callosum (*arrowheads*), which is also contused. **e** On the coronal FLAIR sequence, the injury in the corpus callosum and in the dorsal mesencephalon once again manifests as an increase in signal intensity. The findings are typical of a primary injury in the sense of an axonal injury. (From: *Radiologist* 2003; 43:1004, Fig. 1a–e)

oedema occurs twice as often in children as it does in adults. On CT and MRI, generalised cerebral oedema manifests with a diffuse density reduction and increased signal intensity of the cerebral tissue. The ventricles and the sub-arachnoid cisterns are narrow.

Cerebral swelling may result in herniation syndromes. Here, it is possible to differentiate between different **forms of herniation**:

- The most common is **sub-falcial herniation**. As a result of a unilateral, supra-tentorial space-occupying lesion, the cingulate gyrus and blood vessels under the falx are pressed to the opposite side. On the imaging, the rostral mid-line shift can be seen. If the ipsilateral ventricle is narrow, it may be contra-laterally extended by a blockage of the foramen of Monro. The A2 segments of the anterior cerebral artery are angiographically displaced.
- A bilateral supra-tentorial mass lesion, may result in a **caudal trans-tentorial herniation**. Here, the para-hippocampal gyrus and uncus are unilaterally or bilaterally caudally pressed into the tentorial incisure. On imaging, the supra-sellar and peri-mesencephalic cisterns appear to be narrowed. Compression of the oculo-motor nerve nucleus can lead to dilation of the pupils. The supra-sellar cistern is pressed, and the mid-brain and pons are caudally displaced. This can be best represented in sagittal orientation on MRI. An increase in intra-cranial pressure (e.g. generalised hypoxia), always leads to severe trans-tentorial herniation.
- In rare cases, the mass lesion in the posterior fossa may lead to a **rostral trans-tentorial herniation**. Here, the cerebellar vermis and cerebellar hemispheres are rostrally relocated to the tentorial incisure. The cisterna ambiens is compressed, and compression of the aqueduct can result in acute hydrocephalus.
- A **herniation of the cerebellar tonsils** is found in about half of all patients with caudal trans-tentorial herniation and in two thirds of patients with rostral trans-tentorial herniation. The cerebellar tonsils are displaced caudally into the foramen magnum, and the cisterna magna is compressed.

**Secondary Infarction or Haemorrhaging.** Cerebral infarction and haemorrhaging most often result from herniation syndrome. The branches of the anterior cerebral artery are often pressed against the falx (trans-falcial herniation, see above) or the posterior cerebral artery is pinched against the trans-tentorial edge (trans-tentorial herniation, see above). Infarcts in the basal ganglia arise when the perforating root ganglia arteries are pressed against the base of the skull. Because the brain-stem shifts caudally, the thalamo-perforating arteries from the P1 segment of the communicating artery and the posterior para-median pontine arteries can over-stretch and even tear. This may result in central ischaemia and/or haemorrhaging in the thalamus, mesencephalon and pons (Duret haemorrhage). This Duret haemorrhage is located centrally in the upper pons or in the mid-brain. Distinction from primary brain-stem contusion is possible because contusions are generally located dorso-laterally.

A compression injury with infarction or haemorrhaging of the contra-lateral peduncle arises if this is pressed against the tentorial edge (Kernohan lesion). Here, a reliable differentiation from a primary contusion lesion is not always possible.

Secondary brain infarctions can also be caused by emboli, vascular dissection, fat or air embolism, or venous thrombosis.

**Intra-cranial Infections.** Open cranio-cerebral trauma may result in intra-cranial infections. Open intra-cranial injuries are often recognisable by small intra-cranial air pockets. Smaller fractures of the sphenoid or cribriform plate and dural injuries are mainly assumed to be the cause. Possible infectious complications include meningitis, encephalitis, ventriculitis, sub-dural oedema, osteomyelitis and abscesses. Resulting traumatic CSF leaks are often the starting point for recurrent meningitis. Post-traumatic abscesses may occur even years after the trauma.

After traumatic brain injury, changes can be measured via MRI. These include focal or diffuse regional cerebral atrophy with coarsening of the sulcus, gyral atrophy and enlargement of the ventricular system. Contusion lesions can be detected as cortical gliosis or glial scars. Gliosis in the cerebral white matter results from shear injuries. Haemosiderin deposits, which are mainly seen on the T2\*-weighted gradient-echo sequences, are the result of haemorrhagic residues. Focal gliosis is often the origin of post-traumatic epilepsy, which may occur as a complication in approximately 4% of closed and over 50% of open intra-cranial injuries.

### 9.5.5 Child Abuse

#### ■ ■ Aetiology, Pathogenesis

A trauma is a common cause of death in childhood, and abuse is the most common cause of severe skull and brain injuries in young children. In 1946, in his historic study, Caffey first reported on abused children. In this first study on non-accidental trauma, Caffey reported key findings. These include metaphyseal fractures and intra-cranial injuries with SDH, and the fact that small children are involved. Among the patients, only one child was older than 12 months. In his work, Caffey had not yet clearly shown the pathomechanism of the injury. Because the morbidity and mortality correlate with the extent of intra-cranial injuries, bony injuries of the peripheral skeleton are not discussed any further here.

The common name of the syndrome in the literature attempts to map the aetiology of the injury, although the term "**shaken baby syndrome**" is often used. The infant is taken by the arms or body and shaken. Because of the particular anatomy described above, the head experiences significant accelerations and decelerations with rotational forces. In addition, in the context of abuse, the child can also be thrown against surfaces.

The **pathogenesis of infarcts** is still controversial. Phases of apnoea are discussed because the children are often shaken until they become unconscious and develop breathing disorders. Because of the pressure of the hands on the chest or the abdomen of the child, breathing movements can be impossible. Because unilateral infarcts occur in one third of cases, global hypoxia is

certainly not the only causative factor. The combination of mechanical trauma, haemorrhaging, hypoxia, and convulsions likely overburdens the compensatory capacity of the child's brain, thus resulting in cerebral swelling and the loss of neurons.

**Epidural haematomas** arise as an expression of local trauma to a defined area of the skull. This form of non-accidental trauma is also certainly possible in small children, although it is rather rare.

It is still debatable whether shaking alone can explain all the findings in these children. It is, however, generally accepted that traumas that affect the everyday life of an infant or toddler (e.g. falls from a low height), are not sufficient to trigger "shaken baby syndrome". It must not be forgotten that direct trauma is also possible and that not every mistreated child (especially in the case of older children) was shaken.

### ■ ■ Epidemiology

Epidemiologically, "shaken baby syndrome" only presents itself in children up to the age of 3 years; the vast majority of cases occur in the first 12 months of life. Incidences are reported differently, in children up to 2 years old, about 24% of all head traumas are said to be caused by abuse. Taking into consideration severe traumatic brain injury, this proportion increases significantly.

### ■ ■ Symptoms

In most cases, in the **medical history** no appropriate trauma but rather minor injuries are reported. The data are frequently unreliable and contradictory. The children suffer from cramps, vomiting, breathing problems, lethargy and nutritional disorders. The galea above the fontanelle may bulge as a result of an increase in intra-cranial pressure. In 40–70% of all cases, convulsions are observed. Retinal haemorrhaging is observed in up to 75% of all patients. This occurs either unilaterally or bilaterally; haemorrhaging in the vitreous humour and along the optic nerve or retinal detachments may also occur. It is important to note that retinal haemorrhaging may occur in up to 40% of all vaginal births; this is usually resorbed after 1 month. In the case of accidental trauma, this is much less likely to be detected. This is probably caused by venous hypertension.

Because the abuse is often recurrent, injuries of different ages are typical. SDH are the most common and most consistent finding in abused infants (■ Fig. 9.141).

### ■ ■ Medical Imaging

On **CT** bilateral **SDH** can be found. In the inter-hemispheric fissure, they also appear as typical hyper-dense and/or hypo-dense masses. The density of the haematoma depends on the age of the lesion. Sub-dural haemorrhaging in the posterior inter-hemispheric fissure is practically only observed in maltreated children and is virtually pathognomonic. SDH in infants are otherwise practically only observed in the case of massive trauma (e.g. a car accident). If there is no indication of trauma in an infant, abuse is assumed to be the cause.

Contusions and diffuse axonal injuries in addition to traumatic sub-arachnoid and intra-ventricular haemorrhaging also occur. On **CT**, especially in the latter case, this is often the only indication of diffuse axonal injury with involvement of the corpus callosum or the brain-stem.

On **MRI** these injuries can be represented more sensitively. They contribute to the development of cerebral atrophy with a poor prognosis. Acute brain swelling can occur with a loss of the corticomedullary border and the formation of encephalomalacia defects.

Magnetic resonance imaging is sensitive in the detection of narrow sub-dural haematomas, but is also more sensitive in the detection of surface contusions. It can establish the repeated nature of ill-treatment in SDH by detecting the varying signal behaviour of the different blood degradation products. Non-haemorrhagic axonal shear injuries can also only be represented via MRI.

A **cranial survey radiograph** is indicated in cases of suspected ill-treatment. When X-ray survey radiograph images show simple linear fractures, especially parietal ones, this is non-specific. Multiple or complex fractures, bilateral fractures and fracture lines that cut across the sutures are, however, typical. Approximately 50% of children show cranial fractures. A soft-tissue swelling of the galea may obscure a depressed fracture on clinical inspection.

If there is **any suspicion of "shaken baby syndrome"** a CT must be carried out immediately to exclude large space-occupying haematomas. Because of its greater sensitivity MRI is always indicated for diffuse axonal injuries or narrow SDH. Cranial survey radiographs and scintigraphy of the skeleton are also part of the examination programme.

➤ **Whenever there is a suspicion of child abuse, it is forensically important to document all injuries. The suspicion must be communicated to the colleague in charge of treatment without delay. The child should without fail be admitted to the hospital for further diagnosis and possible therapy, so that a secure environment can be created.**

## 9.6 Inflammatory Diseases of the Brain

Inflammatory diseases of the brain involving the meninges (meningitis) can be differentiated. Here again, both acute and chronic meningitis in addition to septic and aseptic meningitis can be distinguished. Furthermore, a distinction is made between encephalitis and in cases that involve the meninges, meningoencephalitis. Moreover, cerebritis can develop if the brain parenchyma is involved.

The **nomenclature of CNS infections** is organised according to the site of the inflammation. The following distinctions are made:

- Meningitis: inflammation of the meninges, usually the lepto-menix
- Encephalitis/cerebritis: inflammation of the parenchyma
- Meningo-encephalitis: mixed form, mostly spreading from the meninges to the adjacent parenchyma
- Empyema sub-dural empyema: in general, an empyema in a pre-formed cavity
- Abscess: localised inflammation with capsule and abscess cavity
- Ventriculitis: inflammation of the ependyma with/without intra-ventricular pus

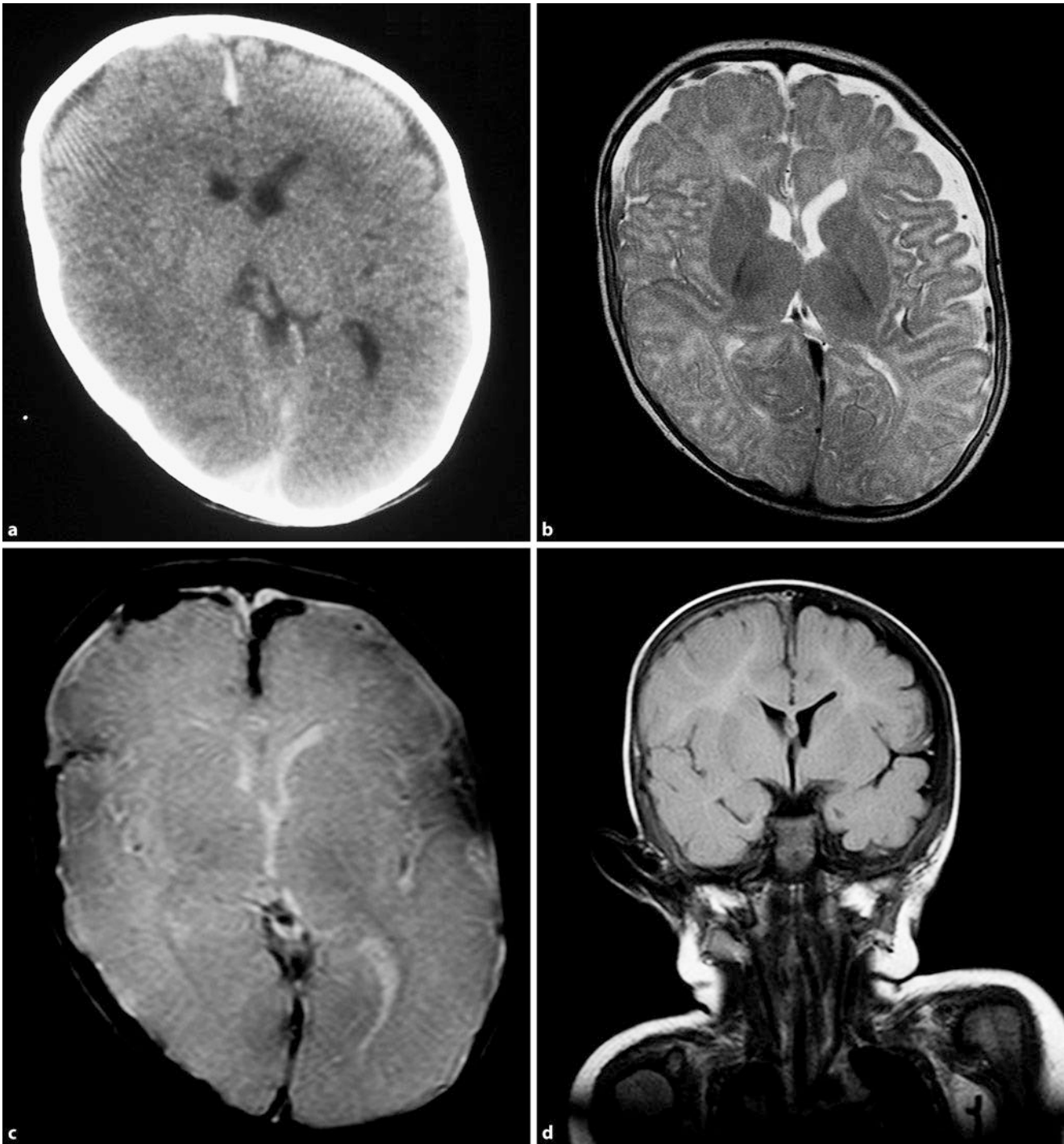


**Fig. 9.141a–d Child abuse.** A 16-month-old child with diminished awareness. The parents reported a fall from a changing table. **a** On the CCT a small sub-dural haemorrhage is shown in the right frontal region, in the anterior inter-hemispheric fissure and on the right on the tentorium. **b** On the T2-weighted MRI the fresh sub-dural haemorrhage shows in the right frontal region in addition to a widening of the external CSF spaces above

the left hemisphere. **c** The T2\* images show the haemorrhage in the right frontal region in addition to the anterior inter-hemispheric fissure and on the tentorium on the right as a hypo-intense space-occupying lesion. **d** On the coronal T1-weighted images the iso-intense sub-dural haemorrhage and the older sub-dural CSF-iso-intense haemorrhage are clearly visible

## 9.6.1 Meningitis

### ■ ■ General

Epidemiology, Aetiology Meningitis is the most common inflammatory disease of the CNS. Meningitis is divided into acute and chronic (hours to a few days versus weeks to months) and purulent or septic and non-purulent or aseptic (with/without granulocytic CSF changes) forms. Acute aseptic meningitis occurs with an incidence of 10–30 per 100,000 people per year. Children are usually affected, mainly in the summer months. The most common causes of aseptic meningitis are viruses. The most common representatives are enteroviruses (echo, coxsackie, Epstein–Barr and arbo viruses).

The **pathogen spectrum** of purulent meningitides is broad; in principle, almost all systemic infections can trigger meningeal involvement. A diagnosis of the pathogen is desirable, but not always successful and often takes too long. In fulminant clinical pictures the patient's life is in acute danger; thus, therapy must begin before the blood/CSF culture is available.

The most common pathogens of purulent meningitis are *Haemophilus influenzae* (septic meningitis) in children < 7 years of age, *Neisseria meningitidis* in older children and *Streptococcus pneumoniae* in adults. The so-called chronic meningitis is caused by tuberculosis or fungi.

A rapid classification of the genesis can be performed by laboratory chemical CSF analysis ■ Table 9.15).

### ■ Acute Bacterial Meningitis

#### ■ ■ Aetiology

The pathogen spectrum of acute bacterial meningitis is age-dependent. The most common pathogen in children and adults is *Neisseria meningitidis*; *Streptococcus pneumoniae* predominates in adults > 50 years (see above). In the peri-natal period purulent meningitis is mainly caused by germs located in the maternal birth canal. The incidence of meningitis caused by *Haemophilus influenzae* has declined by > 80% since the introduction of standardised serial inoculation in 1990. Currently, Hib meningitis effectively plays only a subordinate role.

#### ■ ■ Symptoms

Bacterial meningitis must be considered a **neurological emergency**; mortality is about 25%, morbidity 60%. Clinically, fever, headache, severe photophobia and meningism up to opisthotonus. Convulsions may occur. Within a few hours patients' consciousness can become impaired and they can become comatose. The prognosis correlates with the initial level of consciousness and the time at which therapy is initiated. Overall, the prognosis has been improved in recent years thanks to better intensive medical therapy.

Septic meningitis can occur per continuitatem from a nearby infection site, such as sinusitis, otitis, haematogenously, or via the CSF. They occur less frequently after penetrating trauma and injuries of the dura, such as in neuro-surgery or ENT operations. The pathogens first cause neutrophilic granulocytes to appear. Collections of pus may form in the sub-arachnoidal and sub-pial spaces, which lead to agglutination of the surface.

■ Table 9.15 Cerebro-spinal fluid (CSF) changes in meningitis

	Bacterial meningitis	Viral meningitis	Tuberculous meningitis
CSF	Cloudy	Clear to opal	Spider's web clot
Cell count	> 300/μl	< 100/μl	20–300/μl
Cell type	Granulocytes	Lymphocytes	Lymphocytes
Glucose	Decreased < 40 mg/dl	Normal	Decreased < 40 mg/dl
Protein	Elevated > 120 mg/dl	Normal: < 120 mg/dl	Elevated: > 120 mg/dl
Lactate	Elevated > 3.5 mmol/l	Normal: < 3.5 mmol/l	Elevated: > 3.5 mmol/l

In the accompanying vasculitis secondary circulation disorders can occur.

The clinical symptoms associated with **incipient brain abscesses** as a complication of acute bacterial meningitis (see below) is often non-specific, especially in immunosuppressed patients.

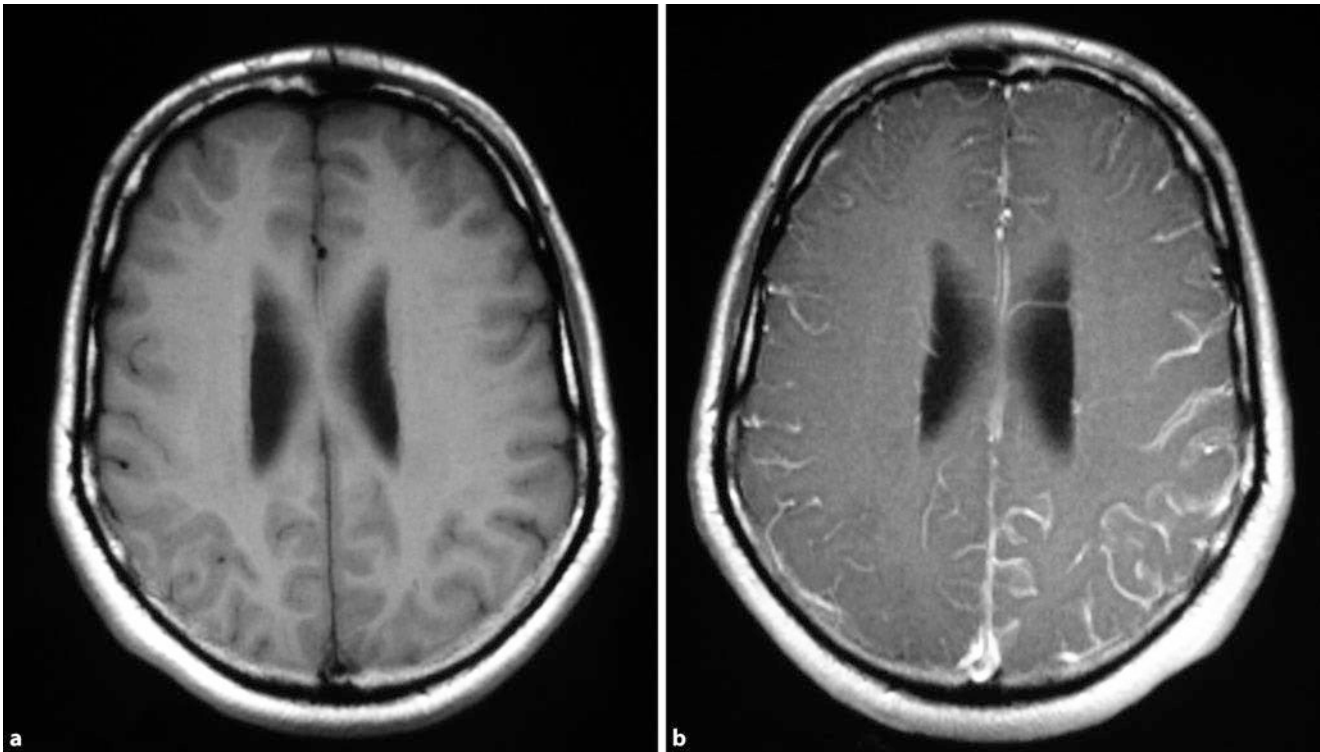
### ■ ■ Clinical Diagnosis

In cases of suspected bacterial meningitis blood and CSF cultures are set up for diagnostic purposes; however, the calculated antibiotic treatment usually begins before the results are in based on an anticipated pathogen spectrum. Once the pathogen has been identified and the susceptibility testing results are in the therapy is then adjusted.

**Medical Imaging.** In septic meningitis medical imaging is often normal; however, increased contrast agent uptake in the lepto- or pachymeninges can be detected (■ Fig. 9.142). In septic and chronic meningitis a thickening of the lepto-meninges may be detectable on T1-weighted images after administration of the contrast agent. If hyper-intensity can be detected in the adjoining brain parenchyma on the FLAIR and T2-weighted sequences, this indicates the spread of the inflammation to the brain parenchyma in accordance with encephalitis. These inflammatory cross-reactions of the meninges and the brain parenchyma are dependent on the location and entry portal of the pathogen. In basal tuberculosis these changes are particularly detectable at the skull base. In this case, it results in early vasculitic changes with corresponding stenoses and occlusions of the basal vessels. In these vasculitic cross-reactions attention must also be paid to brain infarctions, which are detectable as hyper-intensity on diffusion-weighted images. The diagnostically absolutely necessary lumbar puncture should be performed after imaging to detect increased intra-cranial pressure and the risk of entrapment during the puncture in good time.

### ■ ■ Differential Diagnosis

Increased contrast agent uptake in the lepto-meninges may also occur as part of a CSF leak syndrome and after the removal of CSF. In cases of carcinomatous meningitis contrast agent enrichment may occur in the meninges. The meninges are rarely af-



■ **Fig. 9.142a,b Meningitis.** A 68-year-old patient with acute headache, fever and disturbed consciousness. In the lumbar puncture, there are 5,000 granulocytes/ $\mu$ l, the culture was positive for pneumococci. **a** Unenhanced T1-weight-

ed image: inconspicuous. **b** T1-weighted image post-contrast agent: strong cortical and gyral vascular left parietal injections with thickened, strong contrast agent-affine meninges

ected by a lymphoma. The differential diagnosis of other infectious diseases, such as tuberculous meningitis, fungal diseases and non-purulent meningitis from rheumatic conditions, sarcoidosis (see below, ■ Fig. 9.148) and idiopathic pachymeningitis must be considered. In sub-dural hygroma, which are typically iso-intense to CSF, contrast agent uptake is not usually increased in the adjacent meninges.

#### ■ ■ Complications

One of the complications of purulent meningitis is the **sub-dural empyema** (■ Fig. 9.143; see below, ► Sect. 9.6.2). On the CT, a sub-dural empyema is depicted as hypo-density. On the T1-weighted sequences after contrast agent administration, it is usually hypo-intense. The adjacent tissue layers strongly absorb the contrast agent. The contents of the empyema appear, depending on the protein content, usually hyper- or iso-, and more rarely hypo-intense on FLAIR and T2-weighted images.

With septic meningitis **cerebritis and the formation of a brain abscess** may occur (see below, ► Sect. 9.6.2).

#### ■ Viral Meningitis

##### ■ ■ Epidemiology, Aetiology

Acute aseptic meningitis occurs with an incidence of 10–30 per 100,000 people per year and is generally caused by a virus. Children are usually affected, and there is a seasonal increase during the summer months. The most common causative agents are enteroviruses (echo and coxsackie viruses), but also *Herpesviridae* (herpes simplex virus [HSV] I most frequently; however, meningo-encephalitis and EBV also occur) and arboviruses.

#### ■ ■ Symptoms, Therapy

Clinically, fever, headache, photophobia and meningism are the leading symptoms; however, compared with bacterial meningitis the symptomatology is less pronounced. Overall, viral meningitis is usually part of a systemic infection and disease progression is self-limiting in the immunologically healthy as in the underlying disease (mostly respiratory or stomach/intestinal infections). Defect states are rare. A specific therapy is rarely possible or necessary. Supportive measures, such as pain and volume therapy, are useful.

#### ■ ■ Special Form: Tick-borne Encephalitis

The endemic form of viral meningo-encephalitis is triggered by the tick-borne encephalitis (TBE) virus, i.e. a single-stranded RNA virus of the *Flaviviridae* family. The virus multiplies in the salivary glands of ticks and is transferred via the vector during the bite.

In about 70–90% of cases the infection is asymptomatic; symptoms of a flu-like infection occur in only about 10–30%. In 10% of symptomatic patients, a renewed increase in fever occurs approximately 1 week after the defervescence, which is accompanied by signs of meningeal irritation. In the further course disturbances of consciousness progressing to coma and paralysis may occur. The disease is usually self-limiting over some weeks or months and usually leads to a *restitutio ad integrum*.

Tick-borne encephalitis is a notifiable disease in Germany. The Robert Koch Institute issues annual recommendations, e.g. exposure protection and vaccinations in endemic areas.

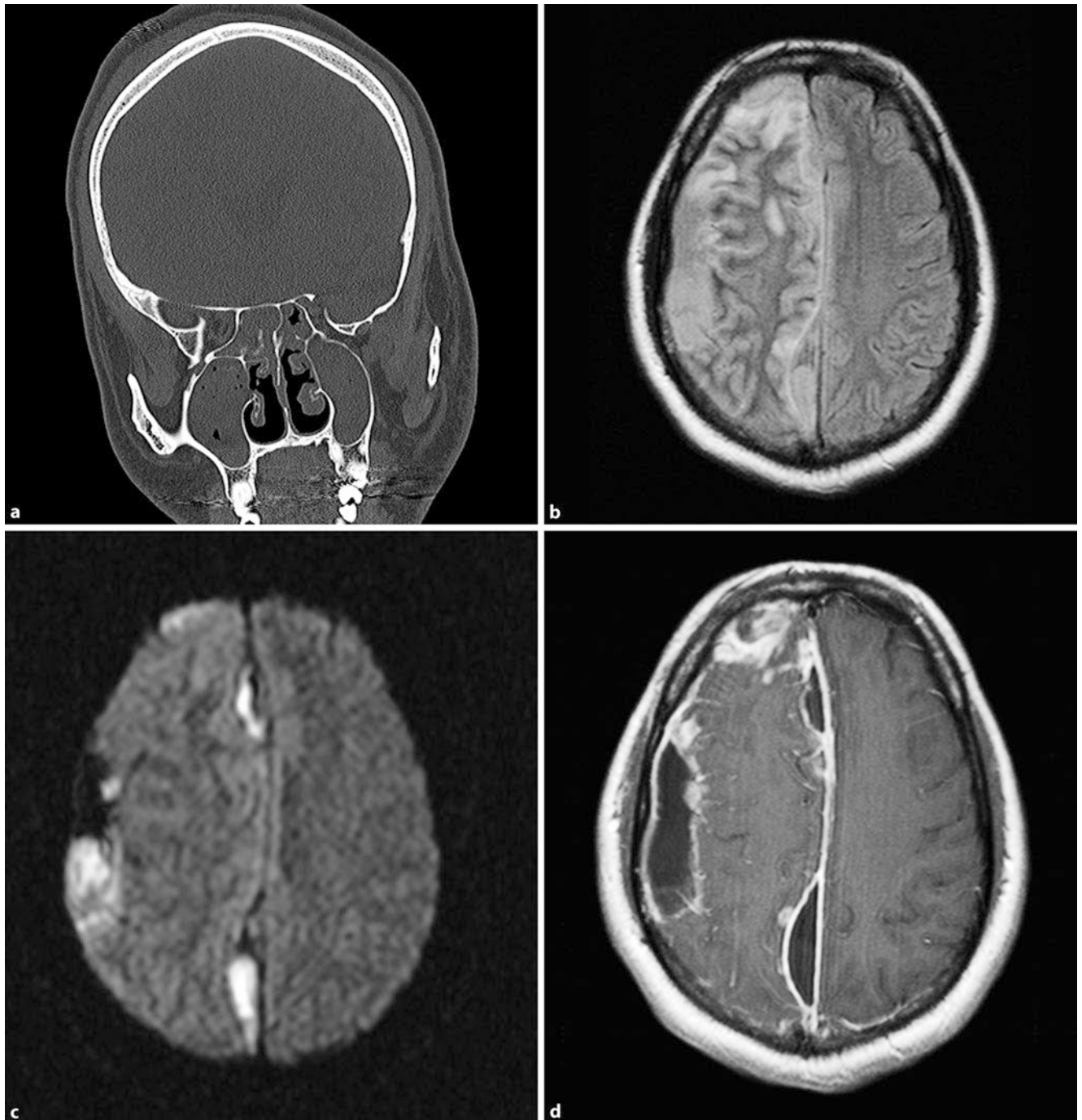


**Fig. 9.143a–d Empyema.** A 29-year-old patient with a history of chronic sinusitis. Acute headache, somnolence, high fever. **a** CCT of the coronary bone space: extensive para-nasal sinusitis with sub-total shading of all para-nasal sinuses; the bony lamella of the frontal skull base is not safely intact. **b** Axial FLAIR sequence: widening of the inter-hemispheric gap by hyperintense (protein-rich) material with accompanying oedema of the adjacent

cortex. **c** Axial diffusion weighting: a signal increase in the inter-hemispheric fissure. **d** Axial T1-weighted post-contrast agent: marginal contrast agent uptake as concomitant meningitis; empyema is hypo-intense, larger areas of uptake in the right frontal region in accordance with cerebritis, which has merged into an abscess over the course of time (not shown)

#### ■ Chronic Meningitis

So-called chronic meningitis is caused by tuberculosis (► Sect. 9.6.3) or fungi. Unlike the partially fulminant acute forms of meningitis, the chronic form shows slow, non-specific progression. Leading clinical symptoms are headache and changes in personality; focal deficits, seizures and decreased vigilance are rare.

#### 9.6.2 Complications in Meningitis or Intra-cerebral Infections

- Abscess
- Epidemiology

In the literature the incidence of brain abscess is recorded at about 1/100,000 people/year. Men are affected 2 to 3 times more



often than women, and the disease occurs more frequently in the 3rd to 4th decade of life. Often, more than one agent can be detected. Owing to the increasing number of immunosuppressed individuals (acquired immunodeficiency syndrome, AIDS, bone marrow or organ transplantation patients), the incidence is rising.

#### ■ ■ Aetiology, Pathogenesis

Most abscesses arise per continuitatem, with sinusitis or otitis (■ Fig. 9.144); in approximately 10% of cases they are caused by dental abscesses in the area of the molars. A highly infectious thrombo-phlebitis is responsible for this. The pathogen spectrum covers the organisms located in the oro-pharyngeal area and invasive fungi, e.g. *Candida* spp. and *Aspergillus* spp. In 70% of cases brain abscesses are caused by streptococci, in 10–30% by staphylococci. Gram-negative bacteria are found in approximately 10–20% of patients.

Twenty per cent of all brain abscesses occur haematogenously in bacterial endocarditis or suppurative pneumonia (so-called septic encephalitis). Often the septic source of the infection cannot be located. Congenital cyanotic heart disease, pulmonary vascular malformations and other diseases carry an increased risk of septic encephalitis. In new-borns bacterial meningitis, usually involving Gram-negative bacteria, can also lead to brain abscesses.

The **abscess development** occurs in different phases (■ Fig. 9.145, ■ Table 9.16). After the invasion of bacteria polymorphonuclear granulocytes find their way into the brain parenchyma from the local capillary bed to the infection focal point. In the early phase of cerebritis no capsule formation can yet be seen; it is difficult to delimit the cerebritis in the surrounding brain parenchyma. This stage lasts about 3–5 days; following on, from the 4th to 14th day, is the late stage of cerebritis. At this stage, smaller areas of necrosis merge into larger ones and the inflammation is circumscribed even more strongly around its focal point. Vascular proliferations, macrophages, granulation tissue and fibroblasts now present as peri-focal. In the early capsule stage towards the end of the 2nd week after the infection, the abscess capsule forms from collagen and reticulin fibres. At the late capsule stage, which may persist for weeks and months, this capsule is complete and consists of an inner layer with inflam-

matory cells, a middle collagen layer and an outer gliosis layer. The chronological progression from the early cerebritis to the late capsule stage is not uniform, but rather depends on the immunological state of the patient and the start of antibiotic therapy.

#### ■ ■ Symptoms, Therapy

The clinical symptoms at the onset of brain abscess are often non-specific, especially in immunosuppressed patients. Along with fever, headache and focal neurological deficits altered states of consciousness and cranial nerve deficits can also occur, especially with septic meningitis. The therapy consists of antibiotics and neurosurgical relief of the abscess. The choice of antibiotics depends on the results of the micro-biological tests. Mortality from brain abscesses before the introduction of a specific antibiotic therapy was 100% and is still 8–10% today. In immunosuppressed patients, especially in organ and bone marrow transplant patients, the mortality rate is still about 90%, even today.

#### ■ ■ Medical Imaging

**Brain abscesses are most commonly detectable** in the frontal and parietal lobes at the cortico-medullary junction (■ Fig. 9.145). Approximately 15% of brain abscesses occur infratentorially. Multiple abscesses mainly show up in immunosuppressed patients. In the early phase of cerebritis a rather poorly circumscribed focal cerebral oedema presents, with increased signal intensity on the T1- and T2-weighted sequences and FLAIR images. After contrast agent administration, if anything, heterogeneous patchy enhancement appears without ring-shaped contrast agent enhancement. Then in the later stages of cerebritis there is increasingly better demarcation of the abscess membrane. On the T1-weighted images after contrast agent administration, the contrast agent usually appears to be strongly and homogeneously absorbed. The abscess cavity is usually hypo-intense on the T1-weighted sequences, hyper-intense on the T2- and FLAIR-weighted sequences. Peri-focally, mostly finger-like oedema with signal increases on the T1-, T2- and FLAIR sequences is also detectable. The contrast agent-absorbing abscess membrane is usually thinner on the side closer to the ventricles than on the cortex-facing one.

Multiple abscesses are common in patients with systemic diseases, such as lymphoma or leukaemia. Under successful antibi-

■ **Table 9.16** Timing of the abscess formation

Phase	Event	Image correlate	Period of time
Early cerebritis	Pathogen invasion, local leucocyte transmigration	Diffuse parenchyma infection poorly definable	1st to 4th day
Late cerebritis	Merging of smaller areas of necrosis into a later abscess cavity, peri-focal vascular proliferation, accumulation of macrophages and fibroblasts, granulation tissue	Inflammation is more highly circumscribed	4th to 14th day
Early capsule stage	Formation of the abscess capsule from collagen and reticulin fibres	Formation of the abscess capsule	2nd to 3rd week
Late capsule stage	Three-layered capsule – Internal inflammatory cells – Collagen middle – External gliosis zone	Good local definability, strong contrast agent-affine capsule	Weeks to months

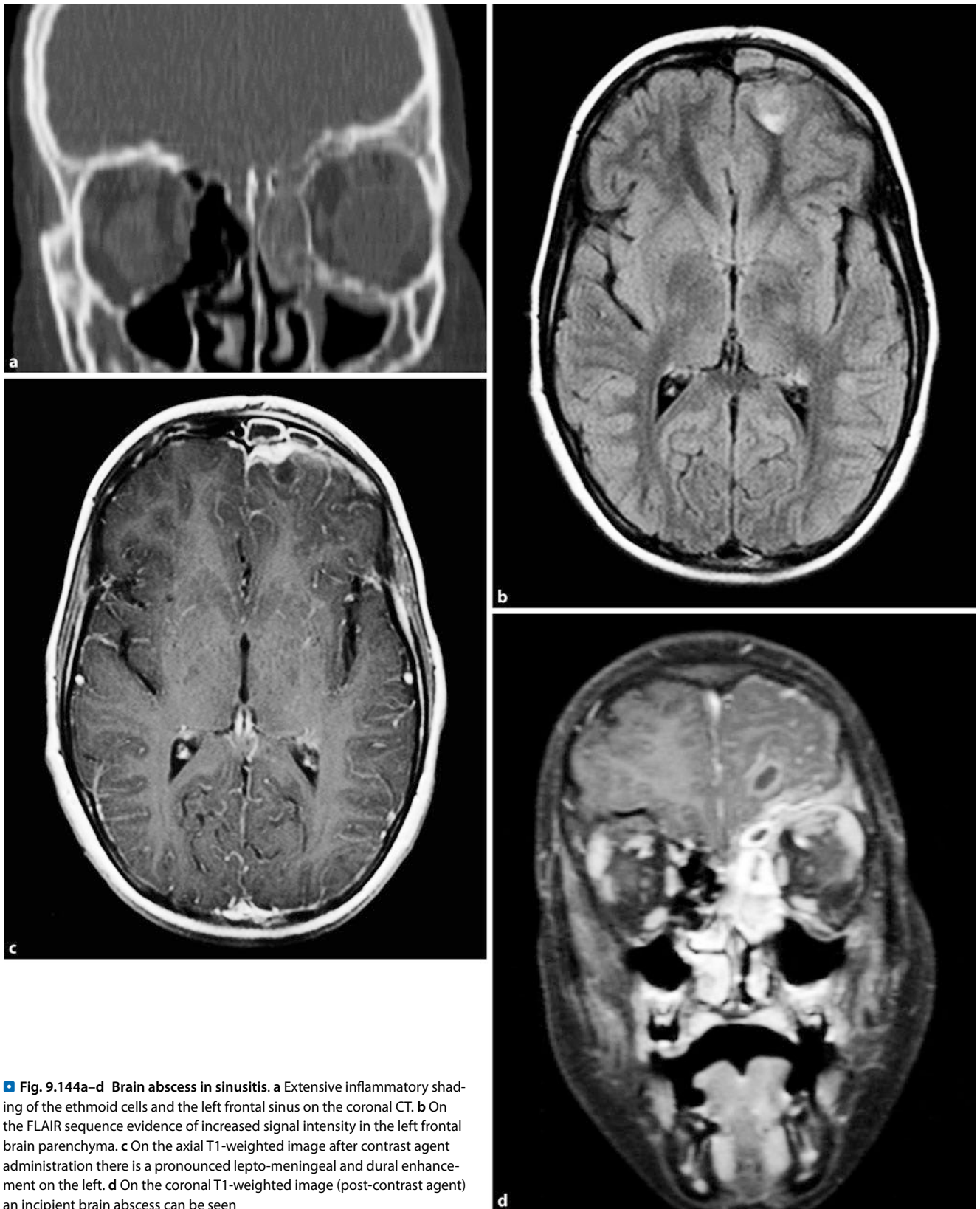
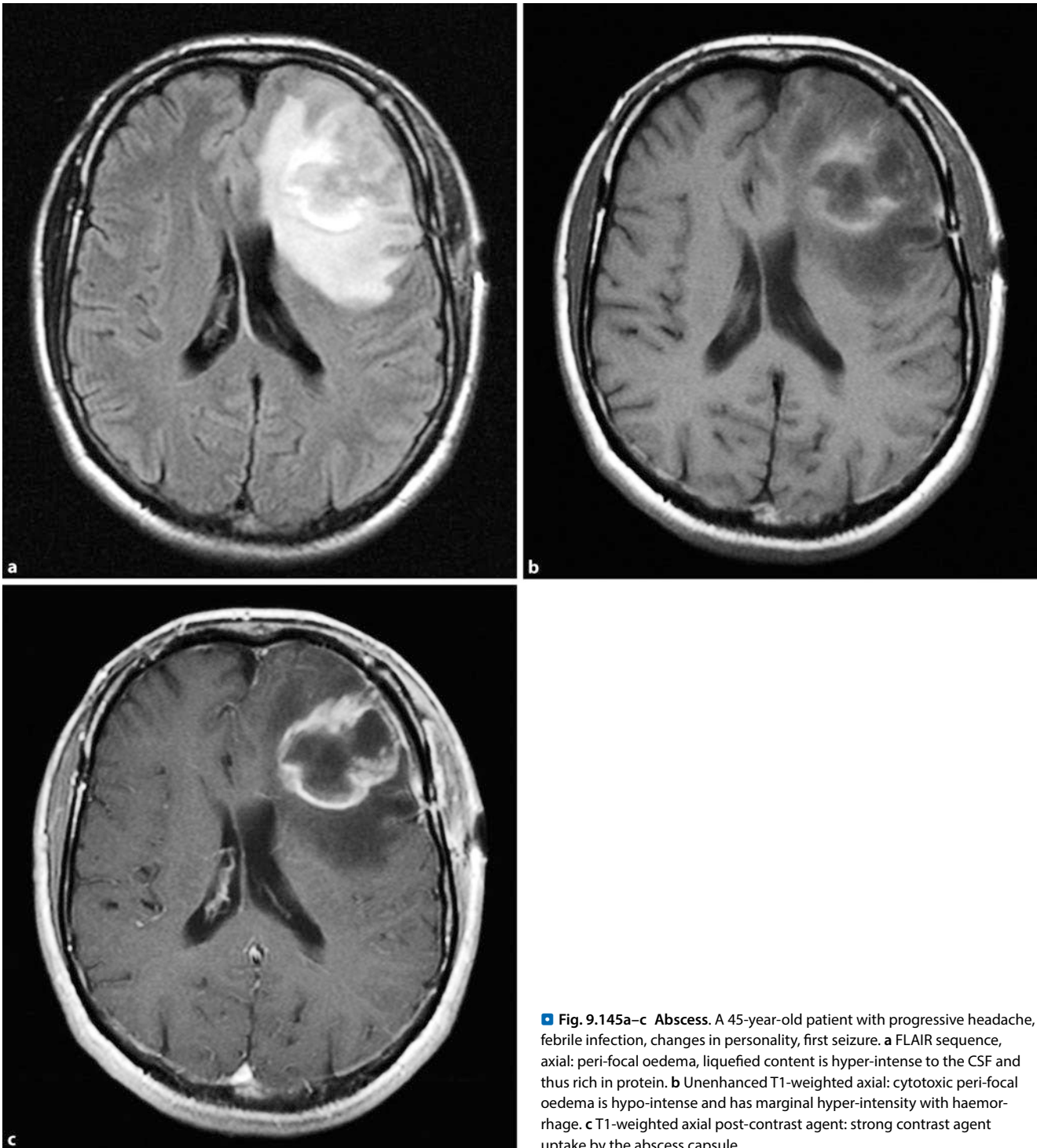


**Fig. 9.144a–d Brain abscess in sinusitis.** **a** Extensive inflammatory shading of the ethmoid cells and the left frontal sinus on the coronal CT. **b** On the FLAIR sequence evidence of increased signal intensity in the left frontal brain parenchyma. **c** On the axial T1-weighted image after contrast agent administration there is a pronounced lepto-meningeal and dural enhancement on the left. **d** On the coronal T1-weighted image (post-contrast agent) an incipient brain abscess can be seen



■ **Fig. 9.145a–c Abscess.** A 45-year-old patient with progressive headache, febrile infection, changes in personality, first seizure. **a** FLAIR sequence, axial: peri-focal oedema, liquefied content is hyper-intense to the CSF and thus rich in protein. **b** Unenhanced T1-weighted axial: cytotoxic peri-focal oedema is hypo-intense and has marginal hyper-intensity with haemorrhage. **c** T1-weighted axial post-contrast agent: strong contrast agent uptake by the abscess capsule

otic treatment, the hyper-intense ring on the T2-weighted images recedes within days.

#### ■ ■ Complications

Complications of a brain abscess are the formation of other abscesses, the development of purulent meningitis or **ependymitis** or **ventriculitis**. In ependymitis or ventriculitis an agglutination of the meninges may occur, leading to the formation of hydrocephalus. Ventriculitis (■ Fig. 9.146, see above) results most commonly from the implantation of CSF drainage catheters,

intra-ventricular neuro-surgical interventions or intra-thecal chemotherapy. On the MRI strong contrast agent uptake shows at the ventricular edge. A spill-over of inflammation to the subependymal brain parenchyma is detectable as a millimetre-wide hyper-intense edge on T2-weighted and FLAIR sequences.

#### ■ ■ Differential Diagnosis

In the differential diagnosis abscesses must be distinguished from central necrotic metastases or primary brain tumours. This reveals that the abscess capsule on T2-weighted images can usually

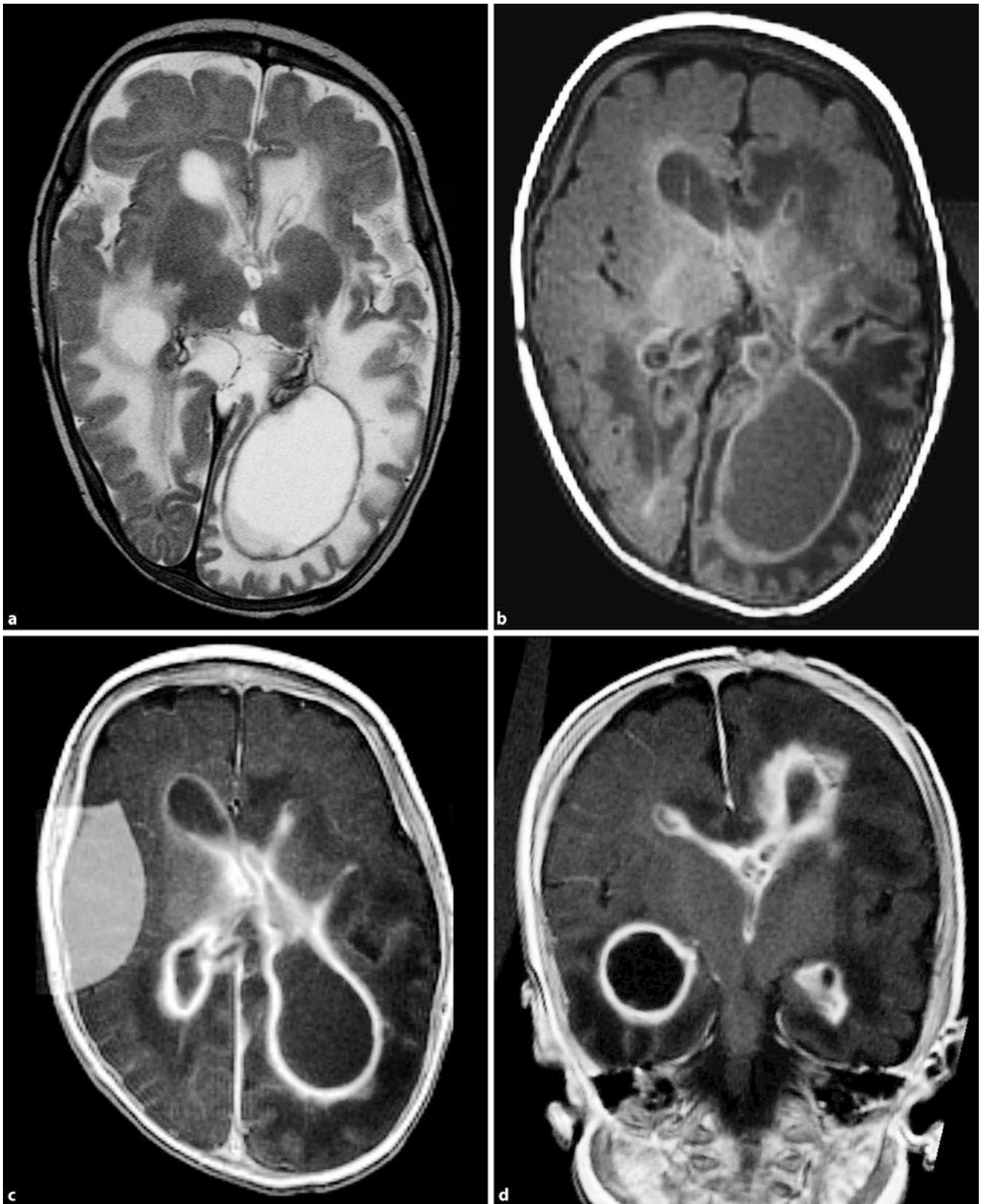


**Fig. 9.146a–d** Ventriculitis. A 12-month-old infant with left parietal peri-natal haemorrhage and consecutive hydrocephalus. State after shunt implantation. Sudden onset of a high fever, a seizure and intra-cranial pressure symptoms. **a** On the T2-weighted images significant widening of the posterior

horn is visible. **b** On the T1-weighted image before contrast agent, incipient hyper-intense ventricular walls. **c, d** After contrast agent administration strong enhancement of the ventricular walls and pronounced lepto-meningeal and dural contrast agent uptake (T1 weighting)

be delineated as an uninterrupted hypo-intense structure, which is less likely to be the case in neoplasia. The perfusion-weighted MRI can also be used to assist with differentiation. In a substantial proportion of higher-grade brain tumours and metastases there is usually an increase in perfusion, whereas in abscesses, radio-necrosis and focal inflammation a decrease in the regional cerebral blood flow is usually detectable. The MR spectroscopy shows a high concentration of amino acids, acetate and succinates in the cyst part, which is not usually the case in centrally necrotic metastases or primary brain tumours. On the diffusion-weighted MRI a reduction in the apparent diffusion coefficient (ADC) shows in the cystic abscess part.

#### ■ Empyema

One of the complications of purulent meningitis or abscesses is the empyema is the sub-dural collection of pus. Rarely, it can also occur directly per continuitatem, e.g. owing to migratory sinusitis or penetrating trauma. The pathogen spectrum is correspondingly different.

Patho-physiologically, there is excessive secretion of activated leucocytes, mostly granulocytes, from the meningeal vessels into the sub-dural space.

**Medical Imaging.** See above (■ Fig. 9.143).

#### ■ Ventriculitis

Ventriculitis is most frequently caused by the implantation of CSF drainage catheters, intra-ventricular neuro-surgical intervention or intra-theal chemotherapy; more rarely, it occurs as a complication of an intra-cranial abscess or meningitis (see above). In cases of leucocyte transmigrating a protein-rich, viscous exudate is produced intra-ventricularly, which can lead to the agglutination of the meninges with formation of hydrocephalus.

**Medical Imaging.** See ■ Fig. 9.146 above.

### 9.6.3 CNS Infections in Immunosuppressed Patients

Pathogen-induced inflammation of the CNS is rare in immunocompetent patients, but more common in immunosuppressed patients. In addition, there is a fundamentally different pathogen spectrum present. Pathognomonic findings in imaging studies do not exist; often, cross-sectional imaging is unremarkable or unspecific, even when clinical symptoms are pronounced. The pathogen spectrum includes the following:

- Bacteria: tuberculosis, syphilis, listeriosis
- Parasites: toxoplasmosis
- Fungi: candidiasis, aspergillosis, cryptococcosis
- Viruses: HIV, HSV, varicella zoster virus (VZV), EBV, CMV

#### ■ Tuberculosis

##### ■ Aetiology and Epidemiology

Tuberculosis is caused by the acid-fast bacterium *Mycobacterium tuberculosis*. The primary infection usually occurs in the lungs

(▶ Chap. 19), more rarely in the skin or the intestine. The so-called primary complex is formed, in which the bacterium can remain asymptomatic during a long latency period. In immunosuppressed situations reactivation can occur, which usually causes a haematogenous, systemic infection.

Involvement of the CNS is one of the most serious complications of tuberculosis. In 2–5% of tuberculosis patients and in approximately 10% of tuberculosis patients with AIDS, there is CNS involvement. Neuro-tuberculosis has a high mortality rate. Neuro-tuberculosis may occur even years after the primary infection. Overall, the incidence of tuberculosis is once again increasing worldwide. The reason for the increase in the incidence of tuberculosis worldwide is the increase in AIDS, an increase in immunosuppressed patients and the incidence of therapy-resistant tuberculosis.

In immunosuppressed patients, however, especially those with an HIV infection at the AIDS stage, other ubiquitous mycobacteria that are usually of low pathogenicity, so-called mycobacteria other than tuberculosis (MOTT) can lead to similar disease patterns: *Mycobacterium avium*, *intercellulare*, *kansasii*, and *fortuitum*.

##### ■ Pathogenesis, Histology

**Tuberculous meningitis** is a granulomatous infection of the lepto-meninges with involvement of the arachnoid and pia mater. Here, a thick exudate forms on the meninges, predominantly at the base of the brain. Cause of the exudate is the rupture of a sub-ependymal or sub-pial granuloma into the sub-arachnoid space or a haematogenous dissemination of a remote focus of tuberculosis. The cell then initiates the immune response for the formation of an exudate on the basal surface of the brain. Later, the lepto-meningitis may spread to the frontal, parietal or occipital brain surface or ependymitis may occur.

With **parenchymal tuberculosis** the most common form is the tuberculous granuloma, more rarely the tuberculous brain abscess, focal cerebritis and allergic tuberculous encephalopathy. Histopathologically, tuberculous granulomas consist of a central zone of necrosis with only a few tuberculosis pathogens and a capsule of collagenous tissue, multi-grained giant cells and mono-nuclear inflammatory cells. Peri-focally cerebral oedema and astrocyte proliferation zones are present. Distinction can be made between caseating granuloma and non-caseating granuloma with and without liquefaction of the contents.

**Tuberculous brain abscesses** are a rare complication. They develop from parenchymal granulomas or meningeal focal points. A focal tuberculous cerebritis occurs mostly in immunosuppressed patients with AIDS. Tuberculous encephalopathy occurs mainly in children and adolescents with pulmonary tuberculosis, and involves excessive destruction of the white matter by peri-vascular demyelination due to a delayed allergic encephalitic type IV immune response.

##### ■ Symptoms, Therapy

The clinical symptoms are fever, headache, varying degrees of disturbances in consciousness, in addition to signs of meningeal irritation, such as neck stiffness, photophobia and vomiting. Additionally, failures often occur on basal cranial nerves along with

signs of focal cerebral ischaemia. The cranial nerve failures can be explained by ischaemic damage to the nerves, lesions and meningeal entrapment. The chronic fibrotic end stage is characterised by the permanent loss of function of these nerves.

In a parenchymal infection the symptoms are less pronounced, mainly consisting of headaches, seizures and focal neurological deficits, but elevated intra-cranial pressure is also detectable.

The **treatment for neuro-tuberculosis** consists of the administration of at least three tuberculostatics (isoniazid, rifampicin, ethambutol). In areas with an epidemic this can be extended to four to five tuberculostatics. The mean duration of treatment is usually 8–16 months.

#### ■ ■ Medical Imaging, Diagnosis

In tuberculous CNS infections, acute or chronic meningitis prevails; more rarely, tuberculomas, abscesses or cerebritis are present.

The **unenhanced CCT** is often inconspicuous or shows non-specific changes, such as hydrocephalus. Often, central calcifications can be found in tuberculomas. As a long-term consequence popcorn-like calcifications can result in the supra-sellar cisterns with or without contrast agent uptake in the surrounding areas.

With **tuberculous meningitis** a strong contrast agent uptake is usually present in the basal meninges on the **MRI**, usually on the T1-weighted sequences. Here, a gelatinous exudate also accumulates, which can lead to a communicating hydrocephalus and which imposes itself as iso- and hyper-intense on T1- and T2-weighted images (■ Fig. 9.147). If the florid inflammation in the CSF spreads to the basal cerebral vessels, it may produce infarcts.

In immunosuppressed patients the contrast agent uptake is often considerably lower. Because of the excessive thickening of the basal meninges the inflammation may spread to the adventitia of the cerebral vessels with the consequences of pan-arteritis with secondary thrombosis and vessel occlusion. Infarcts are usually detectable in the supply area of lenticulo-striate arteries. Increased lepto-meningeal contrast agent uptake may be detectable, even years after successful treatment. In addition, meningeal or ependymal calcifications may persist as residues.

Tuberculomas can form as solitary or multiple features throughout the parenchyma, the meninges and the sub-arachnoid space. The size of the peri-focal oedema is highly variable and dependent on the extent of immunosuppression.

Non-caseating **granulomas** are hyper-intense on the T2-weighted sequences and hypo-intense on T1-weighted images, with homogeneous contrast agent uptake. They show heterogeneous enhancement in the central portion, with annular, interrupted, uniformly thick peripheral contrast agent uptake.

#### ■ ■ Complications, Differential Diagnosis

In the primary infection with immunodeficiency or reactivation with severe immunosuppression, fulminant **mycobacterial Landouzy septicaemia** may occur. On MRI, disseminated, nodular foci of infection can be found, which measure only a few millimetres, so-called milia; contrast agent uptake may be present or absent. Often no changes can be detected, as they fall below the MRI resolution.

Even spinal spread or reactivation with immunosuppression is possible. This can manifest as **spondylodiscitis or vertebral osteomyelitis**. The clinical course is slowly progressive, i.e. over weeks to months (as opposed to the fulminant spondylodiscitis caused by *Staphylococcus aureus*). In a small, retrospective case analysis Smith et al. were able to show that tuberculous spondylodiscitis often resembles a neoplastic event because of large para-vertebral soft-tissue shares with marginalised contrast agent uptake and bony destruction. As a decision criterion calcifications can be detected on the CT. In the spine the infection also spreads along the supplying vessels. In the early stages the front and middle column are most often affected, the posterior column and vertebral arches can be affected later on. A pathognomonic MRI image morphology does not exist. The diagnosis is confirmed by biopsy and pathogen identification.

**For the differential diagnosis** infectious diseases, such as bacterial meningitis and abscesses, fungal infections, non-infectious meningitis from the rheumatic range of diseases, sarcoidosis and idiopathic pachymeningitis must be considered.

However, the **diagnosis** is usually made via the **CSF result**, as in tuberculous lepto-meningitis there is lymphocytosis with increased protein and reduced glucose levels. The final diagnosis is made by culturing and identifying the pathogen; this, however, takes 4–8 weeks. The detection of pathogenic DNA using polymerase chain reaction (PCR) technology is more sensitive, less standardised and not widely available.

#### ■ Sarcoidosis

##### ■ ■ Definition, Epidemiology, Localisation

Although this systemic disease of the connective tissue is not an infectious disease, it is mentioned here, as intra-cranial involvement can occur in up to 15% of patients with sarcoidosis. Typical locations are in the supra-sellar cistern and the hypothalamus, including the tractus opticus. In addition, lesions are also found in the white matter.

##### ■ ■ Medical Imaging

In the diagnosis of sarcoidosis, MRI is clearly superior to CT (■ Fig. 9.148). There are two presentations: mostly granulomatous lepto-meningitis, multiple diffuse parenchymal lesions or a single, intra-cerebral mass lesion are found, corresponding to granulomas. The lepto-meningeal involvement may in a second phase infiltrate the adjoining brain parenchyma along the perivascular spaces. The disease may also show itself as a lesion adjacent to the dura.

In the lepto-meningeal form **the MRI T1-weighted images** show an iso-intense thickening of the sub-arachnoid area, which may extend into the sulci. These can be found both localised and diffusely distributed across the entire brain. On T2-weighted images this lesion usually appears hypo-intense, most likely because of the compact cell structure of the granulomatous process. The presence of oedema in the adjacent brain parenchyma indicates a possible infiltration along the Virchow–Robin spaces or vasculitis of the small vessels. After contrast agent administration, there is diffuse, homogeneous enhancement, which allows a more precise assessment of the spread. The MRI characteristics of the sarcoidosis localised

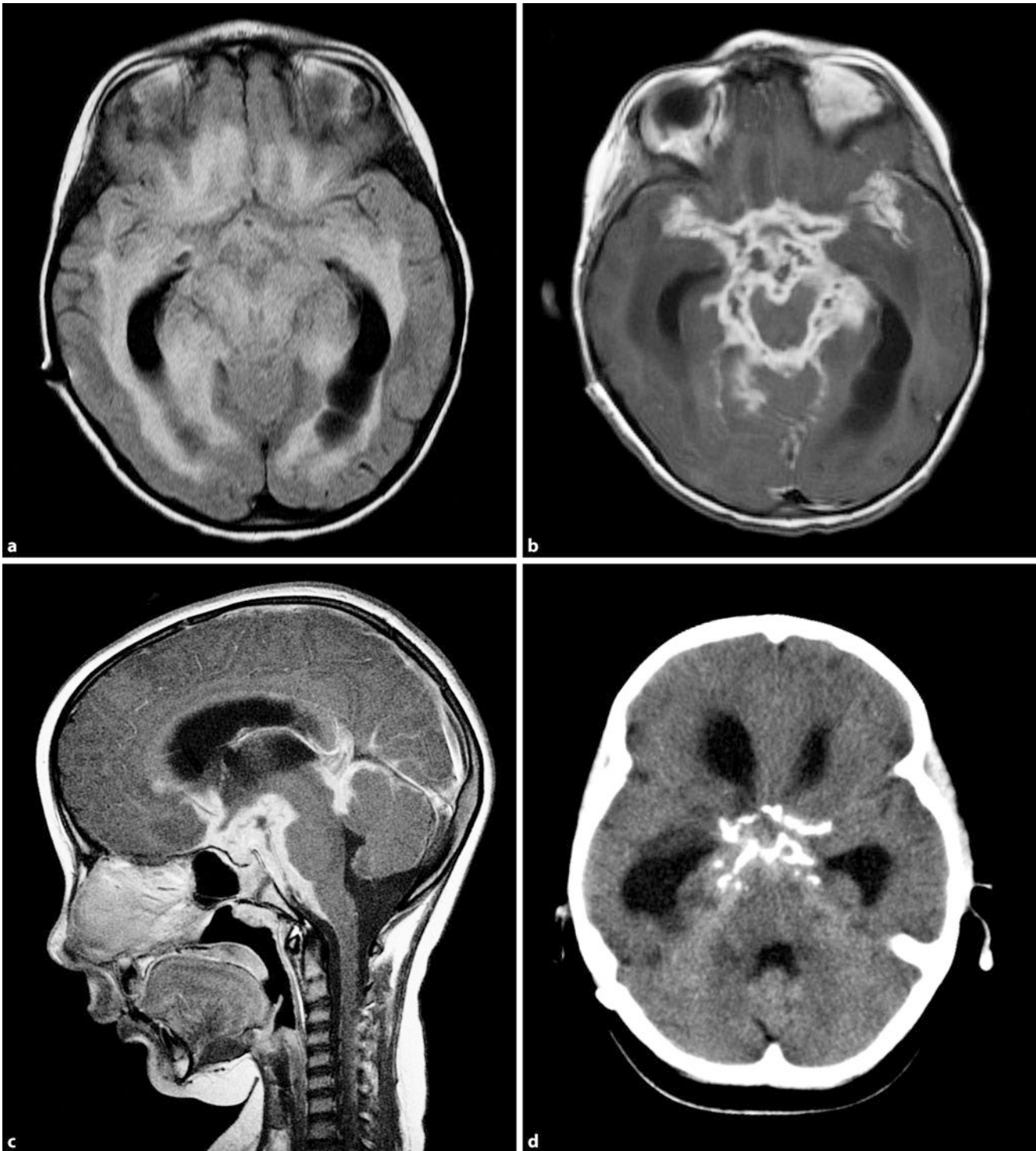


**Fig. 9.147a–d Tuberculosis.** A 12-month-old former twin born prematurely with congenital tubercular infection and disproportionate head growth, dystrophy and lethargy. **a** FLAIR sequence: extensive oedema of the medullary layer and the cortex along with a hydrocephalic configuration of the lateral ventricles. **b** T1-weighted post-contrast agent:

parenchymal contrast agent uptake basal to the brain-stem. **c** T1-weighting of post-sagittal contrast agent: contrast agent uptake anterior and posterior in position to the brain-stem, the aqueduct cannot be delineated. **d** CCT: residual state, clear hydrocephalus internus with popcorn-like supra-sellar calcifications

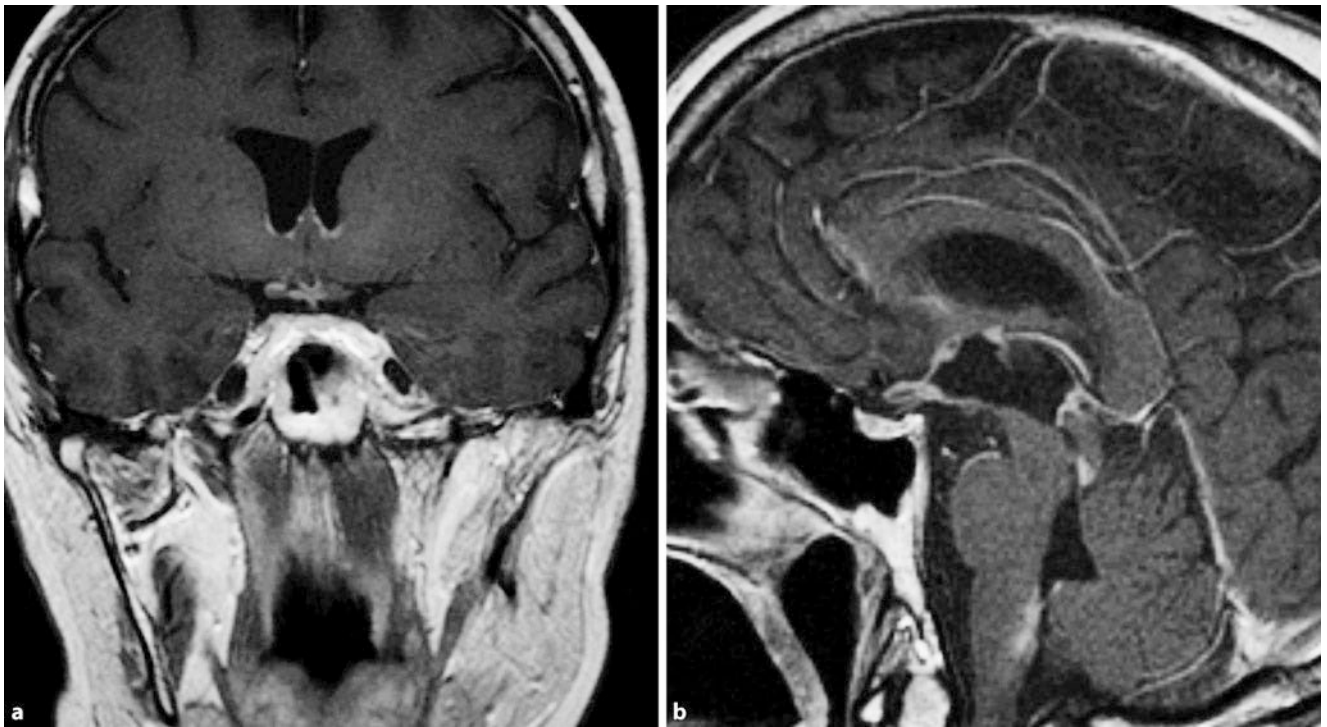


**Fig. 9.148a,b Sarcoidosis.** On the T1-weighted sequences after contrast agent administration a thickened pituitary stalk and contrast agent enhance-

ment are present **a** at the bottom of the lateral ventricles and around the chiasm and **b** in the posterior medulla oblongata

in the dura are similar to that in the sub-arachnoid space. In this location a distinction between the meningioma and dural lymphoma is often difficult; thus, only a biopsy can clarify the final diagnosis.

In neuro-sarcoidosis there is often additional hydrocephalus, parenchymal, homogeneous enhancing nodes in addition to an increased water content in the peri-ventricular, white matter. Often, there is also diffuse enhancement of the basal meninges and the tentorium. The lesions located outside the parenchyma resemble meningiomas. The smoothly definable, parenchymal nodes show no peri-focal oedema, may occur singly or clustered and are either found at the base of the brain or distributed across the hemispheres. On CT they are iso-dense before contrast agent administration, on MRI T1-weighted sequences they are iso-intense similar to grey matter and iso- to hyper-intense on T2-weighted images. They show homogeneous enhancement. After cortisone administration, they rapidly reduce in size and can also disappear completely.

The granulomas are slightly hyper-intense on the MRI, just 1 cm in size, with homogeneous contrast enhancement, slightly hyper-dense on CT, also with clear contrast enhancement. The decreasing size of the infection sites under cortisone therapy is an important criterion.

#### ■ Neuro-syphilis

Lues, or syphilis, is caused by the Spirochete *Treponema pallidum* and is one of the sexually transmitted diseases (STD). This also explains its increased coincidence in relation to HIV infection. Neuro-syphilis can occur at any stage of the disease, on average after about 7 years, at which point an incidence of 5–10% of untreated infected individuals is reported.

Distinction is made among the presentation types illustrated in **Table 9.17**.

Among immunosuppressed patients the acute meningitic form is most common. Often, there are non-specific changes in the medullary layer. As acute stroke is very rare among HIV patients, infectious vasculitis should be considered and a CT or MR angiography should be performed.

#### ■ Borreliosis

##### ■ Definition, Aetiology

The pathogenic agent in Lyme disease, the bacteria *Borrelia burgdorferi*, *Borrelia garinii* and *Borrelia afzelii* are closely related to the syphilis pathogen *Treponema pallidum*. Parallels between the two diseases therefore exist. There are several stages of the disease, which merge into each other, but can also be separated by long symptom-free intervals. These secondary stages are some of the characteristics of borreliosis.

Whether the three borrelia species also present as different diseases and progressions is not yet clear. The disease is transmitted solely by ticks (*Ixodes ricinus* in Europe).

➤ **Borreliosis should not be confused with tick-borne encephalitis (TBE), which is also transmitted by ticks (pathogen: flavivirus; see above, ▶ Sect. 9.6.1). TBE occurs primarily in certain endemic areas (Bavaria, Baden-Württemberg, Austria). In recent years, cases of TBE were also reported in the Rhineland-Palatinate, Hesse and Thuringia. Each year, approximately 200–250 people contract TBE and approximately 50,000–100,000 borreliosis. Active and preventive vaccinations are available against TBE; TBE infection results in lasting**



■ **Table 9.17** Presentation types of neuro-syphilis

Presentation type	Image morphology	Symptoms	Manifestation
Acute meningitis	Thickened contrast agent-affine meninges, exudate	Headache, confusion, neck stiffness, cranial nerve palsy	Within the first 2 years
Cerebro-vascular neuro-syphilis (Heubner vs Nissl arteritis)	Acute stroke, vasculitic co-existence of stenosis and ectasia	Headache, dizziness, personality changes, acute stroke	After 5–7 years
Encephalitis	Diffuse parenchymatous contrast agent enhancement	Slowly progressive dementia, fatigue, intention tremor, delusions	After 10–20 years
Tabes dorsalis	Atrophy of the posterior funiculus, contrast agent uptake is possible	Shooting pains, dysuria, ataxia, areflexia, loss of proprioception, Argyll Robertson pupil	After 15–20 years
Syphilitic gummata	Small, circumscribed nodular lesions originating from the meninges have no space-occupying effect, contrast agent uptake, oedema possible	Focal abnormalities, often combined with meningitis	Manifestation of tertiary syphilis

severe paralysis in about 5–10% of cases. In TBE flu-like symptoms occur 2 weeks after a tick bite. The first nerve inflammation and paralysis occurs about 3 weeks after infection.

#### ■ ■ Epidemiology

Borreliosis exists worldwide; in Germany 0.5% of the population contract the disease for the first time. Many individuals who contract borreliosis cannot recall the tick bite itself; the tick larvae can transmit borrelia.

#### ■ ■ Symptoms

**Stage I.** Local infection. The tick bite initially causes a local skin infection. The classic erythema migrans occurs in about 50% of cases. If there is a direct infection through the blood, the erythema migrans may be missing completely and the disease begins a few days after the bite with flu-like symptoms.

**Stage II.** After a latency of up to 10 weeks, there is a dispersion of the pathogen through the blood and lymph. Extreme sweats, in addition to general symptoms, such as fatigue, night sweats, fever, muscle and joint pain.

**Stage III.** Chronic stage. Formation of antibodies, reduction in the number of borrelia in the body. A small number of *B. burgdorferi* can survive and lead to a resurgence of disease symptoms. This can occur months to years after infection. Typical is an inflammation that jumps from joint to joint. Muscular inflammation, bone and soft tissue pain are also typical. Often, polyneuropathies can also be found. Occasionally, vasculitis can occur jointly with a stroke or cardiomyopathy.

#### ■ ■ Diagnosis

Detection of antibodies in the serum; the humoral immune response requires at least 2 weeks before the first antibodies are detectable.

**Medical Imaging.** Lymphocytic meningitis is associated with strong contrast agent enhancement of the dura and the lepto-

meninges. In borrelia encephalomyelitis, the MRI result can be normal or show pronounced multi-focal, round, partly confluent changes with a high signal on T2-weighted images. On MR imaging the results sometimes cannot be distinguished from acute disseminating encephalomyelitis or MS.

#### ■ Listeriosis

Listeriosis is caused by the Gram-positive anaerobe *Listeria monocytogenes* (*icterohaemorrhagiae* sp.) and usually only affects immunosuppressed individuals. The systemic infection is associated with non-specific, flu-like prodromes. CNS involvement often occurs in the form of meningitis, meningo-encephalitis or abscess formation. An infection of the brain-stem and cerebellum (rhombencephalitis) is typical. Clinically, brain-stem symptoms, such as nystagmus, vertigo, dysphagia, hiccups, even leading to respiratory arrest, occur very early on. The mortality rate is up to 50%.

**Medical Imaging.** Morphological imaging demonstrates the predilection for the rhombencephalon (mostly ponto-medullary) as diffuse oedema and occlusive hydrocephalus in a narrowing of the fourth ventricle. Meningitic or encephalitic contrast agent uptake may be present.

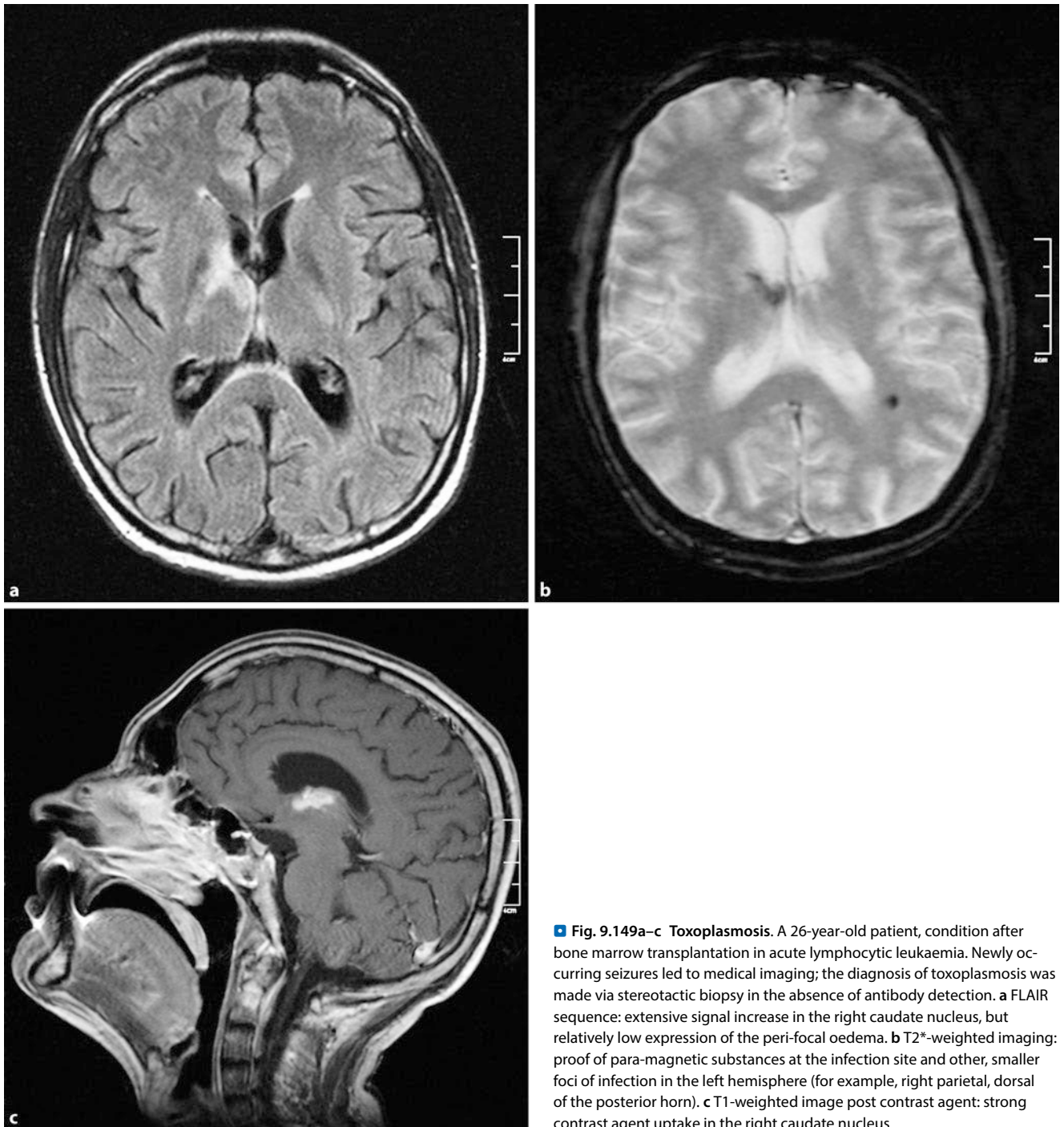
#### ■ Toxoplasmosis

This is the most common opportunistic CNS infection in HIV patients, caused by contaminated food (raw meat) or transmission by cats. The pathogen is *Toxoplasma gondii*.

With immunosuppression, especially in AIDS, the infection can be reactivated and clinically present as encephalitis (■ Fig. 9.149).

➤ **In cases where morphological imaging suggests rhombencephalitis and brain-stem symptoms occur in the immunosuppressed, listeriosis should be considered and therapy should be initiated as soon as possible, even without detected pathogens.**

**Medical Imaging.** Reactivation results in necrotising encephalitis with multiple, thin-walled abscesses. The typical image shows



■ **Fig. 9.149a–c Toxoplasmosis.** A 26-year-old patient, condition after bone marrow transplantation in acute lymphocytic leukaemia. Newly occurring seizures led to medical imaging; the diagnosis of toxoplasmosis was made via stereotactic biopsy in the absence of antibody detection. **a** FLAIR sequence: extensive signal increase in the right caudate nucleus, but relatively low expression of the peri-focal oedema. **b** T2\*-weighted imaging: proof of para-magnetic substances at the infection site and other, smaller foci of infection in the left hemisphere (for example, right parietal, dorsal of the posterior horn). **c** T1-weighted image post contrast agent: strong contrast agent uptake in the right caudate nucleus

multiple, lesions of 1–4 cm in size with marginal oedema and contrast agent uptake.

The multiple lesions, mostly located in the basal ganglia, periventricularly, in the posterior fossa or at the cortico-medullary border, are space-occupying and show peri-focal oedema (hyper-intense on T2-weighted images and the FLAIR sequence, hypo-intense on unenhanced T1-weighted images, hypo-dense on CCT; ■ Fig. 9.149). Typically, there is a strong ring-shaped contrast agent uptake detectable. Depending on the source and extent of immunosuppression, however, contrast enhancement and oedema formation may be weak or absent. The nuclear ( $^1\text{H}$ -

MR) spectroscopy usually shows non-specific inflammatory changes. Rarely, local haemorrhages are found.

The **main differential diagnosis** is the primary CNS lymphoma; toxoplasmosis infection sites are often smaller and disseminated. A response to antibiotics can usually differentiate between toxoplasmosis and lymphoma.

#### ■ **Candidiasis**

The yeast *Candida albicans* is the most common cause of fungal infections overall. However, generalised infections are rare in immunocompetent individuals, AIDS patients and patients

with neutropaenia are at greatest risk. In about 1–6% of cases of systemic candidiasis CNS involvement is found; the mortality rate is estimated at 10–30% with adequate therapy.

Candidiasis may manifest as meningitis or as a micro-abscess. Meningeal symptoms usually occur sub-acutely, an isolated fever is often in the foreground. In the formation of abscesses fever and non-specific encephalopathy are found; focal deficits are rare.

**Medical Imaging.** Because of the poorer resolution of the CT, the CCT may appear unremarkable in spite of disseminated *Candida* micro-abscesses. On the MRI small, ring-shaped lesions with contrast agent uptake, with or without a central haemorrhage at the cortico-medullary border. The rarer macro-abscesses can cause focal neurological deficits because of their space-occupying effect and are most commonly parieto-occipital, less commonly cerebellar, in nature.

#### ■ Aspergillosis

The most important opportunistic fungal infection is caused by *Aspergillus* spp., most commonly by *Aspergillus fumigatus*. Moulds are ubiquitous in the environment. Pre-disposing for invasive aspergillosis are AIDS, cancers and stem cell or organ transplantation. CNS involvement is found in 44–94% of cases of disseminated aspergillosis.

The primary infection occurs via the respiratory tract (lungs, sinuses). The fungus is angio-invasive and haematogenic. With pathogen invasion via the para-nasal sinuses, especially the sphenoid sinus, a CNS infection can occur per continuitatem and present as meningo-encephalitis.

**Medical Imaging.** Mostly, an initial infectious vasculopathy occurs, which can lead to haemorrhage, ischaemia and mycotic aneurysms. Only secondarily does the inflammation spread to the adjacent tissue and manifest as cerebritis or more rarely as an abscess. The **vasculitic distribution pattern is striking**: most commonly the perforating arteries of the front, and more rarely of the rear circulation area, are affected. On MRI the typical picture of septic-embolic cortical–sub-cortical infarctions also emerges (■ Fig. 9.150). In venous vasculitis haemorrhagic congested infarctions may occur. Most frequently, infarctions are found in the basal ganglia and thalami, the corpus callosum and in the brain-stem. The pathogen invasion into infarcted areas occurs rapidly. Depending on the immune status of the organism, circumscribed abscesses, so-called **aspergilloma**, consolidate within a few days, with a characteristic ring enhancement.

In **immunosuppressed patients, however**, it more frequently results in a cerebritic spread with diffuse parenchymal contrast agent uptake. A peri-focal oedema may be present. Lepto-meningeal involvement can be detected post-mortem in almost all cases; however, antemortem there is no morphological image correlate. In the long term, as a residual sign of larger lesions, parenchymal calcifications may be present on the CT or T2- or T2\*-weighted images. On the T2-weighted images active lesions can also show hypo-intense areas due to para-magnetic elements, such as manganese, iron and magnesium, in addition to blood degradation products.

#### ■ Cryptococcosis

The pathogenic agent in cryptococcosis is the encapsulated, yeast-like fungus *Cryptococcus neoformans*. The pathogen occurs ubiquitously and mainly causes infections in the immunosuppressed, typically in AIDS patients. The primary infection takes place in the lungs, from where haematogenous dissemination occurs. The pathogenesis is surprisingly similar to tuberculosis. A differentiation is made between meningitic and the parenchymal infections.

The clinical picture is that of sub-acute meningitis; headache is often the only symptom. The meningitis is mostly basal in nature and most frequently spreads to the brain-stem, mid-brain and basal ganglia.

**Medical Imaging.** It is characterised by a peri-vascular ascending infection, which manifests on morphological imaging as cystic widening of the Virchow–Robin spaces with mucinous secretions. A granulomatous parenchymal reaction to the pathogen invasion is called cryptococcosis. The most common location is in the ependymal cells of the choroid plexus; this may result in obstructive hydrocephalus. In immunosuppressed patients the formation of granulomatous cryptococcosis is, however, rare. On the diffusion-weighted and contrast-enhanced MRI sequences cryptococcosis more closely resembles a necrotic tumour than an abscess.

Even in cryptococcosis vasculitis can cause cerebral infarction in approximately 4% of cases. It was possible to demonstrate that the immediate and delayed contrast-enhanced examination with twice applied, and in total a double amount of contrast agent achieves a higher MRI sensitivity in the immunosuppressed.

#### ■ Mucor Mycosis

In mucor mycosis, there is a direct spread of mucor from the sinuses. The mortality rate is 70%. As with aspergillosis, it often leads to an invasion of the blood vessels with subsequent infarctions.

**Medical Imaging.** Multiple lesions with differently pronounced, peripheral enhancement are detectable, dependent on the immune situation of the patient.

#### ■ Herpesviridae

The group of herpesviridae includes the herpes simplex virus (HSV), human herpesvirus-6 (HHV-6), VZV, CMV and EBV. All herpes viruses have in common that they already have a high prevalence in the general population during adolescence and persist in the organism. With immunosuppression a **reactivation** thus usually **occurs**; a primary infection is rare.

#### ■ HSV

Herpes simplex encephalitis is primarily caused by HSV-1. HSV encephalitis symptoms in immunosuppressed patients can be diffuse and non-specific. A diffuse spread of encephalitis via the fronto-temporal predilection is possible. CSF changes may be absent. The course may be fulminant or protracted over days to weeks.

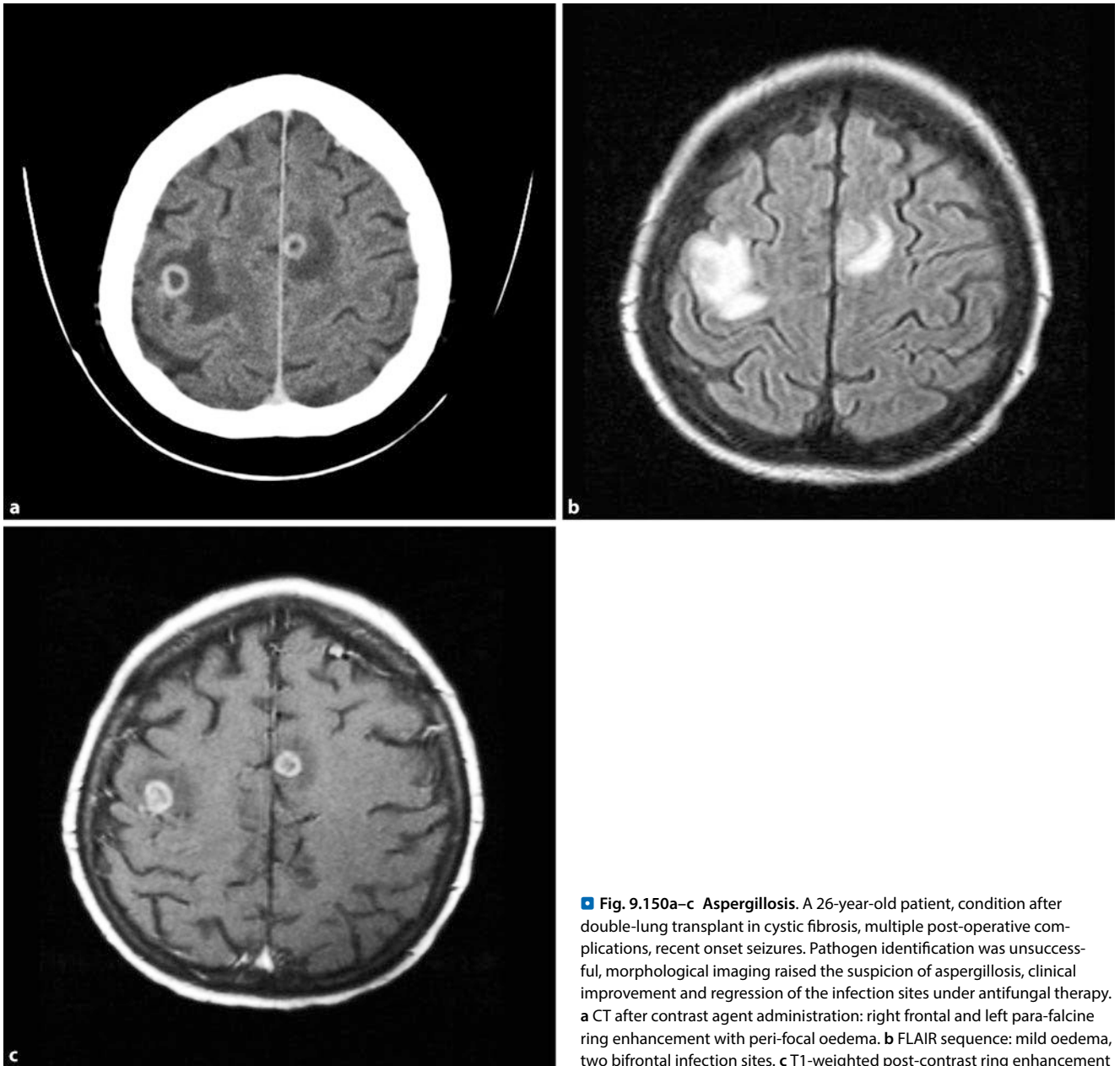


**Fig. 9.150a–c Aspergillosis.** A 26-year-old patient, condition after double-lung transplant in cystic fibrosis, multiple post-operative complications, recent onset seizures. Pathogen identification was unsuccessful, morphological imaging raised the suspicion of aspergillosis, clinical improvement and regression of the infection sites under antifungal therapy. **a** CT after contrast agent administration: right frontal and left para-falcine ring enhancement with peri-focal oedema. **b** FLAIR sequence: mild oedema, two bifrontal infection sites. **c** T1-weighted post-contrast ring enhancement

**Medical Imaging.** As with immunocompetent patients the virus persists mostly in the trigeminal ganglion. The image morphology is also similar: there is a coexistence of cytotoxic and vasogenic oedema usually limited to the limbic system in a bi-temporal to fronto-basal manner (■ Fig. 9.151); DWI and ADC are particularly suitable for distinction. Frequently, micro-bleeds are detectable, whose histopathological correlate is haemorrhagic necrotising inflammation.

#### ■ ■ HHV-6

HHV-6 is the causative pathogen of the childhood disease exanthema subitum (roseola, three-day fever). The symptomatic CNS participation in the primary infection is very rare; however, the persistence of a virus in the brain parenchyma is discussed. In immunosuppressed patients reactivation can lead to bone marrow suppression and pneumonia. Less common are necrotising

or demyelinating forms of meningo-encephalitis. In the literature only a few cases have been described; larger studies are not available.

**Medical Imaging.** On morphological imaging an isolated involvement of the mesial temporal lobe predominates with hyperintensity on T2-weighted and FLAIR sequences. A diffusion restriction on the DWI accompanied by a weakening in the ADC suggests cytotoxic oedema. In addition, an early volume loss of the hippocampus by necrosis is found, which shows as an abnormal increase in signal intensity on the ADC. To illustrate the temporal lobe a coronal section is recommended.

#### ■ ■ Varicella zoster virus

The VZV is the causative pathogen of chickenpox. After the primary infection the virus persists in the brain and spinal nerve

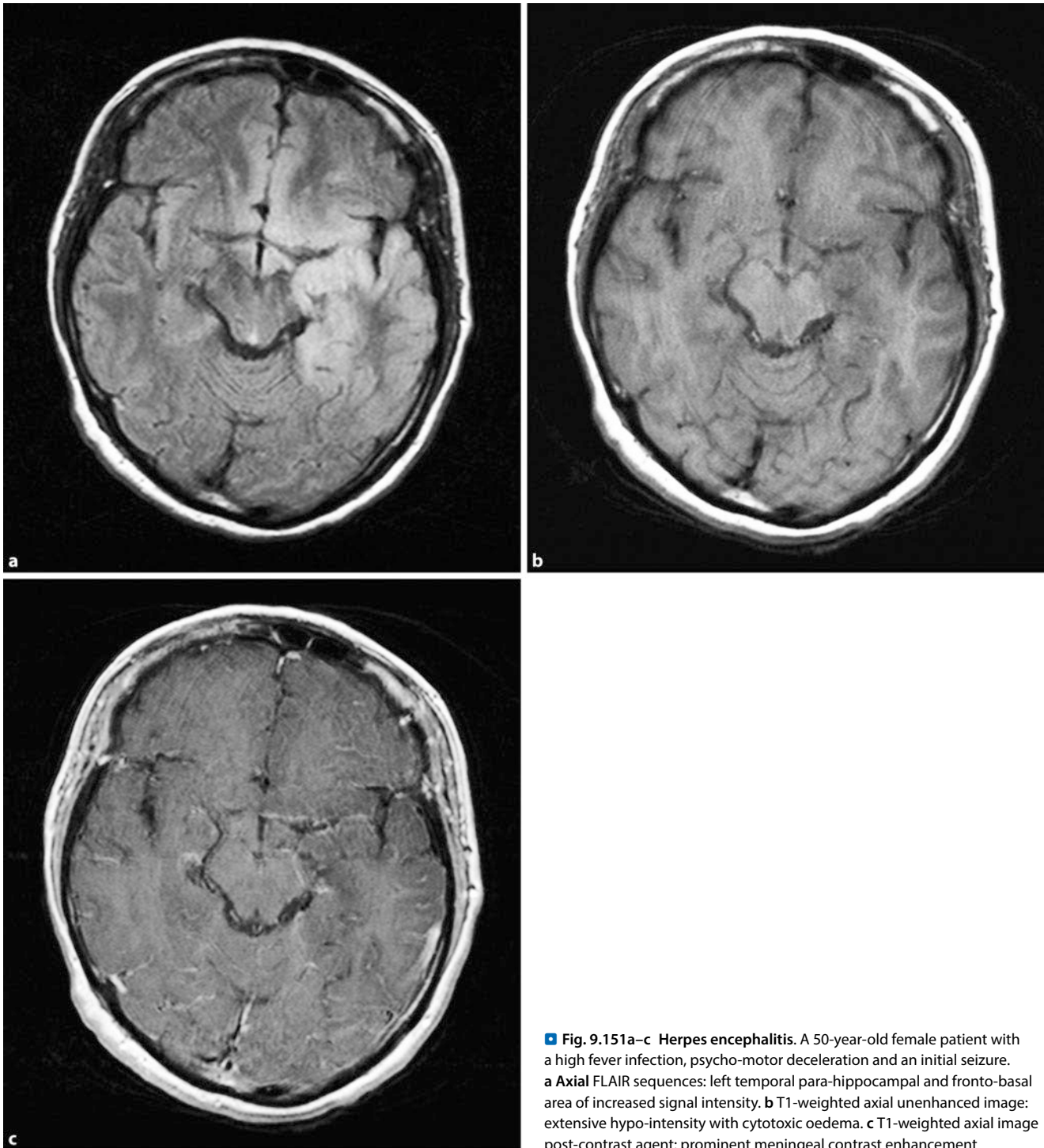


**Fig. 9.151a–c Herpes encephalitis.** A 50-year-old female patient with a high fever infection, psycho-motor deceleration and an initial seizure. **a** Axial FLAIR sequences: left temporal para-hippocampal and fronto-basal area of increased signal intensity. **b** T1-weighted axial unenhanced image: extensive hypo-intensity with cytotoxic oedema. **c** T1-weighted axial image post-contrast agent: prominent meningeal contrast enhancement

ganglia. A later reactivation can lead to the clinical picture of shingles, which can cause chronic neuropathic pains in immunocompetent individuals, CNS involvement is rare, however. In immunosuppressed patients, however, there is a significantly increased risk of CNS invasion with or without dermal manifestation. VZV can cause diffuse meningo-encephalitis, herpes ophthalmicus, neuritis with nerve paralysis and myelitis. The late manifestation as hemiparesis 2–5 weeks after contra-lateral dermal efflorescence (mostly ophthalmic zoster), which may be caused by vasculitic vessel occlusion, is atypical. As a residuum

of vasculitis inflammatory aneurysms are possible. The invasion takes place in a vasogenic manner.

**Medical Imaging.** On morphological imaging haemorrhagic infarctions with an involvement of the large vessels are detectable, a juxtaposition of round or ovaloid demyelination (multi-focal leuko-encephalopathy and progressive multi-focal leuko-encephalopathy [PML] are differential diagnoses) and ischaemia in cases where the smaller vessels are affected. Ventriculitis is rare where the pathogen proliferation takes place in the ependyma. Contrast

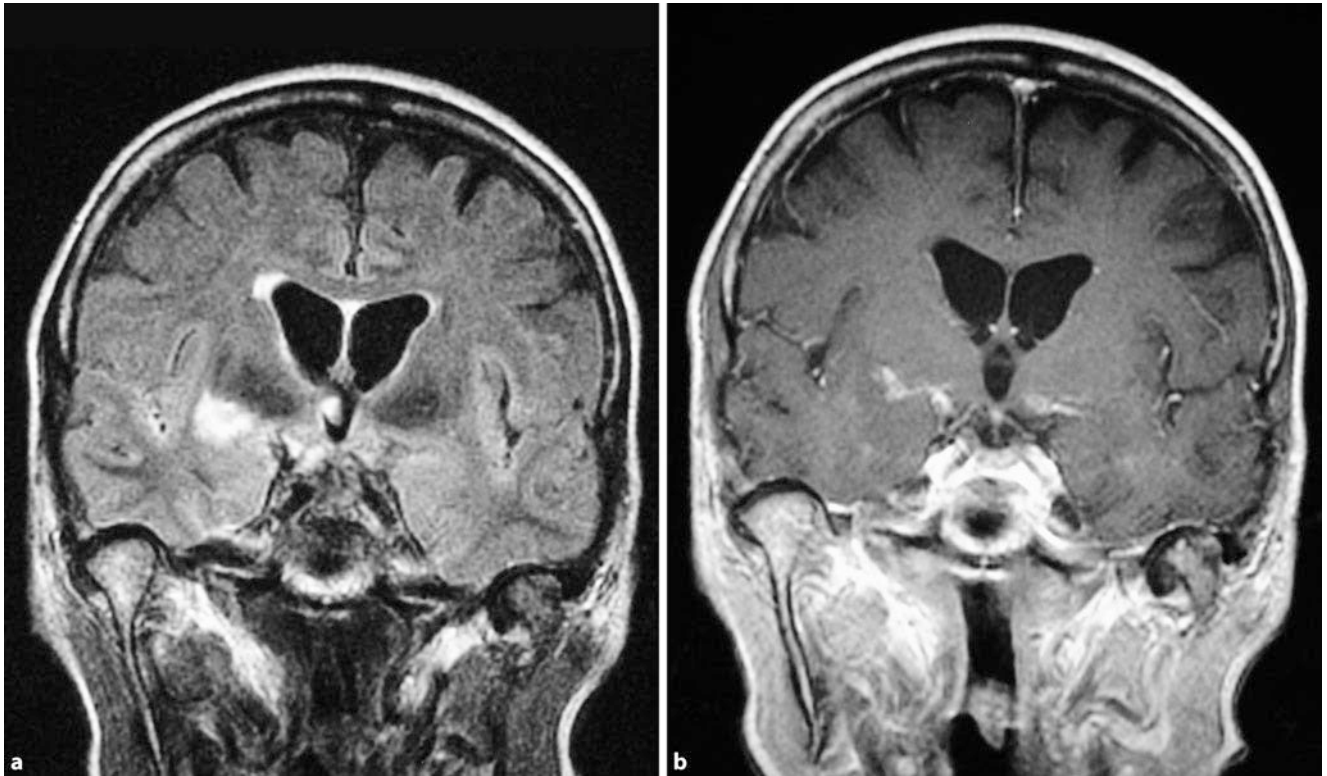


**Fig. 9.152a,b** **Varicella.** a On the FLAIR images there is increased signal intensity in the peri-vascular entry zone, caused by vasculitis; b on the T1-

weighted sequences after contrast agent administration there is peri-vascular enhancement

agent uptake and peri-focal oedema are common (■ Fig. 9.152). The MR angiography can detect characteristic changes; however, it is impossible to rule out vasculitis where an inconspicuous image is produced.

➤ **Also, the clinical pictures of VZV-associated meningomyelodradiculitis and acute necrotising myelitis have been described in AIDS patients.**

#### ■ ■ Cytomegalovirus

The CMV encephalitis is a typical opportunistic infection, which affects 85% of HIV-infected patients, 12% of otherwise immunosuppressed patients and only 3% of immunocompetent patients. It usually occurs only in the late stages of AIDS (CD4 cells < 50/μl); in addition, patients often suffer from other opportunistic infections.

As is the case in VZV a pathogen increase takes place in the ependyma, which, on the one hand causes peri-ventricular necrosis and a disruption of the blood–brain barrier and on the other hand a fibrinous exudate. Owing to the high viscosity of the intra-ventricular exudate CSF circulation may be disrupted with a consequent build-up of hydrocephalus. The clinical symptomatology of encephalitis is usually a sub-acute onset of neurological deterioration progressing over days to weeks; in about 30% of cases, focal brain-stem and cerebellar symptoms occur.

**Medical Imaging.** Most commonly, a CMV infection in HIV manifests as chorio-retinitis (acute visual loss), which can be diagnosed on the fat-suppressed MRI as thickened, clearly contrast agent-affine choroid and retina. Other manifestations in-

clude encephalitis, polyradiculitis, Guillain–Barré syndrome and multi-focal neuropathy. The encephalitis shows peri-ventricular sub-ependymal both on the CT and MRI as delicate contrast enhancement, which sharply delineates the ventricles. In addition, there is diffuse demyelination in the medullary layer as hypodensity on the CT, increased signal intensity on T2-weighted images and the FLAIR sequence.

Microglial nodes and focal parenchymal necroses could be demonstrated as a histopathological correlate.

#### ■ ■ EBV

The EBV has an almost complete prevalence in the normal population by the time they reach young adulthood. Like all herpesviridae, it persists for life. However, not in neurons, but in the B-lymphocytes.

**CNS Lymphoma** Viral DNA can be detected in primary CNS lymphoma, which is a rarity in immunocompetent individuals.

Apparently, EBV-infected lymphocytes are more sensitive to an HIV infection (CD4 cell count < 100/μl); a malignant transformation may take place. Clinically, focal neurological deficits, such as hemiparesis, seizures or aphasia, depending on the topographic location of the tumour, are most notable. The prognosis is unfavourable.

**Medical Imaging.** Morphological imaging usually shows a number (one to three) of multi-focal, space-occupying lesions with strong contrast agent uptake (■ Fig. 9.153). The most common locations are the cerebral cortex, the basal ganglia and the brain-stem.

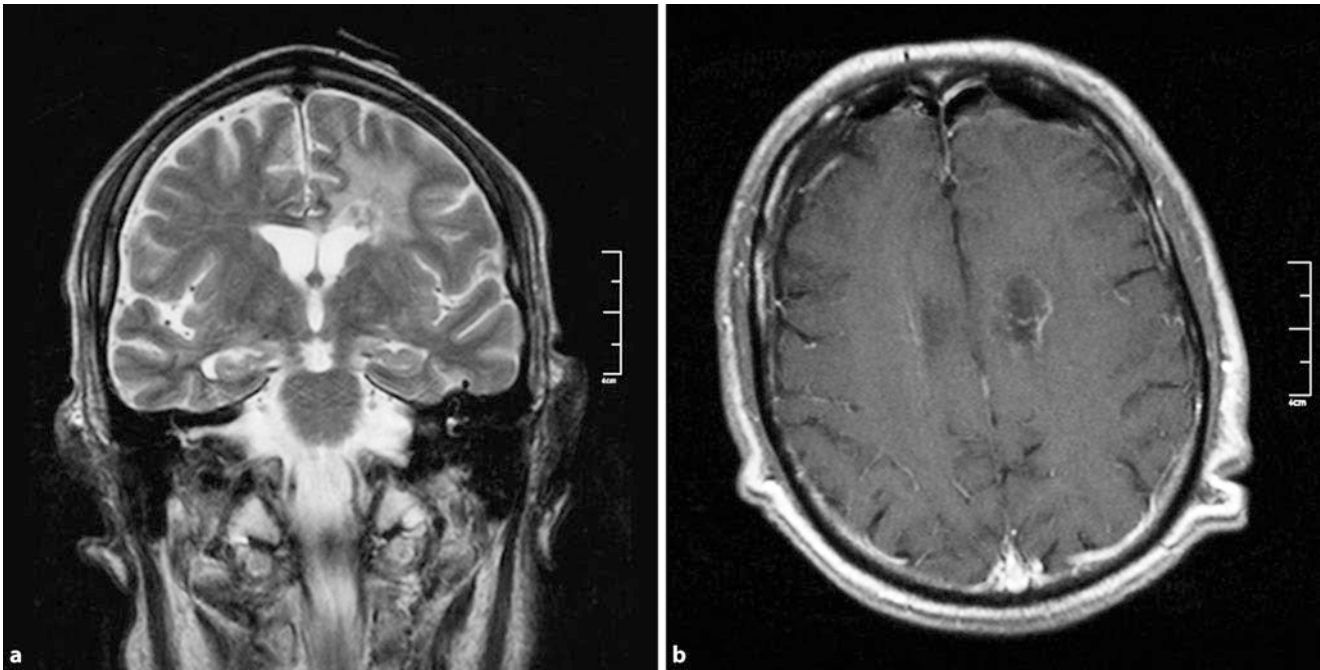


**Fig. 9.153a,b EBV-associated lymphoma.** A 55-year-old male patient, condition after double lung transplantation in advanced chronic obstructive pulmonary disease (COPD). Known generalised CMV and cryptococcal infection. Under therapy fulminant neurological deterioration and exitus letalis after 6 weeks. In the stereotactic biopsy detection of an EBV-associated B-cell

non-Hodgkin's lymphoma. **a** Coronal T2-weighted image: extensive oedema formation in the medullary layer around the left anterior horn with central solid imposing portion. **b** Axial T1-weighted post-contrast agent axial image: marginalised contrast agent uptake around the solid portion, regressive changes centrally

**Post-transplant lymphoproliferative disorder** Because of the iatrogenically limited function of cytotoxic T cells after organ transplantation, there may be a fulminant replication of the EBV virus and infected leukocytes (in the CNS mainly in the B-cell line). The high-grade lymphomas arising in this manner can only be distinguished from primary CNS lymphoma immunohistochemically. This distinction, however, is essential, as the therapy is based on a reduction in the immunosuppressing medication.

In principle, post-transplant lymph-proliferative disorder (PTLD) can affect all organ systems; CNS involvement is rare but associated with a poorer prognosis (■ Fig. 9.154).

#### ■ HIV- and AIDS-defining Infections

Infection with the human immunodeficiency virus (HIV), a capsulated retrovirus with high affinity to the CD4 receptor, leads to a disorder in cellular immunity due to virus replication in CD4<sup>+</sup>lymphocytes. Owing to rapid mutations (molecular mimicry) the virus escapes immune defences. The AIDS stage is defined by an AIDS-defining illness in the United States and also by a decrease in the number of CD4 cells (<200/μl). Many of these diseases are opportunistic infections.

#### Infectious AIDS-defining illnesses with possible CNS involvement

- Systemic candidiasis
- CMV encephalitis, CMV retinitis
- HIV-associated encephalopathy (HIVE)

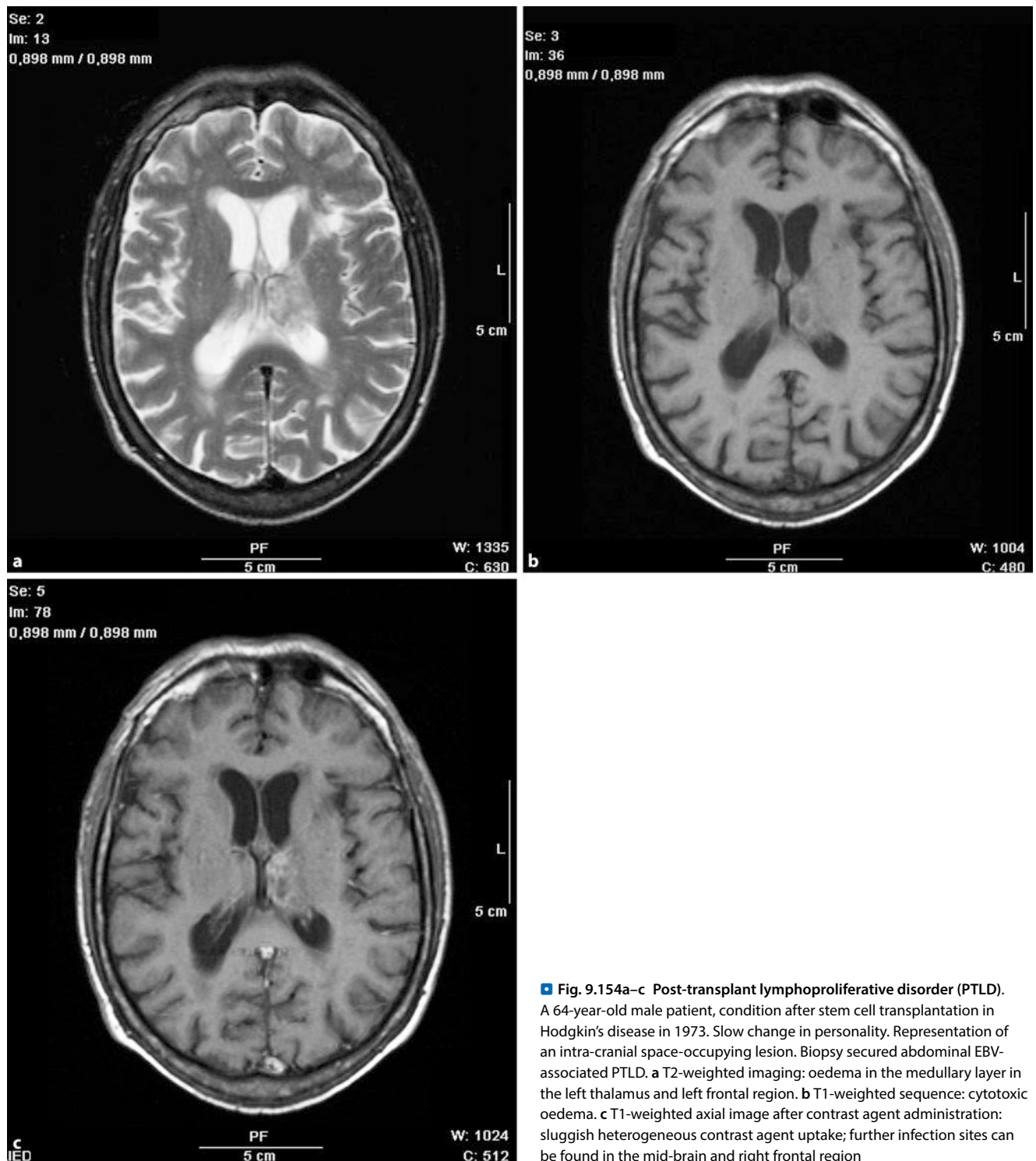
- HSV encephalitis
- Histoplasmosis
- Coccidioidomycosis
- Cryptosporidiosis
- MOTT
- PML
- Tuberculosis
- Toxoplasmosis

#### ■ HIV-associated Encephalopathy

During an HIV infection the brain also becomes the site of virus replication. Cerebral macrophages and glial cells are infected; because of the immunopathogenetic mechanisms there is a disruption to the integrity and function of the neurons. The CNS represents a partially independent compartment of virus replication. Compared with non-affected HIV patients, HIVE patients show a significantly increased viral load in the CSF and parenchyma.

**Clinically**, patients with HIVE stand out because of the so-called **HIV dementia complex**, a slowly progressive sub-cortical dementia similar to Alzheimer's disease, which is clinically divided into stages according to the Memorial Sloan-Kettering Scale (Price 1998).

**Medical Imaging.** In addition to global atrophy morphological imaging shows extended, laterally symmetrical confluent medullary changes, which stand out as hypo-dense on CT, hyperintense on MRI T2-weighted images and FLAIR sequences,



**■ Fig. 9.154a–c Post-transplant lymphoproliferative disorder (PTLD).** A 64-year-old male patient, condition after stem cell transplantation in Hodgkin's disease in 1973. Slow change in personality. Representation of an intra-cranial space-occupying lesion. Biopsy secured abdominal EBV-associated PTLD. **a** T2-weighted imaging: oedema in the medullary layer in the left thalamus and left frontal region. **b** T1-weighted sequence: cytotoxic oedema. **c** T1-weighted axial image after contrast agent administration: sluggish heterogeneous contrast agent uptake; further infection sites can be found in the mid-brain and right frontal region

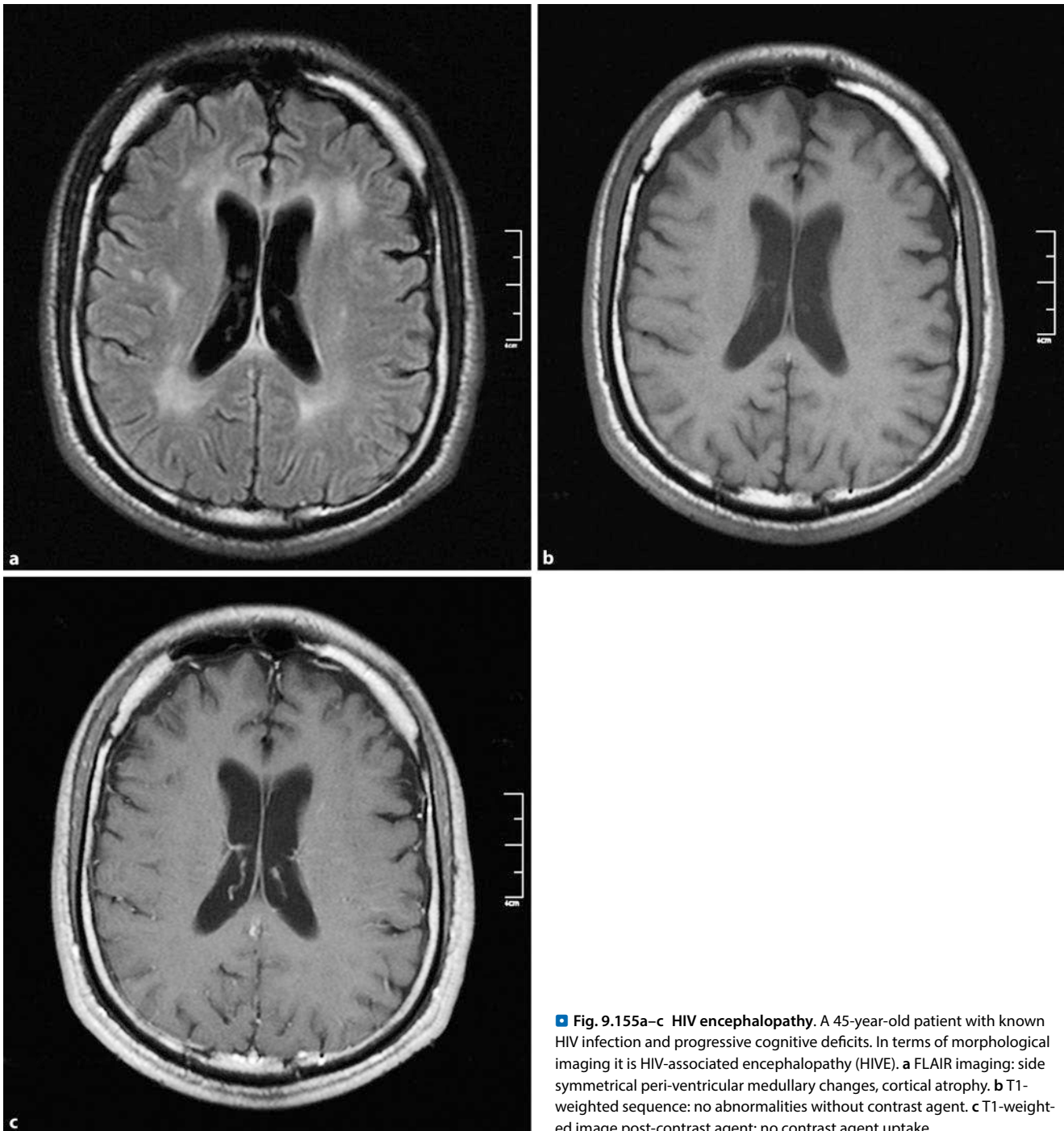
iso-intense without contrast agent on T1-weighted sequences. These changes exclude the cerebral cortex (■ Fig. 9.155). Contrast agent uptake contra-indicates HIVE. On <sup>1</sup>H-MR spectroscopy a small decrease in NAA is detectable, along with a choline increase.

#### ■ Progressive Multi-focal Leukoencephalopathy

Progressive multi-focal leukoencephalopathy (PML) is defined as a rapidly progressive multi-focal demyelinating disease,

which is caused by the reactivation of the John Cunningham (JC) virus, a double stranded DNA (dsDNA) polyomavirus. Approximately 1–10% of HIV-infected individuals contract it; in other immunosuppressed patients PML is much rarer. Time, location and symptoms of the primary infection with the JC virus are unknown; approximately 70–90% of adults have antibodies. PML in HIV-infected patients has a poor prognosis; the survival time after diagnosis is only a few months. It is unclear in which cells the virus persists. At the outbreak of





■ **Fig. 9.155a–c HIV encephalopathy.** A 45-year-old patient with known HIV infection and progressive cognitive deficits. In terms of morphological imaging it is HIV-associated encephalopathy (HIVE). **a** FLAIR imaging: side symmetrical peri-ventricular medullary changes, cortical atrophy. **b** T1-weighted sequence: no abnormalities without contrast agent. **c** T1-weighted image post-contrast agent: no contrast agent uptake

PML replication occurs in the glial cells, which are destroyed during virus release.

The most common **symptoms** are cognitive limitations, aphasic disorders, headache, gait disorders, paralysis, seizures, emotional and visual disturbances.

**Medical Imaging.** On morphological imaging non-enhancing hyper-intense medullary lesions appear without a space-occupying effect on T2-weighted images and FLAIR sequences similar to HIVE. Unlike HIVE an **asymmetrical propagation shows** (■ Fig. 9.156) that the invasive character is expressed through

hypo-intensity on the unenhanced T1-weighted images. The lesions extend to the cortex boundary; the accompanying atrophy is low. Magnetisation transfer (MT) sequences are superior to the standard sequences in the detection of medullary changes because they represent the interaction between free protons and those bound in macro-molecular complexes. The <sup>1</sup>H-MR spectroscopy may show specific changes (significant decrease in NAA and creatine, a lactate peak).

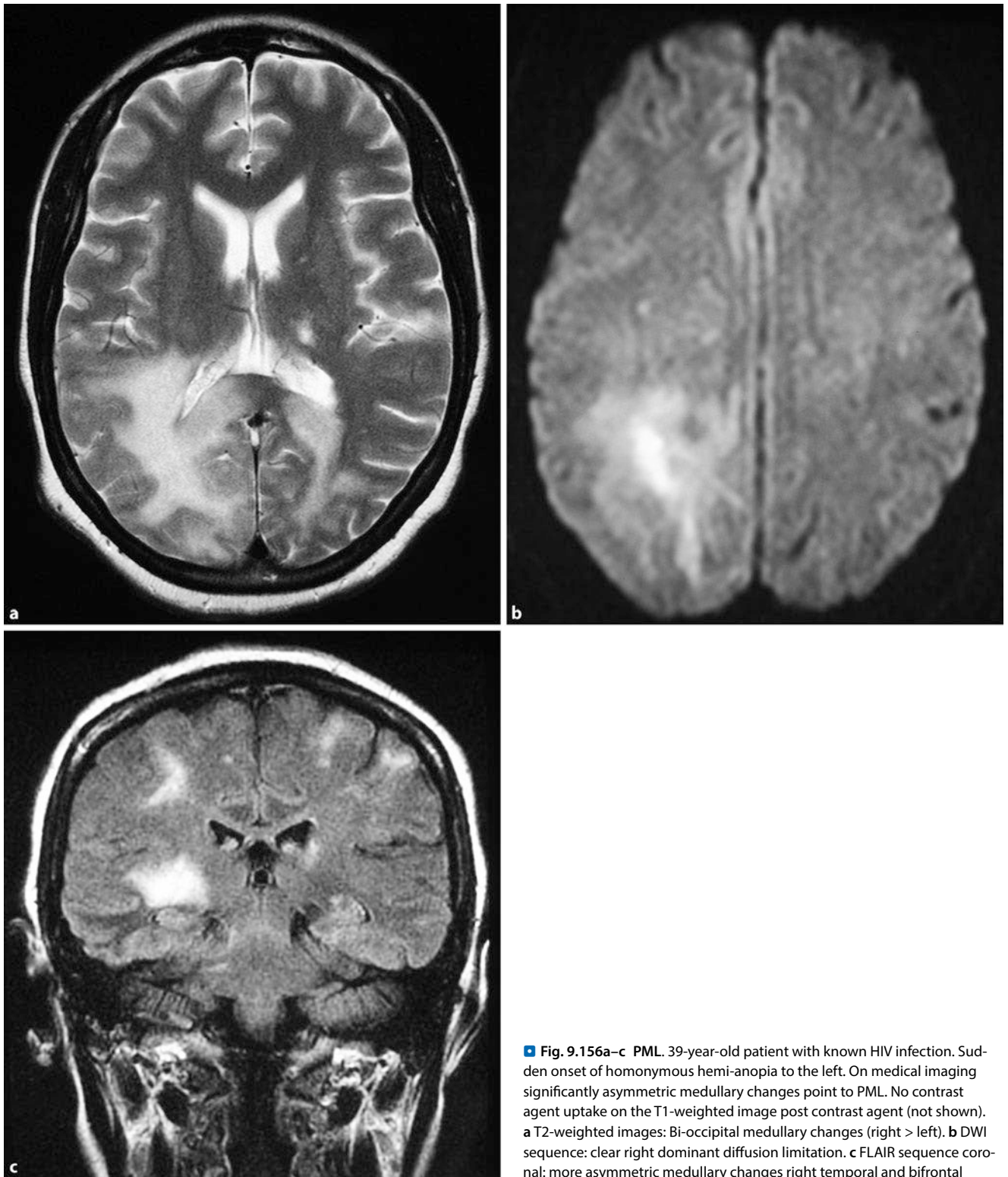


**Fig. 9.156a–c PML.** 39-year-old patient with known HIV infection. Sudden onset of homonymous hemi-anopia to the left. On medical imaging significantly asymmetric medullary changes point to PML. No contrast agent uptake on the T1-weighted image post contrast agent (not shown). **a** T2-weighted images: Bi-occipital medullary changes (right > left). **b** DWI sequence: clear right dominant diffusion limitation. **c** FLAIR sequence coronal: more asymmetric medullary changes right temporal and bifrontal

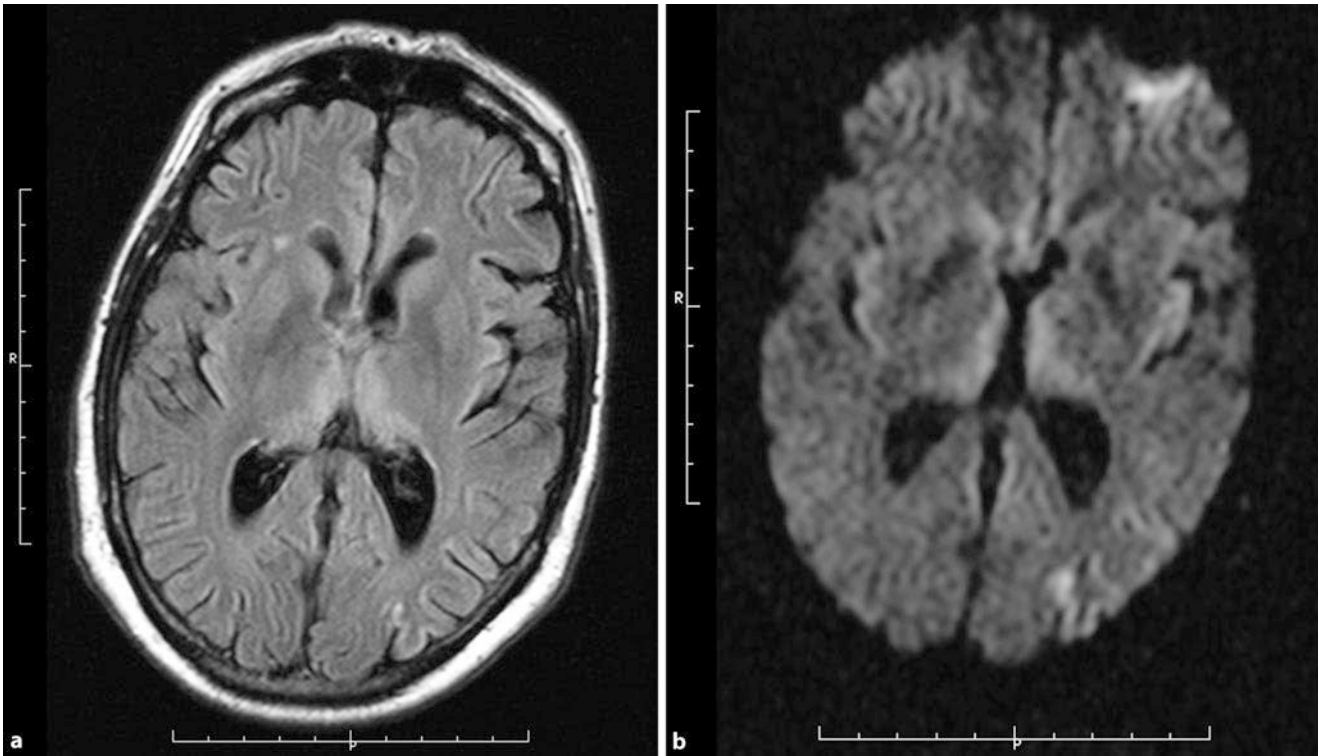
#### 9.6.4 Spongiform Encephalopathy

- **Creutzfeldt–Jakob Disease**
- **Definition, Aetiology, General Information**

Creutzfeldt–Jakob disease (CJD) is caused by a prion (synonym: transmissible spongiform encephalopathy). It is one of the prion diseases that occur in humans and animals, neuropathologically

characterised by spongiform changes, astrocytic gliosis, neuronal loss and deposition of the abnormal form of the prion protein. It can be spread within the affected species or is also transferable between species.

Clinically, progressive dementia, ataxia and myoclonus are present. The diagnosis is made based on the symptoms and EEG changes. Imaging is often normal except for progressive, cortical



■ **Fig. 9.157a,b** Creutzfeldt–Jakob disease. **a** On the axial FLAIR sequences slight hyper-intensity in the basal ganglia is present. **b** On the axial DWI hyperintensity is visible primarily on both sides in the occipital cortex and

the sub-cortical structures. These signal changes are consistent with the typical clinical picture of Creutzfeldt–Jakob disease of the Heidenhain variant. Heidenhain variant patients may become blind

atrophy. On T2-weighted images an increased signal intensity often shows in the basal ganglia (■ Fig. 9.157).

#### ■ ■ Classification, Epidemiology, Symptoms

Prion diseases in humans occur as sporadic (sporadic CJD, sporadic fatal insomnia [FI]), genetic (familial CJD, fatal familial insomnia [FFI], Gerstmann–Sträussler–Scheinker syndrome [GSS]) or transmitted (iatrogenic, variant CJD [vCJD], kuru) forms.

**Sporadic Form.** The sporadic form of CJD is the most common form of the disease occurring worldwide, with an incidence of approximately 1–1.5 cases per year per million inhabitants. The peak incidence is between the 60th and 70th year of life. It is a rapidly progressive disease with a median survival time of approximately 6 months. **Clinically**, rapidly progressive dementia that develops within weeks to months in addition to progressive ataxia dominate; in the course of the disease extra-pyramidal motor disturbances, myoclonus and pyramidal tract signs appear. Finally, an akinetic mutism occurs.

Transmission of the virus from person to person has been hitherto demonstrated only via the iatrogenic route, i.e. via direct contact with infectious tissue. The disease was transmitted in a few cases via contaminated neuro-surgical instruments or intracerebral EEG electrodes. In a few cases there was a case of CJD disease after cornea transplantation. The cornea was from a donor who had died from CJD. Worldwide, most cases, however, are due to contaminated dura mater grafts (most of which occurred in Japan) or IM administration of growth hormone manufac-

tured from cadaver pituitary glands in patients with primary hypopituitarism.

**Variant CJD.** Variant CJD is associated aetiopathogenetically with bovine spongiform encephalitis. To date, approximately 200 cases of the disease have occurred worldwide. The patients are significantly younger than in the sporadic form of CJD (median 30 years). The disease duration is longer (median 14 months). The focus is on psychiatric disorders (mostly depression or psychosis), which can extend over several months without neurological abnormalities. Later, painful dysesthesia and gait ataxia also occur; the dementia occurs late in the disease progression. Unlike the sporadic form of CJD the abnormal prion protein can also be demonstrated in the peripheral lymphoid tissues (appendix, tonsils and lymph nodes). A transfer of this form of disease via blood and blood products has already been observed.

#### ■ ■ Clinical Diagnosis

While the definitive diagnosis of CJD requires a neuro-pathological investigation, the clinical diagnosis of sporadic CJD is supported by the detection of periodic complexes on the EEG (periodic sharp and slow wave complexes), increased concentrations of 14-3-3 protein in the CSF and hyper-intense basal ganglia on MRI T2-weighted images, FLAIR and DWI sequences. Although the MRI has not yet been entered into the diagnostic criteria for sporadic CJD, it is essential for the exclusion of other rapidly progressive forms of dementia.

### ■ ■ Differential Diagnosis

Because of the variable clinical presentation, the differential diagnosis of CJD includes a wealth of neurological and psychiatric disorders. In the elderly the most important differential diagnosis is that of Alzheimer's disease; in younger patients an inflammatory CNS disease must frequently be considered.

## 9.6.5 Parasitic Infections

Parasitic infections are rare in industrialised countries. The most common parasitic infections are cysticercosis, echinococcosis and toxoplasmosis.

### ■ Cysticercosis

#### ■ ■ Taenia Solium

Infection occurs via the ingestion of eggs (*taenia solium*), mostly in inadequately cooked pork. First clinical signs are usually seizures. The parenchyma, meninges, ventricles and spinal cord can be infected.

**Medical Imaging.** Spinal cysticercosis is usually found intradurally, but may have an intra- or extra-medullary location. Intramedullary, it is seen on the MRI as a solid or annular enhanced lesion. Extra-medullary cysts are similar to the sub-arachnoid (racemos) form. In the sub-arachnoid form of the disease, the cysts are usually found in the basal cisterns, the Sylvian fissure and the inter-hemispheric fissure. They grow by wall proliferation. The cysts appear hyper-intense on the FLAIR sequence to CSF, isointense on T2-weighted images. Frequently, there is a marginal enhancement. The vesicle of the intra-axial lesion represents the expanded bubble of the parasite. The cystic lesion in the parenchymatous type contains the head of the worm, the sub-arachnoid type (racemos type) does not. After 5–10 years the parasite dies and the cyst swells after the loss of osmotic regulation. In this situation antigens are released with a resulting inflammatory reaction, oedema and seizures. Subsequently, calcification forms.

In the early phase on the CT or MRI an oedema shows with or without nodular enhancement. Later cysts show (usually < 1 cm) that are iso-intense to CSF. These lesions are usually peripheral to the medullary/cortex border. Sometimes a small node is visible, which represents the scolex.

At this time there is usually no enhancement. Later, the liquid drains from within the cyst, which causes an inflammatory reaction (acute encephalitis). On the imaging an annular enhancing lesion now presents with surrounding oedema. On the CT the cyst has an increased density; on T1- and T2-weighted images its signal is increased to CSF. In the further course of the disease, calcifications form in the area of the cyst. The CT scan shows peripheral calcifications, no oedema and no enhancement. On the MRI these calcifications also show (best on T2- and T2\*-weighted images).

Medical imaging is used for staging and follow-up. In intraventricular cysticercosis cysts also have a signal similar to CSF. They cannot usually be represented by CT. Dependent on the stage, enhancement may be present. The cysts often obstruct the for-

men of Monro, the fourth ventricle or aqueduct, which can lead to hydrocephalus. Ventriculitis results from the rupture of the cysts.

### ■ Hydatid Cyst

Caused by *Echinococcus*, the cysts are usually found in the lungs and liver. CNS involvement occurs in about 2%.

**Medical Imaging.** The cysts are usually solitary, large and smoothly bounded. They are usually located supratentorially in the territory of the middle cerebral artery. On the CT and MRI the cysts are iso-intense to CSF. Unless super-infected, there is usually no contrast enhancement and no marginal oedema.

### ■ Toxoplasmosis

This is the most common opportunistic CNS infection in HIV patients (see above, ► Sect. 9.6.3). In congenital infection there is diffuse encephalitis. Children have microcephalus, mental retardation and chorioretinitis.

**Medical Imaging.** The imaging shows atrophy, dilated ventricles and calcifications in the peri-ventricular white matter, the basal ganglia and the cerebral hemispheres. In the congenital CMV infection the calcifications are usually only peri-ventricular. In patients with AIDS toxoplasmosis mainly results from a reactivated infection (► Sect. 9.6.3). This leads to necrotising encephalitis with multiple, thin-walled abscesses. The typical image shows multiple lesions with contrast agent uptake measuring 1–4 cm in size with marginal oedema. Large lesions often show ring enhancement, while smaller lesions enhance completely. On T2-weighted images they appear mostly hyper-intense, mainly located in the basal ganglia.

The main differential diagnosis is the primary CNS lymphoma. A response to antibiotics can usually differentiate between toxoplasmosis and lymphoma.

## 9.6.6 Multiple Sclerosis and Related Diseases

### ■ Multiple Sclerosis

#### ■ ■ Definition, Epidemiology

Multiple sclerosis is the most common chronic inflammatory disease of the myelin with disseminated lesions in the white matter area of the central nervous system. The pathological lesions were first described in 1835 by Robert Carswell and Jean Cruveilhier, while Jean-Martin Charcot documented the first clinical presentation.

The disease occurs worldwide, but predominates in the northern parts of Canada, the US and Europe. In individual population groups, including the Eskimos, MS has not been described until now. Its incidence is 30–80 persons/100,000 population, with women being affected much more frequently than men (1.7:1.0). Even in children MS has been unequivocally established. Here, girls are also more frequently affected than boys, whereby an early onset of the disease is an adverse prognostic factor. The age of onset lies between the 20th and 40th years of life in one third of the affected individuals. This makes MS one of the most common neurological disorders among young adults.

### ■ ■ Aetiology, Pathogenesis

The pathogenesis of MS is not yet fully understood. Different hypotheses have been given, such as a causative viral infectious disease. A variety of viruses have been discussed as being the triggering MS agent with a subsequent auto-immune T cell response. Causal links between various vaccinations and the subsequent onset of the MS disease have been taken into consideration, just like the above two theories; however, they have not been proven nor have they been completely refuted to this day. Family history and twin studies support the involvement of genetic factors. In addition, an association with human leukocyte antigens (HLA) has been demonstrated. Carriers of the HLA-DR2 allele on chromosome 6p have a 4 times higher risk of the disease.

### ■ ■ Symptoms

Depending on the location of the inflammation that can affect the entire central nervous system MS patients suffer from various focal neurological failures, such as inter alia paresis or paraesthesia, dizziness, ataxia, visual disturbances, but also psycho-pathological deficits. The disease can begin in a mono- or poly-symptomatic manner. It runs mostly in spurts, but can also be chronically progressive.

The optic tract is a common location for the occurrence of inflammation. A disease flare frequently manifests as optic neuritis. The acute visual disturbance of this disease is successfully treated with steroids. However, steroid therapy does not affect the prognosis of the possibly resulting optic atrophy in the later progress of the disease.

### ■ ■ Classification, Therapy

Internationally different rating scales have been introduced to represent the disease stages and progression of MS in a comparable manner. The treatment options were also considered. The most common rating scale is the Kurtzke Expanded Disability Status Scale (EDSS). The scale ranges from 0 to 10 in increments of 0.5, where a value < 3 represents a low-grade constraint and a value > 5 describes severe physical and mental impairment. However, the EDSS is only of limited use for the disease in childhood.

A causal treatment for MS is not known. Physiotherapy, occupational therapy and logopaedics are employed to support immunomodulatory medicines.

### ■ ■ Medical Imaging

The described inflammatory foci form plaques. In the early phase inflammatory cell elements can be detected. In the chronic stage astrogliosis with collagen deposition in the peripheral regions dominates. The requirement for detectable remyelination processes is the presence of oligodendrocytes and intact axons.

In an acute MS episode plaques show partial or complete destruction with loss of the myelin sheath. Axon cylinders are initially spared and only affected in the advanced stages of the disease. At the same time a peri-vascular cell accumulation ("cuffs") can be seen in this acute phase. These precede the myelin sheath disintegration.

**Magnetic Resonance Imaging** The sensitivity of MRI in the detection of known MS is reported to be 76–85%. According to individual studies in the diagnosis of MS, the MRI is more useful for its detection than evoked potentials or CSF results. This primarily concerns patients with isolated spinal cord symptoms. Here MR tomography imaging of the head was shown to be more sensitive than laboratory tests. The best representation of **the plaques** is obtained with FLAIR and T2-weighted spin echo sequences (■ Figs. 9.158, 9.159). In the posterior fossa, T2-weighted images are superior, while in the supra-tentorial region the FLAIR sequence produces better results. Particularly peri-ventricularly near the CSF, which appears with a high signal on the T2-weighted image, FLAIR sequences are appropriate. Occasionally, acute plaques show a thin margin, which is hypo-intense on the T2-weighted images and hyper-intense on the T1-weighted images, caused by free radicals or fat-laden macrophages and protein accumulations (■ Fig. 9.158).

Despite their irregular appearance MS foci usually have a clearly delineated edge. Most peri-ventricular lesions have an oval appearance, where their longitudinal axis aligns itself transversely to the axial images. This also causes the typical picture of the **Dawson's fingers on the sagittal sequences** (■ Fig. 9.158d). MS foci are generally homogeneous in structure without cysts or necrotic components. Haemorrhages do not occur. Furthermore, only in very rare cases are peri-focal oedema or space-occupying effects found.

The main location of the foci is found in the **peri-ventricular white matter**, mostly along the anterior and posterior horns. Long, curved plaques, which affect the inner fibres of the genu of the corpus callosum and splenium can also be seen. Furthermore, wavy plaques along the sub-cortical U-fibres can be detected. In most cases, there is a symmetrical involvement of both cerebral hemispheres, typical predilection sites are the corpus callosum, the corona radiata in addition to the internal capsule and the optic tract. The centrum semi-ovale is usually affected. In principle, however, all myelinated structures can contain MS plaques, including the brain-stem, spinal cord (■ Fig. 9.160) and sub-cortical U-fibres. Brain-stem and cerebellar plaques are more common in adulthood, lesions in the ventro-lateral pons are characteristic, at the entry point of the fifth cranial nerve (■ Fig. 9.161). These are the subject of numerous studies.

Narrow lesions in the corpus callosum, directly adjacent to the ependyma of the lateral ventricle, are clearly visible on sagittal FLAIR sequences in particular.

**Brain atrophy** can be particularly evident in the chronic form. The widening of the lateral ventricles and sulci is striking. Forty per cent of patients also have atrophy of the corpus callosum. This shows up best on T1-weighted sagittal images. However, the exact mechanism is unknown. Possible causes are myelin and axonal loss. The atrophy seems to develop independently of the disease sub-type and the number of focal lesions. In the literature, an annual brain volume loss of 0.5–1%, compared with 0.1–0.3% in the general population, is described. There seems to be a correlation between brain atrophy and clinical impairment, which is stronger than the extent of T2 lesions. A general brain volume reduction in the first 2 years is the best MR predictor of 8-year EDSS scores. An association between brain atrophy and cognitive impairment in MS patients was also discussed.

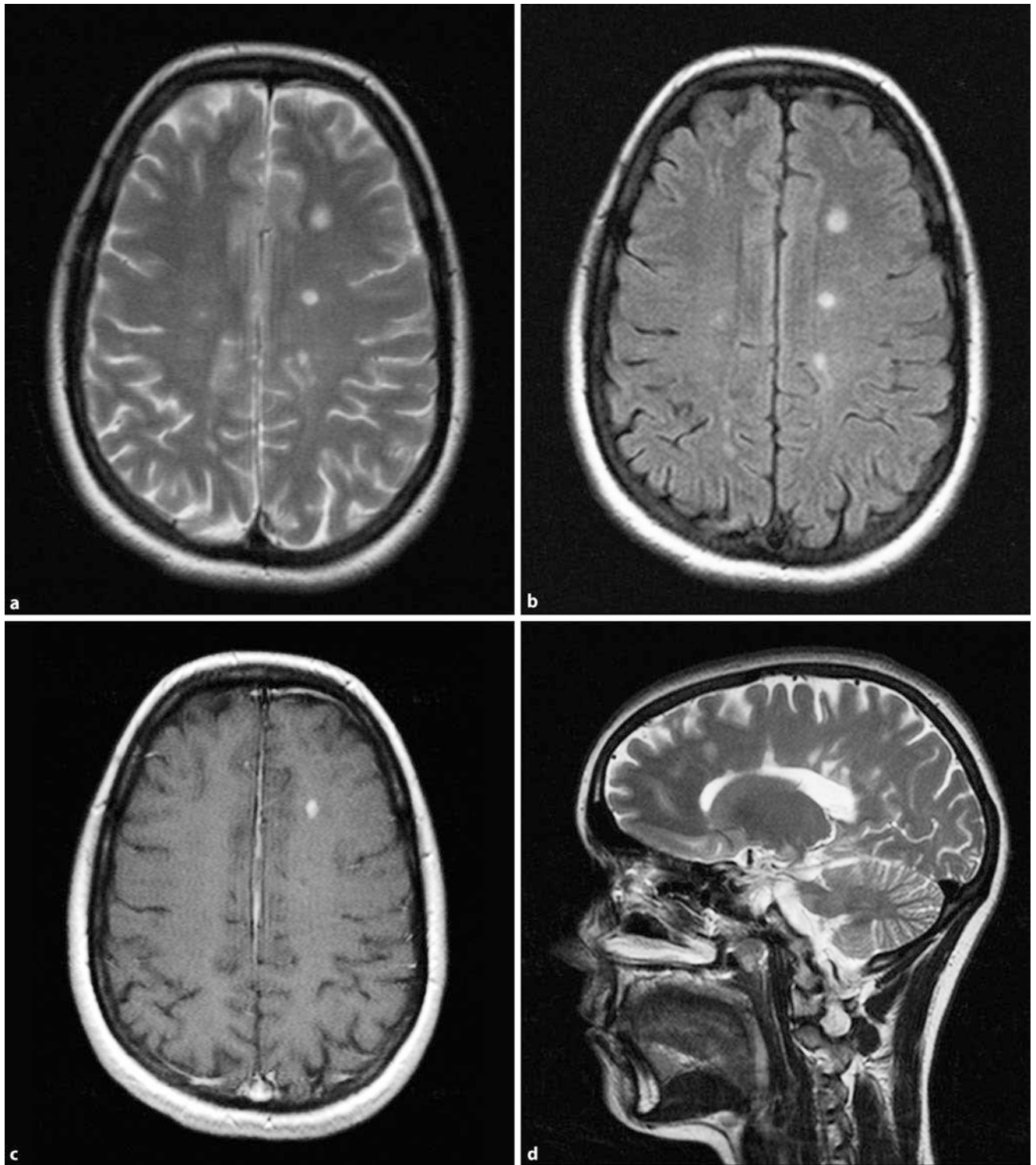
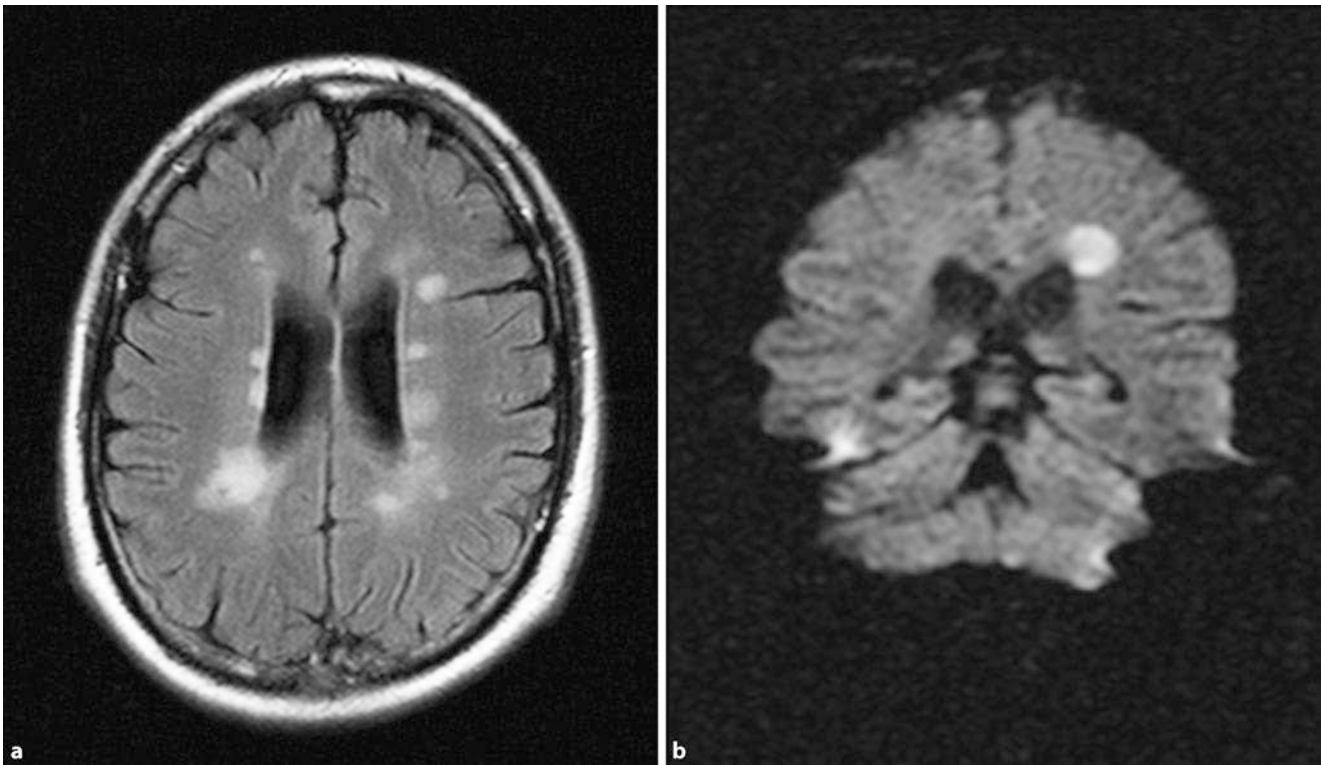
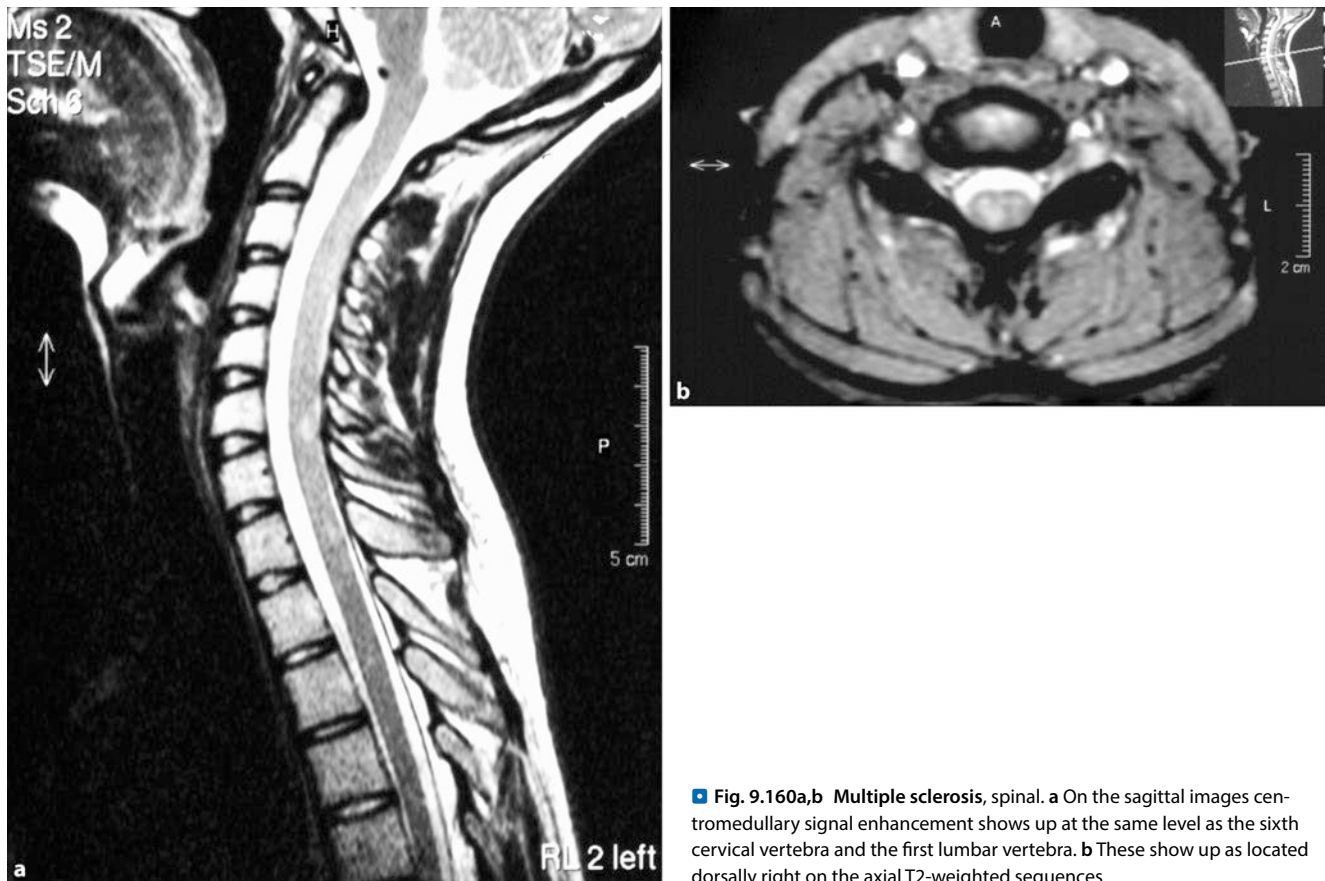


**Fig. 9.158a–d Multiple sclerosis.** **a** Acute plaque, which shows a dark rim on the T2-weighted images. **b** Despite the irregular appearance the edge of the focal point is clearly delineated (→ axial FLAIR). **c** On the axial T1-weighted sequence the contrast agent uptake shows an acute MS focal point. **d** The

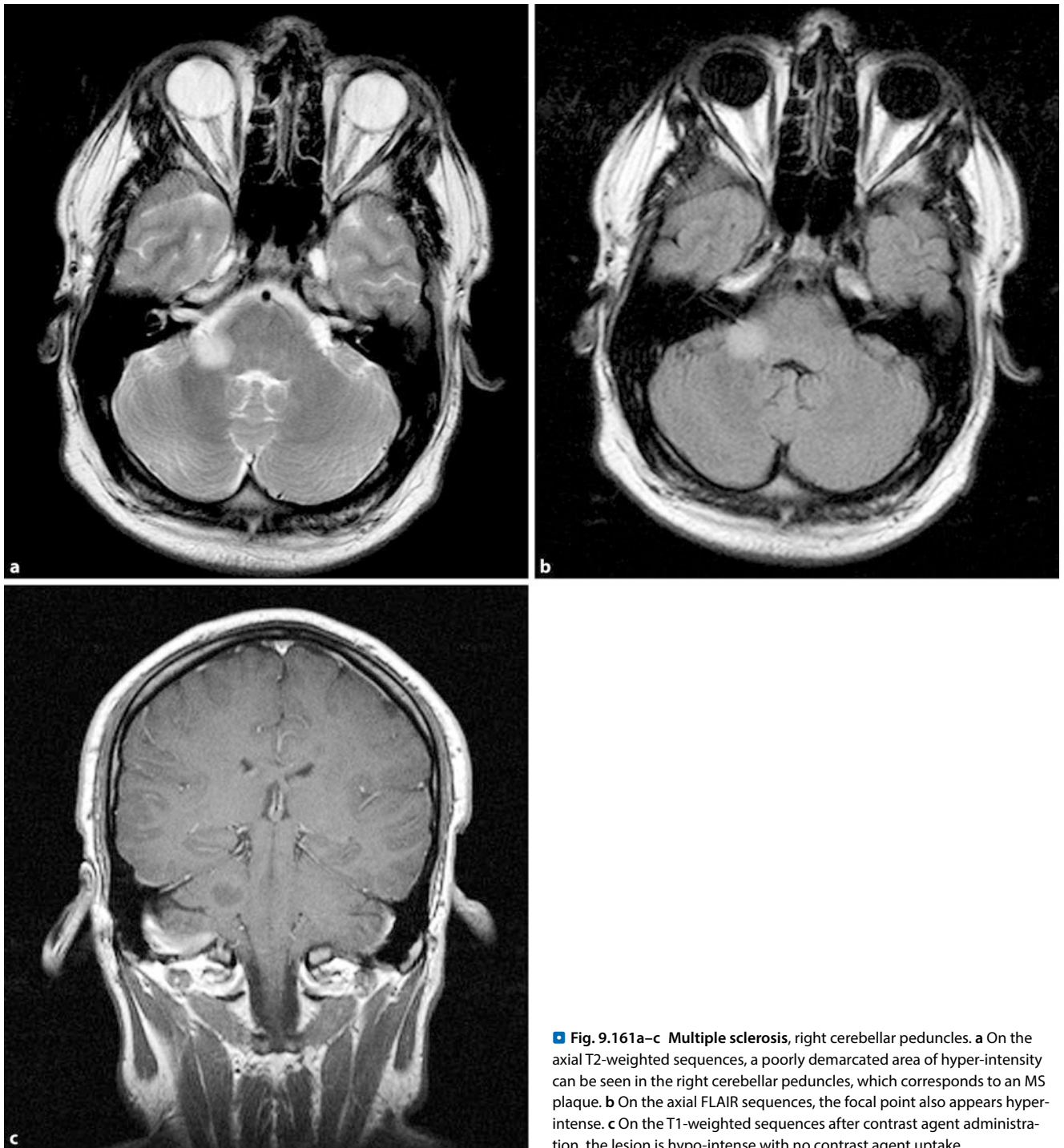
sagittal, thin-slice (3 mm) T2-weighted sequence above the corpus callosum shows the plaques that are typical for multiple sclerosis, which radiate like fingers into the corpus callosum (Dawson's fingers)



■ Fig. 9.159a,b Multiple sclerosis. a Numerous peri-ventricular foci on the axial FLAIR images, b an acute focal point presents as hyper-intensity on the DWI



■ Fig. 9.160a,b Multiple sclerosis, spinal. a On the sagittal images centromedullary signal enhancement shows up at the same level as the sixth cervical vertebra and the first lumbar vertebra. b These show up as located dorsally right on the axial T2-weighted sequences



■ **Fig. 9.161a–c Multiple sclerosis, right cerebellar peduncles.** **a** On the axial T2-weighted sequences, a poorly demarcated area of hyper-intensity can be seen in the right cerebellar peduncles, which corresponds to an MS plaque. **b** On the axial FLAIR sequences, the focal point also appears hyper-intense. **c** On the T1-weighted sequences after contrast agent administration, the lesion is hypo-intense with no contrast agent uptake

Occasionally, a signal decrease (T2 shortening) was observed in the putamen and thalamus on T2-weighted images in advanced stages of the disease. It is assumed that a deposition of iron or other metals occurs here.

An involvement of the visual system, particularly the optic nerve with a clinical picture of an **optic neuritis**, is common. For the detection of acute MS foci in the optic nerve a gadolinium-enhanced, fat-saturated T1-weighted sequence should be made. Partial volume effects are minimised in the direction of the coronal section.

The spinal cord is usually involved in MS, which can lead to a picture of **transverse myelitis** in patients. All levels of the spinal cord may be affected; however, the plaques are mostly found in the cervical region. For diagnostics, STIR sequences are better than T2-weighted spin echo sequences (FSE). The signal resembles that of lesions of the brain. In acute plaques surrounding oedema may occur, which leads to swelling of the spinal cord and can mimic an intra-medullary tumour. In primary and secondary progressive MS diffuse spinal lesions are more common. Even after the acute phase, these foci remain



visible. The quantitative MRI cannot distinguish between old and new lesions.

Interestingly, quantitative brain analysis in MS patients showed a T2 extension not only in acute and chronic plaques, but also diffusely in apparently inconspicuous white matter. This suggests that the involvement of the white matter is not only a focal process, as suggested by the imaging, but rather a diffuse one. The correlation with clinical symptoms is better in the posterior fossa. About 83% of patients with brain-stem or cerebellar plaques show acute neurological deficits.

Although about half of the MS patients show psycho-pathological abnormalities in the course of the disease, these do not correlate in type and extent with the MR changes. However, the extent of the lesions seems to better correlate with cognitive dysfunction than with memory performance. In T1-weighted iso-intense lesions cellular infiltrates with oedema were also shown, but partial preservation of axons. T1 hyper-intensities in MS plaques also correlated better with areas of demyelination, axone loss and the expansion of the extra-cellular space. Thus, it seems that even if it is less sensitive, the T1-weighted image has a higher specificity for damage to the white matter.

In **acute MS plaques** a temporary disruption of the blood–brain barrier occurs, with the subsequent contrast enhancement of the lesion that is detectable for 8–12 weeks after acute demyelination. Both nodular and ring-shaped enhancement are possible. However, on delayed images the previously recessed inner region is filling up. The loss of the blood–brain barrier is most likely due to a migration and infiltration of macrophages. Thus, it was found that the extent of the contrast agent enhancement correlated with the extent of the macrophage infiltration, but not with the infiltration of peri-vascular lymphocytes.

In individual cases lepto-meningeal contrast enhancement has been described in acute MS.

➤ **Differential diagnosis. Occasionally large plaques can cause a space-occupying effect and thus resemble other tumours. However, compared with neoplastic or inflammatory diseases, MS plaques only show minimal peri-focal oedema and almost no space-occupying effect in relation to the size of the lesion. A lack of contrast agent uptake may also help in the further diagnosis. Furthermore, additional peri-ventricular plaques usually exist.**

**Balo's disease** (■ Fig. 9.162), a sub-type of MS, shows a characteristic picture. The plaques are very large, and a concentric annular appearance on T2- and T1-weighted images is typical. After contrast agent administration more enhanced rings can then frequently be seen that alternate with unenhanced regions. Histologically, this correlates with alternating bands of demyelinated and myelinated white matter. It is possible that this represents successive episodes of acute demyelination, where the centre of the lesion represents the oldest core. Contrast-enhanced MR images provide an overview of the activity of the disease; however, they are not a predictor of its future progress.

**Diffusion-weighted Imaging** On DWI, the Brownian molecular motion is measured. This motion is impeded in tissues through cell membranes, vascular structures, axons or chemical interactions with macro-molecules. A low ADC corresponds to high signal intensity (restricted diffusion). It has been shown that the areas without contrast agent uptake of the acute plaques have a higher ADC (decreased anisotropy) compared with the enhanced ring and the homogeneous enhanced lesions. This may reflect a higher degree of demyelination in the centre of the ring-enhanced plaques. Sub-acute or chronic lesions have only a mean ADC increase.

**Diffusion Tensor Imaging** Diffusion tensor imaging (DTI) allows us to make a statement both about the degree of diffusion and the alignment of the diffusion along the three directional axes. Changes in the DTI may precede the formation of focal lesions by at least 6 months.

**MR Spectroscopy** This is used for the characterisation of brain changes. In acute plaques there is a reduction in NAA and an increase in choline values. Free lipids (due to the myelin decay) are also increased. Chronic lesions have decreased NAA and normal choline and creatine levels. Unfortunately, these changes are non-specific and cannot contribute to distinguishing MS plaques from tumours or other inflammatory diseases. A correlation between NAA levels and EDSS in relapsing–remitting MS could not be shown. NAA levels may increase again after 2 years, possibly by remyelination and decrease of the oedema. Creatine levels, which were initially normal, increase between months 3 and 12 months, possibly because of an increased metabolic demand during remyelination. After 12 months, the initially increased choline level returns to normal.

#### ■ Acute Disseminated Encephalomyelitis

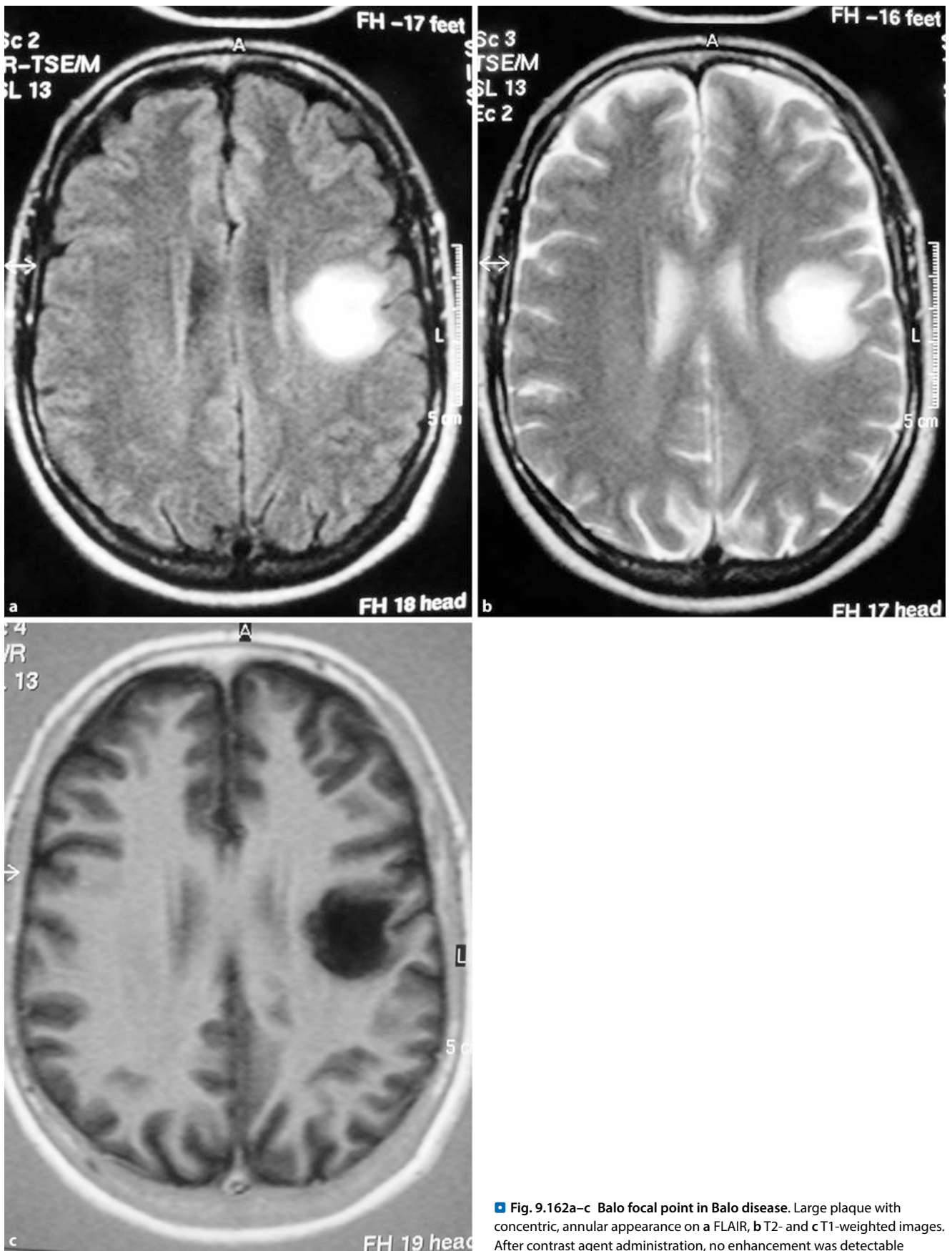
##### ■ Definition

Acute disseminated encephalomyelitis (ADEM) is an acute episode of an autoimmune demyelinating disease of the white matter that mainly affects the brain and spinal cord. It usually occurs after an infection or vaccination. Unlike multiple sclerosis ADEM is a monophasic disease. In rare cases it may recur; then, the term multi-phasic ADEM is used.

Although ADEM is a relatively rare disease, it has gained increasing importance for two reasons. First, in recent years the number of disease cases after vaccinations has increased, especially in children, and second, it can lead to permanent neurological deficits.

##### ■ Epidemiology

Acute disseminated encephalomyelitis is a rare disease, although the exact incidence is unknown. The estimated annual incidence is 0.8/100,000 inhabitants. Children and adolescents are more likely to be affected. Numerous cases have also been reported in adults, even in elderly patients. However, the incidence appears to be significantly lower compared with that in childhood. Children 5–8 years of age are most commonly affected.



■ Fig. 9.162a–c Balo focal point in Balo disease. Large plaque with concentric, annular appearance on a FLAIR, b T2- and c T1-weighted images. After contrast agent administration, no enhancement was detectable

### ■ ■ Aetiology

In approximately 50–75% of cases the clinical manifestation of the disease is preceded by a viral or bacterial infection. Usually this is a non-specific infection of the upper respiratory tract. ADEM may also occur after a vaccination. The symptoms typically begin 6 days to 6 weeks after the infection or vaccination. Pathogens that are associated with ADEM are measles, mumps or the rubella virus in addition to VZV, EBV, hepatitis A and HSV. The most important bacterial pathogen is *Mycoplasma pneumoniae*. Vaccination-associated ADEM is most commonly observed after measles, mumps or rubella immunisations. However, it has also been described after vaccinations against the causative agent of poliomyelitis.

### ■ ■ Pathogenesis, Pathology

The pathogenesis of ADEM is unclear. There are indications that ADEM occurs as a result of a transient auto-immune reaction against myelin or other auto-antigens. This possibly occurs because of a non-specific activation of auto-reactive T lymphocytes.

Acute disseminated encephalomyelitis lesions are observed throughout the brain and spinal cord. Histologically, infiltrates mainly appear in the peri-vascular spaces. Diffuse, often symmetrical peri-venous demyelination occurs. Histologically, the lesions are of the same age. They are mostly localised in the white matter. Lesions can, however, also be found in the cortex, the thalamus, hypothalamus and the remaining grey matter. The inflammatory infiltrates are predominantly composed of lymphocytes, but can also show a mixed picture including lymphocytes, neutrophils and microglia. Most often reactive astrocyte proliferation is present.

### ■ ■ Symptoms

Generalised symptoms, such as fever, myalgia, headache, nausea and vomiting, often precede the neurological symptoms. These symptoms begin 4–21 days after the viral or bacterial event. The development of a focal or multi-focal neurological dysfunction is the hallmark of the clinical presentation of ADEM. The beginning of central neurological dysfunction is rapid. The summit of the dysfunction is achieved within only a few days. Classic clinical features include encephalopathy, which can range from lethargy to coma, and focal or multi-focal neurological symptoms, such as hemiparesis, cranial nerve deficits and paraparesis. Meningism, ataxia and seizures are observed less frequently. Patients with large space-occupying, supra-tentorial or brain-stem lesions occasionally require intensive medical therapy with intubation and mechanical ventilation. When optic neuritis occurs, it is usually bilateral.

Spinal symptoms are found in a minority of patients. In principle, an isolated myelitis can be considered to be ADEM. There is no reason to believe that different pathophysiological mechanisms are present in patients with post-infectious myelitis.

The regression of symptoms often begins within days. Occasionally, a complete remission can take place within only a few days, but it usually takes weeks to months.

### ■ ■ Clinical Diagnosis

**CSF.** In most cases, the CSF examination shows pathological changes; however, a completely normal result is not unusual. Lymphocytic pleocytosis, elevated pressure conditions and protein lev-

els (often <1.0 mg/l) are typical results found in CSF investigations. Oligoclonal bands and intra-theal antibody production are rarer in comparison to MS and other neuro-inflammatory diseases.

**Computed Tomography.** In up to 40% of cases ADEM lesions do not show up on CT. Only when they have reached a sufficient size can they be recognised as hypo-dense areas.

**Magnetic Resonance Imaging.** Magnetic resonance imaging is the method of choice for the presentation of ADEM. The diagnosis cannot be made without MRI. MRI is used not only for the detection of demyelinating lesions, but also to exclude other diseases. Changes on MRI can be identified, particularly on the T2-weighted sequences and on the FLAIR sequence (■ Fig. 9.163). The lesions are detectable as irregular areas of high signal intensity. The lesions are typically large, multiple and asymmetrical. They can be located in the cerebral and cerebellar hemispheres, the brain-stem and spinal cord. The sub-cortical and central white matter are most often affected. Less frequently, the grey matter of the thalami and basal ganglia is affected; in these cases usually symmetrically. Only in 30–60% of cases are the lesions located in the peri-ventricular white matter. Unlike MS, the occurrence of lesions in the corpus callosum is an exception.

On T1-weighted sequences ADEM lesions appear hypointense. The incidence of gadolinium-affine foci is variable and depends on the stage of inflammation. Contrast agent uptake is described in 30–100% of cases. The pattern of uptake varies and may be point-like or peripheral. A complete or incomplete annular uptake is not uncommon.

Acute disseminated encephalomyelitis lesions may have restricted diffusion on the diffusion-weighted sequences, which is particularly the case in acute lesions. MR spectroscopy often shows a reduction in NAA levels in the area of T2 signal-intense lesions, while choline levels are normal. A pathological lactate peak can often be identified.

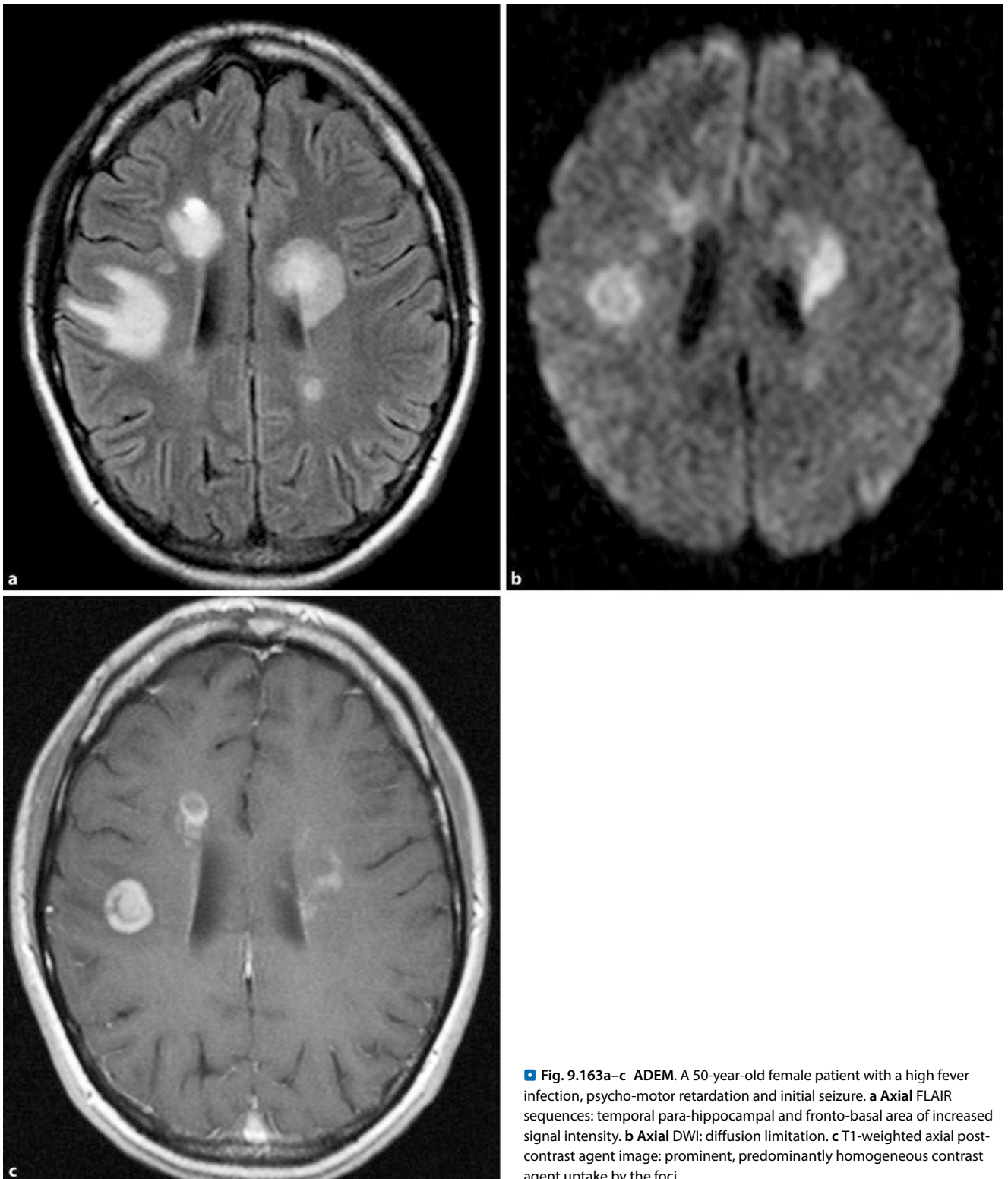
#### MRI Characteristics in ADEM

With cerebral involvement the following MRI patterns are described:

- ADEM with small lesions < 5 mm
- ADEM with large, confluent or tumour-like lesions, which frequently show peri-focal oedema and a space-occupying effect. In these cases the differentiation from a glioblastoma can be very difficult; biopsy confirmation is often required
- ADEM with symmetrical bithalamic lesions
- Acute haemorrhagic encephalomyelitis (AHEM), where a haemorrhage occurs within large foci of demyelination

Involvement of the spinal cord is described in 14–28% of cases. The lesions appear hyper-intense on T2-weighted sequences and may show uptake after gadolinium administration. The foci may be large, and the spinal cord is often swollen. The thoracic region is usually affected.

**Follow-up MRI** plays an important role in the diagnosis of ADEM. In the monophasic ADEM no new foci occur. The com-



■ **Fig. 9.163a–c ADEM.** A 50-year-old female patient with a high fever infection, psycho-motor retardation and initial seizure. **a** Axial FLAIR sequences: temporal para-hippocampal and fronto-basal area of increased signal intensity. **b** Axial DWI: diffusion limitation. **c** T1-weighted axial post-contrast agent image: prominent, predominantly homogeneous contrast agent uptake by the foci

plete regression of MRI lesions is described in 37–75% of patients, a partial regression occurs in 25–53%.

#### ■ ■ Differential Diagnosis: ADEM Versus MS

The differential diagnosis between ADEM and MS is important mainly for prognostic reasons. In children with ADEM, the prognosis is good, while in children with MS, the development of a

significant disability is to be expected in the course of the disease. The most important differences between the clinical manifestation and the CSF analysis are shown in ■ Table 9.18.

In principle, **medical imaging** cannot differentiate ADEM lesions from those caused by MS with any certainty. However, **differences exist** that favour one of the two diagnoses:

**Table 9.18** Acute disseminated encephalomyelitis (ADEM) vs multiple sclerosis (MS): the most important differences in clinical and CSF results

Characteristic features	ADEM	MS
Age	< 10 years	> 10 years
Encephalopathy	Yes	No
Symptoms	Poly-symptomatic	Mono-symptomatic
Optic neuritis	Bilateral	Unilateral
CSF	Lymphocytosis	Intra-thecal IgG

- ADEM lesions often have irregular edges, whereas MS lesions are sharply defined with a “plaque-like” edge
- ADEM lesions are located deep in the white matter and frequently show a recess of the peri-ventricular regions and the corpus callosum. On the other hand, peri-ventricular foci and the corpus callosum lesions are characteristic of MS
- Cortical lesions are far more common in ADEM than in MS
- ADEM lesions are asymmetrical, while in MS the foci show relative symmetry
- Fluid-iso-intense lesions on T1-weighted images, so-called “black holes”, indicate that demyelination has taken place and thus supports the diagnosis of MS
- ADEM lesions of the spinal cord are large with swelling of the spinal cord and usually located in the thoracic spine. Spinal MS foci are smaller, show no swelling and are more likely to occur cervically
- Unlike in MS in ADEM no new lesions occur during the course of follow-up investigations

#### ■ ■ Treatment, Prognosis

Spontaneous complete remission is possible in patients with ADEM. However, this is less common than in patients receiving treatment. High doses of intra-venous cortico-steroids are currently considered first-line therapy. It is hoped that these will cause a reduction in the inflammatory response in the CNS and lead to an improvement in clinical symptoms. If there is no improvement under corticosteroids, immunoglobulins are used. Alternatively, plasmapheresis can be carried out, which is considered a second choice option because of the higher rate of complications.

Mortality of 20% with significant sequelae has been reported in previous studies. Recent studies showed that the prognosis of ADEM is generally favourable. About 70% of patients survive without residual deficits. Even severely affected patients can recover completely. Only a few patients with ADEM require intensive medical therapy.

#### ■ Neuromyelitis Optica (Devic)

With neuromyelitis optica (Devic’s syndrome) there is a combined occurrence of optic neuritis and acute myelitis, which may occur at the same time, but also at different times. Autochthonous IgG production in the CSF may be lacking, but polymorphonuclear leukocytes can also occur.

## 9.7 Metabolic Disorders of the Central Nervous System

### 9.7.1 Basics, Definition

Diseases of the white matter of the brain are called leukodystrophies; they are included in the **group of leuko-encephalopathies**. This term says nothing about their aetiology or pathogenesis. Leuko-encephalopathies form a large group of diseases, which are extremely variable in their clinical symptoms, causes and progression. In childhood, all myelination disorders that have occurred pre-, peri- and post-natally, peri- and para-infectious demyelination, toxic medullary layer damage and genetic diseases of the white matter should strictly be included. Leukodystrophies have been known the longest and have been best defined clinically, morphologically, biochemically and genetically.

**Leukodystrophies** are a group of genetic diseases of the nervous system with involvement of the central and in a few cases peripheral myelin. They represent a disruption in the formation or degradation process of the myelin sheaths. A distinction is made between demyelination, i.e. degradation of normally structured myelin, and dysmyelination, i.e. formation or degradation of myelin of abnormal composition, which thus results in unstable myelin and hypo-myelination. This is a distinction that does not cover all pathogenetic insights, but seems useful while pathogenetic processes are not yet known.

### 9.7.2 Leukodystrophies with Primary Hypo-myelination

#### ■ Pelizaeus–Merzbacher

##### ■ ■ Definition, Epidemiology, Aetiology

Pelizaeus–Merzbacher disease is a rare, sex-linked leukodystrophy, which is characterised by hypo-myelination and patchy demyelination of the brain. The peripheral nervous system is not affected. Its incidence is estimated to be approximately 1:100,000 in boys. In the disease point mutations or duplications of the proteolipid protein gene were detected.

##### ■ ■ Clinic, Diagnosis, Therapy

The **classical form** affects only boys and has a variable clinical beginning. Initial symptoms are nystagmus and muscle hypertonia, mostly in the 1st year of life. Later on, pyramidal and cerebellar symptoms and a spastic dystonic movement disorder develop. The disease is slowly progressive, progressions of the disease up to the age of 14 have been described.

The **Seitelberger’s connatal form** progresses faster; the patients die in the first years of life. Alongside clinical symptoms, pathological brain-stem potentials and MRI are indicative.

**Medical Imaging.** The extent and distribution of **medullary layer changes can be seen well on MRI**. On MRI an increase in NAA levels can be found. The hypomyelination is revealed, especially on the T2-weighted sequences, whereby a signal inversion between grey and white matter can sometimes occur. The genetic defect is also detectable in lymphocytes or fibroblasts.

Causal **treatment** is not possible.

### 9.7.3 Leukodystrophies with an Unknown Metabolic Defect

#### ■ Alexander Disease

##### ■ Epidemiology, Aetiology

This disease is named after Alexander, who described leukodystrophy in a child with megalencephaly in 1949. The disease is very rare; familial cases have been described. The aetiology of the disease is unknown. It is an autosomal recessive hereditary disease.

##### ■ Symptoms

Depending on its start, a distinction is made among the infantile, juvenile and adult forms. Macrocephaly, the cause of which is a real megalencephaly, only develops during the course of the 1st year of life. Patients develop tetraspasticity, less pronounced ataxic symptoms and frequently respond to mild head trauma with seizures and comatose states. Cognitive functions remain good for a relatively long time.

##### ■ Medical Imaging

In the infantile form a diffuse demyelination with a recess around the internal capsule is often found on the imaging. Occasionally, cystic changes in the centrum semi-ovale or frontal region are recognisable. When the brain-stem is predominantly affected a distension of the pons may occur.

**For differential diagnostic purposes** Alexander disease must be distinguished from other megalencephalic leuko-encephalopathies, especially Canavan disease and cystic Van der Knapp leukoencephalopathy.

#### ■ Aicardi–Goutières Disease

##### ■ Definition, Symptoms

This leukoencephalopathy, described in 1984 by Aicardi and Goutières, with cerebral calcifications and persistent CSF pleocytosis, occupies a special position. As early as the 1st year of life the disease manifests as a heavy encephalopathy syndrome with progressive microcephaly, spasticity and dystonia.

##### ■ Medical Imaging

On CT, white matter calcifications are found in the basal ganglia alongside pathological signal changes. The leukoencephalopathy may initially begin frontally and progress rapidly.

#### ■ Myelinopathia Centralis Diffusa

##### ■ Epidemiology, Symptoms

Myelinopathia centralis diffusa known as “vanishing white matter disease” in English, affects children of both sexes. After normal development a mostly intermittent-seeming ataxia appears in the 2nd or 3rd year of life, often at the same time as a slight traumatic brain injury, bronchopulmonary or gastro-intestinal infections. In the following years, the children rapidly lose the ability to walk. At first an ataxia predominates. Between the 6th and 10th year of life increasing tetraspasticity develops. This leads to optic atrophy, seizures and dementia-related deterioration.

##### ■ Medical Imaging

Medical imaging also shows a diffuse change in the entire white matter. On T1- and T2-weighted images the medulla and sub-arachnoid spaces can barely be delimited. Unlike cystic leukoencephalopathy the MR spectroscopy shows a loss of all metabolites and alongside glucose only a lactate increase. The disease is probably much more common than previously thought, various progressive forms ranging from the infantile to the classic to the juvenile type have been observed. The disease is rapidly progressive; patients die between the 14th and 16th years of life. Mutations on chromosomes 3 q27 and 14 q24 have been proven.

#### ■ Megalencephalic Leuko-encephalopathy

##### ■ Definition, Symptoms

Megalencephalic leuko-encephalopathy is one of the macrocephalic leuko-encephalopathies that start slowly but progressively in preschool children. In addition to macrocephaly typical symptoms are spastic/ataxic gait disturbances; later, seizures also appear.

##### ■ Medical Imaging

On MRI a diffuse, almost spongy white substance is shown, with high parietal and temporal cyst formation. It is an autosomal recessive disease whose aetiology is unclear. Patients can reach adolescence. The gene could be located on chromosome 22q.

#### ■ Metachromatic Leukodystrophy

##### ■ Aetiology, Epidemiology

This is a group of autosomal recessive hereditary lipid storage diseases that lead to myelin disintegration where sulfatides accumulate in the brain and other organs, which histochemically react “metachromatically”. They are also called sulfatide lipidosis. The diseases are among the most commonly reported forms of leukodystrophy, with an incidence of 0.6 per 100,000 births.

Sphingo-lipid cerebroside sulfate is a cell membrane component and is found in large quantities, especially in the brain, particularly in myelin membranes. In metachromatic leukodystrophies arylsulfatase A levels are reduced or the enzyme function disrupted. There are numerous mutations of the responsible gene on chromosome 22 q13. The different clinical progression for arylsulfatase A defects is explained by different residual activities of the enzyme.

##### ■ Symptoms

There are several different forms of progression:

**Late infantile metachromatic leukodystrophy** begins at the age of 15–24 months, when children do not make the expected progress in learning to walk and stumble often. Children do not develop further, lose the ability to walk completely and at the age of 2–3 years lose the ability to sit freely. The result is a final non-cerebral state with severe spasticity and loss of all psychomotor skills, from which children will die within 1–7 years after disease onset.

In the **juvenile metachromatic leukodystrophy**, which begins at 4–6 years, the disease progression is similar to that of the late infantile form, but more strongly protracted. Adulthood is rarely achieved. The late juvenile forms begin almost imperceptibly between 6 and 10 years of age with some initial subtle mo-

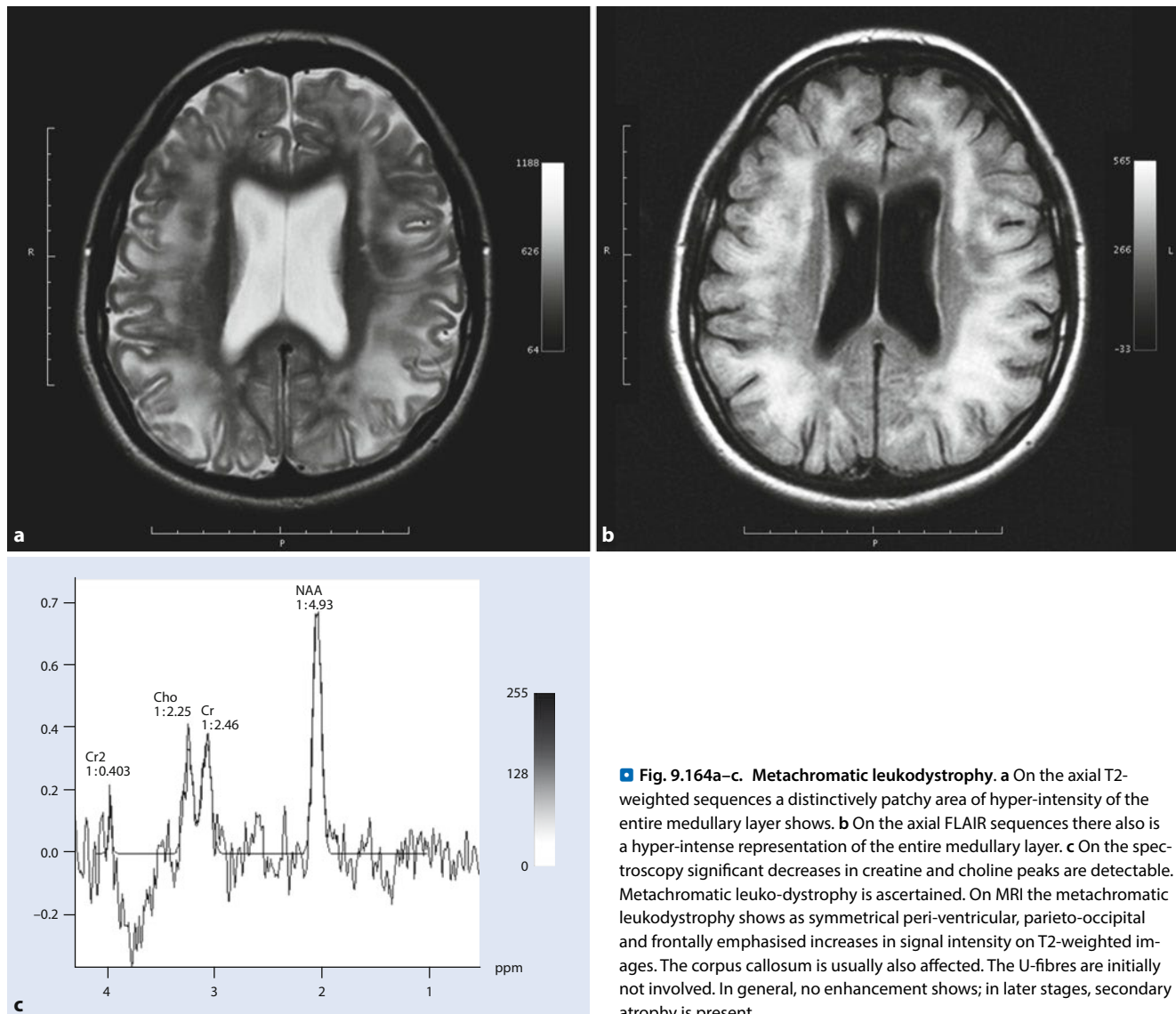


**Fig. 9.164a–c. Metachromatic leukodystrophy.** **a** On the axial T2-weighted sequences a distinctively patchy area of hyper-intensity of the entire medullary layer shows. **b** On the axial FLAIR sequences there also is a hyper-intense representation of the entire medullary layer. **c** On the spectroscopy significant decreases in creatine and choline peaks are detectable. Metachromatic leuko-dystrophy is ascertained. On MRI the metachromatic leukodystrophy shows as symmetrical peri-ventricular, parieto-occipital and frontally emphasised increases in signal intensity on T2-weighted images. The corpus callosum is usually also affected. The U-fibres are initially not involved. In general, no enhancement shows; in later stages, secondary atrophy is present

tor abnormalities, sometimes with mental changes, which when undiagnosed can lead to long periods of difficulties in school and society. The motor and dementia deterioration can progress slowly and can be drawn out into the 4th decade of life.

**Adult metachromatic leukodystrophy** usually begins as early as in adolescence with learning difficulties and conspicuous social behaviour. In time, severe disorders affecting language and mental performance in addition to bizarre behaviour become apparent.

#### ■ ■ Medical Imaging

On MRI a diffuse, progressive demyelination stretching from the ventricles to the periphery can be detected in the early stages, which for a long time omits the sub-cortical U-fibres (■ Fig. 9.164). If peripheral nerves are affected at the same time, leukodystrophy is almost certainly present. The CSF protein content is moderately increased in the late infantile and early juvenile forms, with increasing brain tissue destruction; in the later manifesting forms it is not necessarily pathological. The biochemical detection of the missing activity of arylsulfatase A occurs in the urine or in the leukocytes.

### 9.7.4 Leukodystrophies with a Known Defect

#### ■ Krabbe Disease (Globoid Cell Leukodystrophy)

##### ■ ■ Aetiology, Epidemiology

Krabbe disease is caused by a recessive hereditary deficiency of the lysosomal enzyme galactocerebrosidase. Together with metachromatic and adrenoleukodystrophy it is among the most common forms of leukodystrophy. Galactocerebrosidase normally acts on several substrates. The gene is located on chromosome 14 q31 and shows a large deletion in approximately half of conventional Krabbe patients. In the case of enzyme failure, all substrates fundamentally accumulate that are cytotoxic and destroy the oligodendrocytes.

##### ■ ■ Symptoms

The disease begins in previously inconspicuous infants aged 4–6 months with periods of restlessness, irritability and increasing stiffening of the limbs, which may be accompanied by cramps. The children develop an opisthotonic attitude, are barely

moving and show hyper-acusis and optic atrophy. In the final stage the children are limp and develop bulbar disturbances; they rarely live beyond 1 year.

#### ■ ■ Medical Imaging

In Krabbe disease early-onset hyper-intensities of the thalamus on T2-weighted sequences in addition to progressive medullary layer changes are described in particular. Changes in the cerebellum are also described in the literature.

#### ■ Canavan Disease (Spongy Leukodystrophy)

##### ■ ■ Aetiology

The spongy white matter leukodystrophy is a rare, rapidly progressive, autosomal recessive metabolic disease that occurs mainly in Ashkenazi Jews and which results from a lack of asparto-acylase. NAA is an amino acid that occurs in large quantities, particularly in the grey matter of the brain. Its function is, however, largely unknown. The substance is hydrolysed by asparto-acylase into acetate and aspartate. The relationship between the enzyme defect and the destruction of the white matter is not yet fully understood. The gene for asparto-acylase is located on chromosome 17p13.

##### ■ ■ Symptoms

The clinical onset is variable, in its congenital form the disease occurs immediately after birth. In the most common infantile form this is the case after the 6th month of life. A standstill occurs and a loss of psycho-motor development, optic atrophy and movement disorders develop. Most patients survive the disease only for a few years.

**Medical Imaging.** The MRI shows a sprawling, diffuse, oedematous destruction of the white matter. On MR spectroscopy a greatly increased ratio of NAA to creatine is present, which makes diagnosis possible.

### 9.7.5 Peroxisomal Diseases

The organelle term “peroxisome” was introduced in 1966 by De Dove and Baodhoïn and stems back to the levels of hydrogen peroxides, which are formed by oxidases and degraded by catalases. Peroxisomes exist in all human cells with the exception of erythrocytes.

**Leading symptoms** are intra-uterine growth retardation, severe developmental delay and dysmorphic features, hepatomegaly, contractures of the extremities and renal cysts. All forms of disruptions in the peroxisomal biogenesis are inherited as autosomal recessive traits and have an incidence of 1:25,000–50,000. Peroxisomal metabolic diseases can be divided into **two main groups**:

- Group 1: in developmental peroxisomal disorders peroxisomes are not formed at all or only very incompletely. Defects in multiple peroxisomal metabolic pathways are the result.
- Group 2: in isolated peroxisomal metabolism defects a correct peroxisomal structure exists morphologically, the remaining peroxisomal functions are not affected.

#### ■ Peroxisomal Development Disorders (Group 1)

**Zellweger syndrome** is the prototype of this disease group. Other diseases in this group are neonatal adrenoleukodystrophy, infantile Refsum disease and rhizomelic chondrodysplasia punctata.

The disturbed peroxisome formation in patients is due to errors in the transport system of peroxisomal components. In this group peroxins, the building blocks of the peroxisomal transport system, are disrupted. Peroxins are encoded by PEX genes, mutations cause patients to be unable to import the peroxisomal matrix enzymes synthesised in the cytoplasm.

Patients with classic Zellweger syndrome stand out because of the typical face with a flat, high forehead, deep nasal root, hypertelorism, epicanthus, slightly mongoloid lid axis, micrognathia and dysplastic pinnae. Patients usually die in the first months of life. In Zellweger syndrome a delay in myelination and a gyration disorder with polymicrogyria and a thickened pachygyric cortex are present.

#### ■ Isolated Defects of Peroxisomal Metabolic Pathways (Group 2)

This includes the X-linked adrenoleukodystrophy. Other diseases of this group are the adult type of Refsum disease and hyperoxaluria type 1.

##### ■ ■ Adrenoleukodystrophy

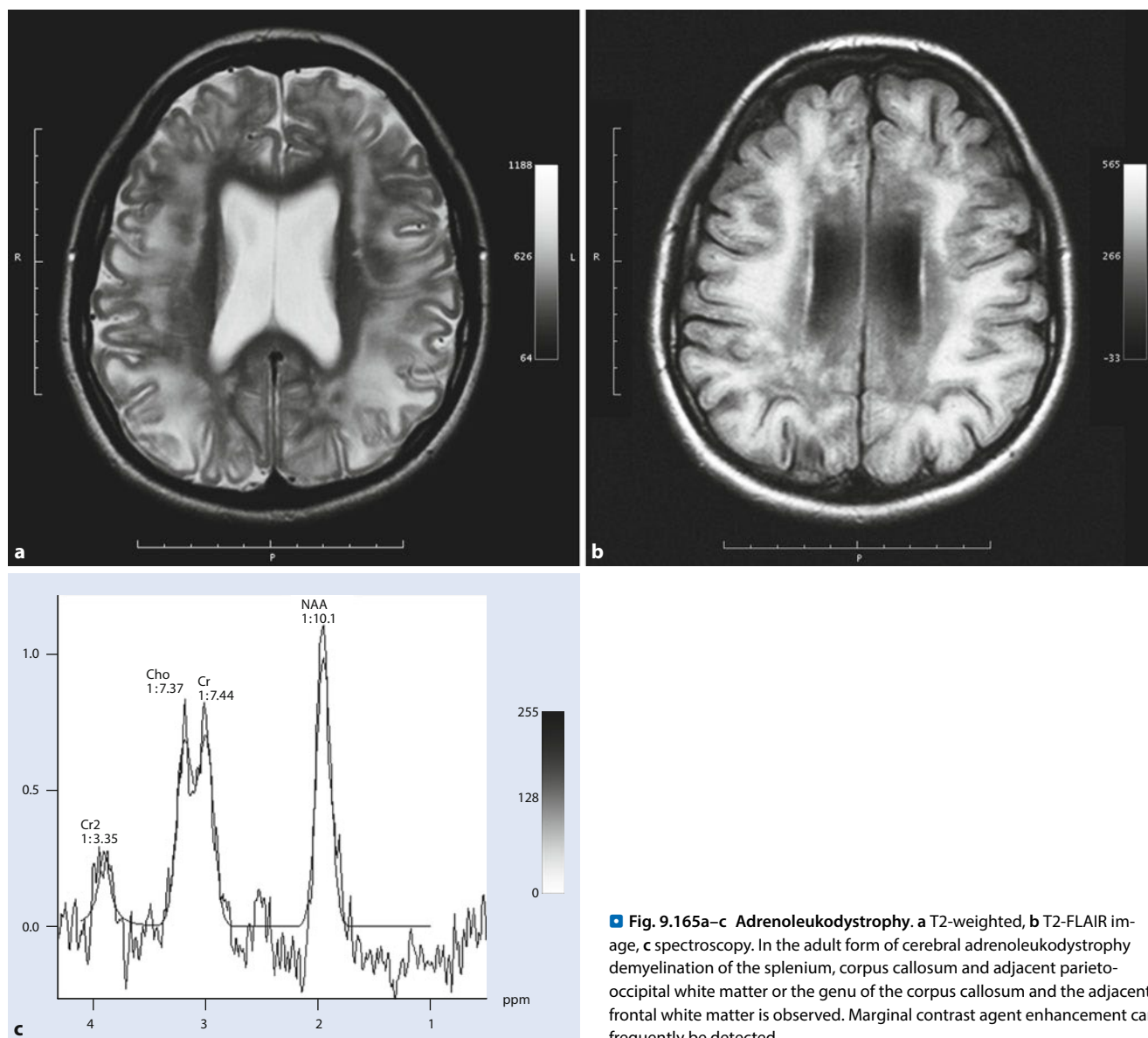
The name adrenoleukodystrophy describes three characteristic features of the disease. They refer to functional impairments of the adrenal cortex (Addison’s disease), to the changes in the white matter of the brain and spinal cord in addition to a progressive destruction of myelin. Characteristic of the X-linked adrenoleukodystrophy are accumulations of very long chains of fatty acids in all body tissues and body fluids, especially in myelin cholesterol esters and the adrenal cortex. It is the most common of the peroxisomal diseases, affecting approximately 1:20,000 boys/men.

**Medical Imaging.** On MRI demyelinations are described, which at first predominantly show symmetrically at the posterior horns of the lateral ventricles. They then expand to include the corpus callosum and spread further to the occipital medullary layer (■ Fig. 9.165). At the edge of the demyelination zones, areas that show contrast enhancement and that are of prognostic importance are often presented, as they point to a rapid progression of the disease. The extent to which the brain regions are affected by X-linked adrenoleukodystrophy can be assessed with an MRI rating scale, which is meaningful for possible therapy using bone marrow transplantation (Loes score). On MR spectroscopy of patients with X-linked adrenoleukodystrophy typical results of NAA reduction and choline increases have also been described.

##### ■ ■ Refsum Disease

Refsum disease is an autosomal recessive disease that occurs because of defects in the peroxisomal enzyme phytanoyl-CoA hydroxylase. It leads to a lack of  $\alpha$ -oxidation of phytanic acid, which in the course of the disease then accumulates in the blood and all lipid-rich tissues, particularly in the neuronal structures. Clinical symptoms are retinitis pigmentosa, peripheral neuropathy, cerebellar ataxia and increased CSF protein levels.





■ **Fig. 9.165a–c Adrenoleukodystrophy.** a T2-weighted, b T2-FLAIR image, c spectroscopy. In the adult form of cerebral adrenoleukodystrophy demyelination of the splenium, corpus callosum and adjacent parieto-occipital white matter or the genu of the corpus callosum and the adjacent frontal white matter is observed. Marginal contrast agent enhancement can frequently be detected

### 9.7.6 Neurolipidoses

Neurolipidoses are diseases of the CNS caused by an inherited enzyme deficiency. Frequently, there is a storage of sphingo-lipids, i.e. lipid molecules and complex carbohydrates.

#### ■ $G_{M1}$ -gangliosidoses

Gangliosides are sphingo-lipids in which the carbohydrate part contains one or more residues of sialic acid.  $G_{M1}$ -gangliosidoses are autosomal recessive hereditary diseases in which a lack of lysosomal  $\beta$ -galactosidase leads to storage phenomena inside and outside the nervous system.

Neuropathological findings primarily concern the grey matter. White matter and peripheral nerves are largely spared. The storage process leads to a decrease and change in the interneural connectivity. The formation of ectopic and strongly thickened neurites, known as **meganeurites**, is characteristic. Clinically, a progressive delay of psycho-motor development can be ob-

served, particularly within the first year of life. Conspicuous facial and skeletal features may already be present at birth. The disease progression rarely lasts longer than 2–3 years, the patients develop muscular hypotonia, spasticity, cerebral seizures and eventually turn blind, deaf and unresponsive.

#### ■ $G_{M2}$ -gangliosidoses

$G_{M2}$ -gangliosidoses are autosomal recessive hereditary diseases that lead to amaurotic dementia, with an accumulation of  $G_{M2}$ -ganglioside in nerve cells. Neuropathological findings are similar to those in  $G_{M1}$ -gangliosidoses, although not as pronounced. Here, too, clinically progressive symptoms are present, such as spasticity, ataxia, dysarthria and blindness.

**Medical Imaging.** Here, similar findings are detected in both  $G_{M1}$ - and  $G_{M2}$ -gangliosidoses. Overall, a generalised myelination delay can be detected; in the infantile form an early involvement of the basal ganglia and the postero-medial thalamus is also characteristic.

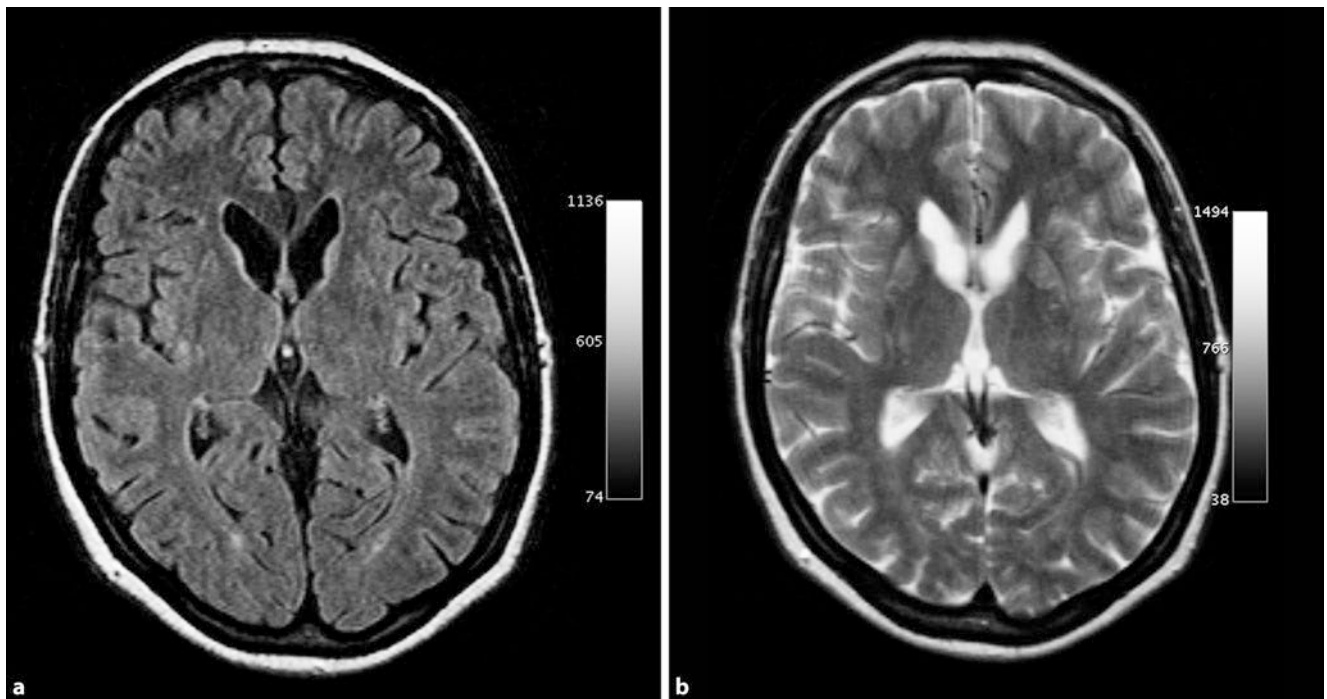


**Fig. 9.166a,b** Niemann–Pick disease, type C. **a** FLAIR image, **b** T2-weighted image. The axial FLAIR and T2-weighted sequences show a slight expansion of the internal CSF spaces, with otherwise normal MRI findings. On MRI and CT of Niemann–Pick disease patients a general, mainly cerebellar

atrophy is often detectable; there are rarely peri-ventricular medullary layer changes. The magnetic resonance spectroscopy often indicates diffuse brain involvement

#### ■ Gaucher Disease

This designation covers three different recessive hereditary sphingo-lipid storage diseases, in which large amounts of glucocerebroside are stored in the phagocytic cells: Gaucher disease type 1, type 2 and type 3. The disease types cause neurological and other symptoms in very different ways.

##### ■ ■ Type 1 Gaucher Disease

Type 1 Gaucher disease is the most common type. Clinical findings in type 1 are highly variable with regard to the disease onset and progression. Splenomegaly, haemorrhagic diathesis, anaemia, leukopaenia and thrombocytopaenia are typical. Neurological symptoms are rare in younger patients and result from complications, such as spinal cord lesions in vertebral fractures, fat embolisms or bleeding into the nervous tissue.

##### ■ ■ Type 2 Gaucher Disease

In this rapidly progressive infantile disease the brain is primarily affected. The pathology is similar to that of type 1. The clinical picture is fairly uniform, hepatosplenomegaly is usually noticed at 3–6 months. Over the course of a few months anaemia, loss of psycho-motor skills, dysphagia and spastic paralyses develop. The children do not usually reach more than 1–2 years of age.

##### ■ ■ Type 3 Gaucher Disease

This type occurs in adolescence or early adulthood. The liver, spleen and bone marrow involvement are similar to those of type 1.

#### ■ Niemann–Pick Disease

The group of Niemann–Pick diseases consists of autosomal recessive hereditary lipid storage diseases with hepatosplenomegaly, which can occur with or without involvement of the nervous system. With regard to the biochemical characteristics of the disease there are two groups:

- Those with intra-cellular storage of sphingo-myelin due to a lack of sphingo-myelinase (Niemann–Pick type A and type B)
- Those with storage of cholesterol due to a cholesterol transport disorder with an only slightly increased content of sphingo-myelin in the organs (Niemann–Pick types C and D)

With **type A** storage vacuoles show up in the nerve cells, the number of neurons in the cortex of the cerebral and cerebellar brain is greatly reduced and a glial proliferation can be found in the grey and white matter. In **general, no CNS symptoms** appear in **type B**. Niemann–Pick disease **type C** is an autosomal recessive hereditary, slowly progressing, neuro-degenerative disease with variable disease onset. Cortical atrophy is detectable; the basal ganglia and brain-stem are particularly strongly affected (■ Fig. 9.166).

#### ■ Fabry Disease

This is a rare, sex-linked hereditary sphingo-lipid storage disease with symptoms that are spread widely across the body; occasionally it can also cause symptoms in girls. Here, a genetic defect of the lysosomal  $\alpha$ -galactosidase A leads to intra-cellular accumulation of ceramide and trihexosides. The disease usually begins in

childhood or the teenage years with intermittent pain crises and acroparaesthesias. The characteristic vascular deposits lead to ischaemias and infarctions in the heart, brain and kidneys and thereby death in the 4th or 5th decade.

- ▶ **Fabry disease should be considered in older boys who suffer from intermittent burning pain in the feet, legs or fingers and whose complaints increase in warm weather.**

### 9.7.7 Fatty Acid Oxidation Disorders

Fatty acid oxidation defects cover all of the disorders involving fatty acids needed in energy formation. As long-chain fatty acids can only be transported across the inner mitochondrial membrane and into the mitochondrial matrix space, the location of the oxidation, as carnitine compounds, this group of diseases includes all congenital **carnitine metabolism disorders**. These include the following **enzyme steps**:

- Acyl-CoA dehydrogenase
- Enoyl-CoA hydratase
- 3-Hydroxyacyl-CoA dehydrogenase
- Hydroxyacyl-CoA dehydrogenase
- 3-ketoacyl-CoA thiolase

Defects in the carnitine transport system are very rare. Most patients clinically manifest at the age of 3 months to 2.5 years with hypoketotic hypoglycaemia, hyper-ammonaemia, transaminase and muscle weakness including cardiomyopathy. On the imaging, intra-cranial peri-ventricular medullary layer changes and cortical infarcts may be detectable.

#### ■ Acyl-CoA Dehydrogenase Deficiency

There are a number of different disorders that affect the  $\beta$ -oxidative degradation of fatty acids. Cardiomyopathies, hypoketotic hypoglycaemia, intolerance to fasting, vomiting, hypoglycaemia, lethargy and coma occur most frequently. Most of these diseases already manifest in the neonatal period. Only a few findings exist for acyl-CoA dehydrogenase defects with regard to imaging technique. The acyl-CoA dehydrogenase defects were previously combined under the term glutaric acidaemia type II. There are reports in the literature of changes in the basal ganglia and in the supra-tentorial medullary layer.

#### ■ Hallervorden–Spatz Disease

Hallervorden–Spatz disease is a neuro-degenerative disease that causes a **basal ganglia disorder**, especially involving the pallidum and the substantia nigra, because of iron deposits. These are caused by a pantothenate kinase disorder, an essential regulatory enzyme in the biosynthesis of the A (CoA) coenzyme. The first description of the disease dates back to Hallervorden and Spatz in 1922, who described an axonal swelling, preferably in the globus pallidus and the zona reticulata of the substantia nigra.

The disease is an autosomal recessive hereditary trait; the gene is located on chromosome 20p12.3-p13.

The disease usually begins towards the end of the first decade of life with a slowly progressive dystonia with additional rigid-

ity and positive pyramidal tract signs in addition to pronounced oro-facial hyperkineses. The disease is accompanied by dementia. In addition, visual disturbances may occur owing to retinopathy or optic atrophy.

**Medical Imaging.** The suspected diagnosis can then be corroborated thanks to MRI and in combination with the neurological symptoms. On the MRI, bilateral signal decreases show in the globus pallidus with a central lightening, which are described as the so-called “**eye of the tiger signs**”. Furthermore, non-specific hyper-density shows up in the pallidum, which are described as “**pseudo-calcifications**”.

### 9.7.8 Heteroglycanosis

#### ■ Mucopolysaccharidoses

##### ■ ■ Definition, Epidemiology

Mucopolysaccharidoses are hereditary storage diseases that are caused by an intra-cellular accumulation of glycosaminoglycans (acid mucopolysaccharides). Glycosaminoglycans are complex carbohydrate chains of uronic acids, amino sugars and neutral sugars. In tissues they are associated with proteins to form large molecular proteoglycans. The incidence of mucopolysaccharidoses is estimated to be about 1:20,000 births.

##### ■ ■ Pathogenesis

Glycosaminoglycans are synthesised intra-cellularly, predominantly excreted into the extra-cellular space and then partially dismantled in lysosomes. If this degradation is disrupted by defective lysosomal enzymes glycosaminoglycan remnants accumulate in lysosomes. Their failure leads to the storage of different degradation products in various tissues and to overall similar but distinguishable symptoms.

##### ■ ■ Symptoms

The most important form of mucopolysaccharidosis is the **mucopolysaccharidosis I**, also known as Pfaundler–Hurler syndrome. This is an autosomal recessive hereditary disease. Patients often show a large skull and stand out because of premature suture synostoses. They are often mentally and physically handicapped. They reach a level of development equivalent to that of a 2- to 3-year-old child. After 4 years of age a further reduction of psycho-motor skills is to be expected.

The **mucopolysaccharidosis II** (Hunter syndrome) is also passed on in an X-linked recessive hereditary manner. The disease is clinically similar to mucopolysaccharidosis I; just like in mucopolysaccharidosis I there are severe, intermediate and lighter progressions.

**Mucopolysaccharidosis III** (Sanfilippo syndrome) is caused by four different enzyme defects, which are each passed on as an autosomal recessive trait. The clinical manifestations resemble one another.

**Other types of mucopolysaccharidoses**, mucopolysaccharidosis IV (Morquio syndrome), mucopolysaccharidosis VI (Marteaux–Lamy syndrome), mucopolysaccharidosis VII (Sly syndrome) and mucopolysaccharidosis IX (hyaluronidase deficiency).

In mucopolysaccharidoses **CNS manifestations also occur**; however, these are similar in all of the different types. The most striking findings are multiple cystic (cryptiform) changes in the medullary layer, which are attributed to a widening of the perivascular spaces due to an accumulation of foam cells filled with mucopolysaccharides. These changes may be found in the periventricular medullary layer, the corpus callosum and the basal ganglia. In addition, widened internal CSF spaces are often present and diffuse pre-ventricular medullary layer changes. In almost all cases of mucopolysaccharidosis radiographs show **bony changes**, which mostly affect the axial skeleton and atlanto-axial joints.

#### ■ Oligosaccharidoses and Related Diseases

Oligosaccharidoses are lysosomal storage diseases. Here, oligosaccharides, short-chain compounds formed from neutral sugars and amino sugars are stored.

The **pathogenesis** corresponds to that of mucopolysaccharidoses.

Autosomal recessive hereditary mutations cause decreased functioning of lysosomal enzymes. Their substrates, oligosaccharide chains consisting of glycoproteins, cannot be properly broken down by a series of specific glycosidases. Depending on the enzyme defect different products accumulate and lead to similar symptoms and course of the illness, but with distinguishable clinical pictures.

**Clinically**, patients suffering from oligosaccharidoses resemble mucopolysaccharidoses cases with varying degrees of coarse facial features, short stature and skeletal changes, liver and spleen enlargement and neuro-degeneration.

### 9.7.9 Disorders Affecting the Oxidative Phosphorylation System

Defects in the oxidative phosphorylation (OXPHOS) system affect one or more components of the terminal substrate oxidation and the transfer of the ATP energy gained in the mitochondria. The incidence of defects in the enzyme complexes, consisting of numerous sub-units, that are organised in the OXPHOS system is estimated to be 1:10,000 live births.

**Classification.** Because of the extremely large phenotypic heterogeneity of this disease, the classification of each case of illness must be determined by consultation of all available clinical, biochemical and genetic criteria. This is the only way to assess the disease prognosis and to evaluate the effectiveness of therapeutic approaches objectively.

#### ■ Encephalomyopathy (Leigh Syndrome)

This is a progressive neuro-degenerative disease with various forms of disease progression. The disease is defined by its neuropathological findings with focal, bilateral and symmetrical necroses, ranging from the thalamus to the pons, and may involve the inferior olive nuclei and the posterior columns (■ Fig. 9.167). At a biochemical level it has a wide range of causes. A number of defects in the OXPHOS system and deficiencies in the pyruvate dehydrogenase can be associated with encephalomy-

opathy (Leigh syndrome). The same enzyme deficiencies in the OXPHOS system can be associated with encephalomyelopathy in one patient, yet lead to a completely different clinical picture in other patients. Why these different disease progressions exist is not yet fully understood.

#### ■ MELAS Syndrome

The abbreviation MELAS stands for mitochondrial encephalomyopathy, lacticidosis and “stroke-like episodes.” Typical symptoms, although these also vary widely, include the signs contained in the name in addition to migraines, hyposomia, increasing dementia and diabetes mellitus.

In the skeletal muscles a lack of activity in complex I or the complexes I and IV of the respiratory chain can be shown, in addition to ragged red fibres in more than half of those affected. After initially normal development progressive myopathy occurs, with reduced physical capacity dominating the picture. The characteristic “stroke-like episodes” with hemiparesis, hemi-anopia, accompanied by vomiting, headaches and seizures usually begin between the ages of 4 and 15 years. However, the symptoms may already occur at the neonatal stage or even later on in adulthood.

**Medical Imaging.** On the MRI, hyper-intense areas show up on the T2-weighted sequences in the parieto-temporal and/or posterior regions of the brain in addition to increasing brain atrophy and calcifications. These changes represent infarcts, which usually regress within hours or days, along with their accompanying neurological symptoms.

#### ■ MERRF Syndrome

Myoclonic epilepsy with ragged red fibres (MERRF) syndrome is characterised by progressive myoclonic epilepsy and mitochondrial myopathy with ragged red fibres and a slowly progressing dementia, with a variable onset of symptoms in late childhood to adulthood. In addition to a wide range of neuro-degenerative signs, there is often numbness and ataxia. Disease progression in MERRF and MELAS can be similar, but it does differ because of the presence of the “stroke-like episodes.”

Clinical entities include Leber’s hereditary optic neuropathy and neuropathy, ataxia and retinitis pigmentosa (NARP) syndrome. NARP syndrome is characterised by the combined occurrence of retinitis pigmentosa, seizures, ataxia, neurogenic proximal muscle weakness, peripheral neuropathy and dementia.

**Medical Imaging.** Here, a similar picture emerges to that in MELAS syndrome, with diffuse atrophy and medullary layer changes. Both of these disease entities stand out not only because of specific clinical phenotypes, but also because of a point mutation in the mtDNA sections, whereby a mutation of the genes involved in the synthesis (Syn genes) of proteins occurs. In addition, there is a group of diseases with a point mutation in mtDNA sections that codes mitochondrial proteins (MIT genes).

#### ■ Chronic Progressive External Ophthalmoplegia

Chronic progressive external ophthalmoplegia (CPEO) is a slowly progressive paresis of the eye and upper eyelid muscles. Kearns–Sayre syndrome (KSS) falls into this group, with disease

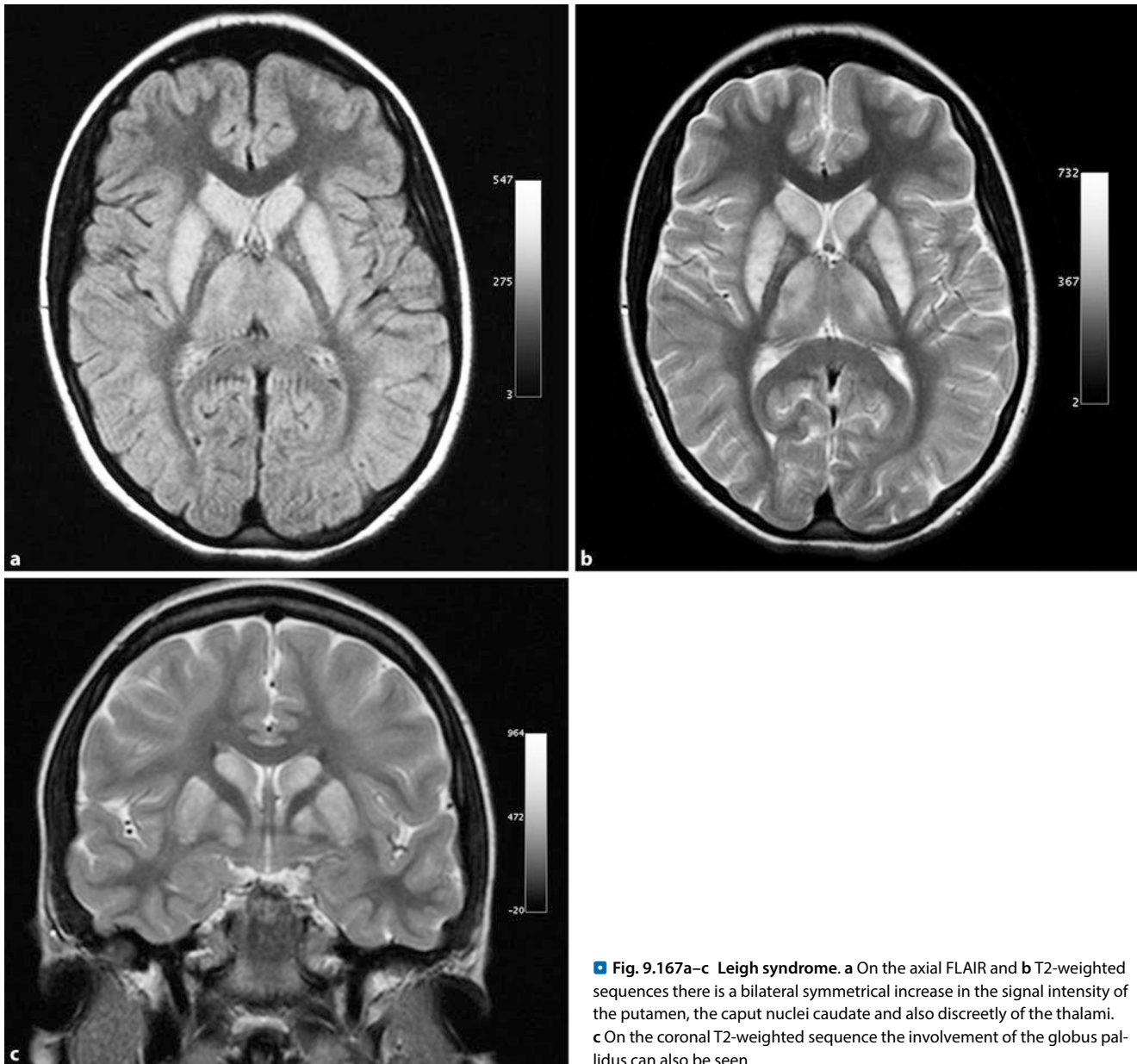


**Fig. 9.167a–c Leigh syndrome.** **a** On the axial FLAIR and **b** T2-weighted sequences there is a bilateral symmetrical increase in the signal intensity of the putamen, the caput nuclei caudate and also discretely of the thalami. **c** On the coronal T2-weighted sequence the involvement of the globus pallidus can also be seen

onset before the 3rd decade of life and CPEO flow syndrome with disease onset in later life. This symptom complex can include a large number of neurological, cardiac, renal and endocrine symptoms in addition to the characteristic signs of ophthalmoplegia, retinitis pigmentosa, myopathy, cerebellar symptoms and increased CSF protein levels.

**Medical Imaging.** With Kearns–Sayre syndrome changes in the medullary layer are present, especially in relation to the O-fibres; furthermore, calcifications occur in the basal ganglia and the cerebellum. In Leber’s hereditary optic neuropathy, optic atrophy is shown with contrast enhancement in the acute stage, in addition to possible brain-stem lesions.

#### ■ Eiper’s Disease

Eiper’s disease (also called Eipers–Hutenlocher syndrome) is a rare autosomal recessive disease with encephalopathy and liver

failure. It is caused by a mitochondrial defect in the respiratory chain. Clinically, there is increased muscle tone with increased reflexes and spasticity and at times therapy-refractory seizures in early childhood.

**Medical Imaging.** This shows cancellous atrophy with neuronal death and astrocyte proliferation with a predilection for the visual cortex. This can lead to cortical blindness.

### 9.7.10 Metabolic Disorders of Amino Acids

#### ■ Phenylalanine Metabolism Disorders

People with a normal protein-containing diet take in much larger quantities of the essential amino acid phenylalanine than is required for protein synthesis. Under normal conditions excess phenylalanine is therefore transformed predominantly by phe-

nylalanine hydroxylase into tyrosine. This enzyme requires an active cofactor. Both a loss of activity or a lack of apoenzyme PAH and a lack of the BH cofactor<sub>4</sub> reduce the activity of the enzyme system. Increased phenylalanine concentrations in infants and small children during the developmental phase cause irreversible brain damage and after completion of brain development lead to reversible functional limitations.

Decreased activity of the phenylalanine hydroxylase complex can lead to the following **metabolic diseases** or abnormalities:

- Classic phenylketonuria requiring treatment
- Mild phenylketonuria with residual activity of the PAH enzyme
- Benign hyperphenylalaninaemia
- Hyperphenylalaninaemia due to a lack of the BH cofactor<sub>4</sub>
- Transient hyperphenylalaninaemia in pre-term infants with a protein-rich diet
- Maternal phenylketonuria, in which the child is damaged in utero by elevated phenylalanine levels in the sense of a toxic embryo-foetopathy

#### ■ ■ Phenylketonuria

Phenylketonuria (PKO) is the most common amino acid metabolism disorder in humans. It is an autosomal recessive hereditary trait. Its frequency differs widely in various ethnic cultures. Phenylketonuria was first described in 1934 as a phenylalanine metabolism disorder and associated with hereditary imbecility.

Hyperphenylalaninaemia affects the development and function of the brain. The cause of this neuro-toxicity is still not fully understood. High phenylalanine levels lead to both acute reversible and chronic irreversible cognitive disorders. If left untreated, the classic PKO will lead to general and focal myelination disorders.

**Medical Imaging.** The delay in myelination, which is present to varying degrees in phenylketonuria, is reflected on the MRI in an area of hyper-intensity in the peri-ventricular medullary layer seen on T2-weighted images. On MR spectroscopy only a discreet reduction of choline is described in the adult form of PKO.

➤ **Thanks to new-born screening almost all PKO patients are diagnosed in time and treated with an appropriate diet.**

#### ■ Homocystinuria

Homocystinuria is caused by an enzyme defect in the homocystein metabolism and occurs at a frequency of 1:300,000. The gene for the defective cytosolic enzyme cystathione- $\beta$ -synthetase (CBS), which causes classical homocystinuria, is located on chromosome 21q22.3. More than 60 known mutations in the CBS gene exist. It is likely that homocystein leads to vascular lesions, subsequent **arterio-sclerotic changes** and thrombo-embolism, in addition to collagen structure malformations. The disease can occur at various stages of life, depending on the severity of the enzyme defect. Hyperhomocysteinaemia leads to atherosclerosis. Accordingly, varying degrees of vascular damage are frequently detectable on the imaging.

### 9.7.11 Wilson's Disease

#### ■ ■ Definition, Aetiology

Wilson's disease, also known as hepatocerebral degeneration or **copper storage disease**, is an autosomal recessive hereditary disorder that disrupts copper discharges by liver cells into the bile. It is caused by a defect in the copper transporting ATPase in the liver cell membrane. The enzyme defect causes excess dietary copper to be stored in liver cells after its resorption and uptake by the liver instead of it being excreted into the bile. This always leads to liver cirrhosis and, in cases of prolonged survival, to characteristic cerebral damage. Without appropriate therapy, the course of the disease is lethal.

#### ■ ■ Epidemiology, Symptoms

The disease incidence is about 1:30,000. Clinically, the neuropsychiatric course predominates in adults, while children < 10 years predominantly show only hepatic symptoms. Clinically, Wilson's disease manifests mostly with non-specific abdominal symptoms, such as hepatosplenomegaly, abdominal pain and vomiting, which are associated with fatigue and loss of performance. Cerebral symptoms are predominantly caused by copper deposition in the basal ganglia and cerebellum. It mainly affects the musculoskeletal system; sensory and cognitive functions are less often affected. Slurred speech, deterioration in writing ability, loss of writing ability, hyper-salivation, extra-pyramidal tremor, chorea, athetosis and dysphagia are typical.

#### ■ ■ Medical Imaging

On MRI, areas of hyper-intensity are detectable in the basal ganglia and brain stem on the T1-weighted sequences and hypo-intensity on T2-weighted images (■ Fig. 9.168).

## 9.8 Disorders of the White Matter

Diseases of the white matter are divided into demyelinating and dysmyelinating diseases:

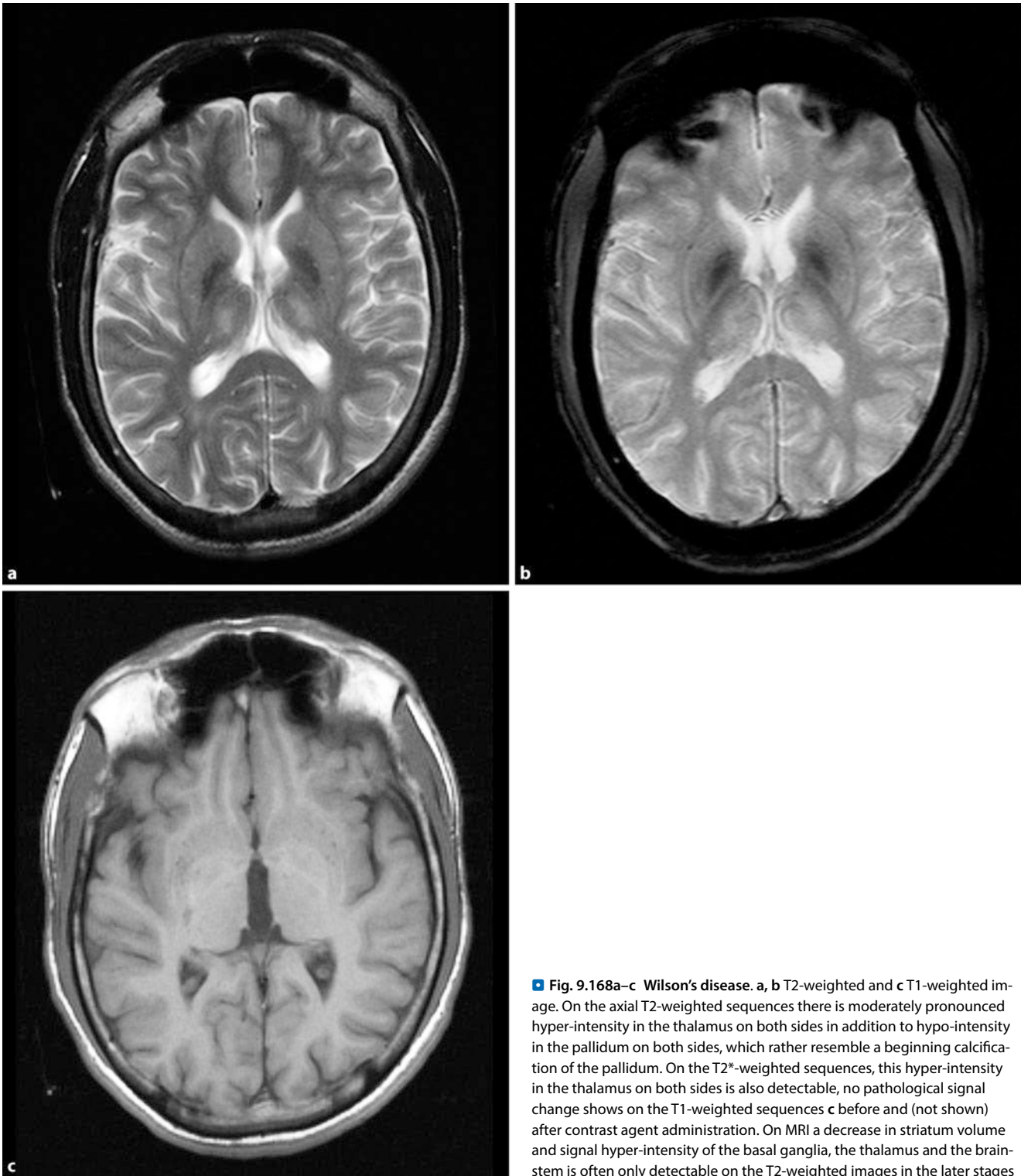
- **Demyelinating diseases** are acquired and affect the myelin
- **Dysmyelinating diseases** are hereditary, affect the formation or maintenance of myelin and are found primarily in children

The **demyelinating diseases** are divided into four groups: primary, ischaemic, infectious and toxic/metabolic.

### 9.8.1 Primary Demyelination

#### ■ Multiple Sclerosis

Multiple sclerosis is the most common demyelinating disease with a predominance in women between the 20th and 40th years of life. Optic neuritis is a common manifestation. For the aetiology, pathogenesis and medical imaging, see ▶ Sect. 9.6.



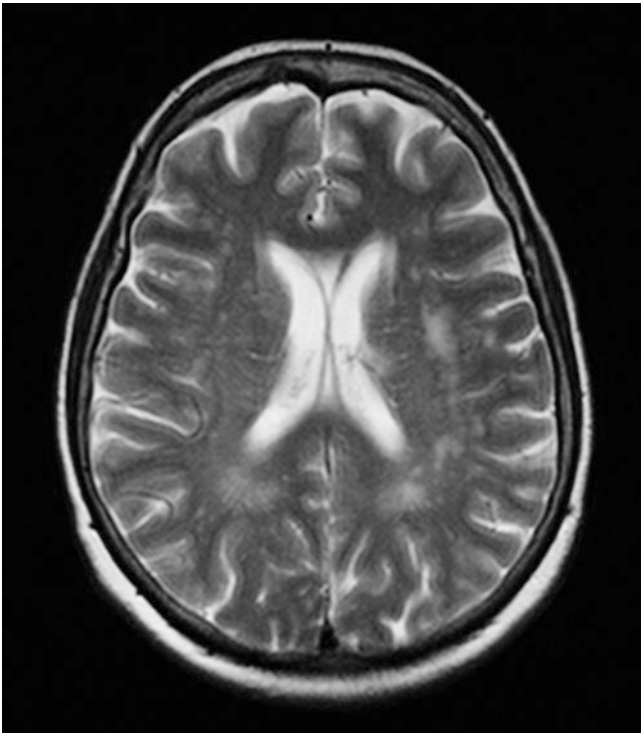
■ **Fig. 9.168a–c Wilson's disease.** **a, b** T2-weighted and **c** T1-weighted image. On the axial T2-weighted sequences there is moderately pronounced hyper-intensity in the thalamus on both sides in addition to hypo-intensity in the pallidum on both sides, which rather resemble a beginning calcification of the pallidum. On the T2\*-weighted sequences, this hyper-intensity in the thalamus on both sides is also detectable, no pathological signal change shows on the T1-weighted sequences **c** before and (not shown) after contrast agent administration. On MRI a decrease in striatum volume and signal hyper-intensity of the basal ganglia, the thalamus and the brainstem is often only detectable on the T2-weighted images in the later stages

### 9.8.2 Ischaemic Demyelination

#### ■ ■ Definition, Pathogenesis

The most common white matter lesions are ischaemic. In older patients these are normal. They reflect arterio-sclerotic vasculopathy. The peri-ventricular white matter and basal ganglia are

most commonly affected. The sub-cortical U-fibres, the corpus callosum, the medulla, the mid-brain in addition to the cerebellar peduncles are usually spared because of their dural blood supply. **Histologically**, the areas affected by the infarction show axonal atrophy and a reduced myelin content.



■ Fig. 9.169 Sub-cortical arterio-sclerotic encephalopathy. T2-weighted image with a peri- and para-ventricular signal increase

#### ■ ■ Aetiology

White matter changes are also known as micro-angiopathic leuko-encephalopathy and sub-cortical arterio-sclerotic encephalopathy (■ Fig. 9.169), which, however, overvalues their importance. The described lesions differ from lacunar infarctions (5–10 mm), which occur in the basal ganglia typically in the upper two thirds of the putamen. The aetiology, however, is similar. Small lesions in the white matter occur predominantly in patients with vasculopathy (caused by arterio-sclerosis or vasculitis). In younger patients vasculitis, embolic disease, hypoxia, dissection and migrainous ischaemia must be considered as possible causes. Distinction between MS lesions and ischaemic lesions is difficult (in 10% of patients MS occurs after 50 years of age). An accurate medical history is important. The corpus callosum and the sub-cortical pathways are usually spared by ischaemic foci.

#### ■ ■ Differential Diagnosis

**Ependymitis granularis** is a standard result. This is a visible signal increase on T2-weighted images, which occurs at the tips of the anterior horns and is up to 1 cm in size. Histologically, this is a loose network of axons with a low myelin content. This porous ependyma allows a trans-ependymal CSF leak, resulting in extended T2 time.

**Virchow–Robin spaces** are typically 1–2 mm in size, but may be significantly larger. Upon entry of blood vessels into the brain parenchyma, they are surrounded by CSF and a thin pial layer. They show up on T2-weighting as a signal increase (■ Fig. 9.170) and are typically found in the centrum semi-ovale, the deep basal ganglia at the level of the anterior commissure, as it is here that

the lenticulo-striate arteries enter. They are a normal variation and become more prominent in old age owing to atrophy. To distinguish between parenchymal lesions and Virchow–Robin spaces, a proton density-weighted (T2-weighted fast echo sequence) or FLAIR sequence may be helpful. CSF (the contents of the Virchow–Robin space) appears iso-intense to the white matter on proton density-weighted sequences. Ischaemic lesions, however, appear hyper-intense on the proton density-weighted images, unless there are cystic changes. On T2-weighted sequences, however, both the infarction and the Virchow–Robin space appear hyper-intense.

**Lacunar infarcts** are usually >5 mm and occur predominantly in the upper two thirds of the corpus striatum. **Peri-ventricular spaces** are smaller, bilateral, often symmetrical, in the lower third of the striatum.

### 9.8.3 Demyelination Caused by Infections

Virally induced demyelination was already covered in the section on CNS infections (▶ Sect. 9.6). **PML** is frequently seen because of the spread of AIDS. It is a reactivation of the latent JC virus. Patients are usually immunosuppressed. As the oligodendrocytes are affected this leads to a pronounced demyelination, especially of the deep white matter, the cerebellum and brain-stem. No contrast medium enhancement, no signs of masses and no bleeding will be detectable. Lesions are asymmetric, predominantly parietal, rapidly progressive and confluent. Involvement of the grey matter or infra-tentorial is possible. Death occurs within a few months.

#### ■ HIV Encephalopathy

This shows up as sub-acute encephalitis with progressive dementia without focal neurological signs. The HIV infection develops in the microglia (macrophages). The resulting cytokines have a toxic effect on neighbouring neurons (▶ Sect. 9.6.3).

**Medical Imaging.** Often a low, cerebral atrophy and focal or diffuse, symmetric signal intensity increases on T2-weighted images are the result. Most often broad, flat areas are affected.

#### ■ Other Infection-related Demyelination

Including:

- ADEM (▶ Sect. 9.6.6)
- Lyme disease (▶ Sect. 9.6.3)
- Sub-acute sclerosing pan-encephalitis (SSPE), a very rare, late and always lethal complication of a measles infection

### 9.8.4 Toxic or Metabolically Related Demyelination

#### ■ Central Pontine Myelinolysis

Central pontine myelinolysis is demyelination that primarily affects those suffering from eating disorders, alcoholism and rapid electrolyte changes, but also infrequently occurs spontaneously. The clinical manifestation is often seen after a very rapid com-



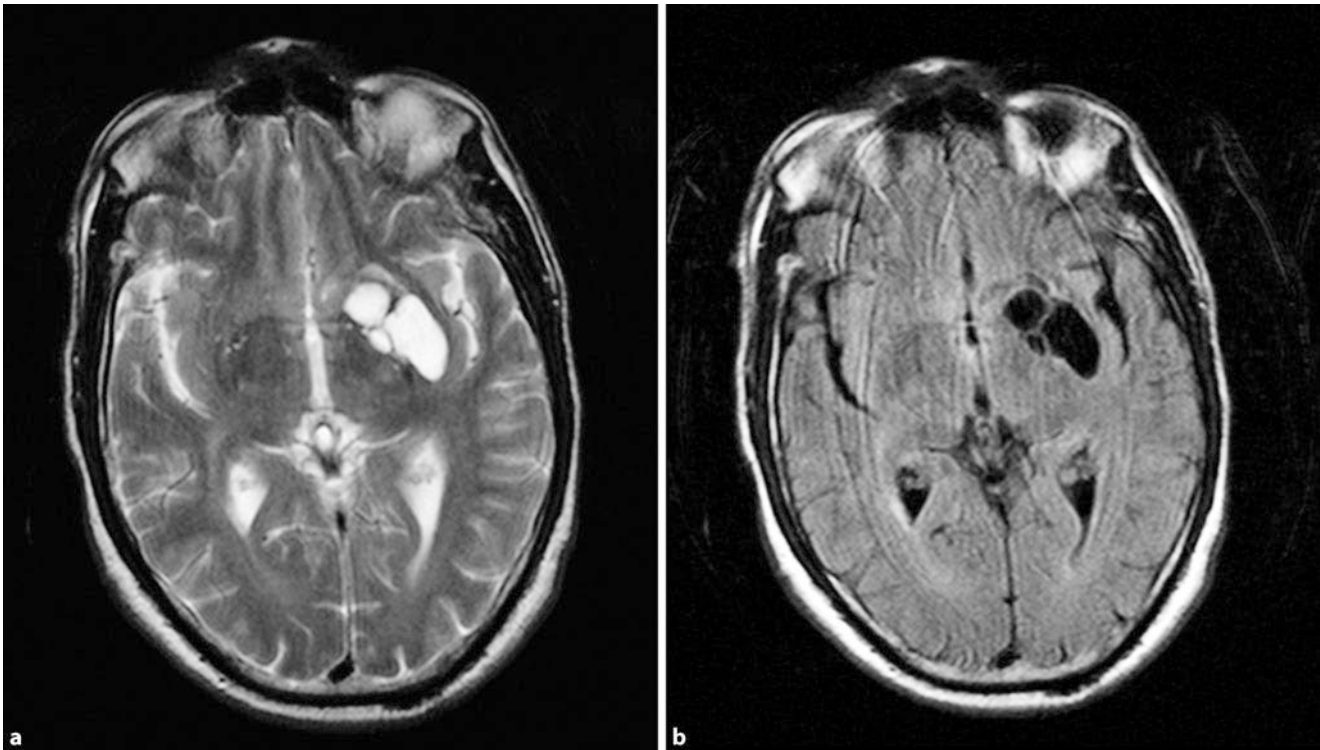


**Fig. 9.170a,b Virchow–Robin space.** **a** On the T2-weighted image there is a CSF-iso-intense change in the area of the basal ganglia on the left. **b** This looks hypo-intense on the FLAIR sequences, compatible with CSF suppression.

compensation of hyponatraemia. Rarely, there is an association with diabetes mellitus, leukaemia or infections. Clinically, cortico-spinal syndromes develop quickly with quadriplegia and “locked-in status” (the patient is mute, cannot move, sometimes comatose). The prognosis is poor.

**Medical Imaging.** On the MRI a central pontine signal increase can usually be detected (■ Fig. 9.171); in some cases contrast agent uptake is detectable. There is a characteristic bilateral pontine involvement with sparing of the superficial brain-stem structures. In about 10% of patients an extra-pontine localisation can be detected.

➤ **Marchiafava–Bignami syndrome is a rare form of demyelination of the central corpus callosum (medial side of the corpus callosum) and is predominantly found in alcoholics. Symptoms include dementia; there is a slow progression leading to death.**

#### ■ **Wernicke–Korsakoff Syndrome**

Although Wernicke’s and Korsakoff’s syndrome are pathologically indistinguishable, there is a clear, clinically significant difference. Both are caused by a thiamine deficiency; dementia is present.

**Medical Imaging.** On MRI, lesions in the basal ganglia, thalamus and brain-stem surrounding the aqueduct are detectable. In addition, there is often atrophy of the mammillary bodies. In the acute phase enhancement can be seen here (■ Fig. 9.172).

tion. Gliosis in the border region does not show up, which fits with a large Virchow–Robin space

#### ■ **Radiation Leuko-encephalitis**

After a cumulative radiation dose of about 40 Gy, radiation-induced vasculopathy with lesions in the white matter often develops 6–9 months after treatment (■ Fig. 9.173).

**Medical Imaging.** On T2-weighted images the lesions appear hyper-intense, confluent and often affect the sub-cortical U-fibres in the region of the irradiated brain. It results from indirect radiation damage owing to arteriitis, caused by hypertrophy, fibrosis and hyalinisation of the endothelium of the small arteries. Patients are usually asymptomatic.

In radiation-induced necrosis and arteriitis, enhancing (partly ring-shaped) lesions with space-occupying effects develop weeks to years after irradiation. These can mimic tumour recurrence. The occurrence is dose-dependent; the necrosis can be progressive and fatal. Predilection locations are situated in the vicinity of the tumour, the tissue here seems to be more sensitive to radiation damage. It is difficult to distinguish between tumour recurrence and radiation-induced necrosis. Here, a follow-up has to take place. Positron emission tomography (PET) can also be used to distinguish the cause because tumour recurrence, unlike radiation necrosis, is metabolically active.

The irradiation also leads to damage to the blood vessels with resultant vasoconstriction.

❗ **Methotrexate and irradiation have a synergistic effect. It is thought that damage to the blood–brain barrier caused by the irradiation leads to neurotoxic levels of methotrexate.**

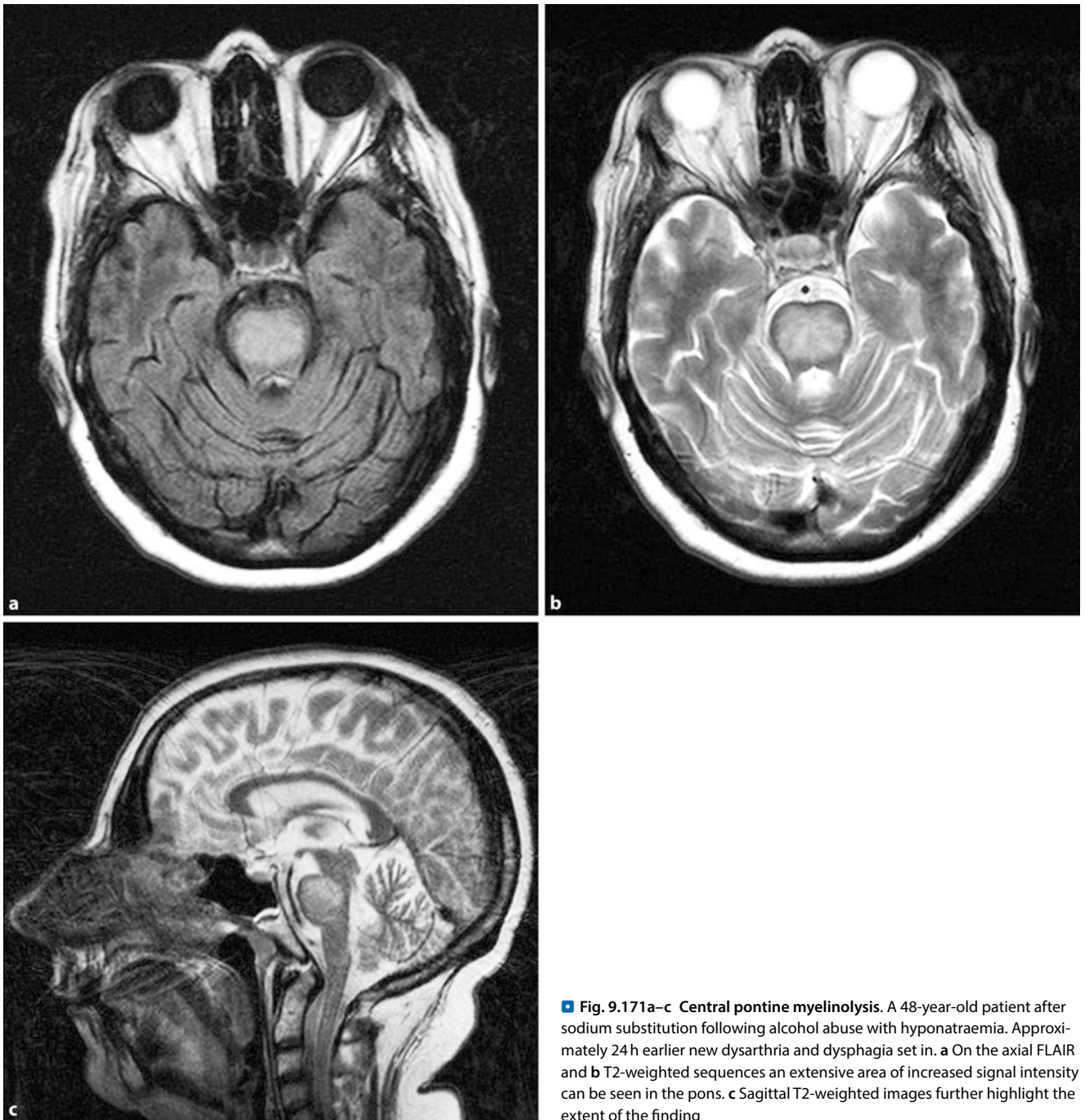


**Fig. 9.171a–c Central pontine myelinolysis.** A 48-year-old patient after sodium substitution following alcohol abuse with hyponatraemia. Approximately 24 h earlier new dysarthria and dysphagia set in. **a** On the axial FLAIR and **b** T2-weighted sequences an extensive area of increased signal intensity can be seen in the pons. **c** Sagittal T2-weighted images further highlight the extent of the finding

#### ■ Wallerian Degeneration

Wallerian degeneration is a secondary degeneration of axons and myelin sheaths distal to a lesion. Unlike the peripheral nerves there is no complete regeneration in the CNS and a glial scar is usually the result. When lesions occur in the CNS, e.g. because of infarctions, haemorrhages etc., degeneration of the affected pyramidal tracts therefore results.

**Medical Imaging.** On MRI this can usually be detected as atrophy, possibly with areas of hyperintensity on T2-weighted images (■ Fig. 9.174).

#### 9.8.5 Dysmyelinating Diseases

These are also called **leukodystrophies** and are very rare. They are characterised by a premature myelin breakdown or faulty formation due to a congenital enzyme or metabolic defect. Diffuse lesions in the white matter are present; distinction is made biochemically or by enzyme analysis. The age of disease onset in addition to the distribution pattern can be of assistance.

**Metachromatic Leukodystrophy.** Most common leukodystrophy, autosomal recessive, error on the enzyme arylsulphatase A. Symptoms: mental deterioration, beginning at 2 years of age. Progress-

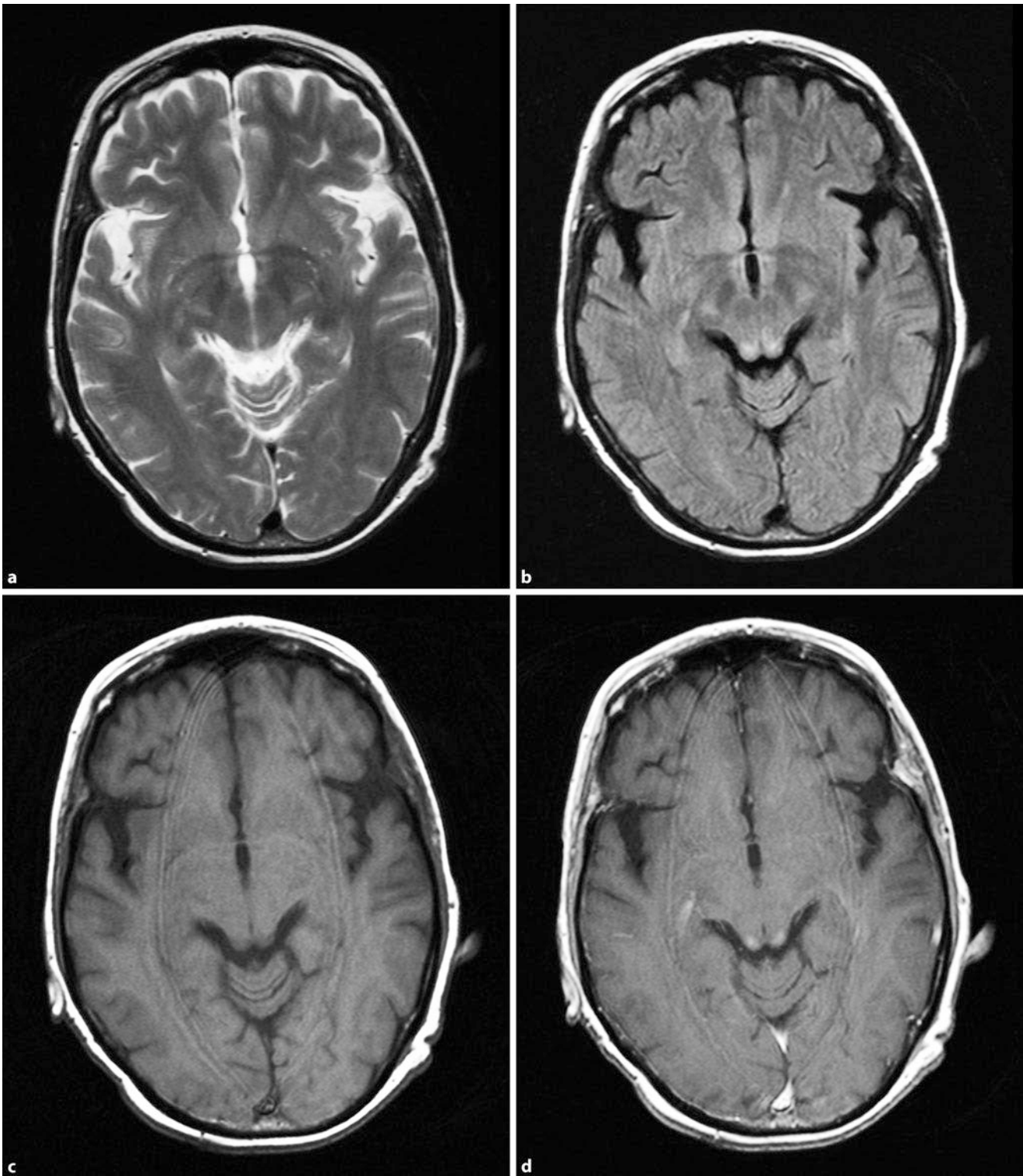


**Fig. 9.172a–d Wernicke's syndrome.** On the **a** T2-weighted and **b** FLAIR sequences a symmetrical signal increase could be detected in the superior colliculus of the lamina tecti mesencephali. **c** On the unenhanced

T1-weighted sequences the lesions appear hypo-intense; **d** after contrast agent administration they show considerable enhancement

sion with death occurring after 5 years. Magnetic resonance imaging: symmetrical areas; the grey matter is not affected.

**Adrenal Leukodystrophy.** Recessive, affects only boys. Disease onset at 5–10 years of age. Frequently abnormal pigmentation,

adrenal insufficiency. Common sites are the peri-atrial white matter with extension into the splenium of the corpus callosum. This leads to a rapid spread to the medial and lateral geniculate nucleus, which explains the children's early visual and auditory disorders. The grey matter is not affected.

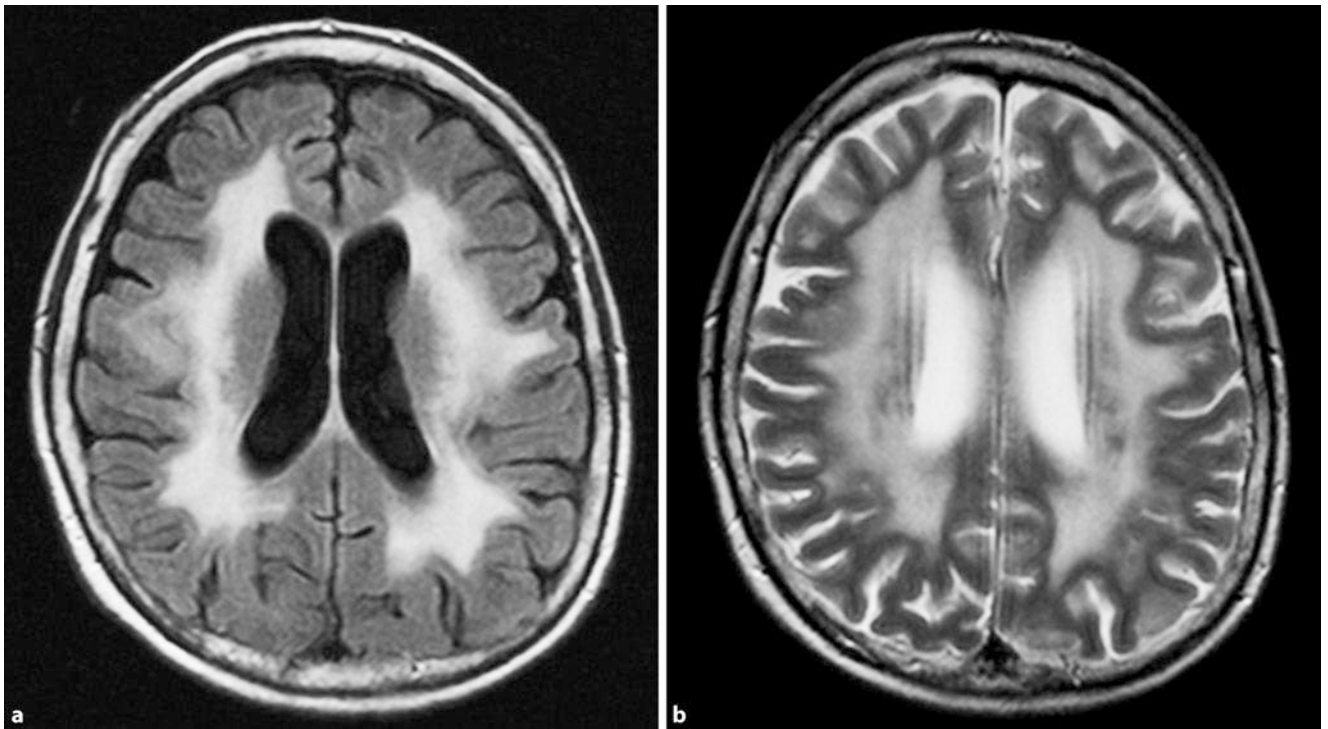


**Fig. 9.173a,b** Radiation damage to the white matter. Confluent increased signal intensity in the medullary layer on the a FLAIR and b T2-weighted sequences following radiation

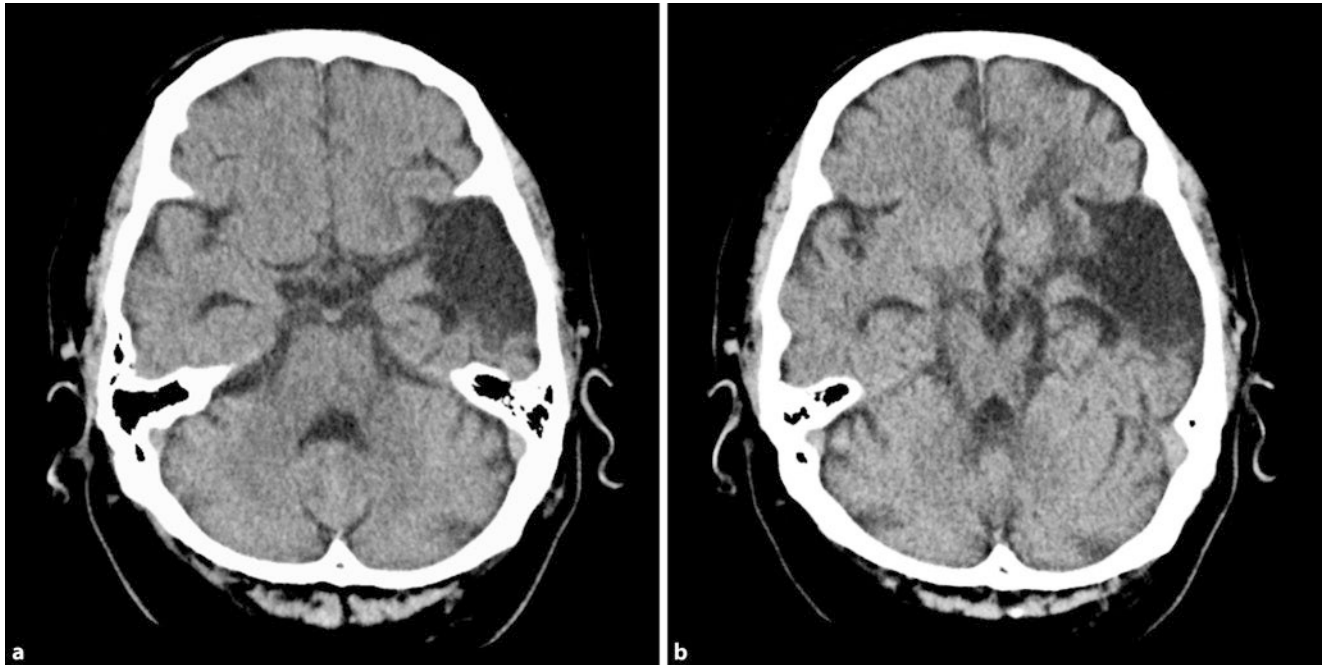


**Fig. 9.174a,b** Wallerian degeneration. On the axial CT images of the skull base, a left temporal substance defect is detectable, in a state following older cranio-cerebral trauma. In the more caudal layers the left crus cerebri presents clearly reduced in size; this is most likely caused by a Wallerian degeneration

**Leigh's Disease.** This is also known as necrotising encephalomyelopathy and affects children <5 years. As the histopathology resembles that of Wernicke's encephalopathy, a congenital defect in the thiamine metabolism is suspected. Symmetrical, focal necroses are found in the basal ganglia, the thalamus and in the

sub-cortical white matter (■ Fig. 9.168). The mid-brain, medulla and the back channels of the spinal cord may also be affected. Involvement of the peri-aqueductal grey matter is characteristic; the mammillary bodies are not affected (but are affected in Wernicke-Korsakoff syndrome).

**Alexander Disease and Canavan Disease.** These diseases are very rare and occur in the first weeks of life. The brain is often enlarged, and patients show macrocephaly.

## 9.9 Neuro-degenerative Disorders

### 9.9.1 Alzheimer's Disease

#### ■ ■ Epidemiology, Symptoms

This is the most common form of dementia. The diagnosis is usually made between 50 and 65 years of age, but the disease can also occur earlier. Death follows 7–10 years after diagnosis.

Dementia syndromes are among the most common diseases in the elderly. In addition to Alzheimer's dementia, also included are vascular dementia, dementia with Lewy bodies and fronto-temporal dementia. Alzheimer's disease (AD) is a progressive neuro-degenerative disease. It is the most common form of dementia and affects about 2–4 million people in the European Union and more than 30 million people worldwide. It is accompanied by a loss or restriction of neuronal function, in particular of cognition. Changes in behaviour are also observed. Age is the biggest risk factor, with a disease frequency of about 8% at age > 65 years and > 30% at age > 85 years. The incidence doubles every 5 years.

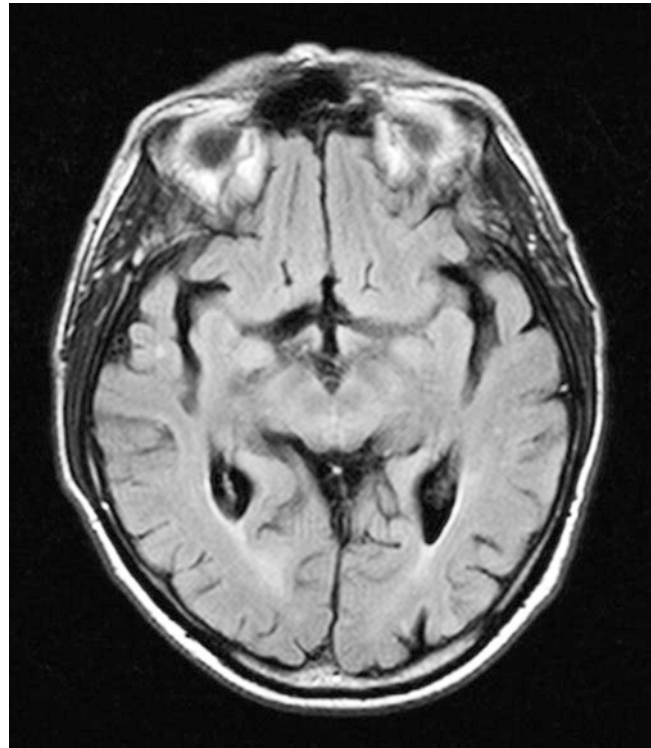
The progression of AD is slow, patients survive the disease on average for 8–10 years after the onset of symptoms. Accordingly, in view of a constant increase in population numbers and an increase in life expectancy, a tripling of dementia cases over the next 50 years is to be expected.

#### ■ ■ Medical Imaging

Diffuse atrophy occurs (■ Fig. 9.175), especially in the area of the hippocampus and temporal lobe (an enlargement of the temporal horns, supra-sellar cisterns and Sylvian fissure can help to distinguish between Alzheimer's disease and normal aging processes). PET shows a reduced glucose metabolism, single photon emission computed tomography (SPECT) and perfusion MRI show reduced cerebral blood flow in these regions. Proton MR spectroscopy shows reduced levels of NAA with increased myo-inositol levels. Increased myo-inositol levels are found only in Alzheimer's disease, and not in other dementias. The ADC in the hippocampus of patients with Alzheimer's disease is also higher than in the control groups.

### 9.9.2 Vascular Dementia, Differential Diagnosis from that of AD

Unlike AD patients, those with vascular dementia (VD) present with a form of multi-infarct dementia, frequently multiple areas of increased signal intensity on T2-weighted sequences, proton density-weighted or FLAIR sequences. These signal increases can occur in the white matter, the basal ganglia and/or the thalamus. Focal infarction areas or lacunae in important areas of the brain may also be associated with VD. Patients with AD may also have



■ Fig. 9.175 Alzheimer's disease. Temporo-parietally accentuated brain atrophy

changes in accordance with lesions in the white matter; there is often an overlap between VD and AD, the so-called mixed form of dementia. The presence of changes in the white matter should therefore not be used to rule out an AD diagnosis.

### 9.9.3 Fronto-temporal Dementia

Frontal atrophy, or Pick's disease, is a rare form of pre-senile dementia and occurs primarily in women. The disease shows a fronto-temporal, predominantly cortical atrophy that spares the posterior two thirds of the superior frontal gyrus. These pathological changes also dominate the imaging findings. The atrophy leads to a consecutive widening of the frontal inter-hemispheric and Sylvian fissures and a rounding of the temporal pole, which is considered an important diagnostic criterion in distinguishing it from AD.

### 9.9.4 Parkinson's Disease

Here, a loss of neurons occurs in the substantia nigra, in particular in the pars compacta. If this loss is greater than 80%, symptoms such as tremor, muscle rigidity and bradykinesia occur. At the time of imaging, the diagnosis is usually established (■ Fig. 9.176).

The imaging helps to distinguish between primary (idiopathic) and secondary (infarction or lesions in the caput nuclei caudate), or when surgery is planned (pallidotomy or thalamot-

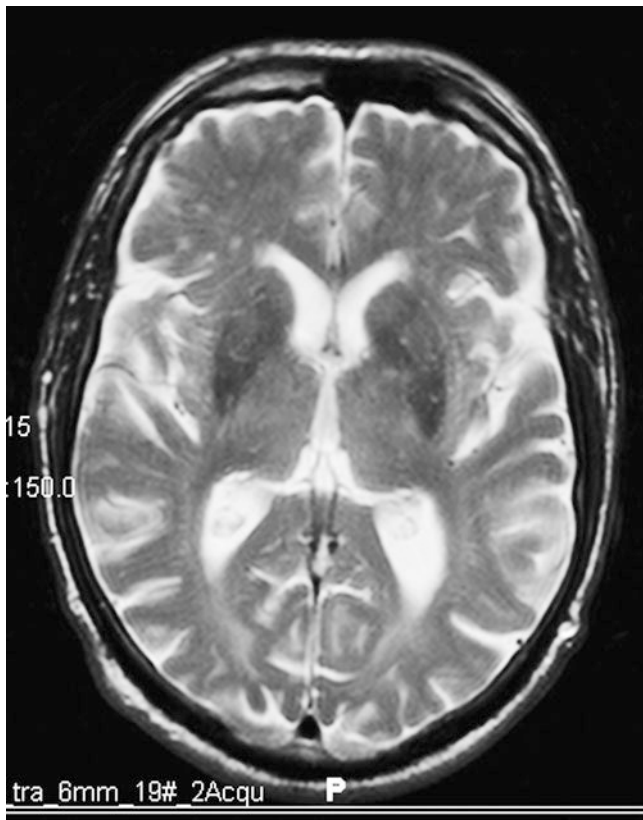


**Fig. 9.176** Parkinson's disease, T2-weighted image. In this 58-year-old patient with known, clinically definite Parkinson's disease a slight hypo-intensity in the lens nucleus and in the nucleus caudatus on both sides is detectable at best. No other abnormalities can be detected

omy). Proton MR spectroscopy detects a reduction in NAA, not only in the basal ganglia but throughout the entire brain. Occasionally, increased iron deposition the mid-brain (hypo-intense) can be detected on gradient echo sequences (T2\*) with a thinning of the pars compacta (the substantia nigra is composed of the pars compacta [hyperintense band on T2-weighted images], which is located between the pars reticularis [anterior] and the red nucleus [posterior]). In general, however, imaging findings are unremarkable. In later stages atrophy is detectable.

### 9.9.5 Multiple System Atrophy

#### ■ ■ Definition, Aetiology

Multiple system atrophy (MSA) is a sporadic neuro-degenerative disease that occurs in middle adulthood and is characterised by a combination of autonomic disorders with Parkinson's symptoms or cerebellar ataxia.

The aetiology of MSA is unknown, and the various symptoms associated with hypotonic blood pressure regulation disorders, sleep disorders, disorders of bladder emptying and movement disorders present interdisciplinary diagnostic and therapeutic challenges to neurologists, internists, urologists and ENT doctors.

The older terms Shy-Drager syndrome, sporadic olivoponto-cerebellar atrophy (OPCA; **Fig. 9.177**) and striato-nigral

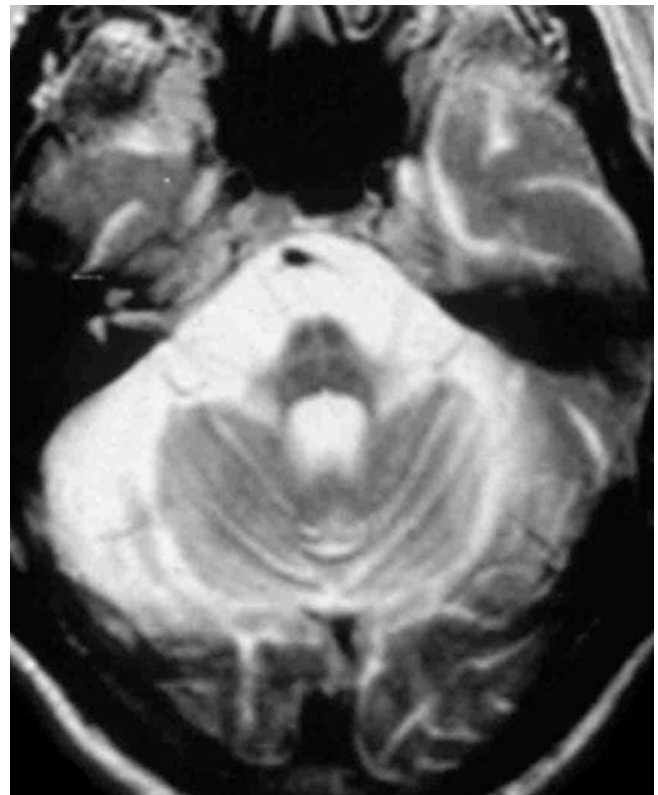


**Fig. 9.177** OPCA/MSA. In this patient with olivoponto-cerebellar atrophy the pons is significantly reduced in size with a so-called "hot-cross bun sign". These changes are predominantly seen in multi system atrophy with cerebellar symptoms

degeneration (SND) denote different manifestations of the clinical neuro-pathological MSA spectrum, whose specific feature is the detection of  $\alpha$ -synuclein-positive deposits in the oligodendrocytes.

The diverse clinical symptoms and a lack of knowledge with regard to the pathogenesis have led to a range of confusing descriptive names, acronyms and proper names that have been previously used for multiple system atrophy (MSA). In the 20th century literature there is an abundance of descriptions of patients with a combination of neurological and autonomic failure of differing degrees and with variable pathomorphological changes. In 1900 Déjérine and Thomas already coined the term "*l'atrophie olivo-ponto-cérébelleuse*" (OPCA), Shy and Drager described two patients in 1960 with a combination of impotence, pronounced orthostatic hypo-tension and Parkinson's syndrome (Shy-Drager syndrome, SDS) and syndromes associated with akinesia, tremor, erectile dysfunction and incontinence were designated striato-nigral degeneration (SND) according to anatomic-pathological aspects. Finally, in 1969 Oppenheimer and Graham made a hypothesis that OPCA, SND and SDS could be different disease spectrums of a single disease and introduced the term MSA, which, however, was not yet defined by exact diagnostic criteria or specific pathological changes and so was rarely used.

The description of MSA as a neuropathological entity only became possible in 1989 thanks to the work of Papp, Kahn and

Lantos, who, in eleven cases with OPCA, SND and SDS, **observed argyrophile glial cytoplasmic inclusions** (glial cytoplasmic inclusions, GCI) in oligodendrocytes and later also in nerve cells. These GCI have proved to be specific and permit a definitive neuro-pathological diagnosis of MSA. What mechanisms lead to the formation of these deposits and the importance they have for the loss of nerve and glial cells is unknown. The GCI themselves consist of aggregated fibrillary structures that measure 10–15 nm in diameter, are similar to microtubules and inter alia contain  $\alpha$ -synuclein,  $\alpha$ - $\beta$ -crystalline and tau. Until now, no mutations in the  $\alpha$ -synuclein gene or in other candidate genes could be proven in MSA patients.

### ■ ■ Epidemiology

With improved neuro-pathological diagnostic options MSA was found in studies of different brain banks in about 5–22% of all autopsies of Parkinson's disease patients. Epidemiological studies continue to be difficult because the clinical diagnosis does not allow us to make definitive statements. The age-adjusted prevalence of MSA is estimated to be 4.4 (2–15):100,000 inhabitants, the incidence is estimated to be ~0.6 per 100,000 inhabitants per year. Until now, no familial incidence has been reported and so far no clear exogenous risk factors have been identified.

### ■ ■ Symptoms, Disease Progression

The mean age at the onset of MSA falls in the 6th decade of life; men and women are affected equally. At the beginning of the disease most patients present with Parkinson's symptoms (46%) or autonomic disorders (41%). Cerebellar disorders are initially found in about 5–10% of patients. The autonomic disorders, in particular erectile dysfunction, but also an increase in urinary frequency, urge incontinence and urinary retention may occur years before motor disturbances occur.

Once neurological symptoms occur, the progression of MSA is swift: the median survival time after diagnosis is 9 years. During this time almost all patients develop a mixed picture consisting of autonomic disorders, Parkinson's symptoms, cerebellar ataxia and signs of pyramidal tract damage in different combinations and states of expression. Autonomic disorders eventually occur in all patients, 50–70% suffer from urinary incontinence, about the same number from vertigo and dizziness. The plurality of MSA patients in the late stages of the disease show signs of Parkinson's disease with bradykinesia, rigidity, hypophonia and dysphagia (90%). Speech and swallowing disorders are often particularly pronounced and cannot be pharmacologically treated. Typical cerebellar signs (gait and extremity ataxia, optokinetic nystagmus and dysarthria) are present in 20–50%, a positive Babinski sign or reflex increases in approximately 60% of the MSA patients. Cognitive impairment is rare.

The most common cause of death is broncho-pneumonia due to pronounced hypokinesia and immobilisation.

### ■ ■ Diagnosis

So far, the definitive diagnosis of MSA can only be made neuro-pathologically. The currently valid, unfortunately quite complex clinical diagnostic criteria distinguish among possible, probable and definite neuro-pathologically secure MSA. Thus, MSA is

likely, if in addition to severe orthostatic hypotension (a drop in blood pressure by at least 30 mmHg systolic or at least 15 mmHg diastolic) or permanent urinary incontinence, Parkinson's syndrome or cerebral dysfunction responds poorly to treatment. Disease onset before 30 years of age or a positive family history exclude MSA. Critical to the diagnosis are a careful medical history and clinical examination, whereas additional diagnostic tools serve primarily to exclude other diseases.

### ■ ■ Differential Diagnosis

The differential diagnosis must set MSA apart from diseases with orthostatic dysregulation, idiopathic Parkinson's disease (IPD), other atypical Parkinson's syndromes in addition to sporadic ataxias that occur in adulthood.

**Orthostatic Dysregulation** Orthostatic dysregulation is confirmed by the Schellong test with a drop in systolic BP of at least 20 mmHg or the diastolic BP 10 mmHg within 3 min after getting up. This drop in blood pressure is often associated with an inadequate increase in heart rate <10 beats/minute. A variety of diseases, especially cardiac and endocrinological disorders in addition to adverse drug side effects can trigger secondary orthostatic hypotension. **Primary autonomic disorders** with orthostatic dysregulation are:

- Reflex syncope
- Postural orthostatic tachycardia syndrome (postural orthostatic tachycardia syndrome, POTS)
- Acute pandysautonomia
- Pure autonomic dysfunction (pure autonomic failure, PAF)
- MSA

The reflex (vasovagal or neurocardiac) syncope and the postural orthostatic tachycardia syndrome are characterised by the complete absence of other symptoms in the (syncope-free) interval. The rare acute pandysautonomia is characterised by the acute development of severe autonomic disorders within weeks, probably as part of an immune-mediated neuropathy. In addition to MSA, only the pure autonomic dysfunction is associated with chronic orthostatic hypotension and autonomic control disorders. Unlike MSA, in which the pre-ganglionic neurons of the spinal cord are primarily affected, PAF is caused by degeneration of peripheral post-ganglionic neurons. This difference can be used for differentiation in diagnostic imaging using MIBG SPECT.

### ■ ■ Idiopathic Parkinson's Disease and Atypical Parkinson's Syndromes

Parkinson's syndromes and symptoms may occur in the context of other neuro-degenerative diseases and as drug side effects. Atypical Parkinson's syndromes are also characterised by symptoms, such as akinesia, rigidity, resting tremor and postural instability occurring to a varying extent. MSA patients, however, differ from IPD patients in a number of ways. Symptoms at disease onset often occur symmetrically, tremor is more rarely present and irregular in many patients and reminiscent of myoclonus. Many MSA patients develop severe hypo-tension. Although orthostasis problems can also occur in the course of IPD, they do not count as early signs and seem to predominantly result from a disturbance in the post-ganglionic autonomic nervous system.

In comparison to IPD the progression of MSA is far more dramatic. A rapid deterioration or even loss of the ability to walk within <5 years practically rules out IPD. Unlike IPD, no more than one third of MSA patients can be satisfactorily treated with L-dopa. A non-responsiveness to L-dopa and orthostatic hypotension early in the disease should therefore always be cause for a critical review of the IPD diagnosis.

While autonomic disorders are characteristic of MSA, falls and cognitive deterioration make a progressive supra-nuclear palsy (PSP, Steele–Richardson–Olszewski syndrome) more likely.

#### ■ ■ Medical Imaging

Magnetic resonance imaging and PET or SPECT can support the diagnosis of MSA and distinguish it from IPD. In later stages the cranial MRI is of definite diagnostic value. The results show pathological signal behaviour found on the T2-weighted sequences in the dorso-lateral parts of the putamen and in the middle cerebellar peduncle. These characteristic findings allow a clear diagnosis in 80% of cases in the advanced stages of the disease. A suitable PET examination, which shows the pre- and post-synaptic areas of the nigro-striatal system, can confirm the diagnosis.

### 9.9.6 Huntington's Disease

This autosomal dominant hereditary disease usually affects patients from the age of 40 onwards. A diffuse cortical atrophy, particularly of the caudate nucleus and the putamen (■ Fig. 9.178). The atrophy of the caudate nucleus causes a widening of the frontal horns.

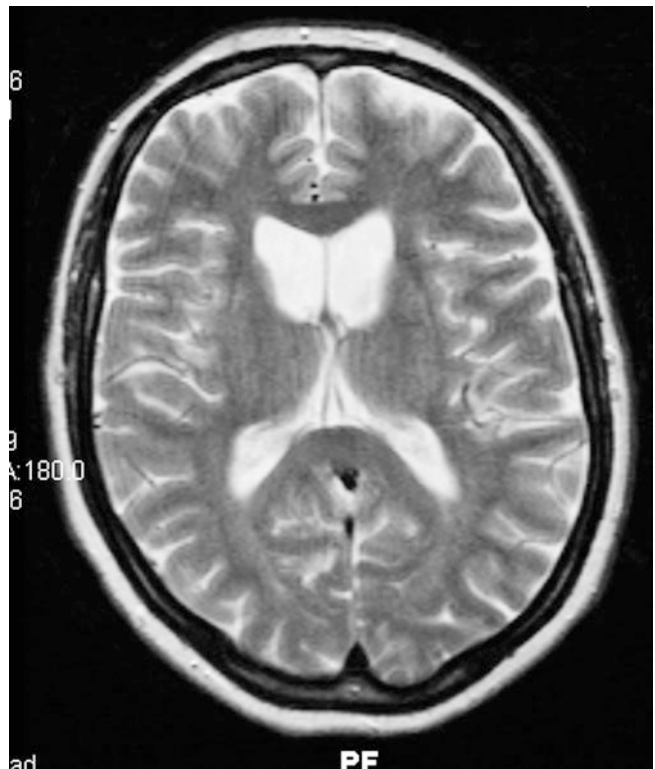
### 9.9.7 Fahr's Disease

#### ■ ■ Definition, Pathogenesis

Symmetrical intra-cerebral calcifications are frequently diagnosed using CT imaging (■ Fig. 9.179) as an often non-specific incidental finding, although the extent of intra-cerebral calcifications differs greatly. The association between symmetrical basal ganglia calcifications and neurological or psychiatric symptoms is generally called Fahr's disease, while the so-called Fahr's syndrome involves pathological changes in the calcium metabolism and a variety of neurological and neuro-psychological deficits.

The clinical picture referred to as Fahr's disease, also known in the literature as symmetrical basal ganglia calcification, non-atherosclerotic vascular calcification, cerebrovascular calcinosis, striato-dental or striato-nigral calcification, was first described as an independent disease post-mortem in 1931 by Thomas Fahr. Predilection sites for calcium deposits are the dentate nucleus and the cerebellar medulla, red nucleus, substantia nigra, globus pallidus, the striatum, the nucleus lateralis of the thalamus (the pulvinar thalamus) and partially the centrum semi-ovale in addition to the capsula interna of the cerebral hemispheres.

**Histologically**, calcification structures could be detected both peri-vascularly and in the tunica adventitia and media of arter-



■ Fig. 9.178 **Huntington's disease.** In Huntington's disease there is atrophy of the basal ganglia, mainly the caudate nucleus, which is less pronounced in the putamen and cerebellum. On these axial T2-weighted sequences of a patient with known Huntington's disease the caudate nucleus is reduced in size on both sides

ies, veins and in particular the capillaries. The calcium deposits consist of hydroxyapatite with quantities of magnesium, iron, silicon, aluminium, zinc and phosphate compounds. As a precursor to the formation of these irreversible areas of calcification, hyalinisation of the vessel walls in addition to a peri-vascular accumulation of polysaccharide–protein complexes, also known as pseudo-calcifications could be proven, which cannot be diagnosed on conventional X-ray investigations and on CT scans.

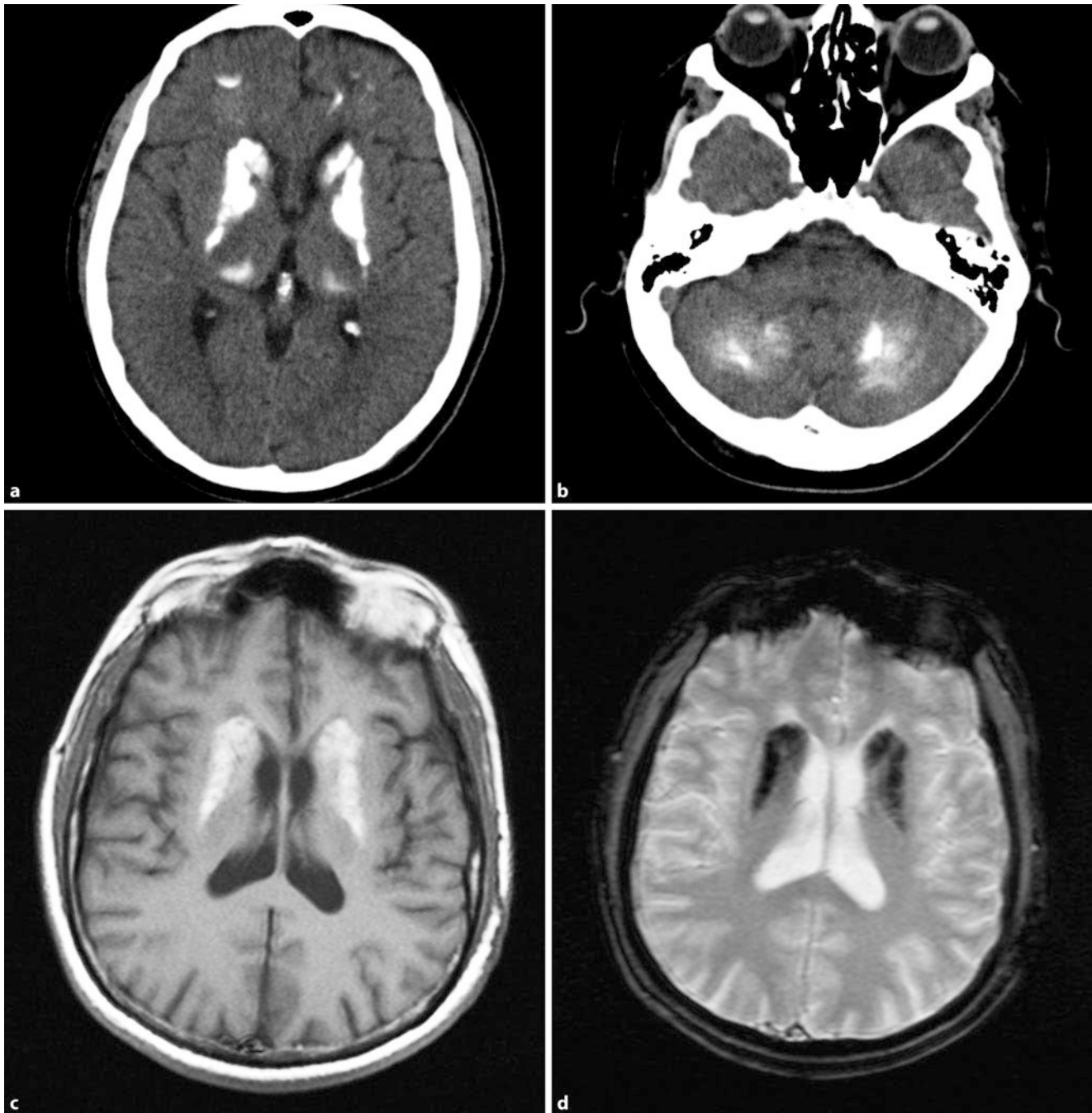
#### ■ ■ Symptoms

The clinical presentation of Fahr's disease is variable and affects all age groups, whereby the disease has a slow progression in most cases. Depending on the location of the calcifications a wide variety of clinical symptoms results, which singularly do not allow a definite diagnosis and make it difficult to differentiate from other possible clinical pictures. In addition to various emergent epileptic seizure equivalents, dominating deficits of the extrapyramidal motor system are in the foreground and can express themselves as hyper- or hypokinesia, and rigidity and spasticity through to Parkinson's syndrome as the most commonly observed movement disorder.

#### ■ ■ Medical Imaging, Diagnosis

In Fahr's disease bilateral calcifications of the basal ganglia, thalamus and the dentate nucleus in addition to the medullary layer of the cerebral hemispheres show up in the full investigation. In addition, infra-tentorial calcifications in the cerebellar hemi-





■ **Fig. 9.179a–d Fahr disease.** a, b CT, c T1-weighted, d T2-weighted images. In this 63-year-old patient pronounced calcification of the basal ganglia shows on both sides, also the thalamus on both sides and both sides of the

cerebellar hemispheres. On the T1-weighted axial images the calcifications appear hyper-intense; on the T2-weighted gradient-echo sequences, the calcifications are hypo-intense

spheres may also occur. More than 50% of patients with symmetrical basal ganglia calcifications that have been investigated with high-resolution CT do not show neurological deficits that match the clinical picture of the disease: the extent of changes that can be evaluated with medical imaging procedures does not correlate with the severity of the neurological and neuro-psychological deficits.

Patients usually show a calcium and phosphate metabolism disorder with serological evidence of hypocalcaemia and hyperphosphataemia.

### 9.9.8 Other Diseases Associated with Degenerative Changes

Some of the diseases discussed in ► Sect. 9.8 can also lead to degenerative changes in the brain.

In **Wilson's disease**, for example (► Sect. 9.7.11, ■ Fig. 9.168) degeneration in the basal ganglia caused by disorders in the copper metabolism are observed. Carbon monoxide and methanol can also cause signal variations in the basal ganglia, particularly

in the globus pallidus (hypo-intense on T1-weighted images, hyper-intense on T2-weighted images).

Even in **Niemann–Pick disease type C** (▶ Sect. 9.7.6) atrophy of the brain is often detectable (■ Fig. 9.166). Neuronal storage processes show up in granular inclusions and cellular outgrowths, for example, in deep cortical layers, basal ganglia, thalamus, substantia nigra and locus coeruleus. The white matter is usually regular, but in some cases there are demyelinations with peri-vascular macrophages. Over longer periods of progression neuro-fibrillary tangles have also been described; however, with a different distribution from that in Alzheimer's dementia.

## 9.10 Hydrocephalus and Intra-cranial Hypotension

### 9.10.1 Hydrocephalus

#### ■ Fundamentals

##### ■ Definition

As a result of an imbalance between CSF production and resorption a widening of ventricles and/or sub-arachnoid CSF spaces results in hydrocephalus (■ Table 9.19). It is a symptom that has a range of causes. In early childhood increased head growth and macrocephaly soon result. A ventricular widening because of a loss of brain substance occurs alongside normal intra-cranial pressure. ■ Table 9.15 shows a schematic representation of the CSF spaces.

##### ■ Epidemiology

In 3–4:1,000 new-born children hydrocephalus can occur. In 25–30% is innate and combined with a spina bifida.

##### ■ Aetiology

The following three mechanisms must be considered as causal mechanisms for hydrocephalus (■ Table 9.19):

- Overproduction of CSF resulting in hyper-secretory hydrocephalus
- Disorder in the CSF passage as a CSF blockage resulting in non-communicating hydrocephalus
- Decreased absorption of CSF resulting in communicating or malresorptive hydrocephalus

Causes of hydrocephalus are deformities, sequelae of infection, bleeding or tumours. Aqueductal stenosis can be caused by a sex-linked recessive mutation. Intra-ventricular haemorrhage in pre-term infants are a common cause. Hyper-secretory hydrocephalus occurs intermittently in cases of inflammation and trauma; it is progressive in cases of choroid plexus papilloma. Resorption disorders usually result from infections and bleeding.

Following the closure of the CSF pathways occlusive hydrocephalus (internus) develops. The obstruction results in the retention of the CSF formed by the choroid plexus and ependyma by ultrafiltration and secretion. As a result there is an increase in intra-cranial pressure and compression of brain tissues. The obstruction site determines the nature and course of emerging symptoms (blockage of the foramen of Monro, aqueduct stenosis, obliteration of the apertures of the fourth ventricle).

In hyper-secretory hydrocephalus cases the increased CSF production leads to a pressure increase; the passage is permeable (communicating hydrocephalus). This also applies to the malresorptive hydrocephalus, which is caused by changes in the arachnoid villi (Pacchioni's granulations) and the impaired resorption (external hydrocephalus). A difference must be made between an acute, active hydrocephalus in which intra-cranial pressure symptoms develop quickly from chronic hydrocephalus, which will occasionally come to a spontaneous stop. "Normal pressure hydrocephalus", in which an intermittent and overall only slight pressure increase causes progressive ventricular widening, presents specific diagnostic problems. Often, various factors occur in combination.

##### ■ Symptoms

As long as **the cranial sutures have not yet fused together**, an increase in intra-cranial pressure will at first lead to increased growth in head circumference. That is why measuring the cranial circumference is one of the important tasks carried out at preventive medical check-ups. Hydrocephalus can be assumed, if the growth curve crosses the percentile curve in an upward direction.

Symptoms of increased pressure are rather limited and non-specific in infants: vomiting, failure to thrive, general restlessness and high-pitched screams. Fontanelles that are tense or bulging, even in an upright posture, dilated cranial sutures, increased venous drawing or a deformation of the head with frontal bossing and a dislocation of the ears are important indicators. The sunset phenomenon of the eyes results from a vertical gaze palsy due to compression of the orbital roof. Papilloedema occurs rarely in early childhood; optic atrophy and strabismus are more likely. In neurological studies, it is not uncommon to find signs of cerebral palsy, statomotor development is often delayed, psychological reactions are mainly altered in acute forms of hydrocephalus.

If the **cranial sutures are closed** signs of raised intra-cranial pressure will be at the fore, right from the beginning. Behavioural changes due to organic psycho-syndrome, headache, vomiting (especially in the morning, on an empty stomach), papilloedema and fundus haemorrhage. If pressure relief does not occur in good time there is a danger of herniation in the area of the foramen magnum, with the occurrence of extensor spasms and autonomic dysregulation.

##### ■ Medical Imaging

**Ultrasound.** Hydrocephalus should always be suspected when increased head growth is noticeable. Ultrasound of the brain and ventricular system, which in infants works well through the open fontanelle, quickly delivers information about ventricular size, bleeding, malformations and other structural changes; thus, a differential diagnosis ruling out other causes of macrocephaly is possible.

**Computed Tomography and Magnetic Resonance Imaging.** This is the best way of assessing the morphological situation. Measurements can be performed with MRI of the CSF flow, to assess CSF dynamics more accurately.

■ **Table 9.19** Hydrocephalus and its causes

Designation	Cause	Location of change	Cause
Hyper-secretory hydrocephalus	Increased CSF production	Choroid plexus	Choroid plexus papilloma, plexus carcinoma
Occlusive/non-communicating hydrocephalus	Reduced CSF flow	Narrowing of the foramen, of Monro, of the aqueduct and more rarely of the foramen of Magendie or Luschka	Aqueductal stenosis, narrowing of the foramen of Monro, Magendie, Luschka space-occupying lesions, e.g. intra-ventricular cysts, colloid cysts, hypophysadenoma, craniopharyngioma, pineal tumours, tectal glioma, cerebellar tumours, cerebellar infarction, epidermoid post-haemorrhagic, post-infectious
Malresorptive hydrocephalus	Reduced CSF resorption	Pacchioni's granulations	Adhesions, post-haemorrhagic and post-infectious Increased venous pressure in cases of venous sinus thrombosis, dural AV malformation, cor pulmonale reverse aetiology in normal pressure hydrocephalus

With an increase in CSF pressure and the onset of ventricular enlargement, dilatation of the temporal horns is usually the first and most sensitive sign of a CSF build-up. As the condition progresses all ventricular sections are then affected by the increase in pressure. The posterior and anterior horns of the lateral ventricles appear blunted and rounded. As a sign of increased CSF pressure, so-called pressure caps (peri-ventricular interstitial oedema) can be detected around the ventricles, usually around the anterior horns in particular. These are expressions of trans-ependymal CSF diapedesis.

➤ **It is often impossible to make a clear distinction between hydrocephalus and a secondary enlargement of the CSF spaces caused by generalised brain atrophy.**

#### ■ ■ Treatment

Medication only has a limited influence on CSF production. An active hydrocephalus cannot be treated in a conservative manner. Instead, the imbalance between production and absorption must be mechanically remedied. Only occasionally can a “wait and see” attitude be justified in situations where regular check-ups are carried out. Congenital hydrocephalus can be diagnosed during a prenatal ultrasound examination.

Trials of intra-uterine treatment have so far had no convincing success.

In cases of acute hydrocephalus rapid relief needs to be ensured.

#### ■ Occlusive Hydrocephalus

##### ■ ■ Aetiology, Diagnosis

Causes of occlusive hydrocephalus are deformities, sequelae of infection or bleeding and tumours. Aqueductal stenosis (■ Fig. 9.180) can be caused by sex-linked, recessive hereditary mutations (■ Table 9.19). Intra-ventricular haemorrhages in pre-term infants are a common cause.

The lateral ventricles are connected to the third ventricle via the foramina of Monro. The foramina of Monro are physiologically narrowed sites in the CSF system. Narrowing of the foramina of Monro in children, e.g. because of pilocytic astrocytomas, germinomas, craniopharyngiomas and supra-sellar arachnoid cysts, occasionally also because of sub-ependymal giant cell

astrocytomas in patients with tuberous sclerosis, can lead to a narrowing or blockage with a corresponding CSF circulation disorder (■ Fig. 9.94).

Colloid cysts are rounded, well-circumscribed, smooth epithelium-lined cysts and usually become symptomatic in the 3rd to 5th decades of life. The contents of colloid cysts usually consist of viscous fluid; the cysts only slowly increase in size, but can result in an acute blockage of the foramen, cranial pressure symptoms then appear suddenly. Typically, colloid cysts are located in the anterior portion of the third ventricle. On MRI, they are spherical and well-defined smooth structures that normally show as hyper-intensity on T1-weighted sequences, and hypo-intensity on T2-weighted sequences (■ Fig. 9.111). In adults, macroadenomas of the pituitary gland, craniopharyngiomas and central neurocytomas are more common, leading to a blockage of the foramen of Monro.

A compression of the aqueduct can be caused by tumours in the pineal region or by tectal tumours (tectal gliomas; ■ Fig. 9.181). The caudal portions of the aqueduct can be blocked by cerebellar tumours.

With Chiari malformations (■ Figs. 9.34, 9.35) aqueductal stenoses are frequently detectable. Significantly enlarged lateral ventricles and the widened third ventricle are characteristic of aqueductal stenoses, with normal width of the fourth ventricle.

#### ■ Non-resorptive Hydrocephalus

Decreased absorption of CSF, e.g. due to adhesions or blockages in the Pacchioni's granulations following sub-arachnoid haemorrhage or meningitis also leads to a CSF build-up. Other causes may be pressure increases in the intra-cranial venous system, such as in sinus vein thrombosis, arterio-venous malformations and dural fistulas. In some patients venous pressure increases are the cause of pseudotumour cerebri. The patients experience headaches, papilloedema, visual loss, even blindness and uni- or bilateral abducens nerve pareses. Venous MR angiography can demonstrate or exclude an outflow obstruction in the sinus or venous system.

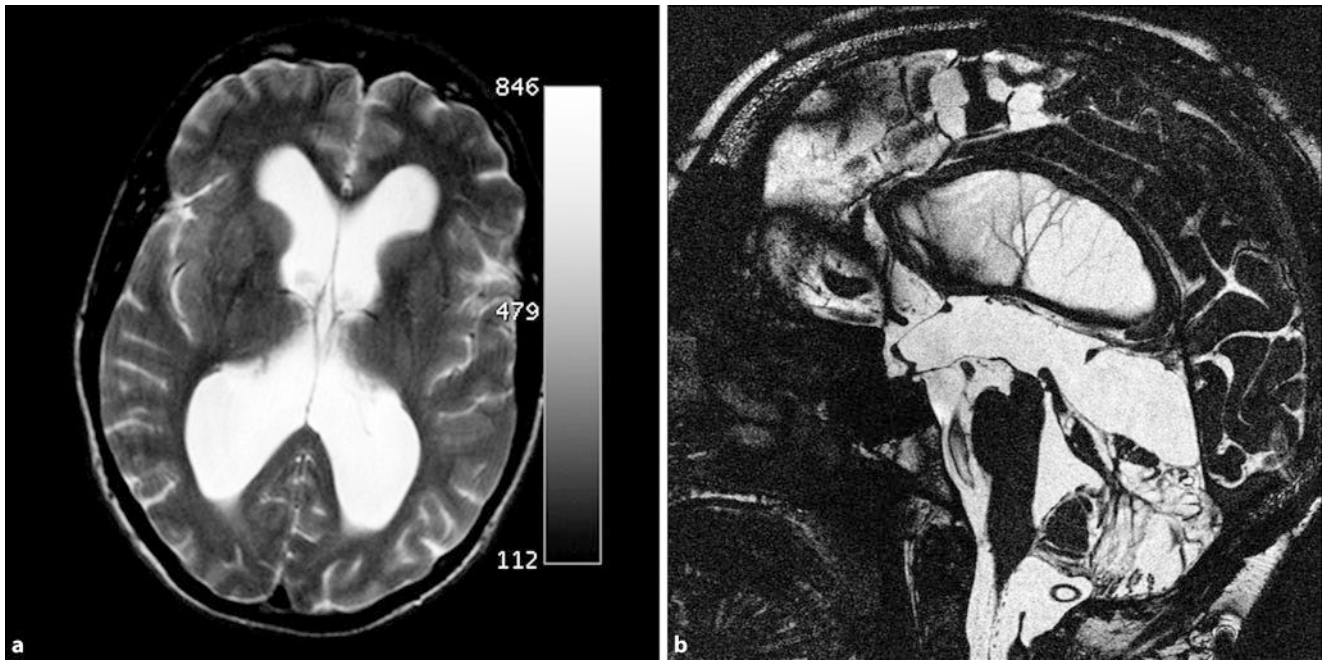


**Fig. 9.180** Aqueductal stenosis. **a** On the axial T2-weighted sequences a significant widening of the internal CSF spaces can be found in combination with an age-appropriate size of the external CSF spaces. **b** On the sagittal

high-resolution T2-weighted sequences (TRUFI) the aqueduct is closed off by a membrane. The commonly seen flow signal above and below the aqueduct in the third and fourth ventricles is not detectable

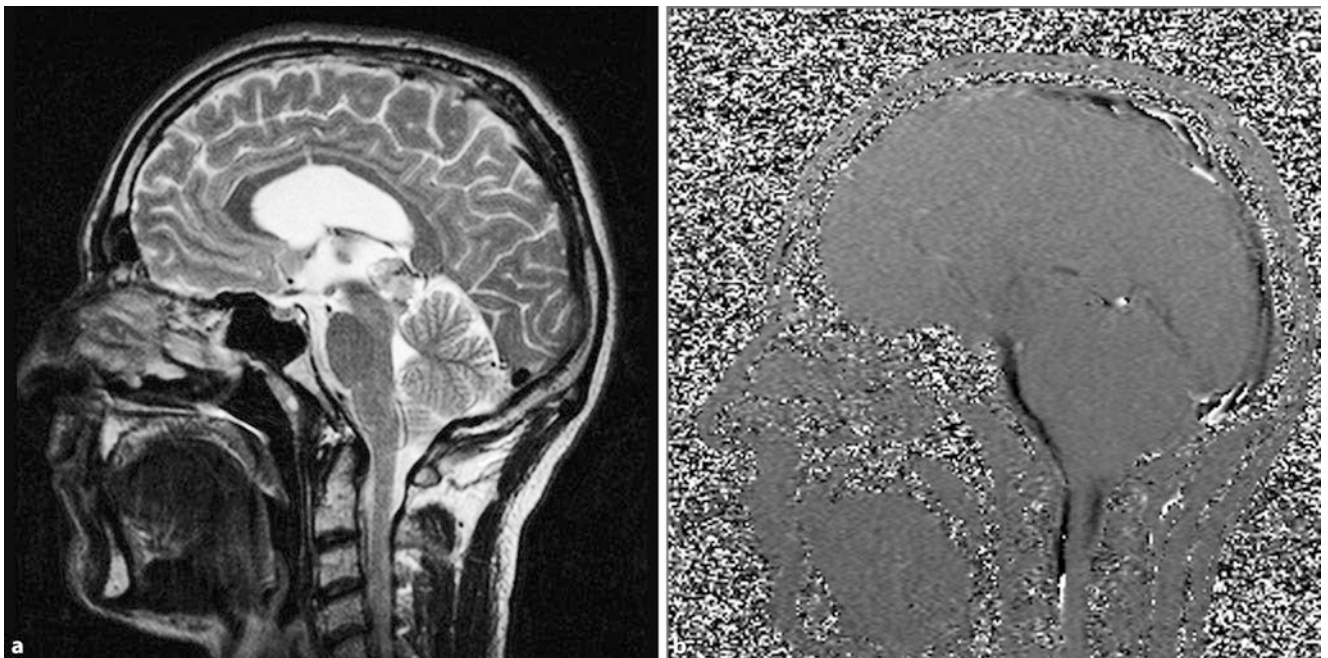


**Fig. 9.181a,b** Tumour of the quadrigeminal plate. **a** On the sagittal T2-weighted sequences a swelling of the lamina tecti, the so-called quadrigeminal plate, is shown. This tumour in the quadrigeminal plate causes

a compression of the aqueduct with a consecutive reabsorption disorder. **b** Measurements of the CSF flow show that flow in the aqueduct is no longer detectable

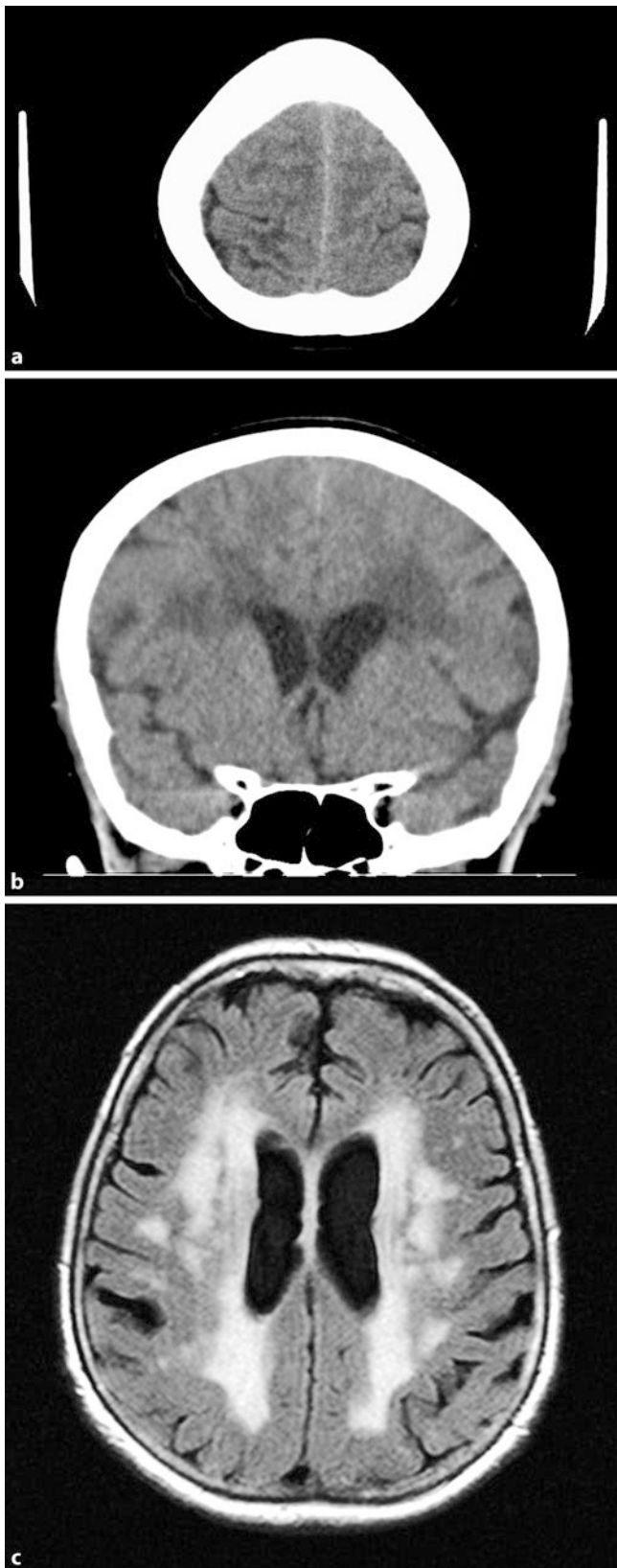
### ■ Normal Pressure Hydrocephalus

#### ■ Definition, Epidemiology, Symptoms

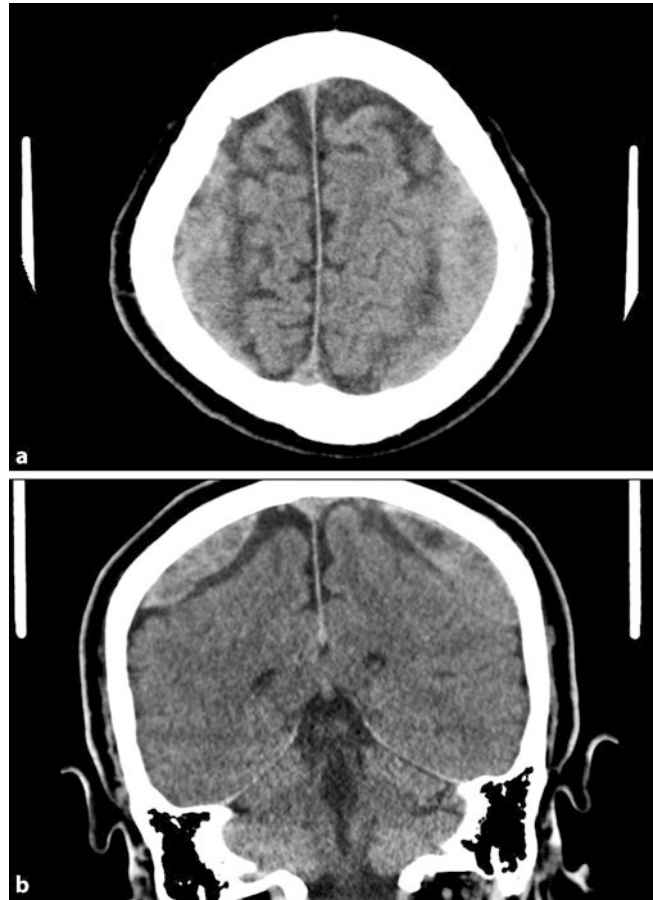
The term normal pressure hydrocephalus (NPH; **Fig. 9.182**) stands for a special form of chronic communicating hydrocephalus. Clinical signs are the triad of: gait disorder, dementia and urinary incontinence. Symptomatic NPH usually occurs after the age of 60, the prevalence is estimated to be 0.4% of over-65s.

#### ■ Aetiology, Pathogenesis

The aetiology of NPH is not yet fully understood. A certain connection between NPH and micro-angiopathic changes seems to exist. The capacity of CSF reabsorption in NPH patients is reduced, without any inflammation or bleeding at Pacchioni's granulations being detectable. The common pathogenetic final pathway of various noxious agents, after which NPH can develop,



■ **Fig. 9.182a,b Normal pressure hydrocephalus.** a On the axial, apical CT images an obliteration of the sulci is detectable. b On the coronal CT images CSF spaces appear to be age-appropriate. Significant discrepancy with the almost completely obliterated apical sulci. c On the axial FLAIR sequences, pronounced medullary layer changes are detectable in addition to the widening of the internal CSF spaces



■ **Fig. 9.183a,b Patient with known hydrocephalus, low CSF pressure.** Because of a change in the pressure setting of the ventricular catheter valve a low CSF pressure with consecutive sub-dural apical haematoma on both sides occurred

is a blockade of the cisternal and/or cortical sub-arachnoid spaces with a consequent increase in CSF resistance. The widening of the ventricular system is caused by the increased trans-cerebral pressure gradient between the intra-ventricular CSF space and the fibrotically altered sub-arachnoid space above the brain convexity (cortical lepto-meningeal fibrosis). CSF pressure is not at all normal in NPH; it is characterised rather by intermittent or periodic pressure increases, and while these do not exceed the limits of physiological autoregulation, they may lead to a reduction of regional cerebral blood flow in the long term.

#### ■ ■ Diagnosis

A distinction between NPH and atrophic ventricular widening is very hard and not possible by means of imaging.

NPH is not a radiological diagnosis; clinical correlation is crucial. The definitive diagnosis can only be made after clinical improvement following ventricular drainage. CSF flow measurements can help predict which patients will benefit from a ventricular shunt. Radio-isotope studies are also performed. Consequences of NPH are a degeneration of the extra-pyramidal nuclei.

#### ■ ■ Treatment

Lasting and drastic improvements can be achieved with shunt surgery. CSF drainage should control periodic CSF pressure

peaks and thus reverse the hydro-dynamic effects of ventricle widening and the ensuing reduction in regional cerebral blood flow and cerebral metabolism, before the trans-ependymal CSF diapedesis has caused irreversible structural lesions in the form of peri-ventricular demyelination and permanent neurological psychiatric deficits.

### 9.10.2 Low CSF Pressure

---

#### ■ ■ Epidemiology, Symptoms

Spontaneous low CSF pressure is a rare clinical picture; however, it is one with increasing tendency. The clinical symptoms are similar to those of post-lumbar puncture syndrome. The leading symptom is the position-dependent headache (especially in the upright position); additionally, nausea, vomiting, tinnitus, cranial nerve palsies and hearing disorders also occur.

#### ■ ■ Aetiology

The cause of spontaneous low-pressure syndrome is a CSF leakage (■ Fig. 9.183), which is mostly situated in a cervical or cervico-thoracic location. The aetiology is still largely unknown. Possible complications are cranial SDH.

#### ■ ■ Medical Imaging

Imaging, particularly MRI, frequently shows diffuse contrast enhancement of the dura, often also accompanied by a caudal shift of the brain-stem. Knowledge of this constellation of radiological findings can be very helpful in making a diagnosis. It is possible that CSF leakage can be detected on the T2-weighted, fat-suppressed sequences. A further possibility is the intra-thecal administration of gadolinium-based contrast agents to better localise the site of CSF leakage.

### References

---

- Lo, Stephens, Fernandez: Statement of correction: paediatric stroke in the United States and the impact of risk factors. *J Child Neurol* 2009; 24: 194
- Naidich, Duvernoy, Sorensen and Haacke (editors). *Duvernoy's atlas of the human brain stem and cerebellum*. Springer, Vienna, 2009
- Price 1998
- Reiser M, Semmler W. *Magnetresonanztomographie*. Springer, Berlin, Heidelberg, New York, 2002
- Tillmann B. *Atlas der Anatomie des Menschen*. 2nd edn, Springer, Berlin, Heidelberg, New York, 2009